


Advances in Experimental Medicine and Biology 1208

Zhiping Xie *Editor*

Autophagy: Biology and Diseases

Technology and Methodology

 Science Press
Beijing

 Springer

Advances in Experimental Medicine and Biology

Volume 1208

Series Editors

Wim E. Crusio, Institut de Neurosciences Cognitives et Intégratives d'Aquitaine,
CNRS and University of Bordeaux, Pessac Cedex, France

Haidong Dong, Departments of Urology and Immunology, Mayo Clinic,
Rochester, MN, USA

Heinfried H. Radeke, Institute of Pharmacology & Toxicology,
Clinic of the Goethe University Frankfurt Main, Frankfurt am Main,
Hessen, Germany

Nima Rezaei, Research Center for Immunodeficiencies, Children's Medical Center,
Tehran University of Medical Sciences, Tehran, Iran

Ortrud Steinlein, Institute of Human Genetics, LMU University Hospital,
Munich, Germany

Junjie Xiao, Cardiac Regeneration and Ageing Lab, Institute of Cardiovascular
Science, School of Life Science, Shanghai University, Shanghai, China

Advances in Experimental Medicine and Biology provides a platform for scientific contributions in the main disciplines of the biomedicine and the life sciences. This series publishes thematic volumes on contemporary research in the areas of microbiology, immunology, neurosciences, biochemistry, biomedical engineering, genetics, physiology, and cancer research. Covering emerging topics and techniques in basic and clinical science, it brings together clinicians and researchers from various fields.

Advances in Experimental Medicine and Biology has been publishing exceptional works in the field for over 40 years, and is indexed in SCOPUS, Medline (PubMed), Journal Citation Reports/Science Edition, Science Citation Index Expanded (SciSearch, Web of Science), EMBASE, BIOSIS, Reaxys, EMBiology, the Chemical Abstracts Service (CAS), and Pathway Studio.


2019 Impact Factor: 2.450 5 Year Impact Factor: 2.324

More information about this series at <http://www.springer.com/series/5584>

Zhiping Xie
Editor

Autophagy: Biology and Diseases

Technology and Methodology

 Science Press
Beijing

 Springer

Editor
Zhiping Xie
Shanghai Jiao Tong University
Shanghai
China

ISSN 0065-2598 ISSN 2214-8019 (electronic)
Advances in Experimental Medicine and Biology
ISBN 978-981-16-2829-0 ISBN 978-981-16-2830-6 (eBook)
<https://doi.org/10.1007/978-981-16-2830-6>

© Science Press 2021

This work is subject to copyright. All rights are reserved by the Publisher, whether the whole or part of the material is concerned, specifically the rights of translation, reprinting, reuse of illustrations, recitation, broadcasting, reproduction on microfilms or in any other physical way, and transmission or information storage and retrieval, electronic adaptation, computer software, or by similar or dissimilar methodology now known or hereafter developed.

The use of general descriptive names, registered names, trademarks, service marks, etc. in this publication does not imply, even in the absence of a specific statement, that such names are exempt from the relevant protective laws and regulations and therefore free for general use.

The publisher, the authors, and the editors are safe to assume that the advice and information in this book are believed to be true and accurate at the date of publication. Neither the publisher nor the authors or the editors give a warranty, expressed or implied, with respect to the material contained herein or for any errors or omissions that may have been made. The publisher remains neutral with regard to jurisdictional claims in published maps and institutional affiliations.

This Springer imprint is published by the registered company Springer Nature Singapore Pte Ltd.
The registered company address is: 152 Beach Road, #21-01/04 Gateway East, Singapore 189721, Singapore

Introduction

This book series consists of three volumes covering the basic science (Volume 1), clinical science (Volume 2), and the technology and methodology (Volume 3) of autophagy. Volume 3 focuses on the technical aspects of autophagy research. It is comprised of two parts. The first part discusses the basic process of autophagy, including its overall classification and individual stages in the life cycle of autophagosomes. The second part discusses the tools, strategies, and model systems in current autophagy research, including cell and animal models, detection and manipulation methods, as well as screening, genomic, proteomic, and bioinformatic approaches. The book is written and edited by a team of active scientists. It is intended as a practical reference resource for interested researchers to get started on autophagy studies.

Contents

Part I Investigating Autophagy: The Basics

1	The Classification and Basic Processes of Autophagy	3
	Tiejian Nie, Lin Zhu, and Qian Yang	
2	Autophagosomal Membrane Origin and Formation	17
	Yi Yang, Li Zheng, Xiaoxiang Zheng, and Liang Ge	
3	Phagophore Closure	43
	Yongheng Liang	
4	The Fusion Between Autophagic Vesicles and Lysosomes	55
	Xiaoxia Liu and Qing Zhong	
5	Autophagosome Trafficking	67
	Jingjing Ye and Ming Zheng	
6	Mechanisms of Selective Autophagy	79
	Qi-Wen Fan and Xiang-Hua Yan	
7	Similarities and Differences of Autophagy in Mammals, Plants, and Microbes	99
	Fu-Cheng Lin, Huan-Bin Shi, and Xiao-Hong Liu	

Part II Investigating Autophagy: Model Systems, Tools and Strategies

8	Monitoring Autophagy by Optical Microscopy	117
	Yanrong Zheng, Xiangnan Zhang, and Zhong Chen	
9	Autophagic Flux Detection: Significance and Methods Involved	131
	Xiao-Wei Zhang, Xiao-Xi Lv, Ji-Chao Zhou, Cai-Cai Jin, Lu-Yao Qiao, and Zhuo-Wei Hu	

10	Gene Manipulation Protocols in Autophagy	175
	Rong Liu, Ren-Peng Guo, and Yue-Guang Rong	
11	MicroRNAs Regulating Autophagy in Neurodegeneration	191
	Qingxuan Lai, Nikolai Kovzel, Ruslan Konovalov, and Ilya A. Vinnikov	
12	Biomarkers of Autophagy	265
	Fang Lin, Yu-Ting Zhu, and Zheng-Hong Qin	
13	Chemical Autophagy Regulators	289
	Ya-Ping Yang, Fen Wang, and Chun-Feng Liu	
14	Cell Models in Autophagy Research	311
	Rui Huang and Shuyan Wu	
15	Autophagy in <i>Drosophila</i> and Zebrafish	333
	Xiuying Duan and Chao Tong	
16	Screening for Genes Involved in Autophagy	357
	Kefeng Lu and Huihui Li	
17	Proteomics and Autophagy Research	373
	Kefeng Lu and Huihui Li	
18	Bioinformatics Technologies in Autophagy Research	387
	Yu Xue, Dong Wang, and Di Peng	

Editorial Committee

Chief Editor

Xie, Zhiping State Key Laboratory of Microbial Metabolism and Joint International Research Laboratory of Metabolic & Developmental Sciences, School of Life Sciences and Biotechnology, Shanghai Jiao Tong University, Shanghai, People's Republic of China

Associate Editors

Backues, Steven K Department of Chemistry, Eastern Michigan University, Ypsilanti, MI, USA

Komduur, Janet A Institute for Life Science and Technology, Department of Biomedical Research, Hanze University of Applied Science, Groningen, The Netherlands

Zhu, Jing State Key Laboratory of Microbial Metabolism and Joint International Research Laboratory of Metabolic & Developmental Sciences, School of Life Sciences and Biotechnology, Shanghai Jiao Tong University, Shanghai, People's Republic of China

Contributors

Zhong Chen College of Pharmaceutical Sciences, Zhejiang University, Hangzhou, Zhejiang, China

Key Laboratory of Neuropharmacology and Translational Medicine of Zhejiang Province, Zhejiang Chinese Medical University, Hangzhou, Zhejiang, China

Xiuying Duan Life Sciences Institute, Zhejiang University, Hangzhou, Zhejiang, China

The Second Affiliated Hospital, School of Medicine, Zhejiang University, Hangzhou, Zhejiang, China

Qi-Wen Fan College of Animal Sciences and Technology, Huazhong Agricultural University, Wuhan, China

Liang Ge School of Life Sciences, Tsinghua University, Beijing, China

Ren-Peng Guo Nanjing Agricultural University, Nanjing, China

Rui Huang Medical School of Soochow University, Suzhou, China

Zhuo-Wei Hu Institute of Materia Medica, Chinese Academy of Medical Sciences & Peking Union Medical College, Beijing, China

Cai-Cai Jin Institute of Materia Medica, Chinese Academy of Medical Sciences & Peking Union Medical College, Beijing, China

Ruslan Kononov Laboratory of Molecular Neurobiology, Sheng Yushou Center of Cell Biology and Immunology, Department of Genetics and Developmental Biology, School of Life Sciences and Biotechnology, Shanghai Jiao Tong University, Shanghai, China

Nikolai Kovzel Laboratory of Molecular Neurobiology, Sheng Yushou Center of Cell Biology and Immunology, Department of Genetics and Developmental Biology, School of Life Sciences and Biotechnology, Shanghai Jiao Tong University, Shanghai, China

Qingxuan Lai Laboratory of Molecular Neurobiology, Sheng Yushou Center of Cell Biology and Immunology, Department of Genetics and Developmental Biology, School of Life Sciences and Biotechnology, Shanghai Jiao Tong University, Shanghai, China

Huihui Li State Key Laboratory of Biotherapy, West China Hospital, Sichuan University, Chengdu, China

Yongheng Liang College of Life Sciences, Nanjing Agricultural University, Nanjing, China

Fang Lin School of Pharmaceutical Science, Soochow University, Suzhou, China

Fu-Cheng Lin Institute of Plant Protection and Microbiology, Zhejiang Academy of Agricultural Sciences, Hangzhou, China

Chun-Feng Liu Department of Neurology, The Second Affiliated Hospital of Soochow University, Suzhou, China

Rong Liu Nanjing Agricultural University, Nanjing, China

Xiao-Hong Liu Institute of Biotechnology, Zhejiang University, Hangzhou, China

Xiaoxia Liu Key Laboratory of Cell Differentiation and Apoptosis of Chinese Ministry of Education, Department of Pathophysiology, Shanghai Jiao Tong University School of Medicine, Shanghai, China

Kefeng Lu State Key Laboratory of Biotherapy, West China Hospital, Sichuan University, Chengdu, China

Xiao-Xi Lv Institute of Materia Medica, Chinese Academy of Medical Sciences & Peking Union Medical College, Beijing, China

Tiejian Nie Department of Experimental Surgery, Tangdu Hospital, The Fourth Military Medical University, Xi'an, Shaanxi, China

Di Peng Key Laboratory of Molecular Biophysics of Ministry of Education, Hubei Bioinformatics and Molecular Imaging Key Laboratory, Center for Artificial Intelligence Biology, College of Life Science and Technology, Huazhong University of Science and Technology, Wuhan, China

Lu-Yao Qiao Institute of Materia Medica, Chinese Academy of Medical Sciences & Peking Union Medical College, Beijing, China

Zheng-Hong Qin School of Pharmaceutical Science, Soochow University, Suzhou, China

Yue-Guang Rong Huazhong University of Science and Technology, Wuhan, China

Huan-Bin Shi China National Rice Research Institute, Hangzhou, China

Chao Tong Life Sciences Institute, Zhejiang University, Hangzhou, Zhejiang, China
The Second Affiliated Hospital, School of Medicine, Zhejiang University, Hangzhou, Zhejiang, China

Ilya A. Vinnikov Laboratory of Molecular Neurobiology, Sheng Yushou Center of Cell Biology and Immunology, Department of Genetics and Developmental Biology, School of Life Sciences and Biotechnology, Shanghai Jiao Tong University, Shanghai, China

Dong Wang Key Laboratory of Molecular Biophysics of Ministry of Education, Hubei Bioinformatics and Molecular Imaging Key Laboratory, Center for Artificial Intelligence Biology, College of Life Science and Technology, Huazhong University of Science and Technology, Wuhan, China

Department of Bioinformatics, School of Basic Medical Sciences, Southern Medical University, Guangzhou, China

Shuyan Wu Medical School of Soochow University, Suzhou, China

Yu Xue Key Laboratory of Molecular Biophysics of Ministry of Education, Hubei Bioinformatics and Molecular Imaging Key Laboratory, Center for Artificial Intelligence Biology, College of Life Science and Technology, Huazhong University of Science and Technology, Wuhan, China

Xiang-Hua Yan College of Animal Sciences and Technology, Huazhong Agricultural University, Wuhan, China

Qian Yang Department of Experimental Surgery, Tangdu Hospital, The Fourth Military Medical University, Xi'an, Shaanxi, China

Ya-Ping Yang Department of Neurology, The Second Affiliated Hospital of Soochow University, Suzhou, China

Yi Yang Hangzhou Normal University, Hangzhou, Zhejiang, China

Jingjing Ye Department of Physiology and Pathophysiology, Peking University Health Science Center, Beijing, China

Xiangnan Zhang College of Pharmaceutical Sciences, Zhejiang University, Hangzhou, Zhejiang, China

Xiao-Wei Zhang Institute of Materia Medica, Chinese Academy of Medical Sciences & Peking Union Medical College, Beijing, China

Li Zheng School of Life Sciences, Tsinghua University, Beijing, China

Ming Zheng Department of Physiology and Pathophysiology, Peking University Health Science Center, Beijing, China

Xiaoxiang Zheng Zhejiang University, Hangzhou, Zhejiang, China

Yanrong Zheng College of Pharmaceutical Sciences, Zhejiang University, Hangzhou, Zhejiang, China

Qing Zhong Key Laboratory of Cell Differentiation and Apoptosis of Chinese Ministry of Education, Department of Pathophysiology, Shanghai Jiao Tong University School of Medicine, Shanghai, China

Ji-Chao Zhou Institute of Materia Medica, Chinese Academy of Medical Sciences & Peking Union Medical College, Beijing, China

Lin Zhu Department of Experimental Surgery, Tangdu Hospital, The Fourth Military Medical University, Xi'an, Shaanxi, China

Yu-Ting Zhu School of Pharmaceutical Science, Soochow University, Suzhou, China

Part I
Investigating Autophagy: The Basics

Chapter 1

The Classification and Basic Processes of Autophagy



Tiejian Nie, Lin Zhu, and Qian Yang

Abstract Autophagy is a general term for the process of the lysosomal degradation of intracellular components, a process occurring exclusively in eukaryotic cells. Based on the way that intracellular substrates are transported to lysosomes, autophagy in mammalian cells can be divided into three main types: macroautophagy, microautophagy, and chaperone-mediated autophagy (CMA). Each type has its unique molecular machinery and is tightly regulated by various cellular signals, helping cells adapt to a changing environment. Autophagy can also be divided into two categories based on cargo selectivity: selective autophagy and nonselective autophagy. Nonselective autophagy refers to the bulk transport of organelles or other cytoplasmic components to lysosomes, while selective autophagy refers to the degradation of a specific substrate. Autophagy plays an essential role in maintaining cellular homeostasis, and dysregulation of it may participate in the pathological process of many human diseases.

Keywords Autophagy · Types · Basic process · Selective autophagy

There are two main degradation routes in cells: the pathway via the proteasome and the autophagy pathway. Proteasomes primarily degrade short-lived proteins, while autophagy is responsible for the degradation of long-lived proteins and damaged or superfluous organelles. Autophagy is also part of the cellular response to intracellular and extracellular stress. In some cases, autophagy can lead to a specific form of cell death (type II programmed cell death) that is considered different from apoptosis (type I programmed cell death). In fact, autophagy rarely occurs in full scale in normal cells unless there is a predisposing factor. These factors range from extracellular forces, such as nutrient deprivation, ischemia, and hypoxia, to intracellular drivers such as metabolic stress, damaged organelles, and unfolded and/or

T. Nie · L. Zhu · Q. Yang (✉)

Department of Experimental Surgery, Tangdu Hospital, The Fourth Military Medical University, Xi'an, Shaanxi, China

e-mail: qianyang@fmmu.edu.cn

© Science Press 2021

Z. Xie (ed.), *Autophagy: Biology and Diseases*, Advances in Experimental Medicine and Biology 1208, https://doi.org/10.1007/978-981-16-2830-6_1

aggregated proteins. Due to the long-term presence of these factors, the cells maintain a very low basal autophagic activity to maintain homeostasis. Autophagy is a conserved phenomenon that exists widely in eukaryotic cells. It is a mechanism for eliminating the excess or damaged organelles that is common to the development and aging process of organisms. This process plays an important role in cellular protein metabolism, waste removal, structural reconstruction, growth, and development (Mizushima et al. 2008).

Based on morphological features and molecular machinery involved, autophagy can be divided into three main types: macroautophagy, microautophagy, and CMA. From the perspective of the substrates, autophagy can also be divided into two categories, selective autophagy and nonselective autophagy, based on the selectivity of autophagic cargo. Nonselective autophagy refers to the random transport of organelles or other cytoplasmic components to lysosomes. Selective autophagy refers to the recognition of a specific substrate to be degraded and is further divided into the following types: mitophagy, pexophagy, reticulophagy, nucleophagy, ribophagy, lipophagy, aggrephagy, and xenophagy. As research advances, other classes of selective autophagy may be discovered in the future.

1.1 The Basic Process of Autophagy

1.1.1 *The Basic Process of Macroautophagy*

Under normal conditions, macroautophagy is maintained at a low level to maintain cellular homeostasis. Under stress conditions such as starvation and hypoxia, it can be induced quickly. This regulation is achieved through posttranslational modifications (such as phosphorylation and acetylation) of key autophagy proteins. In addition, pathological stimuli such as inflammation, oxidative stress, and aggregation of misfolded proteins can activate macroautophagy, which may be a factor in the progression of various diseases. Both the increase and decrease in macroautophagy activity are rapid and tightly regulated processes. The latter is to prevent damage caused by excessive autophagy.

The most typical morphological feature of macroautophagy is the formation of a large number of vesicles in the cytoplasm. First, a free membranous structure appears in the cytoplasm, and then it expands. It is not spherically shaped but rather takes on a bowl-like structure composed of two layers of lipids known as the phagophore, which can be detected by electron microscopy. After enfolding the cargo, this membrane bilayer is called the autophagosome. The origin of the autophagosome membrane is still unclear. Studies have shown that the endoplasmic reticulum, the Golgi apparatus, mitochondria, and the cell membrane may be possible sources of autophagosome membranes (Hamasaki et al. 2013; Hayashi-Nishino et al. 2009). The outer membrane of the autophagosome fuses with the lysosome, and the inner membrane and the encapsulated substances of the autophagosome enter the

lysosome and are hydrolyzed by the lysosomal enzymes. This process breaks down the substances entering the lysosome into various nutrient components (e.g., the protein is broken down into amino acids and the nucleic acids into nucleotides) that are reused by cells. The lysosome that engulfs intracellular components is called an autophagolysosome or autolysosome. Specifically, the process of macroautophagy can be divided into four stages:

1. A separate membrane is formed. Under the stimulation of factors such as starvation, the cup-shaped structure that serves as a separator of the two-layer membrane begins to form around the cytoplasmic components to be degraded.
2. The autophagosome is formed. As the membrane is gradually extended, the cytoplasmic materials are completely surrounded by the newly formed autophagosome.
3. The autophagosome is transported to and fused with a lysosome to form an autolysosome. This process is actively mediated by cytoskeletal structures such as microtubules.
4. The autophagosome is degraded by lysosomal hydrolases, a process that relies on the acidic microenvironment of the lysosome (the pH of mature lysosomes is approximately 4.5, but the pH of the cytoplasm is 7.2).

Since the 1990s, biologists have used yeast as a model to study autophagy. Nearly half of the autophagy-related genes are highly conserved in yeast and multicellular species such as fruit flies, nematodes, and mammals. To unify the standards, in 2003, the autophagy-related genes were collectively named Atg and represent both autophagy genes and their corresponding proteins. The names of mammalian autophagy genes are similar to those of yeast, but there are also differences. The yeast Atg8 in mammals is called microtubule-associated protein light chain 3 (MAP-LC3), while yeast Atg6 in mammals is called Beclin1. Through in-depth research, many yeast Atg homologs have been found in mammals. This finding indicates that autophagy is an evolutionarily conserved process, and its molecular mechanisms are similar for yeasts and mammals.

1.1.2 The Basic Process of Microautophagy

Microautophagy refers to the direct uptake of cytoplasm inclusions (such as glycogen) and organelles (such as ribosomes and peroxisomes) by leaching, invading, or separating the membranes of lysosomes or yeast vacuoles, depending on the form of autophagy. It is different from macroautophagy in that the lysosome deforms itself and encapsulates the substrate in the cytoplasm. Both in macroautophagy and in microautophagy, after the substrate is brought to the lysosome, the membrane wrapped around the substrate is rapidly degraded, and then the substrate is released into the lysosome and dissolved effectively by hydrolases to ensure the reuse of nutrients by the cell (Mukherjee et al. 2016).

During the process of microautophagy, the lysosome/vacuolar membrane is directly invaginated and will eventually extend into the autophagic tube. Vesicles gradually form at the tip of the autophagic tube. The vesicles at the tip of the autophagic tube are always in a dynamic state. After the vesicles fall off the autophagic tube, they move freely in the lysosome/vacuolar and are degraded. Similar to macroautophagy, microautophagy of soluble substances can be induced by nitrogen starvation and/or rapamycin treatment. Furthermore, the process of peroxisome microphagocytosis is dependent on ATG proteins, but there is still no evidence that any ATG protein is directly involved in PMN (piecemeal microautophagy of the nucleus) or the process of microautophagy.

Microautophagy is regulated by the TOR and EGO signaling pathways (Ego1p, Gtr2p, and Ego3p). These pathways control the absorption and degradation of the vesicles. These steps can compensate for the influx of a large amount of membrane caused by macroautophagy. The evidence suggests that, in the absence of nutrients, from rapamycin-induced growth arrest to exponential growth conversion, microautophagy appears to be essential for maintaining organelle size and membrane composition, in addition to contributing to cell survival.

1.1.3 The Basic Process of Chaperone-Mediated Autophagy

Chaperone-mediated autophagy (CMA) refers to a special type of autophagy that selectively degrades certain proteins with the assistance of chaperones. Unlike macroautophagy and microautophagy, CMA is currently thought to exist only in mammalian cells, and CMA does not depend on the formation of membranous structures such as vesicles. The soluble protein substrate in the cytoplasm can directly enter into lysosome. Under physiological conditions, CMA is active in most tissues, such as the liver, brain, and kidneys. In the absence of nutrients (serum and growth factors), CMA can be slowly induced to a maximum activity that can be maintained for a considerable period of time, which makes it quite different from macroautophagy. Therefore, CMA plays a unique role in maintaining a stable intracellular environment.

Before the 1980s, the words “selective” and “lysosome” were never discussed together. It was widely believed that lysosomal degradation was a “bulk” process. However, in 1982, Dice discovered that ribonuclease A (RNase A) can be selectively degraded by lysosomes. This study was the first to confirm the existence of lysosomal-dependent selective degradation of intracellular proteins. Subsequently, Dice and colleagues found that the selective degradation of RNase A is dependent on the KFERQ pentapeptide sequence and that the KFERQ-related motif is also present in other CMA substrates. The presence of the KFERQ pentapeptide is indispensable for the CMA degradation pathway. In 1989, Chiang et al. found that a heat shock cognate protein of 70 KD (Hsc70) can bind to the KFERQ motif and is an essential element of CMA. In 1996, Ana Cuervo et al. found that LAMP2A (lysosome-associated membrane protein type 2A) on the lysosomal membrane is

the receptor involved in this selective degradation pathway, thus identifying another key regulator of CMA. In 1997, Agarraberas et al. found that part of hsc70 is also present in the lysosomal matrix and is critical for CMA. In 2000, Dice officially named this lysosomal-dependent selective degradation method chaperone-mediated autophagy (CMA) (Kaushik and Cuervo 2018).

The process of CMA includes the following steps. First, the hsc70 chaperone protein recognizes and binds to the KFERQ-like amino acid sequence of the substrate protein, together with co-chaperones that include a heat shock protein of 90 KD (Hsp90) and a heat shock protein of 40 KD (Hsp40). Subsequently, the hsc70-substrate-co-chaperone complex binds with LAMP2A to promote the oligomerization of LAMP2A, which forms a passage through which the substrate translocates into the lysosome. Finally, the substrate entering into the lysosomal matrix is resolved by hydrolases, and the LAMP2A bonds are broken such that the oligomers revert to their monomeric components. LAMP2A is considered to be the main rate-limiting factor of CMA. Studies have shown that starvation, oxidative stress, DNA damage, hypoxia, and other stimuli can increase the activity of CMA by promoting the production of the LAMP2A protein. A high-fat diet can reduce the level of LAMP2A on the lysosomal membrane and thus inhibits CMA activity in the liver. Known mutations related to Parkinson's disease lead to gene products that can bind to LAMP2A, block the LAMP2A monomer-to-oligomer cycle, and thus inhibit CMA activity in dopaminergic neurons.

A series of studies have demonstrated that CMA plays a significant role in maintaining neuronal homeostasis, promoting lipid degradation, protecting mitochondrial function, and repairing DNA damage. The CMA activity decreases in aging bodies, mainly due to the decreased level of LAMP2A in the lysosomes, which may underlie the development of aging-related diseases such as Parkinson's disease, Alzheimer's disease, metabolic disorders, and tumors (Cuervo and Wong 2014). Considering the important role of CMA in maintaining cell homeostasis, enhancing CMA activity may be an effective intervention to promote the health of aging organisms (Fig. 1.1).

1.2 Selective Autophagy: The Basics

As early as 1966, Smith et al. observed that a large number of autophagosomes containing prolactin particles appeared in pituitary prolactin cells after the sudden cessation of lactation. De Duve called this phenomenon "crinophagy," which may be the earliest known form of selective autophagy; however, the exact mechanism was not identified at the time. Another known example of selective autophagy is the selective uptake of glycogen by lysosomes, directly after birth, to provide nutrients for the newborn, since it can no longer take up nutrients through the placenta. The intracellular autophagosomes contain a large amount of glycogen but few mitochondria or other organelles (Jin et al. 2013). Selective autophagy relies on specific autophagic receptors that are not necessary for nonselective autophagy.

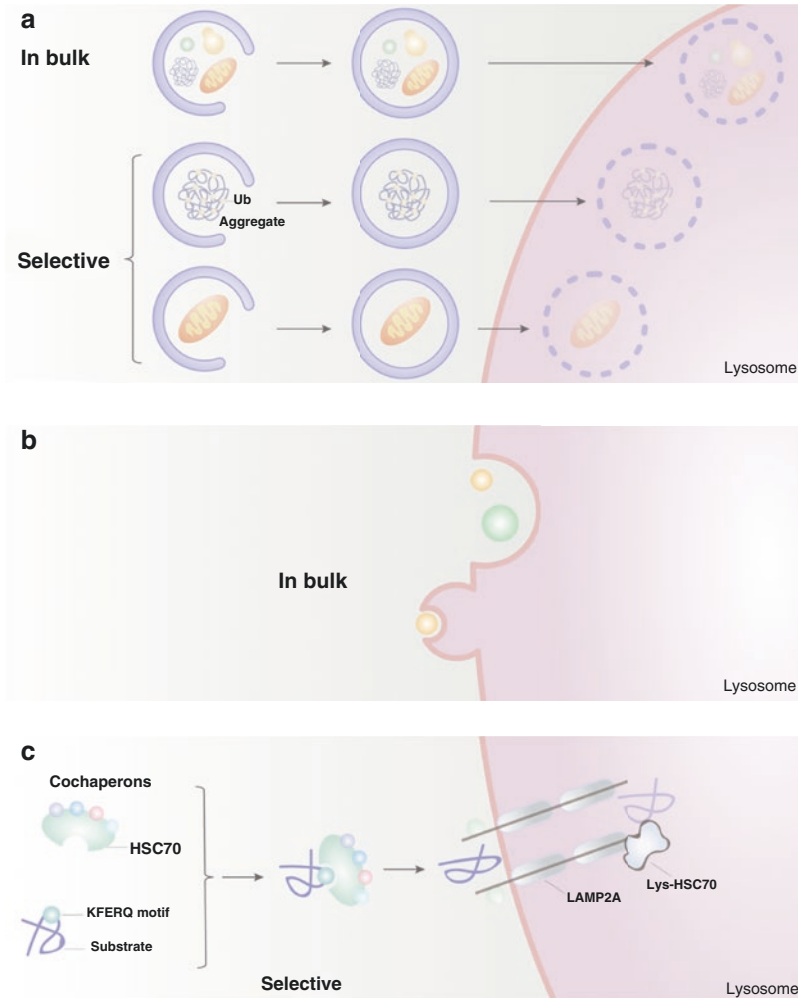


Fig. 1.1 The types and basic processes of autophagy. **(a)** Macroautophagy. **(b)** Microautophagy. **(c)** CMA

In the past few years, researchers have discovered many selective autophagic processes regulated by Atgs: mitophagy, ER-phagy, ribophagy, pexophagy, nucleophagy, aggrephagy, lipophagy, xenophagy, etc. (Anding and Baehrecke 2017).

1.2.1 Mitophagy

Mitophagy refers to the process by which damaged mitochondria are specifically encapsulated into autophagosomes and fused with lysosomes when mitochondria depolarize under stimuli such as ROS, nutrient deprivation, and hypoxia. Mitophagy

is an important process in the maintained balance between mitochondrial quality and cellular energy metabolism. When Elmore et al. treated rat hepatocytes with serum-deficient medium, they found that the spontaneous depolarization rate of mitochondria was significantly elevated, and these depolarized mitochondria were specifically transported to autophagosomes and autolysosomes where they were degraded. The average time for mitochondrial degradation is approximately 7 min. Mitochondria are the primary organelles that produce energy in eukaryotic cells; that is, 80% of the energy required for cell activities is provided by mitochondria. Although oxidative phosphorylation inside mitochondria is a more efficient energy generation process than glycolysis, it is accompanied by the production of reactive oxygen species (ROS). Excessive ROS can cause mitochondrial damage, proapoptotic factor release, and cell death. Even under normal conditions, some mitochondria will be damaged by the accumulation of ROS. Therefore, the timely removal of aging and damaged mitochondria is critical for the health of cells.

Mitophagy is induced via Parkin-dependent and Parkin-independent mechanisms. (1) Under normal conditions, in the Parkin-dependent pathway, protein PINK1 (PTEN-induced putative kinase-1) of the outer mitochondrial membrane is continuously cleaved by protease PARL (Presenilin-associated rhomboid-like protein). When mitochondrial damage occurs, PARL cannot cleave PINK1, causing it to accumulate on the mitochondrial surface. PINK1 can recruit the E3 ubiquitin ligase Parkin to the mitochondria to initiate mitophagy. (2) In sharp contrast with the Parkin-dependent pathway, the Parkin-independent process does not involve the translocation of Parkin to the damaged mitochondria. Instead, proteins containing LIR (LC3-interacting region) motifs in the outer mitochondrial membrane act as receptors that bind to the LC3. These proteins include BNIP3 (BCL2/adenovirus E1B 19 kDa-interacting protein 3), NIX/BNIP3L (BCL2/adenovirus E1B 19 kDa-interacting protein 3-like), FUNDC1 (FUN 14 domain-containing protein 1), and AMBRA1 (autophagy and beclin1 regulator1) (Villa et al. 2018).

1.2.2 Reticulophagy

Bernales and colleagues first named “endoplasmic autophagy (ER-phagy),” which they found in their study of unfolded protein response (UPR). The endoplasmic reticulum is an important site for protein synthesis and lipid metabolism. Its volume and function are consistent with the growth state of cells. Starvation, misfolded proteins, hypoxia, pathogen infection and other stimuli, and certain drug interventions (such as tunicamycin and thapsigargin) can cause dysfunction of the ER, which leads to increased ER volume and ER stress. ER-phagy is activated at the same time that a stimulus is introduced and maintains cellular homeostasis by degrading the damaged ER and its contents, thus constraining ER stress.

As a selective autophagic process, ER-phagy requires activation of a membrane receptor for LC3/GABARAP (γ -aminobutyric acid receptor-associated protein), which in yeast are identified as Atg39 and Atg40. The mammalian counterparts are,

among others, FAM134B (family with sequence similarity 134), SEC62 (translocation protein SEC62), RTN3L (RHD-containing proteins 3L), and CCPG1 (Cell-cycle progression gene 1). Due to different causes of ER-phagy, different membrane receptors are involved. For example, FAM134B and RTN3L are mainly responsible for the ER-phagy induced by starvation conditions, while SEC62 and CCPG1 are involved in ER-phagy caused by ER stress (Wilkinson 2019). Severe ER stress is an important pathological feature of neurodegenerative diseases, tumors, and diabetes. ER-phagy is an important means to regulate ER function and has recently received increasing attention by researchers worldwide. However, the full regulatory network still remains to be elucidated.

1.2.3 Ribophagy

In the case of nutrient deprivation, the removal of organelles is accompanied by specific ribosome degradation. Within yeast, this newly discovered type of selective autophagy is named ribophagy. It has long been believed that the occurrence of ribosomes in autophagosomes was due to the nonselective autophagic process. However, under certain conditions, ribosomes are more susceptible to degradation than are other proteins, which indicates a selective degradation process. Whole genome screening of nonessential genes revealed that ubiquitin protease Ubp3/Bre3 is involved in ribophagy. The degradation of 60S and 40S ribosomes requires core ATG proteins and other special elements (Macintosh and Bassham 2011). Recent studies have shown that, in mammalian cells, NUFIP1 (Nuclear fragile X mental retardation-interacting protein 1) may be an important regulator of ribophagy. When cells were treated with the mTOR inhibitor Torin, NUFIP1 translocated to the cytoplasm from the nucleus and localized to the ribosome as an RNP (ribonucleoprotein) complex together with its partner ZNHIT3 (Zinc finger HIT domain-containing protein 3). NUFIP1 binds to LC3 through its LIR motif to induce ribosome localization to autophagic vacuoles, thus promoting ribophagy (Wyant et al. 2018). However, how mTOR regulates NUFIP1 function and whether there are other ribophagy regulation mechanisms remain to be explored.

1.2.4 Pexophagy

As a kind of organelle that is ubiquitous in eukaryotic cells, peroxisomes contain abundant enzymes, such as peroxidase and catalase, which are important in the regulation of ROS levels. In addition, peroxisomes are involved in the metabolism of purine, fatty acid oxidation and bile acid synthesis. The half-life of peroxisomes is approximately 2 days. When peroxisomes are damaged, they will be removed from the cytoplasm by the autophagy pathway, i.e., pexophagy. Pexophagy is primarily achieved via two pathways: (1) Through autophagy adaptors, a variety of

proteins on the membrane of peroxisomes, such as PEX3, PEX5, and PMP70, can be ubiquitinated to recruit p62 and NBR1, to promote peroxisome degradation, and (2) through autophagy receptors, PEX14 can bind directly with LC3 to induce localization of the peroxisomes to autophagic vacuoles (Eberhart and Kovacs 2018).

Morphologically, pexophagy is divided into micropexophagy and macropexophagy:

1. Micropexophagy. First, the vacuole membrane surrounds the peroxisome cluster. Then, the micropexophagic membrane apparatus (MIPA) structure appears on the rough surface of the cluster. Peroxisome clusters close, which is accomplished by MIPA and vacuolar membrane fusion, to transport peroxisomes to vacuoles.
2. Macropexophagy. When cells grown in methanol medium are transferred to ethanol medium, the peroxisomes are encapsulated in autophagosomes, and delivered to the vacuoles.

1.2.5 Nucleophagy

In some cases, removal of damaged nuclei or nonessential portions of the nucleus, or even the entire nucleus, is critical to promoting cell survival and maintaining proper function. Increasing evidence has shown that part of or even the entire nucleus in eukaryotes is degraded by selective autophagy. Under starvation or other stressful conditions, such as DNA damage and cell cycle arrest, nucleophagy may be induced. Nutrient deprivation can promote nuclear degradation via yeast vacuoles (in PMN). For example, in yeast, a part of the nucleus is swallowed by the vacuole. At the junction of the vacuoles and nucleus, the nucleus gradually enters into the PMN process. The formation of NV (nucleus-vacuole) contact requires Nvj1 and Vac8. Atg11, Atg17, and other core Atg proteins are also essential for PMN function. This process is similar to microautophagy. During PMN initiation, the NV junctions are formed through the interaction of the vacuolar membrane protein Vac8 and the outer nuclear membrane protein Nvj1. Nutrient deprivation leads to an increase in Nvj1. Nvj1 binds with Osh1, and as a result, parts of the NV form a bubble in the vacuole and are released into the vacuole, and are degraded in the process.

After 18–24 h of starvation, another type of nucleophagy may also occur, namely, late nucleophagy (LN), which does not require Nvj1, Vac8, or Atg11. Hitoshi et al. found that Atg39 is the key factor underlying this process in yeast. Atg39 is located on the perinuclear endoplasmic reticulum and contains the LIR motif. When the yeasts are treated with rapamycin, the level of Atg39 is elevated. Then, the autophagic vacuoles containing LC3 are recruited to the nucleus to induce LN. Homologs of Atg39 have not yet been identified in mammals. In addition, micronuclei, which are structures containing ectopic chromosomes or chromosomal fragments produced under genotoxic stress, are also degraded by this selective autophagy pathway (Nakatogawa and Mochida 2015).

In conclusion, nucleophagy is a process that selectively removes nuclei from cells by autophagy. It can be achieved through both macroautophagy and microautophagy, which are called macronucleophagy and micronucleophagy, respectively. During macronucleophagy, autophagosomes engulf the discarded components of the nucleus, and fuse with vacuoles or lysosomes, and finally these nuclear components are degraded. In contrast, during micronucleophagy nuclear components are directly engulfed by invagination, protrusion, and/or vacuole separation or restrictive action of the lysosomal membrane. Whether macroautophagy and microautophagy are involved in nucleophagy in mammals and how either or both are induced remain to be determined by further studies.

1.2.6 Aggrephagy

The concept of aggrephagy, as originally proposed by Overbye, explains the specific removal of aggregates or protein inclusion bodies in cells. Protein aggregation in cells is an ongoing process that is required for key processes of cellular activity; however, some aggregates are produced by protein misfolding under various stress conditions. Those damaged proteins cannot be repaired and are degraded by the proteasome pathway or by lysosomes. These protein aggregates are typically labeled with ubiquitin and recognized by HDAC6, SQSTM1/p62, and NBR1, which function as adaptor proteins.

Effective management of misfolded proteins is beneficial for maintaining the balance between the normal functions of cells. Three systems control the quality of cellular proteins, namely, chaperone-mediated folding, proteasome degradation, and aggrephagy. When the former two pathways fail, aggrephagy is rapidly induced. The first stage of aggresome formation involves aggregation of misfolded proteins or other proteins that fail to refold properly. They form large insoluble aggregates that are transported to the MTOC (microtubule-organizing center) where they are concentrated. These aggresomes can trigger the autophagy degradation pathway, during which proteins that have been labeled with ubiquitin are engulfed by autophagic bilayer membranes that become autophagosomes that are subsequently degraded by lysosomes (Hytinen et al. 2014).

Selective autophagy for protein aggregation has now emerged as an important cellular protein quality control system. In the past decade, scientists have made great progress in understanding aggrephagy. The autophagy receptors p62 and NBR1, as well as the large adaptor protein ALFY, play a major role in aggrephagy. As abnormal aggregation of misfolded proteins is a typical pathological feature of neurodegeneration, autophagy and its signaling cascade provide novel and promising therapeutic targets for the prevention and treatment of neurodegenerative diseases.

1.2.7 Lipophagy

Autophagy plays a role in the degradation of several intracellular components, and recently, cytoplasmic lipid droplets (LDs) were demonstrated to be degraded by autophagy. LDs contain a core consisting primarily of triglycerides and sterol esters and are surrounded by a phospholipid monolayer that includes various proteins. They are highly dynamic organelles, as illustrated by the change in their size and in the number formed, according to different environmental conditions. LDs play an important role in lipid storage and metabolism. They can be degraded by both cytoplasmic and lysosomal pathways, the latter being called lipophagy (Zechner et al. 2017).

Adipose triglyceride lipase (ATGL) and lysosome acid lipase (LAL) are the two enzymes responsible for the hydrolysis of lipids in the cytoplasm and lysosomes, respectively. A decrease in LAL levels causes lipids to accumulate in the lysosome, thereby inhibiting lipophagy. The transcription factors FOXO1 and TFEB are activated when cells lack energy, which promotes the production of LAL. In addition, TFEB also promotes the transcription of other components of lysosomes, thereby activating lipophagy. Due to the large size of LDs, they usually break into several smaller parts before entering autophagosomes, but the specific mechanism of this breakdown remains unclear. Ana et al. found that CMA is responsible for the degradation of proteins PLIN2 and PLIN3, which are located on the LD surface, which promote the translocation of ATGL to the LDs. Therefore, it can facilitate the degradation of LDs via the cytoplasmic pathway. Furthermore, the recruitment of ATGL promotes LDs to break into smaller LDs, which are then swallowed by autophagosomes. This study suggests that there may be complicated regulatory relationships between CMA and lipophagy. LC3, LAMP1, LAMP2B, LAMP2C, and Rab7a may be involved in the fusion between the lipid autophagosomes and the lysosomes, but our current understanding is still limited. In addition, studies have proven that lysosomes and LDs can form transient (“kiss and run”) contacts in a Rab7a-dependent manner, similar to contacts made in the process of microautophagy (Kaushik and Cuervo 2015).

There is a close relationship between the cytoplasmic metabolic pathway of LDs and the lysosomal pathway. ATGL has an LIR motif in a sequence that binds to the autophagic protein LC3. Unlike other forms of selective autophagy, this binding during lipophagy promotes the localization of ATGL to the surface of the LDs to promote lipid hydrolysis, but the specific mechanism remains unclear. In turn, ATGL also promotes the function of PPAR α and SIRT1, which positively regulate the level of autophagy. In addition to being responsible for lipid degradation processes, autophagy-related proteins also play a key role in lipid synthesis. For example, studies have found that LC3 is critical for lipid formation and that knocking out

atg5 or atg7 genes impedes adipocyte differentiation. Given the role of autophagy in lipid metabolism, targeting autophagy-related genes may help in the development of new interventions for the treatment of metabolic diseases such as obesity and diabetes (Christian et al. 2013).

1.2.8 Xenophagy

Xeno stands for “heterologous,” which refers to the selective phagocytosis of bacteria or viruses inside cells. Autophagy represents an important measure for cells to deal with intracellular pathogens. This process has been confirmed in many mammalian experiments. One of the key functions of xenophagy is to serve as the first line of defense against pathogens by targeting intracellular bacteria and viruses for autophagy to control bacteria in the host cell and thus prevent the spread of the infection.

Autophagy constitutes a critical mechanism that cells use to resist pathogen infection, but autophagy is also involved in intracellular microbial infections. On the one hand, autophagy can degrade the pathogen that invades the cell; that is, it can remove intracellular pathogens by xenophagy. On the other hand, some pathogens can escape xenophagy, which facilitates their survival. For example, when the DNA of *Mycobacterium tuberculosis* is released into the cytoplasm, it can be recognized by STING (Stimulator of IFN genes), which promotes ubiquitination of bacterial proteins, and then, they are recognized by the autophagy adaptor proteins p62 and NDP52, which facilitate xenophagy. The PtpA (tyrosine phosphatase A) of *Mycobacterium tuberculosis* inhibits fusion of the autophagosomes and lysosomes by regulating the phosphorylation of VPS33B. In addition, PtpA impairs the function of V-ATPase, hindering the formation of autophagosomes. *Listeria monocytogenes* LLO (listeriolysin O) can directly activate xenophagy, while its other component, ActA, recruits the Arp2/3 complex to inhibit ubiquitination of the bacterial proteins, and subsequently the bacteria are trafficked to autophagosomes (Sharma et al. 2018).

Therefore, in-depth study of the mechanism of xenophagy in infection is expected to help clarify the pathogen invasion process and provide new ideas and methods to prevent and control the occurrence and development of infection through regulated autophagy.

In summary, the discovery of selective autophagy has enriched the knowledge of the forms of autophagic processes, which gives us a fuller understanding of the mechanisms of autophagy. However, the detailed pathways of induction and execution of the autophagy involved in selective autophagic processes have not yet been fully elucidated, and further research is still needed (Fig. 1.2).

	Process	Cargo(Ligand)	Receptor
Fungi	Cvt pathway	Ape1 (propeptide), Ape4, Ams1	Atg19
	Micronucleophagy	Portions of nucleus (Nvj1)	Vac8
	Mitophagy	Mitochondria	Atg32
	Reticulophagy	ER fragments	Atg39, Atg40
	Ribophagy	Ribosomes (Rpl25-Ub)	-
	Pexophagy	Peroxisomes (Pex3/PpPex3, PpPex14)	PpAtg30, Atg36
Mammals	CMA	Cargo protein (KFERQ motif)	Hsc70, LAMP2A
	Mitophagy	Mitochondria (Ub), FUNDC1, BNIP3, BNIP3L, AMBRA1, FKBP8,	OPTN, NDP52, Atg8
	Lipophagy	Lipid droplets	-
	Reticulophagy	FAM134B, RTN3, ATL3	Atg8, GABARAP
	Ribophagy	NUFIP1-ZNHIT3 complex	Atg8
	Glycophagy	STBD1	GABARAPL1
	Pexophagy	Peroxisomes (Ub), PEX14	SQSTM1, NBR1, Atg8
	Aggrephagy	Misfolded proteins (Ub)	SQSTM1, NBR1
	Xenophagy	Viruses (viral capsid proteins), bacteria (Ub)	SQSTM1, CALCOCO2, OPTN

Fig. 1.2 The process and machinery of selective autophagy

1.3 Summary

In the past decade, people have gained a new understanding of the role of lysosomes. The true function of this organelle has evolved from a pure “garbage disposal station” to an active “recycling center” that is involved in protein quality control. Lysosomes are not only responsible for “bulk” degradation but are also key to certain selective degradation processes.

It can be seen from the characteristics of autophagy that are summarized above that once autophagy is initiated, it must be terminated quickly after the crisis has been resolved. Otherwise, the nonspecific removal of the cytoplasmic components can cause irreversible damage to the cells. This time dependence also reminds us that dynamic observations are needed when we are studying autophagy. Snapshots from a single time point are not sufficient to give a holistic view of the important process of autophagy. At present, our knowledge about autophagy and autophagic programmed cell death is still limited. The involved molecules signal transduction pathways, and significance of autophagy requires further research. With the unraveling of these mysteries, the detailed mechanisms of autophagy will be mapped, and the relationship between autophagy and disease will be elucidated. Then, we can find better clinical therapies that promote the well-being of humans.

References

- Anding AL, Baehrecke EH. Cleaning house: selective autophagy of organelles. *Dev Cell*. 2017;41:10–22.
- Christian P, Sacco J, Adeli K. Autophagy: emerging roles in lipid homeostasis and metabolic control. *Biochim Biophys Acta*. 2013;1831:819–24.
- Cuervo AM, Wong E. Chaperone-mediated autophagy: roles in disease and aging. *Cell Res*. 2014;24:92–104.
- Eberhart T, Kovacs WJ. Pexophagy in yeast and mammals: an update on mysteries. *Histochem Cell Biol*. 2018;150:473–88.
- Hamasaki M, Furuta N, Matsuda A, Nezu A, Yamamoto A, Fujita N, Oomori H, Noda T, Haraguchi T, Hiraoka Y, Amano A, Yoshimori T. Autophagosomes form at ER-mitochondria contact sites. *Nature*. 2013;495:389–93.
- Hayashi-Nishino M, Fujita N, Noda T, Yamaguchi A, Yoshimori T, Yamamoto A. A subdomain of the endoplasmic reticulum forms a cradle for autophagosome formation. *Nat Cell Biol*. 2009;11:1433–7.
- Hyttinen JM, Amadio M, Viiri J, Pascale A, Salminen A, Kaarniranta K. Clearance of misfolded and aggregated proteins by aggrephagy and implications for aggregation diseases. *Ageing Res Rev*. 2014;18:16–28.
- Jin M, Liu X, Klionsky DJ. SnapShot: selective autophagy. *Cell*. 2013;152:368–368.e2.
- Kaushik S, Cuervo AM. Degradation of lipid droplet-associated proteins by chaperone-mediated autophagy facilitates lipolysis. *Nat Cell Biol*. 2015;17:759–70.
- Kaushik S, Cuervo AM. The coming of age of chaperone-mediated autophagy. *Nat Rev Mol Cell Biol*. 2018;19:365–81.
- Macintosh GC, Bassham DC. The connection between ribophagy, autophagy and ribosomal RNA decay. *Autophagy*. 2011;7:662–3.
- Mizushima N, Levine B, Cuervo AM, Klionsky DJ. Autophagy fights disease through cellular self-digestion. *Nature*. 2008;451:1069–75.
- Mukherjee A, Patel B, Koga H, Cuervo AM, Jenny A. Selective endosomal microautophagy is starvation-inducible in *Drosophila*. *Autophagy*. 2016;12:1984–99.
- Nakatogawa H, Mochida K. Reticulophagy and nucleophagy: new findings and unsolved issues. *Autophagy*. 2015;11:2377–8.
- Sharma V, Verma S, Seranova E, Sarkar S, Kumar D. Selective autophagy and xenophagy in infection and disease. *Front Cell Dev Biol*. 2018;6:147.
- Villa E, Marchetti S, Ricci JE. No Parkin zone: mitophagy without Parkin. *Trends Cell Biol*. 2018;28:882–95.
- Wilkinson S. ER-phagy: shaping up and destressing the endoplasmic reticulum. *FEBS J*. 2019;286(14):2645–63.
- Wyant GA, Abu-Remaileh M, Frenkel EM, Laqtom NN, Dharamdasani V, Lewis CA, Chan SH, Heinze I, Ori A, Sabatini DM. NUFIP1 is a ribosome receptor for starvation-induced ribophagy. *Science*. 2018;360:751–8.
- Zechner R, Madeo F, Kratky D. Cytosolic lipolysis and lipophagy: two sides of the same coin. *Nat Rev Mol Cell Biol*. 2017;18:671–84.

Chapter 2

Autophagosomal Membrane Origin and Formation



Yi Yang, Li Zheng, Xiaoxiang Zheng, and Liang Ge

Abstract Autophagosome formation is a regulated membrane remodeling process, which involves the generation of autophagosomal membrane precursors (vesicles), the assembly of the autophagosomal membrane precursors to form the phagophore, and phagophore elongation to complete the autophagosome. The sources of the autophagosomal membrane precursors are endomembrane compartments, such as the endoplasmic reticulum (ER), the ER-Golgi intermediate compartment (ERGIC), ER-exit sites (ERES), and endosomes. In response to stress, these structures are remodeled, to generate the early autophagosomal membrane precursors. The phagophore assembly site (PAS), which mainly localizes on the ER, harbors the site for autophagosomal membrane assembly, elongation, and completion. ATG proteins, membrane remodeling factors, and autophagic membranes follow a precise choreography to complete the overall process. In this chapter, we briefly discuss our current knowledge on the membrane origins of the autophagosome, as well as autophagosomal precursor generation, assembly, and expansion.

Keywords Autophagosome · Phagophore · ATG proteins · Membrane remodeling
Endoplasmic reticulum · Mitochondria · Plasma membrane · Endosome
Microfilament

Y. Yang (✉)
Hangzhou Normal University, Hangzhou, Zhejiang, China
e-mail: yyang@hznu.edu.cn

L. Zheng · L. Ge (✉)
School of Life Sciences, Tsinghua University, Beijing, China
e-mail: zhengl20@mails.tsinghua.edu.cn; liangge@mail.tsinghua.edu.cn

X. Zheng
Zhejiang University, Hangzhou, Zhejiang, China
e-mail: zhengxx@zju.edu.cn

© Science Press 2021

Z. Xie (ed.), *Autophagy: Biology and Diseases*, Advances in Experimental Medicine and Biology 1208, https://doi.org/10.1007/978-981-16-2830-6_2

The endomembrane system of eukaryotic cells is a continuous organic whole undergoing dynamic changes. In a narrow sense, the endomembrane system contains the endoplasmic reticulum (ER), the Golgi system, endosomes, lysosomes, peroxisomes, nuclear membranes, etc. Broadly speaking, the endomembrane system consists of all the intracellular organelles with membrane structures, including mitochondria and chloroplasts. The endomembrane system provides unique environments for the initiation of various intracellular biochemical reactions. In addition, the membrane fluidity ensures the coordination of units and maintains the homeostasis of the system. The dynamic changes and the association between the components in the endomembrane system also affect various metabolic pathways in cells. Autophagic vesicles are also part of the dynamic changes of the eukaryotic cell membrane system. Since the discovery of autophagosome in the 1950s, researchers have been working to solve the mystery of the origin and structure of autophagic vesicles. Much progress has been made and the revelation of this mystery is underway. In this chapter, we focus on current opinions about the origin of the autophagosomal membrane and their supporting evidence.

2.1 Vesicular Trafficking in the Endomembrane System

Before introducing the association between intracellular organelles in the endomembrane system and the origin of autophagosomal membrane, we first need to understand the vesicle trafficking processes in the endomembrane system.

Cell compartmentalization is the basic property of the structure and function of eukaryotic cells. Substances are delivered between the various components of the endomembrane system, usually by vesicles. Vesicular transport regulates the delivery of proteins or lipids synthesized in the ER to various locations in the cell. In addition, extracellular materials are internalized through the endocytic pathway. After internalization, these substances are delivered to lysosomes for degradation via trafficking vesicles. Trafficking vesicles bud from a specific area on the plasma membrane in the form of a coated vesicle. To date, three different types of coated vesicles have been identified, namely, Coat Protein Complex (COP) II, COP I, and clathrin. These coated vesicles have varied functions in mediating the transport of materials.

COPII-coated vesicles are believed to mediate the transport of substances from the ER to the Golgi apparatus. In eukaryotic cells, proteins are synthesized in ribosomes in the cytoplasm. Some of the proteins translocate to the ER after the initiation of synthesis. The newly formed proteins are transported from the ER to the Golgi apparatus, and then to the cell surface or other intracellular sites to perform their functions. The protein trafficking route from the ER to the Golgi apparatus is known as early secretory pathway, and is an important phase in the quality control and sorting of proteins. After preliminary processing in the ER, proteins bud from the ER in COPII-coated vesicles at ER-exit sites (ERES). After that, COPII is released and the vesicles fuse with the ER-Golgi intermediate compartment (ERGIC). Protein maturation occurs in the ERGIC. Tubular vesicles leave the ERGIC and are transported to the Golgi apparatus along microtubules. This transport is regulated by motor proteins.

COPI-coated vesicles control the retrograde transport of vesicles from the *cis*-Golgi network to the ER. Clathrin mediates protein transport from the *trans*-Golgi network to the plasma membrane or lysosome. In the process of endocytosis, clathrin also contributes to the trafficking of materials from the plasma membrane to the intracellular compartments.

The process by which trafficking vesicles form, traffic, and fuse with target membranes involves a variety of proteins that regulate the recognition, assembly, and disassembly of these transporters. The mechanism of intracellular vesicle transport has attracted the interest of many scientists. The 2013 Nobel Prize in Physiology or Medicine was awarded jointly to three eminent scientists, James E. Rothman, Randy W. Schekman, and Thomas C. Südhof for their discoveries of the machinery regulating vesicle traffic.

2.2 Membrane Origin of the Autophagosome

Autophagosome formation entails a stepwise membrane remodeling process. It begins with the generation of small autophagosomal membrane precursors. Fusion of these precursors then occurs to form a cup-shaped phagophore followed by phagophore closure to complete a double-membrane autophagosome (Fig. 2.1) (Brier et al. 2016). The appearance of the phagophore is an early event in the formation of autophagic vesicles. Under transmission electron microscope, the phagophore is a crescent- or cup-shaped bilayer structure, and tends to sequester cytoplasmic constituents. The membrane of the phagophore expands and sequesters cytoplasmic materials. After closure, the double-membrane autophagosome is formed. The phagophore is also known as isolation membrane (IM). Regarding the origin of the autophagosomal membrane, at present there are basically two academical views. One view is that the autophagosomal membrane forms de novo in the cytoplasm as the composition of the membrane is simple and the protein content is low. Such an autophagosomal membrane formation is characterized as de novo synthesis.

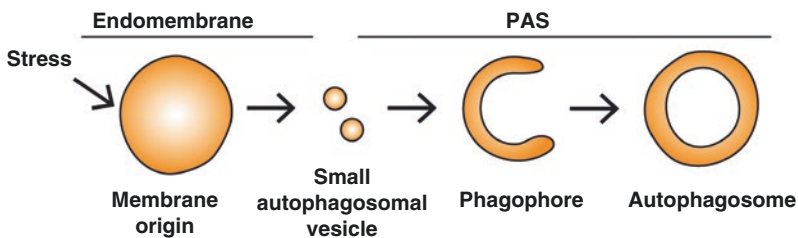


Fig. 2.1 Overview of membrane remodeling in autophagosome formation. Stress signals are transmitted into membrane remodeling signals that act on the autophagosome membrane origin located in the endomembrane. Small autophagosomal vesicles/precursors are then generated as a result of a membrane remodeling process. The precursors are targeted to the phagophore assembly site (PAS) and fuse to form a cup-shaped phagophore. The phagophore further extends and encloses to form the double-membrane autophagosome. The figure is modified from Brier LW et al. (2016)

In another view, autophagic vesicle forms from a pre-existing organelle already containing its cargo. A variety of intracellular organelles with membrane structures in the endomembrane system might contribute material for the generation of the autophagosomal membrane, including the ER, the ER-Golgi intermediate compartment (ERGIC), mitochondria, the plasma membrane, recycling endosomes, the nuclear membrane, etc. The bending, expansion, and closure of the phagophore ultimately contributes to the formation of the autophagosome. The biogenesis and the remodeling of intracellular organelles, as well as material exchange between organelles, occurs mostly at membrane contact sites. This basic principle of cell biology supports the argument that several intracellular organelles participate in the formation of the autophagosomal membrane. Here, we briefly introduce the current prevalent views and experimental evidence regarding the biogenesis of the autophagosomal membrane.

2.2.1 ER: A Major Site for Autophagosomal Membrane Formation

The ER is a fine membrane system in cells that forms an interconnected network of flattened or tubelike structures. Such membrane-enclosed sacs provide a large area for various enzyme reactions within the cells. In addition, the ER continuously associates with the Golgi apparatus as well as the nuclear envelope, supporting material transport in cells. Among the various intracellular organelles in the endomembrane system, the ER is the most likely origin site for autophagosomal membrane formation (Fig. 2.2). However, the ER interacts with other organelles in the cytoplasm and extends to the edge of the cell, and thus it is difficult to identify the exact location of autophagosome nucleation.

Double FYVE domain-containing protein 1 (DFCP1) is a phosphatidylinositol 3-phosphate (PI3P) binding protein. The protein expression of DFCP1 is significantly upregulated in cells under starvation. Microscopic analysis reveals a cup-shaped structure of DFCP1 proteins with a diameter of approximately 1 μm . Microtubule-associated protein light chain 3 (MAP-LC3; aka LC3) is a commonly used biomarker for phagophores. The basal autophagic activity in mammalian cells is relatively low, and the LC3 is dispersed in the cytoplasm. Upon starvation or other stimuli, autophagy is activated and LC3 puncta are formed. Some of the LC3-positive ringlike structures are positive for DFCP1. The DFCP1-positive ringlike structures are located on the ER, and are called the omegasome because of their shape. Three-dimensional tomographic reconstruction reveals the connections between the autophagosomal membrane and ER. The sheet-shaped ER tightly surrounds the cup-shaped phagophore. The phagophore-associated tubular structures are connected to the ER. The formation and extension of phagophore is guided by the ER sheet (Fig. 2.3). The newly formed membrane structure is very narrow, representing a connection between the phagophore and the ER. The Japanese scholars Uemura et al. revealed that the formation of this membrane structure is

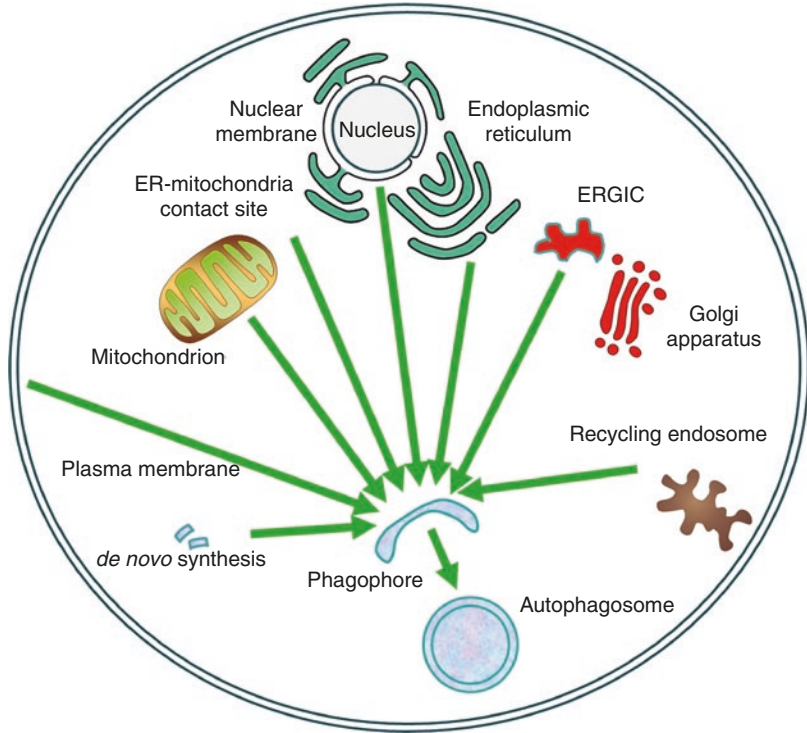


Fig. 2.2 The potential origin for autophagosomal membrane. According to the existing hypotheses, ER, ER-Golgi intermediate compartment (ERGIC), mitochondrion, ER-mitochondria contact site, nuclear membrane, recycling endosome, and plasma membrane may play crucial roles in autophagosome generation. They might be the possible origin sites or important sources for autophagosomal membrane formation. In addition, it is possible that the autophagosomal membrane forms *de novo* in cytoplasm from newly synthesized lipids

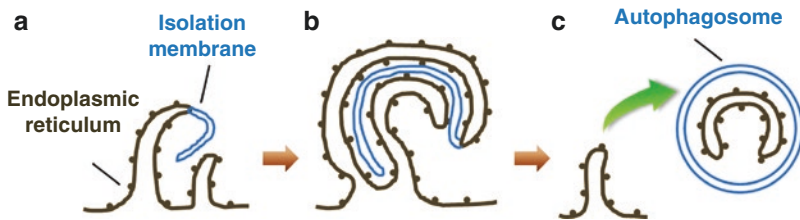


Fig. 2.3 The autophagosomal membrane derived from ER. Generally, the formation of autophagosomal membrane consists of three stages. (a) The ER membrane expands to form the phagophore, which is also known as the isolation membrane. (b) The ER surrounds the phagophore and guides the formation and extension of phagophore. (c) The closure of the phagophore ultimately contributes to the formation of double-membrane autophagosome. After formation, the autophagosome detaches from the ER and becomes an independent double-membrane structure

closely associated with *FIP200*, an important component of the UNC51-like kinase (ULK1) complex, but not the Atg conjugation system (Uemura et al. 2014); membrane formation could still be detected in fibroblasts deficient in *Atg5*, *Atg7*, or *Atg16L1*.

The ER is believed to be a major origin site for autophagosomal membrane formation (Bissa and Deretic 2018). It is possible that the rough ER gives rise to the double-membrane structures at the site where no ribosomes are adhered to form the phagophore. After engulfing part of the cytosol, autophagosomes are formed. This hypothesis has been supported by various experimental evidence. At present, it is known that approximately 70% of the autophagosomes contain content derived from the ER (Hayashi-Nishino et al. 2009). Both sides of the autophagosomal membrane are surrounded by the ER membrane during formation. The inner ER membrane might be degraded after membrane closure, maturation, and fusion with lysosome. Another possibility is that the inner membrane might escape into the cytoplasm through the open side of the phagophore.

2.2.2 Signaling Molecules in the ER Regulate the Biogenesis of the Autophagosomal Membrane

Accumulating evidence suggests that several factors that regulate the biogenesis of the autophagosomal membrane locate on the ER. PI3P plays a crucial role in mediating the formation of autophagosomal membrane. Compared with other intracellular organelles, ER has a relative high level of PI3P. The content of PI3P on the ER is noticeably increased upon starvation. PI3P recruits multiple effectors that control the formation of phagophore coordinately. It is reported that the autophagosomal membrane is derived from sites on the ER enriched with PI3P. Similar to PI3P, Atg14 regulates the autophagosomal membrane origin from the ER. Atg14 contains a cysteine-rich domain at the N-terminal region, which facilitates its specific localization in the ER. The C-terminal region of mammalian Atg14 has a high affinity to PI3P and phosphatidylinositol 4,5-bisphosphate (PI[4,5]P₂) lipids, and also targets to the ER. Under basal condition, Atg14 is uniformly distributed on the ER, while upon starvation, Atg14 puncta accumulate on the ER. The ER localization capability of Atg14 is essential for the biogenesis of the autophagosomal membrane. Atg14 mutants fail to localize on ER or to mediate the formation of autophagosomes. In addition, autophagosomes cannot be formed in cells deficient in Atg14. Based on these findings, Atg14 plays a pivotal role in the biogenesis of autophagosomal membrane originating from the ER. Moreover, ULK1 and Atg5 also form puncta similar to that of Atg14-positive structures. ULK1 and Atg5 can be activated almost synchronously during starvation, followed by ER accumulation and the formation of punctate structures. Subsequently, Atg14 is recruited onto the ULK1/Atg5 complex, which is stabilized by activated PI3K.

2.2.3 *ER-Golgi Intermediate Compartment*

The ERGIC is a docking station in the process of protein sorting and transportation. It receives COPII vesicles from ER as well as COPI vesicles from the Golgi apparatus. Protein sorting occurs in the ERGIC, where tubulovesicular membrane clusters are formed and mature. Driven by motor proteins, the carriers leave the ERGIC, and are transported along the cytoskeleton to the Golgi apparatus or toward the ER via COPI vesicles. Starvation induces the activation of the class III phosphatidylinositol 3-kinase (PI3KC3), which subsequently causes the transport of COPII vesicles to the ERGIC. A close connection between the autophagosomal membrane biomarker LC3 and the ERGIC has been detected. The COPII vesicles derived from the ERGIC provide the source membrane for LC3 lipidation. After lipidation, the LC3 vesicles move to the phagophore assembly site (PAS); fuse with the precursor membranes derived from the ER, cytoplasmic membrane, or Golgi apparatus; and generate the phagophore (Ge et al. 2015).

Several recent studies support the possibility that the ERGIC may serve as a membrane source for the autophagosomal membrane:

1. Nicholas Ktistakis' lab found that the early Atg factor FIP200 localizes adjacent to the ERGIC using a super-resolution Stochastic Optical Reconstruction Microscopy (STORM) approach (Karanasios et al. 2016).
2. Mario Rossi's and Michele Pagano's labs reported that ULK1 phosphorylates SEC23B and promotes its relocation to the ERGIC to generate ERGIC-COPII vesicles (Jeong et al. 2018).
3. The work from Zhijian Chen's lab indicated that cGAS-STING activates autophagy via ERGIC trafficking (Gui et al. 2019). In addition, in studies using *Saccharomyces cerevisiae*, Yoshimori Ohsumi's lab and Jodi Nunnari's lab found that the ERES, which is a *Saccharomyces cerevisiae* equivalent of the ERGIC, is involved in autophagy (Graef et al. 2013; Kuninori et al. 2013). See more details in Sect. 2.3.

2.2.4 *Mitochondrial Outer Membrane*

Mitochondria are the powerhouse of the cell, providing the energy needed for life activities. Mitochondria are double-membrane-bound organelles. The outer mitochondrial membrane is smooth, and the inner mitochondrial membrane is folded to form cristae. The inner mitochondrial membrane separates the mitochondria matrix from the intermembrane space. The mitochondrial membrane is enriched in phosphatidylethanolamine (PE) and phospholipids, and is also the main site for the biosynthesis of PE in cells. Hence, mitochondria may be an important membrane source for the generation of autophagosomal membrane.

In 2010, Jennifer Lippincott-Schwartz's lab raised a novel hypothesis that the autophagosomal membrane may originate from the outer mitochondrial membrane in mammalian cells. They found that under starvation, the LC3-labeled autophagosomal membrane colocalized with a biomarker of the outer mitochondrial membrane, but not biomarkers for the inner mitochondrial membrane or mitochondria matrix. Therefore, the outer mitochondrial membrane might be another source for the biosynthesis of autophagosomal membrane. These results were published in the journal *Cell* that year and have attracted wide attention (Hailey et al. 2010). In 2014, using transmission electron microscopy, immunogold electron microscopy, confocal laser scanning microscope, and flow cytometry, Cook et al. confirmed that mitochondria provide a source for autophagosomal membrane biosynthesis in breast cancer cells (Cook et al. 2014). Under basal condition, or upon drug-induced autophagy activation, the generation of autophagosomal membranes can be seen in breast cancer cells. Some of the autophagosomal membrane interacts with the outer mitochondrial membrane. Hence, membrane lipids such as PE and other phospholipids in mitochondrial membranes may be directly used to synthesize autophagosomal membranes.

2.2.5 ER-Mitochondria Contact Site

It should be noted that organelles in cells are not isolated. Around 20% of the mitochondria surface is close to the ER membrane, with an interval distance of 10–30 nm. The ER-mitochondria contact site plays critical roles in several fundamental physiological processes, such as mitochondrial division, Ca^{2+} signal transduction, lipid metabolism, etc. The region where ER interacts with mitochondria is named as the mitochondria-associated ER membrane (MAM). Outer mitochondrial membrane components may be transferred into the phagophore through ER-mitochondria contact sites. Interruption of the ER-mitochondria contact site significantly blocks the formation of autophagosomes. MAM proteins, including those in the ER-mitochondria contact site, can be collected using subcellular fractionation. After starvation, many autophagy-related proteins, such as Atg14, beclin 1, Vps34, and Vps15, are found in the MAM fraction.

The vesicle-associated membrane protein-associated proteins VAPA and VAPB contribute to the ER-organelle tethering function. The VAPB on ER coordinates with the protein tyrosine phosphatase-interacting protein 51 (PTPIP51) in tethering ER and mitochondria, which regulates the exchange of Ca^{2+} between the ER and mitochondria, and results in the autophagy induction. However, the role of the ER-mitochondria contact site in the generation of the autophagosomal membrane still needs to be further illustrated.

2.2.6 Plasma Membrane

In addition to the aforementioned membrane-rich organelles that play an important role in vesicular transport in the endomembrane system, eukaryotic cells have other membrane-coated vesicular organelles, such as lysosomes, endosomes, and the plasma membrane, all of which are closely associated with the origin of autophagosomal membrane. The plasma membrane mainly consists of membrane lipids and membrane proteins, which are wrapped around the cell surface. The plasma membrane plays an essential role in maintaining the internal environment and homeostasis of the cell. In addition, it also participates in the exchange of material, energy, and signals with the external environment. The surface area of the plasma membrane is large, providing sufficient materials for the formation of autophagosomal membrane.

Autophagy-related 16-like 1 (Atg16L1) is a key regulatory protein for autophagosomal membrane generation. LC3-II-positive vesicles cannot form in cells lacking Atg16. Atg16L1 binds to the Atg12-Atg5 complex, which specifies the site of LC3 lipidation and promotes the formation of mature autophagosome. After the closure of phagophore, the Atg12-Atg5-Atg16L1 complex is released into the cytoplasm. It is generally accepted that the phagophore precursor only expresses Atg16L1; the phagophore expresses both Atg16L1 and LC3; and double-membrane-bound autophagosomes only express LC3. Therefore, Atg16L1 might be used as a biomarker for the early phagophore.

David Rubinsztein and his research group from Cambridge Institute for Medical Research have made great progress in understanding the role of the plasma membrane in the origin of the autophagosomal membrane. In 2010, they for the first time reported that Atg16L1 associates with clathrin-coated vesicles through its interaction with clathrin heavy chain and clathrin adaptor protein 2 (AP2). These vesicles commonly appear in the vicinity of the plasma membrane (Ravikumar et al. 2010). Atg16L1-positive vesicles are internalized and detached from the cytoplasm membrane via endocytosis. Blockage of clathrin-mediated endocytosis decreases the number of Atg16L1-positive vesicles and inhibits autophagosome generation. In addition, suppression of the detachment process results in the accumulation of Atg16L1 precursor structures in cells. Another study indicates that Atg16L1 can be transferred to the phagophore from the plasma membrane and promote autophagosome generation in a clathrin-independent endocytic pathway via Arf6. No matter whether or not protein trafficking from the plasma membrane to autophagosome depends on clathrin, these findings support the hypothesis that the cytoplasm membrane might be an origin of autophagosomal membrane, and suggest that the cytoplasm membrane contributes to the early formation of Atg16L1-containing vesicles.

The Atg16L1-containing vesicles fuse and form an autophagosome in a process regulated by the soluble *N*-ethylmaleimide-sensitive fusion attachment protein receptors (SNAREs), such as vesicle-associated membrane protein 7 (VAMP7),

syntaxin 7, syntaxin 8, or Vti1b. This process involves the fusion between two vesicles with the same origin and properties, and is therefore known as homotypic fusion. The fusion event determines the size of vesicles and promotes the conversion from Atg16L1-containing vesicles to phagophores. Understanding this fusion leads to a new understanding of the origin and formation of autophagosomal membrane, and these data were published on *Cell* in 2011 (Moreau et al. 2011).

2.2.7 *Recycling Endosome*

The endosome is a membrane-bound compartment inside eukaryotic cells. It is a compartment of the endocytic membrane transport pathway. Endosomes are categorized in three different compartments, according to the phases of endocytosis, namely, the early endosome, late endosome, and recycling endosome. Upon endocytosis, the vesicles derived from the plasma membrane fuse with early endosome, and generate late endosome. Some of the late endosomes fuse with lysosomes, and their cargo is degraded inside of lysosomes. Others become recycling endosomes and traffic back to the plasma membrane.

There is some controversy about whether endosomes participate in the origin of autophagic vesicles. After the isolation and purification of autophagic vesicles from rat hepatocytes, immunological examination was carried out, and no lysosomal biomarkers (e.g., lysosomal glycoprotein of 120 kDa, Lgp120) or endosome biomarkers (e.g., early-endosome-associated protein 1 (EEA1)) were detected in the purified contents (Stromhaug et al. 1998). These results suggest that the autophagosomal membrane may not be derived from the membrane structures of lysosomes and endosomes. In contrast, other studies indicate that the autophagosomal membrane-related proteins are found in both early endosome and late endosome (Longatti et al. 2012; Puri et al. 2013). Emerging lines of evidence suggest that the recycling endosome may provide membrane lipids for the biogenesis of autophagosomal membrane.

2.2.8 *Nuclear Membrane*

The nuclear membrane, made up of two lipid bilayer membranes, is located between the cytosol and the nucleus in eukaryotic cells. The nuclear membrane is composed of an inner and outer nuclear membrane, and plays a role in mediating the exchange of material and information between the nucleus and the rest of the cell. The inner and outer membranes connect to each other at several sites, forming nuclear pores, which are the channels by which material is exchanged between the nucleus and the cytoplasm.

In 2009, a Canadian research group found that the curling of nuclear membrane formed phagophores in macrophages infected with herpes simplex type 1 virus

(HSV-1) (English et al. 2009). Under the electron microscope, researchers detected that the nuclear membrane-derived phagophore contains four-membrane structures. Immuno-electron microscopic analysis further confirmed that the phagophores originating from the nuclear membrane express the autophagy-related protein LC3. In addition, Japanese researchers using electronic tomography technology demonstrated in 2018 that phagophore may partially originated from the nuclear membrane in yeast. These vesicular structures were termed the “alphasome” (Baba et al. 2019).

2.3 Endomembrane Remodeling and Autophagosomal Membrane Biogenesis

Autophagosomal membrane biogenesis occurs at specific sites of the endomembrane system. Under steady state, membrane trafficking within the endomembrane system is tightly controlled. Formation of the autophagosome under stress conditions requires redirecting the existing membrane trafficking system. Membrane remodeling events occur to complete the redirection. Similar to membrane trafficking, generation of the autophagosomal membrane includes vesicle budding, trafficking, and fusion. Below, we will discuss two major membrane remodeling events for autophagosomal membrane precursor generation and how these precursors are assembled.

There are at least two portions of membranes that act as early autophagosomal membrane precursors: vesicles that support LC3/Atg8 lipidation and ATG9 vesicles. It has been shown that Atg8 lipidation regulates autophagosome size while Atg9 determines the number of autophagosome in the cell (Jin and Klionsky 2016). In mammals, the ER-Golgi intermediate compartment generates vesicles that support LC3 lipidation (Ge et al. 2013, 2014). ATG9 vesicles primarily come from *trans*-Golgi and endocytic recycling system (Noda 2017). Generation of these vesicles requires endomembrane remodeling.

2.3.1 Remodeling of the ERES-ERGIC-COPII System

The ER harbors majority of the membrane surface area in mammals and plays essential roles in autophagosomal membrane generation and assembly (Lamb et al. 2013). Similar to membrane trafficking, generation of the autophagosomal membrane precursors requires membrane remodeling at specific sites on the ER. The COPII membrane remodeling machinery has been indicated to play a vital role. Under steady state, COPII vesicles are generated from the ER-exit sites (ERES), which is initiated by a type II transmembrane protein SEC12. Upon starvation, the SEC12-positive part of the ERES is enlarged (Fig. 2.4) (Ge et al. 2017). This leads to increased association with the ERGIC and the relocation of a fraction of SEC12

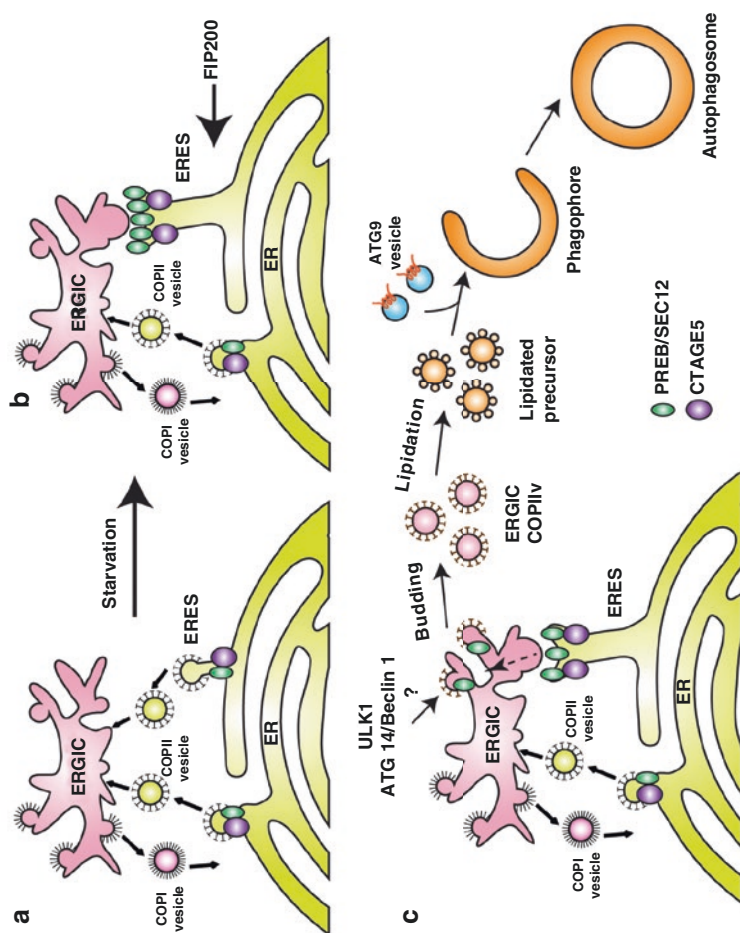


Fig. 2.4 Remodeling of ERES-ERGIC-COPII system. (a) In steady state, SEC12 is enriched in the ERES, which is dependent on its association with CTAGE5. The function of SEC12 on the ERES is for protein cargo transport to the Golgi via packaging COPII vesicles. (b) Upon starvation, a part of the SEC12-positive ERES is enlarged and surrounds the ERGIC. The process is dependent on FIP200 and CTAGE5. (c) The remodeling of SEC12-ERES causes the relocation of SEC12 to the ERGIC (dependent on the ULK1, ATG14, and Beclin1) to promote the assembly of ERGIC-COPII vesicles. These vesicles support LC3 lipidation and nucleate with ATG9-positive vesicles on the PAS. The figure is modified from Ge L. et al. (2017)

to the ERGIC (Ge et al. 2017). The ERGIC-localized SEC12 then initiates COPII assembly on the ERGIC (Fig. 2.4) (Ge et al. 2017). Distinct from the ER-COPII vesicles which are for membrane trafficking between the ER and Golgi, the ERGIC-COPII vesicles associate with autophagic factors and later serve as the template for LC3 lipidation to supply autophagosome biogenesis (Fig. 2.4) (Ge et al. 2014).

How the ERES are remodeled under starvation condition is unclear. Existing evidence indicates that CTAGE5 associates with SEC12 and maintains the concentration of SEC12 on the ERES (Fig. 2.4) (Ge et al. 2017). This is required for the remodeling of the SEC12-ERES. In addition, a population of the autophagic factor FIP200 has been shown to localize on the ERES/ERGIC region (Ge et al. 2017). Via associating with SEC12 through its C-terminus, this population of FIP200 participates in the enlargement of the SEC12-ERES compartment (Ge et al. 2017). The role of FIP200 is independent of its partners ATG13 and ULK1, indicating FIP200 acts independently (Ge et al. 2017). In addition, different ATG protein complexes play differential roles in the remodeling of the ERES-ERGIC-COPII system. Apart from FIP200, ULK1, ATG14, and Beclin1 have been shown to be necessary for the generation of COPII vesicles from the ERGIC (Ge et al. 2014). However, it remains to be determined how these ATG proteins act in each step.

In the yeast (*Saccharomyces cerevisiae*), ERES-COPII plays important roles in autophagosomal membrane formation. Due to the lack of the ERGIC structure, the ERES takes the part of the ERGIC. Nonetheless, a selection mechanism is required to differentiate usual COPII vesicles from autophagic COPII vesicles. The kinase Hrr25 phosphorylates the SEC24 subunit of COPII, which directs COPII vesicles toward autophagosome biogenesis (Davis et al. 2016).

2.3.2 Remodeling of the Trans-Golgi and Endocytic Recycling System

Atg9, an integral membrane protein with six transmembrane domains, is important for autophagosomal membrane biogenesis. During the formation of the autophagosomal membrane in yeast and mammalian cells, Atg9/ATG9 traffics from membrane-bound cellular organelles to phagophores. ATG9 does not stably exist in the autophagosomal membrane. ATG9 is temporarily incorporated into the autophagosomal membrane and is then cycled between the autophagosomes and other compartments. In yeast, Atg9 is distributed in mitochondria, Golgi apparatus, recycling endosomes, and other Atg9 reservoirs. In mammalian cells, Atg9 is detected in Golgi apparatus, primary endosomes, secondary endosomes, recycling endosomes, and other Atg9 reservoirs. Under steady state, the transmembrane protein ATG9 mainly localizes on the *trans*-Golgi and endocytic recycling system (Fig. 2.5) (Noda 2017). Some ATG9 resides on the plasma membrane (Fig. 2.5) (Noda 2017). ATG9 cycles between these compartments (Fig. 2.5) (Noda 2017). Similar to the situation

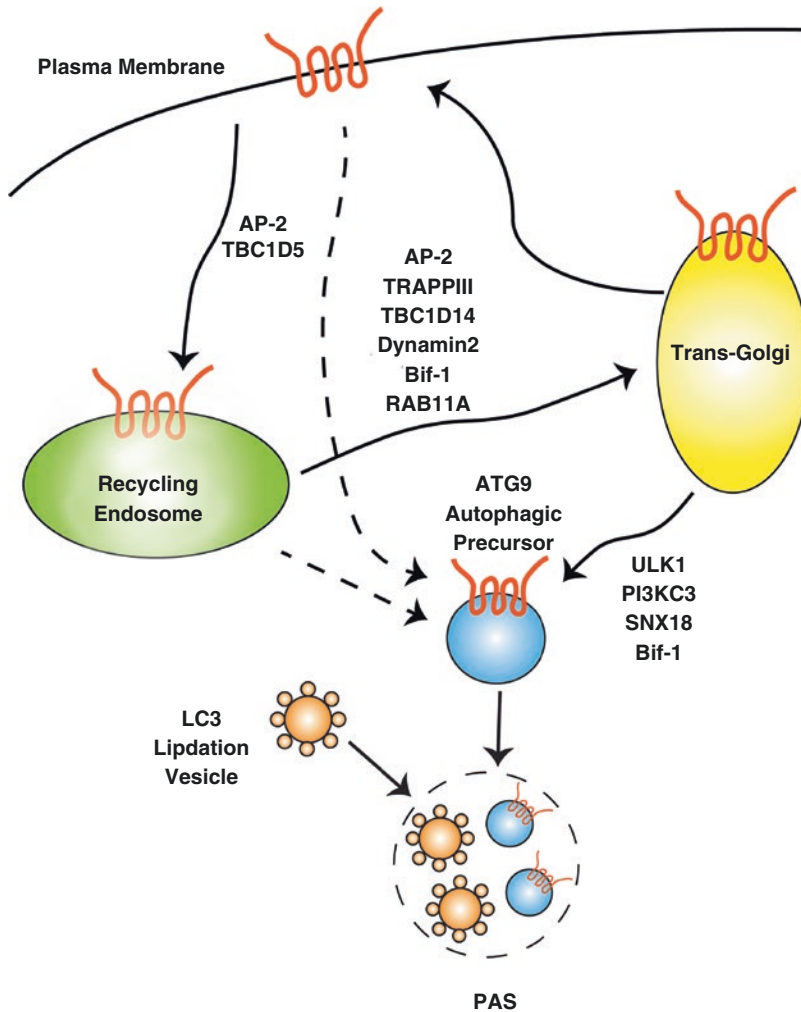


Fig. 2.5 Remodeling of the *trans*-Golgi and endosome system. The transmembrane protein ATG9 cycles among the recycling endosome, the Golgi, and the plasma membrane. AP2 and TBC1D5 are involved in the trafficking of ATG9 from the plasma membrane to the recycling endosome. Multiple proteins, including AP2, TRAPPIII, TBC1D4, RAB11A, Dynamin 2, and Bif-1, regulate the shuttling of ATG9 from the recycling endosome to the Golgi. Upon autophagy induction, ATG9 autophagic vesicles are generated, likely from the Golgi, to nucleate autophagosomal membrane precursors at the PAS. ULK1, PI3KC3, SNX18, and Bif-1 have been shown to regulate the generation of ATG9 autophagic vesicles. The figure is modified from Noda (2017)

with ERGIC-COPII, generation of ATG9 autophagosomal membranes involves membrane remodeling, but of the *trans*-Golgi and endosomes.

It has been shown that the ATG9 located on the *trans*-Golgi relocates to small dispersed vesicles upon starvation (Yoshinori et al. 2011; Young et al. 2006). This

process requires the Bar-domain protein Bif-1 as well as autophagic factors ULK1 and PI3K complex (Yoshinori et al. 2011). The exact molecular details remain elusive.

Several studies shed light on the remodeling of the endosomes upon starvation. The morphological changes include tubulation and fission. Protein factors such as Sorting Nexin 18 (SNX18), Rab11, and TBC1D14 are involved in the tubulation process, and membrane fission is mediated by AP2, Bif-1, Dynamin 2, etc. (Fig. 2.5) (Andrea et al. 2012; Doris and Ivan 2014; Noda 2017).

Similar membrane remodeling also occurs in yeast (*S. cerevisiae*). During starvation, Atg9 distributes from *trans*-Golgi and endosome to vesicles positive for Atg23 and Atg27 (Backues et al. 2015). It has been proposed that these vesicles are intermediates for the formation of Atg9 autophagic membranes. Again, membrane remodeling proteins including Atg24 (a sorting nexin), Retromer, etc. are involved (Hetteema et al. 2014).

2.4 Autophagosomal Membrane Assembly and Expansion

After generation, the autophagosomal membrane precursors are delivered to a specific site called phagophore assembly site (PAS) (Yang and Klionsky 2010). Within the site, the vesicles are tethered and fused to form the cup-shaped phagophore. The process is orchestrated by autophagic factors and membrane remodeling proteins.

2.4.1 PAS Is the Assembly Site for Autophagosomal Membrane

Among autophagy-associated genes (Atgs), atg8 is the primary biomarker for labeling phagophore and autophagosome in yeast cells. Under basal condition, Atg8 is distributed diffusely throughout the cytoplasm of the cells. During starvation, numerous Atg8 puncta appear to accumulate near the vacuoles, though typically not more than one punctum per cell. The morphology of Atg8 puncta is very similar to that of early autophagic vesicles. Using fusion proteins carrying green fluorescent protein (GFP), researchers identified the subcellular localization of other Atgs. Most of the Atgs have been detected to accumulate, or transiently appear at, a certain site near the vacuole, which is termed the pre-autophagosomal structure (PAS). The PAS is mainly localized near the vacuole. Multiple proteins (e.g., Atgs) or protein complexes involved in the formation of autophagic vesicles are recruited to the PAS in an orderly assembly. Atg1 localizes to the perivacuolar PAS. Atg13 functions in the recruitment of Atg1 to the vacuole, where Atg1 clustering and activation occurs (Torggler et al. 2016). Generally, a yeast cell contains only one PAS, while Atg proteins assemble at several sites in mammalian cells. The study of PAS in mammalian cells is just beginning. Assembly of the phagophore occurs at the PAS which supports the nucleation, extension, and closure of the autophagic membrane.

There is one PAS in the yeast (*S. cerevisiae*) which is adjacent to the vacuole and a portion of the ERES, whereas during autophagy in mammalian cells, multiple PASs form. A striking number of PASs are located in a special domain in the ER. This domain of the ER is enriched with PI3P and has a morphology resembling the Greek alphabet “ Ω ”. Therefore, this domain of the ER is termed the “omegasome” (Axe et al. 2011; Sørensen et al. 2018). It has been shown that autophagosomal membranes are assembled at the omegasome, after which the omegasome is disassembled and the completed autophagosome leaves the ER (Axe et al. 2011).

2.4.2 Delivery of Autophagosomal Membrane Precursors to PAS

Recent studies employing biochemical and cell imaging approaches indicate a difference between the sites of autophagosomal precursor generation and assembly. Therefore, it is necessary to deliver the autophagosomal membrane precursors to PAS after generation. The molecular pathways for this are not clear. It has been shown that the site of autophagosomal membrane generation is adjacent to PAS. In the yeast (*S. cerevisiae*), the ERES, the source of autophagic COPII vesicles, is close to the PAS (Kuninori et al. 2013; Young et al. 2006). Moreover, the mammalian ERGIC also locates near the PAS (Karanasios et al. 2016). Regarding ATG9 vesicles, they have been reported to dynamically contact the PAS (Orsi et al. 2012). Therefore, these pieces of evidence indicate that autophagosomal membrane precursors quickly enter the PAS after generation, which is likely to be coupled with the process of assembly.

2.4.3 Assembly of the Phagophore on the PAS

Phagophore assembly starts with a nucleation process. Tethering proteins are required. The protein complex Atg17/Atg13/Atg1 has been indicated as one key factor. In the yeast (*S. cerevisiae*) autophagy, the Atg17/Atg13/Atg1 complex, together with its partners Atg29 and Atg31, is one of the earliest Atg protein complexes that appears on the PAS during starvation-induced bulk autophagy (Hurley and Young 2017). Structural analysis has found that the Atg17 protein is crescent shaped (Fig. 2.6). The curvature of the crescent is the right size to clamp a 30–60-nm-diameter vesicle, which is similar to the size of Atg9 vesicles. The N-terminus and C-terminus of Atg17 reside on each side of the crescent which forms an S-shaped dimer with each other via the C-terminus (Fig. 2.6). The dimer could tether two small vesicles in theory. In addition, in vitro liposome binding assay indicates that the EAT domain of Atg1 binds to highly curved membranes, therefore assisting the

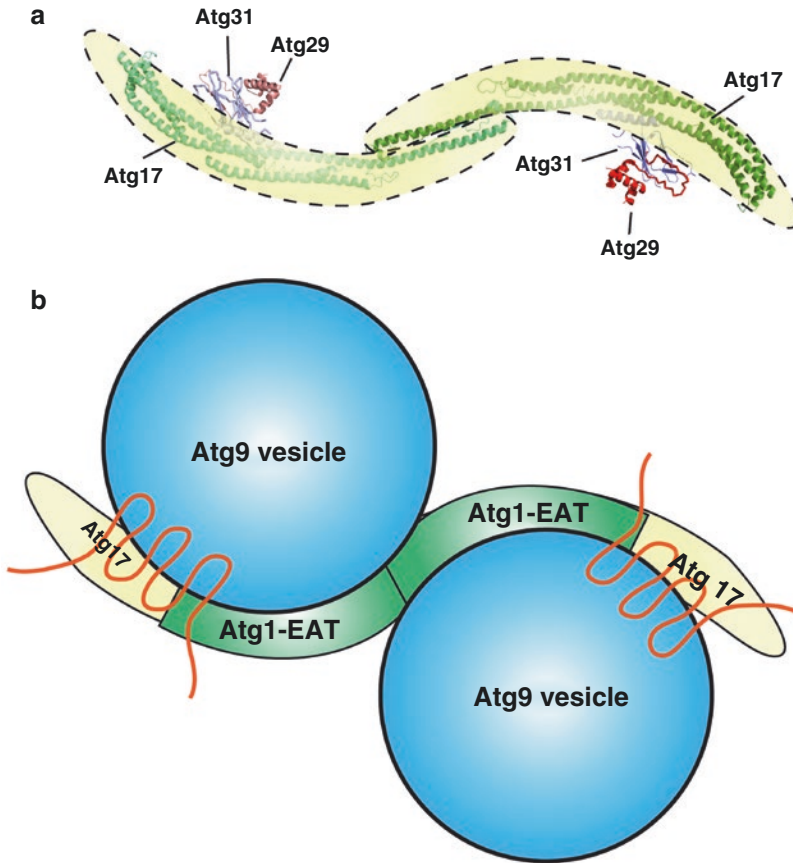


Fig. 2.6 A model for Atg17 complex to tether vesicles. (a) Crystal structure of the Atg17/Atg29/Atg31 dimer. (b) A proposed model for tethering of Atg9 vesicles by the Atg17 complex and Atg1. The figure is modified from Ragusa MJ et al. (2012)

membrane binding and tethering of the Atg17/Atg13/Atg1 complex (Fig. 2.6) (Hurley and Young 2017; Ragusa et al. 2012). The vesicle tethering ability of Atg17/Atg13/Atg1 was partially validated by a following study using in vitro approaches (Rao et al. 2016).

In the yeast (*S. cerevisiae*) autophagy, another tethering factor reported is the TRAPP3 complex. The TRAPP3 complex binds to the Sec23 subunit of COPII (Fig. 2.7) (Tan et al. 2013). Therefore, it recruits COPII vesicles to the site positive for Atg17/Atg13/Atg1 (Fig. 2.7) (Tan et al. 2013). Although pending direct experimental validation, it has been proposed that TRAPP3 may mediate the tethering of COPII and Atg9 vesicles on the PAS.

The mammalian homologues of the Atg17/Atg13/Atg1 and TRAPP3 complexes are FIP200/ATG13/ULK1 and TRAPP3. It has been shown that FIP200/

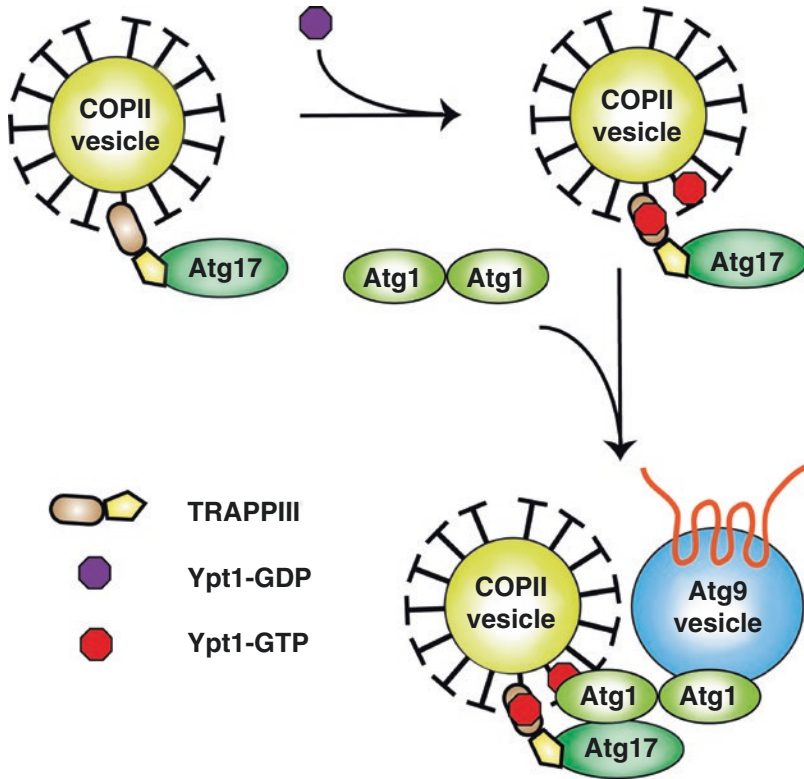


Fig. 2.7 A model for TRAPPIII to tether vesicles. TRAPPIII binds to COPII vesicles and activates Ypt1. Atg17 binds to TRAPPIII and Atg1, which recruits COPII vesicles to the PAS. Atg1 also binds Atg9 vesicles. Through complex formation and likely a dimerization of Atg1, COPII vesicles and Atg9 vesicles are tethered. The figure is modified from Tan D et al. (2013)

ATG13/ULK1 plays a similar role as the Atg17/Atg13/Atg1 complex. Although ULK1 kinase activity is required in the early step of autophagy, it remains to be determined whether the FIP200/ATG13/ULK1 possesses an ability to tether vesicles. Regarding the TRAPPIII complex, it has been shown to regulate ATG9 trafficking in mammalian cells (Noda 2017). However, no direct evidence has been provided to indicate a protein tethering role for it in phagosome assembly.

2.4.4 Elongation of Autophagosomal Membrane

After autophagosomal membrane assembly, multiple rounds of membrane tethering and fusion are required to accomplish autophagosomal membrane extension. As during the assembly process, ATG proteins and non-ATG membrane remodeling factors cooperate to achieve the goal.

2.4.4.1 The PI3KC3 Complex 1

Two PI3KC3 complexes participate in autophagy, of which complex 1 is involved in early autophagosome biogenesis whereas complex 2 is involved in a later stage. Complex 1 consists of ATG14, Beclin1, VPS34, and P150 (Hurley and Young 2017). ATG14 targets complex 1 to the site of autophagosome biogenesis, and VPS34 catalyzes the formation of PI3P. The PI3P recruits downstream factors, e.g., WIPIs (Atg18), which further bring autophagic factors, e.g., ATG16 and ATG2, essential for autophagosomal membrane elongation (Tassula et al. 2015).

2.4.4.2 The Atg9/Atg18/Atg2 Complex

In the yeast (*S. cerevisiae*), Atg9, Atg18, and Atg2 form a protein complex which is essential for autophagosomal membrane elongation. Atg18 binds to PI3P and regulates the localization of the protein complex (Isei 2011). Atg2 possesses membrane tethering activity that it recruits a portion of the adjacent ERES to the PAS to supply lipids for phagophore elongation (Kotani et al. 2018). The structure of mammalian ATG2B has been solved (Zheng et al. 2017; Yang and Klionsky 2010). The structural analysis together with in vitro liposome binding assays suggests a similar function of mammalian ATG2 to the yeast homologue in phagophore maturation.

2.4.4.3 The Atg16 Complex

During autophagy, Atg5 and Atg12 form a protein conjugate, which then forms a complex with Atg16. The complex is essential for efficient Atg8 lipidation. Recent evidence indicates that the complex binds to liposomes via a positively charged region on Atg5. After binding to liposomes, the complex tethers liposomes (Julia et al. 2014). The conclusion is supported by cell imaging studies in mammalian cells, which showed that autophagosome formation required homotypic fusion between ATG16-positive membranes (Moreau et al. 2011). Therefore, it is possible that the Atg5-Atg12/Atg16 (ATG5-ATG12/ATG16) protein complex is involved in tethering membranes during phagophore elongation.

2.4.4.4 Lipidated Atg8

The ubiquitin-like protein Atg8 (LC3) is covalently linked to the PE on autophagosomal membrane precursors. A study using yeast Atg8 indicated that lipidated Atg8 promotes liposome tethering and hemifusion (Nakatogawa et al. 2007). In addition, another study using mammalian LC3 and GABARAPL2 also found that they promote membrane tethering and fusion, and that the ten amino acids at the N-terminus are required for this function (Weidberg et al. 2011). In a yeast genetic study, the expression level of Atg8 correlated with autophagosome size (Xie et al. 2008). Together, these studies indicate the involvement of Atg8/LC3 in regulating autophagosomal membrane elongation.

2.4.4.5 SNARE Proteins

SNARE [soluble *N*-ethylmaleimide-sensitive fusion (NSF) attachment protein receptors] proteins are classified as either R-SNAREs or Q-SNAREs (Moreau et al. 2013). They play a decisive role in membrane fusion. R- and Q-SNAREs localize to different vesicles. One R-SNARE pairs with three Q-SNAREs, which forms an α -helical bundle to merge two membranes together (Wang et al. 2016). Through this way, SNAREs promote membrane fusion.

A special pool of SNARE proteins has been shown to act in autophagosomal membrane elongation. In mammalian cells, VAMP7 (R) pairs with Syntaxin 7 (Qa), Syntaxin 8 (Qc), and Vti1b (Qb), and this is required for ATG16-positive vesicle fusion (Wang et al. 2016). Besides, VAMP2 and VAMP3 were also reported to support phagophore elongation (Sørensen et al. 2018). Yeast genetic studies indicate that the Q-SNAREs Tlg2, Sso1, and Sec9 interact with the R-SNAREs Sec22 and Ykt6 (Sørensen et al. 2018). Together they regulate the membrane trafficking and the fusion of Atg9 vesicles at the PAS.

2.4.4.6 RAB Proteins

RAB proteins are small GTPases essential for membrane trafficking and cargo sorting. Multiple RABs including RAB1 (Ykt1), RAB2, RAB5, RAB11, and RAB33B function in autophagy (Sørensen et al. 2018). RAB1 (Ykt1) regulates the PAS targeting of ULK1 (Atg1) and Atg9; RAB5 activates PI3KC3; RAB11 regulates the membrane remodeling of the endosome and generation of ATG9-positive autophagosomal membrane precursors; RAB33B associates with ATG16. Together, these RAB proteins regulate autophagosomal membrane elongation in different aspects. A recent study reveals the importance of RAB2 in autophagosomal membrane formation. It was shown that the Golgi contributes autophagosomal membrane through RAB2-ATG9-positive vesicles. Under stress conditions, RAB2- and ATG9-positive vesicles dissociate from GM130 on the Golgi. The vesicles subsequently recruit ULK1 to activate autophagosomal membrane initiation. In a later step, RAB2 associates with Pacer and Syntaxin17 to accurately modulate the HOPS complex for autophagosome-lysosome fusion. Together, these RAB proteins regulate different aspects of autophagosomal membrane elongation (Ding et al. 2019).

2.4.5 *The Role of Lipid Synthesis and Transport*

It has been indicated that lipid synthesis and transport also contribute to the membrane supply during autophagosome biogenesis. Evidence for this includes:

1. Lipid droplets contribute to autophagosome biogenesis. Considering that lipid droplets are coated with a single-layer membrane, it is unlikely that lipid droplet

contributes to autophagosome membrane expansion through direct membrane fusion. A solution would be to translocate phospholipids to the autophagosome. In this case, a possible mechanism is membrane contact formation. Indeed, it was shown that lipid droplets directly contact autophagosomes (DuPont et al. 2014).

2. A recent study indicates that phosphatidylinositol synthase (PIS) localizes to the PAS (Nishimura et al. 2017). It is important for the formation of the autophagosome. Therefore, local PI synthesis contributes lipids to the expanding autophagosomal membrane.
3. Structural biology and in vitro biochemical assays indicate that the ATG2 protein contains a lipid-transfer protein-like-hydrophobic-cavity domain which allows it to associate with more than ten kinds of phospholipids and transfer them to the autophagosome. In addition, ATG2 also facilitates the membrane contact between the ER and the autophagosome, which is essential to facilitate lipid transfer (Osawa et al. 2019; Valverde et al. 2019).

2.4.6 The Directionality of Autophagosomal Membrane Elongation and Shape Formation

During the early stage of autophagosomal membrane formation, Atg16L1 binds to Atg12-Atg5 and forms a complex that accumulates at the phagophore precursor and facilitates the LC3 lipidation. Before the autophagosomal membrane closure, the Atg16L1 complex dissociates from the phagophore. Therefore, Atg16L1 is known as a biomarker for early autophagic vacuoles. In 2013, researchers from Norway indicated that SNX18 induced the accumulation of Atg16L1-positive recycling endosomes at the perinuclear region under starvation. Moreover, SNX18 facilitated the recruitment and tubulation of Atg16L1- and LC3-labeled membranes, and contributed to the formation of autophagosomal membrane (Knaevelsrud et al. 2013).

In 2013, David Rubinsztein and his research group further showed that Atg9 and Atg16L1 on the plasma membrane could be engulfed in vesicles and transported to recycling endosomes through different pathways (Puri et al. 2013). Within the recycling endosomes, VAMP3-dependent heterotypic fusion occurs between the Atg9-Atg16L1-containing vesicles, which contributes to the formation of phagophore precursors. Under starvation, the incidence of vesicle fusion is significantly increased. Hence, recycling endosomes might be one of the key links in the transformation of vesicles from different sources into phagophores.

Although Atg16L1 participates in the early formation of autophagosomal membrane, transient overexpression of Atg16L1 in mammalian cells inhibits the biogenesis of autophagosomes, leading to the aberrant accumulation of recycling endosomes in cells. Therefore, transient overexpression of Atg16L1 may not be applicable to studying autophagy in physiological conditions.

2.4.7 The Directionality of Autophagosomal Membrane Elongation and Shape Formation

Autophagosomal membranes elongate to form the cup-shaped phagophore which requires directed membrane extension. In addition, forming the cup-shaped compartment involves scaffolding machinery. It has been shown that ATG proteins regulate the direction of membrane extension and microfilaments build the shape of the phagophore.

2.4.7.1 The Specific Localization of Atg Proteins on the Growing Phagophore

Super-resolution imaging indicates that phagophore elongation in yeast (*S. cerevisiae*) is directional. One side (we name it “side A”) of the phagophore contacts the vacuole to form the vacuole-isolation membrane contact (Fig. 2.8) (Graef et al. 2013; Kuninori et al. 2013). In addition, a portion of the ERES also localizes close to side A (Fig. 2.8). The other side (we name it “side B”) is adjacent to another portion of the ERES. Early autophagosomal membrane assembly factors Atg17, Atg13, and PI3KC3 complex 1 localize on side A (Fig. 2.8). The Atg9/Atg2/Atg18

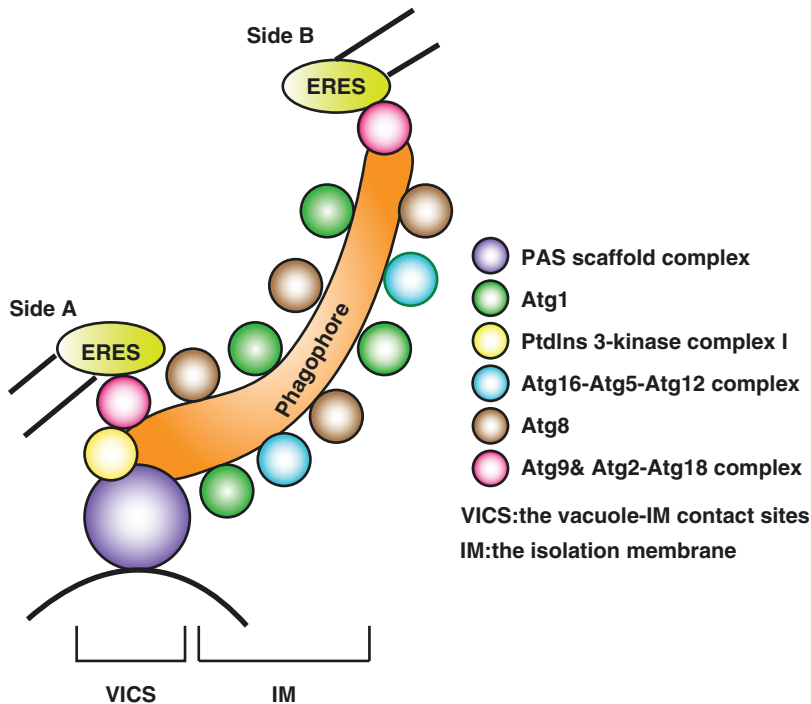


Fig. 2.8 Distribution of Atg proteins on the growing phagophore. The figure is modified from Kuninori S et al. (2013)

complex localizes on both sides (Fig. 2.8). It has been suggested that Atg2 may tether the ERES and the PAS. Therefore, the edge-localized Atg9/Atg2/Atg18 complex may directly tether vesicles to promote phagophore elongation on the edge. The ubiquitin-like machinery, Atg5-Atg12/Atg16 complex, and Atg8 evenly distribute on the phagophore membrane (Fig. 2.8), indicating they may not contribute to the direction of phagophore elongation.

2.4.7.2 Microfilament

Microfilaments, also known as actin filaments, are filaments composed of polymers of actin. Early in 1992, researchers found that autophagosomes could not form in starved cells treated with actin inhibitors such as Cytochalasin D and Latrunculin B. Using immunostaining, actin is found to colocalize with phagophore-related proteins, including Atg14 and Beclin1. In addition, actin is also found in the PI3P-enriched area in cells (Mi et al. 2015). These findings suggest that microfilaments may participate in the early formation of the autophagosomal membrane. Nevertheless, actin does not colocalize with the phagophore closure-related protein Atg5 nor autophagosome maturation-related protein MAP1LC3. Hence, it seems that microfilaments are not involved in the expansion, closure, and maturation of phagophores.

The Arp2/3 complex is an actin nucleator, which functions in promoting actin assembly. Arp2/3 is regulated by nucleation-promoting factors (NPFs). WHAMM (WASP homologue associated with actin, membranes, and microtubules) is a mammalian NPF which mediates Arp2/3-dependent actin assembly. A recent study demonstrates that WHAMM associates with the ER, and colocalizes with the omegasome biomarker DFCP1. WHAMM and DFCP1 comigrate via the actin comet tail motility mechanism, which is a typical process of actin-mediated organelle transport in cells. Disturbance of actin assembly by Latrunculin B or Jasplakinolide blocks the actin comet tail motility of WHAMM and DFCP1, suggesting the formation of autophagosomal membrane is closely associated with actin assembly and disassembly. WHAMM activates the Arp2/3 complex and triggers the formation of branched actin networks, providing mechanical support for omegasome generation. In addition, actin assembly may also rely on functional autophagy. In Atg7-deficient mice, autophagosomes could not form. Moreover, the expression of proteins related to actin assembly is downregulated, and therefore the actin assembly is impaired. Hence, autophagy is closely associated with the dynamic assembly of actin.

Acknowledgement The work is funded by Beijing Natural Science Foundation (JQ20028), National Natural Science Foundation of China (91854114, 31872826), National Key R&D Program of China (2019YFA0508602), and Tsinghua Independent Research Program (2019Z06QCX02).

References

- Andrea L, Christopher AL, Minoo R, Shin-Ichiro Y, Francis AB, Sharon AT. TBC1D14 regulates autophagosome formation via Rab11- and ULK1-positive recycling endosomes. *Autophagy*. 2012;197:659–75.
- Axe EL, Walker SA, Maria M, Priya CH, Llewelyn R, Anja H, Gareth G, Ktistakis NT. Autophagosome formation from membrane compartments enriched in phosphatidylinositol 3-phosphate and dynamically connected to the endoplasmic reticulum. *J Cell Biol*. 2011;182:685–701.
- Baba M, Tomonaga S, Suzuki M, Gen M, Takeda E, Matsuura A, Kamada Y, Baba N. A nuclear membrane-derived structure associated with Atg8 is involved in the sequestration of selective cargo, the Cvt complex, during autophagosome formation in yeast. *Autophagy*. 2019;15(3):423–37.
- Backues SK, Orban DP, Bernard A, Singh K, Cao Y, Klionsky DJ. Atg23 and Atg27 act at the early stages of Atg9 trafficking in *S. cerevisiae*. *Traffic*. 2015;16:172–90.
- Bissa B, Deretic V. Autophagosome formation: cutting the Gordian knot at the ER. *Curr Biol*. 2018;28:R347–9.
- Brier LW, Zhang M, Ge L. Mechanistically dissecting autophagy: insights from in vitro reconstitution. *J Mol Biol*. 2016;428:1700–13.
- Cook KL, Soto-Pantoja DR, Abu-Asab M, Clarke PA, Roberts DD, Clarke R. Mitochondria directly donate their membrane to form autophagosomes during a novel mechanism of parkin-associated mitophagy. *Cell Biosci*. 2014;4:16.
- Davis S, Wang J, Zhu M, Stahmer K, Lakshminarayan R, Ghassemian M, Jiang Y, Miller EA, Ferro-Novick S. Sec24 phosphorylation regulates autophagosome abundance during nutrient deprivation. *Elife*. 2016;5:e21167.
- Ding X, Jiang X, Tian R, Zhao P, Li L, Wang X, Chen S, Zhu Y, Mei M, Bao S, Liu W, Tang Z, Sun Q. RAB2 regulates the formation of autophagosome and autolysosome in mammalian cells. *Autophagy*. 2019;15(10):1774–86.
- Doris P, Ivan D. TBC1D5 and the AP2 complex regulate ATG9 trafficking and initiation of autophagy. *EMBO Rep*. 2014;15:392–401.
- DuPont N, Chauhan S, Arko-Mensah J, Castillo E, Masedunskas A, Weigert R, Robenek H, Proikas-Cezanne T, Deretic V. Neutral lipid stores and lipase PNPLA5 contribute to autophagosome biogenesis. *Curr Biol*. 2014;24:609–20.
- English L, Chemali M, Desjardins M. Nuclear membrane-derived autophagy, a novel process that participates in the presentation of endogenous viral antigens during HSV-1 infection. *Autophagy*. 2009;5:1026–9.
- Ge L, Melville D, Zhang M, Schekman R. The ER–Golgi intermediate compartment is a key membrane source for the LC3 lipidation step of autophagosome biogenesis. *Elife*. 2013;2:e00947–172.
- Ge L, Zhang M, Schekman R. Phosphatidylinositol 3-kinase and COPII generate LC3 lipidation vesicles from the ER–Golgi intermediate compartment. *Elife*. 2014;3:e04135.
- Ge L, Wilz L, Schekman R. Biogenesis of autophagosomal precursors for LC3 lipidation from the ER–Golgi intermediate compartment. *Autophagy*. 2015;11:2372–4.
- Ge L, Zhang M, Kenny SJ, Liu D, Maeda M, Saito K, Mathur A, Xu K, Schekman R. Remodeling of ER-exit sites initiates a membrane supply pathway for autophagosome biogenesis. *EMBO Rep*. 2017;18(9):1586–603. <https://doi.org/10.15252/embr.201744559>.
- Graef M, Friedman JR, Graham C, Babu M, Nunnari J. ER exit sites are physical and functional core autophagosome biogenesis components. *Mol Biol Cell*. 2013;24:2918–31.
- Gui X, Yang H, Li T, Tan X, Shi P, Li M, Du F, Chen ZJ. Autophagy induction via STING trafficking is a primordial function of the cGAS pathway. *Nature*. 2019;567:262–6.
- Hailey DW, Rambold AS, Satpute-Krishnan P, Mitra K, Sougrat R, Kim PK, Lippincott-Schwartz J. Mitochondria supply membranes for autophagosome biogenesis during starvation. *Cell*. 2010;141:656–67.

- Hayashi-Nishino M, Fujita N, Noda T, Yamaguchi A, Yoshimori T, Yamamoto A. A subdomain of the endoplasmic reticulum forms a cradle for autophagosome formation. *Nat Cell Biol.* 2009;11:1433–7.
- Hettema EH, Lewis MJ, Black MW, Pelham HRB. Retromer and the sorting nexins Snx4/41/42 mediate distinct retrieval pathways from yeast endosomes. *EMBO J.* 2014;22:548–57.
- Hurley JH, Young LN. Mechanisms of autophagy initiation. *Annu Rev Biochem.* 2017;86:225–44. <https://doi.org/10.1146/annurev-biochem-061516-044820>.
- Isei T. Autophagosome formation and molecular mechanism of autophagy. *Antioxid Redox Signal.* 2011;14:2201–14.
- Jeong YT, Simoneschi D, Keegan S, Melville D, Adler NS, Saraf A, Florens L, Washburn MP, Cavasotto CN, Fenyo D, Cuervo AM, Rossi M, Pagano M. The ULK1-FBXW5-SEC23B nexus controls autophagy. *Elife.* 2018;7:e42253.
- Jin M, Klionsky DJ. Regulation of autophagy: modulation of the size and number of autophagosomes. *FEBS Lett.* 2016;588:2457–63.
- Julia R, Marta W, Iosune I, Stefan S, Egon O, Claudine K, Sascha M. Mechanism and functions of membrane binding by the Atg5-Atg12/Atg16 complex during autophagosome formation. *EMBO J.* 2014;31:4304–17.
- Karanasios E, Walker SA, Okkenhaug H, Manifava M, Hummel E, Zimmermann H, Ahmed Q, Domart MC, Collinson L, Ktistakis NT. Autophagy initiation by ULK complex assembly on ER tubulovesicular regions marked by ATG9 vesicles. *Nat Commun.* 2016;7:12420.
- Knaevelsrud H, Soreng K, Raiborg C, Haberg K, Rasmuson F, Brech A, Liestol K, Rusten TE, Stenmark H, Neufeld TP, Carlsson SR, Simonsen A. Membrane remodeling by the PX-BAR protein SNX18 promotes autophagosome formation. *J Cell Biol.* 2013;202:331–49.
- Kotani T, Kirisako H, Koizumi M, Ohsumi Y, Nakatogawa H. The Atg2-Atg18 complex tethers pre-autophagosomal membranes to the endoplasmic reticulum for autophagosome formation. *Proc Natl Acad Sci U S A.* 2018;115(41):10363–8.
- Kuninori S, Manami A, Chika KK, Hayashi Y, Yoshinori O. Fine mapping of autophagy-related proteins during autophagosome formation in *Saccharomyces cerevisiae*. *J Cell Sci.* 2013;126:2534–44.
- Lamb CA, Tamotsu Y, Tooze SA. The autophagosome: origins unknown, biogenesis complex. *Nat Rev Mol Cell Biol.* 2013;14:759–74.
- Longatti A, Lamb CA, Razi M, Yoshimura S, Barr FA, Tooze SA. TBC1D14 regulates autophagosome formation via Rab11- and ULK1-positive recycling endosomes. *J Cell Biol.* 2012;197:659–75.
- Mi N, Chen Y, Wang S, Chen M, Zhao M, Yang G, Ma M, Su Q, Luo S, Shi J. CapZ regulates autophagosomal membrane shaping by promoting actin assembly inside the isolation membrane. *Nat Cell Biol.* 2015;17:1112.
- Moreau K, Ravikumar B, Renna M, Puri C, Rubinsztein DC. Autophagosome precursor maturation requires homotypic fusion. *Cell.* 2011;146:303–17.
- Moreau K, Renna M, Rubinsztein DC. Connections between SNAREs and autophagy. *Trends Biochem Sci.* 2013;38:57–63.
- Nakatogawa H, Ichimura Y, Ohsumi Y. Atg8, a ubiquitin-like protein required for autophagosome formation, mediates membrane tethering and hemifusion. *Cell.* 2007;130:165–78.
- Nishimura T, Tamura N, Kono N, Shimanaka Y, Arai H, Yamamoto H, Mizushima N. Autophagosome formation is initiated at phosphatidylinositol synthase-enriched ER subdomains. *EMBO J.* 2017;36:1719–35.
- Noda T. Autophagy in the context of the cellular membrane-trafficking system: the enigma of Atg9 vesicles. *Biochem Soc Trans.* 2017;45:1323–31.
- Orsi A, Razi M, Dooley HC, Robinson D, Weston AE, Collinson LM, Tooze SA. Dynamic and transient interactions of Atg9 with autophagosomes, but not membrane integration, are required for autophagy. *Mol Biol Cell.* 2012;23:1860–73.

- Osawa T, Kotani T, Kawaoka T, Hirata E, Suzuki K, Nakatogawa H, Ohsumi Y, Noda NN. Atg2 mediates direct lipid transfer between membranes for autophagosome formation. *Nat Struct Mol Biol.* 2019;26:281–8.
- Puri C, Renna M, Bento CF, Moreau K, Rubinsztein DC. Diverse autophagosomal membrane sources coalesce in recycling endosomes. *Cell.* 2013;154:1285–99.
- Ragusa MJ, Stanley RE, Hurley JH. Architecture of the Atg17 complex as a scaffold for autophagosome biogenesis. *Cell.* 2012;151:1501–12.
- Rao Y, Perna MG, Hofmann B, Beier V, Wollert T. The Atg1–kinase complex tethers Atg9-vesicles to initiate autophagy. *Nat Commun.* 2016;7:10338.
- Ravikumar B, Moreau K, Jahreiss L, Puri C, Rubinsztein DC. Plasma membrane contributes to the formation of pre-autophagosomal structures. *Nat Cell Biol.* 2010;12:747–57.
- Søreng K, Neufeld TP, Simonsen A. Membrane trafficking in autophagy. *Int Rev Cell Mol Biol.* 2018;336:1–92.
- Stromhaug PE, Berg TO, Fengersrud M, Seglen PO. Purification and characterization of autophagosomes from rat hepatocytes. *Biochem J.* 1998;335(Pt 2):217–24.
- Tassula PC, Zsuzsanna T, Pierre DN, Oliver K. WIPI proteins: essential PtdIns3P effectors at the nascent autophagosome. *J Cell Sci.* 2015;128:207–17.
- Tan D, Cai Y, Wang J, Zhang J, Menon S, Chou HT, Ferro-Novick S, Reinisch KM, Walz T. The EM structure of the TRAPP3 complex leads to the identification of a requirement for COPII vesicles on the macroautophagy pathway. *Proc Natl Acad Sci USA.* 2013;110:19432–7.
- Torggler R, Papinski D, Brach T, Bas L, Schuschnig M, Pfaffenwimmer T, Rohringer S, Matzhold T, Schweida D, Brezovich A, Kraft C. Two independent pathways within selective autophagy converge to activate Atg1 kinase at the vacuole. *Mol Cell.* 2016;64:221–35.
- Uemura T, Yamamoto M, Kametaka A, Sou YS, Yabashi A, Yamada A, Annoh H, Kametaka S, Komatsu M, Waguri S. A cluster of thin tubular structures mediates transformation of the endoplasmic reticulum to autophagic isolation membrane. *Mol Cell Biol.* 2014;34:1695–706.
- Valverde DP, Yu S, Boggavarapu V, Kumar N, Lees JA, Walz T, Reinisch KM, Melia TJ. ATG2 transports lipids to promote autophagosome biogenesis. *J Cell Biol.* 2019;218(6):1787–98.
- Wang Y, Li L, Chen H, Lai Y, Long J, Liu J, Zhong Q, Diao J. SNARE-mediated membrane fusion in autophagy. *Semin Cell Dev Biol.* 2016;60:97–104.
- Weidberg H, Shpilka T, Shvets E, Abada A, Shimron F, Elazar Z. LC3 and GATE-16 N termini mediate membrane fusion processes required for autophagosome biogenesis. *Dev Cell.* 2011;20:444–54.
- Xie Z, Nair U, Klionsky D. Atg8 controls phagophore expansion during autophagosome formation. *Mol Biol Cell.* 2008;19:3290.
- Yang Z, Klionsky DJ. Mammalian autophagy: core molecular machinery and signaling regulation. *Curr Opin Cell Biol.* 2010;22:124–31.
- Yoshinori T, Meyerkord CL, Tsukasa H, Kristin R, Fox TE, Mark K, Loughran TP, Hong-Gang W. Bif-1 regulates Atg9 trafficking by mediating the fission of Golgi membranes during autophagy. *Autophagy.* 2011;7:61–73.
- Young ARJ, Chan EYW, Wen HX, Robert KC, Crawshaw SG, Stephen H, Hailey DW, Jennifer LS, Tooze SA. Starvation and ULK1-dependent cycling of mammalian Atg9 between the TGN and endosomes. *J Cell Sci.* 2006;119:3888–900.
- Zheng JX, Li Y, Ding YH, Liu JJ, Zhang MJ, Dong MQ, Wang HW, Yu L. Architecture of the ATG2B-WDR45 complex and an aromatic Y/HF motif crucial for complex formation. *Autophagy.* 2017;13:1870–83.

Chapter 3

Phagophore Closure



Yongheng Liang

Abstract Phagophore closure is a critical step during macroautophagy. However, the proteins and mechanisms to regulate this step have been elusive for a long time. In 2017, Rab5 was affirmed to play a role in phagophore closure in yeast. Furthermore, in mammalian cells, ESCRT III was reported to have roles in phagophore closure and mitophagosome closure in vivo in 2018 and 2019, respectively. The role of ESCRT in phagophore closure was confirmed in yeast, both in vivo and in vitro, in 2019. Most importantly, the latter paper found that Atg17 recruited the ESCRT III subunit Snf7 to the phagophore to close it under the control of Rab5. To determine the closure characteristics of autophagosome-like membrane structures in ESCRT mutants, a traditional protease protection assay with immunoblotting was used, accompanied by new techniques that were developed, including immunofluorescence assays, autophagosome completion assays, and the optogenetic closure assay. This study delivered our current understanding of phagophore closure and provided more reference methods to detect membrane closure.

3.1 The Status and Difficulties in the Study of Phagophore Closure

Macroautophagy (henceforth autophagy) is mainly regulated by the core Atg proteins. The autophagy process can be roughly divided into five stages: the initiation and phagophore formation, the extension of the phagophore, phagophore closure to enclose cargoes, the fusion of autophagosomes with lysosomes/vacuoles, and degradation and recycling stages. However, the specific process and morphological changes of some stages have not been accurately defined and described. For example, when does a process belong to the stage of extension of the phagophore and when or in what state does a process begin to belong to the phagophore closure stage? Roughly, studies of autophagosome regulation mainly focus on the early

Y. Liang (✉)

College of Life Sciences, Nanjing Agricultural University, Nanjing, China
e-mail: liangyh@njau.edu.cn

© Science Press 2021

Z. Xie (ed.), *Autophagy: Biology and Diseases*, Advances in Experimental Medicine and Biology 1208, https://doi.org/10.1007/978-981-16-2830-6_3

43

stage and the late stage (Tong et al. 2010), even though there are still many unanswered question details for the autophagy process (Lindqvist et al. 2015). A few studies are regarding the middle stage. It was reported that the absence of Atg2 in yeast or the absence of Atg3 in mammalian cells impaired phagophore formation/extension and closure (Sou et al. 2008; Wang et al. 2001). However, since the formation of autophagy-related membrane vesicles and the extension of phagophore in these mutants are affected, it is not possible to define whether the observed defect of phagophore closure is caused by the failure of the early autophagy process or whether Atg2 and Atg3 have unique roles in the closure of phagophores. In addition, the depletion of Atg3 in mammalian cells also leads to the absence of LC3-PE form and the inhibition of Atg12-Atg5 formation, two major ubiquitination conjugation systems, which play very important roles in the formation and extension of phagophores. In the end, the autophagosome-like membrane structures in Atg3-depleted mammalian cells are smaller than normal autophagosomes (Sou et al. 2008), which makes it hard to say that the main role of Atg3 is to regulate phagophore closure. Similarly, there has been a report about an autophagosome closure defect caused by overexpression of inactive Atg4B in mammalian cells, because this overexpression also leads to the failure of LC3 to form LC3-II by normal lipidation (Fujita et al. 2008), so it cannot be excluded that the observed defect of autophagosome closure is not caused by the abnormal early autophagy process in which LC3 is involved. On the other hand, we also cannot exclude the possibility that the yeast Atg8-PE deconjugation process in which Atg4 is involved may play a role in phagophore closure (Nair et al. 2012; Nakatogawa et al. 2012; Yu et al. 2012). However, it will be more appropriate to say that an unmutated protein functions in the process of phagophore closure if the size and shape of autophagosome-like membrane structure from its mutants cannot be simply distinguished from that of normally closed autophagosomes from wild type, and there is no evidence that the early autophagy process is affected, such as the formation of Atg8-PE or the phosphorylation of Atg13, while it is demonstrated that the autophagosome-like membrane structures do not close.

We recently reported that the yeast endocytic Vps21/Rab5 module is required for autophagy (Chen et al. 2014), and found that the absence of these proteins does not affect the production and size of autophagosomes, but it does affect the entry of autophagosomes into vacuoles, resulting in the accumulation of unclosed autophagosomes (Chen et al. 2014). It is further clarified that the protein depletion does not affect the formation of Atg8-PE, but causes the unclosure of autophagosomes (Zhou et al. 2017). As we know, this is the first clear report to observe autophagosome-like membrane structures without defects in initiation and phagophore extension, but with defect in phagophore closure. We further tried to explore the molecular mechanism of Vps21/Rab5 module in phagophore closure and found that the Vps21/Rab5 module regulates phagophore closure through the endosomal sorting complexes required for transport (ESCRT) complex and in a Vps21/Rab5-dependent manner (Zhou et al. 2019). Our results are complementary to the latest finding of mammalian ESCRT in phagophore closure (Takahashi et al. 2018).

The phagophore itself is small in size and spherical; it is impossible to directly observe its open pore to determine whether it is closed by microscopes if the diameter size of the open pore of phagophore is smaller than the maximum resolution

limit of current microscopes. If the diameter size of the open pore of phagophore is bigger than the resolution limit of microscopes, theoretically it is possible to observe the open pore of phagophore through serial-section electron microscopy combined with 3-dimensional reconstruction to determine whether a phagophore is closed. Similarly, multi-slice scanning by super-resolution microscope combined with 3-dimensional reconstruction should also be able to observe the open pore of phagophore to determine whether a phagophore is closed. However, both methods meet difficulties as the platform of the former method is only available in a few labs worldwide, while the latter method is limited by the resolution of super-resolution microscope and by photobleaching during the taking of multiple pictures of the same field. Nonetheless, a few methods have been developed to indirectly determine whether a phagophore is closed or not, based on the differences of accessibility of the contents of autophagosomes between open phagophores and closed autophagosomes. I am going to introduce these methods below.

3.2 Methods to Determine Whether an Autophagosome-Related Structure Is Closed

3.2.1 The Protease Protection Assay

If the accumulation of autophagosome-like structures in cells due to autophagy defects were observed by either fluorescence microscopy or transmission electron microscopy, but researchers are not sure whether they are open or closed autophagosomes, the protease protection assay (Nair et al. 2011) is a common method to determine if the autophagosome-like structures are closed or not. In this assay, different combinations of protease K (PK) and detergent Triton X-100 (TX) are applied to treat the isolated autophagosome-like structures to check the degradation of proteins on or inside the membrane, so that the autophagosome-like structures can be distinguished to be open or closed autophagosomes. In the past, the degradation of proteins associated with the membranes after the above treatment was displayed by immunoblot assay to infer whether the membrane structures are closed. We have recently developed a new method to display whether GFP-Atg8 is still on the membranes after the above treatment by observing GFP fluorescence to infer whether the membrane structures are closed (Zhou et al. 2019).

3.2.1.1 An Immunoblot Assay to Display the Results of Protease Protection Assay

After the isolated autophagosome-like structures from budding yeast were treated with different combinations of protease K and detergent, anti-GFP was used to determine GFP-Atg8 degradation and/or anti-Ape1 to determine prApe1 (Ape1 precursor) maturation to assay whether the autophagosome-like structures are closed.

This method has been widely used to determine the closure characteristics of autophagosome-like structures in cells with obvious GFP-Atg8 accumulation (Cebollero et al. 2012; Yang and Rosenwald 2016; Zhou et al. 2017). Correspondingly, anti-LC3 was used to determine the level of LC3-II, and anti-p62 was used to determine the level of autophagosome cargo protein p62 in mammalian cells, to assay whether the autophagosome-like structures are closed in cells with obvious LC3 accumulation (Takahashi et al. 2018; Velikkakath et al. 2012).

Based on the autophagic phenotypes of a large number of accumulation of autophagosome-like membrane structures in ESCRT mutants *snf7* Δ and *vps4* Δ observed by a fluorescence microscopy and a transmission electron microscopy, the closure characteristics of these autophagosome-like membrane structures were analyzed using the protease protection assay combined with immunoblot assay to demonstrate the application of this method. It is better to set up both positive and negative controls at the same time when applying this method, although one control is often ignored in some studies due to the lack of suitable control or to avoid troubles. In Fig. 3.1, after the strains were induced for autophagy, the autophagosome-associated membrane structures were isolated from them with the same conditions (Zhou et al. 2019). These from *atg1* Δ , which is defective in autophagosome biogenesis, were used as a control of unclosed autophagosomes, while these isolated from *ypt7* Δ were used as a control of closed autophagosomes, to determine the closure characteristics of autophagosome-like membrane structures isolated from *snf7* Δ and *vps4* Δ . The results showed that the autophagosome-like membrane structures isolated from *snf7* Δ and *vps4* Δ are unclosed autophagosomes as GFP-Atg8 was completely degraded to GFP and prApe1 completely matured to mApe1 with protease K without Triton X-100 treatment, similar to the membrane characteristics of autophagosome-associated membrane structures isolated from *atg1* Δ but not to

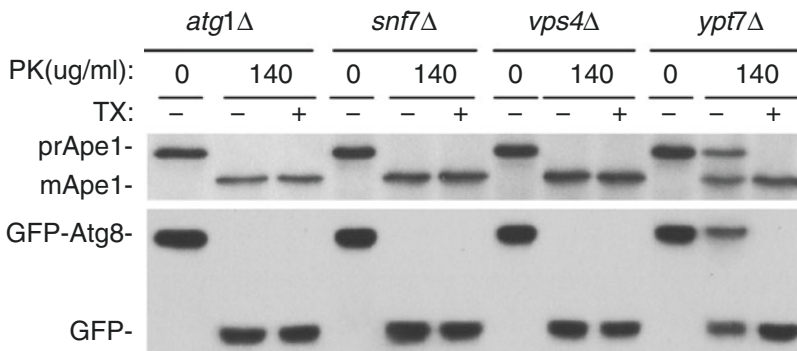


Fig. 3.1 The protease protection assay in combination with immunoblot assay to show the autophagosome-like membrane structures isolated from *snf7* Δ and *vps4* Δ mutants are unclosed autophagosomes. The autophagosome-associated membrane structures isolated from *atg1* Δ and *ypt7* Δ were representing unclosed membrane structures and closed autophagosomes, respectively. For induction of autophagy, the isolation of autophagosome-associated membrane structures and the treatment conditions of protease and detergent, please refer to Zhou et al. (2019). PK protease K, TX Triton X-100

those from *ypt7* Δ , in which GFP-Atg8 was completely degraded to GFP and prApe1 completely matured to mApe1 only if protease K and Triton X-100 were added together. Furthermore, the upstream-downstream relationship between Snf7 and Ypt7 or Vps4 and Ypt7 was determined with constructing double mutants and by using the same protease protection assay to compare the results from single and double mutants (Zhou et al. 2019).

3.2.1.2 Fluorescence Observation to Display the Results of Protease Protection Assay

Atg8 is involved in the whole process of autophagy and distributes at both outer and inner membranes of autophagosomes. GFP-Atg8 is an ideal protein to track autophagosomes at different stages. As stated above, we observed a large number of accumulation of GFP-Atg8-marked autophagosome-like membrane structures outside the vacuoles in *snf7* Δ and *vps4* Δ mutants by fluorescence microscopy (Zhou et al. 2019), obviously different from the large number of accumulation of GFP-Atg8-marked autophagosomes dispersed in cytosol as dots in *ypt7* Δ (Chen et al. 2014). If GFP-Atg8-labeled autophagosomal membrane structures were isolated and subjected to protease protection assay, i.e., when they were treated with protease K and/or Triton X-100 and washed with water, the fluorescence of GFP-Atg8 (GFP unbound to membranes will be lost after washed with water) was observed to display the results of protease protection assay. If the autophagosome-related membrane structures are closed autophagosomes, then GFP-Atg8 fluorescence should be observed for samples treated with protease without detergent. Under the same condition, if the autophagosome-related membrane structures are unclosed autophagosomes, then GFP-Atg8 fluorescence should not be observed. In contrast, GFP-Atg8 fluorescence should be observed for samples which were not treated with both protease and detergent, while not be observed for samples which were treated with both protease and detergent. Thus, the closure characteristics of isolated autophagosome-related membrane structures can be determined. We applied this method to detect the closure characteristics of accumulated autophagosome-like membrane structures in *snf7* Δ , and the conclusion is consistent to that obtained by the immunoblot assay for the protease protection assay, i.e., the accumulated autophagosome-like membrane structures in *snf7* Δ are unclosed autophagosomes.

In Fig. 3.2, fluorescence observation was applied to determine GFP signal for the isolated autophagosome-related membrane structures from *snf7* Δ and *snf7* Δ *ypt7* Δ mutants when the isolated closed autophagosomes from *ypt7* Δ mutant induced under the same condition were used as a control. The results showed that the autophagosome-related membrane structures isolated from *snf7* Δ and *snf7* Δ *ypt7* Δ mutants are unclosed autophagosomes as GFP disappeared when protease K without Triton X-100 was added, indicating that GFP-Atg8 on autophagosome-related membrane structures was accessed and degraded by protease K, not like these isolated from *ypt7* Δ mutant, in which GFP disappeared only when protease K and

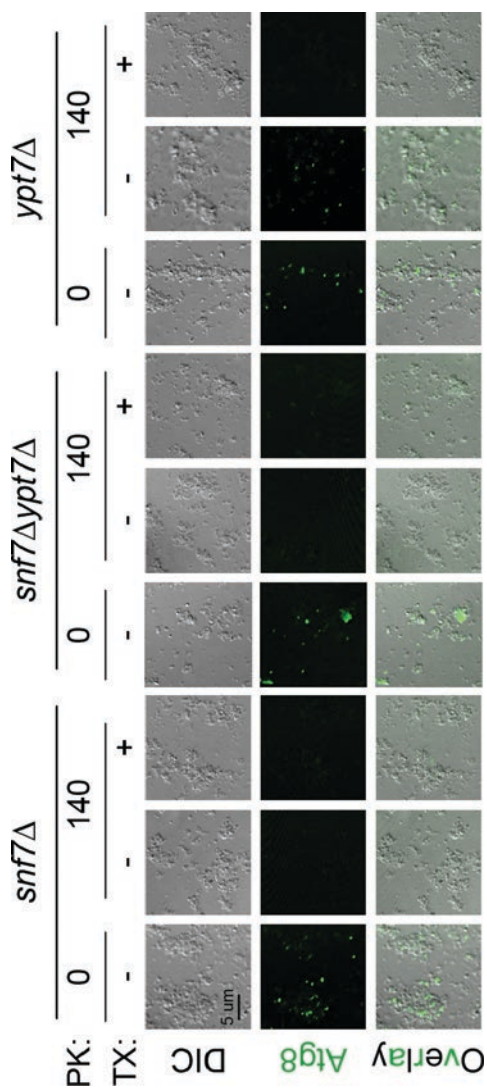


Fig. 3.2 Fluorescence observation for protease protection assay to show the autophagosome-related membrane structures in *snf7Δ* and *snf7Δypt7Δ* mutants are unclosed autophagosomes. The autophagosome membrane-associated structures isolated from *ypt7Δ* represent closed autophagosomes. PK protease K, TX Triton X-100, DIC differential interference contrast

Triton X-100 were added together so that GFP-Atg8 inside closed autophagosomes was accessed and degraded by protease K. As the result in *snf7Δypt7Δ* mutant like that in *snf7Δ* mutant but does not like that in *ypt7Δ* mutant, this method also indicates that Snf7 functions upstream of Ypt7 in autophagy. Please go to our published paper for similar results and more detailed operations (Zhou et al. 2019). Similarly and much earlier, the fluorescence of GFP-fused aminopeptidase I, the best-characterized selective cargo of autophagosomes in *Saccharomyces cerevisiae*, was applied to successfully monitor intact autophagosomes ex vivo to facilitate the fractionation of autophagosomes for biochemical assays (Suzuki et al. 2014).

3.2.2 An Immunofluorescence Assay to Determine Whether Autophagosome-Associated Membrane Structures Are Closed

Immunofluorescence was commonly used for protein localization before live fluorescence was widely used. Based on the fact that autophagosomal membrane structures isolated for the protease protection assay contain GFP-Atg8 on both the outer and inner membranes while the autophagosome interior may contain other cargo proteins, such as Ape1, we designed experiment with corresponding first antibody anti-Ape1 to access cargo Ape1 inside GFP-Atg8-marked unclosed autophagosomes through pores on autophagosome membranes. If the autophagosomes are unclosed, the first antibody rabbit anti-Ape1 can enter unclosed autophagosomes so that the Ape1 inside autophagosomes can be recognized and bound by anti-Ape1, and the second antibody can also enter the unclosed autophagosomes to recognize the first antibody rabbit anti-Ape1 so that the site of Ape1 can be displayed by Alexa Fluor 647-conjugated second antibody anti-rabbit IgG. If the autophagosomes are closed, these processes will not happen on the Ape1 inside closed autophagosomes. By comparing the colocalization of GFP-Atg8 and the Alexa Fluor 647-conjugated second antibody anti-rabbit IgG for Ape1 by immunofluorescence, unclosed autophagosomes will display both red and green colors, and yellow in merge. In contrast, if the autophagosomes are closed, the cargo protein Ape1 inside the GFP-Atg8-labeled autophagosomes cannot be accessed by first antibody rabbit anti-Ape1 and Alexa Fluor 647-conjugated second antibody anti-rabbit IgG, the autophagosomes will only display green color. By observing the colocalization of GFP-Atg8 and Alexa Fluor 647, the autophagosomal membrane structures can be determined to be either closed or unclosed. In Fig. 3.3, with closed autophagosomes isolated from *ypt7Δ* mutant as a control, immunofluorescence combined with GFP-Atg8 showed that the autophagosome-like membrane structures isolated from *snf7Δ* and *snf7Δypt7Δ* mutants are unclosed because the autophagosomal membrane structures are mainly in yellow when the autophagosomal membrane structures isolated from *ypt7Δ* mutant are mainly in green. Furthermore, as the phenotypes in *snf7Δypt7Δ* mutant are similar to these in *snf7Δ* mutant, not to those in *ypt7Δ*

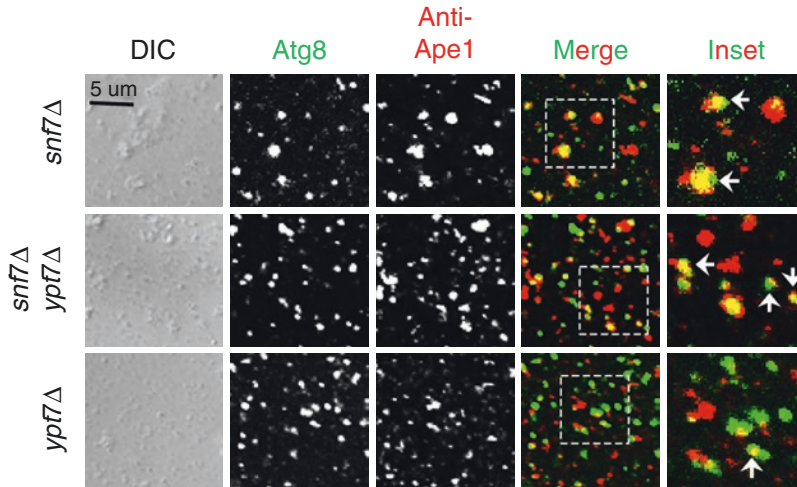


Fig. 3.3 Immunofluorescence combined with GFP-Atg8 tagging showed that the autophagosome membrane-associated structures isolated from *snf7Δ* and *snf7Δypt7Δ* mutants are unclosed autophagosomes. The autophagosome membrane-associated structures isolated from *snf7Δ* and *snf7Δypt7Δ* mutants were displayed with first antibody rabbit anti-Ape1 and second antibody Alexa Fluor 647-conjugated anti-rabbit IgG, representing unclosed autophagosomes. Most of the autophagosome-associated membrane structures isolated from *ypt7Δ* almost cannot be identified with the same first and second antibodies, representing closed autophagosomes. Arrows indicate colocalizations; *DIC* differential interference contrast. The inset pictures indicate the content inside the white dashed frame in merge pictures

mutant, this method also indicates that Snf7 functions upstream of Ypt7 in autophagy. Similar results and more detailed operations were published in our previous paper (Zhou et al. 2019).

3.2.3 The Autophagosome Completion Assay to Determine Phagophore, Nascent Autophagosome, and Mature Autophagosome in Mammalian Cells

In principle, similar to the immunofluorescence microscopy combined with fluorescence tagging we developed above, the lab of Hong-Gang Wang published a HT-LC3 autophagosome completion assay in 2018 to distinguish unclosed and closed phagophores/autophagosomes in mammalian cells (Takahashi et al. 2018). In their method, the authors took advantage of the differential labeling of LC3-II outside and inside autophagosomes by ligand in different colors step by step to distinguish phagophore, nascent autophagosome, and mature autophagosome. The main procedures are: in step 1, autophagy-induced HT-LC3-expressing cells were treated with cholesterol-complexing agents, such as digitonin, to permeabilize the

plasma membrane to release HT-LC-I from the cytosol; in step 2, cells were incubated with a saturating dose of membrane-impermeable Alexa Fluor 488 HT ligand (MIL) to stain membrane-bound HT-LC3-II that is accessible to the cytosol; and in step 3, cells were incubated with a membrane-permeable tetramethylrhodamine HT ligand (MPL) to stain HT-LC3-II sequestered in autophagosomes. After that, the cells were observed with confocal microscope, if the phagophores are only in green color, they are unclosed phagophores; if the phagophores are only in red color, they are closed phagophores, i.e., mature autophagosomes; if the outer layer of a phagophore is only in green color and the inner layer of a phagophore is in red color, that phagophore is closed but immature, i.e., a nascent autophagosome. Through this assay, this research group found that ESCRT-III subunits CHMP2A and AAA-ATPase Vps4 are regulators of phagophore closure in mammalian cells (Takahashi et al. 2018).

3.2.4 The Optogenetic Closure Assay to Distinguish Open and Close Mitophagosomes

During the revision of this manuscript, the Harald Stenmark laboratory in Norway reported a novel optogenetic closure assay for detection of sealed vs open mitophagosomes and found that CHMP2A mediates the closure of mitophagosomes (Zhen et al. 2020). This assay is based on the LOVTRAP system for photoinduced protein dissociation (Wang et al. 2016). The LOVTRAP system takes advantages of the reversible light-sensitive association between the light-oxygen-voltage 2 (LOV2) domain from *Avena sativa* phototropin 1 and the protein A-derived ligand Zdk1 under the 488 nm light. The Stenmark lab fused the N-terminus of the mitochondria outer membrane protein TOMM20 (NTOMM20) with LOV2 and Zdk1 with mCherry to perform the assay. The mitochondria are positive for mCherry because of the association between NTOMM20-LOV2 and cytosolic mCherry-Zdk1. When the cells were exposed to 488 nm wavelength light, the LOV2 domain dissociates from Zdk1, and mCherry-Zdk1 releases from mitochondria to cytosol until the 488 nm light is turned off. The authors reasoned that if mitochondria are enclosed by sealed autophagic membranes, the release of mCherry-Zdk1 into the cytosol should be inhibited. Conversely, if the mitochondria are enclosed by autophagic membranes but unsealed, the release of mCherry-Zdk1 into the cytosol should occur. After confirming the sensitivity and reliability of this assay with control experiments, they found that the proportion of unsealed mitophagosomes in CHMP2A-depleted cells significantly increased, indicating CHMP2A mediates phagophore closure of mitophagosomes (Zhen et al. 2020). This assay can be extended to any organelle inside autophagosomes with organelle-specific protein fusion with LOV2 and compatible fluorescence protein fusion with Zdk1 to determine whether autophagosomes are open or closed in mutants.

Atg proteins change dynamically during the autophagy process, and the compositions of Atg proteins on phagophores and autophagosomes are different. Not like Atg8 existing from the beginning to the end during autophagy, most other Atg proteins, such as Atg2, attach to phagophores and release to be reused after phagophores are closed and mature to be autophagosomes (Noda et al. 2009; Cebollero et al. 2012). If autophagosomes were marked with red fluorescence protein to Atg8 and other Atg proteins were tagged with GFP, at the same time, using a mutant which generated closed mature autophagosomes as a control, then the phagophores/autophagosomes in the target mutant can be determined by observing fluorescence with fluorescence microscopy. If red Atg8 colocalized with green Atgs, then these structures were phagophores or closed immature autophagosomes. If red Atg8 existed and no green Atgs attached to it, just like the fluorescence in the positive control, then the Atg8-marked structures in the target mutant were mature autophagosomes. This method was widely used in yeast and mammalian cells to distinguish or verify whether the autophagosome membrane structures are either phagophores or mature autophagosomes (Cebollero et al. 2012; Takahashi et al. 2018; Zhou et al. 2017, 2019).

3.3 Summary

By using the combination of the above different techniques, we and other groups have determined that Rab5 module proteins and ESCRT complex subunits are regulators for phagophore closure (Takahashi et al. 2018; Zhen et al. 2020; Zhou et al. 2017, 2019), while more experiments are needed to clarify whether some Atg proteins are also required for phagophore closure. However, what's the exact mechanism of these proteins in the regulation of phagophore closure? Till now, we roughly know that Rab5 module regulates the localization of ESCRT subunits on autophagosome and the interactions between Atg protein and ESCRT subunit in yeast, and ESCRT subunits indeed seal unclosed autophagosome in vitro (Zhou et al. 2019). While in mammalian cells, ESCRT-III subunit CHMP2A was recruited to phagophore during autophagy, which further regulates the separation of inner and outer membranes of phagophores to form double-membrane autophagosomes (Takahashi et al. 2018). In addition, CHMP2A also regulates phagophore closure during mitophagy (Zhen et al. 2020). However, the more specific and detailed molecular mechanism of these proteins in phagophore closure remain to be explored.

In addition, are there any other proteins getting involved in phagophore closure? What are the different roles of the same protein or complex from different species in phagophore closure? These are all questions to be answered urgently in the future when studying phagophore closure.

Acknowledgments I thank Janet A. Komduur (Hanze University of Applied Science) for editing this manuscript. This work was supported by grants from the Natural Science Foundation of China (91954125, 31871428).

References

- Cebollero E, van der Vaart A, Zhao M, Rieter E, Klionsky DJ, Helms JB, Reggiori F. Phosphatidylinositol-3-phosphate clearance plays a key role in autophagosome completion. *Curr Biol*. 2012;22:1545–53.
- Chen Y, Zhou F, Zou S, Yu S, Li S, Li D, Song J, Li H, He Z, Hu B, Bjorn LO, Lipatova Z, Liang Y, Xie Z, Segev N. A Vps21 endocytic module regulates autophagy. *Mol Biol Cell*. 2014;25:3166–77.
- Fujita N, Hayashi-Nishino M, Fukumoto H, Omori H, Yamamoto A, Noda T, Yoshimori T. An Atg4B mutant hampers the lipidation of LC3 paralogues and causes defects in autophagosome closure. *Mol Biol Cell*. 2008;19:4651–9.
- Lindqvist LM, Simon AK, Baehrecke EH. Current questions and possible controversies in autophagy. *Cell Death Discov*. 2015;1:15036.
- Nair U, Thumm M, Klionsky DJ, Krick R. GFP-Atg8 protease protection as a tool to monitor autophagosome biogenesis. *Autophagy*. 2011;7:1546–50.
- Nair U, Yen WL, Mari M, Cao Y, Xie Z, Baba M, Reggiori F, Klionsky DJ. A role for Atg8-PE deconjugation in autophagosome biogenesis. *Autophagy*. 2012;8:780–93.
- Nakatogawa H, Ishii J, Asai E, Ohsumi Y. Atg4 recycles inappropriately lipidated Atg8 to promote autophagosome biogenesis. *Autophagy*. 2012;8:177–86.
- Noda T, Fujita N, Yoshimori T. The late stages of autophagy: how does the end begin? *Cell Death Differ*. 2009;16:984–90.
- Sou YS, Waguri S, Iwata J, Ueno T, Fujimura T, Hara T, Sawada N, Yamada A, Mizushima N, Uchiyama Y, Kominami E, Tanaka K, Komatsu M. The Atg8 conjugation system is indispensable for proper development of autophagic isolation membranes in mice. *Mol Biol Cell*. 2008;19:4762–75.
- Suzuki K, Nakamura S, Morimoto M, Fujii K, Noda NN, Inagaki F, Ohsumi Y. Proteomic profiling of autophagosome cargo in *Saccharomyces cerevisiae*. *PLoS One*. 2014;9:e91651.
- Takahashi Y, He H, Tang Z, Hattori T, Liu Y, Young MM, Serfass JM, Chen L, Gebru M, Chen C, Wills CA, Atkinson JM, Chen H, Abraham T, Wang HG. An autophagy assay reveals the ESCRT-III component CHMP2A as a regulator of phagophore closure. *Nat Commun*. 2018;9:2855.
- Tong J, Yan X, Yu L. The late stage of autophagy: cellular events and molecular regulation. *Protein Cell*. 2010;1:907–15.
- Velikkakath AK, Nishimura T, Oita E, Ishihara N, Mizushima N. Mammalian Atg2 proteins are essential for autophagosome formation and important for regulation of size and distribution of lipid droplets. *Mol Biol Cell*. 2012;23:896–909.
- Wang CW, Kim J, Huang WP, Abeliovich H, Stromhaug PE, Dunn WA Jr, Klionsky DJ. Apg2 is a novel protein required for the cytoplasm to vacuole targeting, autophagy, and pexophagy pathways. *J Biol Chem*. 2001;276:30442–51.
- Wang H, Vilela M, Winkler A, Tarnawski M, Schlichting I, Yumerefendi H, Kuhlman B, Liu R, Danuser G, Hahn KM. LOVTRAP: an optogenetic system for photoinduced protein dissociation. *Nat Methods*. 2016;13:755–8.
- Yang S, Rosenwald AG. Autophagy in *Saccharomyces cerevisiae* requires the monomeric GTP-binding proteins, Arl1 and Ypt6. *Autophagy*. 2016;12:1721–37.
- Yu ZQ, Ni T, Hong B, Wang HY, Jiang FJ, Zou S, Chen Y, Zheng XL, Klionsky DJ, Liang Y, Xie Z. Dual roles of Atg8-PE deconjugation by Atg4 in autophagy. *Autophagy*. 2012;8:883–92.
- Zhen Y, Spangenberg H, Munson MJ, Brech A, Schink KO, Tan KW, Sorensen V, Wenzel EM, Radulovic M, Engedal N, Simonsen A, Raiborg C, Stenmark H. ESCRT-mediated phagophore sealing during mitophagy. *Autophagy*. 2020;16(5):826–41.
- Zhou F, Zou S, Chen Y, Lipatova Z, Sun D, Zhu X, Li R, Wu Z, You W, Cong X, Zhou Y, Xie Z, Gyurkovska V, Liu Y, Li Q, Li W, Cheng J, Liang Y, Segev N. A Rab5 GTPase module is important for autophagosome closure. *PLoS Genet*. 2017;13:e1007020.
- Zhou F, Wu Z, Zhao M, Murtazina R, Cai J, Zhang A, Li R, Sun D, Li W, Zhao L, Li Q, Zhu J, Cong X, Zhou Y, Xie Z, Gyurkovska V, Li L, Huang X, Xue Y, Chen L, Xu H, Liang Y, Segev N. Rab5-dependent autophagosome closure by ESCRT. *J Cell Biol*. 2019;218(6):1908–27.

Chapter 4

The Fusion Between Autophagic Vesicles and Lysosomes



Xiaoxia Liu and Qing Zhong

Abstract The autophagosome delivers engulfed substrates to the lysosome for degradation via membrane fusion between the autophagosome and the lysosome. The process of membrane fusion is highly conserved in evolution. It is widely accepted that membrane fusion in general is driven by the zippering of the SNARE complex to form a four-helix bundle. Besides SNAREs, other proteins are required to complete fusion efficiently, including tethering proteins, Rab GTPases, and SM proteins (Sec1/SM family proteins). This chapter will summarize the current knowledge of the key machinery involved in autophagosome-lysosome fusion, including autophagic SNAREs, involved ATG proteins, the HOPS complex, Rab GTPase, and other relevant aspects.

4.1 Autophagosome-Lysosome Fusion

As clarified in the previous chapter, once an autophagophore is closed and matured into autophagosomes, the autophagic process moves into the next step, which is the fusion between autophagosomes and lysosomes. To accomplish this fusion, first the double-membraned autophagosome is tethered to single-membrane lysosomes; then the outer membrane of the autophagosome fuses with the lysosome membranes; and finally, the inner membrane of the autophagosome is hydrolyzed by lysozyme, and the autophagosomal contents are degraded. The process of membrane fusion is highly conserved in evolution. It is widely accepted that membrane fusion in general is driven by the zippering of the SNARE complex to form a four-helix bundle. However, SNARE proteins alone are not enough to complete the process efficiently. Other proteins are required to promote this fusion process, including tethering proteins like Rab GTPase, SM proteins (Sec1/SM family proteins), and others (Wickner

X. Liu · Q. Zhong (✉)

Key Laboratory of Cell Differentiation and Apoptosis of Chinese Ministry of Education, Department of Pathophysiology, Shanghai Jiao Tong University School of Medicine, Shanghai, China

e-mail: xxliu@shsmu.edu.cn; qingzhong@shsmu.edu.cn

© Science Press 2021

Z. Xie (ed.), *Autophagy: Biology and Diseases*, Advances in Experimental Medicine and Biology 1208, https://doi.org/10.1007/978-981-16-2830-6_4

55

and Rizo 2017). Even though a lot of scientists are dedicated to the elucidation of the membrane fusion mechanism between autophagosomes and lysosomes in mammalian cells, our understanding of how these proteins are recruited and regulated and how they are cooperating to facilitate fusion is still limited. This chapter will summarize the current knowledge of the key proteins involved in this fusion step.

4.1.1 SNARE Proteins

SNAREs (soluble *N*-ethylmaleimide-sensitive fusion attachment protein receptors) are membrane proteins. All SNARE proteins contain evolutionarily conserved coiled-coil SNARE motifs (Fig. 4.1a). According to the amino acid that is present in the zero ionic layer of the SNARE domain, SNARE proteins are divided into R-SNAREs (with arginine in the zero ionic layer) and Q-SNAREs (with glutamine in the zero ionic layer) (Fasshauer et al. 1998). There are three Q-SNARE families: Qa, Qb, and Qc. The SNARE complex is formed by a four-helix bundle, including R, Qa, Qb, and Qc (Fig. 4.1b). When all the SNARE protein constituents are anchored to one membrane, the complex is called a *cis*-SNARE complex; otherwise, when the proteins are anchored to two separate membranes, it is called a *trans*-SNARE complex (Fig. 4.1c). Usually, SNARE proteins can form a four-helix bundle by spontaneously zipping from the N-terminal to the C-terminal of the SNARE domain. During this process, the *trans*-SNARE complex pulls and distorts the two membranes on which the proteins are anchored. With the help of other proteins, the membrane lipids are reorganized, and the membranes are eventually fused. After the completion of this fusion, the (now *cis*-) SNARE complex can be hydrolyzed by NSF (*N*-ethylmaleimide-sensitive factor)/ α SNAP. The disassociated SNARE proteins can be reused for the next cycle of fusion (Zhao et al. 2015).

The sets of SNAREs that are available vary between species. Also, the fusion between various membrane structures is regulated by distinctive sets of SNAREs. According to previous studies, in mammalian cells, the fusion between autophagosomes and lysosomes is regulated by STX17 (containing Qa-SNARE domain) and SNAP29 (including both Qb- and Qc-SNARE domains) on autophagosomes and VAMP8 (R-SNARE) on lysosomes (EisukeItakura and Mizushima 2012) (Fig. 4.1a, b). STX17 is recruited to the autophagosomal membrane when an autophagopore is about to close or is already closed (Tsuboyama et al. 2016). However, when SNAP29 and VAMP8 are recruited is still unknown. From an X-ray structure of the STX17-SNAP29-VAMP8 complex, it could be concluded that the three SNARE proteins form a four-helix bundle (Diao et al. 2015). This corresponds to established events in other membrane fusion processes, including for instance the well-described neuronal SNARE complex regulating the fusion between synaptic vesicles and the pre-synaptic membrane and the SNARE complex regulating vacuole fusion in yeast.

Just as in other recognized mechanisms of membrane fusion, *in vitro* reconstitution experiments show that the STX17-SNAP29-VAMP8 complex alone is not enough to drive an efficient fusion. This suggests the requirement of other factors,

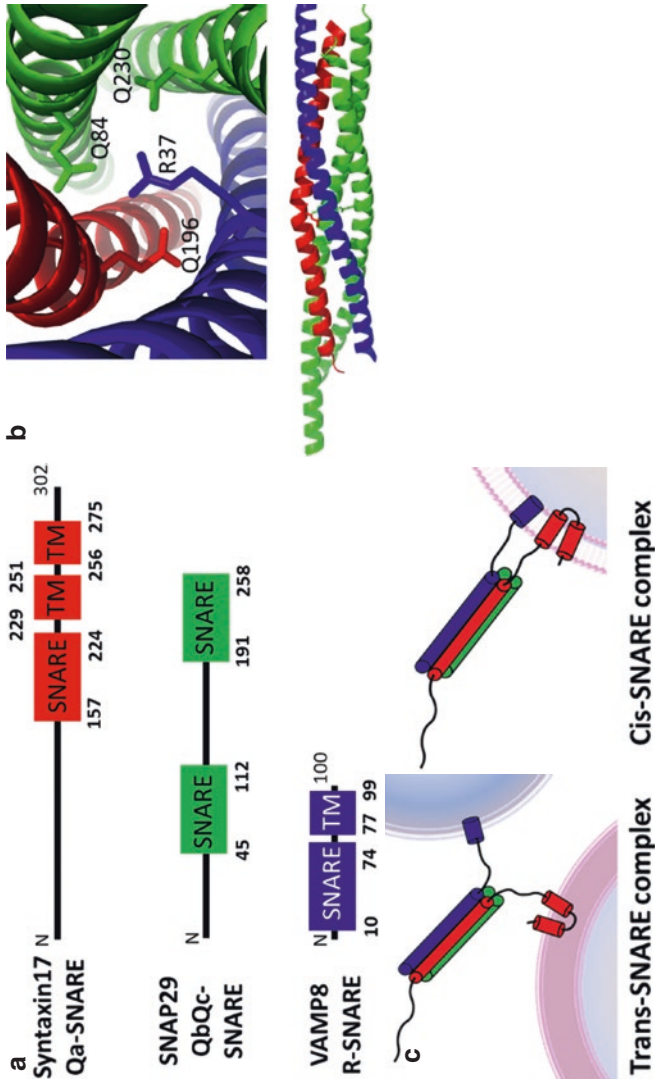


Fig. 4.1 (a) The positions of the SNARE domains in STX17, SNAP29, and VAMP8. (b) Crystal structure (PDB code 4WY4) of the autophagic SNARE complex containing STX17 (red), SNAP29 (green), and VAMP8 (blue). (c) A schematic representation of a *trans*-SNARE and *cis*-SNARE complex

like tethering proteins, Rab GTPase, SM proteins, or others. An example of such a supplementary factor is the tethering protein ATG14. The previous study has demonstrated that ATG14 is able to promote the fusion between autophagosomes and lysosomes driven by STX17-SNAP29-VAMP8 (Diao et al. 2015).

Another interesting fact is that O-GlcNAcylation of SNAP29 can regulate the fusion between autophagosome and lysosome. Also, it has been demonstrated that a knockdown of OGT (O-GlcNAc transferase) and a mutation in the O-GlcNAc-modification site of SNAP29 are able to promote the formation of the SANP29 containing SNARE complex and the fusion between autophagosomes and lysosomes (Guo et al. 2014).

It is also worth mentioning that in STX17 knockout cells, the autophagosome-lysosome fusion is, to some extent, retained. This suggests the involvement of other SNARE proteins in this process. A recent study showed that YKT6 can bind to autophagosomes through its N-terminal longin domain. Together with SNAP29 and lysosomal STX7, a YKT6-SNAP29-STX7 complex can be formed, which drives the fusion between autophagosomes and lysosomes. It was demonstrated that this fusion function is independent from STX17 (Matsui et al. 2018).

4.1.2 Membrane Tethering Factors

Membrane tethering factors can promote membrane fusion by bringing two membranes in close proximity to each other. In some cases, they are also involved in helping in the assembly of the SNARE complex. Membrane tethering factors that have been studied thoroughly are HOPS, ATG14, and Rab GTPase. These factors will be described in the following paragraphs, together with some other, less examined, components.

4.1.2.1 The HOPS Complex

The HOPS complex (homotypic fusion and vacuole protein sorting complex) was found during the study of yeast vacuole fusion. There are six subunits in the HOPS complex, including Vps11, Vps16, Vps18, Vps33, Vps39, and Vps41 (Nakamura et al. 1997; Seals et al. 2000). Cryo-EM structures of the HOPS complex in yeast show that it has a seahorse-like shape with flexible head and tail regions (Fig. 4.2a) (Brocker et al. 2012). In yeast vacuole fusion, Vps39 and Vps41, located on the two ends of the HOPS complex, are able to bind the Rab GTPase Ypt7 from two separate vacuole membranes. This induces the tethering of these two vacuoles. In mammalian cells, the HOPS complex bridges autophagosomes and lysosomes in a more complicated way. So far it's found that HOPS can be recruited to the Rab7 (the homologue of yeast Ypt7)-attached lysosomes through the binding between Vps41 and Rab7 effector protein PLEKHM1 (Pleckstrin homology domain-containing protein) or the binding between Vps39 and another Rab7 effector protein RILP

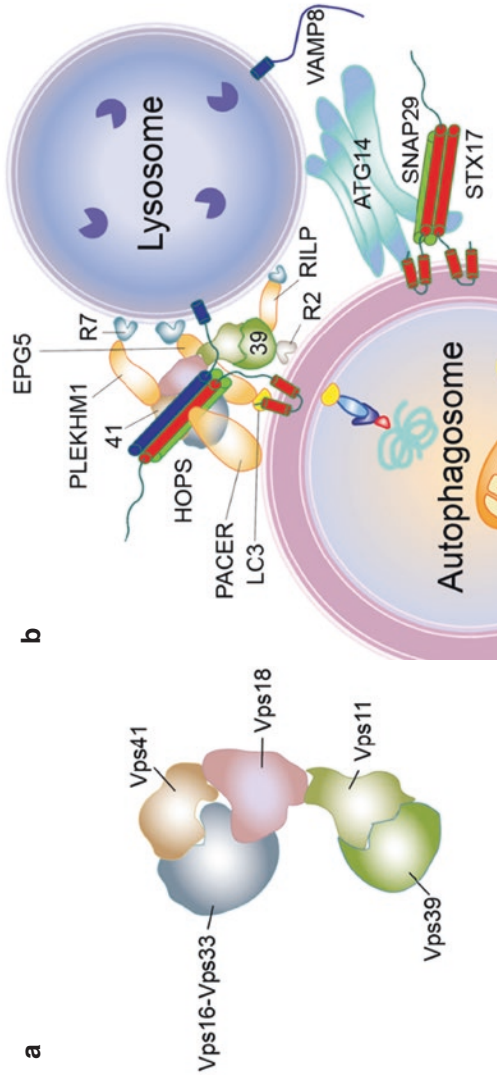


Fig. 4.2 (a) The organization of the HOPS complex (figure cited from (Brocker et al. 2012)). (b) A possible interaction model of SNAREs, HOPS (Vps39 and Vps41 are labeled as 39 and 41), Rab2 (labeled as R2), PLEKHM1, RILP, PACER, EPG5, LC3, and ATG14 in the membrane fusion step between autophagosomes and lysosomes

(Rab-interacting lysosomal protein) (McEwan et al. 2015). On the other hand, HOPS can tether autophagosomes through the binding with STX17 and PACER (protein associated with UVRAG as autophagy enhancer) on autophagosomes. It is possible that PACER enhances the binding between the HOPS complex and STX17 or that PACER, HOPS, and STX17 form a stable complex, to recruit the HOPS complex to autophagosomes and to promote the fusion between autophagosomes and lysosomes (Cheng et al. 2017). Furthermore, the HOPS complex can be recruited to autophagosomes via Rab2. More details about this last mechanism are covered in the following paragraph, about Rab GTPase (Fig. 4.2b).

It is worth noting that one of the HOPS subunits, Vps33, is a SM protein (Sec1/Munc18 protein). It is well known that SNARE complex assembly is the core machinery of membrane fusion. However, the assembly efficiency is not high enough when SNARE proteins are present alone. In a recent study about yeast vacuole fusion, it was found that Vps33 could help in the assembly of the SNARE complex. By overlapping the X-ray complex structures of Vps33-Nyv1 (R-SNARE in yeast) and Vps33-Vam3 (Qa-SNARE in yeast), Nyv1 and Vam3 are observed to register in the correct position for assembling on the Vps33 platform. This suggests that Vps33 and other SM proteins might provide a platform for SNARE assembly (Baker et al. 2015). Even though this hypothesis is not tested in the mammalian cell, there are some hints that Vps33 in mammalian HOPS might have the same function in autophagosome-lysosome fusion. Previous studies showed that Vps33 is able to co-IP with STX17, SNAP29, and VAMP8 (Jiang et al. 2014; Zhen and Li 2015). So the HOPS complex might be able to assist in the assembly of the SNARE complex for the fusion between autophagosomes and lysosomes in mammalian cells. More direct evidence is needed.

Recent studies demonstrated that, besides playing an important role in the tethering of membranes, the HOPS complex has another important function. The HOPS complex is able to promote pore formation during membrane fusion, mainly because of its huge volume (D'Agostino et al. 2017). Pore formation is a speed-limiting step between the hemi-fused state and fully fused state during membrane fusion, which requires a lot of energy. The big HOPS complex (~663 kDa) increases the volume of the SNARE complex, distorts the anchored membranes in the hemi-fusion state, and lowers the energy barrier, which is needed for the formation of the fusion pore in order to promote fusion. The study also proposed that this function of HOPS is conserved in all membrane fusion pathways, which of course includes the fusion between autophagosomes and lysosomes.

4.1.2.2 Rab GTPase

Rab GTPases form a branch of the Ras superfamily. The Ras superfamily is highly conserved in evolution. Rab GTPases play important roles in membrane trafficking. Rab GTPase can switch between the active GTP-bound form and the inactive GDP-bound form (Langemeyer et al. 2018). The function of Rab GTPase is regulated by three important proteins, GAP (GTPase-activating protein), GEF (guanine nucleotide exchange factor), and GDI (GDP dissociation inhibitor). Rab GTPase can be

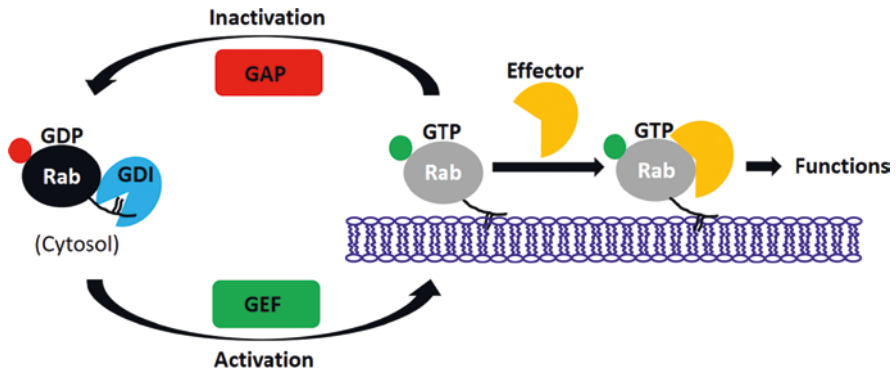


Fig. 4.3 The general model of Rab GTPase activation and inactivation

prenylated on its C-terminal tail and stay in the cytosol through binding with a GDI protein. With the help of GEF, the GDP moiety in Rab GTPase can be switched to GTP. This makes Rab GTPase stably anchored on the membrane and become active to perform its function via the binding of effector proteins. For example, once activated, Rab GTPases can bind cargo adaptors to form transport vesicles, bind motor proteins to transfer vesicles to their target membrane, or bind tethering proteins to promote the fusion between vesicles. At a certain point, bound GTP can be hydrolyzed into GDP by GAP, which makes Rab GTPase lose the binding ability with its effector proteins and become inactive. When needed, Rab-GDP can be activated by GEF again (Fig. 4.3).

So far, the most widely studied Rab GTPases involved in autophagosome-lysosome fusion are Rab7 and Rab2.

The effector proteins of Rab7 include the HOPS complex, PLEKHM1, RILP, EPG5 (ectopic P granules protein 5), and some additional proteins. The PLEKHM1 and RILP were discussed above. EPG5 can be recruited to lysosomes through the binding with Rab7 and VAMP8. On the other hand, EPG5 can interact with LC3 and the STX17-SNAP29 complex on autophagosomes (Fig. 4.2b). Besides, EPG5 is able to stabilize the STX17-SNAP29-VAMP8 *trans*-SNARE complex and to promote the fusion between autophagosomes and lysosomes (Wang et al. 2016).

Rab2 was found to promote membrane fusion in experiments using the *Drosophila melanogaster* model. As a Golgi-resident protein, Rab2 is important for vesicle trafficking from the Golgi. Rab2 is transported on Golgi-derived vesicles to fuse with Rab7-coated autophagosomes, late endosomes, amphisomes, or auto/endolysosomes (Lorincz et al. 2017). In this process, GTP-loaded Rab2 binds to VPS39 in the HOPS complex (Gillingham et al. 2014), while Rab7 binds to VPS41 on the other end of the HOPS complex via PLEKHM1. In this way, Rab2 cooperates with Rab7 to promote the fusion (Fig. 4.2b). In another study, Rab2 was found to locate on autophagosomes and to bind with the HOPS complex, which indicates that Rab2 joins in the autophagosome-lysosome fusion (Fujita et al. 2017).. So far it was found that human Rab2 can co-IP with both VPS39 (Kajiho et al. 2016) and VPS41 (Ding et al. 2019).

4.1.2.3 ATG14

ATG14 is also called Barkor or ATG14L (Sun et al. 2008). In early studies, it was found that ATG14 can regulate the activity of PI3KC3 (class III phosphatidylinositol-3-kinase) and plays an important role in the initiation and extension of autophagosomes (Itakura et al. 2008; Zhong et al. 2009; Matsunaga et al. 2009). ATG14 can sense the membrane curvature by its C-terminal BAT domain [Barkor/Atg14(L) autophagosome-targeting sequence] (Fan et al. 2011). Recently, it was found that ATG14 is also located on mature autophagosomes. It was demonstrated that ATG14 is able to assist STX17 to recruit SNAP29 to autophagosomes in order to promote the assembly of the STX17-SNAP29 complex, and also to tether autophagosomes to lysosomes to promote fusion driven by the STX17-SNAP29-VAMP8 complex (Fig. 4.2b) (Diao et al. 2015). This tethering ability of ATG14 relies on a Cys43/Cys46-dependent self-oligomerization. However, this tethering function is nonspecific, because ATG14 is able to bridge two naked vesicles without SNARE proteins. So far there is very limited knowledge about how other proteins, for example, the HOPS complex, cooperate with ATG14 to regulate this fusion. More research is needed.

4.1.2.4 Other Proteins Involved in the Autophagosome-Lysosome Fusion

In the previous chapter, LC3 (ATG8 in yeast) was mentioned as an important factor in the formation of autophagosomes. There are two forms of LC3, namely, LC3-I and LC3-II. The cytosolic form LC3-I can be switched to the membrane-bound form LC3-II by a truncation process. In this form, LC3 is conjugated to a membrane-resident PE lipid molecule (phosphatidylethanolamine). Recent study showed that the phosphorylation of LC3 also regulates the fusion between autophagosomes and lysosomes. The Thr50 of LC3 can be phosphorylated by Hippo Kinase STK3/STK4. The fusion between autophagosomes and lysosomes is inhibited in the absence of a phosphorylated Thr50. In STK3/STK4 knockout cells, the fusion and autophagy flux can be rescued with a mutation in LC3T50E, which mimics the phosphorylated threonine. Besides, this study proposed that this regulation function of LC3 through phosphorylation is conserved in a variety of species (Wilkinson et al. 2015).

4.1.3 Lipids

PI (phosphoinositides) play an important role in many cellular processes including membrane identity, cell signaling, membrane trafficking, and other processes. The three, four, and five hydroxyl groups of the inositol ring can be phosphorylated by a variety of kinases in different combinations (Fig. 4.4). For example, Vps34 can phosphorylate PI to generate PI3P on omegasomes, which can recruit the PI3P

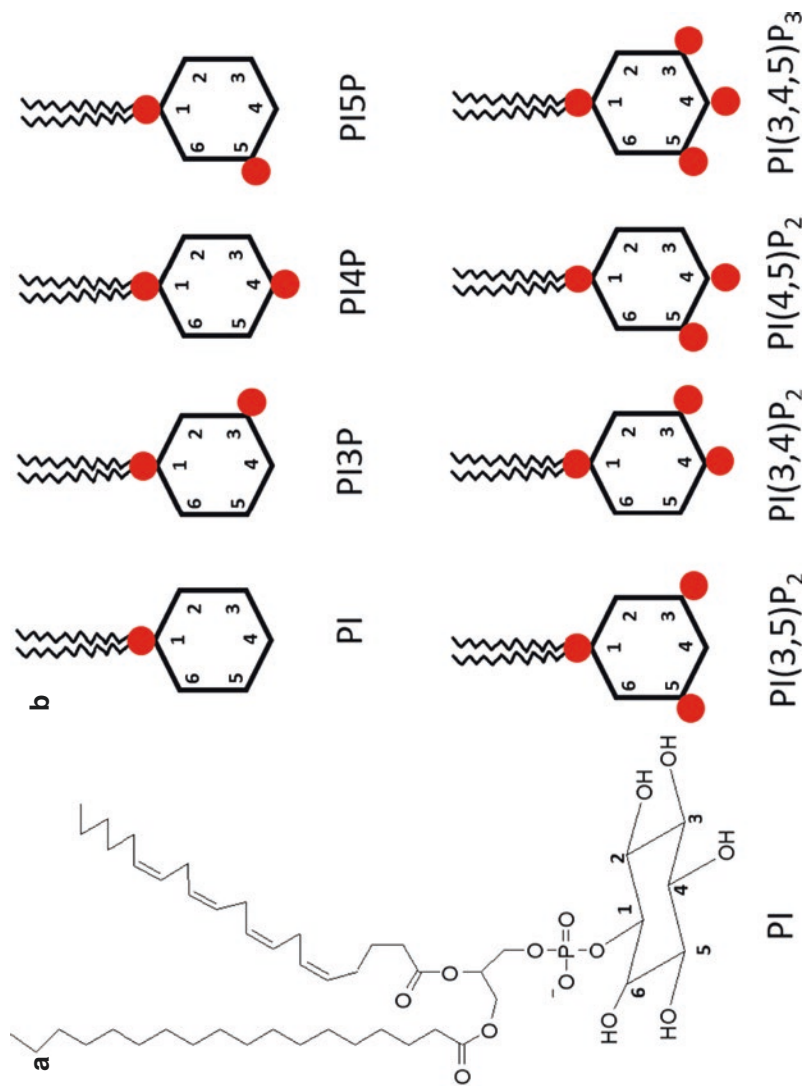


Fig. 4.4 (a) The structure of PI. (b) A schematic view of several PI analogues

effector proteins WIPI2 (WD repeat domain phosphoinositide-interacting protein 2) and DFCP1 (double FYVE-containing protein 1) to the omegasomes. This is important for the recruitment of ATG proteins and the extension of autophagopores.

So far, PI3P, PI4P, and PI(3,5)P₂ have been shown to participate in the fusion between autophagosomes and lysosomes. PI(3,5)P₂ can be dephosphorylated into PI3P by INPPE (inositol polyphosphate-5-phosphatase E), which results in a low concentration of PI(3,5)P₂ on lysosomes. PI(3,5)P₂ can interact with CCTN protein to prevent it from binding with actin. However, once the concentration of PI(3,5)P₂ decreased on the lysosome, CTTN is able to bind with actin and stabilize the actin filament to promote autophagosome-lysosome fusion (Nakamura et al. 2016). Furthermore, other studies found that PI3P can participate in autophagosome-lysosome fusion mediated by TECPR1-ATG5-ATG12 (Chen et al. 2012), and PI4P, generated by PI4K2A/PI4KII α , is also important for this fusion process (Wang et al. 2015).

4.2 Amphisome-Lysosome Fusion

Autophagosomes can fuse with late endosomes to form amphisomes, which can fuse with lysosomes later (Gordon and Seglen 1988; Berg et al. 1998). So far there has been very little research about the fusion mechanism between amphisomes and lysosomes.

It was reported that in the endocytic pathway in K562 cells, Rab11 is associated with MVB (endosomal multivesicular bodies). Some MVB can fuse with the plasma membrane to release their content into the extracellular medium. These intraluminal vesicles are termed exosomes. Upon the induction of starvation, some Rab11-positive MVB fuse with autophagosomes to form amphisomes, which can finally fuse with lysosomes in a Rab7-dependent way (Fader et al. 2008).

Another study pointed out that STX6-VTI1B-VAMP3 can regulate fusion between autophagosome and recycling endosomes to facilitate xenophagy (Nozawa et al. 2017).

4.3 Autophagosome-Plasma Membrane Fusion

Proteins that lack an N-terminal secretion signal are not able to be trafficked through the ER and Golgi, so they are secreted in an unconventional manner, for example, via secretory autophagy. In contrast to degradative autophagy, in secretory autophagy, autophagosomes do not fuse with lysosomes to degrade the engulfed content but fuse with the plasma membrane for secretion/expulsion of the cytoplasmic constituents. It was found that in the secretion of interleukin-1 β , Sec22b on autophagosomes together with STX3/STX4 and SNAP23/SNAP29 on plasma membrane drives the fusion between autophagosomes and the plasma membrane (Kimura et al. 2017). Rab8a is also important for this process. Also, it is worth mentioning

that, in secretory autophagy, autophagosomes can fuse with MVB to form amphisomes before fusion with the plasma membrane (Ponpuak et al. 2015).

References

- Baker RW, et al. A direct role for the Sec1/Munc18-family protein Vps33 as a template for SNARE assembly. *Science (New York, NY)*. 2015;349:1111–4. <https://doi.org/10.1126/science.aac7906>.
- Berg TO, Fengsrud M, Strømhaug PE, Berg T, Seglen PO. Isolation and characterization of rat liver amphisomes. Evidence for fusion of autophagosomes with both early and late endosomes. *J Biol Chem*. 1998;273:21883–92.
- Brockner C, et al. Molecular architecture of the multisubunit homotypic fusion and vacuole protein sorting (HOPS) tethering complex. *Proc Natl Acad Sci U S A*. 2012;109:1991–6. <https://doi.org/10.1073/pnas.1117797109>.
- Chen D, et al. A mammalian autophagosome maturation mechanism mediated by TECPR1 and the Atg12-Atg5 conjugate. *Mol Cell*. 2012;45:629–41. <https://doi.org/10.1016/j.molcel.2011.12.036>.
- Cheng X, et al. Pacer mediates the function of class III PI3K and HOPS complexes in autophagosome maturation by engaging Stx17. *Mol Cell*. 2017;65:1029–1043.e5. <https://doi.org/10.1016/j.molcel.2017.02.010>.
- D'Agostino M, Risselada HJ, Lurick A, Ungermann C, Mayer A. A tethering complex drives the terminal stage of SNARE-dependent membrane fusion. *Nature*. 2017;551:634–8. <https://doi.org/10.1038/nature24469>.
- Diao J, et al. ATG14 promotes membrane tethering and fusion of autophagosomes to endolysosomes. *Nature*. 2015;520:563–6. <https://doi.org/10.1038/nature14147>.
- Ding X, et al. RAB2 regulates the formation of autophagosome and autolysosome in mammalian cells. *Autophagy*. 2019;15(10):1774–86. <https://doi.org/10.1080/15548627.2019.1596478>.
- Eisukeltakura C-I, Mizushima N. The hairpin-type tail-anchored SNARE syntaxin 17 targets to autophagosomes for fusion with endosomes lysosomes. *Cell*. 2012;151:1256–69.
- Fader CM, Sanchez D, Furlan M, Colombo MI. Induction of autophagy promotes fusion of multivesicular bodies with autophagic vacuoles in k562 cells. *Traffic*. 2008;9:230–50. <https://doi.org/10.1111/j.1600-0854.2007.00677.x>.
- Fan W, Nassiri A, Zhong Q. Autophagosome targeting and membrane curvature sensing by Barkor/Atg14(L). *Proc Natl Acad Sci U S A*. 2011;108:7769–74. <https://doi.org/10.1073/pnas.1016472108>.
- Fasshauer D, Sutton RB, Brunger AT, Jahn R. Conserved structural features of the synaptic fusion complex: SNARE proteins reclassified as Q- and R-SNAREs. *Proc Natl Acad Sci U S A*. 1998;95:15781–6.
- Fujita N, et al. Genetic screen in *Drosophila* muscle identifies autophagy-mediated T-tubule remodeling and a Rab2 role in autophagy. *Elife*. 2017;6:e23367. <https://doi.org/10.7554/eLife.23367>.
- Gillingham AK, Sinka R, Torres IL, Lilley KS, Munro S. Toward a comprehensive map of the effectors of Rab GTPases. *Dev Cell*. 2014;31:358–73. <https://doi.org/10.1016/j.devcel.2014.10.007>.
- Gordon PB, Seglen PO. Prelysosomal convergence of autophagic and endocytic pathways. *Biochem Biophys Res Commun*. 1988;151:40–7.
- Guo B, et al. O-GlcNAc-modification of SNAP-29 regulates autophagosome maturation. *Nat Cell Biol*. 2014;16:1215–26. <https://doi.org/10.1038/ncb3066>.
- Itakura E, Kishi C, Inoue K, Mizushima N. Beclin 1 forms two distinct phosphatidylinositol 3-kinase complexes with mammalian Atg14 and UVRAG. *Mol Biol Cell*. 2008;19:5360–72. <https://doi.org/10.1091/mbc.E08-01-0080>.
- Jiang P, et al. The HOPS complex mediates autophagosome-lysosome fusion through interaction with syntaxin 17. *Mol Biol Cell*. 2014;25:1327–37. <https://doi.org/10.1091/mbc.E13-08-0447>.

- Kajiho H, et al. RAB2A controls MT1-MMP endocytic and E-cadherin polarized Golgi trafficking to promote invasive breast cancer programs. *EMBO Rep.* 2016;17:1061–80. <https://doi.org/10.15252/embr.201642032>.
- Kimura T, et al. Cellular and molecular mechanism for secretory autophagy. *Autophagy.* 2017;13:1084–5. <https://doi.org/10.1080/15548627.2017.1307486>.
- Langemeyer L, Frohlich F, Ungermann C. Rab GTPase function in endosome and lysosome biogenesis. *Trends Cell Biol.* 2018;28:957–70. <https://doi.org/10.1016/j.tcb.2018.06.007>.
- Lorincz P, et al. Rab2 promotes autophagic and endocytic lysosomal degradation. *J Cell Biol.* 2017;216:1937–47. <https://doi.org/10.1083/jcb.201611027>.
- Matsui T, et al. Autophagosomal YKT6 is required for fusion with lysosomes independently of syntaxin 17. *J Cell Biol.* 2018;217:2633–45. <https://doi.org/10.1083/jcb.201712058>.
- Matsunaga K, et al. Two Beclin 1-binding proteins, Atg14L and Rubicon, reciprocally regulate autophagy at different stages. *Nat Cell Biol.* 2009;11:385–96. <https://doi.org/10.1038/ncb1846>.
- McEwan DG, et al. PLEKHM1 regulates autophagosome-lysosome fusion through HOPS complex and LC3/GABARAP proteins. *Mol Cell.* 2015;57:39–54. <https://doi.org/10.1016/j.molcel.2014.11.006>.
- Nakamura N, Hirata A, Ohsumi Y, Wada Y. Vam2/Vps41p and Vam6/Vps39p are components of a protein complex on the vacuolar membranes and involved in the vacuolar assembly in the yeast *Saccharomyces cerevisiae*. *J Biol Chem.* 1997;272:11344–9.
- Nakamura S, Hasegawa J, Yoshimori T. Regulation of lysosomal phosphoinositide balance by INPP5E is essential for autophagosome-lysosome fusion. *Autophagy.* 2016;12:2500–1. <https://doi.org/10.1080/15548627.2016.1234568>.
- Nozawa T, Minowa-Nozawa A, Aikawa C, Nakagawa I. The STX6-VTI1B-VAMP3 complex facilitates xenophagy by regulating the fusion between recycling endosomes and autophagosomes. *Autophagy.* 2017;13:57–69. <https://doi.org/10.1080/15548627.2016.1241924>.
- Ponpuak M, et al. Secretory autophagy. *Curr Opin Cell Biol.* 2015;35:106–16. <https://doi.org/10.1016/j.ccb.2015.04.016>.
- Seals DF, Eitzen G, Margolis N, Wickner WT, Price A. A Ypt/Rab effector complex containing the Sec1 homolog Vps33p is required for homotypic vacuole fusion. *Proc Natl Acad Sci U S A.* 2000;97:9402–7.
- Sun Q, Fan W, Chen K, Ding X, Chen S, Zhong Q. Identification of Barkor as a mammalian autophagy-specific factor for Beclin 1 and class III phosphatidylinositol 3-kinase. *Proc Natl Acad Sci U S A.* 2008;105:19211–6.
- Tsuboyama K, et al. The ATG conjugation systems are important for degradation of the inner autophagosomal membrane. *Science (New York, NY).* 2016;354:1036–41. <https://doi.org/10.1126/science.aaf6136>.
- Wang H, et al. GABARAPs regulate PI4P-dependent autophagosome:lysosome fusion. *Proc Natl Acad Sci U S A.* 2015;112:7015–20. <https://doi.org/10.1073/pnas.1507263112>.
- Wang Z, et al. The Vici syndrome protein EPG5 is a Rab7 effector that determines the fusion specificity of autophagosomes with late endosomes/lysosomes. *Mol Cell.* 2016;63:781–95. <https://doi.org/10.1016/j.molcel.2016.08.021>.
- Wickner W, Rizo J. A cascade of multiple proteins and lipids catalyzes membrane fusion. *Mol Biol Cell.* 2017;28:707–11. <https://doi.org/10.1091/mbc.E16-07-0517>.
- Wilkinson DS, et al. Phosphorylation of LC3 by the Hippo kinases STK3/STK4 is essential for autophagy. *Mol Cell.* 2015;57:55–68. <https://doi.org/10.1016/j.molcel.2014.11.019>.
- Zhao M, et al. Mechanistic insights into the recycling machine of the SNARE complex. *Nature.* 2015;518:61–7. <https://doi.org/10.1038/nature14148>.
- Zhen Y, Li W. Impairment of autophagosome-lysosome fusion in the buff mutant mice with the VPS33A(D251E) mutation. *Autophagy.* 2015;11:1608–22. <https://doi.org/10.1080/15548627.2015.1072669>.
- Zhong Y, et al. Distinct regulation of autophagic activity by Atg14L and Rubicon associated with Beclin 1-phosphatidylinositol-3-kinase complex. *Nat Cell Biol.* 2009;11:468–76. <https://doi.org/10.1038/ncb1854>.

Chapter 5

Autophagosome Trafficking



Jingjing Ye and Ming Zheng

Abstract Autophagy is a major intracellular degradation/recycling system that ubiquitously exists in eukaryotic cells. Autophagy contributes to the turnover of cellular components through engulfing portions of the cytoplasm or organelles and delivering them to the lysosomes/vacuole to be degraded. The trafficking of autophagosomes and their fusion with lysosomes are important steps that complete their maturation and degradation. In cells such as neuron, autophagosomes traffic long distances along the axon, while in other specialized cells such as cardiomyocytes, it is unclear how and even whether autophagosomes are transported. Therefore, it is important to learn more about the processes and mechanisms of autophagosome trafficking to lysosomes/vacuole during autophagy. The mechanisms of autophagosome trafficking are similar to those of other organelles trafficking within cells. The machinery mainly includes cytoskeletal systems such as actin and microtubules, motor proteins such as myosins and the dynein-dynactin complex, and other proteins like LC3 on the membrane of autophagosomes. Factors regulating autophagosome trafficking have not been widely studied. To date the main reagents identified for disrupting autophagosome trafficking include:

1. Microtubule polymerization reagents, which disrupt microtubules by interfering with microtubule dynamics, thus directly influence microtubule-dependent autophagosome trafficking
2. F-actin-depolymerizing drugs, which inhibit autophagosome formation, and also subsequently inhibit autophagosome trafficking
3. Motor protein regulators, which directly affect autophagosome trafficking

J. Ye · M. Zheng (✉)

Department of Physiology and Pathophysiology, Peking University Health Science Center, Beijing, China

e-mail: zhengm@bjmu.edu.cn

© Science Press 2021

Z. Xie (ed.), *Autophagy: Biology and Diseases*, Advances in Experimental Medicine and Biology 1208, https://doi.org/10.1007/978-981-16-2830-6_5

Abbreviations

Atg	Autophagy-related gene
CMA	Chaperone-mediated autophagy
GAP	GTPase activation protein
GFP	Green fluorescent protein
JIP1	JNK-interacting protein 1
LC3	Microtubule-associated protein light chain 3
LSD	Lysosomal storage disorders
mTOR	Mammalian target of rapamycin
MYO1C	Myosin IC
MYO6	Myosin VI
NMM2A	Non-muscle myosin IIA
PAS	Phagophore assembly site
PI3K	Phosphatidylinositol 3-kinase
Rab	Ras-related protein in the brain
TGN	<i>Trans</i> -Golgi network
ULK1	UNC51-like kinase
VAMP	Vesicle-associated membrane protein

Autophagy is a major intracellular degradation/recycling system ubiquitous in eukaryotic cells. Autophagy contributes to the turnover of cellular components by engulfing portions of the cytoplasm or organelles and delivering them to the lysosomes/vacuole to be degraded. *Autophagy has been increasingly recognized as essential for cells to maintain homeostasis and is also a conserved mechanism for organisms to adapt to the external environment by recycling their own nutrients.*

There are various types of autophagy, which can be classified according to numerous criteria. In terms of the pathways involved, autophagy can be subdivided into three main categories: macroautophagy, microautophagy, and chaperone-mediated autophagy. Autophagy can also be classified as selective autophagy or nonselective autophagy according to whether or not there is a specific choice of autophagic substrates. Furthermore, autophagy can be classified in terms of cellular purpose as either cellular quality control or nutrient recycling. In macroautophagy, cargo is sequestered into a double-membrane vesicle derived from non-lysosome organelles, termed the autophagosome, which subsequently fuses with an endosome or lysosome or the vacuole. Microautophagy involves the direct engulfment of cargo at the lysosome/vacuole surface by invagination, or protrusion and separation of the lysosome/vacuole. Chaperone-mediated autophagy (CMA) is the process whereby specific amino acid sequences are recognized by chaperones, causing the proteins to be unfolded, transported into the lysosome, and degraded.

Macroautophagy, hereafter simply referred to as autophagy, is mediated by unique double-membrane structures, the autophagosomes, which sequester the

cellular components and then fuse with lysosomes where the captured cargos are degraded. Therefore, the process of autophagy generally includes induction, formation and expansion of the phagophore, fusion of the autophagosome with the lysosome, and breakdown and recycling of contents inside autolysosomes. In this chapter we will focus on the process and molecular mechanisms of the trafficking of autophagosomes to lysosomes.

5.1 Intracellular Movement of Autophagosomes

5.1.1 *Autophagosome, Lysosome, and Vacuole*

Once an autophagic signal has been triggered, autophagic membranes are gradually generated, enlarge, and wrap cytoplasm or organelles to form an autophagosome. There are no lysosomal enzymes in the early autophagosomes. After fusion with lysosome or endosome, the autophagosome becomes a mature autolysosome. Electron microscopic images show that early autophagosomes contain relative complete structures such as morphologically discernable ribosomes, mitochondria, endoplasmic reticulum, etc., while cargos in late autophagosomes are partially or completely degraded, and the electron density in late autophagosomes increases. By approaches such as immune electron microscopy and organelle separation, it has been found that there are many lysosome membrane proteins in late autophagosomes. However, these are less abundant in early autophagosome, and scarcely any lysosome membrane proteins are seen in autophagosome precursors. The early autophagosome has the same pH as the wrapped cargos, but in the process of maturation, the autophagosome is gradually acidified. In mouse liver hepatocytes, the pH of early autophagosome is 6.4, while it is 5.7 in late autophagosome.

Lysosomes are membrane-bound organelles that contain many different hydrolytic enzymes that participate in the disposal of foreign materials and senescent and damaged organelles. All animal cells contain lysosomes except mature red blood cells. Lysosomes are formed by vesicles budding from the Golgi complex containing lysosomal enzymes synthesized in endoplasmic reticulum. The lysosomal membrane proton pump hydrolyzes ATP, transporting cytoplasmic H⁺ ions into lysosome, which leads to a gradual decrease in pH. The lysosome eventually fuses with autophagosome or phagosome to form the mature lysosome. Lysosomes contain more than 60 different acid hydrolytic enzymes such as proteinases, DNAses, RNAses, and glycosidases. The optimal pH for the activity of these enzymes is 5.0 and the pH in lysosome is 3.5–5.5. The acid environment of lysosome plays an important role in the maturation and activity of the hydrolases, and in the degradation of cell contents. If the permeability of lysosome membrane increases, it may lead to the leakage of hydrolytic enzymes from lysosome to cytosol, thus causing severe cell damage. Therefore, maintenance of the homeostasis of the lysosome is essential for normal cell function, and dysfunction of lysosomes leads to diseases including lysosomal storage diseases (LSD).

Vacuoles are large vesicular structures enwrapped by a biological membrane, and are ubiquitous in plants, fungi, protozoa, and some bacteria. Like lysosomes, vacuoles are formed by intracellular biogenesis and endocytosis. Vacuoles are the counterpart of the mammalian lysosomes in the autophagy process, but they are also involved in a wider array of other physiological processes such as in pH and ion homeostasis and in turgor pressure maintenance. The vacuole can also function as storage for ions, metabolites, and proteins. Similar to lysosomes, the vacuole has an acidic internal milieu, which is essential for the optimal activity of acid hydrolases in the lumen.

5.1.2 Autophagosome Trafficking

In yeast, the autophagosome begins to generate at the pre-autophagosomal structure (a.k.a. phagophore assembly site, PAS), a single functional site situated close to the vacuole membrane. In mammalian cells, multiple autophagosome formation sites are detected throughout the cytoplasm. Lysosomes also have different intracellular distributions under different cell conditions. For instance, when nutrients are rich, with sufficient amino acids and growth factors, lysosomes transfer to the periphery of cells, resulting in the activation of mTOR. However, when the cell is lacking nutrients, lysosomes accumulate at the microtubule-organizing center and fuse with autophagosomes transported by microtubules in order to degrade autophagic contents and provide metabolic substrates for cells.

Therefore, autophagosomes must traffic to and then fuse with lysosomes to finish their maturation and degradation. Kimura et al. have shown that autophagosomes do not move far from the sites of formation to lysosomes until they are completed. In neurons, autophagosomes have to move along the axon for a long distance, sometimes more than 1 m. Therefore, it is important to understand how autophagosomes are transported for such long distances to finish the autophagic degradation process. Moreover, in some specialized cells such as cardiomyocytes and skeletal muscle cells, the arrangement of filaments is very strict and tight, and it is unclear how and even whether autophagosomes are transported in these specialized cells. So far, the dynamics and molecular mechanisms underlying autophagosomes' directional traffic and fusion with lysosomes are not fully understood. Although the process of autophagosome formation is unique to this organelle, the trafficking mechanisms used by autophagosomes are similar to that of other organelles in cells, mainly including cytoskeletal systems, motor proteins, and other assistant proteins.

5.2 Molecular Mechanisms of Autophagosome Trafficking

The cytoskeleton is a network structure mainly composed of three basic types of filaments: microfilaments, microtubules, and intermediate filaments. It not only functions to maintain cell shape but also plays important roles in regulating the movement

of cells and organelles and segregating cellular components. During the formation and the trafficking of autophagosomes, it is necessary for them to move along cytoskeletal structures such as microfilaments and microtubules with the assistance of motor proteins and adaptor proteins. Motor proteins are a class of **molecular motors** that use the energy from the hydrolysis of ATP to drive themselves and attached cargo molecules directionally along microfilaments and microtubules. So far, three main motor protein families, myosin, kinesin, and dynein, have been identified.

5.2.1 *Actin*

Microfilaments usually mediate the short-distance transport of autophagosomes within a local area, while microtubules mediate the long-distance transport in the whole cell. Microfilaments, also known as actin filaments or filamentous actin, are important components of the cytoskeleton, and are mainly composed of actin, which mediates cell movement and muscle cell contraction together with myosin. Early studies on actin filaments implicated them in selective autophagy such as mitophagy in yeast but not in mammalian cells. In yeast, blocking actin polymerization did not affect bulk protein degradation by autophagy, indicating that actin is not involved in the nonselective autophagy. However, actin filaments are crucial in the Cvt pathway, the classic pathway of selective autophagy in yeast, where actin mediates the recognition and packaging of prApe1 oligomers into Cvt vesicles and then recruits the Cvt complex to the PAS. Actin filaments also play crucial roles in other types of selective autophagy such as the specific removal of peroxisomes and ER. Blocking actin polymerization inhibits the directional movement of damaged organelles to the PAS and the subsequent removal of damaged organelles. In these actin-mediated selective autophagy processes, autophagy-related protein Atg9 interacts with the Arp2/3 complex via Atg11, coordinately directing the movement of recognized organelles to the PAS and then mediating autophagosome formation.

Later studies found that actin in mammalian cells regulates the recognition and formation of the autophagosome during the initial phase of starvation-induced autophagy. Depolymerizing F-actin with cytochalasin D or Latrunculin B inhibits the formation of autophagosomes. Vice versa, deleting the core factors of autophagy influences assembly of actin filament in starvation-induced autophagy; for instance, F-actin is disassembled in ATG7 knockout MEFs. More recently, a series of studies demonstrated that the dynamics of actin filaments also play a crucial role in autophagosome movement. Actin filaments provide a network for the trafficking of organelles to autophagosome, regulated by the nucleation factors ARP2/3 and actin-capping protein CapZ. This actin-mediated network provides a scaffold to support the expansion, trafficking, and effective fusion of the autophagosome with lysosome. Interestingly, actin-associated autophagosome movement is mediated through actin-comet tail motility. The nucleation-promoting factor WHAMM directly recruits and activates the Arp2/3 complex, resulting in the formation of actin-comet tails on autophagosome. The prompt assembly of actin-comet tails promotes the movement of autophagosomes toward lysosomes.

5.2.2 *Microtubules*

The exact role and mechanism of microtubules in autophagy has been studied for quite a long time. Generally, it has been agreed that microtubules facilitate autophagosome trafficking. Early studies in hepatocytes and kidney epithelial cells indicated that disrupting microtubule polymerization with nocodazole and vinblastine inhibits the fusion of autophagosomes with lysosomes but has no influence on autophagosome biogenesis. Later studies found that these microtubule-depolymerizing reagents increase the intracellular LC3-II concentration, cause the accumulation of autophagosomes, and inhibit autophagy-mediated protein degradation. Together, these data suggest that microtubules mediate the fusion of autophagosomes with lysosomes, and instability of microtubules blocks the transportation and fusion of autophagosomes with lysosomes and results in the accumulation of autophagosomes. However, other findings show that inhibition of the polymerization of microtubules by vinblastine facilitates the formation of the autophagosome without affecting the transfer of hydrolytic enzymes from the lysosome to the autophagosome. In addition, the vinblastine-stimulated autophagosome is independent of nutrient levels and mTOR inactivation but requires the activity of autophagy proteins Atg5 and Atg6. Therefore, the study concluded that microtubules do not mediate the fusion of autophagosomes with lysosomes but instead directly affect the formation of autophagosomes. Visualizing the translocation of LC3, the autophagosomal marker, with green fluorescent protein (GFP) shows that when stable microtubules exist, autophagosomes are transported toward the centrosome in a rapid linear manner, with the average rate of 5 $\mu\text{m/s}$. However, autophagosomes do not only move toward centrosome, but bidirectionally along the microtubule: both forward to and backward away from centrosome. Blocking the N-terminal microtubule binding domain of LC3 by microinjection of anti-LC3 antibody inhibits the linear movement of autophagosomes toward the centrosome and inhibits the fusion of autophagosomes with lysosomes and subsequent degradation. Moreover, depolymerizing microtubules with nocodazole decreases the amount of autophagosomes and slows down the trafficking of autophagosomes toward the centrosome. Collectively, this evidence indicates that microtubule stability is required for the formation of autophagosomes and the trafficking of autophagosomes toward lysosomes but not the fusion of autophagosomes with lysosomes.

Surprisingly, stabilizing microtubules with taxol does not accelerate the movement of autophagosomes toward centrosomes; on the contrary, taxol causes a decreased movement of autophagosomes toward centrosomes, and, an effect similar to microtubule depolymerization, suggesting that while depolymerization and stabilization of microtubules affect autophagosome trafficking, they are not the driving forces for autophagosome movement. So far, the mechanism underlying microtubules in autophagosome trafficking remains an open question. It is generally agreed that microtubule proteins are associated with autophagosome transportation in mammalian cells. However, unlike in mammalian cells, microtubules are not necessary for autophagosome formation and degradation in yeasts. Atg8 is the yeast

homolog of LC3, but the protein structure of Atg8 is different than LC3. Atg8 does not bind to microtubules, whereas the N-terminus of LC3 protein directly binds to microtubules, thus providing additional evidence to support the view that microtubules are not necessary for autophagy in yeast. A possible reason could be that autophagosomes in yeast are generated at the pre-autophagosomal structure (PAS) and mature close to the yeast vacuole membrane, thus the long-distance trafficking toward lysosomes is not required in yeast. This may also explain why actin plays more important roles in the process of autophagosome formation and maturation in yeast.

5.2.3 Motor Proteins

Several motor proteins including actin-based motors such as myosin and microtubule-based motors such as dynein have been implicated in autophagosome trafficking. Interaction of myosin with actin filaments drives a wide range of cellular motility including muscle contraction. So far, several myosins have been shown to play essential roles in specific steps of autophagy. For example, non-muscle myosin IIA (NMM2A) is involved in the early stage of autophagy during the initiation and expansion of the phagophore, and myosin IC (MYO1C) and myosin VI (MYO6) operate in the late stages of autophagy during autophagosome maturation and fusion with the lysosome. NMM2A is encoded by MYH9, and is involved in dynamics of cells such as translocation and migration. Under starvation conditions, NMM2A is activated by the serine/threonine kinase ATG1 (in mammalian cells, ULK1) which is essential for the induction of autophagosome formation. Then NMM2A is recruited to *trans*-Golgi network (TGN) membranes via its interaction with Rab6 and is thus suggested to be involved in transport vesicle formation in the Golgi complex. NMM2A together with actin forms the filament network that provides the tension required for the formation of ATG9 vesicles and serves as the track for the delivery of ATG9 from TGN to phagophore expansion sites within cells. During the maturation stage, MYO6 is the only myosin which directly associates with autophagosomes through adaptor proteins/autophagy receptors, such as NDP52, OPTN, TAX1BP1, and TOM1. MYO1C is widely expressed in eukaryotic cells and associates with the transportation of sphingolipid- and cholesterol-enriched lipid rafts from the *trans*-Golgi network (TGN) to the cell membrane, thus regulating cellular cholesterol homeostasis. Deficiency of MYO1C leads to the accumulation of autophagosomes, which may be due to a requirement for cholesterol in autophagosome-lysosome fusion.

On the other hand, dynein regulates autophagosome movement along the microtubules as a molecular motor connecting autophagosomes and microtubules. Immunofluorescence evidence shows that only mature autophagosomes can move along the microtubules. LC3-labeled mature autophagosomes distribute along microtubules, and LC3 co-localizes with the dynein-dynactin complex. In addition, impairing dynein activity with anti-dynein antibodies by microinjection, or

overexpressing dynamitin which inhibits the activity of dynein-dynactin complex, inhibits the movement of autophagosomes. In cardiomyocytes, H_2O_2 or superoxide anion increases the ATPase activity of dynein, accelerates the movement of autophagosomes, and promotes the fusion of autophagosomes with lysosomes. In neurons, a loss-of-function mutation of dynein causes increased LC3-II, impaired autophagosome degradation, and the accumulation of damaged proteins. Moreover, mutation of dynein aggravates the accumulation of huntingtin protein in Huntington animal models, thus worsening the neurodegenerative symptoms. This evidence suggest that stable microtubule structures mediate the transportation of autophagosomes toward lysosomes, and a motor protein dynein-dynactin complex participates directly in the regulation of autophagosomes movement along microtubules.

5.2.4 Others

The name of LC3, microtubule-associated protein light chain 3, indicates that LC3 participates in the movement of organelles along the microtubules. Although the exact mechanism of LC3 in the regulation of autophagosome movement is unclear, it is no doubt that LC3 plays an important intermediary role in autophagosome trafficking. The 3D structure of LC3 protein reveals two N-terminal α -helices that can directly bind with microtubules. Blocking the N-terminal activity by the microinjection of an anti-LC3 antibody inhibits the linear trafficking of autophagosomes toward lysosomes. In addition, LC3 on the membrane of the autophagosome co-localizes with the middle chain of dynein and the p150 subunit of dynactin. Therefore, LC3 not only recruits motor proteins to bind to the autophagosome membrane but also directly recruits autophagosomes to microtubules and mediates autophagosome movement along microtubules.

LC3 has an established role in mediating autophagosome trafficking in axons in neurons. In neurons, two kinds of motor proteins coexist: the motor protein dynein mediates organelle movement toward nucleus (retrograde), whereas the motor protein kinesin mediates movement away from nucleus (anterograde). Both motor proteins interact with the scaffolding protein JNK-interacting protein 1 (JIP1) to coordinate the direction of movement. The competitive binding of JIP1 with the subunit p150 of dynactin or the heavy chain KHC of kinesin determines the formation of anterograde or retrograde complexes. On the one hand, LC3 on the autophagosome membrane binds to JIP1 via the LIR motif, directly mediating autophagosome trafficking toward the cell body; on the other hand, the binding of LC3 to JIP1 competitively inhibits the binding of JIP1 to kinesin heavy chain KHC, inhibiting the generation of anterograde complexes. In neuronal axons, therefore, LC3 binding to JIP1 makes the autophagosome trafficking retrograde along microtubules toward cell body (Fig. 5.1). In addition, FYVE and coiled-coil domain-containing protein 1 (FYCO1), an effector of Rab7 that localizes on autophagosomes, late endosomes, and lysosomes, is also involved in the regulation of autophagosome trafficking. FYCO1 associates with microtubules by forming complexes with LC3 through the

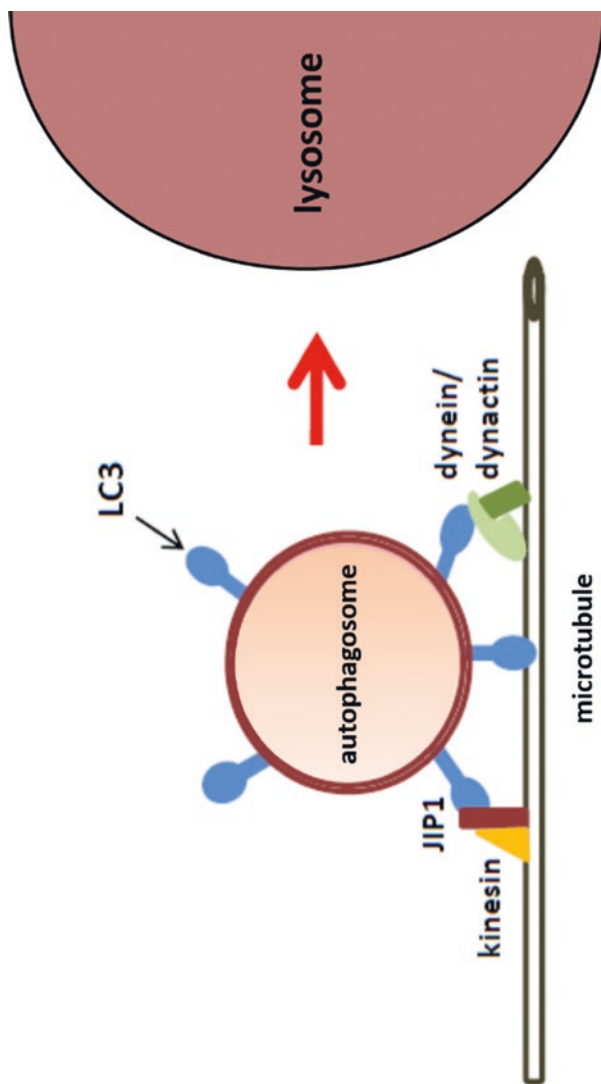


Fig. 5.1 LC3 mediates autophagosome trafficking along the microtubule

LIR motif and Rab7. FYCO1 also interacts with LC3 and PI3P, promoting plus-end-directed transport of autophagosomes through the interaction with kinesin motor protein.

5.3 Regulation of Autophagosome Trafficking

Factors regulating autophagosome trafficking are not well studied. However, there are several types of manipulations widely used in experimental studies so far. (1) Microtubule polymerization reagents, including vinblastine and nocodazole, disrupt microtubules by interfering with microtubule polymerization, thus directly influencing microtubule-dependent autophagosome trafficking. In nocodazole-treated cells, the average speed of autophagosome movement is 1 $\mu\text{m/s}$, far less than the 5 $\mu\text{m/s}$ in untreated cells. Both the total long-distance and linear motions are eliminated by nocodazole. (2) F-actin-depolymerizing drugs such as cytochalasin D and Latrunculin B, which inhibit autophagosome formation, also subsequently inhibit autophagosome trafficking. Under the regulation of nucleation factors arp2/3, actin filaments provide a network for organelles trafficking to autophagosome. The network supports autophagosome expansion, trafficking, and effective fusion with lysosome. The activation of the arp2/3 complex by nucleation promoting factors as WASP (Wiskott-Aldrich syndrome protein (Las-17 in yeast)), WASH (WASP and Scar homolog), WHAMM (WASP homolog associated with actin, membranes, and microtubules), and JMY (junction-mediating and regulatory protein, p53) results in the formation of actin-comet tails on autophagosome. The actin-comet tails promote autophagosome movement toward the lysosomes. Therefore, interrupting actin polymerization by pharmacologically inhibiting ARP2/3 complex, knocking down WHAMM, or using mutagenesis inhibits the formation of comet tails and reduces both the size and amount of autophagosomes. It is proposed that during starvation-induced autophagy, the forces generated by actin polymerization are harnessed to drive autophagosome trafficking. (3) Regulating motor proteins affects autophagosome trafficking directly. Microinjection of anti-dynein intermediate chain antibody (clone 70.1), which is known to impair dynein activity almost completely, impairs the rapid autophagosome movements. Overexpressing dynamitin, a subunit of the dynein-dynactin complex that is known to inhibit dynein- and dynactin-dependent organelle movement, significantly reduces autophagosome movement. Disrupting dynein function by inhibiting the ATPase activity of dynein with adenine analog EHNA (erythro-9-[3-(2-hydroxynonyl)] adenine) results in reduced movement of GFP-LC3-positive autophagosomes. The RAB7 effector protein RILP (RAB7-interacting lysosomal protein) recruits dynein-dynactin motor complexes to RAB7-containing late endosomes to facilitate their transport toward the minus end of microtubules, effectively inhibiting their transport toward the periphery of the cell. Autophagosome transportation along the axon is mediated by binding of JIP1 to the dynein activator dynactin. In addition, the effector of Rab7 FYCO1 also regulates autophagosome trafficking. Regulation of the interaction of

FYCO1 with LC3 and PI3P, or the FYCO1-Rab7 complex, or the binding with kinesin, causes the interruption of autophagosome movement and fusion with lysosomes, thus leading to the accumulation of autophagosomes and impaired autophagy.

Bibliography

- Chua CE, Gan BQ, Tang BL. Involvement of members of the Rab family and related small GTPases in autophagosome formation and maturation. *Cell Mol Life Sci.* 2011;68:3349–58.
- Fass E, Shvets E, Degani I, et al. Microtubules support production of starvation-induced autophagosomes but not their targeting and fusion with lysosomes. *J Biol Chem.* 2006;281:36303–16.
- Fu MM, Nirschl JJ, Holzbaur EL. LC3 binding to the scaffolding protein JIP1 regulates processive dynein-driven transport of autophagosomes. *Dev Cell.* 2014;29:577–90.
- Kast DJ, Dominguez R. The cytoskeleton-autophagy connection. *Curr Biol.* 2017;27(8):R318.
- Kimura S, Noda T, Yoshimori T. Dynein-dependent movement of autophagosomes mediates efficient encounters with lysosomes. *Cell Struct Funct.* 2008;33:109–22.
- Klionsky DJ, Cregg JM, Dunn WA Jr, et al. A unified nomenclature for yeast autophagy-related genes. *Dev Cell.* 2003;5:539–45.
- Köchel R, Hu XW, Chan EY, et al. Microtubules facilitate autophagosome formation and fusion of autophagosomes with endosomes. *Traffic.* 2006;7:129–45.
- Kruppa AJ, Kendrick-Jones J, Buss F. Myosins, actin and autophagy. *Traffic.* 2016;17:878–90.
- Laura G, Leon W, Edmond C. Advances in autophagy regulatory mechanisms. *Cells.* 2016;5:24.
- Mijaljica D, Prescott M, Devenish RJ. The intriguing life of autophagosomes. *Int J Mol Sci.* 2012;13:3618–35.
- Monastyrska I, Rieter E, Klionsky D, et al. Multiple roles of the cytoskeleton in autophagy. *Biol Rev.* 2009;84:431–48.
- Ravikumar B, Acevedo-Arozena A, Imarisio S, et al. Dynein mutations impair autophagic clearance of aggregate-prone proteins. *Nat Genet.* 2005;37:771–6.
- Ravikumar B, Sarkar S, Davies JE, et al. Regulation of mammalian autophagy in physiology and pathophysiology. *Physiol Rev.* 2010;90:1383–435.
- Reggiori F, Ungermann C. Autophagosome maturation and fusion. *J Mol Biol.* 2017;429:486–96.
- Rubinsztein DC, Shpilka T, Elazar Z. Mechanisms of autophagosome biogenesis. *Curr Biol.* 2012;22:R29–34.
- Shibutani ST, Yoshimori T. A current perspective of autophagosome biogenesis. *Cell Res.* 2014;24:58–68.
- Søreng K, Neufeld TP, Simonsen A. Membrane trafficking in autophagy. *Int Rev Cell Mol Biol.* 2018;336:1.
- Yorimitsu T, Klionsky DJ. Autophagy: molecular machinery of self-eating. *Cell Death Differ.* 2005;12:1542–52.
- Yoshinori O. Historical landmarks of autophagy research. *Cell Res.* 2014;24:9–23.

Chapter 6

Mechanisms of Selective Autophagy



Qi-Wen Fan and Xiang-Hua Yan

Abstract Autophagy is a lysosome-dependent degradation process. During autophagy, cytoplasmic components are sequestered and catabolized to supply nutrition and energy under starvation conditions. Recent work has demonstrated that many cargos can be specifically recognized and then eliminated via the core mechanism of autophagy which is termed as selective autophagy. The cargo recognition program provides the basis for the specific degradation of selective autophagy; thus, the exploration of the interaction between the cargo and the receptor is the key for revealing the underlying mechanism. Also, receptor protein complexes are required in various selective autophagy subtypes which process and guide the cargo to the core mechanism. Ubiquitination and phosphorylation are the main methods to modulate the affinity of the receptor toward cargo. Although many key processes of selective autophagy subtypes have been discovered and intensively studied, the precise ways in which the mechanisms of cargo recognition function remain mostly elusive. A fuller mechanistic understanding of selective autophagy will be important for efforts to promote disease treatment and drug development.

The process of autophagy includes four steps: induction, double-membraned formation and elongation, autophagosome formation and maturation, and autolysosome formation. In early studies, autophagy was generally considered a nonselective degradation process. However, the specific degradation of proteins, organelles, and pathogens via selective autophagy processes has greatly expanded the field of autophagy. The specificity of the cargo recognition and the trafficking strategy are key processes for selective autophagy, which requires cargo receptors to link cargos to autophagosomal membranes. In this chapter, we discuss the current view on the molecular mechanisms behind how proteins, organelles, and allogeneic cargo are selected during selective autophagy. Thus, we review the cargo receptors, receptor

Q.-W. Fan · X.-H. Yan (✉)

College of Animal Sciences and Technology, Huazhong Agricultural University,
Wuhan, China

e-mail: xhyan@mail.hzau.edu.cn

© Science Press 2021

Z. Xie (ed.), *Autophagy: Biology and Diseases*, Advances in Experimental
Medicine and Biology 1208, https://doi.org/10.1007/978-981-16-2830-6_6

79

modification, and the mechanisms of cargo recognition and cargo transport in selective autophagy.

6.1 Selective Autophagy

Selective autophagy can be termed as a process to specifically degrade certain components of cells (such as damaged mitochondria, protein aggregates, and invading viruses or bacteria) through the core mechanism of autophagy via specific cargo recognition. Nowadays, selective autophagy has been classified into three categories: selective macroautophagy, selective microautophagy, and chaperone-mediated autophagy (CMA). It is generally expected that the cargo recognition programs might be the same in macroautophagy and microautophagy. Currently, most studies are focusing on exploring the mechanisms of selective macroautophagy. Thus, in this chapter, selective autophagy usually refers to selective macroautophagy.

The process of selective autophagy can be divided into two steps: the first step, cargo recognition and transport and, the second step, cargo degradation in the lysosome. However, selective and nonselective cargo degradation uses the same core mechanism, so the characteristics of selective autophagy are represented in the specific program of cargo recognition and transport, which can be described as a cargo-ligand-receptor-scaffold model.

During autophagy, receptor protein complexes (RPCs) process the cargo. RPCs comprise of a functional tetrad of components: a ligand, a receptor, a scaffold, and an Atg8 family protein (microtubule-associated protein 1 light chain 3 alpha, LC3 in mammals). The ligand is present on the cargo and interacts with the receptor. The autophagy receptor needs to be attached to the cargo to recruit the other components of the RPC; the scaffold protein is recruited to the receptor which guides the cargo to the phagophore assembly site (PAS) and mediates the formation of autophagosomes. It is noteworthy that most of the components in RPCs are replaceable, and some receptors are just an intrinsic component that is present on the surface of the cargo; therefore, ligands are also replaceable parts of RPCs. Moreover, the cargo recognition programs of selective autophagy are usually (1) induction of the cargo degradation signal; (2) modifications of the cargo and the receptor as well as the interaction between the cargo and the receptor; (3) the scaffold which guides the cargo into the PAS by interacting with the receptor; and (4) the receptor and/or scaffold which binds with an Atg8 family protein. Among these processes, the interaction between the cargo and the receptor provides the basis for the specific degradation of selective autophagy, which is also the key for the exploration of the mechanism.

6.1.1 *The Cargo Receptor*

In mammals, the receptors already known to be involved in selective autophagy include sequestosome 1 (p62/SQSTM1), neighbor of BRCA1 (NBR1), calcium binding and coiled-coil domain-containing protein 2/nuclear dot 10 protein 52

(CALCOCO2/NDP52), CALCOCO3/Tax1-binding protein 1 (TAX1BP1), optineurin (OPTN), BCL2/adenovirus E1B-interacting protein 3-like (BNIP3L/NIX), and FUN14 domain-containing 1 (FUNDC1). In yeast, Cue5, Atg19, Atg32, Atg36, Atg39, and Atg40 are known receptors for selective autophagy (Deng et al. 2017). Most of these receptors have both an LC3-interacting region (LIR) and, in yeast, an Atg8 family-interacting motif (AIM) and an ubiquitin-binding domain (UBD). The UBD assists in cargo recognition by its interaction with ubiquitin. Notably, not all receptors involved in selective autophagy are able to interact with members of the Atg8 family. The most important role of the autophagy receptor is to recognize and sort diverse cargo for delivery to the autophagic machinery.

The p62/SQSTM1 protein (hereafter p62) acts as an autophagy receptor in mammals and is widely involved in many types of selective autophagy, including aggrephagy, mitophagy, pexophagy, and xenophagy. Besides containing a LIR and a UBD, p62 includes a Phox and a Bem1p domain (PB1) at the N-terminus. These domains mediate the homopolymerization of p62 and its co-aggregation with the cargo (Stolz et al. 2014). Moreover, this polymerization enables a tight interaction of the p62-coated cargo with lipidated LC3 at the autophagosome. After the discovery of p62, NBR1 was identified as a mammalian autophagy receptor. The structure of NBR1 is highly similar to p62, with a PB1 domain at the N-terminus and a UBD and 2 LIR domains at the C-terminus. NBR1 can also target to ubiquitinated aggregates or organelles, and differs from p62 in its UBD structure which results in a much higher affinity of NBR1 for ubiquitin than p62. NDP52 and TAX1BP1, two SKIP carboxyl homology (SKICH) domain-containing autophagy receptors, play crucial roles in selective autophagy for the recognition and degradation of damaged mitochondria and invading viruses or bacteria. The functions of NDP52 and TAX1BP1 are regulated by TANK-binding kinase 1 (TBK1), which may associate with them through the adapter NAPI1. The SKICH domain of NDP52 and TAX1BP1 can interact with NAPI1, while TBK1 regulates phosphorylation modification of the binding site (Fu et al. 2018). OPTN is also regulated by TBK1 and acts during selective autophagy of intracellular bacteria and damaged mitochondria. NIX and FUNDC1 are the autophagy receptors for mitophagy.

In general, autophagy receptors lack a clear specialization but often cooperate with each other in selecting a specific cargo. NBR1 plays an essential role in p62-dependent sequestration and degradation of aggregated proteins and peroxisomes. On the other hand, during xenophagy, p62 teams up with OPTN and NDP52 to facilitate the removal of invading bacteria. Moreover, the modification of cargo and receptors, such as ubiquitination and phosphorylation, plays an important role in cargo recognition and selective autophagy.

6.1.2 Modification and Cargo Recognition

In order to ensure the accuracy of cargo recognition and thus to prevent unintended degradation, the receptor is usually localized to the cargo in an inactive form and activated as a result of the induction of autophagy. The activation of receptor proteins usually requires phosphorylation and/or ubiquitination, a process necessary

for the formation of PRCs. Therefore, these modification processes can be seen as autophagic targeting signals. In mammals, the most prevalent autophagy targeting signal is ubiquitin, which binds to lysine residues of peptide chains under the action of E3 ubiquitin ligase. The ubiquitination of Lysine 48 or 63 (K48 or K63) in the cargo or intermediate receptor is usually used as an inducer of selective autophagy. In this case, K48-linked chains are always recognized by the proteasome, while K63-linked chains function as a generic autophagy target signal (Khaminets et al. 2016). In fact, the accumulation of all forms of ubiquitin chains in autophagy-deficient cells indicates that autophagy has little selectivity for cargo marked with specific forms of ubiquitin chains.

Phosphorylation of autophagy receptors by different kinases can increase their affinity toward cargo or autophagosomes and thereby regulate the specificity and activity of selective autophagy depending on the cellular condition. The autophagy receptors Atg32 and Atg36 in yeast, whose serine/threonine residues adjacent to the AIM motif are regulated by phosphorylation, affect the activity of mitophagy and pexophagy, respectively. NIX and FUNDC1 have similar phosphorylation processes for the regulation of their activity. Moreover, in 25% of LIR sequences, the key aromatic amino acid sites often are serine or threonine residues, suggesting that phosphorylation may be involved in the regulation of LIR-LC3 interaction (Birgisdottir et al. 2013). The structural studies on OPTN have also shown that the phosphorylation of Ser177 in the LIR structure of OPTN enhances the interaction with Lys51 and Arg11 in the N-terminus of LC3B. Conversely, phosphorylation of some receptors in LIR structures prevents the interaction with LC3s. For example, the phosphorylated LIR sequence (YEVL) of FUNDC1 maintains FUNDC1 in an inactive state, and dephosphorylation under hypoxic conditions allows it to interact with LC3, thereby enabling removal of damaged mitochondria by mitophagy (Liu et al. 2012).

Another example of the involvement of phosphorylation is the mitochondrial outer-membrane Ser/Thr protein kinase PINK1 which can phosphorylate Ser65 in the Parkin ubiquitin-like (Ubl) domain, and the ubiquitin linked at Parkin (Gladkova et al. 2018). The action of PINK1 can promote the capture and the aggregation of receptor-specific cargo. In addition to phosphorylation and ubiquitination, SUMO modification of receptors may be involved in cargo recognition.

6.2 Molecular Mechanisms of Selective Autophagy

6.2.1 *The Selective Autophagy of Proteins*

The degradation of proteins by selective autophagy is mainly directed to misfolded proteins, including aggregates and soluble proteins which have lost efficacy. A misfolded protein present in the cell is initially refolded by the intracellular protein repair pathway. If a misfolded protein cannot be refolded by the chaperone, it needs to be degraded through ubiquitin-proteasome system (UPS), CMA, or other

selective autophagy pathways. Among these three pathways, relatively small and single proteins are usually degraded by the UPS and CMA pathways. However, cargo-like aggregates with a certain spatial structure require aggrephagy for their degradation. The chaperone complex composed of heat shock cognate protein of 70 KDa (Hsc70) and heat shock protein 90 (Hsp90) plays an important role in the quality control of intracellular mature proteins. Recent studies have shown that certain functional proteins can also be selectively degraded by autophagy, such as in ferritinophagy, to modulate cellular ionic levels. This section focuses on the selective autophagy of proteins.

6.2.1.1 The Cytoplasm-to-Vacuole Targeting Pathway

The cytoplasm-to-vacuole targeting (Cvt) pathway is an important regulatory pathway that transports vacuolar enzymes from the cytosol to the vacuole via a selective autophagy-like process. For many vacuolar hydrolases, their zymogens can be transported directly from the cytoplasm to the vacuole via this pathway which contributes to the regulation of vacuolar homeostasis. Klionsky's team has made outstanding contributions to the discovery and mechanisms of the Cvt pathway. Their results have shown that the Cvt pathway has a standardized cargo recognition program (Lynch-Day and Klionsky 2010). The Cvt pathway has strong analogy to the transport of viruslike particles (VLPs) to the vacuole.

The vacuolar hydrolases precursor aminopeptidase I (prApe1), α -mannosidase, (Ams1), aspartyl aminopeptidase (Ape4), and leucine aminopeptidase (Lap3) but also Ty1 VLPs (which are produced by Ty1 retrotransposons in yeast and can be observed as particles by electron microscopy) can be delivered to the vacuolar lumen by the Cvt pathway (Yamasaki and Noda 2017). Atg19 and Atg34 are two important receptors in the Cvt pathway, both of which can recognize substrates and promote the formation of Cvt complexes. Subsequently, the Cvt complex forms a Cvt vesicle under the guidance of the scaffold protein Atg11. In this process, Atg19 has an AIM domain and can bind to Atg8, which helps the Cvt complex to form a Cvt vesicle. A Cvt vesicle has a similar structure to autophagosomes, but the former (about 150 nm) is significantly smaller than the latter (about 500 nm).

At present, the cargo recognition mechanism for Ape1 transportation through the Cvt pathway is relatively clear. The precursor form of Ape1, prApe1, can rapidly oligomerize into a homododecamer, which then assembles into a higher-order complex composed of multiple dodecamers named an Ape1 complex. Atg19 can recognize prApe1 and integrates into the Ape1 complex. Moreover, Atg19 can guide Ams1 to localize to the Ape1 complex to form the Cvt complex. The binding domains of prApe1 and Ams1 on Atg19 are separate, and therefore delivering both prApe1 and Ams1 to the vacuole is a noncompetitive process in the Cvt vesicle. In addition, crystal structure analysis showed that Atg34 can specifically bind to Ams1 to enhance its transport. The vacuolar transport of Ape4 and Lap3 and Ty1 VLPs as well is also carried out by binding to the Cvt complex, and Atg19 can serve as their receptor, but the regulation mechanism is still unclear. A Cvt complex is transported

to the PAS through a mechanism that requires the guidance of Atg11. Atg11 specifically recognizes and binds the C-terminal of Atg19, and this interaction is independent of the cargo, but its localization to PAS relies on prApe1 and Atg19. Therefore, the binding of Atg11 to the Cvt complex is prior to PAS localization. Actin and actin-binding complex (Arp2/3) provide power for the transfer of the Cvt complex to the PAS. Atg11 directly links to actin, pulls the Cvt complex, and finally locates inside the PAS. Upon successful binding of the Cvt complex to the PAS structure, Atg19 binds to Atg8 with its AIM motif to facilitate the assembly of Cvt vesicles. Subsequently, similar to other autophagic cargo receptors, Atg19 binds to the cargo and then enters the lysosome for degradation.

6.2.1.2 Chaperone-Mediated Autophagy

CMA is a type of autophagy distinct from the other autophagic pathways, for its cargo is a single protein with a specific motif. Its degradation function is similar to that of the ubiquitin-proteasome system. Dr. Cuervo and her group are the pioneers of this pathway, and with their work, we have gained a better understanding of the CMA pathway (Kaushik and Cuervo 2018). Owing to its saturability and competitiveness, a subset of long-lived cytosolic soluble proteins is directly delivered into the lysosomal lumen via specific receptors via the CMA pathway. Under nutritional stress, CMA can clear “old” proteins and provide nutrients to cells.

Morphologically, the biggest difference between CMA and other types of selective autophagy is that the cargo transportation from the cytosol to the lysosome occurs without the formation of an autophagosome. This specific transport depends on the function of many chaperones, such as Hsc70 and lysosome-associated membrane protein type 2A (Lamp2A). Hsc70 is a multifunction protein present in the cytoplasmic and lysosomal lumen, and is the sole receptor for the CMA pathway. All the proteins internalized into lysosomes through CMA contain in their amino acid sequence a pentapeptide motif that is always KFERQ motif. Hsc70 remains to be the only chaperone that can directly bind with the KFERQ motif, and many cochaperones, such as the carboxyl terminus of Hsc70-interacting protein (CHIP), Hsp40, and Hsc70-Hsp90 organizing protein (HOP), modulate substrate targeting to lysosomes in an Hsc70-dependent manner. Accurately, CHIP can regulate the refolding of proteins, mainly as a chaperone-associated ubiquitin ligase to stimulate the degradation of the Hsc70 substrate protein; Hsp40 can activate the ATPase activity of Hsp70 and promote the ligation of substrates; Hsp90, in synergy with Hsp70, can recognize unfolded regions of proteins and also prevents the substrate protein aggregation, while HOP acts as an adapter between Hsc70 and Hsp90. In addition, Bcl2-associated athanogene 1 protein (BAG1) and BAG3 are involved in the regulation of CMA substrate transport and can act as a nucleotide exchange factor to stimulate substrate release. The receptor, Lamp2A, is located on the lysosomal membrane and selectively translocates the cargo that is transported by Hsc70 to the lysosome to be degraded. Lamp2A works as a channel protein and has a short

cytosolic tail (GLKRHHTGYEQF) that can bind to the substrate protein. This binding process is a rate-limiting step for the CMA process.

Since the recognition and transport of the substrate proteins by Hsc70 and Lamp2A are carried out in linear steps, a substrate protein is recognized and transported by only one chaperone protein. Chiang et al. found that about 30% of soluble proteins in the cytoplasm have a putative CMA-targeting motif. In addition, Lv et al. have shown that posttranslational modification, such as acetylation, SUMOylation, and other types of modification, may generate additional motifs that increase the number of proteins that can serve as CMA substrates (Lv et al. 2011). Notably, more than one targeting motif does not make proteins better CMA substrates, i.e., a single KFERQ motif can already satisfy the recognition of the substrate by the CMA pathway. So far, CMA has been found only in mammalian cells and in a few bird cells.

6.2.1.3 Aggrephagy

The folding of proteins after their synthesis is essential for the function of proteins in cells. Under normal conditions, the hydrophobic patches of the protein will be buried internally during folding. However, misfolded proteins expose hydrophobic patches on their surface which causes aggregation of intracellular proteins. Protein aggregates cause a waste of energy and nutrition in cells, and seriously interfere with the metabolic activities of cells. Therefore, when protein aggregates appear in cells, they need to be cleared by metabolic pathways, and aggrephagy is described as the selective capture and degradation of aggregates by autophagy.

In addition to p62, NBR1, and OPTN, the Cue5 protein in yeast and its mammalian homologue TOLLIP are newly discovered receptors involved in the clearance of polyglutamine (polyQ protein) aggregates. Two independent pathways have been described for the formation of an aggresome, which use histone deacetylase 6 (HDAC6) and BAG3 as characterizing protein, respectively. These two proteins mediate the transport of aggregates to aggresomes in their respective pathways:

1. HDAC6-dependent transport: HDAC6 promotes dynein-mediated transport of ubiquitinated protein aggregates to aggresomes, and it is also important for the elimination of aggresomes by autophagy (Tan and Wong 2017). HDAC6 can directly link to dynein and ubiquitin substrates and preferentially binds to the K63-linked polyubiquitin chains. Besides, HDAC6 and p62 are involved in the degradation of protein aggregates: while p62 recruits phagophores to the aggregates and participates in the formation of aggresomes, HDAC6 enhances the fusion between aggresomes and lysosomes by remodeling actin.
2. BAG3-dependent transportation: BAG3 and CHIP proteins are both needed for the transport of Hsp70-mediated protein aggregates to the aggresome (Sturner and Behl 2017). BAG3 interacts directly with dynein, which directly transports Hsp70 substrates to the aggresome. This transport does not rely on ubiquitination of the substrate, but the E3 ubiquitin ligase CHIP is essential. Thus, CHIP

induces aggregation of the substrates, while BAG3 mediates the transport of misfolded protein aggregates, which together results in the formation of aggresomes.

After the transport step, the RPC complex which is composed of p62, autophagy-linked FYVE protein (ALFY), and NBR1 can link to the aggresomes by interacting with Atg8. In the complex, p62 is the major constituent and its interaction partners are NBR1 and ALFY. The polymerization of p62 is necessary, and the 400 kDa protein ALFY is a scaffold protein. ALFY contains a BEACH domain, a WD40 repeat region that interacts with Atg5, and a FYVE domain that binds to phosphatidylinositol 3-phosphate (PtdIns(3)P). The presence of these domains suggests potential links and regulatory functions between ALFY and autophagy core components.

6.2.1.4 Ferritinophagy

Ferritinophagy is a newly found selective autophagic process which can participate in the regulation of the iron status in cells. Ferritinophagy can increase the content of the labile iron pool (LIP) by promoting the catabolism of the iron-storage ferritin protein. This process safeguards iron homeostasis during iron depletion. The nuclear receptor coactivator 4 (NCOA4) is an autophagy cargo receptor during low iron levels, which binds ferritin heavy chain 1 (FTH1), and associates with LC3 to recruit cargo-receptor complexes into autophagosomes (Santana-Codina and Mancias 2018). NCOA4 contains an unabled canonical LIR (LC3-interacting region) motif, and its role in ferritinophagy is regulated by HERC2 (HECT and RLD domain-containing E3 ubiquitin protein ligase 2). Mancias et al. found that the C-terminal 383–522 amino acids of NCOA4 are required for binding to ferritin (Mancias et al. 2014). A mutation of I489 or W497 in NCOA4 and R23 in FTH1 abrogated the binding between NCOA4 and FTH1 and induces a block in ferritinophagy. HERC2 is able to interact with NCOA4 in cells, depending on the level of bioavailable iron (Mancias et al. 2015). During a high level of iron, HERC2 selectively binds to NCOA4 to initiate its ubiquitination and degradation. However, during a low level of iron, the combination of HERC2 with NCOA4 is destructed, and stored iron is released through the combination of NCOA4 with FTH1, which can induce ferritinophagy.

Ferritinophagy is important for maintaining an effective iron status in the cell. Ferritinophagy can however lead to the accumulation of ROS. In relation to this, ferritinophagy plays an important role in cellular iron death (ferroptosis). Ferroptosis is an iron and reactive oxygen species (ROS)-dependent form of regulated cell death. The essence of ferroptosis is an abnormal metabolism of cellular iron, which results in a large number of lipids and destroys the intracellular redox balance, thus triggering cell death. Studies have shown that the inhibition of NCOA4 represses ferritin degradation and suppresses ferroptosis, while its overexpression has the opposite effects. Moreover, induction of ferroptosis by erastin was shown to be blocked by a potent inhibitor of autophagy named bafilomycin A1 (BafA1),

indicating ferroptosis as an autophagic cell death program. Ferritinophagy selectively degrades ferritin to release the iron that is stored in cells ensuring cell survival under a depletion of iron.

6.2.2 *The Selective Autophagy of Organelles*

Under normal conditions, cellular organelles need to be maintained at an appropriate number to ensure a normal metabolism. This maintenance usually manifests as a dynamic balance, and autophagy plays an important role in the regulation of organelle renewal and the elimination of damaged organelles. In some extracellular stimulating conditions, such as hypoxia or dramatic changes of the nutrient environment, the organelles become damaged or redundant, and then autophagy participates in the clearance of these organelles. The selective degradation of organelles via the process of autophagy is an adaptive regulation of cells, which is also important for the quality control of intracellular organelles. The RPC model is also suitable for the cargo recognition of organelle autophagy. This section mainly introduces the mechanism of cargo recognition and the physiological significance of various types of organelle autophagy.

6.2.2.1 Mitophagy

Mitophagy refers to the process by which mitochondria are selective degraded by autophagy procedures. Mitophagy occurs in basal mitochondrial quality control, removal of damaged mitochondria, and during the maturation process of immature red blood cells. The substrate of mitophagy is usually a damaged mitochondrion which is accompanied with depolarization of the membrane. This mitochondrial depolarization leads to the accumulation of Parkin on the outer mitochondrial membrane (OMM), which then recruits and binds with the corresponding receptor. This is followed by binding to Atg8 or LC3 under the induction of the scaffold protein. In eukaryotes, the receptors of mitophagy are Atg32 (yeast), OPTN, NDP52, Tax1BP1, BNIP3, NIX/BNIP3L, and FUNDC1 (Liu et al. 2014).

6.2.2.1.1 Mitophagy in Yeast

In yeast, Atg32 is a protein with a single transmembrane span with its N-terminus and C-terminus in the cytoplasmic and mitochondrial intermembrane space (IMS), respectively. The cytosolic N-terminus of Atg32 contains an AIM motif and an I/VLS motif which interact with Atg8 and Atg11, respectively. The interaction with Atg11 is activated by phosphorylation at residues Ser114 and Ser119 in the I/VLS motif of Atg32, and casein kinase 2 (CK2) has been proposed as the Atg32 Ser114 kinase. Under nitrogen starvation, ATP deprivation, or pH-altering conditions,

Atg32 can bind to Atg11. The interaction between Atg32 and Atg11 promotes recruitment of mitochondria to the PAS for sequestration. Notably, Atg32 also interacts with Atg8 through its cytosolic AIM domain. However, mutating the Atg32 AIM causes only a partial mitophagy defect, indicating that the primary role of Atg32 during mitophagy is the recruitment of Atg11 protein.

Because intact mitochondria are larger than autophagosomes, the sequestration of damaged mitochondria might be accompanied with mitochondrial fission. Dnm1 and Fis1 are key proteins that participate in the regulation of mitochondrial fission. It has been shown that deletion of either Dnm1 or Fis1 significantly suppresses mitophagy. Dnm1 can directly bind to Atg11 to promote the recruitment of mitochondria that destined for degradation. Furthermore, the ER-mitochondrial encounter structure (ERMES) plays an important role in the regulation of mitochondrial fission during mitophagy. Nevertheless, the exact mechanism of mitophagy-associated mitochondrial fission is unclear, and more work is still needed.

6.2.2.1.2 Mitophagy in Mammals

In mammals, mitophagy encompasses a more complicated process. So far, the homologous protein of Atg32 in mammals is still controversial. However, there are many mitophagy receptors involved in cargo selection with similar functions to Atg32: OPTN, NDP52, Tax1BP1, NIX, and FUNDC1.

1. NIX, FUNDC1: Nix, a BH3-only member of the Bcl2 family, is a mitochondrial outer-membrane protein and has a LIR domain at the N-terminus that acts as an LC3-binding motif. The exact functions of NIX in mitophagy are still unclear, while the mutation of its LIR domain causes a partial mitophagy defect. The expression of NIX is regulated by hypoxia-inducible factor 1 (HIF-1), which leads to the induction of a variety of processes: pre-processes of mitochondrial clearance, such as Drp1-mediated mitochondrial fission, and induction of the localization of RPCs in mitophagy, such as the localization of Parkin and the initiation of mitophagy. These extensive regulatory functions suggest that NIX might be the core receptor for mitophagy. The study presently carried out in reticulocytes (immature red blood cells) could very well give useful answers about the molecular mechanism of NIX in mitophagy. Mitophagy is involved in the clearance of mitochondria in red blood cells when they develop into mature cells that do not contain mitochondria. NIX functions in the recognition and the transport of mitochondria in this process.

FUNDC1 is a protein with three transmembrane domains and is localized in the mitochondrial outer membrane. Its cytosolic N-terminus contains a typical LIR domain that binds to LC3 and mediates hypoxia-induced mitophagy. A mutation in the LIR domain results in a loss of function of FUNDC1. Phosphorylation plays a key role in the regulation of FUNDC1 function and mitophagy, and FUNDC1 is phosphorylated by SRC kinase, ULK1, and CK2, while more details of the regulatory mechanisms are still unknown.

2. The PINK1-Parkin signaling pathway: The PINK1-Parkin pathway is the most extensively characterized mechanism affecting mitochondrial quality control in most mammalian cells.

PTEN-induced putative protein kinase 1 (PINK1/PARK6) is a kinase acting as a sensor for damaged mitochondria. PINK1 contains a cytosolic C-terminus and a N-terminus passing through the mitochondrial membrane into the matrix. In healthy mitochondria, the N-terminus of PINK1 in the matrix is cleaved by presenilin-associated rhomboid-like protein (PARL) protein and mitochondrial processing proteases (MPP), and subsequently released back into the cytosol for degradation in the proteasome. In compromised mitochondria, the loss of mitochondrial membrane potential ($\Delta\Psi_m$) prevents the translocation of PINK1 into the matrix, and PINK1 is activated and stabilized on the OMM. This activated PINK1 phosphorylates ubiquitin, mitofusin 1 (MFN1), MFN2, and Parkin. Moreover, PINK1 phosphorylates the Ser65 in ubiquitin attached to OMM proteins, generating phospho-ubiquitin, a structure that shows a high affinity to Parkin and thereby recruits Parkin to mitochondria. The phosphorylation of MFN2 mediated by PINK1 also promotes Parkin recruitment.

Parkin/PARK2 contains 465 amino acids and is an E3 ubiquitin ligase that can involve in the ubiquitination of substrates. Mitochondrial depolarization leads to the accumulation of PINK1 in the OMM and the recruitment of Parkin, but the specific mechanism is still unclear. To our knowledge, MFN2, F-box protein 7 (Fbxo7), voltage-dependent anion-selective channel 1 (VDAC1), and mitochondrial movement Rho GTPases (Miro) might be the key regulators for this process.

After abundant Parkin is recruited to the OMM, its E3 ubiquitin ligase activity can mediate the ubiquitination of OMM proteins, such as Mfn1/2, VDAC1, Miro, and hexokinase. Among all these proteins, ubiquitinated VDAC1 acts as the binding signal for HDAC6, p62, NDP52, OPTN, autophagy/beclin-1 regulator 1 (Ambra1), and Beclin, which induce mitophagy.

6.2.2.2 Pexophagy

Peroxisomes are single-membraned organelles present in eukaryotic cells and are necessary for cell survival because of their functions in maintaining redox homeostasis. Pexophagy is the autophagic process for selective removal of peroxisomes. Excess or damaged peroxisomes are recognized by specific receptors which mediate the targeting to autophagosomes. Eventually, the selected peroxisomes are degraded in lysosomes. Due to their important functions, the quantity and quality of peroxisomes need to be highly regulated. In addition, studies have demonstrated that pexophagy is restricted to mature organelles, leaving immature peroxisomes, which still have the ability to incorporate peroxisomal proteins, intact.

The protection of immature peroxisomes may be related to peroxisomal biogenesis factor 3 (Pex3), which is a peroxisome membrane protein that plays a key role in peroxisome synthesis. The removal of Pex3 from the membrane and subsequent

degradation in proteasomal disposal are required for pexophagy. Another key protein that regulates pexophagy is Pex14, which has a key regulatory role for peroxisome matrix input. Its function can be described as a “boat dock” used to immobilize an initiating factor in pexophagy, such as Atg11.

So far, the receptors for pexophagy that have been identified in yeast are PpAtg30 (*Pichia pastoris*) and Atg36 (*Saccharomyces cerevisiae*).

1. Pexophagy in yeast: In *Saccharomyces cerevisiae*, Atg36 mediates the cargo selection in pexophagy when induced by N starvation. Pex3 is required for the recruitment of Atg36 on peroxisomes. Atg36 tethers peroxisomes targeted for degradation. Atg11 is required for pexophagy and Atg36 can bind to Atg11. Moreover, Atg36 contains an AIM motif and can interact with Atg8, but this interaction is unnecessary for pexophagy. Just similar to other receptors, Atg36 is a suicide receptor whose degradation is accompanied by that of the cargo.

PpAtg30 is the pexophagy receptor in *Pichia pastoris*. PpAtg30 binds both Pex3 and Pex14 to localize to the membrane of peroxisomes. Meanwhile, PpAtg30 can interact with PpAtg11 and PpAtg17 which guide the movement of the peroxisome. In addition, the acyl-CoA-binding protein PpAtg37 is an integral peroxisomal membrane protein specifically required for phagophore formation during pexophagy. PpAtg37 is recruited to the RPCs by PpAtg30 to promote the interaction of PpAtg30 with PpAtg11.

2. Pexophagy in mammals: No pexophagy-specific cargo receptor has been found in mammals. Pexophagy in mammals relies on the ubiquitination of peroxisomal proteins and their recognition by SQSTM1 and NBR1. Pex5 is a cytosolic protein that shuttles between the peroxisomal membrane and the cytosol in a ubiquitin-dependent manner. By phosphorylation and subsequent monoubiquitination, Pex5 can localize on the peroxisomal membrane to initiate autophagic degradation that is dependent on the induction of p62. In addition, E3 ubiquitin ligase regulates the ubiquitination process of Pex5 and plays an important regulatory role in starvation-induced pexophagy. Moreover, in response to ROS, ataxia telangiectasia-mutated (ATM) kinase has been found to be involved in the activation of pexophagy (Zhang et al. 2015). ATM can be activated by ROS which then phosphorylates Pex5. This phosphorylation promotes the monoubiquitylation of Pex5, which leads to a colocalization of the peroxisome and Pex5. Subsequently, Pex5 can be recognized by p62, targeting the peroxisomes for pexophagy. The understanding of pexophagy is limited and further studies are still needed.

6.2.2.3 Ribophagy

Ribosome biogenesis and protein translation are the most energy-consuming processes in the cell. Consequently, these two pathways must be tightly controlled upon nutrient conditions. Kraft et al. demonstrated that in *S. cerevisiae*, ribosomes preferentially degrade compared to other cytoplasmic components, indicating that there

is a process that selectively degrades ribosomes, namely, ribophagy (Kraft et al. 2008).

Ubiquitination and deubiquitination are involved in the selective degradation of ribosomes under different nutrition conditions. 60S ribosomal subunits are cleared by the ribophagy pathway under nitrogen starvation. The major partner of the ubiquitin and proteasome system, Cdc48 and its ubiquitin-linked cofactor Ufd3, may act on the ubiquitination of the 60S subunit. The deubiquitinating enzyme Ubp3 and its cofactor Bre5 can mediate the deubiquitination of the 60S subunit, which is required for ribophagy. In addition, both the 60S ribosome-associated E3 ubiquitin ligase Ltn1/Rkr1 and Ubp3 can regulate the ribosomal protein Rpl25, but Ltn1 functions as the opposite of Ubp3 for it is an inhibitor of ribosome autophagy. The regulation of ubiquitination and deubiquitination by Cdc48-Ufd3, Ubp3-Bre5, and Ltn1 is critical for ribophagy of the ribosomal 60S subunit.

Recently, Sabatini's team have shown that nuclear fragile X mental retardation-interacting protein 1 (NUFIP1) is a receptor for starvation-induced ribophagy in mammals (Wyant et al. 2018). NUFIP1 can form a heterodimer with Zinc finger HIT domain-containing protein 3 (ZNHIT3), which is transferred from the nucleus to the lysosome in the cytosol under mTORC1-inhibited conditions. Moreover, NUFIP1 modifies ribosomal RNA and interacts with ribosomes. Therefore, when NUFIP1 accumulates in the cytoplasm, it can carry ribosome substrates. Meanwhile, ZNHIT3 has four potential LIR domains that can bind to LC3; thus, the complex can transport the ribosome to the autophagosome and trigger degradation.

6.2.2.4 Reticulophagy

The endoplasmic reticulum (ER) is an important “assembly plant” that functions to assemble, fold, and transport translated proteins in cells. Reticulophagy is a selective autophagy pathway, which targets aberrant ER as cargo recognized by the specific receptors.

So far, the receptors involving in reticulophagy include Atg39 and Atg40 in yeast and FAM134B, SEC62, RTN3, and CCPG1 in mammals (Nakatogawa and Mochida 2015). In yeast, Atg39 and Atg40 recognize the perinuclear and cytoplasmic ER, respectively. However, in mammals, FAM134B, a reticulon-like protein, can selectively anchor damaged ER and assist the ER to break into “small” fragments. Moreover, FAM134B contains a LIR domain at the C-terminus which can bind to LC3 to guide ER fragments into autophagosomes. Similarly, RTN3 recognizes tubular ER using its C-terminus, and contains multiple LIR domains at the N-terminus that bind to LC3 and participate in the transport of ER fragments. Sec62 is part of the protein translocation apparatus in the membrane of the ER which acts as a receptor for reticulophagy during the steady-state recovery from ER stress. The LIR domain at the C-terminus of SEC62 can be used to interact with LC3s involved in the elimination function during the ER stress recovery phase. CCPG1 is also an ER protein. Its FIP200-interacting region (FIR) and LIR domain allow this protein to bind to RB1CC1/FIP200 and LC3, respectively, which promote the isolation and

degradation of the ER through combination and regulation (Lahiri and Klionsky 2018). Although the receptors for reticulophagy have been found, the research on its regulation mechanism is still lacking, and further studies need to be carried out continuously.

6.2.2.5 Nucleophagy

The nucleus is the key organelle containing the cells' genetic material, and the degradation of the nucleus would generally be detrimental to cells; thus, the autophagic degradation of the nucleus, nucleophagy, involves only a part of the nuclear components, and usually occurs via microautophagy. In *S. cerevisiae*, nucleophagy includes two forms: piecemeal nucleophagy (PMN) and late nucleophagy (LN). PMN takes place under nutrient-rich conditions as well as after a short period of nitrogen starvation, and a nucleus-vacuole junction (NVJ) is needed in this process. The nuclear outer-membrane protein Nvj1p and the vacuolar protein Vac8p are involved in the regulation of binding during the NVJ. Crystal structure analysis performed by Jeong et al. has shown that the N-terminus of Vac8p contains 12 armadillo repeats (ARM), which can bind to the perinuclear ER membrane protein Nvj1p to achieve a mutual anchoring between the nucleus and the vacuole. Thereafter, under induced conditions, the nucleus produces bud-like bulges at the junction region, and part of the nuclear material is delivered to the vacuole by vesicles where it is degraded by vacuolar hydrolases. Therefore, the implementation of PMN requires most of the autophagy core mechanisms, and the proteins that mediate the fusion between the vesicle and the vacuole are indispensable. In addition, the cargos which are selected for PMN are nonessential nuclear components such as portions of the nuclear envelope and the granular nucleolus enriched in pre-ribosomes. The chromosomal DNA, nuclear pore complexes, and the spindle polar bodies are not degraded by this process. However, LN is not piecemeal autophagy which occurs after prolonged periods of nitrogen starvation and is accompanied with changes in the nuclear morphology. The autophagy core mechanism is necessary, but Nvj1p and Vac8p are optional in this process.

At present, the receptor for nucleophagy that has been found in yeast is Atg39 (Mochida et al. 2015). This receptor can be selectively localized to the perinuclear ER or the nuclear membrane, while the degradation of the nuclear outer-membrane protein Hmg1, the nuclear membrane protein Src1, and nucleolar protein Nop1 indicates that Atg39 is the regulator for the breakdown of different nuclear components via autophagy. The homologous protein of Atg39 in mammals has not yet been identified, but some studies in the terminal differentiation of keratinocytes have provided a model for the selective degradation of the nucleus via the autophagy program in mammals. The differentiation of keratinocytes leads to the formation of the stratum corneum, in which process the nucleus gradually dissolves, until the resulting corneocytes have lost their nuclei. The autophagy program might mediate the selective degradation of the nucleus. Incomplete keratinization, which implies that a residue of the nucleus is present in the stratum corneum, is a major

feature of psoriasis. Akinduro et al. have shown that LC3, WIPI1, and ULK1 were reduced in the epidermal keratosis region of psoriasis, suggesting that failure of autophagy may be one of the causes of this disease (Akinduro et al. 2016).

6.2.2.6 Lysophagy

The lysosome is the end point of all autophagy procedures, where the content of autophagosomes is decomposed depending on a large variety of lysosomal hydrolytic enzymes and its internal acidic environment. However, the leakage of lysosomal contents caused by lysosomal membrane rupture is the main cause of lysosomal cell death. Thus, timely cleaning of damaged lysosomes is necessary for the maintenance of cell homeostasis, and the process of selectively degrading lysosomes by autophagy is called lysophagy. Several stimulating factors including bacterial or viral toxins, lipids, β -amyloid, and others can impair lysosomal membranes in vivo and induce the initiation of lysophagy. Galectin-3 can be recruited and bind to glycoproteins exposed on damaged lysosomal membranes (Maejima et al. 2013). This protein can also colocalize with LC3 and might be a lysophagy receptor. In addition, damaged lysosomes typically exhibit colocalization with ubiquitin and p62, suggesting that ubiquitination and subsequent p62 recruitment may be involved in lysophagy. Our knowledge of the mechanisms that control lysophagy are limited; the details remain to be solved.

6.2.2.7 Lipophagy

Lipid droplets (LDs) are organelles composed of a phospholipid monolayer and are mainly used to store neutral lipids such as triglycerides and cholesterol esters in most animal cells. LDs have a strong lipid storage capacity that can form and expand or shrink and dissolve in response to the cellular energy status. There are many proteins presenting on the outside of LDs that can affect the metabolism and be involved in signal transduction. Perilipin (PLIN) family proteins are markers that are typical for fat droplets. In addition, a large number of enzymes related to fat metabolism and cholesterol synthesis or decomposition, such as hormone-sensitive lipase (HSL), adipose triglyceride lipase (ATGL), and diacylglycerol O-acyltransferase 2 (DGAT2), can be recruited to the surface of LDs to participate in their metabolic regulation.

Lipophagy is a selective autophagic procedure that specifically degrades intracellular lipid droplets. The activation of lipophagy is usually coupled to energetic requirements. For example, under fasting conditions, the rapid activation of lipophagy in the liver can rapidly degrade large amounts of fat delivered from fat tissue to meet the energetic requirements of the liver. Similarly, lipophagy can be involved in the production of cellular free fatty acid. Studies of lipophagy were started by Singh et al., who have found that the inhibition of autophagy can lead to the accumulation of lipid droplets in the liver and attenuate the oxidative metabolism of fatty

acids (Singh et al. 2009). Previous studies have shown that PLIN2 and PLIN3 are substrates for CMA, and the degradation of PLINs by CMA allows ATGL to bind to the LD, thereby promoting lipid breakdown. In addition, recent studies have found that the ATGL protein has a LIR domain that can link to autophagosomes. Mutations of the LIR domain lead to the inhibition of ATGL-targeted LD binding, suggesting that ATGL may have important roles in the regulation of lipophagy. At present, research carried out on the mechanism of lipophagy and the procedures of cargo recognition in this process is still lacking.

6.2.3 Selective Autophagy of Xenobiotics

In addition to functioning in maintaining the balance of intracellular proteins and organelles, autophagy is involved in an intracellular innate immune system that removes invading bacteria or viruses. The process of autophagic selective recognition and elimination of intracellular pathogens is termed xenophagy. Moreover, when viral components are degraded via an autophagic process, the term virophagy is used. The next section will focus on the substrate identification procedures for this type of selective autophagy.

6.2.3.1 Xenophagy

Xenophagy refers to the process of autophagic removal of invading pathogens. Ubiquitin is always used as the marker for removal of the pathogens, and xenophagy utilizes autophagy receptors to bind to this marker. Upon entry into the mammalian cytosol, the pathogens become decorated by a layer of polyubiquitinated proteins and are then selectively degraded by the autophagic process. The first step of the autophagic process is the identification of the pathogens by the host cell. It is observed that differing bacteria are linked to differing ubiquitin chains. *Salmonella* is decorated by linear and K63 ubiquitin chains, *Mycobacterium marinum* is surrounded with both K48 and K63 ubiquitin chains, and *Shigella residual* is mainly using ubiquitin chain linkage at the K48 site.

Xenophagy has a similar selection pattern to other types of selective autophagy. The receptors can recognize tags on the cargo and can also bind to LC3s which mediate cargo targeting to the autophagosomes. In this process, intracellular pattern-recognition receptors (PRRs) exhibit a diverse regulatory function for cargo recognition. PRRs include p62-like receptors (SLRs), Toll-like receptors (TLRs), NOD-like receptors (NLRs), RIG-I-like receptors (RLRs), and AIMS2-like receptors (absent in melanoma 2 (AIM2)-like receptors, ALRs). PRRs participate in cargo recognition by pathogen-associated molecular patterns (PAMPs) and damage-associated molecular patterns (DAMPs), and activate autophagy to guide pathogen degradation in lysosomes. SLR is the main receptor type involved in pathogen recognition and acts as the xenophagy receptor. Receptors identified as SLR receptors

involved in xenophagy include p62, NBR1, NDP52, and OPTN. Meanwhile, there are two models to describe the recognition of pathogens which are characterized as ubiquitin-dependent or ubiquitin-independent.

1. Ubiquitin-dependent pathogen recognition: Leucine-rich repeat and sterile alpha motif-containing 1 (LRSAM1) is an E3 ligase involved in the clearance of intracellular *Salmonella*. This protein can localize to bacteria via a leucine-rich repeat (LRR) and promote the ubiquitination of bacteria. In addition, the E3 ubiquitin ligase Parkin plays an important role in xenophagy. The recruitment function of Parkin is necessary to initiate xenophagy to clear intracellular pathogens.

The differences in the affinity of SLRs for distinct types of ubiquitin chains, nonubiquitinated proteins, and LC3 result in SLRs differing in their specificity for invading pathogens. p62, NDP52, and OPTN can participate in the recognition of ubiquitinated *Salmonella*, targeting this pathogen to autophagosomes. Similarly, p62 and NDP52 can recognize residual membrane and *Shigella*, while NBR1 can help p62 and NDP52 to identify *Shigella* in the cytoplasm. Moreover, Mostowy et al. have confirmed that NBR1 blocking can reduce the recruitment of p62 and NDP52, which act as the receptors for autophagic degradation of *Shigella*. For the cytosolic *Salmonella*, the bacterial cell wall component lipopolysaccharide (LPS) activates TBK1 via TLR4, and activated TBK1 phosphorylates the ser177 of OPTN, which contributes to enhance the binding activity with LC3. Furthermore, Cemma and his colleagues have found that during the clearance of *Salmonella* by xenophagy, p62 and NDP52 can simultaneously be recruited into the bacterial microstructure. Even though their functions are independent, both are essential for the clearance process.

2. Ubiquitin-independent pathogen recognition: Galectin-8 can be used to detect the integrity of phagosomes and lysosomes, and sense bacterial infection. The recruitment of galectin-8 to NDP52 is transient, independent on ubiquitination, and NDP52 subsequently enters a ubiquitin-dependent isolation program. Therefore, galectin-8 is an early signal of the infection status of host cells. Diacylglycerol (DAG) is involved in another ubiquitin-free bacteria clearance procedure. Noda et al. modeled the DAG-dependent selective autophagy pathway (Noda et al. 2012). Unlike standard autophagy procedures, after DAG initiates autophagy, LC3 is recruited to pathogens without forming an isolation membrane. Subsequently, the ULK1 complex, ATG9L1, and ATG16L are recruited by LC3 to participate in the formation of *Salmonella*-containing vacuoles (SCV), presenting a distinctive identification and degradation process.

6.2.3.2 Virophagy

Viruses hijack the host to synthesize nucleic acids (DNA or RNA) and other components essential for viral replication or assembly. Such neosynthesized viral components can be recognized by various SLRs and directed to lysosomal degradation. This autophagic elimination of individual viral components is referred to as

virophagy. Although virophagy and xenophagy both present the possibility of eliminating viruses, there is a difference in that virophagy targets neosynthesized viral components rather than the entire viral particles. For instance, p62 has been shown to recognize the Sindbis virus (SINV) capsid and to target it to the autophagosome in an ubiquitination-independent manner. However, an E3 ubiquitin ligase, Smad ubiquitin regulatory factor 1 (SMURF1) is required for the colocalization of p62 with the SINV capsid protein and necessary for virophagy. Recently, Fanconi anemia group C protein (FANCC) was also found to interact with the SINV capsid protein to facilitate virophagy. HSV-1 is another target for SMURF1 and FANCC which mediate the degradation of this virus via a virophagy process, suggesting that those two proteins commonly function as virophagic factors.

In addition, Kim et al. demonstrated that SCOTIN, which is an ER transmembrane protein, can interact with nonstructural protein 5A (NS5A) of the hepatitis C virus (HCV), finally leading to the suppression of viral replication and to autophagic degradation. Picornaviruses, the poliovirus, for example, can be recognized by galectin-8, which restricts viral infection by initiating the autophagic degradation. The cargo recognition program in virophagy shows as a complex system. The exploration of this process can provide direct targets for the biopharmaceutical treatment of disease, so further research is still needed.

6.3 Summary and Prospects

Selective autophagy enables the specific regulation of energy and nutrient metabolism in organisms. The identification of new models of selective autophagy may provide genetic determinants of complex diseases and new targets for drug development. This new version of the chapter is larger than in the previous edition, which reflects the efforts of the experts in life sciences, which rapidly expanded the field of selective autophagy for organelles, viruses, and other cellular metabolically active substances. Unfortunately, our understanding of selective autophagy is still very scarce, and the knowledge of specific receptors and cargo recognition mechanisms is still insufficient. Therefore, many challenges remain for future research, like the identification of new receptors, the elucidation of the mechanisms of cargo recognition, and the mechanisms of posttranslational modification that are involved in specific autophagy.

References

- Akinduro O, Sully K, Patel A, Robinson DJ, Chikh A, McPhail G, Braun KM, Philpott MP, Harwood CA, Byrne C, O'shaughnessy RFL, Bergamaschi D. Constitutive autophagy and nucleophagy during epidermal differentiation. *J Invest Dermatol.* 2016;136:1460–70.

- Birgisdottir AB, Lamark T, Johansen T. The Lir motif—crucial for selective autophagy. *J Cell Sci*. 2013;126:3237–47.
- Deng Z, Purtell K, Lachance V, Wold MS, Chen S, Yue Z. Autophagy receptors and neurodegenerative diseases. *Trends Cell Biol*. 2017;27:491–504.
- Fu T, Liu J, Wang Y, Xie X, Hu S, Pan L. Mechanistic insights into the interactions of NAP1 with the SKICH domains of NDP52 and TAX1BP1. *Proc Natl Acad Sci U S A*. 2018;115:E11651–60.
- Gladkova C, Maslen SL, Skehel JM, Komander D. Mechanism of parkin activation by PINK1. *Nature*. 2018;559:410–4.
- Kaushik S, Cuervo AM. The coming of age of chaperone-mediated autophagy. *Nat Rev Mol Cell Biol*. 2018;19:365–81.
- Khaminets A, Behl C, Dikic I. Ubiquitin-dependent and independent signals in selective autophagy. *Trends Cell Biol*. 2016;26:6–16.
- Kraft C, Deplazes A, Sohrmann M, Peter M. Mature ribosomes are selectively degraded upon starvation by an autophagy pathway requiring the Ubp3p/Bre5p ubiquitin protease. *Nat Cell Biol*. 2008;10:602–10.
- Lahiri V, Klionsky DJ. CCPG1 is a noncanonical autophagy cargo receptor essential for reticulophagy and pancreatic ER proteostasis. *Autophagy*. 2018;14(7):1107–1109.
- Liu L, Feng D, Chen G, Chen M, Zheng Q, Song P, Ma Q, Zhu C, Wang R, Qi W, Huang L, Xue P, Li B, Wang X, Jin H, Wang J, Yang F, Liu P, Zhu Y, Sui S, Chen Q. Mitochondrial outer-membrane protein FUNDC1 mediates hypoxia-induced mitophagy in mammalian cells. *Nat Cell Biol*. 2012;14:177–85.
- Liu L, Sakakibara K, Chen Q, Okamoto K. Receptor-mediated mitophagy in yeast and mammalian systems. *Cell Res*. 2014;24:787–95.
- Lv L, Li D, Zhao D, Lin R, Chu Y, Zhang H, Zha Z, Liu Y, Li Z, Xu Y, Wang G, Huang Y, Xiong Y, Guan KL, Lei QY. Acetylation targets the M2 isoform of pyruvate kinase for degradation through chaperone-mediated autophagy and promotes tumor growth. *Mol Cell*. 2011;42:719–30.
- Lynch-Day MA, Klionsky DJ. The Cvt pathway as a model for selective autophagy. *FEBS Lett*. 2010;584:1359–66.
- Maejima I, Takahashi A, Omori H, Kimura T, Takabatake Y, Saitoh T, Yamamoto A, Hamasaki M, Noda T, Isaka Y, Yoshimori T. Autophagy sequesters damaged lysosomes to control lysosomal biogenesis and kidney injury. *EMBO J*. 2013;32:2336–47.
- Mancias JD, Wang X, Gygi SP, Harper JW, Kimmelman AC. Quantitative proteomics identifies NCOA4 as the cargo receptor mediating ferritinophagy. *Nature*. 2014;509:105–9.
- Mancias JD, Pontano Vaites L, Nissim S, Biancur DE, Kim AJ, Wang X, Liu Y, Goessling W, Kimmelman AC, Harper JW. Ferritinophagy via Nco4 is required for erythropoiesis and is regulated by iron dependent HERC2-mediated proteolysis. *Elife*. 2015;4:e10308.
- Mochida K, Oikawa Y, Kimura Y, Kirisako H, Hirano H, Ohsumi Y, Nakatogawa H. Receptor-mediated selective autophagy degrades the endoplasmic reticulum and the nucleus. *Nature*. 2015;522:359–62.
- Nakatogawa H, Mochida K. Reticulophagy and nucleophagy: new findings and unsolved issues. *Autophagy*. 2015;11:2377–8.
- Noda T, Kageyama S, Fujita N, Yoshimori T. Three-Axis model for Atg recruitment in autophagy against Salmonella. *Int J Cell Biol*. 2012;2012:389562.
- Santana-Codina N, Mancias JD. The role of NCOA4-mediated ferritinophagy in health and disease. *Pharmaceuticals (Basel)*. 2018;11:114.
- Singh R, Kaushik S, Wang Y, Xiang Y, Novak I, Komatsu M, Tanaka K, Cuervo AM, Czaja MJ. Autophagy regulates lipid metabolism. *Nature*. 2009;458:1131–5.
- Stolz A, Ernst A, Dikic I. Cargo recognition and trafficking in selective autophagy. *Nat Cell Biol*. 2014;16:495–501.
- Sturner E, Behl C. The role of the multifunctional BAG3 protein in cellular protein quality control and in disease. *Front Mol Neurosci*. 2017;10:177.

- Tan S, Wong E. Kinetics of protein aggregates disposal by autophagy. *Methods Enzymol.* 2017;588:245–81.
- Wyant GA, Abu-Remaileh M, Frenkel EM, Laqtom NN, Dharamdasani V, Lewis CA, Chan SH, Heinze I, Ori A, Sabatini DM. NUFIP1 is a ribosome receptor for starvation-induced ribophagy. *Science.* 2018;360:751–8.
- Yamasaki A, Noda NN. Structural biology of the Cvt pathway. *J Mol Biol.* 2017;429:531–42.
- Zhang J, Tripathi DN, Jing J, Alexander A, Kim J, Powell RT, Dere R, Tait-Mulder J, Lee JH, Paull TT, Pandita RK, Charaka VK, Pandita TK, Kastan MB, Walker CL. ATM functions at the peroxisome to induce pexophagy in response to ROS. *Nat Cell Biol.* 2015;17:1259–69.

Chapter 7

Similarities and Differences of Autophagy in Mammals, Plants, and Microbes



Fu-Cheng Lin, Huan-Bin Shi, and Xiao-Hong Liu

Abstract Autophagy, a highly conserved metabolic process in eukaryotes, is a widespread degradation/recycling system. However, there are significant differences (as well as similarities) between autophagy in animals, plants, and microorganisms such as yeast. While the overall process of autophagy is similar between different organisms, the molecular mechanisms and the pathways regulating autophagy are different, which is manifested in the diversity and specificity of the genes involved. In general, the autophagy system is much more complicated in mammals than in yeast. In addition, there are some differences in the types of autophagy present in animals, plants, and microorganisms. For example, there is a unique type of selective autophagy called the cytoplasm-to-vacuole targeting (Cvt) pathway in yeast, and a special kind of autophagy, chloroplast autophagy, exists in plants. In conclusion, although autophagy is highly conserved in eukaryotes, there are still many differences between autophagy of animals, plants, and microorganisms.

Abbreviations

CMA	Chaperone-mediated autophagy
Cvt pathway	Cytoplasm-to-vacuole targeting pathway
ERGIC	ER-Golgi intermediate compartment

F.-C. Lin
Institute of Plant Protection and Microbiology, Zhejiang Academy of Agricultural Sciences,
Hangzhou, China
e-mail: fuchenglin@zju.edu.cn

H.-B. Shi
China National Rice Research Institute, Hangzhou, China
e-mail: shihuanbin@caas.cn

X.-H. Liu (✉)
Institute of Biotechnology, Zhejiang University, Hangzhou, China
e-mail: xhliu@zju.edu.cn

ESCRT	Endosomal sorting complexes required for transport
GAPDH	Glyceraldehyde 3-phosphate dehydrogenase
GCN pathway	General control of nutrient
HIF-1	Hypoxia-inducible factor 1
MVB	Multi-vesicle body
PAS	Phagophore assembly site
PE	Phosphatidylethanolamine
PRR	Pattern recognition receptor

Autophagy was first observed by the Belgian biochemist Christian de Duve in the 1950s by electron microscopy. Until the 1990s, it was primarily observed morphologically. Although autophagy was first studied primarily in animal cells, molecular-level studies have mainly been conducted through genetic studies in the yeast *Saccharomyces cerevisiae*. The laboratories of Yoshinori Ohsumi of Japan, Daniel J. Klionsky of the United States, and Michael Thumm of Germany used yeast to screen and identify autophagy-deficient mutants. In 1993, Yoshinori Ohsumi's article published in *FEBS Letters* opened the prelude to the molecular mechanisms of autophagy, and identified 15 key genes involved in autophagy regulation (Tsukada and Ohsumi 1993), which were later renamed "ATG" (Klionsky et al. 2003). The study of the mechanism of autophagy in yeast lays a good foundation for the composition and biological function of autophagy in higher biological cells. Many autophagy genes in yeast have homologous genes in higher organisms. Moreover, these genes are also involved in autophagy and other developmental processes. However, the genetic background of higher organisms is complex, their morphology is diverse, and the autophagy process naturally has many specific features. Therefore, comparing the autophagy processes of different eukaryotic organisms can facilitate a clearer understanding of the functional and biological significance of autophagy in organisms.

Autophagy is generally considered to be a pathway of degradation that recycles intracellular components. The pathway is mainly used to degrade substances, which has a variety of functions (Wen and Klionsky 2016). Cells use autophagy to maintain their viability in the face of starvation. After an organelle is damaged or becomes dysfunctional, it will be degraded by autophagy. The degradation of organelles is also a way for cells to adjust to different nutritional conditions. In addition, autophagy can also be involved in biosynthetic processes. Some hydrolases enter the vacuole through the cytoplasm, allowing their maturation and function. In addition, preliminary observations have revealed that autophagic vacuoles can encapsulate specific signaling molecules and fuse with the plasma membrane, transporting those signaling molecules to the extracellular environment and thus participating in the secretory pathway.

7.1 Microbial Autophagy

7.1.1 *The Process of Microbial Autophagy and Its Molecular Machinery*

7.1.1.1 The Process of Microbial Autophagy

Cell biologists have used *S. cerevisiae* as a model organism to identify *ATG* genes and study their biological functions. At present, yeast has become the best-studied model organism for understanding the molecular mechanism of autophagy. Filamentous fungi are closely related to yeast in evolution, and the autophagy process is similar to that in yeast, but homologs of some proteins or genes are not found in filamentous fungi (Meijer et al. 2007). There are two main types of autophagy in yeast, macroautophagy and microautophagy, which can be divided into selective and non-selective according to their selective cargoes. There are a few studies on non-selective microautophagy, but more on the other three types (Wen and Klionsky 2016). In the methylophilic yeast *Hansenula polymorpha*, non-selective microautophagy was observed under nitrogen starvation, and the absence of *ATG25* activated peroxisomal constitutive degradation (Monastyrska et al. 2005). The processes of selective macroautophagy, non-selective macroautophagy, and selective microautophagy in yeast are generally similar to that in plants and animals, but there are some special processes in yeast, such as cytoplasm-to vacuole-targeting (Cvt) pathway and the nontraditional protein secretion pathway (Thompson and Vierstra 2005).

The autophagy process in yeast mainly includes the following major steps: (1) induction of autophagy; (2) cargo selection and packaging; (3) vesicle aggregation; (4) autophagosome membrane extension and closure; (5) dissociation of autophagy proteins; (6) fusion of autophagosomes and vacuoles; and (7) degradation of autophagosomes (Wen and Klionsky 2016).

7.1.1.2 Molecular Machinery of Autophagy

The origin of autophagosome membrane has been the subject of long-standing debate. Endoplasmic reticulum is one of the sources of membrane. In addition, mitochondria, the ER-Golgi intermediate compartment (ERGIC), the Golgi apparatus (often associated with Atg9 vesicles), recycling endosomes, and the plasma membrane are all proposed sources of the autophagosome membrane (Lemus and Goder 2016). The phosphatidylinositol 3-phosphate kinase (PI3K) complex is involved in the assembly of vesicles, and Atg9 vesicles shuttle back and forth between the phagophore assembly site (PAS) and peripheral membrane structures.

The extension and closure of the autophagy precursor membrane involves two ubiquitin-like conjugation systems, Atg8 and Atg12. These systems are composed of one E1-like protein, Atg7; two E2-like proteins, Atg10 and Atg3; and two ubiquitin-like proteins, Atg8 and Atg12. They play key roles in the maturation of autophagosomes and the recruitment of cargoes. Atg12 is covalently bound to a lysine of Atg5 by the catalysis of Atg7 and Atg10, and the Atg12-Atg5 conjugate forms an oligomer under the action of Atg16. After Atg8 is activated by Atg7 and Atg3, the Atg12-Atg5•Atg16 complex promotes the covalent linkage of the glycine at the C-terminus of Atg8 to phosphatidylethanolamine (PE). Meanwhile, the Atg5 complex can also promote the entry of Atg8-PE into autophagosomes, and Atg8 is involved in the closure of autophagosomes and the recruitment of substrates. After autophagosome formation, the involved autophagy-related proteins will be dissociated and reused, with the exception of Atg8 proteins. Atg2 and Atg18 are involved in the dissociation and recovery of Atg9. The fusion of autophagosomes and vacuoles requires the involvement of SNARE, GTPase, and HOPS complexes. The degradation of autophagosomes is dependent on the acidic environment of the vacuolar cavity and proteases. Atg15 is an esterase involved in the degradation of autophagic bodies (Wen and Klionsky 2016).

7.1.1.3 Nutrient Signaling

In yeast, the main stimulus to induce autophagy is nutritional deficiency. TOR kinase is considered as the main sensing factor of nitrogen sources and amino acids, and negatively regulates the occurrence of macroautophagy. TOR can directly regulate macrophagy by phosphorylating Atg proteins including Atg13. Meanwhile, TOR can also work through a secondary pathway. Tap42 is an effector protein of TOR that forms a complex with PP2A Pph21/22. Overexpression of Pph21 or Pph22 inhibits autophagy, while inactivation of Tap42 or overexpression of Tip41 results in induction of autophagy under well-fed conditions. The downstream target of Tap42-Pph21/22 regulating autophagy is unknown (Yorimitsu et al. 2007). Ksp1 kinase regulates TOR and is also a target of TOR phosphorylation, so the regulatory network is complex. PKA is considered to be a glucose-stimulated protein which regulates TOR by regulating Ksp1 activity (Umekawa and Klionsky 2012).

Yeasts have very complicated mechanisms to perceive and respond to intracellular glucose. High levels of glucose induce the production of cAMP. cAMP binds to the regulatory subunit Bcy1 of PKA and inactivates it. As a consequence, PKA is activated and inhibits macroautophagy. PKA directly phosphorylates Atg1 and Atg13, but the phosphorylation site differs from TOR, and this posttranslational modification regulates these proteins at the PAS. Sch9 is a second glucose-sensing protein, which functions in parallel with PKA. The activity of Sch9 kinase depends on the phosphorylation of TOR, but does not depend on the phosphorylation of Sch9 in the presence of glucose. Similar to PKA, Sch9 inactivation induces autophagy (Yorimitsu et al. 2007). This process is partly regulated by Rim15 (an autophagy-positive regulator), and Msn2/Msn4 (a transcription factor). In the absence of a

nitrogen source, glucose deficiency induces autophagy as a positive regulatory signal. Snf1 kinase is able to sense intracellular energy levels and regulate autophagy induced by energy deficiency. Glucose starvation-induced Snf1-Mec1-Atg1-Atg13 complexes are recruited to the mitochondria, and participate in the autophagy process by regulating mitochondrial respiration (Yi et al. 2017).

The absence of nitrogen can induce autophagy, and one source of nitrogen is amino acids. Indeed, amino acid depletion is another factor that induces autophagy. The general control of nutrient (GCN) pathway modulates autophagy by regulating the synthesis of amino acids. Gcn2 kinase is involved in the sensing of intracellular amino acid levels, which activates the transcription factor Gcn4 via a signaling chain, thereby activating genes involved in amino acid synthesis (Vlahakis et al. 2014). Gcn2 and Gcn4 activated autophagy. Pho85 combines with Pcl5 and phosphorylated (inactivated) Gcn4 and promotes the degradation of these two proteins to achieve negative regulation of autophagy. Pho85 is a cyclin-dependent kinase that can inhibit and activate autophagy, depending on which cyclin is bound to. During phosphate signaling, the Pho85-Pho80 complex inhibits the transcription factor Pho4, which is involved in the activation of transcription of genes involved in the absorption and storage of phosphoric acid. Pho85-Pho80 can also inhibit the activity of Rim15 kinase. In contrast, the Pho85-Clg1 complex inhibits the cyclin-dependent kinase Sic1, thereby activating Rim15 (Yang et al. 2010).

7.1.2 Specific Autophagy in Microbes

7.1.2.1 Cytoplasm-to-Vacuole Targeting (Cvt) Pathway

According to the characteristics of autophagy occurrence in yeast, autophagy is divided into macroautophagy and microautophagy, which are differed in morphology but similar in mechanism. In addition, there is a cytoplasm-to-vacuole targeting (Cvt) pathway, which is similar in mechanism of macroautophagy. This pathway mainly transports vacuolar proteases to vacuoles. The Cvt pathway does not exist in mammals. The Cvt pathway is similar to selective autophagy in morphology. The cargo proteins transported by this pathway are the precursors of aminopeptidase I and alpha-mannosidase. After synthesis of aminopeptidase I in the cytoplasm, it converges to form a dodecamer called aminopeptidase complex, which interacts with the receptor protein Atg19 to form a Cvt complex. The diameter of Cvt vesicle is about 140–160 nm, which is related to the size of Cvt complex. This process can occur under normal physiological conditions. When aminopeptidase I is moderately overexpressed and a larger Cvt complex is formed, it becomes too large to be efficiently taken up by Cvt vesicles, but can still be effectively transferred to the vacuole by means of starvation-induced macroautophagy (GENG 2008). When aminopeptidase I is highly overexpressed, the complex becomes too large even for an autophagosome to envelope, and remains in the cytoplasm (Suzuki et al. 2013).

7.1.2.2 Autophagy-Mediated Protein Secretion Pathway

Studies in *Saccharomyces cerevisiae* and *Pichia pastoris* have found that Acb1, a binding protein of acetyl coenzyme in the cytoplasm, is transported to the extracellular space under starvation conditions, but this is not mediated by known secretory pathways. This transport depends on autophagic proteins. The results of electron microscopy in *S. cerevisiae* showed that the initial transport precursor structure is formed by aggregation of membrane and vesicles, similar to autophagy in morphology. Furthermore, Atg8 and Atg9 are at these sites (Dimou and Nickel 2018). However, in *Aspergillus oryzae* the acetyl coenzyme A binding protein AoAcb2 is also secreted through nontraditional secretion pathways, but does not rely on autophagy system, so it is different from that in yeast (Kwon et al. 2017).

7.2 Similarities and Differences Between Mammalian and Microbial Autophagy Processes

Two major pathways of degradation have been described for most cellular proteins in eukaryotic cells: one is the ubiquitin proteasome pathway, and the other is a macroautophagy process that relies on lysosomes (in animals) or vacuoles (in plants and fungi). Short-lived proteins are degraded and recycled by ubiquitin proteasome system, while long-lived proteins are degraded and utilized by autophagy system. The autophagy process begins with the formation of a double-membrane autophagosome precursor, and it encapsulates cytoplasm as well as aging, misfolded, and redundant proteins to form a complete autophagosome, which is then fused with lysosome, and the cytoplasmic constituents are degraded in the lysosome and recycled. In addition to degrading proteins, the autophagy process also degrades intracellular aging organelles such as mitochondria, peroxisomes, ribosomes, endoplasmic reticulum, etc., as well as infective pathogens in an identical manner. Autophagy activity is at a low basal constitutive level under normal growth conditions, and it is upregulated when the cell encounters intracellular and extracellular stresses or signals, such as starvation, growth factor deficiency, endoplasmic reticulum stress, and pathogen infection. Autophagy can help the organism endure nutrient starvation and stress conditions and eliminate excess or dysregulated organelles. In higher organisms, autophagy plays a role in many physiological processes such as development, proliferation, cell remodeling, aging, tumor suppression, neurodegeneration, antigen presentation, immunity, lifespan modulation, and cell death (Dikic and Elazar 2018).

7.2.1 *Differences of Molecular Machinery in Mammalian Autophagy*

7.2.1.1 **Differences in the Composition of the Autophagy-Related Complex**

In yeasts, there are four conserved signaling transduction complexes regulating the development of autophagy, which are conserved from yeast to plants to animals:

1. The Atg1 protein kinase complex comprises Atg1, Atg11, Atg13, Atg17, Atg29, and Atg31, and the corresponding complex in mammals is a ULK1 complex comprising ULK1, Atg13, FIP200, and Atg101, which regulates an early stage of autophagosome formation. FIP200 performs similar functions as yeast Atg17. The Atg1 complex is in a disassembled state in yeast under the condition of abundant nutrition, but the mammalian ULK1 complex binds directly to mTORC1.
2. The class three phosphatidylinositol 3-phosphate kinase (PI3K) complex contains Vps34, Vps15, Vps30, Atg14, and Atg38, and the corresponding PIK3C3-BECN1 complex in mammals contains Vps34, Vps15, BECN1, Atg14L, and NRBF2, which regulates the production of phosphoinositide signaling, thereby regulating the aggregation of initial autophagic vesicles.
3. A ubiquitin-like conjugation system plays an important role in the maturation of autophagic vesicles and the recruitment of cargo.
4. The Atg9 recycling system, which also includes Atg2, Atg18, and Atg21, is involved in the transfer and recycling of lipids from a hypothetical vesicular source to the forming autophagosome (Mercer et al. 2018).

Although the mechanism of autophagy is similar in many organisms, there are differences in the diversity and specificity of the genes involved. Mammalian autophagy systems are much more complex than yeast. Many autophagy proteins have multiple family members. For example, there is only Atg8 in yeast, but in mammals, the Atg8 gene family has at least seven members including LC3A (two splice variants), LC3B, LC3C, GABARAP, GABARAPL1, and GABARAPL2. Research shows that MAP1LC3 and GABARAP are conjugated to PE and thus bound to autophagic vesicles. The recent studies have shown that GABARAPL1 and GABARAPL2 can also interact with Atg7, Atg3, and Atg5, but the potential significance of mammalian Atg8 family members is still unclear. There are two Atg8 homologs, LGG-1 and LGG-2, *C. elegans*, but only LGG-1 is involved in autophagy (Schaaf et al. 2016). Moreover, Atg101, which is not found in yeast, is present in the autophagy system of mammals.

7.2.1.2 Autophagy Genes Are Involved in Other Biological Processes

Some genes, although conserved, may have additional functions in mammals. For example, yeast Atg6, a component in the PI3K complex, is involved only in vacuolar protein transport and autophagy. BECLIN1, the homologous mammalian protein, not only participates in autophagy regulation but also interacts with bcl-2, a negative regulator of apoptosis, to regulate apoptosis (Booth et al. 2014). Atg4 is also involved in the regulation of Notch signaling pathway in *Drosophila melanogaster*. Therefore, in higher eukaryotes, autophagy genes have both functional separation and functional redundancy.

7.2.2 Differences of Mammalian Autophagy Regulatory Pathways

In mammals, many signals regulate autophagy, and the regulation process is very complicated. Excess or insufficient autophagy will be harmful to the life of the cells. In addition, regulation by different signals also needs to be coordinated. In mammals, intracellular energy levels, nutrients such as amino acids, and growth factors regulate intracellular autophagy levels. AMPK, an AMP-dependent protein kinase, senses intracellular energy levels, and rapamycin targets perceive intracellular nutrient amino acid levels, and growth factors.

Autophagy is a protective response of cells to pathological adversity such as cancer, myocardial ischemia, and pathogen infection. Meanwhile, intracellular stability is maintained by promoting the degradation cycle of intracellular long-lived proteins and organelles. This homeostasis helps cells fight a variety of diseases, such as neurodegeneration, myopathy, liver disease, and obesity. In the face of these stresses, autophagy can maintain the biosynthetic and ATP levels of cells, provide amino acids for de novo synthesis of proteins, and provide the substrates required for the tricarboxylic acid cycle. In mice without Atg5 or Atg7, the level of amino acids in the cytoplasm and tissues is decreased, and these mice die within 1 day after birth (Kuma et al. 2004).

As an important survival metabolic pathway, autophagy has also been demonstrated in cell culture systems. Bax/Bak double-knockout mutant cells cannot undergo apoptosis, so when growth factors are deficient, autophagy protects these cells from death. Silencing Atg7 with RNAi or treating growth factor-deficient cell lines with autophagy inhibitor 3-MA leads to cell death. Supplementing autophagy-deficient cell lines with methyl pyruvate, the substrate required in the tricarboxylic acid cycle, restores ATP synthesis and cell viability. The evidence above shows that autophagy acts as a metabolic pathway to protect cells. However, autophagy cannot protect a cell indefinitely. It can only help cells cope with adversity and fight for time, somewhat like a backup battery (Levine and Kroemer 2008).

7.2.2.1 Regulation of Autophagy by TOR Kinase

TOR was originally identified as a negative regulator of autophagy in yeast and was confirmed to be a major regulator of autophagy in mammals. Mammalian cells contain two complexes: mTORC1 and mTORC2. Each has distinct functions; mTORC1 regulates protein synthesis, cell proliferation, and autophagy, and mTORC2 regulates cytoskeleton, cell metabolism, cell viability, and insulin response. Under conditions with abundant nutrients, phosphorylation of Ulk1 and Atg13 is caused by the binding of mTORC1 to Ulk1 and Atg13 via the subunit Raptor. Under starvation conditions, Ulk1 is dephosphorylated and dissociates from mTORC1. Phosphorylated Atg13 and FIP200 form a complex, thereby activating the initiation of the autophagy. Starvation, amino acid deficiency, or decreased growth factor levels inhibit the activity of mTORC1, thus activating the autophagy process (Noda 2017).

7.2.2.2 Regulation of Autophagy by AMPK Kinase

AMPK is a major positive regulator of autophagy, and AMPK is activated when the ratio of intracellular AMP/ATP increases, indicating that the intracellular energy level is low. Activated AMPK on the one hand phosphorylates and activates Ulk1, and on the other hand phosphorylates Raptor to inhibit mTORC1. Both AMPK and mTOR regulate the growth and metabolism of cells, linking these processes with autophagy (Gallagher et al. 2016).

7.2.2.3 Regulation of Autophagy by Hypoxia

The tissue hypoxia-inducible factor 1 (HIF-1) signaling pathway responds to hypoxia, tissue p53 signaling pathway downstream of DNA damage, and surface pattern recognition receptor (PRR) signaling pathways in response to invasive pathogens. Under the condition of hypoxia, the transcription factor HIF-1 is stabilized, leading to the expression of tissue hypoxia-related gene BNIP3. This protein contains only one functional domain, BH3, is the main target of HIF-1, and is necessary for tissue hypoxia-induced autophagy. Binding of BNIP3 to Bcl-2 blocks the inhibitory interaction of Bcl-2 on Beclin1 and induces autophagy. The tumor suppressor p53 can be induced by many different cellular stresses, including DNA damage, and this factor plays a dual role in the induction of autophagy. Multiple transcriptional targets of p53 activate autophagy, including BAX and PUMA. However, p53 in the cytoplasm can inhibit autophagy independent of transcriptional regulation. The balance between these two effects has not yet been studied in depth. PRRs recognize molecular motifs on the surface of pathogens to induce autophagy, but the mechanism of this signaling pathway is currently unclear, though there is evidence that AMPK and Beclin1 act as downstream effectors (Moloudizargari et al. 2017).

7.2.3 *Mammal-Specific Autophagy Type (Chaperone-Mediated Autophagy, CMA)*

In mammals and birds, in addition to macroautophagy and microautophagy, there is a unique type of autophagy called chaperone-mediated autophagy, which is characterized by direct transport of substrate proteins into lysosomes. Not all proteins can be degraded by this pathway. The substrate protein must contain a specific sequence motif (KFERQ) for recognition by the molecular chaperone HSC70, which is ultimately transported to the lysosomal surface and degraded by entering the lysosome with the transport complex LAMP2A (Kaushik and Cuervo 2018).

7.3 Similarities and Differences of Autophagy Between Plants and Microbes

In the middle of the twentieth century, autophagy in plants was reported through electron microscopy observation. Membrane-encapsulated cytoplasmic components in vacuoles were first observed in the meristem of maize roots. In the late 1970s, Francis Marty and some other researchers found some vesicles wrapping cytoplasm-like cargoes and forming structures like autophagosomes when observing the root meristem cells in *Euphorbia L.* Cytochemical analysis showed that the vesicles were acidic and contained lysosomal acid hydrolases. These morphological studies based on electron microscope provide a primary understanding and definition of autophagy in plants, but these results can only show static processes. Genetic approaches have expanded our understanding of mechanisms and physiological functions of autophagy, especially the identification of *ATG* genes in *S. cerevisiae*, and promoted molecular explanations of autophagy in higher organisms. The analysis of autophagy deletion mutants in plants is advancing the study of autophagy in this field.

Unlike animals, plants are stationary so that they have to endure or overcome stresses from different environmental conditions. For example, seedlings growing in nitrogen-deficient soils or in shade have to face the problems of nitrogen or carbon deficiency. Under the condition of nutrient deficiency, plants need to degrade macromolecular substances in vivo to adapt to the environment. Autophagy is a major system involved in the degradation of organelles and cytoplasmic macromolecules, and therefore plays an extremely important role in the growth and development of plants. Up to now, two types of autophagy have been reported in plants: microautophagy and macroautophagy. The vacuolar membrane can invaginate and envelop cytoplasmic components to form vesicles within the vacuole; these vesicles are degraded by enzymes in the vacuole, and this process is called microautophagy. A large number of cytoplasmic components and organelles can be wrapped in autophagosomes, which fuse with the vacuolar membrane and are then degraded in the vacuole cavity; this process is called macroautophagy. Macroautophagy in

plants is similar to that in animals, but the autophagosome degradation occurs in vacuoles rather than lysosomes. Small vacuolar structures similar to autolysosomes have been found in tobacco suspension cells as well, but it is uncertain whether they exist in all plant cells. In addition to the above two types of autophagy, there are molecular chaperon-mediated autophagy and pathogen autophagy in animals. However, whether these autophagic processes exist in plants has been not known so far (Wang et al. 2018).

7.3.1 Differences in Molecular Machinery of Autophagy in Plants

There are 18 key genes involved in non-selective macroautophagy in yeast: *ATG1–10, 12–14, 16–18, 29, and 31*. In the *Arabidopsis thaliana* genome, there are 30 homologous genes corresponding to the 18 genes above. However, there are no homologous genes for Atg14, 17, 29, and 31. Although the sequences of autophagy proteins in *A. thaliana* are not highly homologous to those of yeast, their functional domains are well conserved, indicating that molecular mechanisms of autophagy in plants and yeast are similar. Autophagy genes have also been identified in many crops such as rice and maize in addition to *A. thaliana*. In addition to the classic autophagy pathway yeast contains, there is a unique autophagy-related pathway called cytoplasm-to-vacuole directed transport pathway, in which aminopeptidase I is transported from the cytoplasm to the vacuole and catalyzed to maturation in the vacuole. The Cvt pathway requires the involvement of most of the key genes in autophagy except Atg29 and Atg31 as well as some other proteins such as Atg19-Atg21 and Atg23. However, there are no definite homologs to these genes in plant genomes. As a result, there seems to be no such pathway in plants. Of course, it is also possible that there are functionally related genes with low sequence homology (Yoshimoto and Ohsumi 2018).

7.3.1.1 Differences in Atg1 Kinase Complex

The Atg1 protein kinase complex comprises Atg1, Atg13, Atg17, Atg29, and Atg31, and is involved in the induction and regulation of autophagy. The TOR complex is the upstream negative regulator of the Atg1 complex. Under nutrient-rich conditions, activated TORC1 in yeast hyper-phosphorylates Atg13, preventing the binding of Atg1 and Atg13 and thus inhibiting the induction of autophagy. In a nutrient-deficient state, TORC1 is inactivated and Atg13 is dephosphorylated, thus binding with Atg1 to initiate autophagy. Homologous proteins of Atg1, Atg13, Atg11, Atg17, and Atg101 in *A. thaliana* were analyzed. Studies showed that AtATG13a and AtATG13b in *A. thaliana* regulate autophagy and AtATG1a interacts with AtATG13b. In *A. thaliana* genome, there are four homologs of Atg1, AtATG1a-1c and AtATG1t, and two homologs of Atg13: AtATG13a and AtATG13b.

Atg17 is not an independent gene in *A. thaliana*, but there is an Atg17-like domain in AtATG11. The Atg1/Atg13 complex is involved in autophagic membrane closure and autophagosome synthesis in yeast and animals, and it is likewise very important for autophagosome formation in plants. Homologs of TORC1 complex subunits TOR, RAPTOR, and LST8 have also been identified in *A. thaliana*, and knockout mutants have also been analyzed. Studies using RNAi to silence *TOR* suggest that *TOR* is also a negative regulator of autophagy in *A. thaliana* (Yoshimoto and Ohsumi 2018).

7.3.1.2 Differences in PI3K Kinase Complex

The PI3K complex is a phosphatidylinositol 3-kinase comprising Vps34, Vps15, Atg6, and Atg14. One of the functions of this complex is to recruit Atg18-Atg2 to autophagic membranes by creating the PI3P required for Atg18 binding. A homolog of Atg14 was not isolated in *A. thaliana*. However, the silencing of *ATG6* in *A. thaliana* and tobacco resulted in decreased autophagy, indicating that the PI3K complex plays an important role in autophagy in plants.

Atg9, as one of the few transmembrane proteins among autophagy-related genes, is currently believed to be involved in the transport of lipid to PAS site and the extension of preautophagosome. Atg9 exists as an oligomer in yeast and interacts with the Atg18-Atg2 complex. The *A. thaliana* T-DNA insertion mutant AtAtg9-1 shows autophagy deficiency phenotypes such as accelerated aging. T-DNA insertion mutants AtAtg2-1 and AtAtg18-1 and transgenic silencing mutant AtAtg18a all show deficiencies in autophagosome formation. There are eight homologs of yeast Atg18 in *A. thaliana*, showing the evolution of a multigene family (Kim et al. 2012).

7.3.1.3 Differences Between Ubiquitin-Like Systems Atg8 and Atg12

Two ubiquitin-like conjugation systems have been extensively studied in a variety of organisms. The Atg8 lipidation system and Atg12 conjugation system play an important role in the extension and closure of autophagosome. After catalysis by the ubiquitin-like E1-activating enzyme Atg7 and ubiquitin-like binding E2 enzyme Atg3, the ubiquitin-like protein Atg8 is covalently attached to the membrane lipid phosphatidylethanolamine (PE). In this process, Atg8 is firstly cleaved by cysteine protease Atg4 to expose the glycine at the C-terminus, activated by Atg7 and Atg3, and then finally combined with the head of PE. This system is also conserved in plants. An *A. thaliana* mutant with a T-DNA insertion in *AtATG7* can be complemented by wild-type AtATG7 protein, but a mutant with a point mutation in *AtATG7* cannot. In addition, there are nine homologs of Atg8 in *A. thaliana*, which can all be cleaved by AtATG4, and the substitution of glycine by alanine results in mislocalization of these proteins. Meanwhile, the intermediate products AtATG8s-PE and

AtATG8-AtATG3 only exist in the wild type, and could not be formed in *Atatg7* and *Atatg4a4b* double-knockout mutants. Atg12 is covalently linked to Atg5 in a reaction catalyzed by the enzymes Atg7 and Atg10. The combination can be detected by antibodies to AtATG5 and AtATG12 in wild-type plants, but not in mutants lacking the proteins AtATG5, AtATG7, AtATG10, and AtATG12a12b (Ryabovol and Minibayeva 2016).

7.3.2 Differences in Autophagy Regulation Pathways in Plants

Negative regulation autophagy by TOR has also been shown to be conserved in plants. TOR regulates the initiation of autophagy by regulating the phosphorylation level of Atg13. But its regulation of Atg1 has not been proven yet. In addition to responding to nutritional deficiency, TOR is also involved in osmotic-induced autophagy activation, but does not participate in oxidative stress and endoplasmic reticulum stress-induced autophagy regulation (Michaeli et al. 2016).

7.3.2.1 Metabolic Components Regulate Autophagy

Glyceraldehyde 3-phosphate dehydrogenase (GAPDH) can negatively regulate autophagy in *A. thaliana*. GAPDH in tobacco can directly interact with Atg3 to inhibit its activity. When plants encounter stress and accumulation of reactive oxygen species, GAPDH relieves the inhibition of Atg3 to activate autophagy (Han et al. 2015).

7.3.2.2 Intracellular Transport Pathways Regulate Autophagy

The exocyst complex regulates the transport of vesicles from the Golgi apparatus to the plasma membrane. Recent studies have shown that mutants of EXO70B1, a component of this complex in *A. thaliana*, are extremely sensitive to nitrogen starvation, and have a decreased number of autophagic bodies in the vacuole. In addition, the EXO70B1 homologous protein EXO70B2 contains an Atg8 interaction domain (AIM) (Kulich et al. 2013). The endosomal sorting complexes required for transport (ESCRT) transports ubiquitinated proteins to the multi-vesicle body (MVB) via the endosome and ultimately to the vacuole for degradation. Studies in mammals have shown that ESCRT is involved in the degradation of autophagosomes, and this conserved function has also been demonstrated in *A. thaliana*. ESCRT in *A. thaliana* regulates the autophagy process by affecting cargo identification, autophagosome transport, and the fusion of autophagosomes and vacuoles (Lefebvre et al. 2018).

7.3.3 *Autophagy Type Specific in Plants*

Recent studies have made great progress in understanding selective autophagy in plants, including peroxisomal autophagy, mitochondrial autophagy, endoplasmic reticulum autophagy, and autophagy of specific proteins, all of which have been shown to exist in *A. thaliana* (Tang and Bassham 2018). Although there are various differences in specific molecular mechanisms of selective autophagy in plants as compared to microorganisms and mammals, here we specifically highlight a type of selective autophagy found only in plants.

7.3.3.1 Chloroplast Autophagy

In the 1980s, studies using transmission electron microscopy showed that autophagy was involved in the degradation of chloroplasts and chloroplasts were degraded in large vacuoles during cell senescence. In addition, autophagy has been speculated to be involved in the quality control of chloroplasts. Autophagy involved in chloroplast regulation depends on two pathways. In one pathway, autophagosomes wrap small bodies containing ribulose biphosphate carboxylase and chloroplast matrix proteins and then enter vacuoles for degradation. In the other pathway, by the help of the receptor protein AT11 which can interact with Atg8 and bind to proteins on the plastid, entire plastids containing thylakoid proteins and matrix proteins can be transported to vacuoles (Xie et al. 2015).

7.4 Conclusion

The synthesis and degradation of proteins in cells is always in a state of dynamic equilibrium. If the balance is broken, this may lead to many problems, so protein degradation plays an important role in intracellular nutrient reuse and the maintenance of intracellular environment stability. The balance of intracellular protein levels is largely dependent on two pathways, one being the ubiquitin proteasome pathway and the other macroautophagy, which involves lysosomes (in animals) or vacuoles (in plants and fungi). Although the mechanism of autophagy is similar in many organisms, there are some differences in the molecular mechanism as well as the pathways that regulate autophagy. One is the diversity and specificity of the genes involved. The other is that, in mammals, the autophagy systems are more complex than in yeast, many signals regulate autophagy, and the regulation process is very complicated. Many autophagy proteins exist as multiple family members, so autophagy genes in higher eukaryotes have both functional separation and functional redundancy. In addition, there are some differences in the types of autophagy in animals, plants, and microorganisms. Autophagy in yeast is divided into two main types, macroautophagy and microautophagy. These two types are classified

according to their selectivity as selective and non-selective autophagy. In addition, there are cytoplasmic to vacuolar pathways, peroxisome autophagy, mitochondrial autophagy, nuclear autophagy, endoplasmic reticulum autophagy, ribosome autophagy, and pathogen autophagy. Chaperone-mediated autophagy appears to be limited to vertebrate animals (Lescat et al. 2020). In plants, there is a unique type of selective autophagy that targets chloroplasts for degradation in the vacuole.

References

- Booth LA, Tavallai S, Hamed HA, Cruickshanks N, Dent P. The role of cell signalling in the cross-talk between autophagy and apoptosis. *Cell Signal*. 2014;26:549–55.
- Dikic I, Elazar Z. Mechanism and medical implications of mammalian autophagy. *Nat Rev Mol Cell Biol*. 2018;19:349–64.
- Dimou E, Nickel W. Unconventional mechanisms of eukaryotic protein secretion. *Curr Biol*. 2018;28(8):R406–R410.
- Gallagher LE, Williamson LE, Chan EYW. Advances in autophagy regulatory mechanisms. *Cells*. 2016;5:24.
- Han S, Wang Y, Zheng X, Jia Q, Zhao J, Bai F, Hong Y, Liu Y. Cytoplasmic glyceraldehyde-3-phosphate dehydrogenases interact with ATG3 to negatively regulate autophagy and immunity in *Nicotiana benthamiana*. *Plant Cell*. 2015;27(4):1316–31.
- Kaushik S, Cuervo AM. The coming of age of chaperone-mediated autophagy. *Nat Rev Mol Cell Biol*. 2018;19:365–81.
- Kim SH, Kwon C, Lee JH, Chung T. Genes for plant autophagy: functions and interactions. *Mol Cells*. 2012;34:413–23.
- Klionsky DJ, Cregg JM, Dunn WA Jr, Emr SD, Sakai Y, Sandoval IV, Sibirny A, Subramani S, Thumm M, Veenhuis M, Ohsumi Y. A unified nomenclature for yeast autophagy-related genes. *Dev Cell*. 2003;5:539–45.
- Kulich I, Pecenkova T, Sekeres J, Smetana O, Fendrych M, Foissner I, Hofberger M, Zarsky V. Arabidopsis exocyst subcomplex containing subunit EXO70B1 is involved in autophagy-related transport to the vacuole. *Traffic*. 2013;14(11):1155–65.
- Kuma A, Hatano M, Matsui M, Yamamoto A, Nakaya H, Yoshimori T, Ohsumi Y, Tokuhisa T, Mizushima N. The role of autophagy during the early neonatal starvation period. *Nature*. 2004;432(7020):1032–6.
- Kwon HS, Kawaguchi K, Kikuma T, Takegawa K, Kitamoto K, Higuchi Y. Analysis of an acyl-CoA binding protein in *Aspergillus oryzae* that undergoes unconventional secretion. *Biochem Biophys Res Commun*. 2017;493:481–6.
- Lefebvre C, Legouis R, Culetto E. ESCRT and autophagies: endosomal functions and beyond. *Semin Cell Dev Biol*. 2018;74:21–8.
- Lemus L, Goder V. A SNARE and specific COPII requirements define ER-derived vesicles for the biogenesis of autophagosomes. *Autophagy*. 2016;12:1049–50.
- Lescat L, Veron V, Mourrot B, Peron S, Chenais N, Dias K, Riera-Heredia N, Beaumatin F, Pinel K, Priault M, Panserat S, Salin B, Guiguen Y, Bobe J, Herpin A, Seiliez I. Chaperone-mediated autophagy in the light of evolution: insight from fish. *Mol Biol Evol*. 2020;37(10):2887–99.
- Levine B, Kroemer G. Autophagy in the pathogenesis of disease. *Cell*. 2008;132(1):27–42.
- Meijer WH, van der Klei IJ, Veenhuis M, Kiel JA. ATG genes involved in non-selective autophagy are conserved from yeast to man, but the selective Cvt and pexophagy pathways also require organism-specific genes. *Autophagy*. 2007;3(2):106–16.
- Mercer TJ, Gubas A, Tooze SA. A molecular perspective of mammalian autophagosome biogenesis. *J Biol Chem*. 2018;293:5386–95.

- Michaeli S, Galili G, Genschik P, Fernie AR, Avin-Wittenberg T. Autophagy in plants—what's new on the menu? *Trends Plant Sci.* 2016;21:134–44.
- Moloudizargari M, Asghari MH, Ghobadi E, Fallah M, Rasouli S, Abdollahi M. Autophagy, its mechanisms and regulation: implications in neurodegenerative diseases. *Ageing Res Rev.* 2017;40:64–74.
- Monastyrska I, Kiel JAKW, Krikken AM, Komduur JA, Veenhuis M, van der Klei IJ. The *Hansenula polymorpha* ATG25 gene encodes a novel coiled-coil protein that is required for macropexophagy. *Autophagy.* 2005;1:92–100.
- Noda T. Regulation of autophagy through TORC1 and mTORC1. *Biomolecules.* 2017;7:52.
- Ryabovol VV, Minibayeva FV. Molecular mechanisms of autophagy in plants: role of ATG8 proteins in formation and functioning of autophagosomes. *Biochemistry (Mosc).* 2016;81:348–63.
- Schaaf MB, Keulers TG, Vooijs MA, Rouschop KM. LC3/GABARAP family proteins: autophagy-(un)related functions. *FASEB J.* 2016;30:3961–78.
- Suzuki K, Akioka M, Kondo-Kakuta C, Yamamoto H, Ohsumi Y. Fine mapping of autophagy-related proteins during autophagosome formation in *Saccharomyces cerevisiae*. *J Cell Sci.* 2013;126:2534–44.
- Tang J, Bassham DC. Autophagy in crop plants: what's new beyond Arabidopsis? *Open Biol.* 2018;8(12):180162.
- Thompson AR, Vierstra RD. Autophagic recycling: lessons from yeast help define the process in plants. *Curr Opin Plant Biol.* 2005;8:165–73.
- Tsukada M, Ohsumi Y. Isolation and characterization of autophagy-defective mutants of *Saccharomyces cerevisiae*. *FEBS Lett.* 1993;333:169–74.
- Umekawa M, Klionsky DJ. Ksp1 kinase regulates autophagy via the target of rapamycin complex 1 (TORC1) pathway. *J Biol Chem.* 2012;287:16300–10.
- Vlahakis A, Graef M, Nunnari J, Powers T. TOR complex 2-Ypk1 signaling is an essential positive regulator of the general amino acid control response and autophagy. *Proc Natl Acad Sci U S A.* 2014;111:10586–91.
- Wang P, Mugume Y, Bassham DC. New advances in autophagy in plants: regulation, selectivity and function. *Semin Cell Dev Biol.* 2018;80:113–22.
- Wen X, Klionsky DJ. An overview of macroautophagy in yeast. *J Mol Biol.* 2016;428:1681–99.
- Xie Q, Michaeli S, Peled-Zehavi H, Galili G. Chloroplast degradation: one organelle, multiple degradation pathways. *Trends Plant Sci.* 2015;20:264–5.
- Yang Z, Geng J, Yen WL, Wang K, Klionsky DJ. Positive or negative roles of different cyclin-dependent kinase Pho85-cyclin complexes orchestrate induction of autophagy in *Saccharomyces cerevisiae*. *Mol Cell.* 2010;38:250–64.
- Yi C, Tong J, Lu P, Wang Y, Zhang J, Sun C, Yuan K, Xue R, Zou B, Li N, Xiao S, Dai C, Huang Y, Xu L, Li L, Chen S, Miao D, Deng H, Li H, Yu L. Formation of a Snf1-Mec1-Atg1 module on mitochondria governs energy deprivation-induced autophagy by regulating mitochondrial respiration. *Dev Cell.* 2017;41:59–71.e4.
- Yorimitsu T, Zaman S, Broach JR, Klionsky DJ. Protein kinase A and Sch9 cooperatively regulate induction of autophagy in *Saccharomyces cerevisiae*. *Mol Biol Cell.* 2007;18:4180–9.
- Yoshimoto K, Ohsumi Y. Unveiling the molecular mechanisms of plant autophagy—from autophagosomes to vacuoles in plants. *Plant Cell Physiol.* 2018;59:1337–44.

Part II
**Investigating Autophagy: Model Systems,
Tools and Strategies**

Chapter 8

Monitoring Autophagy by Optical Microscopy



Yanrong Zheng, Xiangnan Zhang, and Zhong Chen

Abstract Thanks to the advances in optical microscope technology and our knowledge of autophagic biomarkers, single-molecule events of autophagy are now accessible to human eyes. Different proteins are involved hierarchically in the biogenesis and maturation of autophagosomes. Detecting these autophagy-related proteins either by immunostaining or fluorescent protein labelling makes the dynamic autophagic process visible. However, low antibody specificity and weak endogenous expression of autophagy-related proteins in certain tissues limit the applicability of immunostaining in autophagy detection. To cope with this, live-cell imaging combined with various fluorescent probes has been developed and employed in monitoring autophagy. As the most widely used autophagic biomarker, LC3, can be used to visualize autophagosomes, and fluorescent probes targeting LC3, i.e., RFP/mCherry-GFP-LC3, and GFP-LC3-RFP-LC3ΔG, can examine autophagy flux dynamically and quantitatively. In addition, the application of novel fluorophores such as Keima helps to detect the temporal and spatial characteristics of autophagy. Furthermore, selective autophagy can be clarified by labelling corresponding substrates and autophagosomes or lysosomes simultaneously. With the help of two-photon microscopy, the process of autophagy in live animals has been uncovered. Here, we summarize the methods for observing autophagy by optical microscopy and the selection of fluorescent markers.

Keywords Autophagy · Selective autophagy · Immunostaining · Live-cell imaging
Live-animal imaging

Y. Zheng · X. Zhang

Institute of Pharmacology and Toxicology, NHC and CAMS Key Laboratory of Medical Neurobiology, College of Pharmaceutical Sciences, Zhejiang University, Hangzhou, China
e-mail: yanrong_zh@zju.edu.cn; xiangnan_zhang@zju.edu.cn

Z. Chen (✉)

Institute of Pharmacology and Toxicology, NHC and CAMS Key Laboratory of Medical Neurobiology, College of Pharmaceutical Sciences, Zhejiang University, Hangzhou, China

Key Laboratory of Neuropharmacology and Translational Medicine of Zhejiang Province, Zhejiang Chinese Medical University, Hangzhou, China
e-mail: chenzhong@zju.edu.cn

© Science Press 2021

Z. Xie (ed.), *Autophagy: Biology and Diseases*, Advances in Experimental Medicine and Biology 1208, https://doi.org/10.1007/978-981-16-2830-6_8

117

Abbreviations

GABARAP	GABA type A receptor-associated protein
ICC	Immunocytochemistry
IF	Immunofluorescence
IHC	Immunohistochemistry
Lamp-1	Lysosome-associated membrane protein-1
Lamp-2	Lysosome-associated membrane protein-2
MAP1LC3/LC3	Microtubule-associated protein 1 light chain 3
PE	Phosphatidylethanolamine
SIM	Structured illumination microscopy
STED	Stimulated emission depletion microscopy
STORM	Stochastic optical reconstruction microscopy
ZFYVE1	Zinc finger FYVE-type containing 1

8.1 Introduction

Although the observation of double-membrane structures with transmission electron microscope (TEM) serves as a gold standard for autophagy identification, TEM doesn't work when it comes to the detection of autophagy in living cells or animals. In addition, laborious sample preparation and the few probes available also limit the applicability of TEM. To cope with this, techniques for the detection of autophagy with optical microscope have been springing up in recent decades.

Autophagy is characterized by a double-membrane structure called autophagosome. According to the maturity of autophagosome, the process of autophagy can be generally divided into the following stages: phagophore, sealed autophagosome, amphisome, and autolysosome. Different proteins are involved in each special stage, which makes the detection of dynamic processes of autophagy possible. What's more, labelling autophagosomes and autophagy substrates simultaneously can clarify the different types of selective autophagy. Here, we focus on methods of observing autophagy by optical microscope and the selection of fluorescent markers.

8.2 Monitoring Autophagy by Immunostaining

As one basic component of autophagosomes, the Atg8 family is widely employed to visualize autophagy. Once autophagy is activated, Atg8 family members are modified by phosphatidylethanolamine (PE) lipidation at C-terminus. Upon conjugation to PE, diffuse Atg8 in cytosol translocates to autophagosomes, forming punctate structures. Detection of autophagosomes by endogenous Atg8 immunostaining

helps to avoid false positives resulting from overexpression of fluorescent protein-fused Atg8.

The mammalian homologs of Atg8 include microtubule-associated protein 1 light chain 3 (MAP1LC3/LC3) family and GABA type A receptor-associated protein family (GABARAP). The differences in their roles in autophagy are still inconclusive. The LC3 proteins have been reported to participate in phagophore formation, while GABARAP family members contribute more to phagophore elongation and closure (Weidberg et al. 2010). However, other lines of evidence suggest GABARAP rather than LC3 is indispensable for autophagic sequestration of cytosolic substrates in certain cell types (Szalai et al. 2015). Nevertheless, so far, LC3 has been the primary Atg8 mammalian homolog monitored in the most researches. Noteworthy, the LC3 family also has diverse members including LCA, LC3B, and LC3C, and the differences in their functions are poorly understood. A fundamental technical consideration is that some commercialized anti-LC3 antibodies can recognize one special LC3 family member while others cannot. For immunostaining, the antibody can be selected according to the difference in tissue distributions of LC3 family proteins. For example, LC3A is abundant in the brain, allowing immunohistochemical detection, particularly in the Purkinje cells of the cerebellum (Martinet et al. 2013). However, when it comes to the liver as well as the heart, spleen, and lung, transgenic animals may be necessary for immunostaining due to the relatively weak expression of both LC3A and LC3B (Martinet et al. 2006).

To obtain optimal detection of LC3 by immunostaining, different fixatives, embedding media, and antibody concentrations should be tested and optimized. For example, cross-linking fixatives like formalin may be more suitable for fixing LC3 which is not large enough to be precipitated by precipitant fixatives (e.g., methacarn) (Martinet et al. 2013). In addition, immunostaining based on Envision reagent allows signal amplification via a hydrophilic polymer (dextran) conjugated to secondary antibodies and multiple horseradish peroxidase molecules (Fig. 8.1), which may help improve the detection of LC3 by immunohistochemistry (Rosenfeldt et al. 2012).

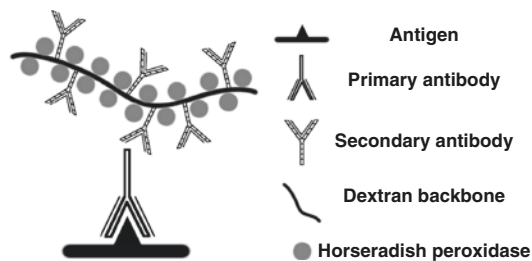


Fig. 8.1 Schematic representation of signal amplification realized by Envision reagent. The dextran backbone of Envision reagent is conjugated to secondary antibodies and multiple horseradish peroxidase molecules. After secondary antibody identifies primary antibody, abundant horseradish peroxidase molecules amplify the signals

8.3 Monitoring Autophagy in Living Cells

Low antibody specificity and weak expression of endogenous LC3 in certain tissues limit the applicability of immunostaining in autophagy detection. To cope with this, optical microscopy has been employed to monitor living cells transfected with fluorescent proteins fused to autophagy-related proteins, which also makes the dynamic processes of autophagy visible.

8.3.1 Live-Cell Imaging of LC3

Similar to immunostaining, LC3 is also the most common autophagic marker examined in live-cell imaging. Here we introduce some methods of LC3 labelling in live-cell imaging.

8.3.1.1 GFP/mCherry-LC3

Single fluorescent protein-fused LC3 (GFP/mCherry-LC3) is the most widely used tool for observing autophagosomes. The fluorescent protein is usually fused to the N-terminus of LC3 since its C-terminus is cleaved during autophagy activation. After autophagy induction in cells expressing GFP/mCherry-LC3, the cytosolic fluorescence signal localizes to punctate structures reminiscent of autophagosomes (Fig. 8.2).

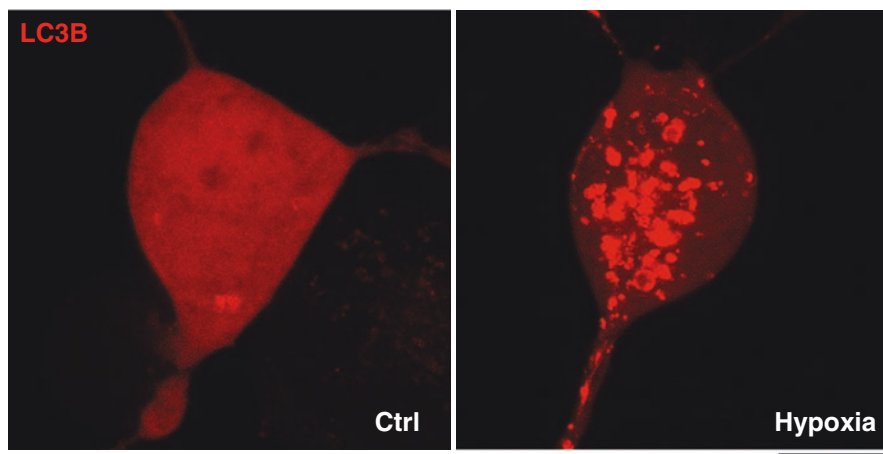


Fig. 8.2 Autophagosomes labelled by mCherry-LC3 in Neuro2a cells. Neuro2a cells were transfected with mCherry-LC3B. In the control group, the signal of mCherry-LC3B is diffuse in the cytosol. However, hypoxia increases the number of punctate structures labelled by mCherry-LC3B, reflecting the activation of autophagy. Scale bar: 10 μ m

The fluorescence of GFP is quenched below pH 7 (Patterson et al. 1997), making GFP undetectable in lysosomes. Thus, it is possible that autophagosomes labelled by GFP-LC3 won't accumulate in certain cell types such as neurons whose lysosomes are relatively active (Adhami et al. 2007). Under such conditions, lysosome inhibitor is necessary to prove autophagy activation. Alternatively, GFP can be replaced by RFP or mCherry which shows stronger acid resistance (Kimura et al. 2007).

One technical concern about single fluorescent protein-fused LC3 is that it by itself cannot indicate the activation of autophagy flux since lysosomal dysfunction can also lead to the accumulation of LC3 puncta. Thus, the use of a lysosome inhibitor is required for determining the increase of autophagy flux (Klionsky et al. 2016); alternatively, one of the following methods of LC3 labelling can be chosen.

8.3.1.2 RFP/mCherry-GFP-LC3

As mentioned above, GFP-LC3 loses fluorescence due to acidic lysosomal conditions, while RFP/mCherry-LC3 does not, allowing the latter to label autophagic compartments both before and after fusion with lysosomes. Taking advantage of this property, RFP/mCherry-GFP tandem fluorescent-tagged LC3 has been devised for dissecting the maturation process of autophagosomes (Kimura et al. 2007). RFP/mCherry-GFP-LC3 shows both GFP and RFP/mCherry signals in the cytosol, but exhibits only the RFP/mCherry fluorescence after fusing with lysosomes (Fig. 8.3), thus allowing visualization of the formation and maturation of individual autophagosomes. In addition, a dramatic increase in the number of puncta with only RFP/mCherry signal as compared to puncta with both GFP and RFP/mCherry signals indicates an accumulation of autolysosomes, and thus the activation of autophagy

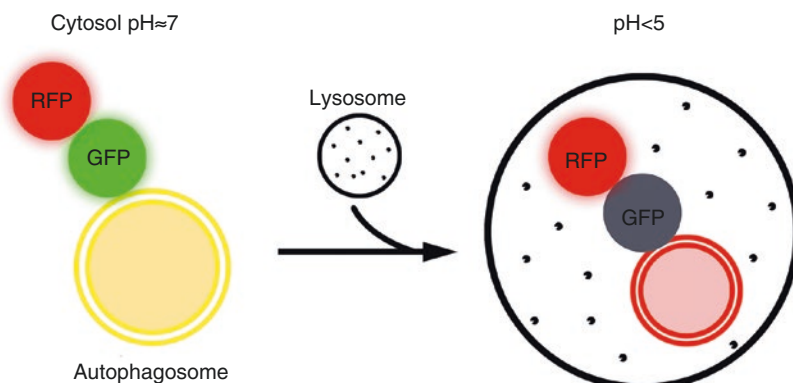


Fig. 8.3 Schematic representation of RFP-GFP-LC3. When autophagy is activated, autophagosomes in the cytosol labelled by RFP-GFP-LC3 show both GFP and RFP signals. However, RFP-GFP-LC3 exhibits only the RFP/mCherry fluorescence after fusing with lysosomes due to the poor acid resistance of GFP

flux. In contrast, lysosome dysfunction stabilizes GFP-LC3 fluorescence and increases GFP-LC3 and mRFP-LC3 co-localization, but reduces the number of puncta with only RFP/mCherry signal.

8.3.1.3 GFP-LC3-RFP-LC3ΔG

Although RFP/mCherry is resistant to acidic conditions, its fluorescence will still be quenched due to the degradation by lysosome, which makes it difficult to access cumulative degradation of an autophagic substrate even with RFP/mCherry-GFP-LC3. To deal with this, another fluorescence probe, GFP-LC3-RFP-LC3ΔG, has been developed (Kaizuka et al. 2016). When autophagy is activated, Atg4 cleaves LC3 precursor to form LC3-I with an exposed glycine residue at C-terminus. LC3-I further undergoes PE conjugation and converts to LC3-II which is recruited to autophagosomes (Fig. 8.4a). In GFP-LC3-RFP-LC3ΔG, GFP-LC3 is fused to the N terminus of RFP-LC3 whose C-terminal glycine is deleted (Kaizuka et al. 2016). When expressed in cells, GFP-LC3-RFP-LC3ΔG is separated into equimolar amounts of GFP-LC3 and RFP-LC3ΔG by endogenous Atg4 proteases. GFP-LC3 localizes to the autophagosomes and is further quenched in lysosomes, while RFP-LC3ΔG stably exists in the cytoplasm due to a lack of PE lipidation (Fig. 8.4b). Thus, RFP-LC3ΔG here serves as an internal control and helps to determine whether the reduction in the GFP intensity is due to autophagy activation or to the decrease of protein synthesis. Autophagic flux can be quantitatively monitored by calculating the GFP/RFP ratio whose reduction reflects an increase of autophagic degradation.

8.3.2 *Live-Cell Imaging of Lysosomes*

The detection of lysosome morphology is also widely employed in autophagy research. However, unlike LC3, lysosomes alone cannot be used to measure the activation of autophagy since the number and size of lysosomes also responds to non-autophagic pathways (Fogel et al. 2012). Thus, lysosomes are usually co-labelled with other autophagy-related proteins to interpret the maturity of autophagosomes or with autophagic substrates to clarify selective autophagy.

8.3.2.1 Acidotropic Dyes

Acidotropic dyes, such as monodansylcadaverine, acridine orange, Neutral Red, LysoSensor Blue, and LysoTracker Red, identify acidified vesicular compartments and therefore can label lysosomes. However, this method cannot distinguish

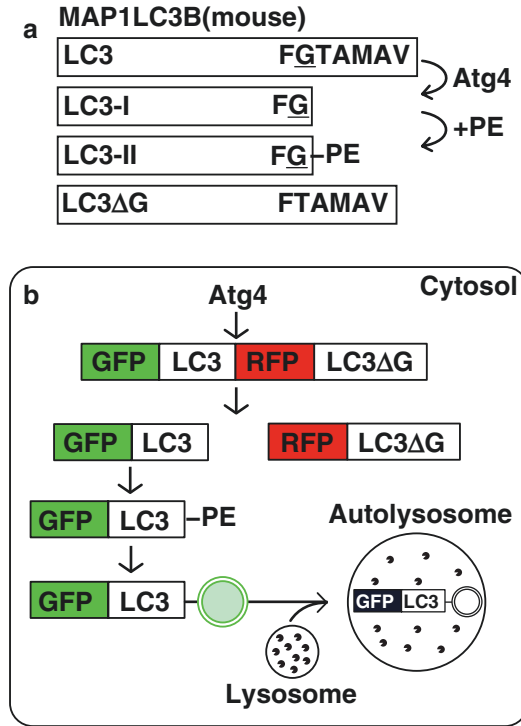


Fig. 8.4 Schematic representation of GFP-LC3-RFP-LC3ΔG. (a). When autophagy is activated, Atg4 cleaves LC3 precursor to form LC3-I with an exposed glycine residue at C-terminus. LC3-I further undergoes PE conjugation and converts to LC3-II. In RFP-LC3ΔG, the glycine residue at C-terminus is deleted. (b) When expressed in cells, GFP-LC3-RFP-LC3ΔG is separated into equimolar amounts of GFP-LC3 and RFP-LC3ΔG by endogenous Atg4 proteases. GFP-LC3 localizes to the autophagosomes and is further quenched in lysosomes, while RFP-LC3ΔG stably exists in the cytoplasm due to a lack of PE lipidation

endosomes, amphisomes, lysosomes, and other acidified organelles and have been gradually replaced by other methods.

8.3.2.2 GFP-Lamp1/Lamp2

Lysosome-associated membrane protein-1 (LAMP-1) and LAMP-2 account for about half of the lysosomal membrane protein (Hunziker et al. 1996) and are the most widely used lysosome marker (Kornfeld and Mellman 1989). Fluorescent protein-fused Lamp-1/2 is useful for indicating the maturity of autophagosomes and monitoring selective autophagy when used in conjunction with other autophagosome or substrate markers.

8.3.3 *Markers for Special Autophagic Stages*

The process of autophagy can be generally divided into the following stages according to the maturity of the autophagosome: phagophore, sealed autophagosome, amphisome, and autolysosome. Different stages of the autophagic process involve different autophagy-related proteins. Some of these proteins localize to autophagosomes for just one particular period of time, which helps in the interpretation of the maturity of autophagosomes. However, the majority of these proteins lack commercial antibodies with high specificity, making live-cell imaging necessary for detection. Here, we introduce some protein markers for different stages of autophagic process.

8.3.3.1 **Phagophore**

Atg5, Atg12, Atg14, and Atg16L1 can serve as phagophore markers. Atg5, Atg12, and Atg16L1 form a protein complex which is critical for the elongation of the phagophore. Downstream inhibition due to LC3/GABARAP deficiency results in an accumulation of the phagophore-associated ATG5, ATG12, and ATG16L1 puncta (Mikhaylova et al. 2012). During autophagosome biogenesis in axons, Atg5 localizes to punctate structure before LC3, and its signal decays from nascent autophagosomes after LC3 translocation (Maday and Holzbaur 2014). Similarly, ATG16L1 is located on phagophores rather than completed autophagosomes (Mizushima et al. 2003; Ravikumar et al. 2010). However, ATG14 is not recruited exclusively to phagophores and can also localize on mature autophagosomes as well as the ER (Fan et al. 2011; Matsunaga et al. 2010). Accordingly, ATG14 should be used in combination with other phagophore and autophagosome markers.

In addition, the ER population of zinc finger FYVE-type containing 1 (ZFYVE1) marks the site of omegasome (Axe et al. 2008) from which phagophores form.

8.3.3.2 **Sealed Autophagosomes**

Numerous proteins including LC3 and WIPI1/2 localize to autophagosomes; however, their punctate signal cannot distinguish elongating phagophores or sealed autophagosomes. Under such circumstances, combination of LC3 and phagophore markers can be employed, and the dissociation of phagophore markers indicates the sealed autophagosomes (Maday and Holzbaur 2014). Additionally, STX17 can serve as a marker of sealed autophagosomes since it is recruited to completely sealed autophagosomes but not to phagophores or autolysosomes (Itakura et al. 2012; Klionsky et al. 2016; Takats et al. 2013).

8.3.3.3 Amphisome and Autolysosome

The autolysosome is produced by the fusion of an autophagosome with a lysosome. Similarly, the convergence of macroautophagy and endocytosis generates an amphisome that further results in an autolysosome upon fusion with a lysosome (Hytinen et al. 2013). Thus, amphisomes and autolysosomes can be labelled by LC3 in combination with endosome markers (such as Rab7) or lysosome marker (such as Lamp-1) (Jager et al. 2004). In addition, tectonin beta-propeller repeat containing 1 (TECPR1) plays a role in autophagosome-lysosome fusion (Chen et al. 2012), thus marking lysosomes and autolysosomes (Klionsky et al. 2016).

8.3.4 Live-Cell Imaging for Selective Autophagy

Selective autophagy refers to the process by which a certain type of substrate is degraded through the autophagy pathway. Accumulated lines of evidence suggest that selective autophagy plays an important role in a variety of physiological and pathological conditions. Selective autophagy can be divided into many subtypes according to diverse substrates, such as mitophagy, ER-phagy, and pexophagy. Although autophagic substrates differ, the observation of different selective autophagic pathways shares some common methods. Here we summarize some strategies for detecting selective autophagy.

8.3.4.1 Co-localization with Atg8 Family Proteins

During selective autophagy activation, substrate of interest is co-localized with Atg8 family members in both transversal and orthogonal views or surrounded by a ringlike structure of Atg8 (Fig. 8.5). Noteworthy, different Atg8 family members

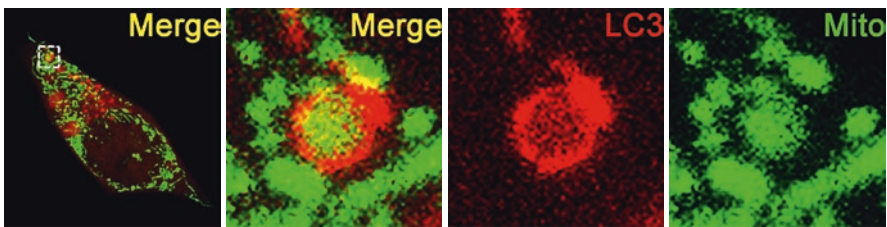


Fig. 8.5 Monitoring mitophagy in Neuro2a cells with confocal microscope. Neuro2a cells were transfected with mCherry-LC3 and MitoGFP to label autophagosomes and mitochondria, respectively. After subjection to hypoxia, mitochondria are engulfed by LC3 puncta, indicating the activation of mitophagy. Scale bar: 2 μ m

should be chosen dependent on their affinity with the substrates. For example, Bnip3L shows stronger interaction with LC3A and GABARAP than LC3B (Novak et al. 2010). Thus, fluorescent protein-fused LC3A or GABARAP should be considered when studying Bnip3L-induced mitophagy.

8.3.4.2 Co-localization with Lysosomes

The co-localization of substrates with lysosomes implies the degradation of the substrate in lysosomes. However, in some cases, the contact between substrates and lysosomes can be induced by non-autophagic pathways. For example, lysosomes interact with mitochondria to mediate mitochondrial fission in HeLa cells (Wong et al. 2018). Thus, the combination of various methods is necessary for the proper interpretation of selective autophagy.

8.3.4.3 pH-Sensitive Fluorescent Probe

Some fluorescent proteins show different spectral properties depending on environmental pH. When fused with a substrate-targeting sequence, the change in the spectral properties of the probe indicates the translocation of the substrate into lysosomes. For example, the red fluorescent protein Keima has a bimodal excitation spectrum peaking at 440 and 586 nm corresponding to the neutral and acidic conditions, respectively, while its emission spectrum peaks at 620 nm (Violot et al. 2009). Thus, mitochondria-targeted Keima (mtKeima) can be employed to detect mitophagy (Katayama et al. 2011). Similarly, MitoQC, an mCherry-GFP tandem fluorescent probe which is fused with mitochondrial targeting sequence, has been developed to monitor mitophagy by taking advantage of weak acid resistance of GFP (Allen et al. 2013).

8.3.4.4 Changes in the Distribution of Key Proteins

In some cases, selective autophagy activation can be indicated by translocation of certain proteins. For example, the loss of mitochondrial membrane potential induces recruitment of Parkin to mitochondria, which triggers the downstream pathway of mitophagy (Youle and Narendra 2011). Thus, the mitochondrial translocation of Parkin reflects the activation of Parkin-mediated mitophagy. Similarly, p62 is recruited to peroxisomes to execute pexophagy (Zhang et al. 2015). Noteworthy, this approach may only be suitable for indicating the activation of certain protein-dependent selective autophagy pathways; a combination of other methods is required for examining general selective autophagy.

8.4 Monitoring Autophagy in Living Animals

Monitoring autophagy *in vivo* is necessary for further investigating the role of autophagy in a variety of physiological and pathological conditions. The biggest obstacle to imaging in living animals is large image depths. Under such circumstances, two-photon excitation microscopy is employed in preference to confocal microscopy. In addition, two-photon microscopy reduces phototoxicity incurred throughout the live samples compared with confocal microscopy. Two-photon microscopy has been reported for visualizing autophagosomes in the cells of retrosplenial dysgranular cortex (RSD) or cerebellar cortex in living mice (Chen et al. 2015). In this study, the cells in RSD and cerebellar cortex were transfected with lentiviral vector expressing EGFP-LC3, and 20 days after virus injection, the mice were investigated by two-photon microscopy with the thin-skull method. In both areas, clustered EGFP-positive vesicles and dispersed fine EGFP-positive dots could be observed, and these structures were further confirmed to be autophagosomes by immunostaining with anti-Lamp-2 antibodies (Chen et al. 2015).

When performing two-photon microscope imaging, virus injection may be necessary for overexpression of fluorescent protein-fused proteins. Inappropriate administration of virus injection results in excessive bleeding and inflammation, both of which undermine the quality of two-photon microscope imaging. In addition, two-photon microscopy has lower spatial resolution than conventional confocal microscope, although it exhibits deeper tissue penetration (<1000 μm) and less phototoxicity. Furthermore, it is difficult to avoid cross talk between fluorophores due to broad excitation bands in two-photon microscope. These disadvantages limit the applicability of two-photon microscope in selective autophagy research. Fortunately, more fluorophores suitable for two-photon imaging have been made available, and a variety of two-photon fluorescent dyes targeting lysosomes have been reported (Jiang et al. 2017; Hou et al. 2018; He et al. 2014), which may contribute to the investigation of autophagy.

Apart from two-photon imaging, macro-zoom fluorescence microscopy has also been employed to observe the activation of autophagy in the whole brain of GFP-LC3 transgenic mice (Tian et al. 2010). In addition, the utilization of model organisms, including *Drosophila*, *C. elegans*, and zebrafish, may help to simplify the detection of autophagy with the use of fluorescence or confocal microscope (Zhou et al. 2015; Xu et al. 2019).

8.5 Perspectives

Advances in optical microscopy techniques have broadened our horizons at scales from a single molecule to tissues. During the last decade, various super-resolution imaging techniques, such as structured illumination microscopy (SIM), stimulated emission depletion microscopy (STED), and stochastic optical reconstruction

microscopy (STORM), have been established to achieve a higher resolution than that imposed by the diffraction limit. The applications of super-resolution methods in the area of autophagy have been considered and have advanced our knowledge of autophagy machinery (Karanasios 2019; Mohan et al. 2019; Ligeon et al. 2015; Graef et al. 2013). The development of novel fluorescent proteins (such as pHRed, Keima, and Dendra2), has allowed the temporal and spatial characteristics of autophagy to be further clarified. In addition, thanks to the deeper understanding of autophagy machinery, more and more biomarkers are available, which promotes in turn the detection of autophagy. However, there are still some bottlenecks in the observation of autophagy with optical microscopy. For example, antibodies against autophagy markers for IHC need further optimization, and fluorescent probes with high specificity and low toxicity are still lacking. What is more, the roles of autophagy need further clarification in living animals. Taken together, breakthroughs in the detection of autophagy will undoubtedly shed light on the molecular mechanisms of autophagy and its roles under physical and pathological conditions.

References

- Adhami F, Schloemer A, Kuan CY. The roles of autophagy in cerebral ischemia. *Autophagy*. 2007;3(1):42–4.
- Allen GFG, Toth R, James J, Ganley IG. Loss of iron triggers PINK1/Parkin-independent mitophagy. *EMBO Rep*. 2013;14(12):1127–35. <https://doi.org/10.1038/embor.2013.168>.
- Axe EL, Walker SA, Manifava M, Chandra P, Roderick HL, Habermann A, Griffiths G, Ktistakis NT. Autophagosome formation from membrane compartments enriched in phosphatidylinositol 3-phosphate and dynamically connected to the endoplasmic reticulum. *J Cell Biol*. 2008;182(4):685–701. <https://doi.org/10.1083/jcb.200803137>.
- Chen DD, Fan WL, Lu YT, Ding XJ, Chen S, Zhong Q. A mammalian autophagosome maturation mechanism mediated by TECPR1 and the Atg12-Atg5 conjugate. *Mol Cell*. 2012;45(5):629–41. <https://doi.org/10.1016/j.molcel.2011.12.036>.
- Chen X, Kondo K, Motoki K, Homma H, Okazawa H. Fasting activates macroautophagy in neurons of Alzheimer's disease mouse model but is insufficient to degrade amyloid-beta. *Sci Rep*. 2015;5:12115. <https://doi.org/10.1038/srep12115>.
- Fan W, Nassiri A, Zhong Q. Autophagosome targeting and membrane curvature sensing by Barkor/Atg14(L). *Proc Natl Acad Sci U S A*. 2011;108(19):7769–74. <https://doi.org/10.1073/pnas.1016472108>.
- Fogel JL, Thein TZT, Mariani FV. Use of LysoTracker to detect programmed cell death in embryos and differentiating embryonic stem cells. *J Vis Exp*. 2012;(68):4254. <https://doi.org/10.3791/4254>.
- Graef M, Friedman JR, Graham C, Babu M, Nunnari J. ER exit sites are physical and functional core autophagosome biogenesis components. *Mol Biol Cell*. 2013;24(18):2918–31. <https://doi.org/10.1091/mbc.E13-07-0381>.
- He L, Tan CP, Ye RR, Zhao YZ, Liu YH, Zhao Q, Ji LN, Mao ZW. Theranostic iridium(III) complexes as one- and two-photon phosphorescent trackers to monitor autophagic lysosomes. *Angew Chem Int Edit*. 2014;53(45):12137–41. <https://doi.org/10.1002/anie.201407468>.
- Hou LL, Ning P, Feng Y, Ding YQ, Bai L, Li L, Yu HZ, Meng XM. Two-photon fluorescent probe for monitoring autophagy via fluorescence lifetime imaging. *Anal Chem*. 2018;90(12):7122–6. <https://doi.org/10.1021/acs.analchem.8b01631>.

- Hunziker W, Simmen T, Honing S. Trafficking of lysosomal membrane proteins in polarized kidney cells. *Nephrologie*. 1996;17(7):347–50.
- Hyttinen JMT, Niittykoski M, Salminen A, Kaarniranta K. Maturation of autophagosomes and endosomes: a key role for Rab7. *BBA-Mol Cell Res*. 2013;1833(3):503–10. <https://doi.org/10.1016/j.bbamcr.2012.11.018>.
- Itakura E, Kishi-Itakura C, Mizushima N. The hairpin-type tail-anchored SNARE syntaxin 17 targets to autophagosomes for fusion with endosomes/lysosomes. *Cell*. 2012;151(6):1256–69. <https://doi.org/10.1016/j.cell.2012.11.001>.
- Jager S, Bucci C, Tanida I, Ueno T, Kominami E, Saftig P, Eskelinen EL. Role for Rab7 in maturation of late autophagic vacuoles. *J Cell Sci*. 2004;117(20):4837–48. <https://doi.org/10.1242/jcs.01370>.
- Jiang JC, Tian XH, Xu CZ, Wang SX, Feng Y, Chen M, Yu HZ, Zhua MZ, Meng XM. A two-photon fluorescent probe for real-time monitoring of autophagy by ultrasensitive detection of the change in lysosomal polarity. *Chem Commun*. 2017;53(26):3645–8. <https://doi.org/10.1039/c7cc00752c>.
- Kaizuka T, Morishita H, Hama Y, Tsukamoto S, Matsui T, Toyota Y, Kodama A, Ishihara T, Mizushima T, Mizushima N. An autophagic flux probe that releases an internal control. *Mol Cell*. 2016;64(4):835–49. <https://doi.org/10.1016/j.molcel.2016.09.037>.
- Karanasios E. Correlative live-cell imaging and super-resolution microscopy of autophagy. *Methods Mol Biol*. 2019;1880:231–42. https://doi.org/10.1007/978-1-4939-8873-0_15.
- Katayama H, Kogure T, Mizushima N, Yoshimori T, Miyawaki A. A sensitive and quantitative technique for detecting autophagic events based on lysosomal delivery. *Chem Biol*. 2011;18(8):1042–52. <https://doi.org/10.1016/j.chembiol.2011.05.013>.
- Kimura S, Noda T, Yoshimori T. Dissection of the autophagosome maturation process by a novel reporter protein, tandem fluorescent-tagged LC3. *Autophagy*. 2007;3(5):452–60.
- Klionsky D, et al. Guidelines for the use and interpretation of assays for monitoring autophagy (3rd edition) (vol 12, pg 1, 2015). *Autophagy*. 2016;12(2):443. <https://doi.org/10.1080/15548627.2016.1147886>.
- Kornfeld S, Mellman I. The biogenesis of lysosomes. *Annu Rev Cell Biol*. 1989;5:483–525. <https://doi.org/10.1146/annurev.cb.05.110189.002411>.
- Ligeon LA, Barois N, Werkmeister E, Bongiovanni A, Lafont F. Structured illumination microscopy and correlative microscopy to study autophagy. *Methods*. 2015;75:61–8. <https://doi.org/10.1016/j.ymeth.2015.01.017>.
- Maday S, Holzbaur EL. Autophagosome biogenesis in primary neurons follows an ordered and spatially regulated pathway. *Dev Cell*. 2014;30(1):71–85. <https://doi.org/10.1016/j.devcel.2014.06.001>.
- Martinet W, De Meyer GR, Andries L, Herman AG, Kockx MM. In situ detection of starvation-induced autophagy. *J Histochem Cytochem*. 2006;54(1):85–96. <https://doi.org/10.1369/jhc.5A6743.2005>.
- Martinet W, Schrijvers DM, Timmermans JP, Bult H, De Meyer GR. Immunohistochemical analysis of macroautophagy: recommendations and limitations. *Autophagy*. 2013;9(3):386–402. <https://doi.org/10.4161/auto.22968>.
- Matsunaga K, Morita E, Saitoh T, Akira S, Ktistakis NT, Izumi T, Noda T, Yoshimori T. Autophagy requires endoplasmic reticulum targeting of the PI3-kinase complex via Atg14L. *J Cell Biol*. 2010;190(4):511–21. <https://doi.org/10.1083/jcb.200911141>.
- Mikhaylova O, Stratton Y, Hall D, Kellner E, Ehmer B, Drew AF, Gallo CA, Plas DR, Biesiada J, Meller J, Czyzyk-Krzeska MF. VHL-regulated MiR-204 suppresses tumor growth through inhibition of LC3B-mediated autophagy in renal clear cell carcinoma. *Cancer Cell*. 2012;21(4):532–46. <https://doi.org/10.1016/j.ccr.2012.02.019>.
- Mizushima N, Kuma A, Kobayashi Y, Yamamoto A, Matsubae M, Takao T, Natsume T, Ohsumi Y, Yoshimori T. Mouse Apg16L, a novel WD-repeat protein, targets to the autophagic isolation membrane with the Apg12-Apg5 conjugate. *J Cell Sci*. 2003;116(9):1679–88. <https://doi.org/10.1242/jcs.00381>.

- Mohan N, Sorokina EM, Verdeny IV, Alvarez AS, Lakadamyali M. Detyrosinated microtubules spatially constrain lysosomes facilitating lysosome-autophagosome fusion. *J Cell Biol.* 2019;218(2):632–43. <https://doi.org/10.1083/jcb.201807124>.
- Novak I, Kirkin V, McEwan DG, Zhang J, Wild P, Rozenknop A, Rogov V, Lohr F, Popovic D, Occhipinti A, Reichert AS, Terzic J, Dotsch V, Ney PA, Dikic I. Nix is a selective autophagy receptor for mitochondrial clearance. *EMBO Rep.* 2010;11(1):45–51. <https://doi.org/10.1038/embor.2009.256>.
- Patterson GH, Knobel SM, Sharif WD, Kain SR, Piston DW. Use of the green fluorescent protein and its mutants in quantitative fluorescence microscopy. *Biophys J.* 1997;73(5):2782–90. [https://doi.org/10.1016/S0006-3495\(97\)78307-3](https://doi.org/10.1016/S0006-3495(97)78307-3).
- Ravikumar B, Moreau K, Jahreiss L, Puri C, Rubinsztein DC. Plasma membrane contributes to the formation of pre-autophagosomal structures (vol 12, pg 747, 2010). *Nat Cell Biol.* 2010;12(10):1021. <https://doi.org/10.1038/ncb1010-1021c>.
- Rosenfeldt MT, Nixon C, Liu E, Mah LY, Ryan KM. Analysis of macroautophagy by immunohistochemistry. *Autophagy.* 2012;8(6):963–9. <https://doi.org/10.4161/auto.20186>.
- Szalai P, Hagen LK, Saetre F, Luhr M, Sponheim M, Overbye A, Mills IG, Seglen PO, Engedal N. Autophagic bulk sequestration of cytosolic cargo is independent of LC3, but requires GABARAPs. *Exp Cell Res.* 2015;333(1):21–38. <https://doi.org/10.1016/j.yexcr.2015.02.003>.
- Takats S, Nagy P, Varga A, Piracs K, Karpati M, Varga K, Kovacs AL, Hegedus K, Juhasz G. Autophagosomal Syntaxin17-dependent lysosomal degradation maintains neuronal function in *Drosophila*. *FEBS J.* 2013;280:269.
- Tian FF, Deguchi K, Yamashita T, Ohta Y, Morimoto N, Shang JW, Zhang XM, Liu N, Ikeda Y, Matsuura T, Abe K. In vivo imaging of autophagy in a mouse stroke model. *Autophagy.* 2010;6(8):1107–14. <https://doi.org/10.4161/auto.6.8.13427>.
- Violot S, Carpentier P, Blanchoin L, Bourgeois D. Reverse pH-dependence of chromophore protonation explains the large Stokes shift of the red fluorescent protein mKeima. *J Am Chem Soc.* 2009;131(30):10356–7. <https://doi.org/10.1021/ja903695n>.
- Weidberg H, Shvets E, Shpilka T, Shimron F, Shinder V, Elazar Z. LC3 and GATE-16/GABARAP subfamilies are both essential yet act differently in autophagosome biogenesis. *EMBO J.* 2010;29(11):1792–802. <https://doi.org/10.1038/emboj.2010.74>.
- Wong YC, Ysselstein D, Krainc D. Mitochondria-lysosome contacts regulate mitochondrial fission via RAB7 GTP hydrolysis. *Nature.* 2018;554(7692):382–6. <https://doi.org/10.1038/nature25486>.
- Xu J, Su T, Tokamov SA, Fehon RG. Live imaging of hippo pathway components in *Drosophila* imaginal discs. *Methods Mol Biol.* 2019;1893:53–9. https://doi.org/10.1007/978-1-4939-8910-2_4.
- Youle RJ, Narendra DP. Mechanisms of mitophagy. *Nat Rev Mol Cell Biol.* 2011;12(1):9–14. <https://doi.org/10.1038/nrm3028>.
- Zhang JW, Tripathi DN, Jing J, Alexander A, Kim J, Powell RT, Dere R, Tait-Mulder J, Lee JH, Paull TT, Pandita RK, Charaka VK, Pandita TK, Kastan MB, Walker CL. ATM functions at the peroxisome to induce pexophagy in response to ROS. *Nat Cell Biol.* 2015;17(10):1259–69. <https://doi.org/10.1038/ncb3230>.
- Zhou YF, Wang Q, Song B, Wu SC, Su YY, Zhang HM, He Y. A real-time documentation and mechanistic investigation of quantum dots-induced autophagy in live *Caenorhabditis elegans*. *Biomaterials.* 2015;72:38–48. <https://doi.org/10.1016/j.biomaterials.2015.08.044>.

Chapter 9

Autophagic Flux Detection: Significance and Methods Involved



Xiao-Wei Zhang, Xiao-Xi Lv, Ji-Chao Zhou, Cai-Cai Jin, Lu-Yao Qiao, and Zhuo-Wei Hu

Abstract Macroautophagy is an important biological process in eukaryotic cells by which longevity proteins, misfolded proteins, and damaged organelles are degraded. The autophagy process consists of three key steps: (1) the formation of autophagosomes; (2) the fusion of the autophagosomes with lysosomes; and (3) the degradation of the contents of autolysosomes. If any of the three steps is impaired, autophagy will not be able to complete its biological function. Dysfunctional or blocked autophagy is closely involved in the pathogenesis of a variety of diseases. The accurate determination of the autophagy activity *in vivo* and *in vitro* has become a challenge in the field of autophagy research. At present, the most widely used detection method to determine autophagy activity in mammalian cells is to quantify LC3B in the cells by Western blot, or to observe the formation and changes of autophagosomes and autolysosomes by immunofluorescence and electron microscopy. However, ignoring the dynamic characteristics of autophagy and only evaluating the number of autophagosomes or the presence of LC3B cannot completely reflect the activation or a blockage of the autophagy system, and objectively analyze its real role in the occurrence and development of a disease. For example, the accumulation of autophagosomes and autolysosomes can occur through an increase in substrate to be degraded after the activation of autophagy, or it may be caused by the partial obstruction or blockage of autophagy. In this chapter, new and familiar ways to detect the autophagic flux are methodically summarized to provide researchers with a multi-angled viewpoint.

Keywords Autophagic flux · Cargo sequestration assay · LC3B · SQSTM1/p62 · TEM

Xiao-Wei Zhang and Xiao-Xi Lv contributed equally to this work

X.-W. Zhang · X.-X. Lv · J.-C. Zhou · C.-C. Jin · L.-Y. Qiao · Z.-W. Hu (✉)
Institute of Materia Medica, Chinese Academy of Medical Sciences and Peking Union Medical College, Beijing, China
e-mail: zhxw@imm.ac.cn; lvxiaoxi@imm.ac.cn; zhoujichao@imm.ac.cn;
jincaicai@imm.ac.cn; qiaoluyao@imm.ac.cn; huzhuowei@imm.ac.cn

Abbreviations

3-MA	3-Methyladenine
BHMT	Betaine-homocysteine methyltransferase
FRET	Fluorescence resonance energy transfer
GFP	Green fluorescent proteins
LDH	Lactate dehydrogenase
LIR	LC3-interaction region
LRS	LC3 recognition sequence
PB1	Phox and Bem1
RFPs	Red fluorescent proteins
TCA	Trichloroacetic acid
TEM	Transmission electron microscopy
UBA	Ubiquitin-associated domain

With the development of knowledge about the molecular mechanisms and functions of autophagy, researchers have realized that autophagic flux disorders can cause a malfunction of the degradation of certain pathogenic proteins, which may be an important mechanism for the development of illnesses such as neurodegenerative diseases, tumors, muscle diseases, cardiovascular diseases, autoimmune diseases, and tissue fibrosis. The key step in the ultimate biological effect of autophagy is the fusion of autophagosomes with lysosomes, which in turn form autolysosomes that degrade the contents of their encapsulation. This process is collectively referred to as autophagic flux. The activation or the obstruction of the autophagic flux can result in distinct biological effects. The detection of the autophagic flux is complicated. It is often impossible to systematically detect autophagic flux by using one of the existing technical methods alone. A combination of a variety of different methods to comprehensively evaluate the activation or obstruction of autophagy is a more objective strategy (Klionsky et al. 2016). At present, the main autophagic flux detection methods include the analysis of the presence of LC3B-II and other autophagy/lysosomal pathway-related proteins, the detection of the autophagic substrate protein SQSTM1/p62, the degradation analysis of autophagy-dependent long-lived proteins, dynamic transmission electron microscopy, cargo sequestration assays, and others. A comprehensive application of these methods can ensure a multi-angle scanning on the occurrence and development of autophagy. In this chapter, we will review the methods that are used to detect the autophagic flux and their significance.

9.1 Evaluating the Presence of LC3B-II and Other Autophagy/Lysosomal Pathway-Associated Proteins in the Cell, to Analyze Autophagic Flux

9.1.1 Detection Methods Using LC3B Protein

The genetic homology of mammalian *LC3B* is as high as 94%, which reflects the conservation and the importance of autophagy in the evolution. The total amount of LC3B in mammalian cells does not fluctuate greatly. Usually, due to lysosomal degradation, only LC3B-I is converted to LC3B-II or LC3B-II is reduced relative to LC3B-I, both of which reflect the existence of autophagic flux. The detection of LC3B-I or LC3B-II alone does not represent the presence of autophagic flux. It is necessary to observe the dynamic changes of the two forms to determine the true activity of autophagy. Western blot is the most common method for the detection of LC3B, and it is also the most important method used to distinguish LC3B-I from LC3B-II. However, many details determine whether the Western blot experiment correctly reflects the autophagic flux state. It is generally believed that LC3B-I is converted to LC3B-II, or that an increased LC3B-II content represents the activation of autophagic flux, while a decreased LC3B-II content represents an inhibition of autophagy. However, there may be two reasons for a decrease in LC3B-II. One is a blockage of autophagic flux, that is, LC3B-I cannot be converted to LC3B-II; the other is the overactivation of autophagic flux, and the clearance of LC3B-II by autophagic lysosomes. In these cases, similar results will be obtained in the Western blot, but they represent distinct biological endpoints. Therefore, how to interpret the differing amounts of the two forms of LC3B, made visible via Western blot, is the key to the determination of autophagic flux activation (Barth et al. 2010).

It is worth noting that there are many technical challenges in the detection of LC3B by Western blot. For example, the choice of antibodies is a determinant of the success of the experiment. Some antibodies have differing binding abilities to the two forms of LC3B, which may result in LC3B-I being difficult to detect. Furthermore, the protein stability of LC3B-I is inferior to LC3B-II, and it is reduced by repeated freeze-thaw cycles or storage in a buffer containing SDS. Therefore, it is necessary to prepare a fresh sample when detecting LC3B-I, and complete the test as soon as possible. When performing Western blot analysis, PVDF is the preferred material used to detect LC3B-II compared to NC, probably due to the different affinity of these two materials for hydrophobic proteins. The use of siRNA for gene interference tends to have little impact on autophagy activity of cells. However, stimulation with the agents used for the transfection with shRNA or overexpression plasmids often results in significant changes in autophagy activity, thus distorting the endpoint.

In addition to the Western blot technique, LC3B protein can be detected by immunofluorescence and flow cytometry. Both assays require labeling with fluorescent dyes or fluorescent proteins. The advantage of immunofluorescence is that point-like aggregations of LC3B can be observed, while flow cytometry can analyze the amount of LC3B present, in a large number of single cells. However, neither of these methods can distinguish between LC3B-I and LC3B-II, and only the total amount of LC3B can be observed. The use of fluorescence for LC3B labeling requires consideration of changes in intracellular pH, which will be explained in detail later.

Changes in the fluorescence intensity of LC3B are usually observed when using flow cytometry to observe the LC3B content in cells (Demishtein et al. 2015). EGFP-LC3B, as a substrate for autophagy, is often used to detect autophagic flux. Through different experimental procedures, flow cytometry can be used to distinguish intracellular free LC3B from bound LC3B, which helps to determine the state of autophagic flux. When the autophagic flux is activated, intracellular LC3B-I will be transformed into LC3B-II, and LC3B-II, which is localized on the surface of the autophagosome or the autolysosomal membrane, will gradually degrade with the activation of autophagy, and then a decreased fluorescence intensity of LC3B will be observed with the flow cytometer. However, since the production of LC3B-I is also increased after autophagy activation, the decrease in fluorescence intensity of LC3B is not very obvious. In order to observe significant fluorescence changes on the flow cytometer, it is necessary to damage the membranes of the cells by using saponin. Saponin produces micropores on the surface of the cell membrane. Since LC3B-I is dispersed in the cytoplasm in a free form, it will leak out of the cell after the cell is treated with saponin. However, LC3B-II mainly binds to the surface of autophagosomes and autolysosome membranes, and these structures cannot pass through the pores, due to their volume. The number of autophagosomes increases when the autophagic flux is activated. Thus, when the autophagic flux is activated, the saponin-treated cells have an increased fluorescence intensity (Fig. 9.1). However, when cells are treated with the autophagy inhibitor bafilomycin A1, the fluorescence intensity of the cells is also enhanced after saponin treatment (Ciechomska and Tolkovsky 2007).

9.1.2 Tools to Detect the Conversion of LC3B-I/LC3B-II in Pharmacological Studies

Also in pharmacological studies, the activity of the autophagic flux can be evaluated by detecting the conversion of LC3B-I to LC3B-II using a Western blot. The core of this assay is the correlation of LC3B-I with LC3B-II, and experiments should be performed to detect drug-associated changes in the LC3B-II conversion with or without the use of a saturating concentration of an autophagy inhibitor. When the autophagic flux is activated, the amount of LC3B-II is significantly increased, when

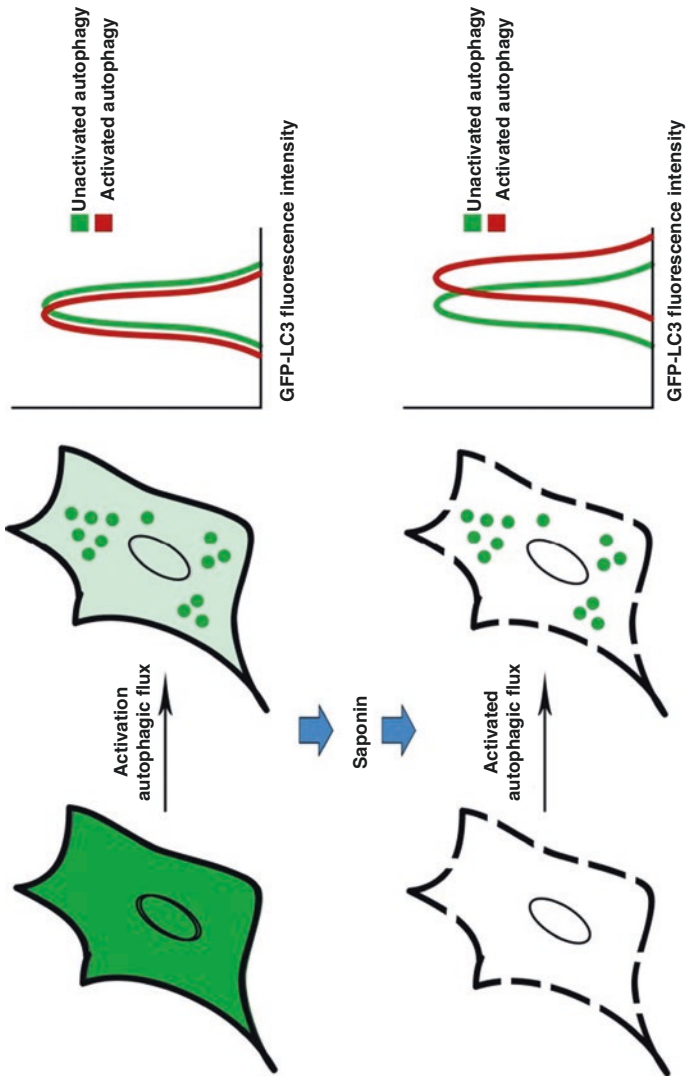


Fig. 9.1 Autophagic flux is detected by flow cytometry. The autophagosomes increase when the autophagic flux is activated. If the membrane rupture treatment is not performed, the fluorescence intensity of the cells is only slightly lowered. If LC3-I leaks out after rupture of saponin, LC3-II in the cells leads to an increase in fluorescence intensity after autophagy activation

autophagy inhibitors are used. Tools for inhibiting autophagy usually include protease inhibitors such as pepstatin A, E-64d, etc., which inhibit lysosomal degradation, or compound inhibitors such as bafilomycin A1, chloroquine, and ammonium chloride, which can alter the lysosomal pH which causes the inhibition of autophagy. Bafilomycin A1 also inhibits the fusion between autophagosomes and lysosomes. The knockdown or knockout of the lysosomal-associated membrane protein 2 (LAMP2) can also inhibit the fusion of autophagosomes and lysosomes, thereby blocking the autophagic flux.

Bafilomycin A1 is currently the most routinely used and recognized autophagy inhibitor, to detect the autophagic flux. Since bafilomycin A1 can effectively inhibit autophagic lysosomal degradation, the amount of LC3B-II detected by Western blot represents the total amount of synthetic autophagosomes and autolysosomes. If the amount of LC3B-II in the treatment condition (test drug + bafilomycin A1) is significantly increased compared to the control condition (only bafilomycin A1 treatment), this reveals that the tested drug increases the formation of autophagosomes or autolysosomes. Conversely, a decrease in LC3B-II compared to the control condition indicates that the treatment drug reduces the formation of autophagosomes (Fig. 9.2a).

Four experimental conditions are usually compared when an autophagic flux detection is implemented using bafilomycin A1. These are condition A, cells without treatment (blank); condition B, cells treated with bafilomycin A1 only; condition C, cells only treated with the drug that is tested; and condition D, cells that are treated with both bafilomycin A1 and the drug (combined treatment). The conversion of LC3B-I to LC3B-II in the untreated cells (condition A) compared to cells treated with the drug (condition C) represents the entire process of autophagic flux, namely, the formation of autophagosomes and the degradation of autophagosomes. The cells treated with bafilomycin A1 (condition B) and the cells that received the combined treatment (condition D) represent the level of the formation of autophagosomes. Therefore, the influence of the drug on the degradation of autophagosome can be partially determined by comparing the cells that have been treated with only the drug (condition C) to the cells that have received the combined treatment (condition D).

In Fig. 9.2b, the results are shown of an experiment that was carried out as described above. The figure demonstrates that the LC3B-II content in condition A (blank) < condition B (inhibitor) = condition C (drug) = condition D (combined). This means that the compound to be tested can reduce autophagosome degradation. Since the amount of LC3B-II in condition B (inhibitor) = condition D (combined treatment), it can be concluded that the test compound does not affect autophagosome formation. And since the amount of LC3B-II in condition A (blank) < condition C (drug), it can be concluded that the test compound inhibits the autophagic degradation without affecting the formation of autophagosomes. Confirming that the role of the tested drug lies solely in the degradation of autophagosomes, no difference in the amount of LC3B-II between condition C (drug) and condition D (combination) is observed (Fig. 9.2b).

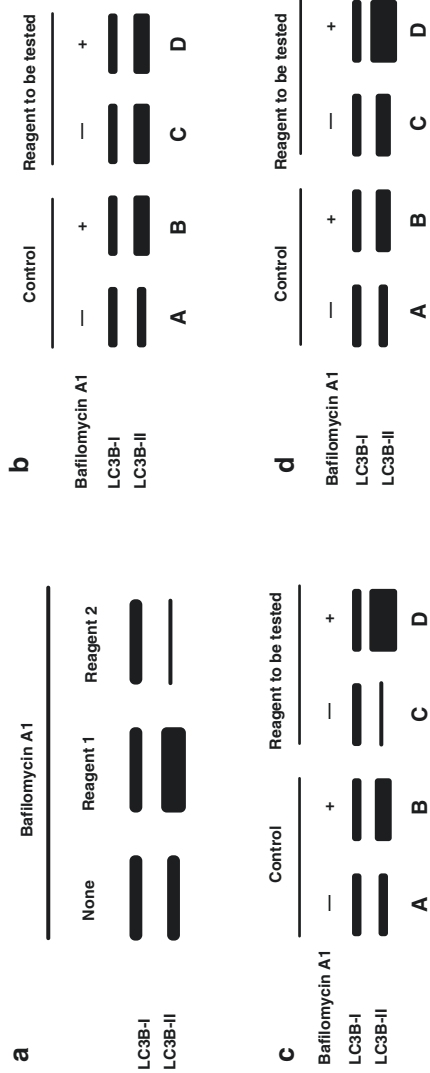


Fig. 9.2 The effect of the autophagy-regulating reagent is determined using Western blot. Detection of reagent 1 increases autophagosome formation, but reagent 2 inhibits autophagosome formation (a). The effect of autophagy-regulating reagent is determined using bafilomycin A1. The test reagent inhibits autophagosome degradation (b). The test reagent increases autophagosome formation and degradation (c). The test reagent increases autophagosome formation (d)

If the results show that the LC3B-II content in the condition C (drug) < condition A (blank) < condition B (inhibitor) < condition D (combination), this means that the test compound can increase the formation and degradation of autophagosomes. When LC3B-II in condition B (inhibitor) < condition D (combination), this indicates that the test compound can increase autophagosome formation; in the case that the test compound can increase autophagosome formation, LC3B-II content in condition C (drug) < condition A (blank), indicating the test compound can increase autophagosome degradation, so LC3B-II content can be observed as condition C (drug) < condition D (combination) (Fig. 9.2c).

If the results show that the LC3B-II content in condition A (blank) < condition B (inhibitor) = condition C (drug) < condition D (combination), this indicates that the test compound increases autophagosome formation. If the LC3B-II content in condition B (inhibitor) < condition D (combination), this indicates that the test compound increases the formation of autophagosomes; in the case that the test compound can increase the autophagosome formation, the LC3B-II content in condition A (blank) < condition C (drug) indicates that the test compounds have the potential to inhibit the degradation of autophagosomes. At this time, it is necessary to compare the difference of LC3B-II content between condition C (drug) and condition D (combination) and the difference of LC3B-II content between condition B (inhibitor) and condition D (combination). If the test compound inhibits autophagosome degradation, the LC3B-II content in condition D (combination)-condition C (drug) should be less than condition D (combination)-condition B (inhibitor); if the test compound only increases autophagosome formation, the LC3B-II content in condition D (combination)-condition C (drug) should be equal to condition D (combination)-condition B (inhibitor) (Fig. 9.2d).

It is usually easy to evaluate the autophagic flux via the above methods except in the last case. Due to the limited accuracy of Western blot experiments, it is difficult to observe whether the accurate LC3B-II content in condition D-condition C is equal to condition D-condition B. Even if there is an equal outcome, this may be an experimental error or a false-positive result. Therefore, it is easier to determine whether the test compound increases the formation of autophagosomes. If it is necessary to simultaneously detect whether it affects degradation, more careful experimentation is needed. When the cells to be detected are blocked in autophagic flux on a long term, due to genotypic changes or other factors, bafilomycin A1 can no longer cause an increase in the content of LC3B-II.

Alternatives for bafilomycin A1 may be useful under some conditions. Since bafilomycin A1 has a great influence on the content of LC3B-II, it may be hard to measure a complementary small effect of the tested drug. If the drug to be detected only weakly regulates autophagy, the change may be occluded by the large effect of bafilomycin A1. In addition, the treatment duration of bafilomycin A1 is critical. The half-life of autophagosomes is only 20–30 min. Usually, bafilomycin A1 completely blocks autophagy after 4 h of stimulation, and short-term bafilomycin A1 stimulation can also prevent the conversion of LC3B-II to LC3B-I in autolysosomes. Long-term (>8–12 h) stimulation with a saturating concentration of bafilomycin A1 is likely to affect the function of the ubiquitin-proteasome pathway as well. When a new autophagy-regulating drug is evaluated, changes in autophagic

flux should be observed for a long time, and multiple time points should be set for judgment. The alternatives for bafilomycin A1 all have their benefits and downsides. Pepstatin A, for example, is a hydrophobic molecule that needs to be dissolved in DMSO or ethanol, thus requiring longer (>8 h) and higher concentrations (>50 µg/mL) of stimulation. With E-64d, on the other hand, only 1 h of stimulation with a concentration of 10 µg/mL is required to inhibit lysosomal activity.

Special attention should be paid to autophagy studies involving viruses, using bafilomycin A1, ammonium chloride, or chloroquine. Since the above autophagy inhibitors inhibit autophagy activity by changing the pH of lysosomes, these drugs will also inhibit the endocytosis of the virus and the virus shelling.

9.1.3 Evaluating the Autophagy Activity by Detecting GFP-LC3B

9.1.3.1 The Construction of Chimeric LC3B

The construction of fluorescent protein tags is one of the most commonly used experimental methods in molecular biology and basic medicine. GFP, RFP, and mCherry are common fluorescent tag proteins. In conventional methods, these fluorescent tags are usually constructed on the C-terminus of the gene of interest, which does not affect the signal peptide function of the N-terminus of the target protein. However, there are strict principles when constructing LC3B fusion proteins. In most organs, LC3B has an extension sequence at the C-terminus, and the final form of LC3B is formed by hydrolysis of this C-terminal sequence by Atg4 protease. When the fluorescent tag is constructed at the C-terminus of LC3B (such as the LC3B-GFP form), the fluorescent tag is cleaved in the cytosol to form an LC3B fragment and a fluorescent tag fragment. This phenomenon can be verified by Western blot experiments, so LC3B-GFP is commonly used to detect the protein activity of Atg4. Another effective method for detecting Atg4 activity is to construct a luciferase reporter gene at the C-terminus of the LC3B protein. Atg4 activity can subsequently be detected by chemiluminescence. Thus, if LC3B is to be detected by a fluorescent fusion protein method, it is more feasible to link the fluorescent protein to the N-terminus of LC3B (such as the GFP-LC3B form).

9.1.3.2 Evaluating the Autophagic Flux by a GFP-LC3B Cleavage Assay

The GFP-LC3B fusion protein is one of the commonly used tools for performing an autophagic flux evaluation. After the GFP-LC3B protein enters autolysosomes, the LC3B portion is more sensitive to proteolytic enzymes in lysosomes than the GFP portion of the fusion protein. However, the lower pH (acidic environment) in the lysosome can cause quenching of the fluorescent signal of GFP, so the autophagic flux is evaluated by a combination of Western blot and immunofluorescence or flow cytometry. In experiments performed by Ni et al., it was demonstrated that the

intensity of green fluorescence in cells expressing GFP-LC3B was decreased when autophagy was activated and three bands of GFP-LC3B-I, GFP-LC3B-II, and GFP alone were detected by Western blot analysis using a GFP antibody. The LC3B antibody can also be used to detect the conversion of endogenous LC3B-I to LC3B-II in a sample (note that the molecular weights detected by Western blots may be different for LC3B antibodies provided by different antibody companies). It is worth noting that the GFP-labeled assay alone is limited to detecting a moderate activation of the autophagic flux and that the GFP band will disappear when the autophagic flux is overactivated. When autophagy is overactivated, the pH in the autolysosomes is further reduced, and its ability to degrade proteins is further enhanced, so the GFP protein is also gradually degraded. At this point, a partial autophagy inhibitor, such as ammonium chloride or chloroquine, is required to observe the GFP band. These drugs neutralize the acidic environment in lysosomes, and GFP bands can be detected in this case. If the GFP band is not observed, it may be either due to the blockage or the excessive activation of autophagic flux. If the presence of green fluorescence signal can be observed through FACS or microscopy, even though the GFP band is not observed via Western blot, this indicates that the fusion of the autophagosomes with lysosomes is blocked. The observation of GFP fluorescence requires consideration of GFP-LC3B protein synthesis, so there is a possibility that the decrease in green fluorescence is not obvious when autophagy is activated. Stimulation with autophagy inhibitors of different concentrations and durations can also effectively distinguish between activation and blockade of autophagic flux (Ni et al. 2011).

The most common methods that are used to activate autophagy are rapamycin stimulation and starvation using EBSS. However, the autophagy processes resulting from the two methods are reflected in quite different ways in the GFP-LC3B Western blot assay. In both cases, GFP fluorescence is quenched and LC3B protein is degraded. Unlike starvation, rapamycin is a mild autophagy activator. When rapamycin is used, a time- and concentration-dependent increase of single GFP bands can be observed via Western blot. However, after inducing autophagy via starvation, the cells require a large amount of endogenous protein to provide the nutrients for survival, so the pH in the lysosome decreases sharply, and the GFP protein is degraded and cannot be observed. However, an increased endogenous LC3B-II content is observed in starvation conditions.

Chloroquine is a commonly used autophagy inhibitor that can block the cellular autophagy activity in a dose-dependent manner. A separate GFP band is still observed when GFP-LC3B-overexpressing cells are treated with low concentrations of chloroquine (about 10 μM). This phenomenon is due to neither experimental error nor enhanced autophagy activity, but caused by the low concentration of chloroquine which partially blocks autophagy, and causes an increase of the pH in lysosomes. Meanwhile, partial autophagy activity can be retained to cause LC3B to degrade. When the chloroquine concentration exceeds 50 μM , the autophagy activity is completely inhibited, so that the GFP band will not be observed. Similarly, GFP bands can be observed with low concentrations of bafilomycin A1 (2.5 nM). This suggests that we need to go through a variety of different methods to get to the bottom of what is going on in the cells (Fig. 9.3).

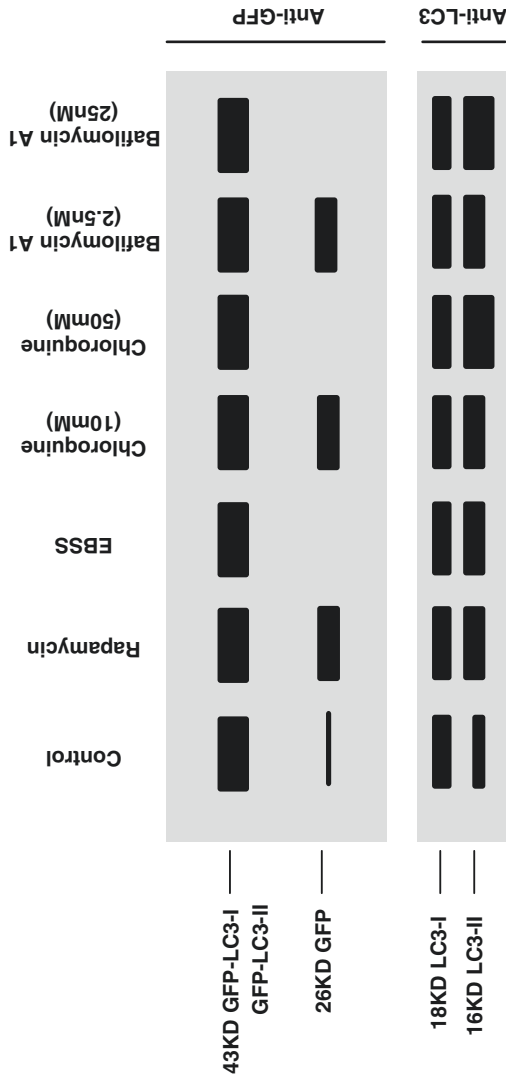


Fig. 9.3 The autophagic flux is detected by Western blot using the GFP-LC3 fusion protein. It can be detected using GFP and LC3 antibodies. After treatment with rapamycin, the activation of endogenous LC3-II by autophagic flux was observed, and a separate GFP band was observed. The autophagic flux was over-activated after culturing the cells with EBSS, and endogenous LC3-II was increased but no separate GFP band was observed. Autophagy was partially blocked with low concentrations of chloroquine or bafilomycin A1, and endogenous LC3-II was increased while a separate GFP band was observed. The use of high concentrations of chloroquine or bafilomycin A1 completely blocked the autophagic flux, and LC3-II was significantly aggregated without the ability to observe individual GFP bands

9.1.3.3 Evaluation of Autophagic Flux Using GFP-LC3B Fluorescence

When the autophagic flux is activated, GFP-LC3B-overexpressing cells will show intracellular GFP-LC3B aggregates under a fluorescence microscope. Calculating the number of GFP-LC3B spots per cell can be used to partially evaluate the activation level of autophagy. Unlike soluble LC3B-I in the cytosol, formed LC3B-II proteins bind to the outside of the autophagosomal membrane, and thus the characteristics of punctate aggregations appear, while LC3B-I in the cytoplasm shows only diffuse fluorescence under the fluorescence microscope. When autophagy is activated, the GFP-LC3B fusion protein is translocated to the autophagosome membrane, and a plurality of bright green fluorescent spots is formed under a fluorescence microscope. Each spot is equivalent to one autophagosome, and the autophagic activity can be partially evaluated by counting. In addition, we can use immunohistochemical methods to perform endogenous LC3B detection without manipulation on the genetic level. Unlike fluorescence microscopy, flow cytometry can be used to rapidly analyze the fluorescence intensity of multiple samples and quantify the fluorescence of GFP-LC3B in each cell, so it is commonly used for high-throughput detection of autophagy activity.

The detection of endogenous LC3B protein demands high requirements of the experimental system and necessitates operational accuracy. If the signal intensity generated by endogenous LC3B is lower than the detection limit, exogenous LC3B gene transfer is required. In this case, a stable transfection of the LC3B gene can reduce the intracellular fluorescence background values and also reduce the experimental bias due to transfection steps or transfection reagents. Usually, in stable transfections, cells are selected and cultured using monoclonal methods, so the intracellular fluorescence intensities can be maintained at the same level. However, the disadvantage of stable transfections with LC3B is that the fluorescence intensity is usually not as high as after transient transfections, and the gene integration site cannot be predicted. The greatest advantage of transiently transfecting cells with LC3B is that it can be used to rapidly express a large number of target genes in cells and thus in multigene co-transfection experiments.

Using fluorescence detection of LC3B requires more complicated processes and equipment than performing Western blots. However, both of these techniques have their advantages and disadvantages, and the combination of the two methods can often lead to more accurate experimental conclusions. It is worth noting that the observation of punctate aggregations of GFP-LC3B alone does not completely evaluate the autophagic flux state. For example, using the autophagy inhibitor bafilomycin A1 to stimulate GFP-LC3B-overexpressing cells can lead to significant LC3B fluorescent dot-like aggregation due to insufficient elimination by autophagosomes. If an immunofluorescence technique is used for detection, it will be found that in bafilomycin A1-induced cells, LC3B punctate aggregation is significantly stronger and brighter than in autophagy-activated cells. Although the GFP-LC3B bright spot volume can be observed and calculated by fluorescence microscopy, the accuracy is still limited.

In addition, an important issue in quantitative analysis of LC3B point aggregation using a fluorescence microscope is that subjective judgment is prone to occur. There is currently no precise standard for the definition of a point-like aggregation. The number of point-like aggregations can be analyzed either by the naked eye or by computer software. Although LC3B punctate aggregation is significantly increased when autophagy is induced, partial punctate aggregation also occurs in uninduced cells. Therefore, such indicators should not be used in determining the activation of autophagic flux, as LC3B punctate aggregation is observed in almost all cells. How to determine the threshold of the number of GFP-LC3B punctate aggregation during autophagy activation is a difficult point in this experiment, and the final result should be “the number of cells with GFP-LC3B punctate aggregation exceeding a certain threshold.” The second difficulty of this method is to distinguish between GFP-LC3B accumulation due to autophagic flux blockade and GFP-LC3B punctate aggregation upon autophagic flux activation (Tabata et al. 2013). Moreover, when the fusion protein of a foreign gene such as GFP-LC3B is overexpressed, the protein expression level may be too high, which may lead to a similar result, which often leads to deviation of the experimental conclusions (Fig. 9.4).

The LC3B punctate aggregation due to overexpression of GFP-LC3B is extremely difficult to distinguish from autophagosomes under fluorescence microscopy. This can however be avoided by some methods. Monoclonal, stably transfected GFP-LC3B cell lines are used as much as possible, and cells which do not show GFP-LC3B punctate aggregation or accumulation during normal growth conditions are selected during the screening of transformants. At present, GFP-LC3B labeling has been successfully applied to the whole animal transgenic level. Transgenic mice with GFP-LC3B under the control of a CAG promoter can be used to evaluate the autophagy activity of target organs *in vivo*. However, this technique is currently unstable, due to the differing inducibility of the CAG promoter in different target tissues or organs. A tissue-specific expression of GFP-LC3B or mRFP/mCherry-LC3B is usually more sensitive and specific than systemic overexpression. Therefore, tissue-specific expression of fluorescently labeled LC3B is currently used in a variety of autophagy-related disease research.

Autophagy is generally thought to be a random degradation system, but there are still some specific substrates that are more prone to degradation by autophagy than others. Therefore, autophagic substrates other than LC3B are also used to evaluate autophagic flux conditions. As a classical selective autophagy substrate, p62 can be used to determine the changes in autophagic flux. Previous experience has shown that intracellular p62 protein levels are negatively correlated with autophagy activity, but recent studies have shown that p62 detection can be done using several techniques and these all have their difficulties, which will be described in detail in the following sections.

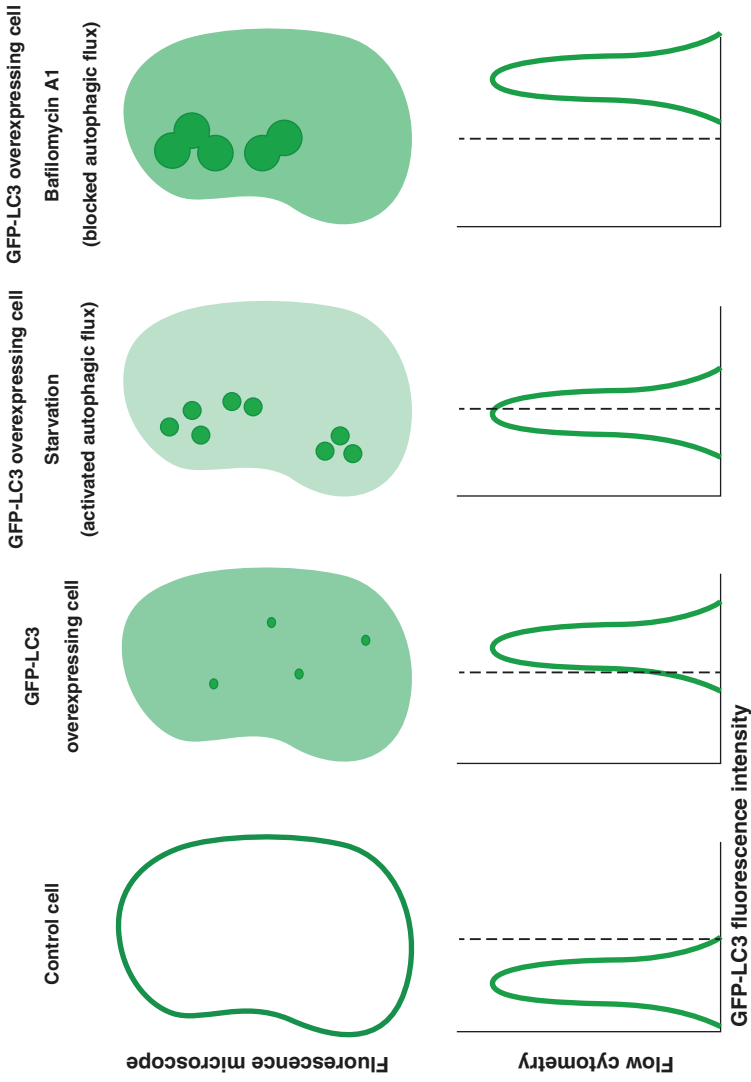


Fig. 9.4 Autophagic flux is observed by GFP-LC3 fluorescence. In GFP-LC3-overexpressed cells, both the intracellular fluorescence intensity and the number of autophagosomes increase following activation of autophagic flux, but the overall cell fluorescence intensity decreases at the same time. Bafilomycin A1 treatment blocks the accumulation of autophagosomes in the autophagic flux unobstructed cells, accompanied with the enhanced fluorescence intensity in overall cells

9.1.3.4 The Isolation and Purification of Autophagic Bodies to Evaluate Autophagic Flux

The analysis of the number of autophagosomes and the related molecules or their contents can not only help to understand the mechanism of autophagosome degradation but also to analyze what contents of the cells are degraded under specific pressure conditions. Traditional methods of isolating autophagosomes require long periods of complex centrifugation steps and a relatively large number of samples. For example, the isolation and extraction of autophagosomes from a mouse liver tissue requires an entire mouse liver, which greatly increases the number of mice that are sacrificed for the experiments. Sorting the autophagosomes of GFP-LC3B transgenic mice with anti-GFP magnetic beads can solve this problem. The basic premise of this technique is that the expressed GFP-LC3B proteins are present in the outer membrane of the autophagosome, and the expression and membrane localization of GFP-LC3B does not affect the autophagy process. Thus, magnetic labeling can be performed using beaded antibodies against GFP to obtain autophagosome of higher purity (Yao et al. 2019).

The specific steps are as follows: First, the tissue sample is homogenized to obtain a suspension, and then the suspension is pushed through pinholes of different diameters to fully lyse the tissue and destroy the outer membranes. Subsequently, the suspension is centrifuged, and the mixed solution is divided into a supernatant fraction containing free GFP-LC3B and a precipitate fraction containing GFP-LC3B-coated autophagosomes. The supernatant is discarded, the pellet is resuspended, and anti-GFP antibody beads are added. The mixture is incubated on ice for 1 h. Finally, the magnetic beads are sorted and eluted to obtain relatively pure autophagosomes for the next step of morphology and protein analysis.

9.1.3.5 Using GFP-LC3B and a Lysosomal Fluorescent Probe to Determine the Autophagic Flux

This method detects the autophagic flux by dynamically assessing the number of autophagosomes, autolysosomes, and lysosomes in a single cell. These three intracellular vesicles can be distinguished by using cells stably expressing GFP-LC3B, plus a lysosomal red fluorescent probe. Since LC3B is a structural component of autophagosomes, autophagosomes can be seen as green spots. The lysosomal red fluorescent probe will stain the acidic vesicle lysosomes in red. Colocalization of the green and red fluorescent signals indicates the presence of autophagosomes, since LC3B is not immediately degraded when autophagosomes fuse to lysosomes. When GFP is degraded, autolysosomes will slowly convert from the initial yellow fluorescence to red fluorescence (du Toit et al. 2018).

The disadvantage of this method is that the concentration of the fluorescent dye has a great influence on the test results. Experiments have shown that the red fluorescence of lysosomes can be quenched by bafilomycin A1, when the concentration of fluorescent probes is less than 75 nM. As bafilomycin A1 can affect the acidity of

lysosomes, the concentration of probe should be greater than 75 nM, and then the red fluorescence can still be maintained for more than 1 h. Another approach is to express an RFP-fluorescent fusion protein of LAMP1 (lysosomal-associated membrane protein 1) instead of a fluorescent probe, which has the same principle as a fluorescent probe and is insensitive to pH changes in lysosomes.

9.1.4 Using Tandem mRFP/mCherry-GFP Fluorescence to Evaluate Autophagic Flux

9.1.4.1 The Characteristics of Fluorophores in Autolysosomes

Many fluorescent dyes can be used to detect the autophagic flux. Unlike GFP or eGFP, which are easily quenched in autophagosomes, RFPs like mCherry are not sensitive to acidic conditions in lysosomes, which makes the red fluorescence still available after entering the autolysosomes. Furthermore, RFPs have a much higher fluorescence intensity and fluorescence stability than GFP, making it easier to perform immunofluorescence. Thus, different fluorophores can be used for autophagy activity detection for different purposes.

9.1.4.2 Tandem Fluorophore Detection of Autophagic Flux

mRFP/mCherry-GFP-LC3B is a fusion protein specifically designed to detect the level of autophagic flux. It is devised to facilitate the observation of autophagy activity in any cell via serial fluorescence. As mentioned above, the GFP fluorescence signal will be quenched due to the decrease of pH after entering the lysosome, but the pH stability of the mRFP or mCherry fluorophore is higher than that of GFP, and it can still be obtained after entering the autolysosomes. Therefore, when the mRFP/mCherry-GFP-LC3B fusion protein is used for cell experiments, the changes in the intensity of red fluorescence and green fluorescence can be observed simultaneously to accurately determine the autophagy activity. If green fluorescence and red fluorescence colocalize in the cells (yellow), this indicates that the mRFP/mCherry-GFP-LC3B fusion protein has not entered the lysosome, meaning that the autophagic flux is blocked. When only red fluorescence occurs, and no green fluorescence is present, it is a steady sign that the mRFP/mCherry-GFP-LC3B fusion protein is localized in a lysosome or in autolysosomes, i.e., the autophagic flux is active. Immunofluorescence microscopes or live-cell workstations are the best instruments for observing this phenomenon, especially live-cell workstations that can dynamically observe changes in intracellular fluorescence color. The greatest advantage of using the mRFP/mCherry-GFP-LC3B tandem fluorescent protein is that the autophagic flux state can be evaluated by a change in fluorescence intensity alone, without using any other autophagy inhibitors or agonists. At the same time, this method can be used to observe the change in autophagic flux of a certain cell

under the living cell workstation for a long time, and also observe the increase of early autophagosomes and late autophagosomes. Cells transfected with the mRFP-GFP-LC3B plasmid show an increase in yellow fluorescence and red fluorescence after starvation treatment, wherein the yellow fluorescence is similar to the green fluorescent dot-like aggregation in the GFP-LC3B-overexpressing cells. At present, this technology is being used for the screening of autophagy regulators (drugs), and the fluorescence intensity of at least 1000 cells can simultaneously be observed by a cytomics cytological microscope to achieve high-throughput screening (Fig. 9.5).

As described above, when the Western blot technique is used to detect the autophagy activity of GFP-LC3B cells, a low-dose chloroquine stimulation can lead to the detection of free GFP protein. This phenomenon is due to the fact that unsaturated autophagy inhibitors increase the pH value of lysosomes. At the same time, the low dose also ensures that part of the autophagy activity is retained. Similarly, when the mRFP/mCherry-GFP-LC3B fusion protein assay is performed, low-dose chloroquine or bafilomycin A1 partially inhibits the increase of lysosomal pH after autophagy while inhibiting lysosomal activity. The green fluorescence signal in these cells is quenched, resulting in red fluorescence. If the cells are stimulated with a high dose or saturated dose of chloroquine or bafilomycin A1, the yellow fluorescence in the cells increases significantly, but the quenching of the green fluorescence is not obvious. The red fluorescence intensity in these cells is very low. This represents that the blockade of the autophagic flux by these high-dosed autophagy inhibitors completely inhibits quenching of GFP fluorescence and degradation of the tagged protein. Evidently, both the activation and a partial blockade of the autophagic flux result in the increase of red fluorescence intensity. The difference between the two is that the intensity of the red fluorescence signal is higher when it is induced by the activation of the autophagic flux than when it is induced by partial autophagy. Given the increase in yellow fluorescent dot-like aggregation in both cases, we can determine the autophagic flux state by the percentage of red fluorescent dots in each cell. When the percentage of red fluorescent dots is increased compared to the control, this represents autophagic flux activation. If the number of red fluorescent dots increases, but the percentage of red dots does not change significantly, it means that the number of yellow fluorescent dots is also increased, that is, the autophagic flux is partially blocked. If the percentage of red fluorescent dots decreases, this means that the autophagic flux is blocked.

Cells transfected with mRFP/mCherry-GFP-LC3B can also be sorted by flow cytometry. The intensity of the emitted light of mRFP or mCherry in each cell is compared with the intensity of GFP emission by using sorting software. The cells with high ratio represent a high autophagic flux activity; the cells with low ratio represent a low autophagic flux activity. Cells with high and low autophagic activity can be sorted (Gump and Thorburn 2014) (Fig. 9.6).

However, the activity of autophagy flow in a cell is not always fixed. After resting for a period of time, the fluorescence ratio of the selected cells with either high or low autophagy flow will shift to the median, which fully indicates that autophagy flow is a dynamic process. The usual experimental means can only detect a certain state of the autophagic flux. To fully evaluate the autophagic flux changes, it is

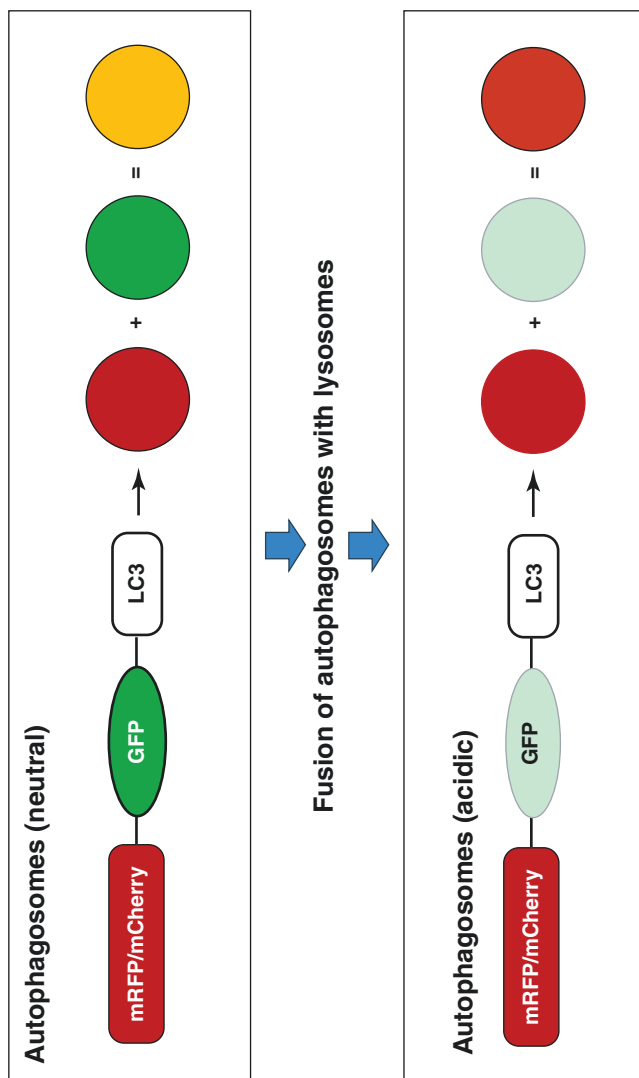


Fig. 9.5 Autophagic flux is detected using the mRFP/mCherry-GFP-LC3 tandem protein. mRFP/mCherry-GFP-LC3-I in the cytoplasm and mRFP/mCherry-GFP-LC3-II on autophagosomes can emit red and green fluorescence under laser excitation, and yellow fluorescence after superposition. When autophagosomes fuse with lysosomes, GFP fluorescence was quenched, so only the red fluorescence of mRFP/mCherry was shown, and the fluorescence will be red after superposition

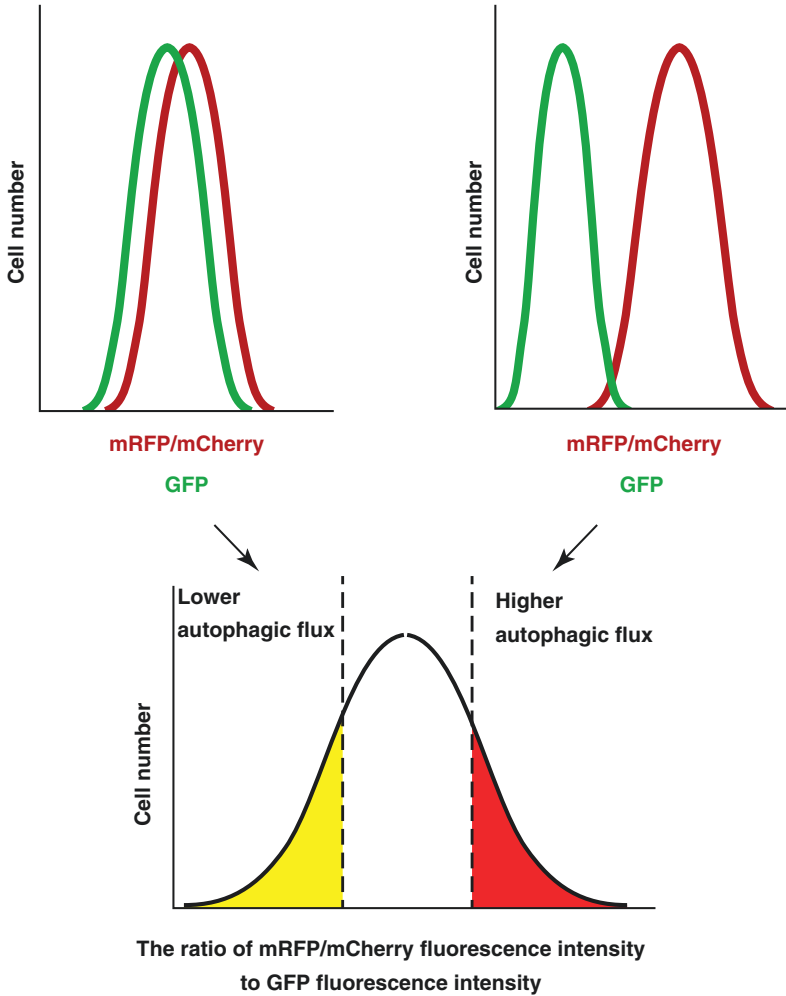


Fig. 9.6 Autophagic flux is determined using the mRFP/mCherry-GFP-LC3 fusion protein in flow cytometry. The ratio of mRFP/mCherry fluorescence intensity to GFP fluorescence intensity is high in autophagic flux-unblocked cells, but is much lower in autophagic flux-obstructed cells

necessary to dynamically observe the autophagy activity in the cells. It is clear that a long-term observation of the changes in intracellular fluorescence intensity of the mRFP/mCherry-GFP-LC3B fusion protein under a live-cell workstation is a good choice for evaluating the autophagic flux.

In summary, as a classical autophagic substrate, the decrease in the total amount of intracellular LC3B-I and LC3B-II usually reflects the level of autophagic flux. Even when LC3B-II is transiently increased when autophagy is activated, LC3B-II undergoes significant degradation over time. Similarly, when GFP-LC3B-overexpressing cells are starved, although a large amount of GFP-LC3B punctate

aggregation occurs in the cells, the total amount of GFP-LC3B in the cytoplasm and nucleus is eventually decreased. With flow cytometry, it is not possible to analyze the intracellular LC3B spot aggregation and cell substructure localization, but is the best choice for analyzing intracellular average fluorescence intensity (Shvets et al. 2008). If the autophagic flux is blocked, there will still be punctate aggregation-like changes, but the degradation of LC3B will be blocked. This can be judged by Western blot or flow cytometry combined with immunofluorescence microscopy. In LC3B degradation experiments, it is best to use Western blot detection at different time points, so that the LC3B-I and LC3B-II transformation can be evaluated, and the degradation of the two types of LC3B molecules can be observed simultaneously. In addition, diverse cell lines have diverse sensitivities to LC3B degradation when the autophagic flux is induced, so preliminary experiments are required to determine the observation conditions.

9.1.4.3 The GFP-LC3B-RFP-LC3B Δ G Probe Can Be Used to Detect Autophagic Flux

In recent years, a new fluorescent probe GFP-LC3B-RFP-LC3B Δ G has been developed to evaluate the autophagic flux. The probe can be hydrolyzed into equimolar amounts of GFP-LC3B and RFP-LC3B Δ G by endogenous Atg4 protease. GFP-LC3B is degraded by autophagy, while RFP-LC3B Δ G remains in the cytoplasm and acts as an internal reference. Therefore, the autophagy effect can be estimated by calculating the GFP/RFP signal ratio.

The probe is constructed by fusing GFP-LC3B to the N-terminus of RFP-LC3B and by deleting the C-terminal glycine of RFP-LC3B to form RFP-LC3B Δ G. After GFP-LC3B binds to PE, it localizes to autophagosomes. The GFP-LC3B in the autophagosome is degraded after fusion with the lysosome, and the GFP-LC3B on the outer autophagosomal membrane is uncoupled by the Atg4 protein and returned to the cytosol. However, RFP-LC3B Δ G cannot be fused to autophagosomes due to the lack of glycine, so it is stably present in the cytoplasm and acts as an internal reference (Kaizuka et al. 2016).

Since it is not necessary to observe the colocalization of two kinds of fluorescence as in tandem probes, the fluorescence intensity of GFP-LC3B and RFP-LC3B Δ G can be determined by a fluorescent microplate reader, which makes it more convenient to do a fast high-throughput screening of autophagy-active drugs.

However, like all other detection techniques, the use of this probe has drawbacks and deficiencies. First, when fused to the genome of the transfected cells, homologous recombination may occur between the two LC3B (i.e., LC3B and LC3B Δ G) sequences, resulting in GFP-LC3B Δ G, thus making the GFP protein unable to be degraded. Therefore, special attention should be taken to avoid this when constructing expression vectors. In theory, RFP-LC3B Δ G would accurately reflect the fate of LC3B-I in the cytoplasm and undergo posttranslational modifications such as phosphorylation and acetylation. It should be noted that the time resolution of the probe is not high. For example, the formation of GFP-LC3B fluorescence

aggregation points can be clearly observed in only 30 min after starvation treatment, but a significant decrease in the GFP/RFP ratio takes 2–4 h. However, such low temporal resolution also has its advantages, such as monitoring the occurrence of underlying autophagy levels using the cumulative effects of RFP. More importantly, if the expression level of the probe is significantly different between cells and tissues, the GFP/RFP ratio does not truly reflect the occurrence of autophagic flux. Therefore, when detecting the occurrence of autophagic flux in different tissues, the fluorescence intensity of RFP should be adjusted to a comparable level between two different cells/tissues.

9.2 Evaluating the Expression of SQSTM1/p62 to Assess the Autophagic Flux

9.2.1 *The Significance of the Role of SQSTM1/p62 in Autophagic Flux*

9.2.1.1 The Biological Functions of SQSTM1/p62

SQSTM1/p62 is the most critical substrate protein for selective autophagy. The protein is also known as the selective autophagy receptor, and forms a bridge between LC3B and the ubiquitinated substrate to be degraded. When the autophagic flux is blocked, a large amount of ubiquitinated proteins accumulates in the cells. The C-terminus of the p62 protein possesses a ubiquitination binding domain (UBA domain) and a short LC3B interaction domain (LIR domain). In addition, the p62 protein includes a PB1 domain for the regulation of its aggregation and binding to other autophagy cargo proteins. The protein level of p62 is usually negatively correlated with autophagic degradation. When autophagic flux is activated, p62 is degraded as an autophagic substrate, and the intracellular p62 level decreases. When some Atg genes are deleted or autophagosomes are blocked from lysosome fusion, p62 is significantly accumulated. In addition, p62 can be used as a carrier to carry the protein to be degraded into the proteasome, but in general its role in the regulation of autophagy is more important (Kraft et al. 2010).

It has previously been accepted that the role of p62 in the activation of autophagic flux was to transfer the substrate to be degraded to the autophagosome membrane surface by binding it to LC3B. However, current experimental results prove that p62 is one of the substrates for autophagy. With the participation of various Atg proteins, p62 and ubiquitinated proteins are involved in the production of autophagosomes. The presence of a structure containing misfolded proteins or to be degraded upstream Atg proteins establishes the initial stage of autophagy development. Subsequently, LC3B recruits autophagic vacuoles around the structure. With the continuous extension of the bilayer membrane structure around the p62 protein, the substrate to be degraded, LC3B, and other Atg proteins autophagosomes are formed. These are necessary processes for the autophagic flux.

9.2.1.2 Structural Characteristics of SQSTM1/p62

The LC3B interaction (LIR) domain of p62 is composed of 11 amino acids and mediates the interaction of p62 with LC3B/GABARAP family proteins. In 2007, Pankiv and his colleagues first mapped the LIR domain on the p62 protein. A mutation in the LIR domain significantly affects the interaction between p62 and LC3B. The researchers confirmed that the LIR domain responsible for interaction with LC3B is the Ser334-Ser344 position, which is also known as the LC3B recognition sequence (LRS). Obtained crystals of the LC3B/p62 interaction site have been subjected to X-ray diffraction, and the LIR domain-defined LC3B binding site was concluded to be positioned between the N-terminal arm and the C-terminal Ub-like domain. In addition to LC3B, the LIR domain interacts with Atg19, NBR1, and Nix. The LIR domain of p62 is important for selective autophagy, and can in this capacity affect the transport of autophagy substrates (Lin et al. 2013).

The C-terminal UBA domain of p62 is composed of 3 α -helices that consist of 50 amino acids. Since the UBA domain contains a ubiquitin Lys-linked side chain, the UBA domain is prone to link to the polyubiquitin Lys side chain of Ub-tagged proteins. Proteins like ubiquinone 1 and NBR1 contain similar motifs. The most important biological function of the UBA domain is to link p62 to polyubiquitinated proteins and mediate subsequent degradation. p62 is involved in the formation of polyubiquitinated protein aggregates through the UBA domain. It has been reported that overexpression of p62 enhances the formation of polyubiquitinated aggregates, but overexpression of p62 may also trigger its own aggregation. It is currently believed that the UBA domain mediates both the formation of aggregates of ubiquitinated proteins and p62 aggregates and that the PB1 domain plays a more important role in p62 self-polymerization than the UBA domain.

The PB1 domain at the N-terminus of the p62 protein is an evolutionarily conserved sequence. The PB1 domain interacts with a variety of signaling molecules such as PKC, MEKK3, MEK5, and ERK1. This implies that the PB1 domain is an important domain, involved in signal transduction. p62 participates in a variety of (patho)physiological processes through the PB1 domain, such as osteoclastogenesis, angiogenesis, early cardiovascular development, and cell polarity formation. In addition, the PB1 domain regulates the activity of the autophagic flux. It is generally believed that the autophagic flux can be obstructed by four reasons: a block in autophagy signaling, inhibition of the formation of autophagosomes, a block in the fusion of autophagosomes to lysosomes, and the inhibition of lysosome activity. However, when the expression of p62 is significantly increased in cells, the p62 will oligomerize due to the interaction between the PB1 domains, and then transform into an insoluble form to accumulate in the cells, resulting in blockade of the autophagic flux. The PB1 domain is also widely present in other autophagy cargo proteins, such as NBR1 and Nix. Therefore, p62 and NBR1 and Nix can also form oligomeric polymers through the PB1 domain, which affects autophagic flux activation negatively.

9.2.1.3 ZZ Domain: Signal Identification Code of N-Terminal Dependent Autophagic Degradation

Since p62 can interact with various signal molecules through its different domains, it plays various important roles in the process of autophagy. The N-terminal degradation process of proteins belongs to the category of autophagy degradation. The main process is that the N-terminal residues of proteins are hydrolyzed or labeled by specific proteases, and finally recognized and degraded by specific N-terminal hydrolyzing proteases. The N-terminal arginine tag (Nt-R) is a protein degradation tag widely found in eukaryotes. Arg-tRNA transferase recognizes the N-terminal aspartic acid or glutamic acid and adds Nt-R label. Eventually, this Nt-R will be recognized and degraded by UBR (ubiquitin ligase N-recognin). The ZZ domain of p62 is a newly discovered Nt-R autophagy degradation signal recognition code. The Nt-R substrate is selectively recognized to induce the occurrence of autophagy. Three sites (D129, D147, and D149) are required for the ZZ domain to interact with NT-R. The ZZ domain of p62 and the UBR-box are the only type I Nt-R signal receptors that have currently been found. Further studies have shown that the ZZ domain of p62 is essential for starvation-induced macroautophagy, but not for the selective autophagy of mitochondria. p62 is also an important regulatory molecule of mTORC1, and acts as a scaffolding protein that recruits mTORC1 to specific locations. Some free amino acids, such as lysine and arginine, are able to activate mTORC1 and promote phosphorylation of p62. However, a mutation of the ZZ domain of p62 would inactivate the mTORC1 signaling pathway, since the ZZ domain of p62 binds to arginine and blocks its interaction with mTORC1. The ZZ domain is also required for p62 to form punctate aggregates during autophagy. It is suggested that the ZZ domain may be involved in the oligomerization of p62. The PB1 domain and the ZZ domain of p62 protein both mediate the formation of oligomers. An *in vitro* p62 protein polymerization experiment found that the self-oligomerization of p62 at the basal level is directly dependent on the PB1 domain, but the accumulation of p62 by disulfide bonds, as occurs during autophagy activation, is dependent on the ZZ domain, suggesting that the ZZ domain is required for regulation of autophagy aggregation of p62 *in vitro* and *in vivo* (Zhang et al. 2018).

9.2.2 SQSTM1/p62 and LC3B Binding Protein Turnover Experiments to Evaluate Autophagic Flux

Although some other autophagy receptors, such as NBR1 and Nix, can also be used as protein markers for autophagy activity assays, p62 is so far the preferred one. It forms a bridge between LC3B and ubiquitinated proteins. The ubiquitinated proteins bound to p62 enter the autophagosomes which finally fuse with lysosomes to form autolysosomes. The p62 content increases when the autophagic flux is

inhibited, whereas the p62 level decreases when the autophagic flux is activated. Phosphorylation of p62 Ser403 regulates the clearance of ubiquitinated proteins by autophagy, a phenomenon that can be detected by using an anti-phospho-p62 antibody.

Current evidence suggests that p62 may also be involved in the regulation of the mTOR signaling pathway. Therefore, p62 may have other biological roles in autophagy in addition to recognizing cargo proteins. Usually, when detection of the p62 protein is used, endogenous amounts of protein should be maintained, as over-expression of p62 will cause an accumulation of p62 protein inclusion bodies. Even when the autophagic flux is blocked, the endogenous p62 will be insoluble, and the protein complexes are unsolvable by Triton X-100. In addition, p62 is involved in the proteasome degradation mechanism, and the p62 content also increases when the proteasome degradation system is blocked. When studying the degradation rate of p62 protein, proteasome degradation system inhibitors should be used appropriately to make sure that only the autophagosomal degradation of p62 is observed; construction of EGFP-p62 with an inducible promoter can also be used to evaluate the degradation of this protein; the radioisotope method can likewise be used to evaluate the degradation of the p62 protein. It is also possible to observe an increase in the p62 content when the autophagic flux is activated, which is due to the compensatory increase in the number of autophagosomes and autolysosomes, and thus the autophagy activity cannot be determined by the expression of p62 alone.

When performing Western blots with the p62 protein, some complications need to be considered. When p62 is overexpressed, it will form aggregates that are sometimes missed during protein isolation, and it is sometimes concluded that the presence of the protein is declining or staying stable when it actually is not. When samples are treated with NP40 or Triton X-100, both the soluble and aggregated forms of p62 are isolated, and an actual comparison of the amount of protein can be made. In most cases, the soluble protein level of p62 does not change significantly during the activation of autophagic flux, which may be due to a simultaneous increase at the transcriptional level. Therefore, the soluble protein level of p62 is not decisively related to autophagic flux. When the autophagic flux is blocked, it is critical to observe the insoluble form p62, using Triton X-100. When the autophagic flux is highly activated, the insoluble form p62 is almost undetectable, and its soluble form may be reduced or may remain unchanged. The experimental bias caused by the above problems can be avoided by choosing the right lysis buffers. If the soluble p62 is detected separately from the insoluble p62, the state of the autophagic flux can be proved more objectively and accurately. In the experimental design, the correct use of autophagy inducers and inhibitors (chloroquine, bafilomycin A1, knockdown LAMP2, etc.) can make it more straightforward to draw conclusions from the detection of soluble and insoluble p62. It should be noted that when the autophagic flux is adjusted, the change of soluble and insoluble p62 has a certain hysteresis, which also poses certain difficulties for interpreting results. When the autophagic flux is activated or inhibited, the protein level of LC3B changes rapidly, but as an autophagic substrate, the adaptation time for p62 is much longer. In each cell line, different detection time points should be tested, and then the optimal

observation time for the change of p62 levels in the cell line can be determined. Assuming that changes in LC3B protein levels can usually be observed 6–24 h after drug treatment, changes in protein levels of p62 may take up to 24 or 48 h, but may also occur at the same time as the changes in LC3B levels.

Another method for detecting p62 is by immunostaining with or without autophagy inhibitors, and the distribution of diffuse p62 and aggregated p62 can be observed. The most accurate method for determining autophagic flux by detecting p62 is to combine Western blot and immunostaining techniques, including immunohistochemistry and immunofluorescence. On one hand, the changes in the content of different forms of p62 in cells can be detected, and on the other hand, the localization of different forms of p62 in cells can be observed. Overall, the increase in LC3B-II is not consistent with the decrease of p62. To correctly evaluate the inhibition of the autophagic flux or the disturbances in the autophagy system, both the LC3B transformation and the changes of soluble and insoluble p62 should be considered.

In recent years, the application of multispectral imaging flow cytometry (MIFC) to detect LC3B and p62 has become increasingly popular. A common method of detecting autophagy is to count LC3B or autophagosome bright spots by dot. The detection of LC3B alone does not reflect the real situation of autophagy in cells. Simultaneous labeling of multiple proteins involved in autophagy can largely avoid false positives or misinterpretations. In the recent MIFC version 6.1 or higher (MilliporeSigma), a new feature is introduced, called Bright Detail Colocalization 3 (BDC 3). With BDC 3 it is possible to compare positive point detail images of three fluorescent probes, quantify the colocalization of the three probes, calculate the Pearson correlation coefficient separately, and expand to three images after correction. By converting the BDC 3 correlation coefficient, Rajan et al. proposed a new analytical method that combines the three most commonly used fluorescent markers to simultaneously measure the state of autophagy. Three autofluorescence markers, p62, LC3B, and lysosome (LAMP1), were detected in autophagy-activated cells. MIFC was used to analyze cell clusters that were treated with several autophagy inhibitors. The coincidence points of the highlights of the three autophagy markers were compared, which was combined with the LC3B-positive dot counting function, and in this way the authors were able to objectively and quantitatively assess the autophagic flux (Pugsley 2017).

The LC3B dots were counted using MIFC, and the colocalization of three autophagy markers was determined, to measure the autophagy flux. Under basal conditions (control samples), the number of autophagosomes was small, and there were only a few cells with “highlighted spots.” After the addition of the autophagy inhibitor chloroquine, which causes inhibition of the fusion between the autophagosome and the lysosome, the number of LC3B highlights increased. Since the lysosomes were unable to degrade the formed autophagosomes and p62 is located in autophagosomes, this resulted in an increased colocalization of LC3B, p62, and LAMP1. This phenomenon was further amplified under the condition of nutritional deficiencies. If chloroquine was not added, the number of autophagosomes did not increase significantly, mainly due to starvation-induced autophagic flux activation and accelerated metabolic turnover.

9.2.3 Other Applications of SQSTM1/p62 in the Detection of Autophagic Flux

p62 is important for the selective degradation of for instance protein aggregates during autophagy. In fluorescence imaging assays, the reduction of GFP-p62 and an increased colocalization of GFP-p62 with lysosomes are typical manifestations of the activation of selective autophagy. The presence of GFP-p62 and the occurrence of GFP-p62- and LAMP2-positive lysosomes can be assessed by using cell staining and high-throughput time-lapse imaging experiments. The colocalization of the GFP-p62 and lysosomes, the average fluorescence intensity of GFP-p62, and the fusion number of autophagosomes and lysosomes can be assessed in this way. Christopher M. Hale et al. obtained ten target genes via this method by siRNA screening. Knockout verification confirmed the role of these targets in the upregulation of autophagic flux via multiple assays. The retrieved targets include transcriptional regulators, lysine acetylase and ubiquitinase. The discovery of new autophagy regulatory pathways by means of high-throughput autophagy screening may be a viable way to find therapeutic targets for autophagy-related diseases (Hale et al. 2016).

9.3 Other Methods for the Measurement of Autophagic Flux

9.3.1 Autophagic Degradation of Long-Lived Proteins

Intracellular proteins are mainly degraded through two pathways, the proteasome pathway and the autophagy pathway, in which the proteasome pathway is mainly responsible for the degradation of short-lived proteins, while the long-lived proteins and some organelles are mainly degraded via the autophagy pathway. In recent years, more and more researchers have realized that simply observing the number of autophagic lysosomes is not enough to evaluate the changes in the autophagic flux, while monitoring the degradation of long-lived proteins could be very helpful. Autophagy acts as a lysosomal-dependent degradation pathway widely present in eukaryotic cells, and its activation includes the formation of autophagosomes, the fusion of autophagosomes with lysosomes, and the degradation of the autophagosomal contents in autolysosomes. Under starvation or stress conditions, autophagy can effectively regulate the degradation of intracellular long-lived proteins and key organelles, providing a material basis for cells to preserve or promote cellular immunity, development, and tissue remodeling. Under pathological conditions, a blocked or overactivated autophagic flux can lead to abnormal degradation of long-lived proteins, resulting in an abnormal cell function and morphology, disruption of cell homeostasis, and further deterioration of tissue and organ function (Yoshimori 2004). Here, we will introduce the conventional methods to assess autophagic flux, based on the detection of long-lived protein degradation in cell lines and primary cells.

9.3.1.1 Degradation of Long-Lived Proteins in Cell Lines

Observing the degradation of long-lived proteins is a classical method for the dynamic quantitative analysis of autophagy. Researchers have used the detection of the degradation of large-scale and isotope-labeled long-lived proteins to evaluate the autophagic flux as early as the 1970s. The assay typically involves the incorporation of radioactive amino acids in cellular proteins and the quantification of protein degradation by the detection of radiolabeled amino acids. The methods in this direction that are currently being used have been re-optimized and are based on various tumor cell line platforms such as the human colon cancer cell line HT-29 and the human breast cancer cell line MCF7. These methods have been established by Lavieu and Scarlatti, respectively. The operation can be adjusted according to the characteristics of the cell type.

Specifically, the procedure is to incubate cultured cells with an isotope-labeled amino acid (usually ^{14}C - or ^3H -labeled leucine or valine or ^{35}S -labeled methionine) for several hours or even days. The radioactive material that is not incorporated into proteins is removed by incubation of the cells with the non-isotopically labeled amino acid for a short period of time (usually 1 h, for some cells this step may be extended to 24 h), and the proteasome will rapidly degrade the excess of non-labeled and radioactive amino acids. HBSS- or EBSS-induced autophagy activation is stimulated for 4 h, during which 3-MA can also be added to inhibit the formation of autophagosomes. Finally, 10% trichloroacetic acid (TCA) is added to the cells overnight, the lysate is centrifuged at $470 \times g$ for 10 min, and the amount of radioactive signal in the acidic supernatant is detected by means of a liquid scintillation spectrometer. The pellets are washed twice, dissolved in 0.2 M NaOH solution, incubated at 37°C for 2 h, and then subjected to isotope detection as well, using a liquid scintillation spectrometer. The ratio of the isotope in the supernatant and the isotope in the precipitated protein is the degradation rate of long-lived proteins.

In the operation process, the following problems should be noted:

1. The selection of amino acids is particularly critical. In some cells, an isotope-labeled amino acid (such as leucine) may directly inhibit the autophagy activity; the best choice would be to use a more common amino acid that does not interfere with autophagy activity in most cells, like valine.
2. Unlike with bicarbonate containing EBSS, do not place cells in a CO_2 -containing environment when incubating cells with HBSS as $\text{HCO}_3^-/\text{CO}_2$ cannot regulate the pH of cell culture media.
3. 3-MA is the most common autophagy inhibitor, which can inhibit the formation of the PI3K3c complex (including Beclin 1, Atg6, Vps30, Vps15, and Vps34). It is worth noting that 3-MA also exerts a strong inhibitory effect on PI3K, interfering with other signal transduction pathways in the cell that depend on PI3K, thereby affecting certain physiological properties and functions of the cell. In addition, 10 mM 3-MA is not specific for autophagy inhibition, but also inhibits membrane transport processes such as endocytosis, the phosphorylation of important signaling molecules like JNK and p38, and the permeability of mitochondrial membranes. 3-MA also inhibits protein degradation in $\text{Atg5}^{-/-}$ cells,

suggesting that 3-MA also partially inhibits other protein degradation pathways. Therefore, when performing autophagic flux studies, especially using simultaneous detection of apoptosis or death, 3-MA should be used appropriately, and other methods of identification should be used to jointly evaluate the true state of the autophagic flux.

This method has high sensitivity but low specificity and cannot distinguish between autophagy-dependent degradation and non-autophagy-dependent degradation. Therefore, it is usually necessary to add a lysosomal antagonist such as chloroquine, ammonium chloride, or bafilomycin A1. The specificity of the method is usually investigated by analyzing the release of isotopically labeled amino acids before and after the addition of lysosomal antagonists. This is important since autophagic degradation plays a large role but is not exclusively responsible for the degradation of long-lived proteins. For example, when *Atg5*^{-/-} embryonic stem cells undergo nutritional starvation, the degradation of long-lived proteins is reduced to 30–40% of wild-type cells, suggesting that other protein degradation pathways are also involved in the degradation of long-lived proteins. Possibly, this role is overestimated due to the upregulation of other proteolytic pathways after *Atg5* deletion.

9.3.1.2 Degradation of Long-Lived Proteins in Primary Hepatocytes

Since the process of autophagy is relatively active in hepatocytes and rat primary liver cells are easy to obtain, the study of long-lived protein degradation is most conveniently performed in rat primary hepatocytes.

In the study of autophagy, in order to obtain reliable and accurate experimental results, rat primary hepatocytes need to be obtained from the liver of a fasted rat. The specific cell preparation process is as follows:

1. Rats are fasted for 18–24 h and then anesthetized with pentobarbital (45 mg/kg). The portal vein is dissected, and the liver is perfused with 50 mL of KH sodium bicarbonate buffer containing 10 mM Na⁺-HEPES and no Ca²⁺; the blood is drained, and then inverted from the inferior vena cava at a perfusion rate of 40 mL/min, for 10 min.
2. 0.1 mL of 1.3 M CaCl₂ and 20 mg collagenase are added to 100 mL of the above perfusate, and simultaneously filled with oxygen-containing 5% CO₂, and the liver is perfused for 10–15 min in the same direction.
3. After perfusion, the liver is placed in a sterile cell culture dish and cut into small pieces (diameter about 1 mm) with medical scissors. The tissue blocks are, with an appropriate amount of medium, transferred to a 250 mL cell culture flask, and gently shaken for 2–3 min.
4. All obtained cells are transferred through a 120 μm nylon mesh to filter out cell debris. The cells are washed three times with ice-cold KH buffer (containing 1.3 M CaCl₂ and 10 mM Na⁺-HEPES) to remove collagenase and are then placed on ice.

During the culture of rat primary liver cells, KH bicarbonate buffer (pH = 7.4) is used as a basal medium, containing Na⁺-HEPES and glucose at a final concentration of 10 mM and cycloheximide at a final concentration of 20 μM. The liver cells are cultured in a 25 mL sealed culture flask, at 37 °C, placed in a 70 rpm shaker to ensure sufficient oxygen supply. The cell samples are collected at different time points, and the amino acid products after protein degradation are obtained by denaturation and neutralization. The corresponding amino acids can be analyzed and compared using high-performance liquid chromatography. The specific steps are as follows:

1. Before adding the cells to the sealed culture flask, make sure that the bottle is filled with oxygen-containing 5% CO₂ and equilibrated in a water bath for at least 10 min. Once the fully mixed liver cells are added, the bottle cap is tightened in time.
2. When the cells are cultured for a suitable time (such as 0, 30, 60, 90, or 120 min), 1 mL of the cell suspension is pipetted into a centrifuge tube containing 0.3 mL of 14% HClO₄ to stop the reaction and placed on ice.
3. The suspension is incubated for at least 15 min to ensure complete denaturation of the cells and is then centrifuged. 1 mL of supernatant is pipetted into a sterile centrifuge tube, and the pH is adjusted to 7.0 with a solution containing 2 M KOH and 0.3 M MOPS to neutralize the amino acid sample.
4. The neutralized amino acid samples can be analyzed by amino acid pre-column derivatization high-performance liquid chromatography (RP-HPLC) to measure the proline (or other amino acid) content, and the degradation of long-lived proteins in mutant cells and normal cells can be compared after the autophagic flux is blocked.

A mixed solution of amino acids or 3-MA is often added to the basal medium to achieve inhibition of autophagy activity, and proline-free amino acid solution to achieve autophagy. The solutions contain 60 μM asparagine, 100 μM isoleucine, 250 μM leucine, 300 μM Lysine, 40 μM methionine, 50 μM phenylalanine, 100 μM proline, 180 μM threonine, 70 μM tryptophan, 400 μM alanine, 30 μM aspartic acid, 100 μM glutamic acid, 350 μM glutamine, 300 μM glycine, 60 μM cysteine, 60 μM histidine, 200 μM serine, 75 μM tyrosine, and 100 μM ornithine. The content of various amino acids is equivalent to the amino acid content in venous blood of fasted 24-h rats, and the solution is adjusted to pH 7.4 with 1 M NaOH. The solution is usually stored as a 20× concentrated stock at -20 °C and can be used for several weeks.

In the actual operation process, the following problems should be noted:

1. In order to effectively inhibit protein synthesis, 20 μM of cycloheximide should be added to the culture medium. The concentration of cycloheximide should be strictly controlled since higher concentrations of cycloheximide inhibit mitochondrial electron transport and autophagy.
2. Because isoleucine and proline do not inhibit autophagy activity, it is possible to use radioactively labeled isoleucine to replace the labeled proline.

3. Before livers are isolated, ensure that the rats are fasted for more than 18 h, because the glycogen reserve in the liver cells has a great influence on the metabolism of the cells.

Unfortunately, the detection sensitivity of conventional radioisotope labeling assays is low. The latest studies propose a new method for the quantitation of long-lived protein degradation, based on L-azido-based high alanine (AHA) labeling in mouse embryonic fibroblasts (MEF) and human cancer cells. AHA is a substitute for L-methionine and contains a bis-naphthoic acid moiety. AHA is added to the cultured cells and is incorporated into actively synthesized proteins. The azide group of AHA can be stained with alkyl-labeled fluorescent dyes. After staining, the content of azide-containing proteins is assessed by measuring the fluorescence intensity by flow cytometry. Activation of autophagy by starvation or rapamycin (mTOR) can trigger a significant decrease in fluorescence intensity. At the same time, studies have confirmed that in cells containing autophagy disorders caused by the deletion of *Atg* genes, or when using certain pharmacological agents, the decrease in fluorescence intensity is reduced, indicating a clear negative correlation between fluorescence intensity and autophagy activity. Compared with traditional radioisotope pulse labeling methods, this method is more sensitive, more accurate, safer, and easier to operate (Zhang et al. 2014).

9.3.2 Monitoring Autophagic Flux with Dynamic Transmission Electron Microscopy

In the 1950s, researchers observed autophagy in cells by transmission electron microscopy (TEM). For more than half a century, TEM has been considered a gold indicator for the occurrence of autophagy. The formation of phagophores with a bilayer membrane structure is of great significance during the morphological changes through autophagy. Many autophagy structures were first discovered by TEM and finally confirmed by other methods. TEM has many advantages: It has a high resolution, which is specifically important during the early stages of autophagy, and can also observe a variety of autophagic ultrastructures, such as phagocytic vesicles, autophagosomes (amphisomes, hybrid vacuoles that fused by autophagosomes and late endosomes), and autolysosomes. However, autophagy is a dynamic and continuous process in cells. The use of TEM to examine the morphology of autophagy in fixed cells is not sufficient to completely and objectively analyze the changes in autophagic flux. However, based on the static detection of TEM, an autophagy inhibitor can be used to observe the number and morphology of autophagy ultrastructures at different time points to achieve dynamic detection of autophagic flux (Eskelinen et al. 2011).

9.3.2.1 Accurate Sampling Is the Key to the Detection of Autophagy via TEM

The key to the detection of autophagic flux via TEM is to accurately quantify the autophagy ultrastructures in a cell or tissue sample. Compared with optical microscopy, TEM has higher resolution, but TEM requires that the sample volume is very small. Also the preparation requirements for the sample are higher. Since it is necessary to cut the cells into coupes of about 70–80 nm, it is very difficult to obtain a desired field of view, which causes a large bias in the TEM detection sample. When samples are collected from cultured cell clumps, it is relatively easy to obtain parallel results, since it is possible to ensure a more uniform distribution and similar cell state during the culture process; for tissue sample collection, the entire organ needs to be sampled. A recommended method is called “uniform random sampling.” The first principle of this method is to ensure that each area used for sectioning in the sample has an equal opportunity to be collected. In the following figure, we take kidney tissue as an example to briefly explain how to adopt it (Fig. 9.7).

We know that the advantage of TEM is that autophagy can be observed at the initial stage of autophagic vacuole formation. The traditional slice used in TEM is 50–80 nm, but the X-ray tomography technique can be used to perform 200 scans for samples that are about 250 nm thick. Through analysis and image reconstruction, the three-dimensional structure of autophagy ultramicrocytoids can be fairly clearly observed at an accuracy of 1–2 nm.

When using TEM for autophagy studies, particular concerns need be noticed:

1. Many organelles exhibit a microscopic morphology similar to autophagosomes and autolysosomes, particularly when cells are in special states, such as stress or cell death. In these states, the endoplasmic reticulum will be swollen and deformed, and can be easily confused with autophagic organelles.
2. Due to the different positions where individual cells are cut to produce usable slices, a double-layer membrane structure containing cytoplasm can be observed under some circumstances without designating autophagy.
3. The use of immunoelectron microscopy to specifically label specific autophagy markers will greatly improve the accuracy of the observations.

9.3.2.2 Reasonable Quantification Is the Basis of Using TEM for the Detection of Autophagic Flux

At present, TEM is the most sensitive method to observe autophagic subcellular structures. It can be used to observe the aggregation of various ultrastructures that are formed during autophagy (such as early and late autophagy vesicles). When the ratio of these vesicles to autolysosomes is analyzed, the dynamic process of autophagic flux can be objectified. If the proportion of autophagosomes is significantly

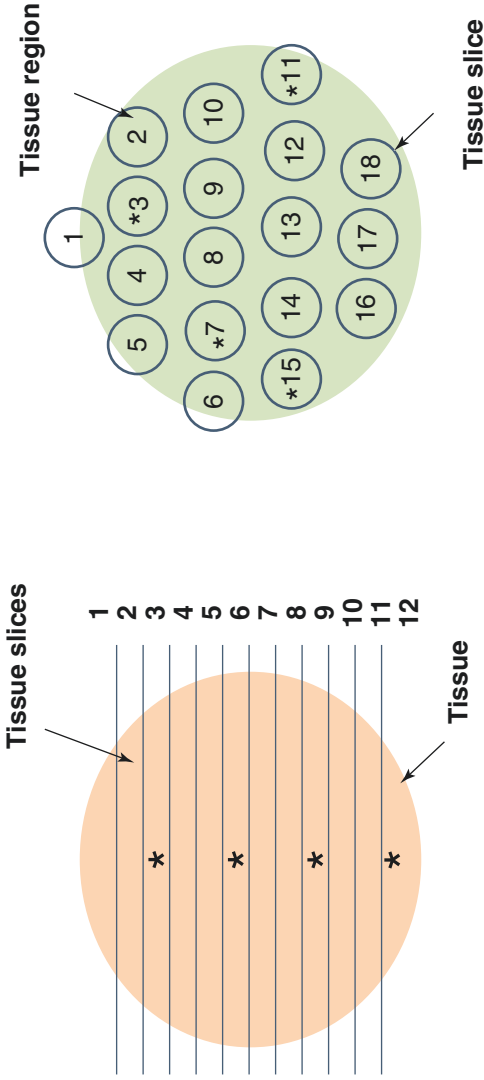


Fig. 9.7 The kidneys were sampled using uniform random sampling. First, the tissue is sliced at the same thickness and spacing (12 pieces in total), one piece randomly selected from one out of every three pieces, and then one piece is selected every two pieces, so the total number of samples is 4. (The 3rd, 6th, 9th, and 12th pieces are selected as the target slices here.) Second, for each piece of the slice, the uniform random sampling method should also be used, and 18 areas should be uniformly selected in the tissue section, randomly between 1 and 4. Select one area out of every three areas, so the total sampling area is 4 (the 3rd, 7th, 11th, and 15th pieces are selected as the destination area here)

higher than that of autolysosomes, it may mean that the upstream of the autophagic stream is overactivated or that there are obstacles in the formation or maturation of autophagic endosomes or autolysosomes. In addition, a massive accumulation of autophagy late-stage structures may be due to obstacles in the process of autolysosome degradation.

It should be noted that since the lifespan of autolysosomes is very short, most of the downstream structures of autophagic flux observed by TEM are amphisomes. Of course, the detection of autolysosomes can be achieved by blocking the degradation of autolysosomes using lysosomal inhibitors such as leupeptin, pepsin, and E-64d.

It has been confirmed that by application of autophagy inhibitors, it is possible to reveal the dynamic changes of individual subcellular structures of autophagy at different time points. The selection of the time point of observation after autophagy induction is very important. For example, when autophagy occurs unhindered, the lifespan of an autophagy ultrastructure in rat or mouse cells is only 6–8 min. The addition of vinblastine, an autophagy downstream inhibitor, can prolong the lifespan of autophagic flux components to 27–30 min. During this time, a large number of autophagosomes can be observed under TEM. However, if the time point is not properly selected, the autophagy turnover rate will be too high to be able to truly reflect the activity of autophagy.

Using TEM to detect the autophagic flux still requires an overall evaluation in conjunction with other assays. When the presence of a large number of autophagosomes is observed, it may be caused by excessive activation of the autophagy upstream signal. Of course, the obstruction of autolysosome degradation is not excluded. Similarly, when autophagosomes are reduced, it does not necessarily result from the inhibition of autophagic flux, since it may also be the result of overactivation of the lysosomal degradation mechanism. Therefore, in the actual research process, an autophagy signal protein such as LC3B, Beclin 1, or p62 should also be considered to determine whether the autophagic flux is obstructed and in which step.

9.3.3 The Cargo Sequestration Assay to Evaluate Autophagic Flux

The technique referred to as the cargo sequestration assay involves the detection of the conversion of a probe protein from the soluble form (cytosolic) to the insoluble form (in organelles). In this technique, protease inhibitors are used to block the proteolytic inactivation and degradation of the probe protein in the autophagic vesicles or lysosomes. The cargo sequestration assay is one of the most direct and accurate methods for detecting autophagy activity and autophagic flux (Engedal et al. 2019).

9.3.3.1 Endogenous Cytoplasmic Proteins as Probes to Detect Autophagic Flux

Many proteins in the cell can be used as probes for the detection of autophagy. However, when choosing the ideal endogenous probe to use with the cargo sequestration technique, three necessary conditions need to be met: (1) it should be a long-lived protein in the cytoplasm; (2) the lysosomal pathway should be the only pathway by which the protein is degraded; and (3) the activity of the target protein is not destroyed during the aggregation process, since the measurement of the protein activity is used in order to quantify the amount of protein present, using the corresponding biochemical methods. The most commonly used probe is lactate dehydrogenase (LDH).

Protease inhibitors are indispensable in the cargo sequestration assay. A necessary precondition for the used inhibitor is that the degradation of the probe of interest can be completely inhibited by it. If other proteases can also participate in the breakdown of the target protein, the corresponding protease inhibitors also need to be added to the cells. Kopitz et al. found that using a buffer with 0.3 mM leupeptin can rapidly and effectively prevent the inactivation and degradation of LDH in lysosomes and ensure a sustainable and stable aggregation of active probe proteins in lysosomes. Comparing the insoluble form of LDH in the lysosome of protease inhibitor-treated hepatocytes with the total LDH activity in the control cells will represent the aggregation rate of the target protein probe (LDH), which usually is 2.5–4%/h in primary hepatocytes.

Activity tests for probe proteins by an enzymatic assay are preferable to immunoblotting, allowing much more accurate quantification at specific time points. After autophagosome formation, any inhibitor that blocks its fusion with lysosomes, such as the tubulin inhibitor vinblastine or 3-MA, can result in linear aggregation of LDH in prelysosomal autophagic vacuolar compartment. Kopitz et al. found that 3-MA can completely inhibit the accumulation of LDH in autophagosomes in leupeptin-treated hepatocytes.

Other targets that are used in cargo sequestration assays are subtypes of betaine-homocysteine methyltransferase (BHMT). BHMT is a liver injury marker abundantly expressed in the liver. During degradation, BHMT is split into a variety of subtypes, some of which specifically bind to autophagic organelle membranes, especially autophagosomes. These subtypes can be used as specific probes for autophagy sequestration assays. Since they are only present in autophagic vesicles, there is no need to consider autophagic vesicles and other organelles (or even whole cells) when processing sequestered products. At present, the most widely used BHMT subtype is the amino-terminal hydrolyzed fragment p10, with a molecular weight of approximate 10 kD. P10 is a product of BHMT after hydrolyzation by serine protease and another leupeptin peptide-sensitive protease. Since BHMT is easily hydrolyzed to produce p10, it is necessary to add a high concentration of the serine protease inhibitor AEBSF (4-(2-aminoethyl) benzenesulfonyl fluoride) during the extraction and analysis of the target probe, to prevent further production of new p10. Due to the autophagy specificity of p10, a low background, and a

consistently stable sequestration rate (approximately 2%/h), good results can be obtained within 4 h, in autophagy sequestration experiments. Immunoblotting can be used for the quantification of p10.

An important tool in autophagy sequestration assays is electrodisruption technology. The technique is used to separate the cell fluid from the cell organelles. The cell sample is placed in a $1 \times 1 \times 5$ cm ionization chamber in the cell ionization instrument, a 2 kV/1.2 mF pulse is applied, and then the cells are placed on a Nycodenz density separation buffer (containing 8% Nycodenz, 2.2% sucrose, 50 mM sodium dihydrogen phosphate, 1 mM dithiothreitol, and 1 mM EDTA, pH = 7.5), centrifuged at 3750 rpm for 30 min at 4 °C, and finally all the organelles and autophagy components are obtained by precipitation.

The sequestration rate of the probe protein can be calculated by quantifying the isotope, measuring the enzyme activity, or assessing the amount of marker protein present in the cells.

9.3.3.2 Labeled Exogenous Sugar as a Probe to Detect Autophagic Flux

When endogenous proteins are used to determine the sequestration and the autophagic flux, autophagy inhibitors are necessary to distinguish between autophagic degradation and the degradation via the proteasome pathway. Because of this, the results are inevitably affected by high background. However, when exogenous autophagic substrates are used as a probe, the autophagic flux study is more reliable, and the interference factors are relatively few. Examples of such exogenous cargo probes are isotopically labeled disaccharides or trisaccharides. The sugars are transferred into the cells via electroporation or mechanical force. Raffinose is a widely used probe. In addition, sucrose (which is hydrolyzed by sucrase in amphisomes and lysosomes) and lactose (which is hydrolyzed by endogenous β -galactosidase in lysosomes) can be used in the detection of various stages of autophagic flux.

The main reasons for the selection of disaccharides or trisaccharides as probes for autophagic flux studies include: (1) most di-/trisaccharides are relatively easily labeled with isotopes; (2) di-/trisaccharide molecules are small and easy to use with electroporation; (3) after the cell membrane is closed, the bis-/trisaccharide does not easily escape from the cytoplasm; and (4) di-/trisaccharides are usually not synthesized and metabolized in mammalian cells, which precludes the interference by endogenous saccharides. In addition, the degradation processes of di-/trisaccharides are often compartmentalized. Lactose is for instance hydrolyzed by a specific β -galactosidase only present in lysosomes. Because of this, the fusion of autophagosomes with lysosomes and the biological functions of autophagosomes can be conveniently studied.

Raffinose, also known as melitriose, is the best-known trisaccharide in nature. Raffinose is composed of galactose, fructose, and glucose. As early as in 1986, ^3H -labeled raffinose was used as a probe for autophagy studies. Unlike disaccharides, raffinose is not sequestered by non-autophagic organelles, so is only present in the soluble form in cytoplasm and in the insoluble form in autophagosomes and lysosomes. Therefore, it can be accurately used to quantify the autophagic flux.

After electroporation, and re-closure of hepatocytes at 37 °C, raffinose is maintained in an insoluble form, sequestered in autophagosomes, and 3-MA completely inhibits this sequestration.

Sucrose is another exogenous probe that is used in autophagy sequestration studies, and commercial sucrose is mostly labeled with ^{14}C . Unlike raffinose, sucrose can be sequestered not only by autophagy subcellular organelles but also by mitochondria. The use of sequestered sucrose to measure autophagic flux requires a special selective extraction process in order to distinguish between mitochondria-separated sucrose and autophagy (including autophagosomes, amphisomes, and autolysosomes). Compared to autophagic organelles, mitochondrial membranes contain very little cholesterol and are tolerant of digitonin. Low concentrations of digitonin (0.2–0.5 mg/mL) can effectively lyse the membrane of autophagic organelles without destroying the mitochondrial membrane.

Invertase is a sucrose hydrolase expressed in yeast cells. For the studies of mammalian cellular autophagy, it can be taken up by cells via endocytosis and intracellular phagocytosis. Researchers have found that hepatocyte lysosomes can sequester autophagy-derived sucrose and endocytosed invertase. Gordon et al. showed that sucrose aggregated in amphisomes (vacuoles that formed with autophagosomes and late endosomes in hepatocytes) can be completely degraded by endocytic invertase. However, even in the presence of 3-MA, sequestered sucrose in lysosomes is also degraded by endocytic invertase, suggesting that lysosome endocytosis of invertase exists in both autophagy-dependent and autophagy-independent manners.

Just like sucrose, lactose can be taken up and cleaved by lysosomes. Interestingly, the lactose metabolism in the cytoplasm is extremely slow, but once taken up by lysosomes, lactose is eventually hydrolyzed by β -galactosidase which is specifically located in lysosomes. As a result, lactose can be used as a biomarker to distinguish amphisomes from autolysosomes: Obstruction of the fusion between autophagic compartments and lysosomes in hepatocytes causes lactose to accumulate in the autophagic compartments, but exogenous administration of β -galactosidase, which is endocytosed into endosomes, prevents such an accumulation, indicating sequestered lactose and endocytosed β -galactosidase are delivered to the same prelysosomal vacuoles, i.e., amphisomes.

Electroinjected lactose can be used to detect the final stage of the autophagy-lysosomal pathway and to evaluate the entire autophagic flux. The following is a brief introduction to a lactose sequestration test:

1. Introduce ^{14}C -labeled lactose to the cell, add 10% cold trichloroacetic acid, and place the cells on ice for 30 min.
2. Centrifuge the cells at 5000 rpm for 30 min, pass the supernatant through a 0.45 μm filter, and then separate using 5 μm Supelcosil LC-NH2 high-performance liquid phase column (25 \times 4.6 mm).
3. The first eluted product will contain ^{14}C -labeled glucose; the next will contain ^{14}C -labeled lactose. The efficiency of autophagy degradation is indicated by the radiation activity of glucose compared to the total radiation activity of the glucose and lactose. Using this method, Hoyvik et al. found that 3-MA completely inhibits the degradation of lactose.

9.3.3.3 The Autophagy Sequestration Assay to Evaluate Autophagic Flux in Yeast Cells

Because the metabolism of carbohydrates in yeast cells is fast, the electroinjection of oligosaccharides is not suitable for the detection of autophagic sequestration in yeast cells. Researchers have designed a series of unique methods for autophagic flux detection in yeast. The most classic method is the ALP (alkaline phosphatase) Pho8 Δ 60 assay. The yeast gene PHO8 encodes the only alkaline phosphatase that is present in vacuoles (vacuoles are the equivalent of lysosomes in mammalian cells). Normally, the N-terminus of Pho8 contains a transmembrane domain consisting of 60 amino acids which ensures the successful translocation to the endoplasmic reticulum, subsequently to the Golgi, and eventually to the vacuole, where its C-terminal peptide is hydrolyzed in order to form the active form of ALP. When the N-terminal sequence is cleaved off (Pho8 Δ 60) Pho8 cannot enter the endoplasmic reticulum and stagnates in the cytosol. Because of this, the autophagy route is the only way to transport Pho8 Δ 60 into the vacuole and to attain hydrolase activity. When nonselective autophagy activity is activated, Pho8 Δ 60 is transported to vacuoles via autophagosomes. Once here, it is hydrolyzed to exert alkaline phosphatase activity, which can be quantitatively analyzed by a corresponding enzyme activity assay or by SDS-PAGE. Under nutritional sufficiency conditions, the activity of Pho8 Δ 60 is usually very low, which reflects the basal level of autophagy. A significant increase of its activity can be detected after the induction of autophagy. Activation involves the step of autophagosomal transport of Pho8 Δ 60 to the vacuole, so in the absence of fusion of the autophagosome with the vacuole, no activity will be measured.

9.3.3.4 Issues That Need to Be Considered in Autophagy Cargo Sequestration Assays

To date, in most of the autophagic flux studies, autophagy has been demonstrated by detecting various autophagic markers. Only a few accurate quantitative methods have been used to detect autophagic flux activity in a short period. The autophagy cargo sequestration assay provides researchers with more choices. The following issues should however be considered in the actual experimental design:

1. Cells with strong adherence are not easily injected, and exogenous probes are difficult to introduce into the cells.
2. When endogenous probes are used, it is better to select long-lived proteins that are only degraded through the autolysosomal pathway.
3. Choose simple, rapid, and mature methods to detect the endogenous probe activity.
4. Electrolytic separation is a simple and effective method for separating soluble and insoluble forms of probe proteins, but it is not suitable for all applications. It is recommended to try other dissociation methods, such as homogenization and density gradient centrifugation.

5. The detection of p10 can very well be used in cargo sequestration assays in hepatocytes because the expression of BMTH is high in these cells. In cells with little or no expression of BHMT, transfection of a GST-BHMT expression vector can improve the autophagy sequestration assay.

Autophagy is a multistage cellular biological process influenced by many factors. The process is regulated via several processes, including a long-term regulation of autophagy, employing several gene expression systems, and a short-term regulation of autophagy activity, which is regulated by the substrate sensitivity of some enzymes that are involved. For the long-term regulation of autophagic flux, an intuitive and accurate method is essential. Autophagy cargo sequestration assays combined with other methods will help researchers to more fully understand and accurately determine the autophagic flux.

9.3.4 Application of Nanoparticles for the Detection of Autophagic Flux Research

Nanoparticles (NPs) are artificial particles with a diameter of 1–100 nm. Nanoparticles can penetrate into cells and can be transmitted via nerve cell synapses, blood, and lymphatic vessels. At the same time, nanoparticles can selectively accumulate in specific cell types and in specific cell structures. Recent studies have found that a specific range of nanoparticles can act as potential autophagy activators and are cleared by autophagic flux, which makes it possible to apply nanoparticles in autophagy studies (Remaut et al. 2014).

Researchers have found that semiconductor fluorescent nanoparticles with a particle size of less than 10 nm can activate autophagy in a particle size-dependent manner. Since the electronic energy levels of the particles can be quantized, they are called quantum dots (QDs). Transmission electron microscopy images show that QDs in the cytoplasm are processed analogously to autophagic substrates. They are sequestered in autophagosomes, and are transported to autolysosomes. While using TEM, and observing the quantum dots that appear as specific dot-like structures in the cell, LCB3 can be visually observed in the cells by immunocytochemistry.

Using QD has the following advantages: (1) QDs have a special brightness and imageability; (2) QDs have a broad excitation wavelength and a narrow particle size-dependent emission wavelength; (3) QDs are opaque under electron microscopy; and (4) QDs can be combined with various commercialized biomolecules, medium molecular weight proteins, and bio-modifying complexes (Seleverstov et al. 2009). Because of these advantages, QDs are more and more applied to the research of autophagy.

9.3.4.1 The Detection of Autophagic Flux in Living Cell by Using Fluorescent Nanoparticles of Differing Sizes

Seleverstov et al. have tried to observe the autophagic flux using fluorescent nanoparticles with different particle sizes. They found that QDs with small particle sizes are more suitable for autophagic flux research, as the fluorescence intensity of large particles is more easily affected by cellular biological activities such as cell division and cytoplasmic flux (secretion and exocytosis).

Combined with other autophagic flux detection methods, the researchers found that using a Qtracker Cell Labeling Kit to label multiple cells with a smaller particle size QD (QD525, green) which has an emission wavelength of 525 nm, the fluorescence clearance rate consistently reflects the autophagic flux. When the cells are labeled with QD (QD605, red) which has a larger particle size and an emission wavelength of 605 nm, the fluorescence clearance rate more appropriately reflects a non-autophagy-dependent QD clearance pathway. Usually, the autophagic flux has a clearance time of about 72 h for QD, while the non-autophagy-dependent QD clearance takes longer (20–50 days).

When performing a fluorescence QD detection of autophagic flux, the following notes should be considered:

1. For long-term fluorescence observation, it is recommended to use adherent cells. This makes it easier to observe cells.
2. Observation time point recommendations are 0, 4, 8, 12, 24, 36, 48, and 72 h and several days after induction.
3. Normally, green fluorescent QDs require a stronger excitation intensity than red fluorescent QDs. Although fluorescently labeled QDs do not undergo fluorescence decay, it is still important to ensure that the fluorescence excitation intensity is consistent at each time point.
4. Single cells and tissues that are labeled with fluorescent QDs can also be used in immunocytochemistry/histochemistry so that a multi-label approach is possible.

9.3.4.2 Prospects for the Application of Nanoproducts in the Research of Autophagic Flux

Nanoparticles are a new biomedical tool. Many conventional experimental techniques such as immunoblotting can benefit from the application of nanoparticles, and their sensitivity gives these techniques a qualitative lift. Metal (gold or silver) nanoparticles can increase the detection sensitivity of small (less than 10 kD) proteins and peptides by 10,000 times. In addition, the application of fluorescent QD technology allows the direct detection of degraded proteins in the cytosol, thereby avoiding the process of immunoprecipitation and quantification. It has been reported that nanoparticles are used for the detection of high-sensitivity protein activities (such as enzyme activity and phosphorylation) on protein chips. Although the above technologies are still in the early stages of development, their application will greatly promote autophagy research.

Some research institutes have used nanoparticles to label mitochondria and other organelles in damage-related mechanism studies. Although there is currently no reliable method that uses nanoparticles in the study of autophagic degradation of damaged organelles, we believe that nanoparticle labeling technology has great potential in this area.

Cellular reactions are accompanied by energy consumption and production. Temperature-sensitive QDs can be used to detect these changes. At present, QD can sensitively deliver information about intracellular temperature changes, and these specific changes can be accurately quantified by a specific high-sensitivity photometer. The QD technology can potentially be applied in the research for autophagic flux by detecting dynamic temperature changes in autophagic organelles.

9.3.5 *The Cyto-ID Autophagic Flux Assay*

The current list of autophagy assays lacks rapid and accurate quantitative assays. This hinders the development and implementation of autophagy-targeted therapies for a variety of diseases. A variety of autophagy assays have been developed to date, but only a few of them are suitable for both quantitative and high-throughput assays, and these methods are cumbersome to perform and still not accurate enough. The newly developed Cyto-ID fluorescent dye provides an accurate and simple assay for autophagy research. Cyto-ID is a cationic amphiphilic tracer dye that specifically labels autophagosomes but not lysosomes and endosomes. The Cyto-ID assay is a spectrophotometric assay based on this specific fluorescent dye. It has excellent performance and can be used to measure the size of the autophagy vesicles. This allows the monitoring of the autophagic flux and the identification of novel genes or compounds that regulate autophagy in a more convenient and faster manner (Guo et al. 2015). In the following paragraphs, the Cyto-ID assay is compared to the main traditional autophagy assays.

LC3B is an autophagic marker widely used for the detection of autophagic flux. Cyto-ID assays can be used as an alternative to LC3B immunoblot assays to distinguish between activated and impaired autophagic flux at steady state. The drawbacks of LC3B analysis are:

1. Measuring LC3B-II only gives information about autophagosomes, while Cyto-ID dye labels most autophagy vesicles.
2. The levels of the LC3B-II protein are not sufficiently stable, while the Cyto-ID assay is equally sensitive to the LC3B immunoblotting but more stable.
3. LC3B-based assays do not provide accurate digital readings associated with autophagic vesicles, where Cyto-ID assays do. Cyto-ID assays may be the most accurate quantitative analysis of all autophagy analysis techniques to date.

LC3B conjugated to GFP is also commonly used for fluorescent autophagy detection. A disadvantage of this approach is that ectopically expressed GFP-LC3B

typically forms aggregates that are difficult to distinguish from the characteristic subcellular structures of autophagosomes, resulting in false-positive results. Cyto-ID dye, on the other hand, specifically labels autophagosomes with minimal staining of lysosomes and endosomes, which can improve the accuracy of detection greatly.

MCD labels are also often used to monitor autophagic flux. Similar to other acidic fluorescent dyes such as acridine orange and LysoTracker Red, MCD labels will stain acidic vesicles formed during autophagy but also lysosomes. In contrast, Cyto-ID stains very little or even negligibly on lysosomes or amphisomes. Therefore, Cyto-ID can perform autophagy detection with more specificity and sensitivity.

As the most common method for detecting autophagy, electron microscopy can obtain images of early or late autophagy vesicles in cells, but often does not provide quantitative data and is not suitable for clinical applications. Cyto-ID assays, however, make it not only possible to conveniently measure the size of autophagic compartments but also allow quantification of fluorescent dots, which makes them a good candidate to be applied in drug screening assays and clinical detection methods.

Taken together, this new Cyto-ID fluorescence spectrophotometry method provides a fast and reliable quantification of autophagy vesicles and autophagic flux, which can be used for autophagy-related research on drugs and therapies.

9.3.6 High-Throughput Screening of Autophagy Regulatory Compounds by a Split-Luciferase Assay and the AlphaLISA Assay

Autophagy is a lysosomal degradation pathway that plays an important role in cellular immunity, tumor suppression, metabolism, prevention of neurodegeneration, and prolonged lifespan. The development of new compounds that specifically induce or inhibit autophagy has become a key research activity. Two reliable assays have been established to identify autophagic flux: the split luciferase assay and the AlphaLISA assay (Amplified Luminescent Proximity Homogeneous Assay) (Chiang et al. 2018).

The beclin 1/Bcl-2 split luciferase assay relies on two nonfunctional fragments of NLuc (amino acids 2–416) and CLuc (amino acids 398–550), which can form a luciferase after binding to their corresponding partner. To measure Beclin 1/Bcl-2 interactions with the split luciferase assay, a HeLa cell line expressing N-terminal NLuc-tagged Beclin 1 (NLuc-Beclin 1) and CLuc-labeled Bcl-2 (CLuc-Bcl-2) was used. A renilla luciferase was designed as an internal control. The interaction of Beclin 1/Bcl-2 was measured in relative luminescence units (RLU), which is the calculated ratio of split luciferase and renilla luciferase. In addition, the AlphaLISA method can be used to evaluate protein-protein interaction *in vitro*, for example, using purified recombinant Beclin 1 and Bcl-2 proteins.

9.3.7 *The Identification of Autophagy-Related Proteins with Single-Particle Low-Temperature Electromagnetic Technology*

Single-particle low-temperature electromagnetic technology is an emerging powerful EM technique that is able to present a detailed electron microscope structure of protein complexes at different resolutions. Single-particle low-temperature electromagnetic technology requires only a small amount of sample, avoids the need for crystallization, and has wide applicability in autophagy research. Recently, research using this technique has provided detailed image data of protein complexes involved in the initiation, development, and substrate targeting process of autophagic flux, including ATG1 protein kinase complexes and all class III phosphatidylinositol 3-phosphate complexes I (Hurley and Nogaes 2016). In addition, this technology will be applied for image acquisition of the mTORC1 complex, Ape1 particles (the main substrate for selective autophagy in yeast), and p62. Single-particle low-temperature electromagnetic technology requires only a small amount of sample, avoids the need of crystallization, and shows great potential in autophagy research. The latest breakthroughs in low-temperature electromagnetic technology will enhance our possibilities to understand the structure of autophagy proteins and the autophagic regulation characteristics of biological macromolecules.

References

- Barth S, Glick D, Macleod KF. Autophagy: assays and artifacts. *J Pathol.* 2010;221:117–24.
- Chiang WC, Wei Y, Kuo YC, Wei S, Zhou A, Zou Z, Yehl J, Ranaghan MJ, Skepner A, Bittker JA, Perez JR, Posner BA, Levine B. High-throughput screens to identify autophagy inducers that function by disrupting Beclin 1/Bcl-2 binding. *ACS Chem Biol.* 2018;13:2247–60.
- Ciechomska IA, Tolkovsky AM. Non-autophagic GFP-LC3 puncta induced by saponin and other detergents. *Autophagy.* 2007;3:586–90.
- Demishtein A, Porat Z, Elazar Z, Shvets E. Applications of flow cytometry for measurement of autophagy. *Methods.* 2015;75:87–95.
- du Toit A, Hofmeyr JS, Gniadek TJ, Loos B. Measuring autophagosome flux. *Autophagy.* 2018;14:1060–71.
- Engedal N, Luhr M, Szalai P, Seglen PO. Measurement of bulk autophagy by a cargo sequestration assay. *Methods Mol Biol.* 2019;1880:307–13.
- Eskelinen EL, Reggiori F, Baba M, Kovacs AL, Seglen PO. Seeing is believing: the impact of electron microscopy on autophagy research. *Autophagy.* 2011;7:935–56.
- Gump JM, Thorburn A. Sorting cells for basal and induced autophagic flux by quantitative ratio-metric flow cytometry. *Autophagy.* 2014;10:1327–34.
- Guo S, Liang Y, Murphy SF, Huang A, Shen H, Kelly DF, Sobrado P, Sheng Z. A rapid and high content assay that measures cyto-ID-stained autophagic compartments and estimates autophagy flux with potential clinical applications. *Autophagy.* 2015;11:560–72.
- Hale CM, Cheng Q, Ortuno D, Huang M, Nojima D, Kassner PD, Wang S, Ollmann MM, Carlisle HJ. Identification of modulators of autophagic flux in an image-based high content siRNA screen. *Autophagy.* 2016;12:713–26.

- Hurley JH, Nogales E. Next-generation electron microscopy in autophagy research. *Curr Opin Struct Biol.* 2016;41:211–6.
- Kaizuka T, Morishita H, Hama Y, Tsukamoto S, Matsui T, Toyota Y, Kodama A, Ishihara T, Mizushima T, Mizushima N. An autophagic flux probe that releases an internal control. *Mol Cell.* 2016;64:835–49.
- Klionsky DJ, Abdelmohsen K, Abe A, Abedin MJ, Abeliovich H, Acevedo Arozena A, Adachi H, Adams CM, Adams PD, Adeli K, Adhihetty PJ, Adler SG, Agam G, Agarwal R, Aghi MK, Agnello M, Agostinis P, Aguilar PV, Aguirre-Ghiso J, Airoidi EM, Ait-Si-Ali S, Akematsu T, Akporiaye ET, Al-Rubeai M, Albaiceta GM, Albanese C, Albani D, Albert ML, Aldudo J, Algul H, Alirezaei M, Alloza I, Almasan A, Almonte-Beceril M, Alnemri ES, Alonso C, Altan-Bonnet N, Altieri DC, Alvarez S, Alvarez-Erviti L, Alves S, Amadoro G, Amano A, Amantini C, Ambrosio S, Amelio I, Amer AO, Amessou M, Amon A, An Z, Anania FA, Andersen SU, Andley UP, Andreadi CK, Andrieu-Abadie N, Anel A, Ann DK, Anoopkumar-Dukie S, Antonioni M, Aoki H, Apostolova N, Aquila S, Aquilano K, Araki K, Arama E, Aranda A, Araya J, Arcaro A, Arias E, Arimoto H, Ariosa AR, Armstrong JL, Arnould T, Arsov I, Asanuma K, Askanas K, Asselin E, Atarashi R, Atherton SS, Atkin JD, Attardi LD, Auberger P, Auburger G, Aurelian L, Autelli R, Avagliano L, Avantiaggiati ML, Avrahami L, Awale S, Azad N, Bachetti T, Backer JM, Bae DH, Bae JS, Bae ON, Bae SH, Baehrecke EH, Baek SH, Baghdiguian S, Bagniewska-Zadworna A, et al. Guidelines for the use and interpretation of assays for monitoring autophagy (3rd edition). *Autophagy.* 2016;12:1–222.
- Kraft C, Peter M, Hofmann K. Selective autophagy: ubiquitin-mediated recognition and beyond. *Nat Cell Biol.* 2010;12:836–41.
- Lin X, Li S, Zhao Y, Ma X, Zhang K, He X, Wang Z. Interaction domains of p62: a bridge between p62 and selective autophagy. *DNA Cell Biol.* 2013;32:220–7.
- Ni HM, Bockus A, Wozniak AL, Jones K, Weinman S, Yin XM, Ding WX. Dissecting the dynamic turnover of GFP-LC3 in the autolysosome. *Autophagy.* 2011;7:188–204.
- Pugsley HR. Assessing autophagic flux by measuring LC3, p62, and LAMP1 co-localization using multispectral imaging flow cytometry. *J Vis Exp.* 2017;(125):55637.
- Remaut K, Oorschot V, Braeckmans K, Klumperman J, De Smedt SC. Lysosomal capturing of cytoplasmic injected nanoparticles by autophagy: an additional barrier to non viral gene delivery. *J Control Release.* 2014;195:29–36.
- Seleverstov O, Phang JM, Zabinnyk O. Semiconductor nanocrystals in autophagy research: methodology improvement at nanosized scale. *Methods Enzymol.* 2009;452:277–96.
- Shvets E, Fass E, Elazar Z. Utilizing flow cytometry to monitor autophagy in living mammalian cells. *Autophagy.* 2008;4:621–8.
- Tabata K, Hayashi-Nishino M, Noda T, Yamamoto A, Yoshimori T. Morphological analysis of autophagy. *Methods Mol Biol.* 2013;931:449–66.
- Yao J, Qiu Y, Jia L, Zacks DN. Autophagosome immunoisolation from GFP-LC3B mouse tissue. *Autophagy.* 2019;15(2):341–6.
- Yoshimori T. Autophagy: a regulated bulk degradation process inside cells. *Biochem Biophys Res Commun.* 2004;313:453–8.
- Zhang J, Wang J, Ng S, Lin Q, Shen HM. Development of a novel method for quantification of autophagic protein degradation by AHA labeling. *Autophagy.* 2014;10:901–12.
- Zhang Y, Mun SR, Linares JF, Ahn J, Towers CG, Ji CH, Fitzwalter BE, Holden MR, Mi W, Shi X, Moscat J, Thorburn A, Diaz-Meco MT, Kwon YT, Kutateladze TG. ZZ-dependent regulation of p62/SQSTM1 in autophagy. *Nat Commun.* 2018;9:4373.

Chapter 10

Gene Manipulation Protocols in Autophagy



Rong Liu, Ren-Peng Guo, and Yue-Guang Rong

Abstract Macroautophagy (referred to as autophagy hereafter) is a highly conserved catabolic process in eukaryotic cells. Autophagy is essential for cellular homeostasis through elimination and recycling of large cytoplasmic components, such as abnormal protein aggregates and damaged organelles, via lysosomal degradation. Since being originally identified by genetic screening in yeast, autophagy-related (ATG) genes have played a central role in autophagy research in different organisms, including plants, worms, flies, and mammals. Mouse models for monitoring autophagic activity or clarifying its biological functions have also been established. These mice are powerful tools to investigate roles of autophagy *in vivo*. Owing to the rapid technological advances in molecular biology, it is ever more efficient and simpler to manipulate autophagy-associated genes. Herein, we will introduce some commonly used approaches of gene silencing in mammalian cells, including CRISPR/Cas9-mediated gene knockout and siRNA- and shRNA-mediated gene knockdown. We also summarized the common mouse models used for assessing autophagy. We hope to bring the researchers some useful information as they study autophagy.

R. Liu · R.-P. Guo
Nanjing Agricultural University, Nanjing, China
e-mail: liurong010@njau.edu.cn

Y.-G. Rong (✉)
Huazhong University of Science and Technology, Wuhan, China
e-mail: rongyueguang@hust.edu.cn

10.1 The Genetic Information and Mouse Models Used in Autophagy

10.1.1 The Genetic Information Used in Autophagy

In the 1990s, a series of autophagy-related (*ATG*) genes were discovered through yeast genetic screening, which makes it possible to study the autophagic machinery at a molecular level. To date, more than 35 *ATG* genes have been identified in yeast. Among them, *ATG1-10*, *ATG12-14*, *ATG16*, and *ATG18* are highly conserved in mammals (Nakatogawa et al. 2009). These *ATG* genes, together with additional essential factors, form the core autophagy machinery and are indispensable for the process of autophagy. Herein, we will summarize the information about the central genes (or proteins) involved in autophagy induction, autophagosome formation, and autophagosome-lysosome fusion.

10.1.1.1 The ULK1 Complex in Autophagy Induction

Autophagy can be induced via various types of extra- or intracellular stimuli, including nutrient deficiency, withdrawal of growth factors, reduced ATP levels, hypoxia, and other stresses (He and Klionsky 2009). Depletion of amino acids or growth factors (e.g., insulin) is most effective for autophagy induction, and both of these signals converge on the mechanistic target of rapamycin complex 1 (mTORC1, also known as mammalian target of rapamycin complex 1), a central protein kinase of the nutrient-sensing pathway.

The induction of autophagy requires the ULK1 kinase complex. In mammals, the ULK1 complex consists of Unc-51-like kinase 1 (Ulk1, mammalian homolog of yeast Atg1), Atg13, FIP200, and Atg101. Unlike the Atg1 complex in yeast, the ULK1 complex is stably formed, and nutrient-dependent complex disassembly is not observed in mammalian cells. Activities of the ULK1 complex are regulated by mTORC1. Under nutrient-rich conditions, active mTORC1 phosphorylates ULK1 and Atg13 to prevent the membrane targeting of the ULK1 complex. During starvation condition, mTORC1 is inhibited and dissociates from the ULK1 complex. Then, the ULK1 complex is free to phosphorylate other components, such as Atg13 and FIP200, leading to autophagy induction. In addition, the 5'-AMP-activated protein kinase (AMPK) coordinates with mTORC1 to regulate autophagy induction through the phosphorylation of ULK1 at distinct serine residues. Under starvation conditions, AMPK phosphorylates ULK1 at Ser 317 and Ser 777 to disrupt the interaction between mTORC1 and ULK1, leading to the activation of autophagy.

10.1.1.2 The Class III PI3K Complex in Autophagosome Formation

Autophagy induction is followed by autophagosome formation, which is composed of isolation membrane formation, elongation, and completion (Mizushima et al. 2011). In mammals, the class III phosphatidylinositol 3-kinase (PI3KC3) complex is required for isolation membrane formation and assembly. Vacuolar protein sorting 34 (Vps34), the catalytic subunit, is associated with Beclin1 (coded by the *Becn1* gene, homolog of yeast *ATG6*) and Vps15, to form the core elements of PI3KC3 complex (Mizushima and Komatsu 2011). Vps34 is recruited by the ULK1 complex and produces phosphatidylinositol 3-phosphate (PI3P) at initiation sites. PI3P is critical for autophagosome formation and is considered a marker of autophagosome membranes.

Beclin1 play vital roles in autophagosome formation. Its interaction with Vps34 promotes the catalytic activity of Vps34 and increases production of PI3P. Several factors are reported to interact with Beclin1 to regulate the activity of PI3KC3 complex. (1) Atg14L (the mammalian homolog of yeast *Atg14*) is an essential component of Beclin1-Atg14L-Vps34-Vps15 complex that senses membrane curvature and regulates the activity and localization of Vps34. (2) UV radiation resistance-associated gene (UVRAG) is located in the Beclin1-Vps34-Vps15 complex in a mutually exclusive manner with Atg14L, and is involved in trafficking of mature autophagosomes to lysosomes. (3) RUN domain- and cysteine-rich domain containing Beclin1-interacting protein (Rubicon) negatively regulates endosome maturation and autophagy by inhibiting PI3KC3 complex activity. Additional Beclin1-interacting components, including activating molecule in Beclin1-regulated autophagy (AMBRA1); Bax-interacting factor 1 (Bif1); PTEN-induced putative kinase 1 (PINK1); neuronal isoform of protein interaction, specifically with TC10 (nPIST); IP3 receptor (IP3R); the pancreatitis-associated protein; vacuole membrane protein 1 (VMP1); and high mobility group box 1 (HMGB1), are also identified as participating in autophagosome formation (reviewed in (Pyo et al. 2012)). Recently, Cheng et al. reported that a protein associated with UVRAG as autophagy enhancer (Pacer) antagonizes Rubicon to stimulate Vps34 kinase activity to positively regulate autophagosome maturation.

10.1.1.3 Ubiquitin-Like Conjugation Systems in Autophagosome Expansion and Maturation

During expansion of autophagosome membranes, two ubiquitin-like conjugation systems are involved: the Atg12 system and the microtubule-associated protein 1 light chain 3 (LC3) system.

In the first conjugation system of Atg12-Atg5-Atg16L, Atg12 is conjugated to Atg5. Atg12 contains a carboxyl-terminal glycine residue, which is activated by ubiquitin-activating enzyme (E1)-like enzyme Atg7 in an ATP-dependent manner (Mizushima et al. 1998). Atg12 is then transferred to ubiquitin-conjugating enzyme (E2)-like enzyme Atg10, and finally conjugated to Atg5. The Atg12-Atg5 conjugate interacts with Atg16L to form a multimeric Atg12-Atg5-Atg16 protein complex through homodimerization of Atg16L. The Atg12 system has no deconjugating enzyme, and the Atg12-Atg5-Atg16 complex is formed constitutively irrespective of nutrient conditions.

The modification of LC3 by phosphatidylethanolamine (PE) is the second ubiquitin-like conjugation system that is essential for the formation of autophagosomes. LC3 is cleaved by the cysteine protease Atg4 to form cytosolic LC3-I and then conjugated with PE by E1-like enzyme Atg7 and E2-like enzyme Atg3. The last step in Atg3 conjugation requires Atg12-Atg5-Atg16L complex, which serves as an ubiquitin ligase enzyme (E3)-ligase. The resulting LC3-PE (LC3-II) associates with newly forming autophagosome membranes and remains on autophagosomes even after their fusion with lysosomes (Burman and Ktistakis 2010). Thus, the conversion of LC3-I to LC3-II is widely regarded as a marker indicating autophagy induction or fusion of autophagosomes with other organelles.

10.1.1.4 Participants in Autophagosome-Lysosome Fusion

Sequestration of cytoplasmic cargos into the autophagosome is followed by the fusion of the vesicle with a late endosome or lysosome to form the autolysosome. Upon fusion, the cargos are degraded by hydrolases inside the autolysosomes and recycled to the cytoplasm for re-utilization (Nakamura and Yoshimori 2017). Three major participants are involved in this process: Ras-related GTP-binding protein (Rab) GTPases, soluble *N*-ethylmaleimide-sensitive fusion attachment protein receptors (SNARE) proteins, and membrane-tethering complexes.

Rab GTPases are evolutionally conserved regulators of membrane trafficking in eukaryotic cells. Each Rab protein localizes to a distinct membrane area, and thus is thought to provide specificity to membrane trafficking. Rab7 plays a pivotal role in the process of autophagosome-lysosome fusion. Rab7 is localized on late endosomes and lysosomes, and is essential for endocytic membrane trafficking from late endosomes to lysosome, autophagosome-lysosome fusion, and the subsequent degradation of autophagosomal components. Other GTPases, such as Rab33b, Rab22, and Rab24, also participate in regulation of the fusion step.

SNARE proteins play a key role in autophagosome-lysosome fusion. In mammals, there are more than 60 SNARE proteins that mediate the specific recognition and fusion of vesicle trafficking. Functionally, SNAREs can be divided into two categories: vesicle-SNAREs (v-SNAREs) and target-SNAREs (t-SNAREs). v-SNAREs are generally found on vesicles, and t-SNAREs are often localized in targeting membranes. Each v-SNARE or t-SNARE has a helical domain that can be intertwined to form a SNARE complex, enabling specific recognition and efficient fusion of vesicles and target membranes (Zhao and Zhang 2018). During autophagy,

Syntaxin 17 (Stx17) is recruited to the outer membrane of mature autophagosomes and combines with another v-SNARE protein Snap29 to form a complex, which binds to the t-SNARE protein Vamp8 on lysosomes, promoting anchoring and fusion of autophagosomes and lysosomal membranes. Correspondingly, gene silencing of *Stx17*, *Snap29*, and *Vamp8* results in intracellular accumulation of autophagosomes. In addition, Atg14 binds to the binary complex formed between Stx17 and Snap29, promotes its interaction with Vamp8, and promotes the fusion of autophagosomes and lysosomes.

The HOPS complex regulates the endocytic pathway, and also acts as a tethering factor for autophagosome-lysosome fusion. All HOPS components, including Vps33a, Vps16, Vps11, Vps18, Vps39, and Vps41, interact with Stx17. In line with this, these HOPS subunits are recruited to Stx17-positive autophagosomes upon autophagy induction. Furthermore, knockdown of *Vps33a*, *Vps16*, or *Vps39* blocks autophagic flux and causes accumulation of Stx17- and LC3-positive autophagosomes, indicating that HOPS promotes autophagosome-lysosome fusion with Stx17. Ectopic P granules protein 5 (Epg5) is another tethering factor that determines the fusion specificity of autophagosomes with lysosomes. Epg5 stabilizes and facilitates the assembly of the Stx17-Snap29-Vamp8 SNARE complex to promote the fusion between autophagosomes and lysosomes.

Mammalian cells utilize autophagy to maintain homeostasis of materials and energy. In the past decades, owing to the rapid development of molecular biology, increasing numbers of autophagy-associated genes have been investigated. These genes and their products are precious resources for better understanding the mechanism of the autophagy process, and are summarized in Table 10.1. Continued

Table 10.1 The major autophagy machinery and autophagy-associated genes in mammals

Autophagy machinery	Autophagy-associated genes	Corresponding proteins	Features or functions
ULK complex	<i>Ulk1/2</i>	Ulk1/2	Ser/Thr kinase; phosphorylated by mTORC1; recruits ATG proteins to isolation membrane
	<i>Atg13</i>	Atg13	Phosphorylated by mTORC1; modulates the activity of ULK complex
	<i>Rb1cc1</i>	FIP200	Scaffold for ULK1/2 and Atg13
	<i>Atg101</i>	Atg101	Binds and stabilizes Atg13
	Class III PI3K complex	<i>Pik3c3</i>	Vps34
<i>Pik3r4</i>		Vps15	PI3K regulatory subunit
<i>Becn1</i>		Beclin1	Key regulator of Vps34 activity
<i>Atg14</i>		Atg14	Senses membrane curvature; regulates the activity and localization of Vps34
<i>Uvrag</i>		UVRAG	Interacts with Beclin1, activates PI3K complex
<i>Rubcn</i>		Rubicon	Interacts with Beclin1, inhibits PI3K complex activity

(continued)

Table 10.1 (continued)

Autophagy machinery	Autophagy-associated genes	Corresponding proteins	Features or functions
Atg12 conjugation system	<i>Atg12</i>	Atg12	Ubiquitin-like protein; conjugated to Atg5
	<i>Atg7</i>	Atg7	E1-like enzyme
	<i>Atg10</i>	Atg10	E2-like enzyme
	<i>Atg5</i>	Atg5	Atg12 is conjugated to Atg5
	<i>Atg16l1/2</i>	Atg16l1/2	Homodimer; interacts with Atg5
LC3 conjugation system	<i>Map1lc3a/b/c</i>	LC3a/b/c	Ubiquitin-like; conjugated to PE
	<i>Atg4a-d</i>	Atg4a-d	LC3 C-terminal hydrolase; deconjugating enzyme
	<i>Atg7</i>	Atg7	E1-like enzyme
	<i>Atg3</i>	Atg3	E2-like enzyme
Rab GTPases	<i>Rab7a/b/11</i>	Rab7a/b/11	Localizes to late endosomes and lysosomes; recruits tethering complexes to promote fusion
SNARE complex	<i>Stx17</i>	Stx17	v-SNARE
	<i>Snap29</i>	Snap29	v-SNARE, forms binary complex with Stx17 on autophagosomes
	<i>Vamp8</i>	Vamp8	t-SNARE, interacts with binary complex of Stx17 and Snap29
Membrane-tethering complexes	<i>Vps33a</i>	Vps33a	Components of HOPS complex, help SNARE proteins to physically drive the fusion of autophagosomes and lysosomes
	<i>Vps16</i>	Vps16	
	<i>Vps11</i>	Vps11	
	<i>Vps18</i>	Vps18	
	<i>Vps39</i>	Vps39	
	<i>Vps41</i>	Vps41	
	<i>Epg5</i>	Epg5	Stabilizes and facilitates the assembly of Stx17-Snap29-Vamp8 SNARE complex to promote fusion

studies to identify key molecules regulating autophagy and underlying molecular mechanisms are still required to better understand this process.

10.1.2 The Mouse Models Used in Autophagy

As a highly conserved cellular metabolic process, autophagy plays crucial roles in the progress of both physiological and pathological conditions. In the past decade, an increasing number of mouse models have been established to measure autophagic activity and clarify its biological functions. Here, we will summarize currently available autophagy-monitoring mouse models and autophagy-deficient mouse models.

10.1.2.1 Monitoring and Measuring Autophagy Using Transgenic Mice

Among the ATG proteins, LC3 is present on newly forming autophagosome membranes and remains on autophagosomes even after their fusion with lysosomes. Thus, LC3 is widely used as an autophagosome marker. Green fluorescent protein (GFP)-tagged LC3 (GFP-LC3) is the first molecular probe used to monitor autophagy. When GFP-LC3 is expressed, punctate signals can be easily observed by fluorescence microscopy. In 2004, a transgenic mouse ubiquitously expressing GFP-LC3 was developed in Mizushima's lab. The appearance of autophagosomes in mouse tissues can be directly measured by fluorescence microscopy analysis of cryosections. It should be noted that the enrichment of autophagosomes might be ascribed to higher rates of autophagosome induction or impaired autophagosome-lysosome fusion or lysosomal degradation. Thus, without lysosomal inhibition, GFP-LC3 alone cannot indicate autophagic flux. In addition, the fluorescent signal of GFP is quenched quickly under the acidic conditions in lysosomes, and more quantitative systems were developed afterwards.

Transgenic mRFP-GFP-LC3 mice have been developed and validated by examining their response to starvation or autophagy-regulating drugs such as rapamycin. Specifically, mice carrying an mRFP-GFP-LC3 reporter under the control of the CAG promoter were developed to study the autophagic flux in the heart and kidney after ischemia-reperfusion injury. The limitation of the mRFP-GFP-LC3 system is that the identification of RFP/GFP-double positive and single positive puncta is technically difficult *in vitro* and *in vivo*, limiting accurate measurement of autophagic flux.

Mice expressing GFP-LC3-RFP-LC3 Δ G were generated by Mizushima and colleagues in 2016. In addition to monitoring autophagic flux without using lysosomal inhibitors, this system can also be used to measure basal autophagic activity. A key limitation of GFP-LC3-RFP-LC3 Δ G is that the time resolution is poor, requiring over 2 h to detect a clear reduction of the GFP:RFP ratio, which is the relevant measurement for monitoring autophagy.

Selective degradation of mitochondria via mitophagy is critical for mitochondrial quality control. However, reliable methods to monitor mitophagy *in vivo* are quite limited. So far, two reporter systems are available for detecting mitophagic flux in mouse models: mt-Keima and *mito-QC*.

mt-Keima is targeted to mitochondria by fusion to the COX8 subunit. Keima is a pH-dependent fluorescent protein that is resistant to lysosomal hydrolysis. In a neutral environment (mitochondria), mt-Keima is excited predominantly by 458-nm light and produces red signal. When delivered into acidic lysosomes, mt-Keima is activated by 561-nm light and fluoresces red. The ratio of mt-Keima-derived fluorescence (561 nm/458 nm) indicates the activity of mitophagy. Mice expressing the mt-Keima reporter have been developed for the *in vivo* assessment of mitophagy in tissues under a wide range of experimental conditions. It should be noted that freshly sectioned tissue and rapid visualization are required when using mt-Keima, as the Keima protein signal is lost upon conventional fixation. Another disadvantage of mt-Keima is that the emission spectra between acidic and neutral environments

are not completely separated, but this problem may be improved by genetic alterations in the structure of Keima in the future.

Another pH-sensitive mitochondrial fluorescent probe, *mito-QC*, has been generated. *mito-QC* is developed by fusing the tandem mCherry-GFP tag to the mitochondrial targeting sequence of the outer mitochondrial membrane protein FIS1. Like mRFP-GFP-LC3 system, the mitochondria display both red and green signals under steady-state conditions. When mitophagy occurs, mitochondria are delivered to lysosomes, where mCherry fluorescence remains stable, but GFP fluorescence becomes quenched by the acidic pH. A transgenic mouse model harboring *mito-QC* was generated to monitor mitochondrial turnover in a range of tissues. Interestingly, basal mitophagic activity differs among tissues and cell types as indicated by *mito-QC*. The kidney is a major organ of mitophagy, and cardiomitophagy is activated during development in mice. Compared to mt-Keima transgenic mice, the *mito-QC* mice display some advantages such as no overlap in emission spectra and a better compatibility with a variety of labeling techniques.

Together, thanks to fluorescent reporters coupled to LC3 or mitochondrial proteins, various mouse models have been developed to monitor autophagy and mitophagy flux in vivo. The molecular probes, detection methods, and main limitations/advantages of these mouse models are summarized in Table 10.2.

10.1.2.2 Analyzing Autophagy Using ATG Gene Knockout Mice

The majority of ATG genes identified in yeast are highly conserved in mammals, allowing analyses of the roles of autophagy using genetic techniques. Autophagy-deficient mice generated by knockout of core ATG genes are powerful tools to investigate physiological roles and pathological effects of autophagy. Here, we will summarize these mouse models and their phenotypes.

Table 10.2 Transgenic mouse models for monitoring autophagy and mitophagy

Molecular probes	Detection and evaluation	Limitations or advantages
GFP-LC3	GFP-LC3 puncta	Cannot indicate autophagic flux; GFP is quenched in lysosomes
mRFP-GFP-LC3 or mCherry-GFP-LC3	GFP+, RFP+ puncta indicate autophagosomes and GFP-, RFP+ puncta indicate autolysosomes	Indicates autophagic flux; technically difficult to distinguish double positive from single positive puncta
GFP-LC3-RFP-LC3ΔG	The ratio of GFP signal to RFP signal	Measures basal autophagic activity; time resolution is poor
mt-Keima	The ratio of the 561–458 nm excited fluorescence intensity	Measures mitophagic flux; emission spectra overlap; incompatible with fixed tissues
<i>mito-QC</i>	GFP+, RFP+ puncta indicate cytoplasmic mitochondria and GFP-, RFP+ puncta indicate mitophagy	No overlap in emission spectra and compatible with a variety of labeling techniques

Table 10.3 Knockout mice of autophagy-related genes

Genes	Survival time	Phenotypes
<i>Becn1</i>	E7.5 or earlier	Defects in proamniotic canal closure
<i>Rb1cc1</i>	E13.5–E16.5	Defective heart and liver development
<i>Pik3c3</i>	E8.5	Fail to form mesoderm; reduced cell proliferation
<i>Atg9a</i>	Before E14.5	Growth retardation
<i>Atg13</i>	E17.5	Growth retardation; defective heart development
<i>Ulk1/2</i>	Neonatal lethal	Impaired lung function
<i>Atg3, Atg5, Atg7, Atg12, Atg16L1</i>	Neonatal lethal	Die within 1 day after birth, morphologically normal, reduced amino acid levels, suckling defect
<i>Atg4b</i>	Viable	Balance dysfunction
<i>Atg4c</i>	Viable	Fertile, increased susceptibility to carcinogen-induced fibrosarcoma
<i>Ulk1</i>	Viable	Increased reticulocyte number with delayed mitochondrial clearance
<i>Ulk2, Map1lc3b, Gabarap</i>	Viable	No obvious phenotypic defects

In mammals, approximate 20 core autophagy-related genes are involved in autophagosome formation, and 14 of them have been deleted in mice (Kuma et al. 2017). These ATG gene-deficient mice exhibit different phenotypes: some die during embryogenesis, some causes neonatal lethality (within 1 day) despite almost normal appearance at birth, and some show no obvious abnormalities (Table 10.3).

Conventional *Atg5*^{-/-} mice survive early development, but this is owing to the residual maternally inherited *Atg5* protein in *Atg5*^{-/-} oocytes. Oocyte-specific *Atg5*^{-/-} knockout results in embryonic lethality at the four-cell to eight-cell stages. Mice deficient in genes functioning upstream of the ATG conjugation systems, including *Becn1*^{-/-}, *Rb1cc1/FIP200*^{-/-}, *Pik3c3/Vps34*^{-/-}, *Atg9a*^{-/-}, and *Atg13*^{-/-} mice, die during embryonic development. The ULK-deficient mouse is an exception. *Ulk1*^{-/-} or *Ulk2*^{-/-} mice are viable, probably due to the redundant effect, and *Ulk1*^{-/-} *Ulk2*^{-/-} double knockout mice are neonatal lethal. Mice deficient in genes involved in *Atg12* and *LC3* conjugation systems (except *Atg10*) have been generated. Among them, *Atg3*^{-/-}, *Atg5*^{-/-}, *Atg7*^{-/-}, *Atg12*^{-/-}, and *Atg16L1*^{-/-} embryos survive the entire embryonic period and are born at Mendelian frequency but die within 1 day of birth. Mice deficient in redundant genes involved in the two conjugation systems, including *Lc3b*^{-/-}, *Gabarap*^{-/-}, *Atg4b*^{-/-}, and *Atg4c*^{-/-} mice, exhibit no obvious (or weak) abnormalities. Why the phenotypes of different ATG gene knockout mice vary a lot is not completely understood. It may depend on the step in autophagy at which each gene functions, and accordingly, mice lacking upstream autophagy genes may show more severe phenotypes. In addition, the ATG genes may have functions other than autophagy regulation. The

functional redundancy or compensatory mechanisms between different ATG genes can also influence the readouts of knockout mice.

Although embryonic or neonatal lethality is observed in conventional ATG gene knockout mice, it is still possible to investigate autophagy in adult mice by using *Atg5*^{-/-}: NSE-*Atg5* mice. Mizushima and colleagues demonstrate that re-expression of *Atg5* in the brain is sufficient to rescue *Atg5*-null mice from neonatal lethality, suggesting that neuronal dysfunction, including suckling failure, is the primary cause of neonatal death. The majority of these rescued mice survive between 8 weeks and 8 months. Further analysis of this mouse model revealed previously unappreciated roles for *Atg5* in multiple processes, including regulation of the hypothalamic-pituitary-gonadal axis and iron absorption in the intestine. These mice provide a valuable resource for understanding the physiological roles of autophagy in the whole body.

Analysis of autophagy-associated gene knockout mice has greatly contributed to clarifying the physiological functions of autophagy *in vivo*. Currently, studies of autophagy are mainly centered on ATG genes, and mouse models for other autophagy-regulating genes, especially regulators of autophagosome-lysosome fusion, are largely lacking. In the future, combined usage of different mouse models will improve the understanding of the role and mechanism of autophagy.

10.2 Gene Manipulation Techniques in Mammalian Cells

10.2.1 Gene Knockout Techniques in Mammalian Cells

Precise modification of genetic information is essential to understanding the function of a given gene. In the past decades, gene knockout techniques have enabled the elucidation of the role of specific genes in various biological processes.

Traditionally, gene knockout is mainly achieved via homologous recombination, which requires creating a DNA construct containing the desired mutations. This method is inefficient, as homologous recombination accounts for only 10^{-2} – 10^{-3} of DNA integrations, and limited to certain organisms. More recently, technological breakthroughs in genome editing and regulation have significantly improved the efficiency and specificity of gene knockout. Generally, two major parts are required for a molecular machinery to precisely edit DNA sequences: a DNA-binding domain to specifically recognize and bind DNA and an effector domain to mediate DNA cleavage or other effects. Thus, sequence-specific nucleases can be engineered to perform gene knockout. Zinc-finger nucleases (ZFNs) are one type of programmable genome editing machines. ZFNs contain a common Cys₂-His₂ DNA-binding domain, which recognizes codons of a desired DNA sequence, and a DNA cleavage domain of the FokI restriction endonuclease. Another genome editing platform is transcription activator-like effector nucleases (TALENs). TALENs also contain a DNA-binding domain and a nuclease that causes a double-stranded break (DSB) in the DNA.

Though both ZFNs and TALENs can be programmed to target specific DNA sequences, the complicated and time-consuming protein engineering, selection, and validation required restricts their wide application. The clustered regularly interspaced short palindromic repeats (CRISPR)/CRISPR-associated protein 9 (Cas9) is emerging as a powerful system for genome editing, and especially for gene knock-out in diverse organisms.

10.2.1.1 The Principle of CRISPR/Cas9

The CRISPR/Cas system was initially described as an adaptive immune system in bacteria and archaea. The type II CRISPR system is one of the best characterized and has now been engineered as RNA-guided endonucleases for genome editing. The Cas9 protein can be directed to specific DNA regions via a 20-nt single-guide RNA (sgRNA) to create DSBs. The selection of Cas9 target sites requires the presence of a protospacer adjacent motif (PAM) sequence directly 3' of the 20-bp target sequence. For Cas9 nuclease from *S. pyogenes* (SpCas9), the target sequence must immediately precede a NGG-3' PAM, e.g., 5'-GTGCCGAAATGACCGAGTTCGG-3'. By simply purchasing a pair of oligos encoding the 20-nt guide sequence, Cas9 can be easily retargeted to new DNA sequences, which makes customization easier. The DSBs generated by Cas9 activate DNA repair mechanisms of nonhomologous end joining (NHEJ) or homology-directed repair (HDR). Error-prone NHEJ is activated without a template, resulting in insertions and/or deletions (indels) that lead to frameshift mutations and premature stop codons, causing a gene knockout. If a donor template with homology to the target sites exists, the HDR pathway is activated to allow for precise repair. At present, the CRISPR/cas9 system is the most efficient platform for genome editing and popularly used in diverse organisms, though potential off-target effects cannot be ignored (Wang et al. 2016).

10.2.1.2 Applications and Protocol of CRISPR/Cas9

ATG genes can be efficiently manipulated via the CRISPR/Cas9 system to investigate their functions. As essential components of Atg12 and LC3 conjugation systems, Atg5 and Atg7 are required for autophagosome formation (see introduction above). Thus, either Atg5 or Atg7 is commonly removed through Cas9 or other methods to block autophagy and reveal the roles of autophagy in various mammalian cells.

Similar to other mammalian genes, CRISPR/Cas9-mediated gene knockout of Atg5 or Atg7 mainly includes:

1. Target selection for sgRNA. When searching for target sites in the genome, one requirement is that a PAM immediately follows the target DNA locus. However, this does not severely restrict the targeting range of Cas9, as PAM sequences can

be found on average every 8–12 bp in the human genome. It is recommended to use an online CRISPR Design Tool (<http://tools.genome-engineering.org>) to select sgRNAs that offer suitable target sites. Possible off-target effects of Cas9 should also be considered, and at least two distinct sgRNAs are required for each gene.

2. sgRNA construction and delivery. Expression plasmids for sgRNA are always used to deliver sgRNA. The plasmids, such as the widely used pSpCas9(BB)-2A-Puro (PX459), are engineered to express Cas9 and sgRNA simultaneously. The purchased oligo pairs encoding the 20-nt guide sequences can be ligated into the plasmid after annealing. Other transfection plasmids enabling virus production *in vivo* are also used, such as LentiCRISPRv2.
3. Clonal isolation. Clonal isolation of transfected cells is necessary to establish pure and stable knockout cell lines. Serial dilutions and flow cytometry can be used to isolate single cells after transfection and antibiotic selection.
4. Knockout validation of cell lines. The SURVEYOR nuclease assay is commonly used in detecting editing efficiency of CRISPR/Cas9. SURVEYOR nuclease or other endonucleases, such as T7 Endonuclease I, are able to recognize and cleave non-perfectly matched DNA, cruciform DNA structures, Holliday structures or junctions, and heteroduplex DNA to detect mutants. Genomic amplicons of the target region can be cloned into a plasmid, and a set of clones can be prepared for Sanger sequencing to determine the genotype of modified cell lines. In addition, western blot or other functional tests are required to validate gene knockout mediated by CRISPR/Cas9.

10.2.2 Gene Knockdown Techniques in Mammalian Cells

In addition to gene knockout, gene knockdown techniques are widely used for genetic functional analysis. Expression of one or more of an organism's genes is reduced in knockdown experiments. The reduction can occur via genetic modification or by treatment with a short DNA or RNA oligonucleotide that is complementary to either a gene or a messenger RNA (mRNA) transcript (Summerton 2007). Small interfering RNA (siRNA) and short hairpin RNA (shRNA) are two commonly used methods of gene knockdown.

10.2.2.1 Autophagy Gene Knockdown by siRNA

10.2.2.1.1 The Principle of siRNA

siRNA is also known as short interfering RNA or silencing RNA. It is a short (typically 20–24 bp) double-stranded RNA (dsRNA) with phosphorylated 5' ends and hydroxylated 3' ends with two overhanging nucleotides. siRNAs are easily

designed and synthesized and introduced into the cell. In the cytoplasm, exogenous siRNAs are processed by the RNA-induced silencing complex (RISC), in which the sense strand of siRNA is degraded and ejected from RISC, and the remaining antisense strand binds to its complementary mRNA to trigger mRNA degradation by RISC.

10.2.2.1.2 The Application of siRNA

RNA interference (RNAi) mediated by siRNA can be used to silence a specific autophagy gene to identify its function or to measure the role of autophagy in various mammalian cells. Further, the genome-wide siRNA screen is a powerful tool to reveal the mechanism of autophagy and identify novel autophagy regulators:

1. In a genome-wide human siRNA screen, Lipinski et al. (2010) demonstrated that upregulation of autophagy requires the type III PI3K, but not inhibition of mTORC1 under normal nutrient conditions. They also show that a group of growth factors and cytokines, which positively regulate cell growth and proliferation, including MAPK-ERK1/2, Stat3, Akt/Foxo3, and CXCR4/GPCR, inhibit the type III PI3K. This study suggests that autophagy and cell proliferation may represent two alternative cell fates that are regulated in a mutually exclusive manner.
2. Orvedahl et al (2011). performed a high-content, image-based, genome-wide siRNA screen to detect mammalian genes required for selective autophagy. They identified 141 candidate genes required for viral autophagy, which were enriched for pathways of mRNA processing, interferon signaling, vesicle trafficking, cytoskeletal motor function, and metabolism. Among these gene products, SMURF1, a C2-domain-containing protein, was determined to be a novel mediator of both viral autophagy and mitophagy.
3. Continuing with Orvedahl et al.'s work, Mauthe et al. (2016) also determined the effects of ATG proteins on the replication of six different viruses through siRNA screening. An undocumented role for Atg13 and FIP200 in picornavirus replication, which is independent of their function in autophagy as components of the ULK complex, is revealed in this paper.
4. To find new proteins that modulate starvation-induced autophagy, McKnight et al. (2012) performed a genome-wide siRNA screen in a stable human cell line expressing GFP-LC3. They identified nine novel autophagy regulators and studied two of them in depth. SCOC is found to form a complex with UVRAG and FEZ1 to regulate ULK1 complex activities. Another candidate, WAC, is required for starvation-induced autophagy but also acts as a potential negative regulator of the ubiquitin-proteasome system.

Together, these genome-wide siRNA screens on autophagy-regulating genes are valuable resources to understand the mechanisms and novel roles of autophagy.

10.2.2.1.3 The Protocol of siRNA

1. Design siRNA
2. Plate $0.2\text{--}1.0 \times 10^6$ cells per well in a six-well plate 24–48 h before transfection, so they will be 20–70% confluent.
3. Dilute 10–30-pmol siRNA in 50–100- μL serum-free medium; incubate at room temperature for 5 min.
4. Add transfection reagent to 50–100 μL serum-free medium (1:2–1:3 ratio); incubate at room temperature for 5 min.
5. Add diluted siRNA to diluted transfection reagent; incubate at room temperature for 20 min.
6. Add siRNA-lipid complex to cells; rock the plate gently back and forth to evenly distribute the complexes.
7. After transfection, incubate the cells at 37 °C under normal cell culture conditions for 24–48 h. Then, analyze transfected cells for knockdown efficiency.

10.2.2.2 Autophagy Gene Knockdown by shRNA

10.2.2.2.1 The Principle of shRNA

Synthesized siRNA-mediated gene silencing is simple and fast. However, siRNAs have a major drawback of a short lifespan, which weakens their ability to regulate gene expression. The shRNA approach overcomes this limitation and inhibits gene expression more stably.

A shRNA is an artificial RNA molecule that can spontaneously form a hairpin structure, and is widely applied to silence expression of genes in mammals. shRNAs can be delivered into cells through plasmids or various viral vectors. Once introduced into the cell, the shRNA is transcribed via the promoter on the vector. The product mimics pri-microRNA (pri-miRNA) and is processed by Drosha. The formed pre-shRNA is exported from the nucleus by Exportin 5, and then recognized by the cellular RNAi machinery and processed to form active siRNAs. After that, the task of gene silencing can be completed via siRNAs as introduced above.

10.2.2.2.2 The Application of shRNA

In mammalian cells, knockdown of ATG genes via shRNA approach is quite common to block autophagy. Similar to the siRNA technique, a genome-wide shRNA screen can also be utilized to search novel autophagy regulators. Strohecker et al. (2015) developed a high-content image-based shRNA screening system via monitoring levels of the autophagy substrate p62/SQSTM1. They identified 186 putative autophagy inhibitors and 67 potential autophagy stimulators. Among them, PFKFB4 was shown to regulate autophagy through influencing redox balance in the cell. Recently, Cassidy et al. (2018) developed an inducible shRNA mouse model

targeting *Atg5*, termed ATG5i mice. Unlike conventional and conditional whole-body knockout mouse models of key autophagy genes, which display perinatal death and lethal neurotoxicity, respectively, ATG5i mice make dynamic inhibition of autophagy in vivo possible. The researchers find that ATG5i mice recapitulate many of the previously described phenotypes of tissue-specific knockouts. They also demonstrate that hepatomegaly and other pathologies associated with autophagy deficiency can be rescued with restoration of autophagy; however, this leads to the development of hepatic fibrosis. These ATG5i mice are good resources to investigate the pathological consequences of autophagy inhibition and restoration.

10.2.2.2.3 The Protocol of shRNA

1. Design and construct the shRNA expression plasmid.
2. Plate $0.2\text{--}1.0 \times 10^6$ cells per well in a six-well plate 24–48 h before transfection, so they will be 20–70% confluent.
3. Dilute 2–10- μg plasmid in 50–100- μL serum-free medium; incubate at room temperature for 5 min.
4. Add transfection reagent to 50–100- μL serum-free medium (1:1–1:2 ratio); incubate at room temperature for 5 min.
5. Add diluted plasmid to diluted transfection reagent; incubate at room temperature for 20 min.
6. Add plasmid-lipid complex to cells; rock the plate gently back and forth to evenly distribute the complexes.
7. After transfection, incubate the cells at 37 °C under normal cell culture conditions for 24–48 h. Then, analyze transfected cells for knockdown efficiency.

In this chapter, we reviewed what is known about the main autophagy-associated genes in mammals and commonly used mouse models of autophagy. We also introduced some popular approaches to gene manipulation in the field of autophagy research, including CRISPR/Cas9-mediated gene knockout and siRNA- and shRNA-mediated gene knockdown. Autophagy-related genes can be manipulated through the abovementioned methods at both the genomic and transcriptional levels. Mouse models with modified autophagy genes have also been established to provide more in vivo evidence for better understanding the roles of autophagy in both physiological and pathological conditions.

References

- Burman C, Ktistakis NT. Autophagosome formation in mammalian cells. *Semin Immunopathol.* 2010;32(4):397–413.
- Cassidy LD, et al. A novel *Atg5*-shRNA mouse model enables temporal control of Autophagy in vivo. *Autophagy.* 2018;14(7):1256–66.

- He C, Klionsky DJ. Regulation mechanisms and signaling pathways of autophagy. *Annu Rev Genet.* 2009;43:67–93.
- Kuma A, Komatsu M, Mizushima N. Autophagy-monitoring and autophagy-deficient mice. *Autophagy.* 2017;13(10):1619–28.
- Lipinski MM, et al. A genome-wide siRNA screen reveals multiple mTORC1 independent signaling pathways regulating autophagy under normal nutritional conditions. *Dev Cell.* 2010;18(6):1041–52.
- Mauthe M, et al. An siRNA screen for ATG protein depletion reveals the extent of the unconventional functions of the autophagy proteome in virus replication. *J Cell Biol.* 2016;214(5):619–35.
- McKnight NC, et al. Genome-wide siRNA screen reveals amino acid starvation-induced autophagy requires SCOC and WAC. *EMBO J.* 2012;31(8):1931–46.
- Mizushima N, Komatsu M. Autophagy: renovation of cells and tissues. *Cell.* 2011;147(4):728–41.
- Mizushima N, et al. A protein conjugation system essential for autophagy. *Nature.* 1998;395(6700):395–8.
- Mizushima N, Yoshimori T, Ohsumi Y. The role of Atg proteins in autophagosome formation. *Annu Rev Cell Dev Biol.* 2011;27:107–32.
- Nakamura S, Yoshimori T. New insights into autophagosome-lysosome fusion. *J Cell Sci.* 2017;130(7):1209–16.
- Nakatogawa H, et al. Dynamics and diversity in autophagy mechanisms: lessons from yeast. *Nat Rev Mol Cell Biol.* 2009;10(7):458–67.
- Orvedahl A, et al. Image-based genome-wide siRNA screen identifies selective autophagy factors. *Nature.* 2011;480(7375):113–7.
- Pyo JO, Nah J, Jung YK. Molecules and their functions in autophagy. *Exp Mol Med.* 2012;44(2):73–80.
- Stroecker AM, et al. Identification of 6-phosphofructo-2-kinase/fructose-2,6-bisphosphatase as a novel autophagy regulator by high content shRNA screening. *Oncogene.* 2015;34(45):5662–76.
- Summerton JE. Morpholino, siRNA, and S-DNA compared: impact of structure and mechanism of action on off-target effects and sequence specificity. *Curr Top Med Chem.* 2007;7(7):651–60.
- Wang HF, La Russa M, Qi LS. CRISPR/Cas9 in genome editing and beyond. *Annu Rev Biochem.* 2016;85:227–64.
- Zhao YG, Zhang H. Formation and maturation of autophagosomes in higher eukaryotes: a social network. *Curr Opin Cell Biol.* 2018;53:29–36.

Chapter 11

MicroRNAs Regulating Autophagy in Neurodegeneration



Qingxuan Lai, Nikolai Kovzel, Ruslan Konovalov, and Ilya A. Vinnikov

Abstract Social and economic impacts of neurodegenerative diseases (NDs) become more prominent in our constantly aging population. Currently, due to the lack of knowledge about the aetiology of most NDs, only symptomatic treatment is available for patients. Hence, researchers and clinicians are in need of solid studies on pathological mechanisms of NDs. Autophagy promotes degradation of pathogenic proteins in NDs, while microRNAs post-transcriptionally regulate multiple signalling networks including autophagy. This chapter will critically discuss current research advancements in the area of microRNAs regulating autophagy in NDs. Moreover, we will introduce basic strategies and techniques used in microRNA research. Delineation of the mechanisms contributing to NDs will result in development of better approaches for their early diagnosis and effective treatment.

11.1 Introduction

Neurodegenerative diseases (NDs) represent a major threat to the modern society, affecting tens of millions of people worldwide with a particular increase of incidence among the elderly (GBD 2015 Neurological Disorders Collaborator Group 2017). The most common NDs are caused by misfolding and accumulation of disease-specific proteins. Depending on the protein causing such accumulation, NDs can be further classified as tauopathies if such a prion-like protein is represented by phosphorylated tau protein, amyloidoses for amyloid β ($A\beta$) protein pathology, synucleinopathies for α -synuclein (SNCA), transactive response DNA

Qingxuan Lai and Nikolai Kovzel contributed equally to this work.

Q. Lai · N. Kovzel · R. Konovalov · I. A. Vinnikov (✉)
Laboratory of Molecular Neurobiology, Department of Genetics and Developmental Biology,
Sheng Yushou Center of Cell Biology and Immunology, School of Life Sciences and
Biotechnology, Shanghai Jiao Tong University, Shanghai, China
e-mail: i.vinnikov@sjtu.edu.cn

binding protein 43 (TDP-43) proteinopathies and prion diseases for scarpie isoform of the prion protein and others (Dugger and Dickson 2017). Tauopathies include progressive supranuclear palsy, corticobasal syndrome, frontotemporal dementia and parkinsonism linked to chromosome 17 (FTDP-17), chronic traumatic encephalopathy and Alzheimer's disease (AD) to name just a few (Orr et al. 2017). The latter can also be categorized as amyloidosis which is characterized by extracellular deposition of A β (Dogan 2017; Koo et al. 1999; Kametani and Hasegawa 2018). Synucleinopathies include Parkinson's disease (PD), PD-like dementia, dementia with Lewy bodies and multiple system atrophy (MSA) (Valera et al. 2017). Accumulation of TDP-43, a 43-kDa protein involved in transcription repression, splicing and RNA metabolism, can lead to amyotrophic lateral sclerosis (ALS) and ubiquitin-positive, and tau- and alpha-synuclein-negative frontotemporal dementia (FTLD-TDP) (Neumann et al. 2006; Yu et al. 2020). All the above examples include NDs involving pathogenic accumulation of misfolded proteins (often referred to as prion-like proteins) which can be counteracted by the autophagy pathway (Dugger and Dickson 2017). Currently, the cause of most of the NDs is unknown which complicates their diagnosis and treatment. Genetic, epigenetic, hormonal and environmental factors can contribute to these pathologies. This chapter discusses studies about autophagy-regulating microRNAs in NDs (Fig. 11.1, Table 11.1).

11.1.1 Autophagy in Neurodegenerative Diseases

Autophagy is a complex process for repurposing the energy flows, degradation and recycling of intact and malfunctioning proteins and organelles within the cell. Autophagy is subdivided into macroautophagy, chaperon-mediated autophagy and microautophagy (Fig. 11.1). The major proteins regulating this process are called 'autophagy-related' (Atg). Many NDs are accompanied by autophagy abnormalities (Nixon 2013; Harris and Rubinsztein 2012). Prion-like proteins involved in NDs pathogenesis such as A β (Stöhr et al. 2012), phosphorylated tau (Sanders et al. 2014), SNCA (Woerman et al. 2018), mutant huntingtin (Jeon et al. 2016) and TDP43 (Nonaka et al. 2013) can aggregate into complex structures with long half-lives, while autophagy can counteract accumulation of such aggregates (Dugger and Dickson 2017). Neurons are highly differentiated post-mitotic cells and hence are vulnerable to autophagy dysfunction due to their limited ability to regenerate and because the accumulating prion-like proteins cannot be diluted by cellular division (Finkbeiner 2020).

11.1.1.1 Autophagy in Alzheimer's Disease

Alzheimer's disease (AD) is the most common ND affecting primarily the neocortex and hippocampus (Calderon-Garcidueñas and Duyckaerts 2017) and characterized by aggregation of A β protein, tau protein and some other proteins leading to a

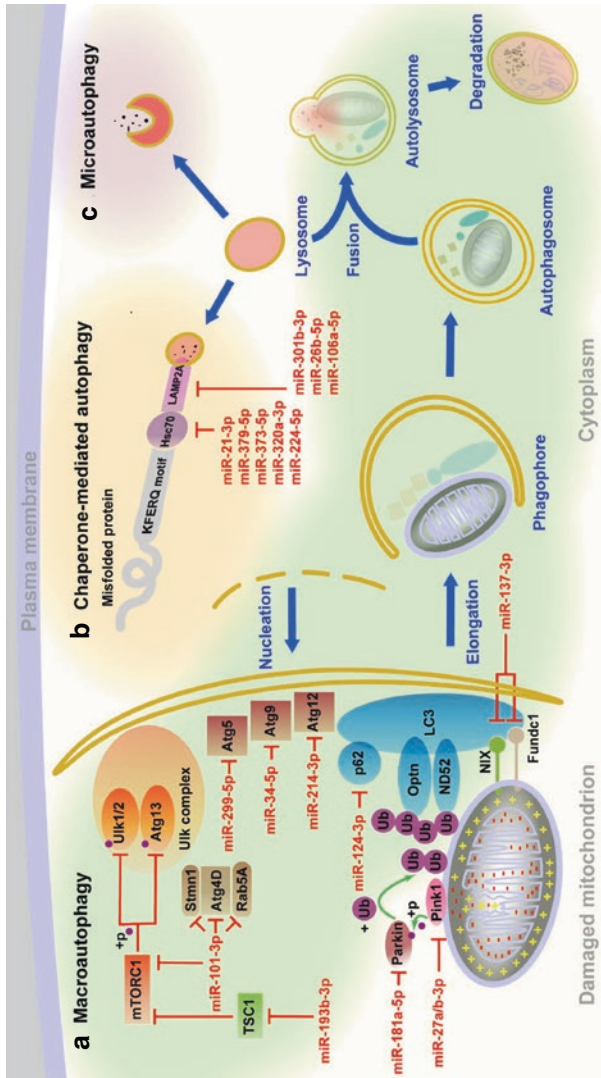


Fig. 11.1 MicroRNAs regulating autophagy in neurodegeneration. The scheme depicts mitophagy as one of the forms of macroautophagy (a), chaperone-mediated autophagy (b) and microautophagy (c) pathways and neurodegeneration-related microRNAs targeting the critical regulators of these pathways. (a) Upon membrane potential loss in the damaged mitochondria, Parkin is being recruited to PINK1 (PTEN-induced putative kinase 1) followed by ubiquitinylation of the proteins on the outer mitochondrial membrane which are recognized by macroautophagy receptors optineurin (Optn) and nuclear dot protein (NDS2). These receptors bind LC3 (microtubule-associated protein1 light chain 3) to initiate the formation of autophagosome. The key regulators involved in the initiation include also Atg (autophagy-related), NIX (also known as Bnip3L, BCL2 interacting protein 3 like), Fundc1 (FUN14 domain containing 1), Ulk (Unc-51 like autophagy activating kinase), cargo receptor p62, mTORC1 (mammalian/mechanistic target of rapamycin complex 1) and other proteins not depicted here for simplicity. (b) In chaperone-mediated autophagy, misfolded proteins are recognized by Hsc70 (heat shock cognate protein 70) chaperone through a pentapeptide motif (KFERQ). This complex then binds to LAMP2A (lysosomal-associated membrane protein 2A) on the lysosome for further degradation. The acidic content of lysosome and autolysosome (a–c) is depicted with crimson. For more details, see Table 11.1

Table 11.1 Studies on microRNAs regulating autophagy in neurodegenerative diseases

MicroRNA	Target	Prediction tools	Validation <i>in vitro</i>	Validation <i>in vivo</i>	Behaviour tests	Age-related changes in miR/target expression	Expression level in neurodegeneration	References
• miR-34a-5p	• Atg9	• TargetScan	• Dual luciferase assay on HeLa cells	• Atg9, autophagy and lifespan \nearrow upon loss of miR-34a-5p in <i>C. elegans</i>	• Movement assay	• miR-34a-5p \nearrow in WI-38 human fibroblasts with induced growth arrest (qRT-PCR) and in <i>C. elegans</i> (microarray)	• miR-34a-5p \nearrow in AD model APP ^{swe} /PSΔE9 mice (RT-PCR)	Yang et al. (2013); Ibañez-Ventoso et al. (2006); Maes et al. (2009); Wang et al. (2009a)
• miR-214-3p	• Atg12	• miRDB • microRNA.org	• Dual luciferase assay on undifferentiated SH-SY5Y cells • Microarray profiling and Western blot analysis on primary hippocampal neurons from SAMP8 mice using mimics and antagoniRs	• Atg12 \searrow (western blot) upon injection of mimics to the third ventricle of SAMP8 mice	• Morris water maze	• miR-214-3p \nearrow in extremely old liver tissues of C57BL/6J mice (microarray hybridization) • Atg-12 inactivation using RNAi shortened lifespan in <i>C. elegans</i>	• miR-214-3p \nearrow in STHdhQ111/HdhQ111 cell model of Huntington's disease (qRT-PCR) • miR-214-3p \searrow in the serum of PD patients • miR-214-3p \searrow in cerebrospinal fluid of sporadic AD patients • miR-214-3p \nearrow in grey matter of temporal cortex in AD patients (microarray)	Zhang et al. (2016a); Wang et al. (2011); Sinha et al. (2010); Maes et al. (2008); Dong et al. (2016); Hars et al. (2007)
• miR-299-5p	• Atg5	• TargetScan	• Atg5 \searrow upon mimics treatment (western blot) • Atg5 \nearrow upon miR-299-5p antagoniR treatment of primary hippocampal neurons from APP ^{swe} /PS1ΔE9 mice	• Atg5 \searrow (immuno fluorescence) and \nearrow cognitive performance upon injection of mimic to the third ventricle of APP ^{swe} /PS1ΔE9 mice	• Fear conditioning test • Cued conditioning test • Morris water maze	• miR-299-5p \searrow in aged human peripheral blood mononuclear cells (RT-PCR) • Atg5 \searrow due to hypermethylation in aged mouse macrophages	• miR-299-5p \nearrow in cerebrospinal fluid of AD patients • miR-299-5p \searrow in PD dopaminergic neurons upon starvation and in hippocampi of APP ^{swe} /PS1ΔE9 mice • miR-299-5p \searrow in hippocampus of AD mice model APP ^{swe} /PS1ΔE9 • miR-299-5p \searrow in temporal cortex of AD patients (microarray)	Zhang et al. (2016b); Wang et al. (2011); Noren Hooten et al. (2010); Tolosa et al. (2018); Khalil et al. (2016)

<ul style="list-style-type: none"> • miR-124-3p 	<ul style="list-style-type: none"> • p62 	<ul style="list-style-type: none"> • TargetScan 	<ul style="list-style-type: none"> • p62 \searrow in HEK293 cells transfected with miR-24-3p mimic (qRT-PCR, western blot) 	<ul style="list-style-type: none"> • p62 and neuroinflammation \searrow in SNpc of MPTP-induced mouse neurodegeneration model upon exosomal delivery of miR-124-3p (RT-PCR, cytokine assay) 	<ul style="list-style-type: none"> • N/A 	<ul style="list-style-type: none"> • BACE1 activity (but not expression levels) \nearrow in aged brains of humans, rhesus monkeys and mice. However, the enzyme concentration remains unchanged • miR-124-3p \nearrow in aged human skin (RT-PCR) 	<ul style="list-style-type: none"> • See above for miR-124-3p 	<p>Yao et al. (2019)</p>
<ul style="list-style-type: none"> • miR-101-3p 	<ul style="list-style-type: none"> • mTOR • STMN1 • RAB5A • Atg4D 	<ul style="list-style-type: none"> • MIRANDA • TargetScan 	<ul style="list-style-type: none"> • α-Synuclein \nearrow, autophagy \searrow upon treatment of oligodendrocytes with the mimic-equipped lentiviral construct • α-Synuclein \searrow, autophagy \nearrow upon treatment of oligodendrocytes with the antagomiR-equipped lentiviral construct 	<ul style="list-style-type: none"> • Oligodendrocyte α-synuclein \searrow (qRT-PCR and Western blot) and autophagy \nearrow (immunocytochemistry, western blot) upon injection of antagomiR-equipped lentiviral construct to striatum of the MBP-α-synuclein transgenic mouse model of MSA 	<ul style="list-style-type: none"> • N/A 	<ul style="list-style-type: none"> • miR-101-3p \searrow in aged human T cells foreskin cells • mTORC1 activity \nearrow with aging 	<ul style="list-style-type: none"> • miR-101-3p \searrow in cortex of AD patients • mTORC1 expression \nearrow in hippocampus of patients with severe AD • mTORC1 \searrow in cardiac cells of mouse Huntington's disease model 	<p>Nunez-Iglesias et al. (2010); Sun et al. (2014a); Child et al. (2018); Guillén and Benito (2018); Valera et al. (2017)</p>

(continued)

Table 11.1 (continued)

MicroRNA	Target	Prediction tools	Validation <i>in vitro</i>	Validation <i>in vivo</i>	Behaviour tests	Age-related changes in miR/target expression	Expression level in neurodegeneration	References
<ul style="list-style-type: none"> miR-193b-3p 	<ul style="list-style-type: none"> TSC1 	<ul style="list-style-type: none"> N/A 	<ul style="list-style-type: none"> Dual luciferase assay on NSC-34 cells qRT-PCR/western blot on NSC-34 cells using miR-mimics, inhibitors or scrambled oligonucleotides GFP-LC3 puncta imaging on NSC-34 cells transfected with GFP-LC3 plasmids and mimics, inhibitors or scrambled oligonucleotides 	<ul style="list-style-type: none"> Western blot on spinal cord in the SOD1G93A mouse model of ALS 	<ul style="list-style-type: none"> N/A 	<ul style="list-style-type: none"> TSC1 \nearrow in aged skin cells (Illumina Human HT-12 V3 BeadChips) 	<ul style="list-style-type: none"> miR-193a-3p \searrow in serum of PD patients miR-193a-3p \searrow in serum of AD patients and <i>in vitro</i> AD model in PC12 and undifferentiated SH-SY5Y cell lines TSC1 \searrow in brain tissue of AD patients miR-193a-3p \searrow in white matter of temporal cortex in AD patients (microarray) 	<ul style="list-style-type: none"> Wang et al. (2011); Dong et al. (2016); Li et al. (2017b, 2018b); Cao et al. (2020); Glass et al. (2013)
<ul style="list-style-type: none"> miR-27a/b-3p 	<ul style="list-style-type: none"> PINK1 	<ul style="list-style-type: none"> TargetScan PicTar miRanda 	<ul style="list-style-type: none"> Dual luciferase assay on HeLa cells Western blot on HeLa and M17 cells using LNA-containing antagomiRs 	<ul style="list-style-type: none"> N/A 	<ul style="list-style-type: none"> N/A 	<ul style="list-style-type: none"> miR-27a-3p and miR-27b-5p \searrow in human aged T-cells and aged foreskin cells miR-27a-3p concentration \searrow in aged peripheral blood mononuclear cells (RT-PCR) PINK1 \searrow in aged murine lung tissue 	<ul style="list-style-type: none"> miR-27a-3p \nearrow in blood plasma of PD patients miR-27a-3p \searrow in cerebrospinal fluid of AD patients miR-27b-5p \nearrow in blood monocytes and macrophages of AD patients miR-27a-3p and miR-27b-5p \nearrow in the following brain regions of AD patients: cerebellum, medial frontal gyrus, hippocampus (qRT-PCR) 	<ul style="list-style-type: none"> Kim et al. (2016a); Noren Hooten et al. (2010); Chen et al. (2018); Guedes et al. (2016); Sosulski et al. (2015); Sala Frigerio et al. (2013); Haackl et al. (2010)

<ul style="list-style-type: none"> miR-181a-5p 	<ul style="list-style-type: none"> Parkin 	<ul style="list-style-type: none"> TargetScan miRanda FindTar 	<ul style="list-style-type: none"> Dual luciferase assay on undifferentiated SH-SY5Y cells Western blot on undifferentiated SH-SY5Y cells using LNA-modified antagonomiRs 	<ul style="list-style-type: none"> N/A 	<ul style="list-style-type: none"> N/A 	<ul style="list-style-type: none"> miR-181a-5p in aged mice brain miR-181a-5p in aged human serum 	<ul style="list-style-type: none"> miR-181a-5p in white matter of temporal cortex in AD patients (microarray testing) 	<p>Cheng et al. (2016); Wang et al. (2011); Noren Hooten et al. (2013); Smith-Vikos and Slack (2012)</p>
<ul style="list-style-type: none"> miR-137-3p 	<ul style="list-style-type: none"> FUNDC1 NIX 	<ul style="list-style-type: none"> TargetScan DIANA microT-CDS 	<ul style="list-style-type: none"> Dual luciferase assay on HEK-293 cells Western blot on SH-SY5Y, HEK293, HeLa and MEF cells using mimics, and antagonomiRs 	<ul style="list-style-type: none"> N/A 	<ul style="list-style-type: none"> N/A 	<ul style="list-style-type: none"> miR-137-3p in plasma of PD patients (qRT-PCR analysis) miR-137-3p in brain samples of AD patients (qRT-PCR analysis) miR-137-3p in blood serum of AD patients (qRT-PCR analysis) miR-137-3p in Hdh 109/109 cell Huntington's disease model (RT-PCR) 	<ul style="list-style-type: none"> miR-137-3p in plasma of PD patients (qRT-PCR analysis) miR-137-3p in brain samples of AD patients (qRT-PCR analysis) miR-137-3p in blood serum of AD patients (qRT-PCR analysis) miR-137-3p in Hdh 109/109 cell Huntington's disease model (RT-PCR) 	<p>Li et al. (2017b); Geekiyange and Chan (2011); Geekiyange et al. (2012)</p>
<ul style="list-style-type: none"> miR-26b-5p miR-106a-5p miR-301b-3p 	<ul style="list-style-type: none"> Hsc70 	<ul style="list-style-type: none"> N/A 	<ul style="list-style-type: none"> Dual luciferase assay on undifferentiated SH-SY5Y cells 	<ul style="list-style-type: none"> N/A 	<ul style="list-style-type: none"> N/A 	<ul style="list-style-type: none"> miR-106a-5p in foreskin, mesenchymal stem cells and CD8+ T-cells from old donors (LNA microarrays) 	<ul style="list-style-type: none"> All 3 microRNAs (RT-PCR), while Hsc70 (RT-PCR and western blot) in PD SNpc 	<p>Alvarez-Erviti et al. 2010, 2013; Hackl et al. (2010); Mimura et al. (2014)</p>

(continued)

Table 11.1 (continued)

MicroRNA	Target	Prediction tools	Validation <i>in vitro</i>	Validation <i>in vivo</i>	Behaviour tests	Age-related changes in miR/target expression	Expression level in neurodegeneration	References
<ul style="list-style-type: none"> miR-21-5p miR-224-5p miR-379-5p miR-373-3p miR-320a-3p 	<ul style="list-style-type: none"> LAMP2A 	<ul style="list-style-type: none"> N/A 	<ul style="list-style-type: none"> Dual luciferase assay on undifferentiated SH-SY5Y cells 	<ul style="list-style-type: none"> N/A 	<ul style="list-style-type: none"> N/A 	<ul style="list-style-type: none"> No change of LAMP-2A in the human cerebrospinal fluid during aging 	<ul style="list-style-type: none"> miR-21-3p, miR-224, miR-373-5p (RT-PCR) while LAMP-2A (RT-PCR and western blot) miR-224-5p, miR-373-5p (RT-PCR) while LAMP-2A (RT-PCR and western blot) 	<ul style="list-style-type: none"> Alvarez-Erviti et al. (2010, 2013); Kiffin et al. (2007)

AD Alzheimer's disease, *ALS* amyotrophic lateral sclerosis, *APP^{swe/PS1ΔE9}* a double-transgenic AD mouse model expressing a chimeric mouse/human amyloid precursor protein Mo/HuAPP695^{swe} and mutated PSEN 1 (PS1ΔE9) protein in the neurons of the central nervous system, *Atg* autophagy-related, *Fundc1* FUN14 domain containing 1, *Hsc70* heat shock cognate protein 70, *HD* Huntington's disease, *LAMP-2* lysosomal-associated membrane protein 2, *LNA* locked nucleic acid, a stable nucleotide analogue containing a methylene bridge between the 2' and 4' oxygen of the ribose ring, *MBP* myelin basic protein, *MEF* mouse embryonic fibroblast, *MPTP* 1-methyl-4-phenyl-1,2,3,6-tetrahydropyridine, *MSA* multiple system atrophy, *mTORC1* mammalian (or mechanistic) target of rapamycin complex 1, *N1X* (or *Binp3L*) BCL2 interacting protein 3 like, *NSC-34* mouse motor neuron-like diploid cells, *PC12* a cell line derived from a pheochromocytoma of the rat adrenal medulla, *PD* Parkinson's disease, *PINK1* PTEN-induced putative kinase 1, *qRT-PCR* (real time) quantitative reverse-transcription polymerase chain reaction, *SAMP8* a sporadic AD mouse model established on the basis of *AKR/J* line, *SH-SY5Y* dopaminergic neuroblastoma cells, *SNpc* substantia nigra pars compacta

progressive loss of neurons (Blennow et al. 2006; Hardy and Selkoe 2002). AD is associated with impaired lysosomal, autophagosome and autolysosome function (Yu et al. 2005; Boland et al. 2008). As evidenced by experiments in mice (Spilman et al. 2010), primary rat neurons (Boland et al. 2008; Tian et al. 2011), mouse embryonic fibroblasts (Tian et al. 2011) and murine neuroblastoma N2a cells (Tian et al. 2011), autophagy can effectively counteract A β accumulation. Indeed, knock-out of autophagy-promoting protein Atg7 (autophagy-related 7) reduces the extracellular secretion of A β and plaque formation in APP (amyloid precursor protein) transgenic mice and increases intracellular accumulation of A β aggravating neurodegeneration (Nilsson et al. 2013; Komatsu et al. 2007). Moreover, downregulation of autophagy-regulator beclin-1 in the brains of AD patients (Salminen et al. 2013) is supported by *in vitro* and *in vivo* experiments demonstrating the protective effect of beclin-1 against A β accumulation (Salminen et al. 2013; Uddin et al. 2019) suggesting that autophagy plays a vital role in counteracting AD pathology (Salminen et al. 2013; Uddin et al. 2019; Chung et al. 2019).

11.1.1.2 Autophagy in Parkinson's Disease

Parkinson's disease (PD) is the second most common ND and the most common ND affecting the motor system (Aboud et al. 2015) with the main symptoms comprising tremor, rigidity, bradykinesia and postural instability (Tysnes and Storstein 2017). The key pathology hallmarks of PD are represented by the loss of dopaminergic neurons in the substantia nigra pars compacta (SNpc) and accumulation of intracellular SNCA-containing deposits, also called Lewy bodies (Takahashi et al. 2018; Rocha et al. 2018). Similar to A β and tau, SNCA has prion-like properties (Stöhr et al. 2012; Sanders et al. 2014; Woerman et al. 2018) and can be cleared by autophagy (Poehler et al. 2014; Dehay et al. 2012). The process of mitophagy, one of the types of macroautophagy (Fig. 11.1), plays a crucial role in the maintenance of dopaminergic neurons and the pathogenesis of PD. Indeed, there are PD-associated mutations G309D (Valente et al. 2004a), G502C, G275T, G1391A (Valente et al. 2004b) and T167A, C245A, G758A, C823T, C1310T (Jankovic et al. 2018) in two critical mitophagy-related proteins: phosphatase and tensin homolog (PTEN)-induced kinase 1 (PINK1) and parkin, respectively (Gómez-Suaga et al. 2018).

11.1.1.3 Autophagy in Multiple System Atrophy

Affecting both neurons and oligodendrocytes, multiple system atrophy (MSA) represents another SNCA-associated ND which is manifested by parkinsonism, ataxia and dysfunction of the autonomous nervous system (Fanciulli and Wenning 2015). Proteasomal clearance of myeloid proteins is impaired in MSA, while upregulation of autophagy is often observed in MSA as a compensatory mechanism opposing the SNCA buildup, indicating the abnormalities in autophagy could be related to MSA pathology (Schwarz et al. 2012; Pukaß and Richter-Landsberg 2015; Tanji et al. 2013).

11.1.1.4 Autophagy in Huntington's Disease

Huntington's disease (HD) develops when trinucleotide (CAG) repeat expansion of a mutated huntingtin protein gradually damages striatal and cortical neurons leading to chorea, dystonia, balance disorders and cognitive decline (Walker 2007; Bates 2005). The function of huntingtin is not fully understood, but it was shown to be involved in the intracellular transport and can act as a scaffold for macroautophagy (Ochaba et al. 2014; Martin et al. 2015; Rui et al. 2015). Moreover, autophagy can prevent intracellular accumulation of mutated huntingtin aggregates (DiFiglia et al. 1997; Jin et al. 2016). This prompted the development of autophagy-promoting strategies to halt HD progression by inhibition of the mammalian target of rapamycin (mTOR) pathway, a key cellular regulator of energy homeostasis, growth and autophagy (Williams et al. 2008; Sabatini 2017).

11.1.1.5 Autophagy in Amyotrophic Lateral Sclerosis

Main pathological feature of amyotrophic lateral sclerosis (ALS) is degeneration of motor neurons associated with accumulation of misfolded proteins such as TDP43, superoxide dismutase 1, NIMA-related kinase 1, fused in sarcoma and C9orf72 (Kiernan et al. 2011). ALS is associated with impaired autophagosome and autolysosome formation (Hara et al. 2006; Barmada et al. 2014; Shen et al. 2015; Teyssou et al. 2013; Crippa et al. 2010). For example, in superoxide dismutase 1 G93A mutant ALS mouse model, this protein is cleared from neurons by autophagy (Crippa et al. 2010). Generally, autophagy modulates cell death rate so that its suppression leads to neurodegeneration (Hara et al. 2006; Barmada et al. 2014). In turn, mitophagy receptor mutations are also linked to ALS development (Wong and Holzbaur 2014).

11.1.1.6 Autophagy in Frontotemporal Dementia

Frontotemporal dementia (FTD) is a general term for a class of NDs characterized by abnormalities in behaviour and language (Tanji et al. 2013; Krasniak and Ahmad 2016; Lee and Gao 2009; Bang et al. 2015). FTD progression is linked to Valosin-containing proteins (VCPs) which are critical for autophagic vesicles maturation (Halawani and Latterich 2006; Wong et al. 2018; Ju et al. 2009). The VCP research and other evidence indicate the role of autophagy in FTD (Lee and Gao 2009).

11.1.2 RNA Interference and MicroRNAs

As mentioned above, NDs progression is often modulated by autophagy activity, which in turn is regulated by multiple mechanisms including RNA interference (RNAi), a process of mRNA inhibition by antisense RNA molecules such as small interfering (siRNAs) or microRNAs (Wang et al. 2018; Ye et al. 2013). In mammals, primary microRNAs (pri-microRNAs) are typically transcribed by the DNA-directed RNA polymerase II (RNAPol II) (Lee et al. 2004; Cook et al. 2020) or, in rare cases, (RNAPol III) (Borchert et al. 2006). Such hairpin-loop-structured pri-microRNAs are then recognized and cleaved by microprocessor complex containing one Drosha and two DGCR8 (DiGeorge syndrome critical region 8) proteins to produce precursor microRNAs (pre-microRNAs) (Lee et al. 2003). The latter is exported into the cytoplasm by exportin V and finally cleaved by Dicer ribonuclease producing mature 20–25 bp long double-stranded microRNAs with 3'-overhangs on both 5'- and 3'-(called 5p and 3p) strands (counting from the transcription start site in the pri-microRNA). Mediated by Dicer, one of these strands, called a guide strand, will be typically incorporated into the Argonaute 2 (Ago2)-containing RNA-mediated silencing complex (RISC), while the passenger strand will be rapidly degraded (Lee et al. 2004; Ambros et al. 2003). The guide strand directs binding of RISC to the target mRNA leading to its degradation or translation repression (Rand et al. 2005). There are more than 5000 microRNAs in human genome, at least half of which being unique to humans (Londin et al. 2015) (Table 11.2). Due to only partial sequence complementarity, single microRNA can regulate multiple transcripts while a single gene is often regulated by several microRNAs (Krek et al. 2005; Lim et al. 2005). MicroRNAs regulate the majority of human protein-coding genes (Lewis et al. 2005) including those important for functionality of the nervous system (Schratt 2009) (Table 11.2). MicroRNAs can be pre-loaded into RISC complexes and remain stable in the processing bodies (P-bodies) in the neuronal terminals for later context-dependent degradation of mRNAs and inhibition of their translation (Corbin et al. 2009; Parker and Song 2004). Such interaction occurs in the 3'-untranslated region (UTR) of the target mRNA (Hausser et al. 2013) with rare exceptions when microRNAs bind to 5'-UTR or coding sequence (CDS) (Fang and Rajewsky 2011). In the latter cases, microRNAs can stabilize target transcripts and increase their half-life instead of neutralizing them (Atambayeva et al. 2017) (Table 11.2).

Table 11.2 Bioinformatics tools in microRNA research

Tools (more details at https://tools4mirs.org/)	Identification and analysis of known microRNAs	Analysis of microRNA isoforms (isoMirs)	Identification of novel microRNAs and their precursors	Analysis of differential expression of microRNAs	Target prediction ^b	Function al annotation and analysis of microRNA targets	Single nucleotide polymorphisms (SNP) in microRNAs	Comments	References
ADmiRE							√	Annotative Database of miRNA Elements is a microRNA variant annotation tool which combines miRNA sequence features derived from conservation and variation with biologically important annotations. Framework for microRNA variant annotation and prioritization using human population and disease datasets	Oak et al. (2019)
miRDB					√			Recently updated features of miRDB include 2.1 million predicted gene targets regulated by 6709 microRNAs. In addition to presenting precompiled prediction data, a new feature is the web server interface that allows submission of user-provided sequences for miRNA target prediction. In this way, users have the flexibility to study any custom microRNAs or target genes of interest	Chen and Wang (2019); Liu and Wang (2019)
miRGator						√		miRGator aims to be the microRNA portal encompassing microRNA diversity, expression profiles, target relationships and various supporting tools. By keeping datasets and analytic tools up to date, miRGator should continue to serve as an integrated resource for biogenesis and functional investigation of microRNAs	Cho et al. (2012)

miRNA SniPer									✓	An online tool for the detection of microRNA polymorphisms in vertebrates. miRNA SniPer accepts a list of miRNA genes and returns a table of variations within different regions of miRNA genes: pre-miRNA, mature, seed region	Zorc et al. (2012)
MirSNP									✓	MirSNP is a collection of human SNPs in predicted miRNA-mRNA binding sites	Liu et al. (2012b)
miRSystem								✓		A database which integrates seven well-known microRNA-target gene prediction programs: DIANA, miRanda, miRBridge, PicTar, PITA, rna22 and TargetScan. This database contains validated data from TarBase and miRecords on interaction between miRNA and its target genes	Lu et al. (2012)
BioVLAB-MMIA-NGS								✓	✓	BioVLAB-MMIA-NGS is Cloud-based microRNA mRNA integrated analysis system using NGS data. System computes differentially/significantly expressed miRNAs (DEmiRNAs) and mRNAs/genes (DEGs), and with targeting information, DEGs targeted by DEmiRNAs and having negative correlation between them are extracted	Chae et al. (2014)

(continued)

Table 11.2 (continued)

	Identification and analysis of known microRNAs	Analysis of microRNA isoforms (isoMirs)	Identification of novel microRNAs and their precursors	Analysis of differential expression of microRNAs	Target prediction ^b	Function annotation and analysis of microRNA targets	Single nucleotide polymorphisms (SNP) in microRNAs	Comments	References
Tools (more details at https://tools4mirs.org/)	✓		✓	✓				Comprehensive analysis pipeline for deep microRNA sequencing (CAP-miRSeq) integrates read preprocessing, alignment, mature/precursor/novel microRNA qualification, variant detection in microRNA coding region and flexible differential expression between experimental conditions. According to computational infrastructures, users can run samples sequentially or in parallel for fast processing. In either a case, summary and expression reports for all samples are generated for easier quality assessment and downstream analyses	Sun et al. (2014b)
Chimira	✓			✓				Chimira is a web-based system for miRNA analysis from small RNA-Seq data. Sequences are automatically cleaned, trimmed, size selected and mapped directly to microRNA hairpin sequences. This generates count-based microRNA expression data for subsequent statistical analysis. Moreover, it is capable of identifying epi-transcriptomic modifications in the input sequences. Supported modification types include multiple types of 3'-modifications, 5'-modifications and also internal modifications or variation	Vitisos and Enright (2015)

CleaveLand4	√									<p>CleaveLand is a generalizable computational pipeline for the detection of cleaved miRNA targets from degradome data. CleaveLand takes as input degradome sequences, small RNAs and a miRNA database and outputs small RNA targets</p>	<p>Addo-Quave et al. (2008)</p>
CPSS	√	√	√	√	√	√	√	√	√	<p>CPSS is a computational platform for the analysis of small RNA deep sequencing data), designed to completely annotate and functionally analyse microRNAs (miRNAs) from NGS data on one platform with a single data submission</p>	<p>Zhang et al. (2014)</p>
DARIO	√			√						<p>A free web server for the analysis of short RNAs from high-throughput sequencing data</p>	<p>Fasold et al. (2011)</p>
DeAnnIso			√					√		<p>DeAnnIso is an online tool, designed for detection and annotation of isomiRs from small RNA sequencing data. The detected isomiRs will be classified into different categories. The isomiRs will be aligned with canonical microRNA and will be annotated with expression, constitution, SNP and an in-house dataset. It can also extract differentially expressing isomiR between two samples. In addition, IsomiR Bank provides targets prediction and enrichment analysis to evaluate the effects of isomiRs on target selection</p>	<p>Zhang et al. (2016c)</p>

(continued)

Table 11.2 (continued)

Tools (more details at https://tools4mirs.org/)	Identification and analysis of known microRNAs	Analysis of microRNA isoforms (isoMirs)	Identification of novel microRNAs and their precursors	Analysis of differential expression of microRNAs	Target prediction ^b	Function al annotation and analysis of microRNA targets	Single nucleotide polymorphisms (SNP) in microRNAs	Comments	References
eRNA	✓		✓	✓				eRNA focuses on the common tools required for the mapping and quantification analysis of miRNA-seq and mRNA-seq data. The software package provides an additional choice for scientists who require a user-friendly computing environment and high-throughput capacity for large data analysis	Yuan et al. (2014b)
iMir	✓	✓	✓	✓	✓			iMir is a modular pipeline for comprehensive analysis of small RNA-Seq data, comprising specific tools for adapter trimming, quality filtering, differential expression analysis, biological target prediction and other useful options by integrating multiple open-source modules and resources in an automated workflow	Giurato et al. (2013)

isomiR2Function				✓	✓	✓	✓	<p>IsomiR2Function allows for the high-throughput detection of plant isomiRs from any miRNA-seq profiling study. IsomiR2Function not only allows for the identification of the templated and non-templated 5'-isomiRs and 3'-isomiRs but also allows for the expression quantification. Since, the prediction of biologically relevant target is an important criterion for the identification of isomiRs and their targets—IsomiR2Function identifies target as well. Following target prediction, it allows for functional enrichment of the identified targets. In parallel, isomiR2Function provides support for the visualization of read mapping on corresponding precursor sequences</p>	Yang et al. (2017)
IsomiRage	✓	✓						<p>A workflow for the characterization and analysis of microRNAs and their variants in next-generation sequencing datasets. IsomiRage permits the deconvolution of miRNA heterogeneity and could be used to explore the functional role of miRNA isoforms</p>	Muller et al. (2014)
isomiReX	✓	✓		✓				<p>IsomiRage is an open-access web platform to identify isomiRs and on the fly graphical visualization of the differentially expressed microRNAs in control as well as treated library</p>	Sablak et al. (2013)

(continued)

Table 11.2 (continued)

Tools (more details at https://tools4mirs.org/)	Identification and analysis of known microRNAs	Analysis of microRNA isoforms (isoMirs)	Identification of novel microRNAs and their precursors	Analysis of differential expression of microRNAs	Target prediction ^b	Function al annotation and analysis of microRNA targets	Single nucleotide polymorphisms (SNP) in microRNAs	Comments	References
LeARN/smallA	✓		✓		✓			A platform based on LeARN, dedicated to analyse data generated by RNAseq small RNA projects	Noirrot et al. (2008)
MAGI	✓		✓	✓	✓	✓		MAGI is a web service for fast microRNA-Seq data analysis in a graphics processing unit (GPU) infrastructure. Using just a browser, users have access to results as web reports in just a few hours—>600% end-to-end performance improvement over state of the art	Kim et al. (2014)
miR-PREFeR	✓		✓					MIR-PREFeR uses expression patterns of microRNA and follows the criteria for plant microRNA annotation to accurately predict plant miRNAs from one or more small RNA-Seq data samples of the same species	Lei and Sun (2014)
miRA			✓					miRA is a new tool to identify miRNA precursors in plants, allowing for heterogeneous and complex precursor populations. miRA requires small RNA sequencing data and a corresponding reference genome, and evaluates precursor secondary structures and precursor processing accuracy; key parameters can be adapted based on the specific organism under investigation	Evers et al. (2015)

miRge	✓	✓	✓	✓				miRge is a logical, ultrafast, small RNA-seq solution to process samples in a highly multiplexed fashion, resulting in dramatically decreased computational requirements when processing sets of samples in a single run. It utilizes a unique sequential alignment algorithm for annotation of small RNA-seq data. Output is given for microRNAs as raw reads and reads per million (RPM) in addition to isomiR data and reads for all other RNA species (tRNA, rRNA, snoRNA, mRNA). IsomiR entropy can be determined for each sample or across samples in a multiplex run	Baras et al. (2015)
miRanalyser	✓	✓	✓	✓				miRanalyser—a web server and stand-alone tool for the detection of known and prediction of new microRNAs in high-throughput sequencing experiments	Hackenberg et al. (2011)
miRDeep-P	✓		✓					miRDP can be used to identify microRNA genes in plant species, even for those without detailed annotation. It is also designed to assign expression status to individual microRNA genes, which is critical as more miRNAs in plants belong to paralogous families with multiple members encoding identical or near-identical miRNAs	Yang and Li (2011)

(continued)

Table 11.2 (continued)

Tools (more details at https://tools4mirs.org/)	Identification and analysis of known microRNAs	Analysis of microRNA isoforms (isoMirs)	Identification of novel microRNAs and their precursors	Analysis of differential expression of microRNAs	Target prediction ^b	Function al annotation and analysis of microRNA targets	Single nucleotide polymorphisms (SNP) in microRNAs	Comments	References
miRDeep2	✓		✓					miRDeep2 is a completely overhauled tool which discovers microRNA genes by analysing sequenced RNAs. The tool reports known and hundreds of novel microRNAs with high accuracy in seven species representing the major animal clades	Friedländer et al. (2011)
miRIdentify	✓		✓					A stringent approach to confidently predict novel miRNAs in animals	Hansen et al. (2014)
MIREAP	✓		✓					MIREAP combines small RNA position and depth with a model of microRNA biogenesis to discover microRNAs from deeply sequenced small RNA library	Qibin and Jiang (2008)
MIRENA	✓		✓					MIRENA looks for miRNA sequences by exploring a multidimensional space defined by only five (physical and combinatorial) parameters characterizing acceptable pre-miRNAs. MIRENA validates pre-miRNAs with high sensitivity and specificity, and detects new miRNAs by homology from known miRNAs or from deep sequencing data	Mathelier and Carbone (2010)
miRExpress	✓							A stand-alone software package implemented for generating microRNA expression profiles from high-throughput sequencing of RNA without the need for sequenced genomes	Wang et al. (2009b)

miRNA Digger	✓	✓	✓	✓	miRNA Digger was developed for systematical discovery of miRNA candidates through genome-wide screening of cleavage signals based on degradome sequencing data	Yu et al. (2016)
miRNAkey			✓		miRNAkey is a software package designed to be used as a base-station for the analysis of microRNA deep sequencing data. It implements common steps taken in the analysis of such data, as well as adds unique features, such as data statistics and multiple mapping levels, generating a novel platform for the analysis of microRNA expression. The tabular and graphical output contains detailed reports on the sequence reads and provides an accurate picture of the differentially expressed microRNAs in paired samples	Ronen et al. (2010)
MIRPIPE				✓	MIRPIPE represents a new pipeline for the quantification of microRNA based on small RNA sequencing reads. In opposition to present algorithms that generally rely on genomic data to identify microRNAs, MIRPIPE focuses on niche model organisms that lack such information. Among the MIRPIPE features are automatic trimming and adapter removal of raw RNA-Seq reads originating from various sequencing instruments, clustering of isomiRs, and quantification of detected microRNAs by homology search versus public or user uploaded reference databases	Kuennen et al. (2014)

(continued)

Table 11.2 (continued)

Tools (more details at https://tools4mirs.org/)	Identification and analysis of known microRNAs	Analysis of microRNA isoforms (isoMirs)	Identification of novel microRNAs and their precursors	Analysis of differential expression of microRNAs	Target prediction ^b	Function annotation and analysis of microRNA targets	Single nucleotide polymorphisms (SNP) in microRNAs	Comments	References
mirPro	✓	✓	✓					mirPro is a tool for miRNA-seq analysis. It can quantify known and novel microRNAs in single-end RNA-seq data and provide useful functions such as IsomiR detection and ‘arm switching’ identification, microRNA family quantification, and read cataloging in terms of genome annotation. mirPro only works for species that has reference genome	Shi et al. (2015)
miRSeqNovel	✓	✓	✓	✓				An R/Bioconductor based workflow for novel microRNA prediction from deep sequencing data	Qian et al. (2012)
miRTarCLIP					✓			From miRTarCLIP scratch, it automatically removes adaptor sequences from raw reads, filters low-quality reads, reverts C to T, aligns reads to 3'-UTRs, scans for read clusters, identifies high confidence microRNA-target sites and provides annotations from external databases. With multi-threading techniques and our novel C to T reversion procedure, miRTarCLIP greatly reduces the running time comparing to conventional approaches	Chou et al. (2013)

mirTools 2.0	✓	✓	✓	✓	✓	✓	✓	✓	<p>MirTools 2.0 is updated version of mirTools, which was developed to comprehensive characterize the small RNA transcriptome obtained from high-throughput sequencing. It enables user to detect and profile non-coding RNA (lRNA, snRNA, snoRNA, rRNA and piRNA); obtain detailed annotation information about known miRNA (absolute/relative reads count and most abundant tags); identify the microRNA-target genes; and their detailed functional annotate; perform the comparison of many samples; and identify the differentially expressed non-coding RNAs between experimental groups; discover novel microRNAs</p>	Wu et al. (2013)
MTide	✓			✓	✓	✓	✓	✓	<p>MTide is an integrated pipeline designed to parse sRNA-seq and degradome data for microRNA-target identification in plant. It can quantify the known microRNA expression and identify novel microRNA from sRNA-seq data, identify the target of microRNA from degradome data signature, predict target of microRNA precisely, prioritize predicted target according to GO similarity to known or validated target, and identify the expressed microRNA between two samples</p>	Zhang et al. (2014)

(continued)

Table 11.2 (continued)

Tools (more details at https://tools4mirs.org/)	Identification and analysis of known microRNAs	Analysis of microRNA isoforms (isoMirs)	Identification of novel microRNAs and their precursors	Analysis of differential expression of microRNAs	Target prediction ^b	Function al annotation and analysis of microRNA targets	Single nucleotide polymorphisms (SNP) in microRNAs	Comments	References
ncPRO-seq	✓							ncPRO-seq is a tool for annotation and profiling of ncRNAs using deep-sequencing data. This comprehensive and flexible ncRNA analysis pipeline, aims in interrogating and performing detailed analysis on small RNAs derived from annotated non-coding regions in miRBase, Rfam and repeatMasker, and regions defined by users. The ncPRO-seq pipeline also has a module to identify regions significantly enriched with short reads that cannot be classified as known ncRNA families	Chen et al. (2012)
Oasis 2.0	✓		✓	✓	✓	✓		Oasis is a web application that allows for the fast and flexible online analysis of small-RNA-seq (sRNA-seq) data. Oasis' exclusive selling points are a differential expression module that allows for the multivariate analysis of samples, a classification module for robust biomarker detection and an advanced programming interface that supports the batch submission of jobs. Both modules include the analysis of novel miRNAs, miRNA targets and functional analyses including GO and pathway enrichment	Capecce et al. (2015)

Omics Pipe	√			√				<p>A computational framework that automates multi-omics data analysis pipelines on high performance compute clusters and in the cloud. It supports best practice published pipelines for RNA-seq, miRNA-seq, Exome-seq, whole-genome sequencing, CHIP-seq analyses and automatic processing of data from The Cancer Genome Atlas (TCGA). Omics Pipe provides researchers with a tool for reproducible, open-source and extensible next-generation sequencing analysis</p>	Fisch et al. (2015)
PIPmir			√					<p>PIPmir is an algorithm to identify novel plant miRNA genes from a combination of deep sequencing data and genomic features. The algorithm can be used as the full pipeline, as just a classifier, or as just a plant precursor sequence predictor.</p>	Breakfield et al. (2012)

(continued)

Table 11.2 (continued)

Tools (more details at https://tools4mirs.org/)	Identification and analysis of known microRNAs	Analysis of microRNA isoforms (isoMirs)	Identification of novel microRNAs and their precursors	Analysis of differential expression of microRNAs	Target prediction ^b	Functional annotation and analysis of microRNA targets	Single nucleotide polymorphisms (SNP) in microRNAs	Comments	References
Prost!	√	√						Prost! (PROcessing Of Short Transcripts) analyses any source of small RNA sequencing data. Prost! does not rely on existing annotation to filter sequencing reads but instead starts by aligning all the reads on a user-provided genomic reference, allowing the study of miRNAs in any species. Additionally, any number of samples can be studied together in a single Prost! run, allowing a more accurate analysis of an entire dataset. After grouping the processed reads by genomic location, Prost! then annotates the reads using a user-defined annotation database (public or personal annotation database). Genomic alignment, grouping and then annotation enable the study of potentially novel miRNAs, as well as permitting the retention of all the isomiRs that a microRNA may display. Finally, Prost! contains additional features such as grouping by seed sequence for a more functional approach of the dataset, provides automatic discovery of potential mirror-microRNAs, and analyses the frequency of various types of post-transcriptional modifications at each genomic location. Each step of the Prost! analysis is provided in a Excel file for the user to have all information in hand for deeper analysis of specific cases	Desvignes et al. (2019)

RandA	✓			✓					RandA is a tool for deep-sequencing data analysis. It performs various RNA-seq analysis steps including adapter clipping; alignment against a database derived from Rfam; multiple mapping handling; read count normalization and differential expression testing for each transcript detected in the samples	Isakov et al. (2012)
SeqBuster	✓	✓							A command-line bioinformatic tool useful for the analysis of deep sequencing data, namely known microRNAs and isomiRs annotation	Pantano et al. (2009)
Shortran	✓		✓	✓					Shortran provides an efficient and user-friendly tool for flexible analysis of sRNA-seq data. Using shortran, user is able to quickly generate and combine annotation and profiling information from a complex sRNA-seq experiment	Gupta et al. (2012)
sPARTA							✓		A powerful tool for plant miRNA target prediction and PARE validation. It can search for targets in unannotated genomic regions, which is useful to discover novel regulatory modules, independent of genome annotations that may be incomplete	Kakrana et al. (2014)

(continued)

Table 11.2 (continued)

	Identification and analysis of known microRNAs	Analysis of microRNA isoforms (isoMirs)	Identification of novel microRNAs and their precursors	Analysis of differential expression of microRNAs	Target prediction ^b	Function al annotation and analysis of microRNA targets	Single nucleotide polymorphisms (SNP) in microRNAs	Comments	References
Tools (more details at https://tools4mirs.org/)	✓	✓	✓	✓	✓	✓		sRNAtoolbox is aimed to provide small RNA researchers with several useful tools including sRNA expression profiling from deep sequencing experiments and several downstream analysis tools. The centre piece of sRNAtoolbox is sRNAbench, which allows the expression profiling and prediction of novel microRNAs in deep sequencing experiments. The other tools can be either launched on sRNAbench results or independently using the appropriate file formats	Rueda et al. (2015)
UEA sRNA Workbench	✓		✓	✓	✓			The UEA sRNA workbench is a simple to use, downloadable sRNA software package based on algorithms developed for the original UEA sRNA Toolkit that will perform a complete analysis of single or multiple-sample small RNA datasets from both plants and animals to identify interesting landmarks (such as detection of novel microRNA sequences) or other tasks such as profiling small RNA expression patterns in genetic data	Stocks et al. (2012)

wapRNA	✓		✓	✓	✓	✓		wapRNA provides an integrated tool for RNA sequence, refers to the use of high-throughput sequencing technologies to sequence cDNAs in order to get information about a sample's RNA content. wapRNA provides researchers with efficient ways to measure RNA sequence experimentally, allowing them to get information such as how different alleles of a gene are expressed, detect post-transcriptional mutations or identifying gene fusions, annotate the known miRNAs or predict the news and so on	Zhao et al. (2011)
--------	---	--	---	---	---	---	--	--	--------------------

^aTools4miRs (<https://tools4mirs.org>) is a manually curated platform comprising over 170 tools for microRNA analysis

^bComputational methods for putative microRNA target prediction. The pipelines may employ thermodynamic, evolutionary, probabilistic, or sequence-based approaches

11.2 Regulatory Interplay of RNA Interference and Autophagy in Neurodegenerative Diseases

Despite the absence of conclusive evidence of a crucial role of the microRNA pathway in NDs (Lai et al. 2019), several *in vitro* and *in vivo* models demonstrate the contribution of this pathway to neurodegeneration. In line with the upregulation of miR-34c-5p in the AD patients' hippocampus, researches have detected high levels of this microRNA, decreased levels of its target sirtuin 1 and memory deterioration in 24-month-old mice and in a double-transgenic mouse model of AD co-expressing chimeric mouse-human amyloid precursor protein (APP) and a mutant human pre-senilin (PS1) in neurons of the central nervous system (APP^{swe}/PS1 Δ E9 mice) (Jankowsky et al. 2004; Zovoilis et al. 2011). Accordingly, injection of miR-34c-5p mimics into the hippocampus negatively affects learning ability while the rescue of the memory function by target protectors directly demonstrates the critical role of sirtuin 1 as a functional target of miR-34c-5p in this phenotype (Zovoilis et al. 2011). This study shows inter-relation of microRNA functions in aging and neurodegeneration (Verheijen et al. 2018). Age is the major risk factor for most NDs, while autophagy may affect both aging and neurodegeneration (Finkbeiner 2020; Rubinsztein et al. 2011). Knockout of miR-34 which targets Atg9, a critical gene in autophagosome formation, prolongs the lifespan of *C. elegans* (see Table 11.1) (Yang et al. 2013).

Expression of Drosha, a critical ribonuclease for microRNA maturation, is reduced in some cases of ALS indicating the control of microRNA biogenesis by autophagy (Gonçalves et al. 2018). Normally, Ago2 which is not occupied by microRNAs is degraded by the autophagy pathway. Interestingly, experiments in cell culture, in mouse models and in HD autopsy samples revealed that aggregation of mutated huntingtin causes Ago2 accumulation and dysfunction of the microRNA pathway which can be alleviated by activation of autophagy (Pircs et al. 2018). HD is often associated with abnormal autophagy (Martinez-Vicente et al. 2010; Petersén et al. 2001), while stimulation of autophagy pathway can alleviate this pathology (Floto et al. 2007).

RNAi is a promising therapeutic tool to regulate disease-associated genes (Adams et al. 2018). In contrast to microRNAs, siRNAs are fully complementary to their targets (Elbashir et al. 2001), thus strongly inducing transcript degradation (Piatek and Werner 2014). The first RNAi-based drug on the market, patisiran, was developed against one of the NDs and targets amyloid transthyretin (Adams et al. 2017, 2018). The genes targeted by microRNAs are involved in different autophagy stages (Finkbeiner 2020) (see Fig. 11.1), while RNAi tools are widely applied to study autophagy in NDs (see Table 11.1). Below, we will discuss the roles of specific autophagy-regulating microRNAs in NDs.

11.2.1 Macroautophagy-Regulating MicroRNAs in Neurodegeneration

Macroautophagy involves several key autophagy-related (Atg) regulators to engulf organelles or proteins to be degraded by a phagophore, followed by its maturation to a double-membrane structure called autophagosome. Finally, autophagosome transports the cargo towards the lysosome in order to fuse with the latter and degrade the contents with the means of acidic lysosomal hydrolase (see Fig. 11.1) (Nixon 2013; Yang et al. 2013; Walczak and Martens 2013). Below, we discuss three microRNAs involved in regulation of macroautophagy initiation in AD models: miR-214-3p, miR-299-5p and miR-124-3p. All of them are highly expressed in the central nervous system with the miR-124-3p being the most abundant neuronal microRNA (Zhang et al. 2016a, b; Gascon et al. 2014) (see Fig. 11.1, Table 11.1).

11.2.1.1 MicroRNAs Regulating Macroautophagy Initiation

Transfection of Atg12-targeting miR-214-3p into mouse primary hippocampal neurons reduces autophagosome formation as evidenced by LC3B (microtubule-associated protein 1 B light chain 3) and beclin1 decrease and p62 increase (Zhang et al. 2016a). Moreover, miR-214-3p mimics injection into the third ventricle of SAMP8 (senescence accelerated mouse prone 8) AD mouse model (see Table 11.1) decreases expression of Atg12 while also reducing apoptosis which phenotypically leads to restored spatial learning and memory (Zhang et al. 2016a). In another AD model, APP^{swe}/PS1 Δ E9 mice (see above, and Table 11.1), miR-299-5p is neuroprotective via targeting Atg5, suppressing autophagy and decreasing caspase-dependent apoptosis (Zhang et al. 2016b).

As previously mentioned, miR-124-3p is the most abundant and one of the critical microRNAs in the central nervous system. Its upregulation improves learning and slows down pathology development in the same APP^{swe}/PS1 Δ E9 AD model. One of the proposed mechanisms for these effects of miR-124-3p is regulation of its putative target amyloid precursor protein (APP) cleaving enzyme 1 (BACE1) (Du et al. 2017). BACE1 cleaves APP to produce A β (Fukumoto et al. 2010) leading to its aggregation, and formation of fibrils and plaques (Nixon 2007; Wu et al. 2016; Feng et al. 2017). Interestingly, in a widely used PD mouse model causing a severe neurodegeneration of dopamine neurons, injection of MPTP (1-methyl-4-phenyl-1,2,3,6-tetrahydropyridine) toxin results in reduced expression of miR-124-3p and upregulation of its targets p62 (also known as sequestosome 1) and p38 (also known as mitogen-activated protein kinase 14, MAPK14) reflecting suppressed autophagy and activation of microglia (Yao et al. 2019). While knockdown of p62 suppresses the levels of phosphorylated p38 and pro-inflammatory responses in glial BV2 cells, application of miR-124-3p mimics to the lateral cerebral ventricle rescues the toxin-induced phenotype and promotes autophagy by attenuating the activities of p62 and phosphorylated p38 (Yao et al. 2019) (see Fig. 11.1, Table 11.1).

11.2.1.2 MicroRNAs Regulating the mTOR Pathway

The mammalian (or mechanistic) target of rapamycin (mTOR) pathway is a key pathway inhibiting macroautophagy (see Fig. 11.1). In the condition of high nutritional supply, mTOR complex 1 inhibits Unc-51 like autophagy activating kinase (Ulk) complex consisting of FIP200 (also known as RB1 inducible coiled-coil 1, Rb1cc1), Ulk1/2 (analogues of Atg1) and Atg13 via direct phosphorylation of Atg13 and Ulk1/2 (Kim et al. 2011). Inhibition of the mTOR pathway upon metabolic stress or deficiency of nutrients leads to dephosphorylation of Ulk1/2 and Atg13, which in turn leads to phosphorylation of FIP200 by Ulk and autophagy initiation (Rabinowitz and White 2010).

This pathway is regulated by microRNAs abundant in the central nervous system, such as miR-101-3p (Valera et al. 2017; Li et al. 2017a; Wong et al. 2013; Lee et al. 2012). In the MSA mouse model expressing myelin basic protein promoter-driven SNCA (MBP- α -syn), striatal expression of miR-101-3p is elevated (Krismer et al. 2013) leading to inhibition of autophagy (Valera et al. 2017). The study identified several targets of miR-101-3p: Rab5A, Atg4D, stathmin 1 (STMN1) and mTOR with the first three being autophagy-promoting genes and the latter being autophagy inhibitor, as such, miR-101-3p is a potent regulator of autophagy. In this model, upregulation of miR-101-3p correlates with SNCA accumulation, which can be attenuated by microRNA inhibitor administration (Valera et al. 2017). Another microRNA regulating autophagy is miR-193b-3p. It activates mTOR via targeting its negative regulator tuberous sclerosis complex 1 (TSC1) (Li et al. 2017a). Downregulation of this microRNA and mTOR, and as a result activation of autophagy and cell survival, was detected both in ALS patients (Chen et al. 2016) and in G93A mutant superoxide dismutase 1 ALS mouse model.

11.2.1.3 The Role of Mitophagy-Related MicroRNAs in Neurodegeneration

Mitochondrial autophagy, or mitophagy, is a type of macroautophagy when the phagophore initiation machinery is recruited to damaged mitochondria in order to maintain the pool of healthy organelles in the cell. Such balance may be severely disturbed in PD (Banerjee et al. 2010), AD (Fang et al. 2019), ALS (Wong and Holzbaur 2014) and other NDs. Indeed, single nucleotide polymorphisms (SNPs) in Pink1 (PTEN-induced putative kinase 1) and parkin are strongly associated with PD (Klein et al. 2005; Ibáñez et al. 2006). Pink1 is accumulated on the damaged outer mitochondrial membrane and recruits cytoplasmic parkin initiating mitophagy via autophagy receptors optineurin (Optn) and ND52 (nuclear dot protein 52) receptors (Deas et al. 2011; Ruimeng et al. 2019) (see Fig. 11.1). This process can be directly inhibited by parkin-targeting miR-181a-5p and Pink1-targeting miR-27a/b-3p (Kim et al. 2016a; Cheng et al. 2016). Interestingly, miR-27a/b-3p are induced by mitophagy (Kim et al. 2016a) and thus are capable of forming a negative feedback loop in SNpc, where these microRNAs are highly abundant (Landgraf et al. 2007). This region located in the ventral midbrain comprises the majority of dopaminergic

neurons which are known to be particularly vulnerable to oxidative stress, aging and mitochondrial damage. Notably, miR-27a-3p also reduces huntingtin levels in R6/2 HD mouse model via a different mechanism (Ban et al. 2017).

Another microRNA abundant in SNpc, miR-137-3p, (Landgraf et al. 2007) targets autophagy receptors located on the outer mitochondrial membrane Fundc1 (FUN14 domain containing 1) and NIX (Poursadegh Zonouzi et al. 2017) which promote autophagy in hypoxic conditions via binding to LC3 (Poursadegh Zonouzi et al. 2017; Liu et al. 2012a; Bruick 2000; Sandoval et al. 2008; Schweers et al. 2007) (Fig. 11.1). Inhibition of mitophagy by miR-137-3p is prevented by expression of synthetic Fundc1, and NIX variants lacking the microRNA binding site in their 3'-UTR cannot bind to miR-137-3p, thus preventing the inhibition of mitophagy by miR-137-3p (Poursadegh Zonouzi et al. 2017).

11.2.2 MicroRNAs Regulating Chaperone-Mediated Autophagy in Neurodegeneration

The key proteins in chaperone-mediated autophagy (CMA): LAMP-2A and heat shock cognate protein 70 (Hsc70) are downregulated in PD. They are directly targeted by eight of microRNAs that are highly abundant in the brain (Kim et al. 2007): miR-21-3p, miR-379-5p, miR-373-5p, miR-320a-3p, miR-224-5p, miR-301b-3p, miR-26b-5p and miR-106a-5p, which was validated for all microRNAs except miR-320a-3p (see Fig. 11.1 and Table 11.1). Interestingly, transfection of these microRNAs reduces the expression of LAMP-2A and Hsc70 and upregulates the SNCA levels in SH-SY5Y dopaminergic neuroblastoma cells (Alvarez-Erviti et al. 2013). Accordingly, since six of these microRNAs are upregulated in SNpc of PD patients and two other microRNAs are upregulated in amygdala of PD patients with correspondingly reduced expression of their targets LAMP-2A or Hsc70 in these regions (Alvarez-Erviti et al. 2010), inhibition of CMA may contribute to accumulation of Lewy bodies (Alvarez-Erviti et al. 2013) in these patients. In addition, the age-related decline in CMA is also associated with a decline in LAMP2A expression, a rate-limiting regulator for this type of autophagy (Cuervo et al. 2004; Zhang and Cuervo 2008).

11.3 Techniques Used in MicroRNA Research

11.3.1 Techniques for MicroRNA Identification

11.3.1.1 Next-Generation Sequencing

Next-generation sequencing (NGS) detects short DNA molecules in a sample (Voelkerding et al. 2009) and as such is well suited for microRNA research. NGS is a method of choice for discovery of novel microRNAs and microRNA isoforms as

well as for characterization of expression patterns in various cell populations. MicroRNA and other transcripts must first be reverse-transcribed to produce cDNA for subsequent sequencing. Once generated, NGS data require bioinformatical analysis (see Table 11.2 for examples of relevant tools) and have to be verified by reverse transcription real-time quantitative PCR (qRT-PCR).

11.3.1.2 Quantitative Reverse-Transcription PCR for Identification of MicroRNAs

Semi-quantitative PCR analysis can be done by comparing band sizes after electrophoresis of DNA products produced by different number of cycles (Marone et al. 2001). A quantitative PCR (qPCR) uses fluorescent reporter sequence to monitor the amount of replicated DNA for relative or absolute quantification (Dhanasekaran et al. 2010). Similar to NGS, microRNAs must be reverse-transcribed using linear (Sharbati-Tehrani et al. 2008; Raymond et al. 2005), usually random hexamer primers (Stangegaard et al. 2006) to generate cDNA and increase the length of the product to enhance the effectivity of subsequent PCR-based assay (Chen et al. 2005; Zhang et al. 2008).

Both the fluorescent dye SYBR-green and Taqman fluorescent probes can be used for qRT-PCR quantifications. The former integrates into the double-stranded PCR product, while the latter binds specifically to defined nucleotide sequences. Both methods allow quantification of replicated product via an increase of fluorescence signal. TaqMan assay utilizing microRNA-specific fluorescent probes or universal probes exhibits high accuracy and sensitivity (Luo et al. 2012). In contrast, strategies SYBR-green-based qRT-PCR are prone to false-positive results (e.g. detecting primer dimers). Data from qPCR need to be normalized (Chugh and Dittmer 2012). Optimal approach is to use a set of genes expressed throughout the body as a normalization reference (Chugh and Dittmer 2012). For large-scale qRT-PCR experiments, at least three stably expressed housekeeping genes are used, and the geometric mean is generated as an accurate normalization factor (Vandesompele et al. 2002; Meyer et al. 2010; Peltier and Latham 2008). Some stably expressed microRNAs can also be used as references (Peltier and Latham 2008). In addition, researchers should set up experimental replicates to ensure the credibility of microRNA expression data. Different replicates of each group should be scattered in different positions of the cell plate to avoid experimental errors (Chugh and Dittmer 2012). We usually use a 1:1, 1:5, 1:25, 1:125 and 1:625 dilutions of one of the samples for both the studied microRNA and the reference gene (e.g. U6 RNA) in the conventional (not large scale) qRT-PCR assays. This helps us ensure the dynamics of Ct fluorescent curves. Additionally, quenching a known amount of a specific RNA in such assays may also allow an absolute quantification of specific RNAs in the samples.

11.3.1.3 In Situ Hybridization

In situ hybridization (ISH) method utilizes RNA probe markers to detect microRNA expression in tissue samples (Jin and Lloyd 1997). ISH also allows to specify the location and specific cell groups expressing microRNA of interest. This method requires thorough preparation of samples, especially in slicing, cross-linking and fixation steps, but allows to precise target detection. Visualization can be performed with use of hapten markers (Nielsen 2012). A common control used in ISH approach is a tissue with target microRNA knockout.

11.3.1.4 Northern Blot

Northern blot consists of size-based separation of RNA samples by gel electrophoresis with a consequent transfer of RNA aggregates onto a nylon membrane. As transfer is completed, RNA samples are fixed by heat or UV-induced covalent linkage and hybridized with labelled nucleotide probes, which allow further imaging. Originally used markers were ^{32}P -DNA probes (Trayhurn 1996), and current alternatives are represented by hapten-labelled RNA probes used in combination with anti-hapten antibody conjugated with phosphatase. Phosphatase chemiluminescent substrate is then used for visualization (Ramkissoon et al. 2006). Using locked nucleic acids (LNA) as a probe increases sensitivity and specificity (Válóczi et al. 2004). LNA nucleotides have additional linkage between 2' oxygen and 4' carbon, while remaining natural B-type conformation possesses more stable and nuclease-resistant structure. Use of LNA also enhances complementary base pairing and hence the binding of probe to target.

11.3.1.5 Nuclease Domain-Deficient Cas9-Based Fluorescent Reporter System

CRISPR-Cas9 system is widely used in microRNA research (Wang et al. 2019). The CRISPR (Clustered Regularly Palindromic Short Interspersed Repeats) includes an AT-rich leader sequence, a repeat sequence capable of forming a stem-loop structure after transcription and an interval sequence (Chang et al. 2016). CRISPR-Cas9 gene editing tool is targeted by single guide RNA (sgRNA) molecule and cleaves target sequence Cas9 nuclease. Firstly, functional complex is formed between sgRNA backbone and Cas9 (Loureiro and da Silva 2019). Spacer sequence then guides Cas9 complex to PAM sequence, which initiates interaction with DNA molecule. If this molecule contains target sequence, complementary to sgRNA, it is processed by Cas9 (Loureiro and da Silva 2019). After nucleolytic cleavage, target sequence is repaired by cell and occurring mistakes cause mutations, leading to synthesis of non-functional transcripts (Loureiro and da Silva 2019). The CRISPR-Cas9 system is currently the most widely used gene editing technology.

Nuclease domain-deficient Cas9 (dCas9) is a modified Cas9, which can be guided by sgRNA but does not possess nucleolytic activity. One of its implementations is a microRNA-detecting fluorescent sensor. It is delivered as two transgenes: one codes for fusion protein dCas9-VPR (VPR is a type of transcriptional activator construct) and sgRNA, and the other contains a marker gene (usually fluorescent protein) with sgRNA-responsive sequence within the promoter. The sgRNA is supplied in precursor form with a 5'cap, 3'tail and a binding site for microRNA of interest. Precursor sgRNA can't interact with dCas9, but can pair with specific microRNA to be processed by RISC complex into mature guiding form. Mature sgRNA then targets fusion protein to the marker gene's promoter, where expression is activated by VPR (Wang et al. 2019).

11.3.1.6 Hybridization Strategies for Binding Site Identification

High-throughput sequencing of RNA isolated by cross-linking immunoprecipitation (HITS-CLIP) strategy allows identification of microRNA-target pairs. After cross-linking, a pull-down of Ago2 complexes is performed to isolate microRNA-target complexes for identification by sequencing. Cross-linking ligation and sequencing of hybrids (CLASH) is another strategy for high-throughput identification of microRNA-target pairs and their binding sites (Helwak and Tollervey 2014). It is performed in cell cultures by UV-induced cross-linking tagged bait protein with RNA, thus stabilizing RNA-RNA interactions. Originated RNA-RNA duplexes are partially truncated by nucleases, then ligated and resultant chimeric molecules are used as templates to reverse-transcribe cDNA library. Further high-throughput sequencing of the produced library allows identification of interaction sites (Helwak and Tollervey 2014).

Photoactivatable ribonucleoside-enhanced cross-linking and immunoprecipitation (PAR-CLIP) is a modified version of HITS-CLIP, in which photoactivated nucleotide 4-thiouridine is added to the sample prior to UV exposure (Hafner et al. 2010). Upon activation by light, 4-thiouridine incorporates into cross-linked sites and promotes conversion of thymine to cytosine, hence 'labelling' the binding site for following deep sequencing step (Hafner et al. 2010). Another high-throughput sequencing strategy, microRNA tagging and affinity-purification (miRAP) are also based on the binding of microRNA to Ago2 protein within RISC complex. It implements modified Ago2 with added tag, so microRNA-Ago2 complexes can be purified from tissue homogenates using tag-specific antibodies (He 2012). MiRAP solves the problem of cell heterogeneity in neural tissues and can detect microRNA expression profile of any genetically established cell group.

11.3.1.7 RNA Microarray

Microarray is one of the earliest techniques for high-throughput analysis of RNA expression (Dong et al. 2013). The strategy is based on detection of microRNAs by a sequence-specific probes spatially organized on solid surfaces (usually glass slides or silicon membranes). Each microRNA of interest becomes localized on a specific site and then is visualized by fluorescent markers (Schena et al. 1995). The strategy can't distinguish between pre-microRNA and mature microRNA. Hybridization can be performed directly with microRNAs or with generated cDNA library (Li and Ruan 2009). As multiple microRNAs are detected on the same chip, hybridization parameters must be suitable for all the microRNAs of interest (Yin et al. 2008). Use of LNA allows to solve the latter issue, as well as increasing overall sensitivity and precision (Castoldi et al. 2006). Microarray results need to be verified by more sensitive methods, such as TaqMan qRT-PCR.

Various microRNA detection technologies described above have different dynamic ranges. NGS and qRT-PCR with possess large dynamic ranges and can detect small changes, hence are suitable for in-depth study of microRNA functions.

11.3.2 *MicroRNA-Target Verification Tools*

11.3.2.1 Dual Luciferase Reporter System

The dual luciferase reporter system is a simple, reliable and well-established strategy for target verification. MicroRNA is co-expressed with fluorescent marker bearing 3'-UTR sequence of its predicted target. Depending on experimental design, a fluorescent marker without 3'-UTR, a fluorescent marker with an inverted 3'-UTR or a fluorescent marker with mutated 3'-UTR can be used as a control (Martin et al. 2013). If microRNA binds cloned 3'-UTR sequence, decrease of the fluorescence signal will be observed. Specific mutations in binding sites of microRNAs and their targets are used to additionally verify the binding location within 3'-UTR sequence. A potential disadvantage of this strategy is that microRNA and reporter interaction context and their concentrations can be different from physiological (Kuhn et al. 2008). Results can be verified with qRT-PCR or western blot.

11.3.2.2 Reverse-Transcription Quantitative Real-Time PCR

The abovementioned qRT-PCR method can also be used to identify microRNAs effect on their target expression. Random hexamer but not dT-polynucleotide (oligo(dT)) primers can be used to amplify mature microRNAs, while the oligo(dT) primers can be used to quantify target genes of these microRNAs.

11.3.2.3 Western Blot

Western blot is a well-established method to assess protein expression levels. Protein samples are segregated by size via gel electrophoresis, transferred to membrane, detected by primary antibodies and visualized by secondary antibodies (Burnette 1981). Western blot is a robust and reliable method to monitor expression levels of microRNA targets. Interdependence of microRNA and protein concentrations allow to judge whether there is a regulatory link: decrease of microRNA expression would normally increase concentration of target's protein and vice versa. Western blot allows direct detection of protein levels, which reflects functional activity of the gene better than assessment of mRNA levels.

11.3.2.4 ELISA

Western blot can be used for semi-quantitative or, if carefully analysed, quantitative detection of protein levels. Unlike Western blot, enzyme-linked immunosorbent assay (ELISA) detects the precise concentration of proteins in body fluids such as plasma, serum and cerebrospinal fluid. In ELISA, the protein of interest is immobilized on a solid surface and is detected by enzyme-bound antibody. Enzyme conjugated to antibody allows quantification, usually by colour change produced by catalytic reaction. Most commonly used enzymes are alkaline phosphatase and horseradish peroxidase.

ELISA may utilize primary antibody for target detection and secondary enzyme-conjugated antibody for quantification. Another variation is 'sandwich ELISA', which captures target by solid surface immobilized antibody and then applies a set of antibodies for quantification.

In microRNA research both ELISA and western blot can be used to detect concentrations of target protein (Li and Ruan 2009; Zhang et al. 2010). However, the former is easier for quantitative applications, and the latter is able to detect changes in protein size and hence track target's multimerization, degradation or digestion.

11.3.3 *Gain-of-Function Research Strategies*

11.3.3.1 Classical Transgenesis

11.3.3.1.1 Systemic MicroRNA Overexpression

Pol III promoters are active throughout whole body and, hence, can be cytotoxic if used for transgene expression. Pol II promoters are less active and tissue-specific (Giering et al. 2008). For expression of transgene microRNAs, Pol III promoters U6 and H1 can be used, which naturally control expression of small nuclear RNAs. The

Pol III promoters do not require regulators upstream of the gene to function effectively (Paddison et al. 2002). This allows constitutive expression of any sequence under 400 bp, fitting microRNA expression needs (Tuschl 2002). Pol III promoters are rarely inducible, although there are examples of temporal control via tetracycline (Tet) administration (Szulc et al. 2006). Some natural microRNAs are transcribed under control of Pol II system, and it can also be used for expression of transgenes and artificially designed siRNAs (Zeng et al. 2002). Apart from the classical transgenesis, delivery of the gene of interest in a viral vector under a promoter of choice is a widely accepted technique for the *in vivo* gain-of-function studies. For Pol III-driven transcription microRNAs are usually inserted downstream in the form of shRNA, which undergoes maturation upon transcription (Brummelkamp et al. 2002; Miyagishi and Taira 2002). In Pol II constructs microRNA is inserted upstream of another gene, usually used as a marker (e.g. fluorescent protein) (Miyagishi and Taira 2002). Pol II allows polycistronic expression of multiple microRNAs inserted onto 3'-UTR of a reporter gene (Stegmeier et al. 2005; McLaughlin et al. 2007).

For a precise control over transgene expression, implementing all natural regulatory elements (promoters, insulators, enhancers) artificial chromosomes can be used. Artificial chromosomes are represented by yeast artificial chromosomes, bacterial artificial chromosomes, human artificial chromosomes and some other vectors. Yeast artificial chromosome is a linear eukaryotic vector with functional elements, which is amplified in yeast cells and delivered to transgenic animal by pronuclear injection or transfection. It is suitable for large-segment transgenes and can carry fragments above 1 Mb. Bacterial artificial chromosomes are derived from bacterial F-factor plasmids, which can only hold approximately 300 kb fragments, but are more stable (Giraldo and Montoliu 2001). Human artificial chromosomes are produced from truncated natural chromosomes or by de novo construction. Human artificial chromosomes can accommodate up to 10 Mb fragments and contain functional elements such as centromeres and telomeres, allowing it to remain stable during mitotic cycle in human or mouse cells (Kouprina et al. 2013). Artificial chromosomes can be implemented for microRNA transgenesis in model organisms (Casola 2010), but are more commonly used for genetic screening (Tagawa et al. 2007; Chaubey et al. 2009; Zhang et al. 2007).

11.3.3.1.2 Conditional MicroRNA Overexpression

11.3.3.1.2.1 *Conditional Overexpression Driven by Tissue-Specific/Cell Type-Specific Promoters*

All promoters of this type are Pol II promoters. This strategy was used for common model organisms like mice, *C. elegans* and *Drosophila* for tissue-specific (Giering et al. 2008; Qadota et al. 2007; Welborn et al. 2015) and cell type-specific (Calixto et al. 2010; Cullere et al. 2008) microRNA expression.

11.3.3.1.2.2 *Cre-loxP-Driven Conditional Overexpression*

Another way to induce spatially specific expression of transgenic microRNAs is to use the Cre-loxP system. The loxP site contains two 13 bp inverted repeats and an 8 bp spacer (Missirlis et al. 2006). The repeats act as recognition sites for P1 phage-derived Cre recombinase (Missirlis et al. 2006). Cre recombinase binds to the first and the last 13 bp regions of each loxP site, forming a dimer. These dimers then combine into tetramer (Missirlis et al. 2006). The sequence between loxP sites is cut out by Cre, and DNA ends are re-joined by ligase (Missirlis et al. 2006). Transcriptional control on the basis of Cre-loxP system is achieved with loxP-Stop-loxP (LSL) construct inserted after Pol II promoter, before transgene-encoding sequence with microRNA inserted into its 3'-UTR. The LSL construct terminates transcription, and hence, no transcript is produced until LSL is cut out by Cre activity. This limits transgene transcription to cells and tissues expressing Cre recombinase (Piovan et al. 2014). Transgenesis utilizing this strategy can be achieved with means of classical transgenesis or by viral vector delivery.

11.3.3.1.2.3 *CreERT2-loxP-Driven Conditional Overexpression*

Another variation of Cre-based control is Cre fusion with mutated oestrogen receptor (ER). Mutated ER (ERT2) has low affinity to its natural ligand and preferentially binds synthetic ligand tamoxifen (Erratum 1996) (Indra et al. 1999). Before tamoxifen activation, the fusion protein remains in cytoplasm where it tends to bind heat shock protein (hsp). Upon binding to tamoxifen, conformational change occurs, uncoupling CreERT2 from hsp and exposing its nuclear-localization sequence, inducing its translocation to nucleus, where Cre interacts with genomic loxP sites (Zhang et al. 2012). CreERT2 system is widely used as a mean of spatiotemporal expression control, applicable to microRNA transgene studies (Abram et al. 2014). The limitation of this strategy is tamoxifen inability to pass blood-brain barrier. There is currently a wide choice of mouse models implementing CreERT2 system, and the common strategy for recombination induction is administration of 1 µg of tamoxifen every day for five consecutive days (Che et al. 2020).

Somewhat similar approach to expression control is taken in so-called 'FLP-out' strategy. It utilizes sequence-specific recombinase FLP and FLP-recognition targets (FRT) spaced by STOP sequence. FLP-induced recombination removes transcription-interrupting construct and allows expression of transgene (Basler and Struhl 1994). FLP is often designed under control of heat shock promoter, thus limiting its application to suitable model organisms. FLP-out approach is mainly used in *Drosophila* microRNA research (Caygill and Johnston 2008; Tyler et al. 2008; Wong et al. 2002); however, there are mutant mouse strains available (Lewandoski 2001).

11.3.3.1.2.4 *Tet-Off and Tet-On Conditional Overexpression Systems*

Tetracycline (Tet) is an antibiotic used in several strategies for controlled transcription. Tet-off system shuts down expression upon sensing Tet and is based on Tet resistance operon from *E. coli* and Herpes simplex virion protein 16 (VP16). Fusion protein called tetracycline-controlled transactivator (tTA) consisting of tetracycline repressor (tetR) and VP16 activation domain (AD) binds to tetracycline operon (tetO) in the coding sequence, where VP16 AD activates expression. Administered Tet binds to tetR sequence in tTA, inhibiting its activating effect on tetO in dose-dependent manner (Gossen and Bujard 1992). In recent years, doxycycline is often used as a Tet alternative (Das et al. 2016). There is an example of miR-21 expression under the control of Nestin (neural stem cell marker) promoter through Tet-off strategy in the brain of NesCre8 mouse (Medina et al. 2010). Similarly, another study used the Tet-off system to upregulate the expression of miR-150 (Hoareau-Aveilla et al. 2015).

Classical transgenesis or viral vectors can be used for integration of Tet-based control system into model organism (Dickins et al. 2007). Potential downside is impermeability of blood–brain barrier to Tet, which is why doxycycline can be preferred (Beard et al. 2006). Further modification of the strategy is Tet-on system, which is reported to have better responsiveness and lesser expression leakage than Tet-off (Kafri et al. 2000). The Tet-on system utilizes mutated version of tetR, reverse TetR (rTetR) within reverse tTA (rtTA). Due to mutated conformation, rtTA is unable to bind to tetO. In turn, binding to Tet induces conformational change, restoring rtTA affinity to tetO and, hence, initiating transcription activation by VP16 AD (Gossen et al. 1995).

11.3.3.2 **Viral Vectors**

Viral vectors are another mean of transgenic microRNA delivery. The most commonly used in *in vivo* studies are adeno-associated viruses and lentiviral vectors. This system can be targeted in tissue-specific manner by manipulating proteins expressed by viral capsule. Although there are some shortcomings in viral vectors, such as possible interferon response (Bridge et al. 2003), it is still one of the most commonly used methods for microRNA transgenesis (Couto and High 2010).

Adeno-associated virus (AAV) is unable to propagate in absence of co-infection, and after genome integration, it remains silent, replicating only upon activity of viral proteins of ‘helper’ virus. AAV can infect both dividing and non-dividing cells; however, transduction efficiency of S-phase cells is much higher (Russell et al. 1994). Important limitation of AAV vectors is their relatively small load capacity, limited to 5 kb (Wu et al. 2010); however, there are approaches utilizing head-to-tail UTR recombination of two separate AAV vectors, allowing to deliver longer sequences (Sun et al. 2000; Duan et al. 2000). AAV also requires several weeks to start expression. However, it remains active within infected cells for months, expressing transgene. Co-infection of multiple vectors is possible. Pseudotyping

(modification of the surface peptides of the capsid) can mediate entry to either specific cell types or broad range of cells, and even effective crossing of the blood–brain barrier (e.g. AAV-PHP.eB serotype).

Lentiviral vectors are the most widely used retroviral system, usually utilizing HIV-1 protein machinery with deleted accessory genes. There are further safety precautions: capsid of the non-retroviral VSV is used to construct lentiviral vectors on the basis of non-human pathogens such as SIV, FIV and EIAV. In addition, viral genes *env*, *rev*, *gag* and *pol* are dispersed on different plasmids for packaging. In this way, a total of four different plasmids are used for the packaging of virions, with the fourth plasmid containing the transgenic sequence of the LTR spacer. There are also modified pseudotyped vectors, constructed via application of glycoprotein of vesicular stomatitis virus to expand host range of lentiviral vectors (Burns et al. 1993).

Viral vectors are suitable for spatially and temporally controlled transgenesis, example of which is provided below.

11.3.3.2.1 Pol II-Driven Overexpression

11.3.3.2.1.1 Overexpression Driven by Tissue-Specific/Cell Type-Specific Promoters

Tissue-specific Pol II promoters were successfully utilized as a part of viral vectors for tissue-specific and stable expression of microRNAs, e.g. liver-specific expression (Giering et al. 2008), vascular endothelium (Nicklin Stuart et al. 2001), neurons (Nielsen et al. 2009), macrophages and muscle cells (Pichard et al. 2012).

11.3.3.2.1.2 Cre-loxP-Driven Overexpression

Cre-loxP strategy described above can be utilized in viral vectors, for a controllable deletion of transcription-ablating insertion (Iovino et al. 2005). Further modification of Cre-loxP system delivered by viral vectors includes utilization of mutated loxP sites, which have to be paired with the same type of loxP mutant in order to allow recombination. Recombination outcome, being either inversion or complete excision of loxP-flanked sequence, depends on the relative orientation of the loxP pair. The FLIP cassette (Stern et al. 2008), for example, consists of two different pairs of mutated loxP (loxP-2272 and 5171), initially oriented in inversion-inducing manner, dual selection cassette and microRNA-expressing cassette reverted into antisense position. A loxP-2272 pair flanks both cassettes, while loxP-5171 flanks microRNA cassette. First recombination by Cre flips microRNA transgene into sense position, switching relative position of loxP pair flanking selection cassette into excision-inducing. Consequently, next recombination cuts out the selection cassette (Stern et al. 2008). Such ‘flip’ construction prevents leakage of microRNA from usual LSL construct and allows inducible expression of several transgene vectors. On the other hand, contrary to coding genes, the transcription of shRNAs, when designed with such a flipping system, might still be leaky due to inverted

complementarity of shRNA hairpin (hence, LSL might be preferable for expression of shRNA). Therefore, when choosing between flipping and LSL-based expression systems, the researcher must keep it in mind to prevent the possibility of leakage events.

11.3.3.2.2 Pol III-Driven Overexpression

11.3.3.2.2.1 *Unconditional Overexpression*

On average, expression from Pol III promoters is more active, which results into higher degree of silencing, but can also lead to cytotoxicity and impairment of endogenous microRNA expression and maturation. Nevertheless, vectors bearing unconditionally expressed Pol III-driven microRNAs constructs can be convenient for studies using cell line models (Guda et al. 2015).

11.3.3.2.2.2 *Conditional Overexpression*

Pol III promoter benefits make them a desirable target for further modifications, and so systems for conditional Pol III expression were developed. For example, a Tet-off strategy was implemented for temporal control of microRNA tandem expression; however, the system suffered from noticeable expression leakage (Zhou et al. 2008). Tet-on and doxycycline-based systems (Amar et al. 2006) are also used in inducible Pol III-driven viral vectors for microRNA expression (Pluta et al. 2007). However, this system usually exhibits varying degrees of expression leakage, which may be caused by high activity of the Pol III promoter (Pluta et al. 2007).

Also, a modified Tet-on system has been created by producing a fusion protein tTRKRAB, containing tetracycline-sensing tTR and Krüppel-associated box (KRAB) domain. The latter, once targeted to tetO-neighbouring promoter by tTR, induces a local heterochromatin state by initiating histones deacetylation and methylation, leading to epigenetic silencing of the transgene-encoding region. Both transgene and transactivating fusion protein can be delivered on single lentiviral vector in both Tet-on and Tet-off configurations. This strategy was shown to work with both Pol II and Pol III promoters, and was successfully tested in human embryonic and hematopoietic stem cells, in tumour cells and *in vivo* upon direct intrastriatal injection into rat brains (Szulc et al. 2006). The system allows conditional transgene expression and can be used for microRNA-induced knockdown.

11.3.3.2.3 Transduction of Single Guide RNAs for Cas9-Driven Epigenetic Enhancement of MicroRNA Promoters

Nuclease-free dCas9 systems are widely used as a targeting tool for various functional domains to manipulate transcriptional activity in a controllable way (Gjaltema and Schulz 2018). Application of dCas9 targeting system can be roughly divided

into CRISPR interference (CRISPRi) for gene silencing by blocking transcription initiation or elongation (Qi et al. 2013) and CRISPR-mediated gene activation (CRISPRa), achieved by fusion of dCas9 to various transcriptional activation domains for expression enhancement (Gilbert et al. 2013). For gain-of-function microRNA research, various CRISPRa tools can be utilized for increased expression of microRNAs of choice or to enhance expression of whole polycistronic microRNA clusters (Mong et al. 2020).

One of the first CRISPRa systems was dCas9-VP64 (tetramer of virion protein 16 activation domain) and dCas9-p65 fusions (Gilbert et al. 2013). Soon there was further improvement in efficiency and accuracy variations, e.g. dCas9-VPR (employing tripartite activator VP64-p65-Rta) (Chavez et al. 2015). Next, there was synergistic activation mediator (SAM), utilizing so-called sgRNA2.0, which is a sgRNA designed in a way to fold into several loops, not affecting dCas9-VP64 targeting, but providing a recruiting scaffold for additional activators (p65-HSF1 guided to sgRNA by MS2 protein). Altogether, SAM allows a synergistic effect from three activating factors: VP64, p65 and HSF1 (Zhang et al. 2015).

Another valuable CRISPRa technology is a dCas9-SunTag. The latter fuses dCas9 to a repeating peptide array which binds multiple antibody-fusion proteins. These can be aforementioned VP64 activation domains, thus creating a multimer activating platform with single sgRNA provided. This strategy was shown to induce 25 times greater transcription activation than dCas9-VP64 (Tanenbaum et al. 2014).

Finally, there is a dCas9-SPH technology, combining SunTag multidomain scaffold strategy with p65-HSF1 transactivators from dCas9-VPR. It was successfully tested *in vivo* in nervous system of transgenic mice to activate expression of several genes and non-coding RNAs, and a comparative study on fluorescent reporter has shown it to be the most potent from the dCas9-based epigenetic activators described here (Zhou et al. 2018). As a versatile research model, mice expressing Cre-dependent dCas9-SPH with a fluorescent reporter EGFP were bred (Zhou et al. 2018).

11.3.3.3 Transfection of MicroRNA Mimics

11.3.3.3.1 Transfection of Unmodified MicroRNA Analogues

MicroRNA mimics are synthetic nucleic acids capable of producing microRNA-emulating molecules which target a unique mRNA sequence, regulating its protein product by the microRNA mechanism. One of the forms of mimicking microRNA is utilization of exogenous siRNA or shRNA, where the former would mimic mature microRNA duplex and the latter would be processed as pre-microRNA, with possibility of utilizing non-canonical maturation pathways to lower enzyme competition with endogenous microRNAs (Ma et al. 2014). Mimics can be designed for narrower, single gene targeting and hence may be preferential for gene silencing. Mimics can also alleviate consequences of lowered microRNA expression (e.g. in

disease state) or be used for gain-of-function studies by overexpressing or introducing novel microRNA-mimic to the model. Some modifications allow to further increase efficiency of mimics.

Unmodified mimics are often used for *in vitro* transient transfection of cell cultures as a relatively simple and economical way to get an insight on specific microRNA function. This approach has its obvious limitations due to only temporal presence of the mimics in cells and possible deviations from natural microRNA pathways (Jin et al. 2015; Lu and Rothenberg 2018). Currently, there are multiple commercially available transfection kits allowing relatively simple transfection procedure of various nucleotide (DNA or microRNA mimics) quantities with high efficiency and negligible cytotoxicity (Park et al. 2011).

11.3.3.3.2 Sugar Motif Modifications

Modifications of 2' sugar moieties have been shown to be well tolerated, exert no negative effect on silencing function and increase microRNA/mimic stability against endogenous nucleases (Czaderna et al. 2003; Chiu and Rana 2003). An example is 2'-*O*-methyl (2'-*O*-Me) modification for increased target binding affinity and nuclease resistance (Manoharan 1999). There are various modifications available (Prakash et al. 2005): 2'-*O*-allylation (Amarzguioui et al. 2003), 2'-*O*-ethylamine and 2'-*O*-cyanoethyl (Bramsen et al. 2009) are used for higher silencing activity. However, these modifications, if overused, can lead to targeting deterioration and increased toxicity (Mook et al. 2007). Hence, a scale of modifications and their positioning should be carefully considered. Even single position-specific sequence-independent 2'-*O*-Me modification of a guiding strand can reduce construct's ability to target unwanted transcripts with partial complementarity, without affecting its affinity to perfectly matching targets (Jackson et al. 2006). Similarly, precise localization of a very few LNA-modified moieties allows to substantially increase construct's functionality. For example, a construct was developed, utilizing two LNA moieties at 3' end of both strands of double-stranded mimic for increased resistance to nucleases and one LNA moiety at 5' end of the passenger strand, to promote preferential recruitment of guide strand into silencing complex (Vinnikov et al. 2017). Upon liposome delivery to cell cytoplasm, these oligonucleotide constructs can remain in the target tissue for several weeks (Vinnikov et al. 2014). The LNA-modified mimics are conformationally stable and nuclease-resistant (Wahlestedt et al. 2000) and have weak immunostimulatory properties (Whitehead et al. 2011).

11.3.3.3.3 Backbone Modifications

Incorporation of phosphorothioate linkage into the RNA nucleotides allows further increase in nuclease stability (Altmann et al. 1996) and enhances *in vivo* biodistribution of microRNAs in some organs (Braasch et al. 2004). This modification reduces mimic affinity to its target (Krützfeldt et al. 2007), but it can be compensated by implementation of sugar moieties modifications discussed above (Yu et al. 2012). Alternative, and often considered as more potent than phosphorothioate, modification is a replacement of one non-bridging phosphodiester oxygen by an isoelectric borane to produce a boranophosphate (Jack and Barbara Ramsay 2001). Boranophosphates can be incorporated into natural DNA or RNA sequence by innate polymerases, show increased resistance to nucleases and have higher activity and potency than both phosphodiester and phosphorothioate mimics (Hall et al. 2004).

Another modification is achieved by replacing 3'-OH by amine group, producing N3' phosphoramidate (NP) linkages (Chen et al. 1995). Nucleotide mimics with incorporation of NP into backbone are resistant to nuclease hydrolysis and still functionally pair with intrinsic DNA and RNA sequences (Gryaznov 2010). Other backbone modifications include phosphonoacetate (PACE) linkages with non-bridging oxygen substituted by acetic acid group for increased nuclease resistance (Dellinger et al. 2003), which, however, might slightly impair affinity to targets (Sheehan et al. 2003), and sulphur incorporation, as a substitute for non-bridging oxygen, leading to largely similar to PACE characteristics (Sheehan et al. 2003). Sugar and backbone modifications of accurately chosen nucleotides in the construct can greatly improve its stability and overall RNAi efficiency. Optimal modifications combination may result in drastic increase of stability and RNAi efficiency, while reducing cytotoxicity.

11.3.3.3.4 Other Modifications

There are other modifications as well, improving microRNA uptake and structural stability, e.g. cholesterol-conjugated microRNA with polyethylene imine for *in vivo* tumour targeting (Mun et al. 2019) and cationic liposome complexes, which allow *in vivo* delivery of constructs with prolonged stability (Vinnikov et al. 2014, 2017; Lujan et al. 2019).

11.3.4 Loss-of-Function Research Strategies

Cells and animal models are effective tools for studying the function of specific microRNAs in the context of neurodegeneration and aging. In order to study the loss of function in these models, the following methods are currently available.

11.3.4.1 Knock Out of Key Genes in MicroRNA Biosynthesis

11.3.4.1.1 Dicer Knockout

Dicer plays an important role in microRNA biosynthesis. It possesses double-stranded RNA-specific nuclease activity. Pre-microRNAs are produced by Drosha and DGCR8 (DiGeorge syndrome critical region 8) in the nucleus (Wilson and Doudna 2013; Emde et al. 2015; Shan et al. 2008). In the cytoplasm, Dicer and Ago2, PACT (protein kinase RNA activator) and TRBP (TAR RNA-binding protein 2) cleave pre-microRNA into mature microRNA. Dicer knockout results in early arrest of development (Zhang et al. 2011). Expression of Dicer in brain, heart and adipose tissue decreases during aging (Boon et al. 2013; Mori et al. 2012), leading to decline of mature microRNA levels (Mori et al. 2012; Dimmeler and Nicotera 2013). This decrease was directly observed in brain (Inukai et al. 2012). Knockout of Dicer removes all microRNAs, producing drastic phenotypic changes. Modified mimics can be administrated exogenously in different combinations to test possible functional roles of corresponding microRNAs. Narrowing spectrum of microRNAs delivered can allow to specify certain functional interconnections in such Dicer-depleted models.

11.3.4.1.1.1 Classic Transgenic Methods

Classical transgenesis can be used successfully to produce Dicer-knockout models, and there are multiple works on mice utilizing this strategy. However, Dicer ablation has very wide physiological consequences, leading to death in uterus (Yang et al. 2005). For specific phenotype study, the knockout must be conditional, restricted to certain cell types (Kobayashi et al. 2008) or additionally controlled by one of the temporal regulation methods described above (Chmielarz et al. 2017; Wu et al. 2012).

11.3.4.1.1.2 Viral Delivery of sgRNAs to Knockout Dicer Using Cas9

Another approach is to deliver sgRNA-guided Cas9 nuclease by viral vectors. CRISPR/Cas9 system is well established in the context of KO induction and was implemented for Dicer studies (Berrens et al. 2017). There are strategies for simultaneous delivery of both nuclease and sgRNA on a single viral vector construct. In case of vectors with smaller loading capacities, e.g. AAV, standard SpCas9 (*Streptococcus pyogenes* Cas9) can't be co-expressed with sgRNA, and its smaller orthologs can be used, e.g. SaCas9 (*Staphylococcus aureus* Cas9) (Ran et al. 2015) or some other smaller genome-editing nucleases currently explored (He et al. 2018). Alternatively, larger lentiviral vector can fit spCas9 together with several sgRNAs for increased targeting efficiency (Choi et al. 2016). Members of Cas13 protein family target RNA molecules specifically and, hence, can be a valuable tool for targeted gene knockdowns (Zhou et al. 2020).

11.3.4.2 Systemic Knockout of Specific MicroRNAs and Their Families

Systemic knockout of microRNA means complete removal of microRNA from the experimental model. Systemic knockout can be achieved by impairing all or several key exons of the target gene (Guo et al. 2019) by deletion or replacing with another gene (usually positive selection marker) via recombination (Hall et al. 2009). Results of systemic microRNA knockout can be very prominent: deafness (Lewis et al. 2009), tumour formation (Mitsumura et al. 2018), embryonic (Kuhnert et al. 2008) or quick postnatal death (Ventura et al. 2008). Moreover, systemic microRNA knockout is not specific in terms of temporal or spatial characteristics, while microRNA expression is generally a tissue-specific, cell lineage-specific or developmental stage-specific (Geisler and Fechner 2016). Therefore, conditional knockout is usually preferred for microRNA research.

11.3.4.3 MicroRNA Conditional Knockout

11.3.4.3.1 Classic Transgenesis

Conditional knockout is restricted to a certain cell group or defined by time period. It allows to produce more meaningful experimental data. The Cre-loxP system is used to generate knockout mice (Schwenk et al. 1995). The conditional knockout mouse model uses a cell type-specific promoter to drive Cre expression. To produce the Cre-loxP conditional system, firstly a microRNA gene flanked by loxP sequences should be introduced *in vitro*. This is usually achieved by transfection of embryonic stem cells, to replace the wild-type gene in the process of homologous recombination (Prosser et al. 2011). Embryonic stem cells then are implanted into uterus of pseudo-pregnant mouse to develop a transgenic animal (Prosser et al. 2011). Another mouse line is made to express Cre under control of specific gene promoter (Prosser et al. 2011). Offspring of these two mice, which will inherit both transgenes, will have a specific microRNA knocked out in tissues where Cre is expressed. Cre-loxP system has the advantages of high efficiency and strong specificity. But there are obvious disadvantages when applied to microRNA research. Many microRNAs are produced from different loci, but share seed sequences. There can be several copies of the same microRNA encoded from different chromosomal loci. Moreover, there are species of highly similar microRNAs (microRNA families), usually expressed from the same cluster, which can share the seed region and, hence, target similar transcripts. So it is sometimes critical to knock out whole cluster (or multiple clusters on different chromosomes), in order to suppress the function of a specific microRNA group.

11.3.4.3.2 Viral Transduction of Cassettes for Cas9-sgRNA-Driven Knockout

Currently, microRNA knockout strategies implement adenovirus (Jiang et al. 2018), lentivirus (Huang et al. 2018) and adeno-associated virus (Huang et al. 2019), and can be used in various models. They induce RNAi to silence microRNA gene expression. In mice, the Cre-loxP-based CRISPR-Cas9 system can be used for conditional knockout. In this strategy, CRISPR activity is restricted to cells which express Cre. Cas9 is usually placed under control of CAG promoter, and LSL construct is inserted between them. Hence, excision of LSL by Cre induces transcription (Zhou et al. 2018; Platt et al. 2014). Both Cre and sgRNA can be delivered by viral vectors or plasmids. Using tissue-specific or cell-specific Cre lines allows precise spatially conditional knockout (Zhou et al. 2018; Platt et al. 2014).

11.3.4.4 MicroRNA Knockdown in *In Vitro* Models

Just as in case of gain-of-function transfection of unmodified microRNA-mimicking oligonucleotides, antisense oligonucleotides can be transfected into cultured cells for inhibition of specific microRNAs. This approach usually utilizes unmodified oligonucleotides for *in vitro* experiments, in combination with gain-of-function transfection for further insight into specific microRNA functions (Li et al. 2018a; Wu et al. 2014; Xu et al. 2019; Chen et al. 2017). However, for sufficient inhibition much higher concentrations of such antisense oligonucleotides are required, comparing to gain-of-function mimics transfection: sometimes up to fivefold difference (Zeng et al. 2016). All the limitations of microRNA mimics transfection apply to transfection of microRNA inhibitors, requiring researcher to carefully design the experiment and view results critically in terms of their relation to *in vivo* conditions. However, it is still a valuable and relatively simple approach.

11.3.4.5 MicroRNA Knockdown in *In Vivo* Model

11.3.4.5.1 AntagomiRs/MicroRNA Inhibitors

MicroRNA antagonists (antagomiRs) in the form of unmodified oligonucleotides usually have poor stability. Modification of ribose by 2'-*O*-methyl, terminal phosphorothioate linkages and 3' addition of cholesterol molecule are standard for increased stability of antagomiR (Ling and Calin 2014). Other stabilizing modifications include 2'-*O*-methylation, 2'-*O*-methoxyethylation and 2'-fluoro substitution (Garzon et al. 2010). Addition of cholesterol molecule assists entrance into cell (Krützfeldt et al. 2005). The 2'-*O*-methylation increases binding efficiency (Majlessi et al. 1998) and stability (Rettig and Behlke 2012). The 2'-fluoro substitution enhances both microRNA mimics (Deleavey et al. 2009) and antagomiRs (Kawasaki et al. 1993), possibly due to enthalpy shift of negatively charged fluorine (Pallan et al. 2010). However, 2'-fluorine substitution does not increase nuclease resistance

significantly (Manoharan 1999). AntagomiRs bind their target microRNAs, inhibiting their silencing function. Delivery can be performed by lipofectamine transfection or viral infection (Krützfeldt et al. 2005). AntagomiR provides knockdowns with high specificity, high efficiency and long duration. However, antagomiRs cannot cross the blood–brain barrier (Kuhn et al. 2013). Therefore, direct injection of the vector into the corresponding brain area is required.

Both oligonucleotides transfection and viral vectors can be applied with the following methods. At present, methods for knocking down microRNA based on adenovirus (Jiang et al. 2018), lentivirus (Huang et al. 2018) and adeno-associated virus (Huang et al. 2019) are used in different models.

11.3.4.5.2 MicroRNA-Sponges

MicroRNA sponge binds to specific microRNA (Carè et al. 2007). Transgene encoding microRNA sponge can block the activity of all microRNAs with the corresponding seed sequence (Ebert et al. 2007). Sponge is usually designed as an oligonucleotide with four to ten binding sites corresponding to the targeted microRNA (Santulli 2016). Sponge efficiency is determined by number of binding sites and their affinity to the microRNA. As targeted by seed sequence only, unlike whole sequence-specific antagomiRs, a single sponge can target a whole microRNA family with similar seed sequence, which can be a useful characteristic for some studies, but a drawback for others (Ebert and Sharp 2010). Delivered by viral vectors or inserted by means of classic transgenesis, sponges, unlike antagomiRs, can bear no enhancing chemical modifications and, however, are constantly persistent in cells (Ebert et al. 2007). In order to repress target microRNAs, sponges must be expressed on a constant rate, which can be costly to the cell and requires strong promoters. There is a strategy modification for higher effectivity of inhibition at the same doses of sponges: sponges bearing imperfect complementarity to microRNA seeds ('bulged' binding sites) produce greater microRNA silencing effect, possibly due to increased stability against RISC-mediated RNA degradation pathway (Ebert et al. 2007; Gentner et al. 2009). MicroRNA sponges are one of the simplest ways to inhibit microRNA function.

11.3.4.5.3 Tough Decoys

Tough decoys were invented in 2009, when various RNA decoy designs carried by lentiviral vectors were tested (Haraguchi et al. 2009). Tough decoys are the most accurate and potent constructs for microRNA inhibition (Haraguchi et al. 2009). The effectiveness of miR-25-3p tough decoy inhibition has been evaluated *in vitro* and *in vivo* (Jeong et al. 2018). Their advantages include resistance to endonucleases, high microRNA binding efficiency and convenient delivery. Although the

original study utilized lentiviral vector and Pol III promoter for tough decoy production [201], later study comparing several microRNA inhibiting approaches proposed Pol II promoter as a more desirable choice, because inhibitory activity of tough decoys transcribed from Pol III and Pol II promoters remained the same, while Pol II promoters are overall more convenient for temporal and spatial expression control (Bak et al. 2013). The same study comparatively identified tough decoys as overall the most potent microRNA inhibitors from seven tested (Bak et al. 2013).

11.3.5 In Vivo Validation of MicroRNA-Target Interactions

11.3.5.1 Target Protectors

Target protectors block target sites on mRNA, preventing microRNA pairing with its target. Protectors are usually designed to complementary pair seed sequence and about 10–20 nucleotides flanking each side of it (Vasudevan 2012). Modifications by LNA bases and 2'-*O*-methylation, as well as non-oligonucleotide formats (discussed below) of protectors allow to avoid Ago-mediated degradation of mRNA paired with protector (Choi et al. 2007).

11.3.5.1.1 Morpholino Format

Morpholino oligonucleotides (MO) are artificially synthesized antisense molecules. Due to their chemical modifications (phosphorodiamidate-linked morpholine rings with attached bases), they are resistant to endogenous nucleases and are able to induce gene silencing by blocking RNA splice junctions or translation start sites (Pattanayak et al. 2019). MO ability to target specific nucleotide sequence allows them to be used as a target protector by blocking 3'-UTR binding sequence on target mRNA, hence interfering with microRNA pairing and consequent biodegradation. This also allows to verify predicted binding sites. An important advantage of morpholino formats is negligible cytotoxicity.

11.3.5.1.2 Other Forms

Peptide nucleic acids (PNAs) are another tool for target protection. PNAs are DNA derivatives with sugar backbone replaced by achiral peptide chain. PNAs are not recognized by nucleases, can form stable heteroduplexes with complementary natural nucleotides and hence are used for both direct microRNA blockage and for target mRNA protection (Zarrilli et al. 2017).

11.3.6 Further Notes Related to MicroRNA Research

Apart from the classical microRNA methods mentioned before, the researchers sometimes need to face complex biological events associated with complex biogenesis and functional interactions of microRNAs. In this section, we discuss some of those.

11.3.6.1 Base Modifications

Evidence exists for methylation of m⁶A (Berulava et al. 2015) and m⁷G (Yuan et al. 2014a) in microRNAs, the functional meaning of which remains vague. There is study of methylation of primary, precursor and mature forms of human miR-125b by tRNA methyltransferase NSun2, which leads to overall repression of the microRNA silencing effect by inhibiting maturation of pri- and one of the pre-forms and lowering ability of mature microRNA to interact with RISC complex (Yuan et al. 2014a). These findings correspond to another massive study, which concluded that knockdown of demethylase FTO leads to lowered concentration levels of 92% of 239 potentially methylated microRNAs; moreover, methylated microRNAs were found to bear several conserved motifs, possibly discriminating them from non-methylated ones (Berulava et al. 2015). However, 42 microRNAs were also found to be significantly increased upon FTO knockdown (Berulava et al. 2015). Uncertainty is further added by a recent study of m⁷G methylation of let-7 by METTL1, which seemed to result in enhanced microRNA maturation rate (Pandolfini et al. 2019). To conclude, methylation seems to exert some functional effect on microRNAs, which, however, is not fully understood yet.

11.3.6.1.1 Other Modifications

Another common modification found in microRNAs is adenylation of 3' end, the data for which also shows some contradictions, or maybe rather still unknown patterns. Non-canonical polymerase Gld2 was directly shown to adenylate miR-122, miR-134 and let-7a, but not their pre-mature forms; moreover, adenylation resulted into almost twofold increase in half-lives of microRNAs, except for let-7a, which has shown much higher stability in non-adenylated form than other microRNAs, and did not change it significantly upon adenylation. Higher target silencing followed the increased stability of adenylated microRNAs (D'Ambrogio et al. 2012). The same study went further to test global *in vivo* effect of Gld2 and produced a fibroblast culture with its depletion. While control cells tested by deep-sequencing have shown 50 microRNAs (~8.7%) to be adenylated, Gld2-depleted fibroblasts had 46 of these showing an average 2.1-fold decrease in adenylated species. Interestingly, not all of the microRNAs fell in concentration upon adenylation fading, but the ones did had either pre-mature or mature form mostly destabilized. Finally, sequence

analysis has shown that nucleotide context of 3' end largely affects the degree of stabilization effect exerted by adenylation (D'Ambrogio et al. 2012). In conclusion, the study has shown that some, but not all microRNAs, are stabilized by 3' adenylation.

However, the other study concerning specifically cancer-related miR-21 has shown that its 3' adenylation by PAPD5 results in consequent 3'-5' direction trimming and exoribonuclease degradation, with disruption of this pathway being a highlight of multiple cancers (Boele et al. 2014). Furthermore, another study looked into separate knockdowns of PAPD5, PAPD4 and PAPD7 in human cell cultures and found reduction in microRNA adenylation levels to be the highest for the second protein, limited for the former and not present for the latter. Moreover, further tests have shown an increase of microRNAs silencing upon reduction of adenylation levels and overall lowered ability of adenylated microRNAs to recruit protein members of RISC complex (Burroughs et al. 2010). Overall, these lines of evidence propose opposite effects of adenylation on microRNA functions. However, a strong influence of nucleotide context was mentioned, and the studies bringing conflicting results manipulated with different enzymes in different cellular models. Hence, it is possible to conclude that adenylation effect on microRNAs stability and silencing potential is quite variable depending of biological context, the exact patterns behind which are still unknown.

11.3.6.2 Drosha-Independent MicroRNA Maturation

The first example of Drosha-independent pathway was mirtrons (microRNA-intron) pathway. Mirtrons are small intronic RNA hairpins produced during gene splicing in as a pre-microRNAs. Therefore, they skip Drosha cleavage and follow otherwise canonical pathway: get exported to cytoplasm by Exportin5 and undergo Dicer-dependent maturation (Okamura et al. 2007). Originally identified in *Drosophila* and *C. elegans* (Ruby et al. 2007), mirtrons were soon found to be broadly present in mammals (Berezikov et al. 2007). Two other Drosha-independent sources of microRNAs are some small nucleolar RNA (snRNA) (Taft et al. 2009) and tRNA (Babiarz et al. 2008): upon processing by Dicer, both provide microRNA-like molecules with functional activity.

11.3.6.2.1 Dicer-Independent Maturation of miR-451

Highly conserved among vertebrates miR-451 is an example of Dicer-independent maturation. Although its primary transcript is processed by Drosha, the derived pre-miR-451 hairpin molecule is not cleaved by Dicer. Experiments have shown that Dicer knockout does not ablate processing of mature miR-451, which becomes depleted only in case of Ago2 protein knockdown (Yang et al. 2010). Vice versa, miR-451 was lost in infant-lethal Ago2 knockdown mice (Cheloufi et al. 2010).

Moreover, biochemical engineering of Dicer-dependent pre-miR-430c in Zebrafish allowed to produce its alternative pre-mature form, mimicking hairpin of miR-451. This mimic was successfully processed in Dicer-depleted cells following Ago2 pathway, which points to several important conclusions: first, secondary structure of microRNAs might be detrimental to its maturation pathway *in vivo*; second, it is possible to engineer hairpin molecules which will be processed *in vivo* by Dicer-independent pathway (Cifuentes et al. 2010). This significantly expands our capabilities to genetically manipulate and rescue Dicer-deficient phenotype. Further research derived a list of functional parameters for design of effective Dicer-independent microRNA mimics, among which there were base-pairing requirements, specific length of hairpin and G:C content of distal stem (Yang et al. 2012).

11.3.6.2.2 Ago2-Dependent MicroRNA Maturation

A study analysing separate knockouts of Drosha, Exportin5 and Dicer pointed to the fact that Dicer knockout leads to decrease in 3p microRNAs to more severe extent than in 5p, which points to the maturation by means of 3'-5' trimming of pre-microRNAs (Jeon et al. 2016). This corresponded to previous observations (Cifuentes et al. 2010; Ravi et al. 2012), which might mean a much more broad utilization of Ago2-dependent microRNA maturation pathway, than it is known from the specific described examples.

11.3.6.2.3 Cluster Assistance in MicroRNA Maturation

Another example of unusual organization of microRNAs maturation process is cluster-assisted maturation, when certain primary hairpin ('recipient') is only processed by Drosha in pair with another hairpin ('helper'). Some microRNAs are spatially organized into genomic clusters, which results into them being transcribed as a single multi-hairpin transcript, separated into distinct pre-microRNAs upon Drosha complex processing. However, certain structural characteristics (e.g. small loops and short stems) can make microRNA primary hairpin a sub-optimal Drosha substrate. It was recently found that processing of such sub-optimal pri-microRNAs is often dependent on cleavage of neighbouring pri-microRNA hairpin from the same transcript. This requires incorporation of specific molecular actors into the microprocessor complex and can be demonstrated on the examples of: pri-miR-15a, only processed in presence of pri-miR-16-1 (Hutter et al. 2020) and already mentioned miR-451, maturation rate of which increases greatly when its pri-hairpin is co-processed with pri-miR-144 (Shang et al. 2020). Cluster co-processing seems to require both 'helper' and 'recipient' hairpins to originate from single transcript, and happens upon microprocessor's recognition of helper microRNA and the linker sequence joining it to the recipient one.

11.3.6.2.4 Non-classical MicroRNA Maturation Pathways Provide New Ideas for Genetic Manipulation

A m⁷G cap has been implemented into artificial constructs in order to bias guide strand choice and avoid unwanted and unpredictable targeting (Xie et al. 2013). Moreover, by combining knowledge of non-canonical microRNA maturation pathways, strategies have been developed to generate microRNA-like molecules which bypass both Drosha and Dicer processing (Maurin et al. 2012). This discovery can be promising in developing gene-silencing constructs which would not compete with endogenous microRNAs for canonical maturation pathway.

11.3.6.3 Non-canonical MicroRNA-Target Interactions

11.3.6.3.1 Transcript-Dependent MicroRNA Degradation

Transcript-dependent microRNA degradation (TDMD) causes microRNA degradation upon binding to target. TDMD seems to require high degree of complementarity in 3' end of microRNA and seed sequence, with mismatches present in central microRNA region (Fuchs Wightman et al. 2018). This changes conformation of Ago-microRNA silencing complex, followed by enzymatic degradation of exposed microRNA.

A very illustrative example of TDMD functioning and importance comes from an *in vivo* study of two possibly evolutionary-related genes: lncRNA *libra* in Zebrafish and protein-coding gene *Nrep* in mouse (Bitetti et al. 2018). Both are almost exclusively brain-specific and highly complementary to miR-29/miR-29b (with archetypical for TDMD central mismatches). *Nrep* shows high conservation with *libra* in its 3' non-coding region, which together with their common expression pattern raised a hypothesis that both transcripts may exert regulatory functions via non-coding elements. Zebrafish with inverted or ablated *libra* have shown significant changes in explorative and anxiety-like behaviour (Bitetti et al. 2018). Further *in vitro* testing has shown TDMD effect exerted by *Nrep* on miR-29b (Bitetti et al. 2018). Overall, the study illustrates how crucial could be TDMD control not just on molecular, but also on behavioural level.

11.3.6.3.2 Other Non-classical MicroRNA-Target Interactions

In animals, only partial complementarity is observed between microRNA and its target. Strong binding of microRNA with a specific short (~6–8 nt) region of target mRNA is usually detrimental for further partial annealing and microRNA-target hybridization (Bartel 2009). This short sequence of initial contact is called 'seed sequence' and is located at the 5' end region of microRNA (Lewis et al. 2003). Canonical pairing is usually represented by complete annealing of microRNA to 6–8 nucleotides in seed sequence (called, self-explanatory, 6-mer, 7-mer and 8-mer

pairings) and, when combined with evolutionary conservation data, secondary structure analysis and some other parameters, pairing within a seed sequence can be a valuable tool for microRNA-target predictions (Mourelatos 2008). However, there are multiple examples of non-canonical target binding.

There are cases in which non-perfect alignment within seed sequence is present in microRNA-target interaction ('functional wobble'), but the pairing still occurs due to so-called 'supplementary region/element': a near-complete complementary pairing in the region outside of the seed sequence. Such is the pairing of human miR-196a and miR-196b to HOXB8 mRNA, which produces G:U wobble in the middle of the seed sequence, but shows almost complete sequence matches in seed's flanking regions (Yekta et al. 2004). In turn, *C. elegans* let-7 binds lin-41 mRNA, producing a bulb because of uneven base pairing, but such imperfect pairing is compensated by complementarity region shifted to the 3' end of microRNA (Vella et al. 2004). Examples of incomplete seed binding are quite diverse and even include targeting of a completely 'seedless' transcripts, as in case of human miR-24-3p (Lal et al. 2009).

As non-canonical target pairing, unpredictable by standard seed pairing rules, was found to be more and more broadly present, a need for a suitable model has appeared to explain and predict such pairing. For this, a 'pivot pairing' rule was proposed (Chi et al. 2012). In short, by analysis of thermodynamics of microRNA-target interactions and statistical analysis of data available on most common non-canonical targets, authors suggested that there is a certain type of seed mispairing, 'functional bulge', which appears on either fifth or sixth (starting from 3' seed sequence end) nucleotide of mRNA and allows robust binding of sixth nucleotide of microRNA seed sequence. This sixth nucleotide pairing appears to be critical for stabilization of a transitional state of microRNA-target duplex. Moreover, this spatial organization of 'functional bulge' turned out to be conserved throughout microRNA targets (although to the lesser extent, than canonical pairing) (Chi et al. 2012). These examples of non-canonical binding demonstrate how limited are the currently available tools and how many more interaction patterns may occur in RNA interference. Accumulation of more data and creating new models may allow us to deepen our understanding and predict such interactions with growing confidence and precision.

11.4 Conclusions

The critical role of autophagy-related genes in ND (Kim et al. 2016b) and ability of autophagic clearance of abnormal misfolded proteins (Berger et al. 2005; Webb et al. 2003; Ravikumar et al. 2002) in the healthy and diseased brain make studies about regulation of this pathway by microRNAs highly relevant both for basic research and clinical practice. Indeed, novel RNAi-based approaches to treat ND are already on the market and will gain more and more attention in the future (Shah et al. 2018). In this chapter, we highlighted 18 autophagy-regulating microRNAs

related to aging and neurodegeneration. However, neither of the discussed studies had proven a causative role of these macroautophagy- and CMA-targeting microRNA in neurodegenerative diseases. This doesn't preclude the researchers from further exploration of these pathways. Instead, more *in silico*, *in vitro*, *in vivo* and *ex vivo* data will allow researchers to gain solid evidence to either rule out or confirm the contribution of the RNAi/autophagy interplay to neurodegeneration and the human pathology.

Funding This study was supported by the SJTU startup fund for junior researchers #AF0800059 to Q.L. and the joint grant from ShengYushou Center of Cell Biology and Immunology to I.A.V.

References

- About AA, et al. PARK2 patient neuroprogenitors show increased mitochondrial sensitivity to copper. *Neurobiol Dis.* 2015;73:204–12.
- Abram CL, et al. Comparative analysis of the efficiency and specificity of myeloid-Cre deleting strains using ROSA-EYFP reporter mice. *J Immunol Methods.* 2014;408:89–100.
- Adams D, et al. Trial design and rationale for APOLLO, a Phase 3, placebo-controlled study of patisiran in patients with hereditary ATTR amyloidosis with polyneuropathy. *BMC Neurol.* 2017;17(1):181.
- Adams D, et al. Patisiran, an RNAi therapeutic, for hereditary transthyretin amyloidosis. *N Engl J Med.* 2018;379(1):11–21.
- Addo-Quaye C, Miller W, Axtell MJ. CleaveLand: a pipeline for using degradome data to find cleaved small RNA targets. *Bioinformatics.* 2008;25(1):130–1.
- Altmann K-H, et al. Second generation of antisense oligonucleotides: from nuclease resistance to biological efficacy in animals. *CHIMIA Int J Chem.* 1996;50(4):168–76.
- Alvarez-Erviti L, et al. Chaperone-mediated autophagy markers in Parkinson disease brains. *Arch Neurol.* 2010;67(12):1464–72.
- Alvarez-Erviti L, Seow Y, Schapira AHV, Rodriguez-Oroz MC, Obeso JA, Cooper JM. Influence of microRNA deregulation on chaperone-mediated autophagy and α -synuclein pathology in Parkinson's disease. *Cell Death Dis.* 2013;4(3):e545.
- Amar L, et al. Control of small inhibitory RNA levels and RNA interference by doxycycline induced activation of a minimal RNA polymerase III promoter. *Nucleic Acids Res.* 2006;34(5):e37.
- Amarzguioui M, et al. Tolerance for mutations and chemical modifications in a siRNA. *Nucleic Acids Res.* 2003;31(2):589–95.
- Ambros V, et al. A uniform system for microRNA annotation. *RNA.* 2003;9(3):277–9.
- Atambayeva S, et al. The binding sites of miR-619-5p in the mRNAs of human and orthologous genes. *BMC Genomics.* 2017;18(1):428.
- Babiarz JE, et al. Mouse ES cells express endogenous shRNAs, siRNAs, and other Microprocessor-independent, Dicer-dependent small RNAs. *Genes Dev.* 2008;22(20):2773–85.
- Bak RO, Hollensen AK, Primo MN, Sørensen CD, Mikkelsen JG. Potent microRNA suppression by RNA Pol II-transcribed 'Tough Decoy' inhibitors. *RNA.* 2013;19(2):280–93.
- Ban JJ, et al. MicroRNA-27a reduces mutant huntingtin aggregation in an in vitro model of Huntington's disease. *Biochem Biophys Res Commun.* 2017;488(2):316–21.
- Banerjee R, Beal MF, Thomas B. Autophagy in neurodegenerative disorders: pathogenic roles and therapeutic implications. *Trends Neurosci.* 2010;33(12):541–9.
- Bang J, Spina S, Miller BL. Frontotemporal dementia. *Lancet.* 2015;386(10004):1672–82.
- Baras AS, et al. miRge—a multiplexed method of processing small RNA-Seq data to determine microRNA entropy. *PLoS One.* 2015;10(11):e0143066.

- Barmada SJ, et al. Autophagy induction enhances TDP43 turnover and survival in neuronal ALS models. *Nat Chem Biol.* 2014;10(8):677–85.
- Bartel DP. MicroRNAs: target recognition and regulatory functions. *Cell.* 2009;136(2):215–33.
- Basler K, Struhl G. Compartment boundaries and the control of *Drosophila* limb pattern by hedgehog protein. *Nature.* 1994;368(6468):208–14.
- Bates GP. History of genetic disease: the molecular genetics of Huntington disease—a history. *Nat Rev Genet.* 2005;6(10):766–73.
- Beard C, et al. Efficient method to generate single-copy transgenic mice by site-specific integration in embryonic stem cells. *Genesis.* 2006;44(1):23–8.
- Berezikov E, et al. Mammalian mirtron genes. *Mol Cell.* 2007;28(2):328–36.
- Berger Z, et al. Rapamycin alleviates toxicity of different aggregate-prone proteins. *Hum Mol Genet.* 2005;15(3):433–42.
- Berrens RV, et al. An endosRNA-based repression mechanism counteracts transposon activation during global DNA demethylation in embryonic stem cells. *Cell Stem Cell.* 2017;21(5):694–703.
- Berulava T, et al. N6-adenosine methylation in miRNAs. *PLoS One.* 2015;10(2):e0118438.
- Bitetti A, et al. MicroRNA degradation by a conserved target RNA regulates animal behavior. *Nat Struct Mol Biol.* 2018;25(3):244–51.
- Blennow K, de Leon MJ, Zetterberg H. Alzheimer's disease. *Lancet.* 2006;368(9533):387–403.
- Boele J, et al. PAPD5-mediated 3' adenylation and subsequent degradation of miR-21 is disrupted in proliferative disease. *Proc Natl Acad Sci.* 2014;111(31):11467–72.
- Boland B, et al. Autophagy induction and autophagosome clearance in neurons: relationship to autophagic pathology in Alzheimer's disease. *J Neurosci.* 2008;28(27):6926–37.
- Boon RA, Iekushi K, Lechner S, Seeger T, Fischer A, Heydt S, Kaluza D, Tréguer K, Carmona G, Bonauer A, Horrevoets AJG, Didier N, Girmatsion Z, Biliczki P, Ehrlich JR, Katus HA, Müller OJ, Potente M, Zeiher AM, Hermeking H, Dimmeler S. MicroRNA-34a regulates cardiac ageing and function. *Nature.* 2013;495(7439):107–10.
- Borchert GM, Lanier W, Davidson BL. RNA polymerase III transcribes human microRNAs. *Nat Struct Mol Biol.* 2006;13(12):1097–101.
- Braasch DA, et al. Biodistribution of phosphodiester and phosphorothioate siRNA. *Bioorg Med Chem Lett.* 2004;14(5):1139–43.
- Bramsen JB, et al. A large-scale chemical modification screen identifies design rules to generate siRNAs with high activity, high stability and low toxicity. *Nucleic Acids Res.* 2009;37(9):2867–81.
- Breakfield NW, et al. High-resolution experimental and computational profiling of tissue-specific known and novel miRNAs in *Arabidopsis*. *Genome Res.* 2012;22(1):163–76.
- Bridge AJ, et al. Induction of an interferon response by RNAi vectors in mammalian cells. *Nat Genet.* 2003;34(3):263–4.
- Bruick RK. Expression of the gene encoding the proapoptotic Nip3 protein is induced by hypoxia. *Proc Natl Acad Sci U S A.* 2000;97(16):9082–7.
- Brummelkamp TR, Bernards R, Agami R. A system for stable expression of short interfering RNAs in mammalian cells. *Science.* 2002;296(5567):550–3.
- Burnette WN. "Western Blotting": electrophoretic transfer of proteins from sodium dodecyl sulfate-polyacrylamide gels to unmodified nitrocellulose and radiographic detection with antibody and radioiodinated protein A. *Anal Biochem.* 1981;112(2):195–203.
- Burns JC, et al. Vesicular stomatitis virus G glycoprotein pseudotyped retroviral vectors: concentration to very high titer and efficient gene transfer into mammalian and nonmammalian cells. *Proc Natl Acad Sci.* 1993;90(17):8033.
- Burroughs AM, Ando Y, de Hoon MJL, Tomaru Y, Nishibu T, Ukekawa R, Funakoshi T, Kurokawa T, Suzuki H, Hayashizaki Y, Daub CO. A comprehensive survey of 3' animal miRNA modification events and a possible role for 3' adenylation in modulating miRNA targeting effectiveness. *Genome Res.* 2010;20(10):1398–410.
- Calderon-Garcidueñas AL, Duyckaerts C. Alzheimer disease. *Handb Clin Neurol.* 2017;145:325–37.
- Calixto A, et al. Enhanced neuronal RNAi in *C. elegans* using SID-1. *Nat Methods.* 2010;7(7):554–9.

- Cao F, Liu Z, Sun G. Diagnostic value of miR-193a-3p in Alzheimer's disease and miR-193a-3p attenuates amyloid- β induced neurotoxicity by targeting PTEN. *Exp Gerontol.* 2020;130:110814.
- Capece V, et al. Oasis: online analysis of small RNA deep sequencing data. *Bioinformatics.* 2015;31(13):2205–7.
- Carè A, Catalucci D, Felicetti F, Bonci D, Addario A, Gallo P, Bang M-L, Segnalini P, Gu Y, Dalton ND, Elia L, Latronico MVG, Høydal M, Autore C, Russo MA, Dorn GW 2nd, Ellingsen O, Ruiz-Lozano P, Peterson KL, Croce CM, Peschle C, Condorelli G. MicroRNA-133 controls cardiac hypertrophy. *Nat Med.* 2007;13(5):613–8.
- Casola S. Mouse models for miRNA expression: the ROSA26 locus. In: Monticelli S, editor. *MicroRNAs and the immune system: methods and protocols.* Totowa: Humana Press; 2010. p. 145–63.
- Castoldi M, Schmidt S, Benes V, Noerholm M, Kulozik AE, Hentze MW, Muckenthaler MU. A sensitive array for microRNA expression profiling (miChip) based on locked nucleic acids (LNA). *RNA.* 2006;12(5):913–20.
- Caygill EE, Johnston LA. Temporal regulation of metamorphic processes in *Drosophila* by the let-7 and miR-125 heterochronic microRNAs. *Curr Biol.* 2008;18(13):943–50.
- Chae H, et al. BioVLAB-MMIA-NGS: microRNA–mRNA integrated analysis using high-throughput sequencing data. *Bioinformatics.* 2014;31(2):265–7.
- Chang H, et al. CRISPR/cas9, a novel genomic tool to knock down microRNA in vitro and in vivo. *Sci Rep.* 2016;6(1):1–12.
- Chaubey A, et al. MicroRNAs and deletion of the derivative chromosome 9 in chronic myeloid leukemia. *Leukemia.* 2009;23(1):186–8.
- Chavez A, et al. Highly efficient Cas9-mediated transcriptional programming. *Nat Methods.* 2015;12(4):326–8.
- Che X, et al. MicroRNA-1 regulates the development of osteoarthritis in a Col2a1-Cre-ERT2/GFPfl/fl-RFP-miR-1 mouse model of osteoarthritis through the downregulation of Indian hedgehog expression. *Int J Mol Med.* 2020;46(1):360–70.
- Cheloufi S, et al. A dicer-independent miRNA biogenesis pathway that requires Ago catalysis. *Nature.* 2010;465(7298):584–9.
- Chen Y, Wang X. miRDB: an online database for prediction of functional microRNA targets. *Nucleic Acids Res.* 2019;48(D1):D127–31.
- Chen J-K, et al. Synthesis of oligodeoxyribonucleotide N3' \rightarrow P5' phosphoramidates. *Nucleic Acids Res.* 1995;23(14):2661–8.
- Chen C, et al. Real-time quantification of microRNAs by stem–loop RT–PCR. *Nucleic Acids Res.* 2005;33(20):e179.
- Chen C-J, et al. ncPRO-seq: a tool for annotation and profiling of ncRNAs in sRNA-seq data. *Bioinformatics.* 2012;28(23):3147–9.
- Chen Y, et al. Aberration of miRNAs expression in leukocytes from sporadic amyotrophic lateral sclerosis. *Front Mol Neurosci.* 2016;9:69.
- Chen Y, et al. MicroRNA-133 overexpression promotes the therapeutic efficacy of mesenchymal stem cells on acute myocardial infarction. *Stem Cell Res Ther.* 2017;8(1):1–11.
- Chen L, et al. Identification of aberrant circulating miRNAs in Parkinson's disease plasma samples. *Brain Behav.* 2018;8(4):e00941.
- Cheng M, et al. MicroRNA-181a suppresses parkin-mediated mitophagy and sensitizes neuroblastoma cells to mitochondrial uncoupler-induced apoptosis. *Oncotarget.* 2016;7(27):42274–87.
- Chi SW, Hannon GJ, Darnell RB. An alternative mode of microRNA target recognition. *Nat Struct Mol Biol.* 2012;19(3):321–7.
- Child DD, et al. Cardiac mTORC1 dysregulation impacts stress adaptation and survival in Huntington's disease. *Cell Rep.* 2018;23(4):1020–33.
- Chiu YL, Rana TM. siRNA function in RNAi: a chemical modification analysis. *RNA.* 2003;9(9):1034–48.
- Chmielarz P, et al. Dicer and microRNAs protect adult dopamine neurons. *Cell Death Dis.* 2017;8(5):e2813.

- Cho S, et al. miRgator v3.0: a microRNA portal for deep sequencing, expression profiling and mRNA targeting. *Nucleic Acids Res.* 2012;41(D1):D252–7.
- Choi W-Y, Giraldez AJ, Schier AF. Target protectors reveal dampening and balancing of Nodal agonist and antagonist by miR-430. *Science.* 2007;318(5848):271–4.
- Choi JG, et al. Lentivirus pre-packed with Cas9 protein for safer gene editing. *Gene Ther.* 2016;23(7):627–33.
- Chou C-H, et al. A computational approach for identifying microRNA-target interactions using high-throughput CLIP and PAR-CLIP sequencing. *BMC Genomics.* 2013;14(1):S2.
- Chugh P, Dittmer DP. Potential pitfalls in microRNA profiling. *Wiley Interdiscip Rev RNA.* 2012;3(5):601–16.
- Chung KM, et al. Alzheimer's disease and the autophagic-lysosomal system. *Neurosci Lett.* 2019;697:49–58.
- Cifuentes D, Xue H, Taylor DW, Patnode H, Mishima Y, Cheloufi S, Ma E, Mane S, Hannon GJ, Lawson ND, Wolfe SA, Giraldez AJ. A novel miRNA processing pathway independent of Dicer requires Argonaute2 catalytic activity. *Science.* 2010;328(5986):1694–8.
- Cook GA-O, et al. Structural variation and its potential impact on genome instability: novel discoveries in the EGFR landscape by long-read sequencing. *PLoS One.* 2020;15(1):e0226340.
- Corbin R, Olsson-Carter K, Slack F. The role of microRNAs in synaptic development and function. *BMB Rep.* 2009;42(3):131–5.
- Couto LB, High KA. Viral vector-mediated RNA interference. *Curr Opin Pharmacol.* 2010;10(5):534–42.
- Crippa V, Sau D, Rusmini P, Boncoraglio A, Onesto E, Bolzoni E, Galbiati M, Fontana E, Marino M, Carra S, Bendotti C, De Biasi S, Poletti A. The small heat shock protein B8 (HspB8) promotes autophagic removal of misfolded proteins involved in amyotrophic lateral sclerosis (ALS). *Hum Mol Genet.* 2010;19(17):3440–56.
- Cuervo AM, et al. Impaired degradation of mutant α -synuclein by chaperone-mediated autophagy. *Science.* 2004;305(5688):1292–5.
- Cullere X, et al. Neutrophil-selective CD18 silencing using RNA interference in vivo. *Blood.* 2008;111(7):3591–8.
- Czauderna F, et al. Structural variations and stabilising modifications of synthetic siRNAs in mammalian cells. *Nucleic Acids Res.* 2003;31(11):2705–16.
- D'Ambrogio A, et al. Specific miRNA stabilization by Gld2-catalyzed monoadenylation. *Cell Rep.* 2012;2(6):1537–45.
- Das AT, Tenenbaum L, Berkhout B. Tet-On systems for doxycycline-inducible gene expression. *Curr Gene Ther.* 2016;16(3):156–67.
- Deas E, Wood NW, Plun-Favreau H. Mitophagy and Parkinson's disease: the PINK1–parkin link. *Biochim Biophys Acta.* 2011;1813(4):623–33.
- Dehay B, Ramirez A, Martinez-Vicente M, Perier C, Canon M-H, Doudnikoff E, Vital A, Vila M, Klein C, Bezard E. Loss of P-type ATPase ATP13A2/PARK9 function induces general lysosomal deficiency and leads to Parkinson disease neurodegeneration. *Proc Natl Acad Sci U S A.* 2012;109(24):9611–6.
- Deleavey GF, Watts JK, Damha MJ. Chemical modification of siRNA. *Curr Protoc Nucleic Acids Chem.* 2009;39(1):16.31–16.322.
- Dellinger DJ, et al. Solid-phase chemical synthesis of phosphonoacetate and thiophosphonoacetate oligodeoxynucleotides. *J Am Chem Soc.* 2003;125(4):940–50.
- Desvignes T, et al. miRNA analysis with Prost! reveals evolutionary conservation of organ-enriched expression and post-transcriptional modifications in three-spined stickleback and zebrafish. *Sci Rep.* 2019;9(1):3913.
- Dhanasekaran S, Doherty TM, Kenneth J. Comparison of different standards for real-time PCR-based absolute quantification. *J Immunol Methods.* 2010;354(1):34–9.
- Dickins RA, et al. Tissue-specific and reversible RNA interference in transgenic mice. *Nat Genet.* 2007;39(7):914–21.

- DiFiglia M, et al. Aggregation of huntingtin in neuronal intranuclear inclusions and dystrophic neurites in brain. *Science*. 1997;277(5334):1990–3.
- Dimmeler S, Nicotera P. MicroRNAs in age-related diseases. *EMBO Mol Med*. 2013;5(2):180–90.
- Dogan A. Amyloidosis: insights from proteomics. *Annu Rev Pathol*. 2017;12:277–304.
- Dong H, et al. MicroRNA: function, detection, and bioanalysis. *Chem Rev*. 2013;113(8):6207–33.
- Dong H, et al. A panel of four decreased serum microRNAs as a novel biomarker for early Parkinson's disease. *Biomarkers*. 2016;21(2):129–37.
- Du X, et al. miR-124 downregulates BACE 1 and alters autophagy in APP/PS1 transgenic mice. *Toxicol Lett*. 2017;280:195–205.
- Duan D, et al. A new dual-vector approach to enhance recombinant adeno-associated virus-mediated gene expression through intermolecular cis activation. *Nat Med*. 2000;6(5):595–8.
- Dugger BN, Dickson DW. Pathology of neurodegenerative diseases. *Cold Spring Harb Perspect Biol*. 2017;9(7):a028035.
- Ebert MS, Sharp PA. MicroRNA sponges: progress and possibilities. *RNA (New York, NY)*. 2010;16(11):2043–50.
- Ebert MS, Neilson JR, Sharp PA. MicroRNA sponges: competitive inhibitors of small RNAs in mammalian cells. *Nat Methods*. 2007;4(9):721–6.
- Elbashir SM, et al. Duplexes of 21-nucleotide RNAs mediate RNA interference in cultured mammalian cells. *Nature*. 2001;411(6836):494–698.
- Emde A, et al. Dysregulated miRNA biogenesis downstream of cellular stress and ALS-causing mutations: a new mechanism for ALS. *EMBO J*. 2015;34(21):2633–51.
- Erratum. *Nucleic Acids Res*. 1996;24(7):1389.
- Evers M, et al. miRA: adaptable novel miRNA identification in plants using small RNA sequencing data. *BMC Bioinformatics*. 2015;16(1):370.
- Fanciulli A, Wenning GK. Multiple-system atrophy. *N Engl J Med*. 2015;372(3):249–63.
- Fang Z, Rajewsky N. The impact of miRNA target sites in coding sequences and in 3'UTRs. *PLoS One*. 2011;6(3):e18067.
- Fang EF, et al. Mitophagy inhibits amyloid- β and tau pathology and reverses cognitive deficits in models of Alzheimer's disease. *Nat Neurosci*. 2019;22(3):401–12.
- Fasold M, et al. DARIO: a ncRNA detection and analysis tool for next-generation sequencing experiments. *Nucleic Acids Res*. 2011;39(Suppl 2):W112–7.
- Feng T, et al. Autophagy-mediated regulation of BACE1 protein trafficking and degradation. *J Biol Chem*. 2017;292(5):1679–90.
- Finkbeiner S. The autophagy lysosomal pathway and neurodegeneration. *Cold Spring Harb Perspect Biol*. 2020;12(3):a033993.
- Fisch KM, et al. Omics Pipe: a community-based framework for reproducible multi-omics data analysis. *Bioinformatics*. 2015;31(11):1724–8.
- Floto RA, Sarkar S, Perlstein EO, Kampmann B, Schreiber SL, Rubinsztein DC. Small molecule enhancers of rapamycin-induced TOR inhibition promote autophagy, reduce toxicity in Huntington's disease models and enhance killing of mycobacteria by macrophages. *Autophagy*. 2007;3(6):620–2.
- Friedländer MR, et al. miRDeep2 accurately identifies known and hundreds of novel microRNA genes in seven animal clades. *Nucleic Acids Res*. 2011;40(1):37–52.
- Fuchs Wightman F, et al. Target RNAs strike back on microRNAs. *Front Genet*. 2018;9:435.
- Fukumoto H, et al. A noncompetitive BACE1 inhibitor TAK-070 ameliorates A β pathology and behavioral deficits in a mouse model of Alzheimer's disease. *J Neurosci*. 2010;30(33):11157–66.
- Garzon R, Marcucci G, Croce CM. Targeting microRNAs in cancer: rationale, strategies and challenges. *Nat Rev Drug Discov*. 2010;9(10):775–89.
- Gascon E, et al. Alterations in microRNA-124 and AMPA receptors contribute to social behavioral deficits in frontotemporal dementia. *Nat Med*. 2014;20(12):1444–51.
- GBD 2015 Neurological Disorders Collaborator Group. Global, regional, and national burden of neurological disorders during 1990–2015: a systematic analysis for the Global Burden of Disease Study 2015. *Lancet Neurol*. 2017;16(11):877–97.

- Geekiyana H, Chan C. MicroRNA-137/181c regulates serine palmitoyltransferase and in turn amyloid β , novel targets in sporadic Alzheimer's disease. *J Neurosci*. 2011;31(41):14820–30.
- Geekiyana H, et al. Blood serum miRNA: non-invasive biomarkers for Alzheimer's disease. *Exp Neurol*. 2012;235(2):491–6.
- Geisler A, Fechner H. MicroRNA-regulated viral vectors for gene therapy. *World J Exp Med*. 2016;6(2):37–54.
- Gentner B, et al. Stable knockdown of microRNA in vivo by lentiviral vectors. *Nat Methods*. 2009;6(1):63–6.
- Giering JC, et al. Expression of shRNA from a tissue-specific pol II promoter is an effective and safe RNAi therapeutic. *Mol Ther*. 2008;16(9):1630–6.
- Gilbert LA, et al. CRISPR-mediated modular RNA-guided regulation of transcription in eukaryotes. *Cell*. 2013;154(2):442–51.
- Giraldo P, Montoliu L. Size matters: use of YACs, BACs and PACs in transgenic animals. *Transgenic Res*. 2001;10(2):83–103.
- Giurato G, et al. iMir: an integrated pipeline for high-throughput analysis of small non-coding RNA data obtained by smallRNA-Seq. *BMC Bioinformatics*. 2013;14(1):362.
- Gjaltema RAF, Schulz EG. CRISPR/dCas9 switch systems for temporal transcriptional control. In: Jeltsch A, Rots MG, editors. *Epigenome editing: methods and protocols*. New York: Springer; 2018. p. 167–85.
- Glass D, et al. Gene expression changes with age in skin, adipose tissue, blood and brain. *Genome Biol*. 2013;14(7):R75.
- Gómez-Suaga P, et al. ER–mitochondria signaling in Parkinson's disease. *Cell Death Dis*. 2018;9(3):1–12.
- Gonçalves IdCG, et al. Neuronal activity regulates DROSHA via autophagy in spinal muscular atrophy. *Sci Rep*. 2018;8(1):1–15.
- Gossen M, Bujard H. Tight control of gene expression in mammalian cells by tetracycline-responsive promoters. *Proc Natl Acad Sci*. 1992;89(12):5547–51.
- Gossen M, et al. Transcriptional activation by tetracyclines in mammalian cells. *Science*. 1995;268(5218):1766–9.
- Gryaznov SM. Oligonucleotide N3' \rightarrow P5' phosphoramidates and thio-phosphoramidates as potential therapeutic agents. *Chem Biodivers*. 2010;7(3):477–93.
- Guda S, et al. miRNA-embedded shRNAs for lineage-specific BCL11A knockdown and hemoglobin F induction. *Mol Ther*. 2015;23(9):1465–74.
- Guedes JR, et al. MicroRNA deregulation and chemotaxis and phagocytosis impairment in Alzheimer's disease. *Alzheimers Dement*. 2016;3(1):7–17.
- Guillén C, Benito M. mTORC1 overactivation as a key aging factor in the progression to type 2 diabetes mellitus. *Front Endocrinol*. 2018;9:621.
- Guo Y-P, et al. Global gene knockout of Kcnip3 enhances pain sensitivity and exacerbates negative emotions in rats. *Front Mol Neurosci*. 2019;12:5.
- Gupta V, et al. shortran: a pipeline for small RNA-seq data analysis. *Bioinformatics*. 2012;28(20):2698–700.
- Hackenberg M, Rodríguez-Ezpeleta N, Aransay AM. miRanalyzer: an update on the detection and analysis of microRNAs in high-throughput sequencing experiments. *Nucleic Acids Res*. 2011;39(Suppl 2):W132–8.
- Hackl M, et al. miR-17, miR-19b, miR-20a, and miR-106a are down-regulated in human aging. *Aging Cell*. 2010;9(2):291–6.
- Hafner M, Landthaler M, Burger L, Khorshid M, Hausser J, Berninger P, Rothballer A, Ascano M Jr, Jungkamp A-C, Munschauer M, Ulrich A, Wardle GS, Dewell S, Zavolan M, Tuschl T. Transcriptome-wide identification of RNA-binding protein and microRNA target sites by PAR-CLIP. *Cell*. 2010;141(1):129–41.
- Halawani D, Latterich M. p97: the cell's molecular purgatory? *Mol Cell*. 2006;22(6):713–7.
- Hall AHS, et al. RNA interference using boranophosphate siRNAs: structure–activity relationships. *Nucleic Acids Res*. 2004;32(20):5991–6000.

- Hall B, Limaye A, Kulkarni AB. Overview: generation of gene knockout mice. *Curr Protoc Cell Biol.* 2009;44(1):19.12.1–19.12.17.
- Hansen TB, et al. miRdentity: high stringency miRNA predictor identifies several novel animal miRNAs. *Nucleic Acids Res.* 2014;42(16):e124.
- Hara T, Nakamura K, Matsui M, Yamamoto A, Nakahara Y, Suzuki-Migishima R, Yokoyama M, Mishima K, Saito I, Okano H, Mizushima N. Suppression of basal autophagy in neural cells causes neurodegenerative disease in mice. *Nature.* 2006;441(7095):885–9.
- Haraguchi T, Ozaki Y, Iba H. Vectors expressing efficient RNA decoys achieve the long-term suppression of specific microRNA activity in mammalian cells. *Nucleic Acids Res.* 2009;37(6):e43.
- Hardy J, Selkoe DJ. The amyloid hypothesis of Alzheimer's disease: progress and problems on the road to therapeutics. *Science.* 2002;297(5580):353–6.
- Harris H, Rubinsztein DC. Control of autophagy as a therapy for neurodegenerative disease. *Nat Rev Neurol.* 2012;8(2):108–17.
- Hars ES, et al. Autophagy regulates ageing in *C. elegans*. *Autophagy.* 2007;3(2):93–5.
- Hausser J, et al. Analysis of CDS-located miRNA target sites suggests that they can effectively inhibit translation. *Genome Res.* 2013;23(4):604–15.
- He M. miRNA tagging and affinity-purification (miRAP). *Bio Protoc.* 2012;2(19):e265.
- He X, et al. Basic and clinical application of adeno-associated virus-mediated genome editing. *Hum Gene Ther.* 2018;30(6):673–81.
- Helwak A, Tollervey D. Mapping the miRNA interactome by cross-linking ligation and sequencing of hybrids (CLASH). *Nat Protoc.* 2014;9(3):711–28.
- Hoareau-Aveilla C, Valentin T, Daugrois C, Quelen C, Mitou G, Quentin S, Jia J, Spicuglia S, Ferrier P, Ceccon M, Giuriato S, Gambacorti-Passerini C, Brousset P, Lamant L, Meggetto F. Reversal of microRNA-150 silencing disadvantages crizotinib-resistant NPM-ALK(+) cell growth. *J Clin Invest.* 2015;125(9):3505–18.
- Huang H, et al. Transduction with lentiviral vectors altered the expression profile of host microRNAs. *J Virol.* 2018;92(18):e00503–18.
- Huang JA-O, et al. The microRNAs miR-204 and miR-211 maintain joint homeostasis and protect against osteoarthritis progression. *Nat Commun.* 2019;10(1):2876.
- Hutter K, et al. SAFB2 enables the processing of suboptimal stem-loop structures in clustered primary miRNA transcripts. *Mol Cell.* 2020;78(5):876–89.
- Ibáñez P, et al. Mutational analysis of the PINK1 gene in early-onset parkinsonism in Europe and North Africa. *Brain.* 2006;129(3):686–94.
- Ibáñez-Ventoso C, et al. Modulated microRNA expression during adult lifespan in *Caenorhabditis elegans*. *Aging Cell.* 2006;5(3):235–46.
- Indra AK, et al. Temporally-controlled site-specific mutagenesis in the basal layer of the epidermis: comparison of the recombinase activity of the tamoxifen-inducible Cre-ERT and Cre-ERT2 recombinases. *Nucleic Acids Res.* 1999;27(22):4324–7.
- Inukai S, de Lencastre A, Turner M, Slack F. Novel microRNAs differentially expressed during aging in the mouse brain. *PLoS One.* 2012;7(7):e40028.
- Iovino N, et al. A loxP-containing pol II promoter for RNA interference is reversibly regulated by Cre recombinase. *RNA Biol.* 2005;2(3):86–92.
- Isakov O, et al. Novel insight into the non-coding repertoire through deep sequencing analysis. *Nucleic Acids Res.* 2012;40(11):e86.
- Jack SS, Barbara Ramsay S. Boranophosphates as mimics of natural phosphodiesterases in DNA. *Curr Med Chem.* 2001;8(10):1147–55.
- Jackson AL, et al. Position-specific chemical modification of siRNAs reduces “off-target” transcript silencing. *RNA.* 2006;12(7):1197–205.
- Jankovic MZ, et al. Identification of mutations in the PARK2 gene in Serbian patients with Parkinson's disease. *J Neurol Sci.* 2018;393:27–30.
- Jankowsky JL, Fadale DJ, Anderson J, Xu GM, Gonzales V, Jenkins NA, Copeland NG, Lee MK, Younkin LH, Wagner SL, Younkin SG, Borchelt DR. Mutant presenilins specifically elevate

- the levels of the 42 residue beta-amyloid peptide in vivo: evidence for augmentation of a 42-specific gamma secretase. *Hum Mol Genet.* 2004;13(2):159–70.
- Jeon I, et al. Human-to-mouse prion-like propagation of mutant huntingtin protein. *Acta Neuropathol.* 2016;132(4):677–592.
- Jeong D, et al. miR-25 tough decoy enhances cardiac function in heart failure. *Mol Ther.* 2018;26(3):718–29.
- Jiang X, et al. Targeting hepatic miR-221/222 for therapeutic intervention of nonalcoholic steatohepatitis in mice. *EBioMedicine.* 2018;37:307–21.
- Jin L, Lloyd RV. In situ hybridization: methods and applications. *J Clin Lab Anal.* 1997;11(1):2–9.
- Jin HY, et al. Transfection of microRNA mimics should be used with caution. *Front Genet.* 2015;6:340.
- Jin P, et al. Autophagy-mediated clearance of ubiquitinated mutant huntingtin by graphene oxide. *Nanoscale.* 2016;8(44):18740–50.
- Ju J-S, Fuentealba RA, Miller SE, Jackson E, Piwnicka-Worms D, Baloh RH, Wehl CC. Valosin-containing protein (VCP) is required for autophagy and is disrupted in VCP disease. *J Cell Biol.* 2009;187(6):875–88.
- Kafri T, et al. Lentiviral vectors: regulated gene expression. *Mol Ther.* 2000;1(6):516–21.
- Kakrana A, et al. sPARTA: a parallelized pipeline for integrated analysis of plant miRNA and cleaved mRNA data sets, including new miRNA target-identification software. *Nucleic Acids Res.* 2014;42(18):e139.
- Kametani F, Hasegawa M. Reconsideration of amyloid hypothesis and tau hypothesis in Alzheimer's disease. *Front Neurosci.* 2018;12:25.
- Kawasaki AM, et al. Uniformly modified 2'-deoxy-2'-fluoro-phosphorothioate oligonucleotides as nuclease-resistant antisense compounds with high affinity and specificity for RNA targets. *J Med Chem.* 1993;36(7):831–41.
- Khalil H, et al. Aging is associated with hypermethylation of autophagy genes in macrophages. *Epigenetics.* 2016;11(5):381–8.
- Kiernan MC, et al. Amyotrophic lateral sclerosis. *Lancet.* 2011;377(9769):942–55.
- Kiffin R, et al. Altered dynamics of the lysosomal receptor for chaperone-mediated autophagy with age. *J Cell Sci.* 2007;120(5):782.
- Kim J, Inoue K, Ishii J, Vanti WB, Voronov SV, Murchison E, Hannon G, Abeliovich A. A MicroRNA feedback circuit in midbrain dopamine neurons. *Science (New York, NY).* 2007;317(5842):1220–4.
- Kim J, Kundu M, Viollet B, Guan K-L. AMPK and mTOR regulate autophagy through direct phosphorylation of Ulk1. *Nat Cell Biol.* 2011;13(2):132–41.
- Kim J, et al. MAGI: a Node.js web service for fast microRNA-Seq analysis in a GPU infrastructure. *Bioinformatics.* 2014;30(19):2826–7.
- Kim J, et al. miR-27a and miR-27b regulate autophagic clearance of damaged mitochondria by targeting PTEN-induced putative kinase 1 (PINK1). *Mol Neurodegener.* 2016a;11(1):1–16.
- Kim M, et al. Mutation in ATG5 reduces autophagy and leads to ataxia with developmental delay. *elife.* 2016b;5:e12245.
- Klein C, et al. PINK1, Parkin, and DJ-1 mutations in Italian patients with early-onset parkinsonism. *Eur J Hum Genet.* 2005;13(9):1086–93.
- Kobayashi T, et al. Dicer-dependent pathways regulate chondrocyte proliferation and differentiation. *Proc Natl Acad Sci U S A.* 2008;105(6):1949–54.
- Komatsu M, Wang QJ, Holstein GR, Friedrich VL Jr, Iwata J-i, Kominami E, Chait BT, Tanaka K, Yue Z. Essential role for autophagy protein Atg7 in the maintenance of axonal homeostasis and the prevention of axonal degeneration. *Proc Natl Acad Sci U S A.* 2007;104(36):14489–94.
- Koo EH, Lansbury PT Jr, Kelly JW. Amyloid diseases: abnormal protein aggregation in neurodegeneration. *Proc Natl Acad Sci U S A.* 1999;96(18):9989–90.
- Kouprina N, et al. A new generation of human artificial chromosomes for functional genomics and gene therapy. *Cell Mol Life Sci.* 2013;70(7):1135–48.

- Krasniak CS, Ahmad ST. The role of CHMP2B (Intron5) in autophagy and frontotemporal dementia. *Brain Res.* 2016;1649:151–7.
- Krek A, et al. Combinatorial microRNA target predictions. *Nat Genet.* 2005;37(5):495–500.
- Krismer F, et al. Intact olfaction in a mouse model of multiple system atrophy. *PLoS One.* 2013;8(5):e64625.
- Krützfeldt J, Rajewsky N, Braich R, Rajeev KG, Tuschl T, Manoharan M, Stoffel M. Silencing of microRNAs in vivo with ‘antagomirs’. *Nature.* 2005;438(7068):685–9.
- Krützfeldt J, et al. Specificity, duplex degradation and subcellular localization of antagomirs. *Nucleic Acids Res.* 2007;35(9):2885–92.
- Kuenne C, et al. MIRPIPE: quantification of microRNAs in niche model organisms. *Bioinformatics.* 2014;30(23):3412–3.
- Kuhn DE, et al. Experimental validation of miRNA targets. *Methods.* 2008;44(1):47–54.
- Kuhn DE, Nuovo GJ, Terry AV Jr, Martin MM, Malana GE, Sansom SE, Pleister AP, Beck WD, Head E, Feldman DS, Elton TS. Chromosome 21-derived microRNAs provide an etiological basis for aberrant protein expression in human down syndrome brains. *J Biol Chem.* 2013;288(6):4228.
- Kuhnert F, Mancuso MR, Hampton J, Stankunas K, Asano T, Chen C-Z, Kuo CJ. Attribution of vascular phenotypes of the murine *Egfl7* locus to the microRNA miR-126. *Development.* 2008;135(24):3989–93.
- Lai Q, et al. Chapter 8—Roles of microRNAs in Parkinson’s and other neurodegenerative diseases. In: Mallick B, editor. *AGO-driven non-coding RNAs.* San Diego: Academic; 2019. p. 209–32.
- Lal A, et al. miR-24 inhibits cell proliferation by targeting E2F2, MYC, and other cell-cycle genes via binding to “seedless” 3’UTR microRNA recognition elements. *Mol Cell.* 2009;35(5):610–25.
- Landgraf P, Rusu M, Sheridan R, Sewer A, Iovino N, Aravin A, Pfeffer S, Rice A, Kamphorst AO, Landthaler M, Lin C, Socci ND, Hermida L, Fulci V, Chiaretti S, Foà R, Schliwka J, Fuchs U, Novosel A, Müller R-U, Schermer B, Bissels U, Inman J, Phan Q, Chien M, Weir DB, Choksi R, De Vita G, Frezzetti D, Trompeter H-I, Hornung V, Teng G, Hartmann G, Palkovits M, Di Lauro R, Wernet P, Macino G, Rogler CE, Nagle JW, Ju J, Papavasiliou FN, Benzing T, Lichter P, Tam W, Brownstein MJ, Bosio A, Borkhardt A, Russo JJ, Sander C, Zavolan M, Tuschl T. A mammalian microRNA expression atlas based on small RNA library sequencing. *Cell.* 2007;129(7):1401–14.
- Lee JA, Gao FB. Inhibition of autophagy induction delays neuronal cell loss caused by dysfunctional ESCRT-III in frontotemporal dementia. *J Neurosci.* 2009;29(26):8506–11.
- Lee Y, et al. The nuclear RNase III Droscha initiates microRNA processing. *Nature.* 2003;425(6956):415–9.
- Lee Y, et al. MicroRNA genes are transcribed by RNA polymerase II. *EMBO J.* 2004;23(20):4051–60.
- Lee S-T, et al. MiR-206 regulates brain-derived neurotrophic factor in Alzheimer disease model. *Ann Neurol.* 2012;72(2):269–77.
- Lei J, Sun Y. miR-PREFeR: an accurate, fast and easy-to-use plant miRNA prediction tool using small RNA-Seq data. *Bioinformatics.* 2014;30(19):2837–9.
- Lewandoski M. Conditional control of gene expression in the mouse. *Nat Rev Genet.* 2001;2(10):743–55.
- Lewis BP, Shih I-h, Jones-Rhoades MW, Bartel DP, Burge CB. The microRNA.org resource: targets and expression. *Cell.* 2003;115(7):787–98.
- Lewis BP, Burge CB, Bartel DP. Conserved seed pairing, often flanked by adenosines, indicates that thousands of human genes are microRNA targets. *Cell.* 2005;120(1):15–20.
- Lewis MA, Quint E, Glazier AM, Fuchs H, De Angelis MH, Langford C, van Dongen S, Abreu-Goodger C, Piipari M, Redshaw N, Dalmay T, Moreno-Pelayo MA, Enright AJ, Steel KP. An ENU-induced mutation of miR-96 associated with progressive hearing loss in mice. *Nat Genet.* 2009;41(5):614–8.
- Li W, Ruan K. MicroRNA detection by microarray. *Anal Bioanal Chem.* 2009;394(4):1117–24.
- Li C, et al. Downregulation of microRNA-193b-3p promotes autophagy and cell survival by targeting TSC1/mTOR signaling in NSC-34 cells. *Front Mol Neurosci.* 2017a;10:160.

- Li N, et al. Plasma levels of miR-137 and miR-124 are associated with Parkinson's disease but not with Parkinson's disease with depression. *Neurol Sci.* 2017b;38(5):761–7.
- Li Y-H, et al. The E3 ligase for metastasis associated 1 protein, TRIM25, is targeted by microRNA-873 in hepatocellular carcinoma. *Exp Cell Res.* 2018a;368(1):37–41.
- Li H, et al. FTO is involved in Alzheimer's disease by targeting TSC1-mTOR-Tau signaling. *Biochem Biophys Res Commun.* 2018b;498(1):234–9.
- Lim LP, et al. Microarray analysis shows that some microRNAs downregulate large numbers of target mRNAs. *Nature.* 2005;433(7027):769–73.
- Ling H, Calin GA. Chapter 25—The role of microRNAs and ultraconserved non-coding RNAs in cancer. In: Dellaire G, Berman JN, Arceci RJ, editors. *Cancer genomics.* Boston: Academic; 2014. p. 435–47.
- Liu W, Wang X. Prediction of functional microRNA targets by integrative modeling of microRNA binding and target expression data. *Genome Biol.* 2019;20(1):18.
- Liu L, Feng D, Chen G, Chen M, Zheng Q, Song P, Ma Q, Zhu C, Wang R, Qi W, Huang L, Xue P, Li B, Wang X, Jin H, Wang J, Yang F, Liu P, Zhu Y, Sui S, Chen Q. Mitochondrial outer-membrane protein FUNDC1 mediates hypoxia-induced mitophagy in mammalian cells. *Nat Cell Biol.* 2012a;14(2):177–85.
- Liu C, et al. MirSNP, a database of polymorphisms altering miRNA target sites, identifies miRNA-related SNPs in GWAS SNPs and eQTLs. *BMC Genomics.* 2012b;13(1):661.
- Londin E, et al. Analysis of 13 cell types reveals evidence for the expression of numerous novel primate- and tissue-specific microRNAs. *Proc Natl Acad Sci U S A.* 2015;112(10):E1106–15.
- Loureiro A, da Silva GJ. CRISPR-Cas: converting a bacterial defence mechanism into a state-of-the-art genetic manipulation tool. *Antibiotics (Basel).* 2019;8(1):18.
- Lu TX, Rothenberg ME. MicroRNA. *J Allergy Clin Immunol.* 2018;141(4):1202–7.
- Lu T-P, et al. miRSystem: an integrated system for characterizing enriched functions and pathways of microRNA targets. *PLoS One.* 2012;7(8):e42390.
- Lujan H, et al. Synthesis and characterization of nanometer-sized liposomes for encapsulation and microRNA transfer to breast cancer cells. *Int J Nanomedicine.* 2019;14:5159–73.
- Luo X, et al. PolyA RT-PCR-based quantification of microRNA by using universal TaqMan probe. *Biotechnol Lett.* 2012;34(4):627–33.
- Ma H, Zhang J, Wu H. Designing Ago2-specific siRNA/shRNA to avoid competition with endogenous miRNAs. *Mol Ther Nucleic Acids.* 2014;3:e176.
- Maes OC, et al. Murine microRNAs implicated in liver functions and aging process. *Mech Ageing Dev.* 2008;129(9):534–41.
- Maes OC, Sarojini H, Wang E. Stepwise up-regulation of MicroRNA expression levels from replicating to reversible and irreversible growth arrest states in WI-38 human fibroblasts. *J Cell Physiol.* 2009;221(1):109–19.
- Majlessi M, Nelson NC, Becker MM. Advantages of 2'-O-methyl oligoribonucleotide probes for detecting RNA targets. *Nucleic Acids Res.* 1998;26(9):2224–9.
- Manoharan M. 2'-Carbohydrate modifications in antisense oligonucleotide therapy: importance of conformation, configuration and conjugation. *Biochim Biophys Acta Gene Struct Express.* 1999;1489(1):117–30.
- Marone M, et al. Semiquantitative RT-PCR analysis to assess the expression levels of multiple transcripts from the same sample. *Biol Procedures online.* 2001;3(1):19–25.
- Martin MM, Lee EJ, Buckenberger JA, Schmittgen TD, Elton TS. MicroRNA-155 regulates human angiotensin II type 1 receptor expression in fibroblasts. *J Biol Chem.* 2013;288(6):4226.
- Martin DD, et al. Autophagy in Huntington disease and huntingtin in autophagy. *Trends Neurosci.* 2015;38(1):26–35.
- Martinez-Vicente M, Talloccy Z, Wong E, Tang G, Koga H, Kaushik S, de Vries R, Arias E, Harris S, Sulzer D, Cuervo AM. Cargo recognition failure is responsible for inefficient autophagy in Huntington's disease. *Nat Neurosci.* 2010;13(5):567–76.
- Mathelier A, Carbone A. MIRENA: finding microRNAs with high accuracy and no learning at genome scale and from deep sequencing data. *Bioinformatics.* 2010;26(18):2226–34.

- Maurin T, et al. RNase III-independent microRNA biogenesis in mammalian cells. *RNA*. 2012;18(12):2166–73.
- McLaughlin J, et al. Sustained suppression of Bcr-Abl-driven lymphoid leukemia by microRNA mimics. *Proc Natl Acad Sci*. 2007;104(51):20501–6.
- Medina PP, Nolde M, Slack FJ. OncomiR addiction in an in vivo model of microRNA-21-induced pre-B-cell lymphoma. *Nature*. 2010;467(7311):86–90.
- Meyer SU, Pfaffl MW, Ulbrich SE. Normalization strategies for microRNA profiling experiments: a ‘normal’ way to a hidden layer of complexity? *Biotechnol Lett*. 2010;32(12):1777–88.
- Mimura S, et al. Profile of microRNAs associated with aging in rat liver. *Int J Mol Med*. 2014;34(4):1065–72.
- Missirlis PI, Smailus DE, Holt RA. A high-throughput screen identifying sequence and promiscuity characteristics of the loxP spacer region in Cre-mediated recombination. *BMC Genomics*. 2006;7(1):73.
- Mitsumura TA-O, et al. Ablation of miR-146b in mice causes hematopoietic malignancy. *Blood Adv*. 2018;2(23):3483–91.
- Miyagishi M, Taira K. U6 promoter-driven siRNAs with four uridine 3’ overhangs efficiently suppress targeted gene expression in mammalian cells. *Nat Biotechnol*. 2002;20(5):497–500.
- Mong EF, et al. Chromosome 19 microRNA cluster enhances cell reprogramming by inhibiting epithelial-to-mesenchymal transition. *Sci Rep*. 2020;10(1):3029.
- Mook OR, Baas F, de Wissel MB, Fluiter K. Evaluation of locked nucleic acid-modified small interfering RNA in vitro and in vivo. *Mol Cancer Ther*. 2007;6(3):833–43.
- Mori MA, Raghavan P, Thomou T, Boucher J, Robida-Stubbs S, Macotela Y, Russell SJ, Kirkland JL, Blackwell TK, Kahn CR. Role of microRNA processing in adipose tissue in stress defense and longevity. *Cell Metab*. 2012;16(3):336–47.
- Mourelatos Z. The seeds of silence. *Nature*. 2008;455(7209):44–5.
- Muller H, Marzi MJ, Nicassio F. IsomiRage: from functional classification to differential expression of miRNA isoforms. *Front Bioeng Biotechnol*. 2014;2:38.
- Mun B, et al. Efficient self-assembled microRNA delivery system consisting of cholesterol-conjugated microRNA and PEGylated polycationic polymer for tumor treatment. *ACS Appl Bio Mater*. 2019;2(5):2219–28.
- Neumann M, Sampathu DM, Kwong LK, Truax AC, Micsenyi MC, Chou TT, Bruce J, Schuck T, Grossman M, Clark CM, McCluskey LF, Miller BL, Masliah E, Mackenzie IR, Feldman H, Feiden W, Kretzschmar HA, Trojanowski JQ, Lee VM. Ubiquitinated TDP-43 in frontotemporal lobar degeneration and amyotrophic lateral sclerosis. *Science*. 2006;314(5796):130–3.
- Nicklin Stuart A, et al. Analysis of cell-specific promoters for viral gene therapy targeted at the vascular endothelium. *Hypertension*. 2001;38(1):65–70.
- Nielsen BS. MicroRNA in situ hybridization. In: Fan J-B, editor. *Next-generation microRNA expression profiling technology: methods and protocols*. Totowa: Humana Press; 2012. p. 67–84.
- Nielsen TT, et al. Neuron-specific RNA interference using lentiviral vectors. *J Gene Med*. 2009;11(7):559–69.
- Nilsson P, et al. A β secretion and plaque formation depend on autophagy. *Cell Rep*. 2013;5(1):61–9.
- Nixon RA. Autophagy, amyloidogenesis and Alzheimer disease. *J Cell Sci*. 2007;120(23):4081–91.
- Nixon RA. The role of autophagy in neurodegenerative disease. *Nat Med*. 2013;19(8):983–97.
- Noirot C, et al. LeARN: a platform for detecting, clustering and annotating non-coding RNAs. *BMC Bioinformatics*. 2008;9(1):21.
- Nonaka T, Masuda-Suzukake M, Arai T, Hasegawa Y, Akatsu H, Obi T, Yoshida M, Murayama S, Mann DMA, Akiyama H, Hasegawa M. Prion-like properties of pathological TDP-43 aggregates from diseased brains. *Cell Rep*. 2013;4(1):124–34.
- Noren Hooten N, et al. microRNA expression patterns reveal differential expression of target genes with age. *PLoS One*. 2010;5(5):e10724.
- Noren Hooten N, et al. Age-related changes in microRNA levels in serum. *Aging*. 2013;5(10):725–40.

- Nunez-Iglesias J, et al. Joint genome-wide profiling of miRNA and mRNA expression in Alzheimer's disease cortex reveals altered miRNA regulation. *PLoS One*. 2010;5(2):e8898.
- Oak N, et al. Framework for microRNA variant annotation and prioritization using human population and disease datasets. *Hum Mutat*. 2019;40(1):73–89.
- Ochaba J, et al. Potential function for the Huntingtin protein as a scaffold for selective autophagy. *Proc Natl Acad Sci U S A*. 2014;111(47):16889–94.
- Okamura K, et al. The mirtron pathway generates microRNA-class regulatory RNAs in *Drosophila*. *Cell*. 2007;130(1):89–100.
- Orr ME, Sullivan AC, Frost B. A brief overview of tauopathy: causes, consequences, and therapeutic strategies. *Trends Pharmacol Sci*. 2017;38(7):637–48.
- Paddison PJ, Caudy AA, Bernstein E, Hannon GJ, Conklin DS. Short hairpin RNAs (shRNAs) induce sequence-specific silencing in mammalian cells. *Genes Dev*. 2002;16(8):948–58.
- Pallan PS, et al. Unexpected origins of the enhanced pairing affinity of 2'-fluoro-modified RNA. *Nucleic Acids Res*. 2010;39(8):3482–95.
- Pandolfini L, et al. METTL1 promotes let-7 microRNA processing via m7G methylation. *Mol Cell*. 2019;74(6):1278–90.
- Pantano L, Estivill X, Martí E. SeqBuster, a bioinformatic tool for the processing and analysis of small RNAs datasets, reveals ubiquitous miRNA modifications in human embryonic cells. *Nucleic Acids Res*. 2009;38(5):e34.
- Park J-S, et al. Comparative nucleic acid transfection efficacy in primary hepatocytes for gene silencing and functional studies. *BMC Res Notes*. 2011;4(1):8.
- Parker R, Song H. The enzymes and control of eukaryotic mRNA turnover. *Nat Struct Mol Biol*. 2004;11(2):121–7.
- Pattanayak S, et al. Chapter 4—Combinatorial control of gene function with wavelength-selective caged morpholinos. In: Deiters A, editor. *Methods in enzymology*. Academic; 2019. p. 69–88.
- Peltier HJ, Latham GJ. Normalization of microRNA expression levels in quantitative RT-PCR assays: identification of suitable reference RNA targets in normal and cancerous human solid tissues. *RNA (New York, NY)*. 2008;14(5):844–52.
- Petersén A, Larsen KE, Behr GG, Romero N, Przedborski S, Brundin P, Sulzer D. Expanded CAG repeats in exon 1 of the Huntington's disease gene stimulate dopamine-mediated striatal neuron autophagy and degeneration. *Hum Mol Genet*. 2001;10(12):1243–54.
- Piatek MJ, Werner A. Endogenous siRNAs: regulators of internal affairs. *Biochem Soc Trans*. 2014;42(4):1174–9.
- Pichard V, et al. Specific micro RNA-regulated TetR-KRAB transcriptional control of transgene expression in viral vector-transduced cells. *PLoS One*. 2012;7(12):e51952.
- Piovan C, et al. Generation of mouse lines conditionally over-expressing microRNA using the Rosa26-Lox-Stop-Lox system. In: Singh SR, Coppola V, editors. *Mouse genetics: methods and protocols*. New York: Springer; 2014. p. 203–24.
- Pircs K, et al. Huntingtin aggregation impairs autophagy, leading to argonaute-2 accumulation and global microRNA dysregulation. *Cell Rep*. 2018;24(6):1397–406.
- Platt RJ, et al. CRISPR-Cas9 knockin mice for genome editing and cancer modeling. *Cell*. 2014;159(2):440–55.
- Pluta K, et al. Lentiviral vectors encoding tetracycline-dependent repressors and transactivators for reversible knockdown of gene expression: a comparative study. *BMC Biotechnol*. 2007;7(1):41.
- Poehler A-M, et al. Autophagy modulates SNCA/ α -synuclein release, thereby generating a hostile microenvironment. *Autophagy*. 2014;10(12):2171–92.
- Poursadegh Zonouzi AA, Shekari M, Nejatizadeh A, Shakerizadeh S, Fardmanesh H, Poursadegh Zonouzi A, Rahmati-Yamchi M, Tozhi M. Impaired expression of Drosha in breast cancer. *Breast Dis*. 2017;37(2):55–62.
- Prakash TP, et al. Positional effect of chemical modifications on short interference RNA activity in mammalian cells. *J Med Chem*. 2005;48(13):4247–53.
- Prosser HM, et al. A resource of vectors and ES cells for targeted deletion of microRNAs in mice. *Nat Biotechnol*. 2011;29(9):840–5.

- Pukaš K, Richter-Landsberg C. Inhibition of UCH-L1 in oligodendroglial cells results in microtubule stabilization and prevents α -synuclein aggregate formation by activating the autophagic pathway: implications for multiple system atrophy. *Front Cell Neurosci.* 2015;9:163.
- Qadota H, et al. Establishment of a tissue-specific RNAi system in *C. elegans*. *Gene.* 2007;400(1):166–73.
- Qi LS, et al. Repurposing CRISPR as an RNA-guided platform for sequence-specific control of gene expression. *Cell.* 2013;152(5):1173–83.
- Qian K, et al. miRSeqNovel: an R based workflow for analyzing miRNA sequencing data. *Mol Cell Probes.* 2012;26(5):208–11.
- Qibin L, Jiang W. MIREAP: microRNA discovery by deep sequencing. 2008.
- Rabinowitz JD, White E. Autophagy and metabolism. *Science.* 2010;330(6009):1344–8.
- Ramkissoon SH, Mainwaring LA, Sloand EM, Young NS, Kajigaya S. Nonisotopic detection of microRNA using digoxigenin labeled RNA probes. *Mol Cell Probes.* 2006;20(1):1–4.
- Ran FA, et al. In vivo genome editing using *Staphylococcus aureus* Cas9. *Nature.* 2015;520(7546):186–91.
- Rand TA, et al. Argonaute2 cleaves the anti-guide strand of siRNA during RISC activation. *Cell.* 2005;123(4):621–9.
- Ravi A, et al. Proliferation and tumorigenesis of a murine sarcoma cell line in the absence of DICER1. *Cancer Cell.* 2012;21(6):848–55.
- Ravikumar B, Duden R, Rubinsztein DC. Aggregate-prone proteins with polyglutamine and polyalanine expansions are degraded by autophagy. *Hum Mol Genet.* 2002;11(9):1107–17.
- Raymond CK, Roberts BS, Garrett-Engele P, Lim LP, Johnson JM. Simple, quantitative primer-extension PCR assay for direct monitoring of microRNAs and short-interfering RNAs. *RNA.* 2005;11(11):1737–44.
- Rettig GR, Behlke MA. Progress toward in vivo use of siRNAs-II. *Mol Ther.* 2012;20(3):483–512.
- Rocha EM, De Miranda B, Sanders LH. Alpha-synuclein: pathology, mitochondrial dysfunction and neuroinflammation in Parkinson's disease. *Neurobiol Dis.* 2018;109:249–57.
- Ronen R, et al. miRNAkey: a software for microRNA deep sequencing analysis. *Bioinformatics.* 2010;26(20):2615–6.
- Rubinsztein DC, Mariño G, Kroemer G. Autophagy and aging. *Cell.* 2011;146(5):682–95.
- Ruby JG, Jan CH, Bartel DP. Intronic microRNA precursors that bypass Drosha processing. *Nature.* 2007;448(7149):83–6.
- Rueda A, et al. sRNAToolbox: an integrated collection of small RNA research tools. *Nucleic Acids Res.* 2015;43(W1):W467–73.
- Rui YN, et al. Huntingtin functions as a scaffold for selective macroautophagy. *Nat Cell Biol.* 2015;17(3):262–75.
- Ruimeng L, Jin Z, Yan L. PINK1/Parkin-mediated mitochondrial autophagy. *Chin J Biochem Mol Biol.* 2019;35(10):1072–9.
- Russell DW, Miller AD, Alexander IE. Adeno-associated virus vectors preferentially transduce cells in S phase. *Proc Natl Acad Sci.* 1994;91(19):8915–9.
- Sabatini DM. Twenty-five years of mTOR: uncovering the link from nutrients to growth. *Proc Natl Acad Sci.* 2017;114(45):11818–25.
- Sablok G, et al. isomiRex: web-based identification of microRNAs, isomiR variations and differential expression using next-generation sequencing datasets. *FEBS Lett.* 2013;587(16):2629–34.
- Sala Frigerio C, et al. Reduced expression of hsa-miR-27a-3p in CSF of patients with Alzheimer disease. *Neurology.* 2013;81(24):2103–6.
- Salminen A, Kaamiranta K, Kauppinen A, Ojala J, Haapasalo A, Soininen H, Hiltunen M. Impaired autophagy and APP processing in Alzheimer's disease: the potential role of Beclin 1 interactome. *Prog Neurobiol.* 2013;106:33–54.
- Sanders DW, et al. Distinct tau prion strains propagate in cells and mice and define different tauopathies. *Neuron.* 2014;82(6):1271–88.
- Sandoval H, Thiagarajan P, Dasgupta SK, Schumacher A, Prchal JT, Chen M, Wang J. Essential role for Nix in autophagic maturation of erythroid cells. *Nature.* 2008;454(7201):232–5.

- Santulli G. MicroRNAs and endothelial (dys) function. *J Cell Physiol.* 2016;231(8):1638–44.
- Schena M, Shalon D, Davis RW, Brown PO. Quantitative monitoring of gene expression patterns with a complementary DNA microarray. *Science.* 1995;270(5235):467–70.
- Schrott G. microRNAs at the synapse. *Nat Rev Neurosci.* 2009;10(12):842–9.
- Schwarz L, et al. Involvement of macroautophagy in multiple system atrophy and protein aggregate formation in oligodendrocytes. *J Mol Neurosci.* 2012;47(2):256–66.
- Schweers RL, Zhang J, Randall MS, Loyd MR, Li W, Dorsey FC, Kundu M, Opferman JT, Cleveland JL, Miller JL, Ney PA. NIX is required for programmed mitochondrial clearance during reticulocyte maturation. *Proc Natl Acad Sci U S A.* 2007;104(49):19500–5.
- Schwenk F, Baron U, Rajewsky K. A cre-transgenic mouse strain for the ubiquitous deletion of loxP-flanked gene segments including deletion in germ cells. *Nucleic Acids Res.* 1995;23(24):5080.
- Shah SZA, et al. Regulation of microRNAs-mediated autophagic flux: a new regulatory avenue for neurodegenerative diseases with focus on prion diseases. *Front Aging Neurosci.* 2018;10:139.
- Shan G, Li Y, Zhang J, Li W, Szulwach KE, Duan R, Faghihi MA, Khalil AM, Lu L, Paroo Z, Chan AWS, Shi Z, Liu Q, Wahlestedt C, He C, Jin P. A small molecule enhances RNA interference and promotes microRNA processing. *Nat Biotechnol.* 2008;26(8):933–40.
- Shang R, et al. Genomic clustering facilitates nuclear processing of suboptimal pri-miRNA loci. *Mol Cell.* 2020;78(2):303–16.
- Sharbati-Tehrani S, et al. miR-Q: a novel quantitative RT-PCR approach for the expression profiling of small RNA molecules such as miRNAs in a complex sample. *BMC Mol Biol.* 2008;9(1):34.
- Sheehan D, et al. Biochemical properties of phosphonoacetate and thiophosphonoacetate oligodeoxynucleotides. *Nucleic Acids Res.* 2003;31(14):4109–18.
- Shen WC, et al. Mutations in the ubiquitin-binding domain of OPTN/optineurin interfere with autophagy-mediated degradation of misfolded proteins by a dominant-negative mechanism. *Autophagy.* 2015;11(4):685–700.
- Shi J, et al. mirPro—a novel standalone program for differential expression and variation analysis of miRNAs. *Sci Rep.* 2015;5(1):14617.
- Sinha M, et al. Altered microRNAs in STHdhQ111/HdhQ111 cells: miR-146a targets TBP. *Biochem Biophys Res Commun.* 2010;396(3):742–7.
- Smith-Vikos T, Slack FJ. MicroRNAs and their roles in aging. *J Cell Sci.* 2012;125(1):7–17.
- Sosulski ML, et al. Deregulation of selective autophagy during aging and pulmonary fibrosis: the role of TGFβ1. *Aging Cell.* 2015;14(5):774–83.
- Spilman P, et al. Inhibition of mTOR by rapamycin abolishes cognitive deficits and reduces amyloid-β levels in a mouse model of Alzheimer's disease. *PLoS One.* 2010;5(4):e9979.
- Stangegaard M, Høgh Dufva I, Dufva M. Reverse transcription using random pentadecamer primers increases yield and quality of resulting cDNA. *BioTechniques.* 2006;40(5):649–57.
- Stegmeier F, et al. A lentiviral microRNA-based system for single-copy polymerase II-regulated RNA interference in mammalian cells. *Proc Natl Acad Sci U S A.* 2005;102(37):13212–7.
- Stern P, et al. A system for Cre-regulated RNA interference in vivo. *Proc Natl Acad Sci.* 2008;105(37):13895–900.
- Stocks MB, et al. The UEA sRNA workbench: a suite of tools for analysing and visualizing next generation sequencing microRNA and small RNA datasets. *Bioinformatics.* 2012;28(15):2059–61.
- Stöhr J, Watts JC, Mensinger ZL, Oehler A, Grillo SK, DeArmond SJ, Prusiner SB, Giles K. Purified and synthetic Alzheimer's amyloid beta (Aβ) prions. *Proc Natl Acad Sci U S A.* 2012;109(27):11025–30.
- Sun L, Li J, Xiao X. Overcoming adeno-associated virus vector size limitation through viral DNA heterodimerization. *Nat Med.* 2000;6(5):599–602.
- Sun Y-X, et al. Differential activation of mTOR complex 1 signaling in human brain with mild to severe Alzheimer's disease. *J Alzheimers Dis.* 2014a;38(2):437–44.
- Sun Z, et al. CAP-miRSeq: a comprehensive analysis pipeline for microRNA sequencing data. *BMC Genomics.* 2014b;15(1):423.
- Szulc J, et al. A versatile tool for conditional gene expression and knockdown. *Nat Methods.* 2006;3(2):109–16.

- Taft RJ, Glazov EA, Lassmann T, Hayashizaki Y, Carninci P, Mattick JS. Small RNAs derived from snoRNAs. *RNA*. 2009;15(7):1233–40.
- Tagawa H, et al. Synergistic action of the microRNA-17 polycistron and Myc in aggressive cancer development. *Cancer Sci*. 2007;98(9):1482–90.
- Takahashi H, et al. Comprehensive MRI quantification of the substantia nigra pars compacta in Parkinson's disease. *Eur J Radiol*. 2018;109:48–56.
- Tanenbaum ME, et al. A protein-tagging system for signal amplification in gene expression and fluorescence imaging. *Cell*. 2014;159(3):635–46.
- Tanji K, et al. Alteration of autophagosomal proteins in the brain of multiple system atrophy. *Neurobiol Dis*. 2013;49:190–8.
- Teyssou E, et al. Mutations in SQSTM1 encoding p62 in amyotrophic lateral sclerosis: genetics and neuropathology. *Acta Neuropathol*. 2013;125(4):511–22.
- Tian Y, Bustos V, Flajolet M, Greengard P. A small-molecule enhancer of autophagy decreases levels of Abeta and APP-CTF via Atg5-dependent autophagy pathway. *FASEB J*. 2011;6:1934–42.
- Tolosa E, et al. MicroRNA alterations in iPSC-derived dopaminergic neurons from Parkinson disease patients. *Neurobiol Aging*. 2018;69:283–91.
- Trayhurn P. Northern blotting. *Proc Nutr Soc*. 1996;55(1B):583–9.
- Tuschl T. Expanding small RNA interference. *Nat Biotechnol*. 2002;20(5):446–8.
- Tyler DM, Okamura K, Chung W-J, Hagen JW, Berezikov E, Hannon GJ, Lai EC. Functionally distinct regulatory RNAs generated by bidirectional transcription and processing of microRNA loci. *Genes Dev*. 2008;22(1):26–36.
- Tysnes OB, Storstein A. Epidemiology of Parkinson's disease. *J Neural Transm (Vienna)*. 2017;124(8):901–5.
- Uddin MS, Al Mamun A, Labu ZK, Hidalgo-Lanussa O, Barreto GE, Ashraf GM. Autophagic dysfunction in Alzheimer's disease: cellular and molecular mechanistic approaches to halt Alzheimer's pathogenesis. *J Cell Physiol*. 2019;234(6):8094–112.
- Valente EM, Abou-Sleiman PM, Caputo V, Muqit MMK, Harvey K, Gispert S, Ali Z, Del Turco D, Bentivoglio AR, Healy DG, Albanese A, Nussbaum R, González-Maldonado R, Deller T, Salvi S, Cortelli P, Gilks WP, Latchman DS, Harvey RJ, Dallapiccola B, Auburger G, Wood NW. Hereditary early-onset Parkinson's disease caused by mutations in PINK1. *Science*. 2004a;304(5674):1158–60.
- Valente EM, Salvi S, Ialongo T, Marongiu R, Elia AE, Caputo V, Romito L, Albanese A, Dallapiccola B, Bentivoglio AR. PINK1 mutations are associated with sporadic early-onset parkinsonism. *Ann Neurol*. 2004b;56(3):336–41.
- Valera E, et al. MicroRNA-101 modulates autophagy and oligodendroglial alpha-synuclein accumulation in multiple system atrophy. *Front Mol Neurosci*. 2017;10:329.
- Válóczi A, Hornyik C, Varga N, Burgyán J, Kauppinen S, Havelda Z. Sensitive and specific detection of microRNAs by northern blot analysis using LNA-modified oligonucleotide probes. *Nucleic Acids Res*. 2004;32(22):e175.
- Vandesompele J, et al. Accurate normalization of real-time quantitative RT-PCR data by geometric averaging of multiple internal control genes. *Genome Biol*. 2002;3(7).
- Vasudevan S. Functional validation of microRNA-target RNA interactions. *Methods*. 2012;58(2):126–34.
- Vella MC, et al. The *C. elegans* microRNA let-7 binds to imperfect let-7 complementary sites from the lin-41 3'UTR. *Genes Dev*. 2004;18(2):132–7.
- Ventura A, Young AG, Winslow MM, Lintault L, Meissner A, Erkland SJ, Newman J, Bronson RT, Crowley D, Stone JR, Jaenisch R, Sharp PA, Jacks T. Targeted deletion reveals essential and overlapping functions of the miR-17 through 92 family of miRNA clusters. *Cell*. 2008;132(5):875–86.
- Verheijen BM, Vermulst M, van Leeuwen FW. Somatic mutations in neurons during aging and neurodegeneration. *Acta Neuropathol*. 2018;135(6):811–26.
- Vinnikov IA-O, et al. Hypothalamic miR-103 protects from hyperphagic obesity in mice. *J Neurosci*. 2014;34(32):10659–74.

- Vinnikov IA, Domanskyi A, Konopka W. Continuous delivery of oligonucleotides into the brain. In: Kye MJ, editor. *MicroRNA technologies*. New York: Springer; 2017. p. 89–117.
- Vitsios DM, Enright AJ. Chimira: analysis of small RNA sequencing data and microRNA modifications. *Bioinformatics*. 2015;31(20):3365–7.
- Voelkerding KV, Dames SA, Durtschi JD. Next-generation sequencing: from basic research to diagnostics. *Clin Chem*. 2009;55(4):641–58.
- Wahlestedt C, et al. Potent and nontoxic antisense oligonucleotides containing locked nucleic acids. *Proc Natl Acad Sci*. 2000;97(10):5633–6638.
- Walczak M, Martens S. Dissecting the role of the Atg12-Atg5-Atg16 complex during autophagosome formation. *Autophagy*. 2013;9(3):424–5.
- Walker FO. Huntington's disease. *Lancet*. 2007;369(9557):218–28.
- Wang X, et al. miR-34a, a microRNA up-regulated in a double transgenic mouse model of Alzheimer's disease, inhibits bcl2 translation. *Brain Res Bull*. 2009a;80(4):268–73.
- Wang W-C, et al. miRExpress: analyzing high-throughput sequencing data for profiling microRNA expression. *BMC Bioinformatics*. 2009b;10(1):328.
- Wang W-X, et al. Patterns of microRNA expression in normal and early Alzheimer's disease human temporal cortex: white matter versus gray matter. *Acta Neuropathol*. 2011;121(2):193–205.
- Wang X, et al. RNA interference of long noncoding RNA HOTAIR suppresses autophagy and promotes apoptosis and sensitivity to cisplatin in oral squamous cell carcinoma. *J Oral Pathol Med*. 2018;47(10):930–7.
- Wang X-W, et al. A microRNA-inducible CRISPR-Cas9 platform serves as a microRNA sensor and cell-type-specific genome regulation tool. *Nat Cell Biol*. 2019;21(4):522–30.
- Webb JL, Ravikumar B, Atkins J, Skepper JN, Rubinsztein DC. Alpha-Synuclein is degraded by both autophagy and the proteasome. *J Biol Chem*. 2003;278(27):25009–13.
- Welborn JP, et al. RhoX8 ablation in the Sertoli cells using a tissue-specific RNAi approach results in impaired male fertility in Mice1. *Biol Reprod*. 2015;93(1):1–14.
- Whitehead KA, et al. Silencing or stimulation? siRNA delivery and the immune system. *Annu Rev Chem Biomol Eng*. 2011;2(1):77–96.
- Williams A, et al. Novel targets for Huntington's disease in an mTOR-independent autophagy pathway. *Nat Chem Biol*. 2008;4(5):295–305.
- Wilson RC, Doudna JA. Molecular mechanisms of RNA interference. *Annu Rev Biophys*. 2013;42:217–39.
- Woerman AL, et al. α -synuclein: multiple system atrophy prions. *Cold Spring Harb Perspect Med*. 2018;8(7):2157–1422.
- Wong YC, Holzbaur EL. Optineurin is an autophagy receptor for damaged mitochondria in parkin-mediated mitophagy that is disrupted by an ALS-linked mutation. *Proc Natl Acad Sci*. 2014;111(42):E4439–48.
- Wong AM, Wang JW, Axel R. Spatial representation of the glomerular map in the *Drosophila* protocerebrum. *Cell*. 2002;109(2):229–41.
- Wong H-KA, Veremeyko T, Patel N, Lemere CA, Walsh DM, Esau C, Vandenburg C, Krichevsky AM. De-repression of FOXO3a death axis by microRNA-132 and -212 causes neuronal apoptosis in Alzheimer's disease. *Hum Mol Genet*. 2013;22(15):3077–92.
- Wong TH, et al. Three VCP mutations in patients with frontotemporal dementia. *J Alzheimers Dis*. 2018;65(4):1139–46.
- Wu Z, Yang H, Colosi P. Effect of genome size on AAV vector packaging. *Mol Ther*. 2010;18(1):80–6.
- Wu D, et al. Dicer-microRNA pathway is critical for peripheral nerve regeneration and functional recovery in vivo and regenerative axonogenesis in vitro. *Exp Neurol*. 2012;233(1):555–65.
- Wu J, et al. mirTools 2.0 for non-coding RNA discovery, profiling, and functional annotation based on high-throughput sequencing. *RNA Biol*. 2013;10(7):1087–92.
- Wu Q, et al. Methylation of miR-129-5p CpG island modulates multi-drug resistance in gastric cancer by targeting ABC transporters. *Oncotarget*. 2014;5(22):11552.

- Wu Q, et al. The protective role of microRNA-200c in Alzheimer's disease pathologies is induced by beta amyloid-triggered endoplasmic reticulum stress. *Front Mol Neurosci*. 2016;9:140.
- Xie M, et al. Mammalian 5'-capped microRNA precursors that generate a single microRNA. *Cell*. 2013;155(7):1568–80.
- Xu R, et al. MicroRNA-1246 regulates the radio-sensitizing effect of curcumin in bladder cancer cells via activating P53. *Int Urol Nephrol*. 2019;51(10):1771–9.
- Yang X, Li L. miRDeep-P: a computational tool for analyzing the microRNA transcriptome in plants. *Bioinformatics*. 2011;27(18):2614–5.
- Yang WJ, Yang DD, Na S, Sandusky GE, Zhang Q, Zhao G. Dicer is required for embryonic angiogenesis during mouse development. *J Biol Chem*. 2005;280(10):9330–5.
- Yang J-S, Maurin T, Robine N, Rasmussen KD, Jeffrey KL, Chandwani R, Papapetrou EP, Sadelain M, O'Carroll D, Lai EC. Conserved vertebrate mir-451 provides a platform for Dicer-independent, Ago2-mediated microRNA biogenesis. *Proc Natl Acad Sci U S A*. 2010;107(34):15163–8.
- Yang J-S, Maurin T, Lai EC. Functional parameters of Dicer-independent microRNA biogenesis. *RNA*. 2012;18(5):945–57.
- Yang J, et al. MiR-34 modulates *Caenorhabditis elegans* lifespan via repressing the autophagy gene *atg9*. *Age*. 2013;35(1):11–22.
- Yang K, et al. isomiR2Function: an integrated workflow for identifying microRNA variants in plants. *Front Plant Sci*. 2017;8:322.
- Yao L, et al. MicroRNA-124 regulates the expression of p62/p38 and promotes autophagy in the inflammatory pathogenesis of Parkinson's disease. *FASEB J*. 2019;33(7):8648–65.
- Ye L, et al. Knockdown of TIGAR by RNA interference induces apoptosis and autophagy in HepG2 hepatocellular carcinoma cells. *Biochem Biophys Res Commun*. 2013;437(2):300–6.
- Yekta S, Shih I-H, Bartel DP. MicroRNA-directed cleavage of HOXB8 mRNA. *Science*. 2004;304(5670):594–6.
- Yin JQ, Zhao RC, Morris KV. Profiling microRNA expression with microarrays. *Trends Biotechnol*. 2008;26(2):70–6.
- Yu WH, et al. Macroautophagy—a novel Beta-amyloid peptide-generating pathway activated in Alzheimer's disease. *J Cell Biol*. 2005;171(1):87–98.
- Yu D, et al. Single-stranded RNAs use RNAi to potently and allele-selectively inhibit mutant huntingtin expression. *Cell*. 2012;150(5):895–908.
- Yu L, et al. miRNA Digger: a comprehensive pipeline for genome-wide novel miRNA mining. *Sci Rep*. 2016;6(1):18901.
- Yu CH, et al. TDP-43 triggers mitochondrial DNA release via mPTP to activate cGAS/STING in ALS. *Cell*. 2020;183(3):636–49.
- Yuan S, et al. Methylation by NSun2 represses the levels and function of microRNA 125b. *Mol Cell Biol*. 2014a;34(19):3630.
- Yuan T, et al. eRNA: a graphic user interface-based tool optimized for large data analysis from high-throughput RNA sequencing. *BMC Genomics*. 2014b;15(1):176.
- Zarrilli F, et al. Peptide nucleic acids as miRNA target protectors for the treatment of cystic fibrosis. *Molecules*. 2017;22(7):1144.
- Zeng Y, Wagner EJ, Cullen BR. Both natural and designed micro RNAs can inhibit the expression of cognate mRNAs when expressed in human cells. *Mol Cell*. 2002;9(6):1327–33.
- Zeng Q, et al. Overexpression of miR-155 promotes the proliferation and invasion of oral squamous carcinoma cells by regulating BCL6/cyclin D2. *Int J Mol Med*. 2016;37(5):1274–80.
- Zhang C, Cuervo AM. Restoration of chaperone-mediated autophagy in aging liver improves cellular maintenance and hepatic function. *Nat Med*. 2008;14(9):959–65.
- Zhang R, Peng Y, Wang W, Su B. Rapid evolution of an X-linked microRNA cluster in primates. *Genome Res*. 2007;17(5):612–7.
- Zhang J, et al. The cell growth suppressor, mir-126, targets IRS-1. *Biochem Biophys Res Commun*. 2008;377(1):136–40.

- Zhang G-L, et al. Suppression of hepatitis B virus replication by microRNA-199a-3p and microRNA-210. *Antivir Res.* 2010;88(2):169–75.
- Zhang Q, Kandic I, Kutryk MJ. Dysregulation of angiogenesis-related microRNAs in endothelial progenitor cells from patients with coronary artery disease. *Biochem Biophys Res Commun.* 2011;405(1):42–6.
- Zhang J, et al. Conditional gene manipulation: cre-ating a new biological era. *J Zhejiang Univ Sci B.* 2012;13(7):511–24.
- Zhang Z, et al. MTide: an integrated tool for the identification of miRNA–target interaction in plants. *Bioinformatics.* 2014;31(2):290–1.
- Zhang Y, et al. CRISPR/gRNA-directed synergistic activation mediator (SAM) induces specific, persistent and robust reactivation of the HIV-1 latent reservoirs. *Sci Rep.* 2015;5(1):16277.
- Zhang Y, et al. MiR-214-3p attenuates cognition defects via the inhibition of autophagy in SAMP8 mouse model of sporadic Alzheimer’s disease. *Neurotoxicology.* 2016a;56:139–49.
- Zhang Y, et al. MiR-299-5p regulates apoptosis through autophagy in neurons and ameliorates cognitive capacity in APPswe/PS1dE9 mice. *Sci Rep.* 2016b;6(1):1–14.
- Zhang Y, et al. DeAnnIso: a tool for online detection and annotation of isomiRs from small RNA sequencing data. *Nucleic Acids Res.* 2016c;44(W1):W166–75.
- Zhao W, et al. wapRNA: a web-based application for the processing of RNA sequences. *Bioinformatics.* 2011;27(21):3076–7.
- Zhou H, Huang C, Xia XG. A tightly regulated Pol III promoter for synthesis of miRNA genes in tandem. *Biochim Biophys Acta.* 2008;1779(11):773–9.
- Zhou H, et al. In vivo simultaneous transcriptional activation of multiple genes in the brain using CRISPR–dCas9-activator transgenic mice. *Nat Neurosci.* 2018;21(3):440–6.
- Zhou H, et al. Glia-to-neuron conversion by CRISPR-CasRx alleviates symptoms of neurological disease in mice. *Cell.* 2020;181(3):590–603.
- Zorc M, et al. Catalog of microRNA seed polymorphisms in vertebrates. *PLoS One.* 2012;7(1):e30737.
- Zovoilis A, et al. microRNA-34c is a novel target to treat dementias. *EMBO J.* 2011;30(20):4299–308.

Chapter 12

Biomarkers of Autophagy



Fang Lin, Yu-Ting Zhu, and Zheng-Hong Qin

Abstract Biomarkers (short for biological markers) are biological measures of a biological state. Autophagy biomarkers play an important role as an indicator of autophagy during normal physiological processes, pathogenic processes or pharmacological responses to drugs. In this chapter, some biomarkers of different types of autophagy, including macroautophagy, selective autophagy, chaperone-mediated autophagy, and microautophagy, as well as the lysosomal biomarkers are introduced. The described biomarkers may be used to detect the level of autophagy in cells or tissues in a dynamic, real-time, and quantitative manner. However, each biomarker has its specific significance and limitation. Therefore, the analysis of the autophagy level in cells or tissues through the detection of autophagy biomarkers should be carried out carefully.

Abbreviations

3-MA	3-Methyladenine
AMP	Adenosine monophosphate
AMPK	5' AMP-activated protein kinase
Atg	Autophagy-related gene
BNIP3	Bcl-2 and adenovirus E1B 19-KDa interacting protein 3
CMA	Chaperone-mediated autophagy
CNS	Central nervous system
DFCP1	Double FYVE-containing protein 1
DRAM1	Damage-regulated autophagy modulator 1
GABARAP	Gamma-aminobutyric acid receptor-associated protein
GFP	Green fluorescent protein
GTP	guanosine triphosphate

F. Lin · Y.-T. Zhu · Z.-H. Qin (✉)
School of Pharmaceutical Science, Soochow University, Suzhou, China
e-mail: linfang-1@suda.edu.cn; qinzhenhong@suda.edu.cn

© Science Press 2021

Z. Xie (ed.), *Autophagy: Biology and Diseases*, Advances in Experimental Medicine and Biology 1208, https://doi.org/10.1007/978-981-16-2830-6_12

MFN1	Mitofusion 1
MFN2	Mitofusion 2
mTOR	mammalian target of rapamycin
PE	Phosphatidylethanolamines
PI3K	Phosphatidylinositol 3-kinase
PtdIns	Phosphatidylinositol
TGN	Trans-Golgi network
VPS	Vacuolar protein sorting
ZFYVE1	Zinc finger FYVE domain-containing protein 1

Autophagy includes several major aspecific degradation routes, such as macroautophagy, microautophagy, chaperone-mediated autophagy, and some types of selective autophagy, such as pexophagy, mitophagy, ferritinophagy, and aggrephagy. In this chapter, contemporarily used biomarkers for macroautophagy, microautophagy, chaperone-mediated autophagy, and mitophagy will be discussed (Galluzzi et al. 2017; Klionsky et al. 2016) (Table 12.1).

Table 12.1 The biomarkers of autophagy

Type	Process	Biomarkers
Macroautophagy	Autophagosome formation	Atg5-Atg12 Atg16L LC3 Atg9 BECN1/Beclin1/Vps30/Atg6 Atg14/Bakor DRAM1 ZFYVE1/DFCP1
	Substrate of macroautophagy	p62
Chaperone-mediated autophagy		LAMP-2a HSC70
		Rab7 Vac8 Atg18 ESCRT(VPS4) HSC70
Lysosome		LAMP-1 LAMP-2

12.1 Biomarkers of Macroautophagy

Macroautophagosomes are sourced from the membrane of the endoplasmic reticulum, the Golgi or from the cell membrane. The sourced membrane forms a cup-like structure and wraps proteins, organs, and other autophagic cargos, subsequently forming a closed double-layer membrane vesicle in the cell, which is named an autophagosome (Mizushima et al. 2002). Next, the autophagosome fuses with the lysosome, and the proteins or organelles in the autophagic body are degraded by lysosomal enzymes. Therefore, the biomarkers of this process include three categories, namely, biomarkers of autophagosomes, biomarkers of lysosomes, and autophagic substrate biomarkers.

12.1.1 Biomarkers of Autophagosomes

Autophagy-related (ATG) proteins are proteins involved in autophagy. Several key Atg proteins can be used as biomarkers of autophagy.

12.1.1.1 Atg5-Atg12

In the classical ubiquitin theory, ubiquitin is produced as a precursor and is subsequently cleaved by specific proteases to expose certain carboxy-terminal glycine residues. The ubiquitin is then activated by the E1 enzyme and transferred to the E2 enzyme via the formation of a thioester bond. After identifying the target protein, E3 ubiquitin ligase transfers the ubiquitin molecule from the E2 enzyme to the target protein via the formation of a connection between the glycine of ubiquitin and a lysine residue of the target protein (Scheffner et al. 1995). Atg12 is the first identified ubiquitin-like Atg protein. Autophagy-associated protein Atg7 is an E1-like activase and Atg10 is an E2 binding enzyme. Atg12 is first activated by Atg7, then transported to Atg10, and then covalently linked to a lysine residue of the substrate protein Atg5 to form a Atg12-Atg5 complex. Substrate-specific E3 ligase is not required in this process. The formation of the Atg12-Atg5 complex is not affected by environmental stress such as nutritional deficiencies. The presence of the Atg12-Atg5 complex is crucial for the formation of autophagosomes. The absence of Atg12-Atg5 will cause defects in autophagy complex (Shao et al. 2007; Hanada and Ohsumi 2005; Mizushima et al. 1998).

Detection method: The Western blotting technique can be used to detect the level of Atg5 and Atg12. The anticipated molecular weight of Atg12 is 15 kD, and appears to be about 19 kD on SDS-PAGE gel. The molecular weight of Atg5 is about

32 kD. The molecular weight of Atg12 is small and quite difficult to detect with Western blot. However, Atg12-connected Atg5 stays bound to Atg12 during the sample preparation process, making the complex of Atg12-Atg5 easier to detect. The Atg12-Atg5 complex is about 55 kD on a SDS-PAGE gel. Both antibodies can be used to detect the complex.

Limitations: In certain mammalian cells, almost all Atg5 and Atg12 are present as part of the complex so the level of atg12-atg5 does not change significantly in the short-term starvation state. In this case, autophagy may be wrongly estimated to be at a low level. However in hepatocytes, human fibroblasts and mouse fibroblasts, assessing the presence of the Atg12-Atg5 complex will give a good indication of the occurrence of autophagy.

12.1.1.2 Atg16L1

The coiled-coil protein Atg16L1 interacts with the Atg12-Atg5 complex, and causes the formation of Atg12-Atg5-Atg16 tetramers by its own oligomerization. These tetramers play a role in the extension of the autophagy precursor membrane. The Atg12-Atg5-Atg16L1 complexes adhere to the surface of the autophagosome. The complex distributes more pronounced in the membrane of the convex, and less in the concave part of the membrane. This means that the Atg12-Atg5-Atg16L1 complex is mainly located on the outside of the membrane of autophagosomes. The complexes are released from the autophagosomal membrane after the structure is completely closed, and redistributes in the cytoplasm. In the meanwhile, Atg8-PE, which is distributed on both sides of the membrane, stays present on the autophagosomal membrane, and is transported to the lysosomes and degraded after fusion with the lysosome (Romanov et al. 2012) (Fig. 12.1). In summary, during the process of membrane transfer, Atg16L1 locates on the early autophagic membrane, but it is not present on the complete autophagic lysosome membrane (Zavodszky et al. 2013). Therefore, Atg16L1 is used to detect the formation of early autophagosomes.

Detection methods: Atg5, Atg12 or Atg16L1 can be detected by immunotransmission electron microscopy and immunohistochemistry staining. Under normal conditions, these endogenous proteins are dispersed in the cytoplasm, but when autophagy is induced by environmental stress such as starvation, a dot-like aggregation or plaques of Atg5, Atg12 or Atg16L1 in cells will be significantly increased. When autophagy is inhibited, this point aggregation of Atg5, Atg12 or Atg16L1 is reduced.

Limitations: if the downstream extension of autophagosomal membrane is inhibited, such as in LC3/GABARAP mutants, the Atg5, Atg12 or Atg16L1 aggregation will be increased. When the fusion between autophagosomes and lysosomes is inhibited or when lysosomes are alkalinized, the dot-like aggregation of Atg5, Atg12 or Atg16L1 will also increase, so it is necessary to design good controls and detect other autophagic substrates for screening as well, depending on the goal of the experiment.

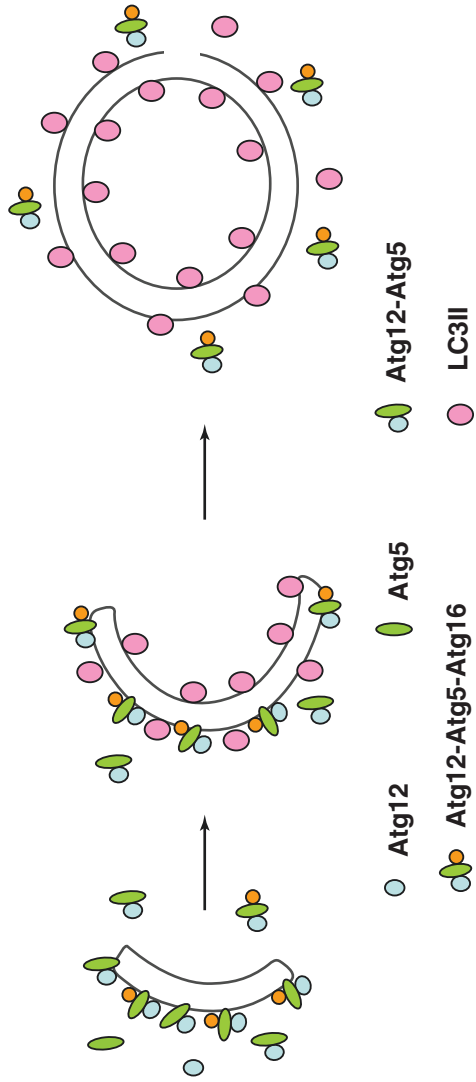


Fig. 12.1 Atg12-Atg5-Atg16L Complex and the formation of autophagosome

12.1.1.3 Atg8/LC3

Atg8/LC3 is the most widely used molecular biomarker in current autophagy research. In yeast, Atg8 is coupled to phosphatidylethanolamine (PE) to form Atg8-PE. In mammalian cells, the analogs of Atg8 are divided into two categories, MAP1LC3/LC3 (Microtubule-associated proteins 1A/1B light chain 3B) and GABARAP (Gamma-aminobutyric acid receptor-associated protein). The category MAP1LC3/LC3 includes the proteins LC3A, LC3B, LC3B2, and LC3C; and the GABARAP group includes the proteins GABARAP, GABARAPL1, and GABARAPL2. The distribution of these subtypes of molecules can differ between cell types. LC3A and LC3B have high homology. Commercial LC3B antibodies can be used to detect both LC3A and LC3B. The background level of GABARAP is usually very low and increases only after autophagy is induced. The occurrence of mitochondrial autophagy induced by NIX/BNIP3L is more dependent on GABARAP than on LC3 protein (Novak et al. 2010). In addition, LC3 is involved in the formation of autophagosomal membrane, and GABARAP is involved in the extension and closure of the membrane (Dancourt and Melia 2014).

LC3-II and LC3-I are two forms of LC-3 that can be transformed into each other. Newly synthesized LC3 in cells is first processed to LC3-I, which is the soluble form that is located in the cytoplasm. Then, after a ubiquitination process, ubiquitinated LC3-I binds to phosphatidylethanolamine (PE) which exists on the surface of the autophagosomal membrane, and forms the membrane bound form LC3-II. The ubiquitination process takes place as follows: Atg4/Atg4B, a cysteine protease, cleaves the carboxyl terminus of Atg8/LC3 at Arg117, which leads to the exposure of Gly116. Gly116 of Atg8 forms a thioester bond with Cys507 of Atg7. Atg7 is an E1-like enzyme that subsequently transfers Atg8 to Atg3 (Noda et al. 2011). Atg3 is an E2-like protein that also binds to Atg8 in the form of a sulfur-ester bond. Finally, Atg8 binds to PE through Gly116 (Yu et al. 2012).

LC3-II, as distributed on the autophagosomal membrane, is a biomarker of autophagosomes. The LC3-II content or LC3-II/LC3-I ratio positively correlates with the number of autophagosomes, and can be used to assess the level of autophagy in cells. Atg8 concentrations can increase tenfold when autophagy is activated in yeast. However, in mammalian cells, sometimes the total increase in LC3 is not significant. For example, when autophagy is activated in human SH-SY5Y cells, the LC3-II level increases a little, but the LC3-I clearly decreases. This phenomenon is associated with high autophagy flow. The reason is that LC3-I is transformed to LC3-II and LC3-II is transferred to the lysosome and degraded.

Detection methods:

1. The Western blot method. After SDS-PAGE electrophoresis, the apparent molecular weight of LC3-I is 18 kD and the apparent molecular weight of LC3-II is 16 kD. Because of coupling with PE, the molecular weight of LC3-II is larger than LC3-I. However, the mobility of LC3-II in SDS-PAGE is faster than that of LC3-I. Levels of LC3 or the ratio of LC3-II/LC3-I can be used as a marker to compare the level of autophagy between different experimental groups.

Limitations: Because LC3 is easily degraded in a lysis buffer with SDS, it is better to perform Western blot experiments within 2 weeks after the samples are prepared. The samples should not be frozen and thawed repeatedly. When transfection experiments with exogenous LC3 are carried out in cultured cells, the transfection heterogeneity should also be considered. If the transfection efficiency is not very high, even if the autophagy level is significantly changed in the transfected cells, the detection results may be covered by other unsuccessfully transfected cells present in the sample. At this point, it is necessary to use immunohistochemical methods for verification.

It has long been thought that if the autophagosome number is high, then the autophagic activity of the cell is also elevated. However, it should be noted that the activation of the autophagy pathway does not only cause an increase in the formation of autophagosomes, but also the degradation of these autophagosomes and their contents. Therefore, when assessing the autophagy flux in cells that are in a pathological state, several aspects should be kept in mind, including: whether the autophagosomes fuse with lysosomes, and whether the degradation of proteins or organelles in autophagosomes really occurs. A strategic use of chemicals that block the process of autophagy in specific stages, may help in determining these aspects. Chemicals that are currently used are lysosomal alkalizers (such as chloroquine and ammonium chloride), lysosomal inhibitors (such as the cysteine protease inhibitor E-64d and the aspartic proteinase inhibitor pepstatin A), and autophagosome and lysosome fusion inhibitors (such as bafilomycin). Incomplete proteolysis, abnormal lysosomal acidification, or slowed autophagy-lysosomal fusion are common in neurons in disease states. Therefore, only the increase of LC3-II is no evidence for the activation of autophagy.

In addition, the LC3-II levels in cell types, sometimes even inside the same tissue, can differ greatly. This can cause difficulties to identify the LC3-II level. For example, in neurons, the level of LC3-II is very low and difficult to detect, and the ratio of LC3-I and LC3-II is extraordinarily high, because LC3-II-positive autophagy bodies are quickly degraded once they are produced. Therefore, LC3-I cannot be ignored because it may provide a more complete picture of the cellular autophagic response.

2. Immunohistochemistry: Immunohistochemistry is widely used to detect LC3, but it should be noted that an increase of the level of autophagy should be evaluated not by the increase of protein staining density in cells, but by the increase of plaque or dot-like staining. The levels of LC3 can be detected in paraffin sections or frozen sections. When autophagy is at a low level, the localization of LC3 in most tissues is dispersed in the cytoplasm. In some tissues, the localization of LC3 is not limited to the cytoplasm and autophagosomes. For example, in liver cells, endogenous LC3 is also present on lipid droplets, when the cells are in a state of starvation. Likewise, in Atg-deficient mouse neurons, LC3 accumulates in ubiquitin/p62-positive aggregates. Therefore, sometimes the punctate aggregation of LC3 is not located on the autophagosome. In general, researchers will connect GFP to LC3 to facilitate the observation of the distribution and level of LC3 in order to value the situation of autophagy in real time. However, it should

be noted that if GFP is attached to the carboxy terminal of LC3, it will be cut off by Atg4, after autophagy is induced, to form GFP independent of LC3. After this procedure, the fluorescence of GFP does not represent LC3 anymore. If the GFP is attached to the amino terminus of LC3, the GFP moiety will not be cut off, and will represent LC3 and autophagy vesicles. Therefore, GFP-LC3 or GFP-Atg8 should be used instead of LC3-GFP or Atg8-GFP when constructing GFP fusion expression genes (Klionsky 2011).

LC3-II is crucial in the autophagy process, so generally LC3-II is a very good marker for autophagosomes, but there are some important aspects that should be paid attention to: (1) Studies also have shown that LC3-II aggregates can also form in the condition of autophagosome deficiency (Runwal et al. 2019). (2) The LC3-II level alone cannot explain the situation of autophagic flow.

12.1.1.4 Atg9

Atg9 is an evolutionarily highly conserved protein, present in eukaryotes, ranging from yeast to mammalian cells. Atg9 is the only transmembrane protein of all the identified Atg proteins so far. Atg9 has six transmembrane domains. Both the N-terminal and the C-terminal domain are exposed to the cytoplasm. In yeast, Atg9 is located on monolayer vesicles of 30–60 nm in diameter, which are derived from the Golgi membrane and that move rapidly around inside the cytoplasm. Under the induction of starvation or after the addition of rapamycin, the expression of Atg9 is up-regulated, and the amount of Atg9 vesicles increases. Available evidences from yeast suggest that Atg9 may be involved in the transport of lipids to form autophagosomes.

Atg9 vesicles have not been shown in mammalian cells, but the co-localization of mammalian Atg9 (mAtg9), the autophagosome marker LC3, and the advanced endosomal protein Rab7 was detected by immunofluorescence. Studies have shown that mAtg9 is necessary for the formation of DFCP1-positive autophagic precursors, but does not rely on some early autophagic proteins such as ULK1 and WIPI2. In fact, mAtg9 and autophagic vesicles are in dynamic interaction. After the formation of mature autophagosomes, mAtg9 does not integrate into the autophagosome, but dissociates into the cytoplasm. mAtg9 locates to endosomes and endosomal sites, and it is speculated that it is active between various cell structures, including the recycled endosome, and plays a critical role in the initiation process of autophagy. For example, mAtg9 interacts with adaptor protein-1 and mannose-6-phosphate receptor, helps the lysosomal hydrolases transport from trans-Golgi network to endosome (Jia et al. 2017). Multiple studies have shown that mAtg9 plays an important role in the extension of the autophagosome precursor membrane system (Zavodszky et al. 2013; Mari et al. 2010).

Detection methods: the level and distribution of Atg9 can be detected by Western blot and immunohistochemistry. Atg9 is 839aa and has an expected molecular weight of 105 kD. In SDS-PAGE electrophoresis, the band of Atg9 is present at about 130 kD.

12.1.1.5 BECN1/Beclin-1/Vps30/Atg6

Mammalian Beclin-1 is a homolog of the Apg6/Vps30 gene of yeast. It functions in the signal transduction route that regulates the initiation of autophagy. In equilibrium conditions, Beclin-1 interacts with Bcl-2 and autophagy is inhibited. When cells are facing autophagy inducing conditions, the proapoptotic molecule BH3 dissociates Beclin-1 from Bcl-2 (Xu and Qin 2019). Beclin-1 binds to PIK3C3/Vps34, a class III phosphatidylinositol-3 kinase, and then autophagy is activated.

Beclin-1 was originally discovered when the protective role of Bcl-2 in the central nervous system was explored. Beclin-1 contains 450 amino acid residues and has a relative molecular weight of 60 kD. Beclin-1 is mainly located on the trans face of the Golgi apparatus, on the endoplasmic reticulum and on mitochondria. Beclin-1 protein has four important domains: the Bcl-2-homology binding (BH3) domain, a coiled-coil Domain (CCD), the Evolutionarily Conserved Domain (ECD), and a nuclear export signal domain. Beclin-1 binds to Vps34 by its ECD domain to form the Class III PI3K complex, and Vps15 (also known as Phosphoinositide 3-kinase regulatory subunit 4, PI3KR4 in human) can anchor Vps34 to the cell membrane. Vps34 phosphorylates phosphatidylinositol to produce phosphatidylinositol 3-phosphate (PI3P), which binds other autophagy-related proteins in the preautophagosomal membrane. This process plays an important role in the early stage of autophagosome formation (Wirth et al. 2013). PI3K inhibitor (3-MA, Wortmannin) can interfere with the formation of autophagosomes.

Detection methods: The level and the location of Beclin-1 can be detected by Western blot and immunohistochemistry. Dot-like aggregation or plaques of GFP-Beclin-1 have been detected as signs of autophagy by fluorescence microscopy or transmission electron microscopy. However, it should be noted that Beclin-1 itself has a nuclear export signal. Fluorescence microscopy of cells expressing Beclin-1-GFP also showed that Beclin-1 exports from the nucleus during autophagy activation (Wu et al. 2012). Researchers have shown that the localization of the GFP fusion protein is interfered by the presence of the GFP moiety, and fluorescence microscopy shows a nuclear localization tendency. Therefore, there may be interference when GFP-Beclin1 is used to indicate the activation of autophagy. Beclin1-related PtdIns3K activity is crucial in autophagosome formation in Beclin1-dependent autophagy. Therefore, the determination of PtdIns3K activity in a Beclin-1 immunoprecipitation can be used to monitor the regulatory effect on autophagy.

Limitations: Beclin-1 levels are very high in some tissue cells. This will cause only little changes in the quantity of Beclin-1, even when autophagy is induced. Additionally, Beclin1-independent autophagy also occurs in cells, and under this condition, autophagy cannot be blocked by a PtdIns3K inhibitor.

12.1.1.6 Atg14/Barkor

Atg14 is located on the autophagosome. The carboxyl terminal of Atg14 is named Barkor/Atg14 Autophagosome Targeting Sequence (BATS). The BATS region is of great significance in the recruitment and activation of Beclin-1 (Mei et al. 2016) during autophagy. Bioinformatics and mutation analysis have revealed that the BATS domain of Atg14 is bound to autophagy vesicle membranes through the hydrophobic surface of the alpha helix. It is inclined to bind to the autophagy vesicle membrane with a higher curvature, containing PI3P. Immunofluorescence analysis showed that the localization of BATS overlaps with Atg16, LC3, and part of DFCP1 under environmental stress (Fan et al. 2011). Atg14-GFP or BATS-GFP may be used as autophagy markers in the detection of autophagy level by fluorescence microscopy or electron microscopy.

Detection method: Atg14 localization can be detected by immunohistochemistry.

Limitations: Atg14 is located not only in autophagosomes, but also in autophagolysosomes and the endoplasmic reticulum. Therefore, it is better to identify autophagy with other markers.

12.1.1.7 DRAM1

DRAM1 is a small hydrophobic protein with six transmembrane structures. It is mainly located in the cis Golgi body, co-located with the Golgi membrane protein GM30, and giantin. DRAM1 also localizes in early and late endoplasm and lysosomes, co-located with EEA1, and LAMP-2. DRAM1 is activated by p53 under environmental stress. DRAM1 gene silencing can block autophagy (Crighton et al. 2006).

Detection methods: Western blots are used to detect protein expression. However, DRAM1 is highly hydrophobic, which leads to difficulties with the preparation of antibodies. Western blots with DRAM1 antibodies show weak bands and some non-specific bands. Constructing a tagged DRAM1 could be a solution that would help with the detection of DRAM1. In addition, real-time quantitative PCR could be used to detect the gene transcription level of DRAM1.

12.1.1.8 ZFYVE1/DFCP1

ZFYVE1 (Zinc finger FYVE domain-containing protein 1), also known as DFCP1 (Double FYVE-containing protein 1), contains two zinc-combined FYVE domains. ZFYVE1/DFCP1 consists of 777aa. Besides these two FYVE structure domains, which are placed in tandem on the C-terminus, it also contains a zinc finger domain on the N-terminus. FYVE domains have the capacity to bind to membranes, via PI3P. ZFYVE1 can recruit other proteins to this position. In this way, ZFYVE1 is involved in membrane transport and cell signaling. ZFYVE1/DFCP1 is located at the endoplasmic reticulum and the Golgi apparatus. Starvation induces the

translocation of ZFYVE1 to the rough-endoplasmic reticulum and co-localization with the omegasome. ZFYVE1/DFCP1 appears in the early stage of autophagy (Nascimbeni et al. 2017).

Detection methods: The level of ZFYVE1/DFCP1 can be detected by Western blot. On SDS-PAGE, ZFYVE1/DFCP1 is located at a molecular weight of about 95 kD. The distribution of ZFYVE1/DFCP1 in cells can be detected by immunohistochemistry. When autophagy is activated, ZFYVE1/DFCP1 changes in allocation, from a weak disperse distribution to a bright dot-like aggregation.

12.1.1.9 p62/SQSTM1

p62, also known as SQSTM1, is degraded through autophagy. p62 is expressed in a variety of cells and tissues and is involved in several signal transduction processes as a scaffold protein. Immunohistochemical results have shown that the localization of p62 overlaps with that of LC3. p62 can bind to LC3 with its LIR domain and bind to ubiquitin-containing proteins through the ubiquitin-associated domain (UBA). p62 and its bound polyubiquitinated protein are contained in autophagosomes and degraded in the autolysosome. When autophagy is inhibited, autophagosomes accumulate and the level of p62 level will increase. Therefore, p62 can be used as an indicator of autophagy, and a decrease of the p62 level can reflect the degree of autophagy activity (Bartlett et al. 2011).

In addition, p62 can accumulate with ubiquitinated protein aggregates. Although the degradation of intracellular substances by macroautophagy is generally considered as nonselective, recent studies have found that macroautophagy has some selectivity to ubiquitinated proteins in a p62-dependent way. The serine 403 of p62 plays an important role in binding this ubiquitinated substrate.

Detection methods: Western blot can be used to detect the level of P62 protein. The band of p62 on SDS-PAGE is about 62 kD.

Limitations: The following aspects should be considered:

1. Cell types and conditions. Levels and level changes of p62 may be different in different cell species and conditions. In some cells, although the Western Blot experimental data of LC3II show strong autophagy induction, the p62 level does not change significantly. Sometimes the level of p62 in cell lysates does not decrease even if autophagic degradation of p62 occurs, which is caused by an increased gene transcription. In some conditions, the p62 protein level or the amount of p62 mRNA will temporarily increase when autophagy is induced. In prolonged starvation, the increased transcription level of p62 may restore p62 intensities to the prestarvation level (Sahani et al. 2014).
2. Time of sample collection for the protein assay. Because the transformation from LC3-I to LC3II is rapid, but the substrate removal takes a longer time, the change of p62 levels may be later than that of the increase of the LC3II level. Prolonging the sample collection time to assess p62 levels would be advantageous.

3. p62 is also a substrate of the proteasome and of some proteases.

Because p62 is also involved in the degradation process via the proteasome, the p62 level increases when the proteasome function is inhibited (Demishtein et al. 2017). In addition, p62 is also a substrate of calpain 1, a calcium-dependent nonlysosomal protease, so it is difficult to explain the significance of the p62 level in autophagy and the detection of cell death. Therefore, in autophagy research, protease inhibitors, autophagy inhibitors (including chloroquine, bafilomycin A1), or gene manipulation (including gene overexpression, knock down or knock-out) should be utilized to fully evaluate the relationship between the changes in p62 level and autophagy level.

4. The concentration of detergent in the lysis buffer.

p62 aggregates are insoluble in lysis buffers that contain the detergents NP40 or Triton X-100. Therefore, only the free form of p62 is detected in Western blot analysis if these detergents are used. When high autophagy flux occurs, the aggregation level of the insoluble p62 may decrease, while the soluble part in the lysate, which is detected by Western blot, may also decrease, or remain unchanged. The state of p62 oligomerization can be checked by comparing samples that have been prepared with Triton X-100 (free form of p62) to samples prepared using 1% SDS (total amount of p62). When p62 is used as the indication of the level of autophagy, positive and negative controls are very necessary, and the mRNA level of p62 should be evaluated at the same time.

5. p62 can enhance the formation of autophagosome in selective autophagy. p62 and NBR1 can either work independently or as hetero-oligomers to recruit target cargoes to the autophagosome (Kirkin et al. 2009; Cha-Molstad et al. 2017).

In summary, although the decrease of p62 level and the increase of LC3II level may be not significantly correlated when autophagy flux increases, as a substrate of autophagy, p62 is an important biomarker for autophagy flux. p62 should only be used to evaluate autophagy flow in combination with other autophagy biomarkers, such as LC3II.

12.2 Biomarkers of Selective Autophagy

12.2.1 Biomarkers of Mitophagy

Mitophagy is mitochondrial autophagy. Mitochondria can get damaged by ROS, nutritional deficiency, cell aging, and other external stimuli. In the processes of mitophagy, impaired mitochondria are engulfed into an autophagosome, which then fuse with the lysosome for degradation by lysosomal enzymes. Mitophagy is a crucial process, important for maintaining a proper mitochondrial morphology and regulation of the mitochondrial function, for a proper response to apoptotic stimuli, and for monitoring of mitochondrial quality (Twig et al. 2008).

Mitochondrial markers and autophagy markers such as LC3 are commonly used to display mitochondrial autophagy. In addition, several mitochondrial autophagy receptors can also be considered as markers of mitochondrial autophagy (Liu et al. 2014).

12.2.1.1 Atg32

In yeast, Atg32 is a core molecule in mitochondrial degradation. It recruits Atg8 and Atg11 as protein receptors. Atg8, the LC3 homolog of mammalian cells, is coupled with phosphatidylethanolamine (PE) and located on autophagy vesicles, participating in the autophagy process. Atg11 is a scaffold protein, providing a platform for the assembly of Atg protein in selective autophagy. Atg32 is a transmembrane protein and is located on the outer membrane of mitochondria. The molecular weight of Atg32 is about 59 kD. The amino terminal 43 kD of Atg32 is exposed to the cytoplasm. The carboxyl terminal 13 kD is exposed to mitochondrial intermembrane space (IMS). Atg8 and Atg11 can be recruited at the amino terminal of Atg32, which plays an important role in the occurrence of mitochondrial autophagy. The carboxyl terminal may play a role in regulating mitochondrial autophagy. Inhibition of Atg32 expression will reduce the efficiency of mitochondrial autophagy. Similarly, overexpression of Atg32 will increase the efficiency of mitochondrial autophagy. Researchers have considered that Atg32 is the limiting step of mitochondrial autophagy in yeast.

Limitations: Although mitochondrial autophagy is an evolutionarily conserved phenomenon, no Atg32 homologous gene has been found in mammalian cells.

12.2.1.2 BNIP3 and NIX/BNIP3L

The autophagy receptors BNIP3 and Nix in mitochondria can also interact with LC3 to remove damaged mitochondria through autophagy. BNIP3 (Bcl-2 and adenovirus E1B 19 kD interacting protein 3) and NIX/BNIP3L (BNIP3-like) are linked to Bcl-2 with their BH3 domain. The sequence of NIX/BNIP3L has 56% homology with BNIP3. NIX/BNIP3L and BNIP3 are located in mitochondria and the endoplasmic reticulum. They regulate apoptosis and programmed necrosis by affecting mitochondrial respiration and ROS levels. When BNIP3 inserts into the outer membrane of a mitochondrion, the amino terminus is in the cytoplasm, while the carboxyl terminus is in the mitochondrion. BNIP3 induces the disappearance of the mitochondrial crest and promotes the release of cytochrome c. Meanwhile, both NIX/BNIP3L and BNIP3 contain a LIR domain, which can bind to LC3, so they are also known as the receptors of mitophagy. For example, hypoxia induces the expression of NIX/BNIP3L and BNIP3, and induces mitophagy. In addition, NIX/BNIP3L interacts with small GTPase—Rheb of the Ras family to promote mitophagy. Phosphorylation of BNIP3 at serine 17 and serine 24 promotes its binding to LC3

and facilitates the occurrence of mitophagy. In addition, NIX/BNIP3L can promote Parkin to locate to the damaged mitochondria, and Parkin also ubiquitinates the proteins on the mitochondrial membrane, thus leading to the interaction between p62 and LC3 and the occurrence of mitochondrial autophagy.

Detection methods: the levels of NIX/BNIP3L and BNIP3 can be detected by Western blot. The predicted size of BNIP3 amino acid sequence is 22 kD. However, in SDS-PAGE gels, besides the 22 kD band, a BNIP3 dimer is present at about 60 kD.

12.2.1.3 PINK1/Parkin

Interaction between PINK1 and Parkin is crucial for the regulation of mitophagy in mammalian cells. PTEN-induced putative kinase 1 (PINK1) is a serine/threonine protein kinase present in the cytosol but it can also be targeted to the outer mitochondrial membrane. Mitochondria with normal mitochondrial membrane potential ($\Delta\psi_m$) import and degrade PINK1, preventing the accumulation of PINK1 on the outer mitochondrial membrane. PINK1 accumulates on impaired mitochondria with a decreased $\Delta\psi_m$. Parkin, a component of a multiprotein E3 ubiquitin ligase complex, binds to PINK1 that is accumulated on the impaired mitochondria and tags the damaged mitochondria with ubiquitin for degradation through mitophagy (Durcan and Fon 2015).

Detection method: Western blot can be used to check PINK1 and Parkin levels.

Limitation: Mitophagy can also occur in a Parkin-independent way. Without the participation of Parkin, some other proteins, such as NIX, FUNDC1, and BNIP3, or cardiolipin also directly interact with the LC3 protein and cause engulfment of the dysfunctional mitochondria into an autophagosome. Meanwhile, other E3 ubiquitin ligases such as SMURF1 and MUL1 also can ubiquitinate the damaged mitochondria and promote mitophagy.

12.2.2 Biomarkers of ER Autophagy

The endoplasmic reticulum is the largest membrane organelle in eukaryotic cells. It plays a key role in protein synthesis and secretion, lipid metabolism, calcium homeostasis, and signal transduction between organelles. The endoplasmic reticulum is built up as a series of connected flattened sacs and tubular structures. The endoplasmic reticulum can change its morphology and function to respond to different physiological and pathological conditions. ER-phagy is an autophagic degradation pathway that uses ER-resident receptors. These receptors are also involved in the regulation of the morphology and function of the endoplasmic reticulum. Mammalian ER-phagy receptors have been found, including FAM134B, Sec62, RTN3, CCPG1, and ATL3. FAM134B is the first ER-phagy receptor that was discovered. FAM134B deficiency blocks hunger-induced ER fragmentation and subsequent lysosomal degradation. Another endoplasmic reticulum autophagy receptor,

ATL3, was more recently discovered. ATL3 is specifically located in the tubular endoplasmic reticulum and mediates the degradation of the tubular endoplasmic reticulum, but does not affect the flattened sac structure of endoplasmic reticulum. ATL3 interacts specifically with the GABARAP subfamily of the ATG8 protein family through two GABARAP-interacting motif (GIM) structure domains. In patients with hereditary sensory and autonomic neuropathy type I (HSAN), two types of point mutations (Y192C and P338R) have been found in ATL3. Y192C is exactly in the GIM domain of ATL3. This study found that the two ATL3 mutations associated with this disease disrupted the interaction between ATL3 and GABARAP, blocking endoplasmic reticulum autophagy mediated by ATL3. These mutations in ATL3, but also mutations occurring in FAM134B, affect ER-phagy in neurons, causing endoplasmic reticulum stress, which then affects the survival of sensory and autonomic neurons and causes the disease symptoms of HSAN.

In the area of selective substrate degradation via autophagy, some other domains besides the above-mentioned mitophagy and ER-phagy have been discovered, such as aggregate autophagy (aggrephagy), ribosome autophagy (ribophagy), nucleus autophagy (nucleophagy), xenophagy, lysosome autophagy (lysophagy), lipid autophagy (lipophagy), and iron autophagy (ferritinophagy). Some markers of selective autophagy are listed in Table 12.2. The research in this field is lagging

Table 12.2 The biomarkers of several kinds of selective autophagy

Selective autophagy	Autophagy receptors	Literatures
Aggrephagy	p62/SQSTM1	Bjorkoy G., et al., <i>J. Cell Biol.</i> 2005, 171(4): 603–614
Mitophagy	PINK/Parkin	Geisler S, et al., <i>Nat Cell Biol</i> , 2010, 12:119–131
	BNIP3, NIX/ BNIP3L	Schweers RL, et al., <i>Proc Natl Acad Sci USA</i> . 2007, 104:19500–19505 C’Sullivan T., et al., <i>Immunity</i> ., 2015, 43:331–342 Chourasia A., <i>EMBO reports</i> , 2015,16:1145–1163
	Atg32	Kanki T., et al., <i>Developmental Cell</i> ., 2009,17:98–109
Ribophagy	NUFIP1	Wyant GA, et al., <i>Science</i> . 2018, 360(6390): 751–758
	Ubp3p/Bre5p	Kraft C, et al., <i>Nat Cell Biol</i> . 2008, 10(5): 602–10
Reticulophagy (ER-phagy)	FAM134B/ RETREG1	Khaminets, A., et al., <i>Nature</i> . 2015, 522: 354–358
	Sec62	Fumagalli F, et al., <i>Nat Cell Biol</i> . 2016, 18(11): 1173–1184
	RTN3	Grumati, P., et al., <i>eLife</i> , 2017, 6 , e25555
	CCPG1	Smith, M. D, et al., <i>Dev. Cell</i> , 2018, 44 , 217–232
	TEX264	An, H., et al., <i>Mol Cell</i> . 2019, 74(5):891–908 Chino H., et al. <i>Mol Cell</i> . 2019, 74(5):909–921
Ferritinophagy	ATL3	Chen Q., et al., <i>Curr Biol</i> . 2019, 29(5):846–855
	NCOA4	Mancias J.D., et al., <i>Nature</i> , 2014. 509(7498): 105–109

behind that of general autophagy. With the deepening of research, more markers will certainly be found in the future.

12.3 Biomarkers of Chaperone-Mediated Autophagy (CMA)

Chaperone-mediated autophagy is a process in which proteins in the cytoplasm bind to a molecular chaperone, such as heat shock cognate protein of 70 kD (HSC70), and then recognize lysosome-associated protein type2a (Lamp-2a). The complex is subsequently transported to the lysosome for degradation by lysosomal enzymes (Fig. 12.2). Compared with macroautophagy and microautophagy, the main feature of CMA is that proteins in the cytoplasm are directly transported into the lysosomal cavity via the lysosomal membrane, without the need to form autophagosomes. In addition, unlike macroautophagy, according to the substrates, CMA is a form of selective autophagy. CMA can degrade about 30% of the soluble protein molecules in the cytoplasm. All proteins that can function as a substrate of CMA contain a KFERQ-like amino acid sequence, which is the only amino acid sequence that can be recognized by HSC70 (Cuervo and Wong 2014). There are three subtypes of Lamp-2, namely, Lamp-2a, Lamp-2b, and Lamp-2c. Using RNAi technology, researchers have concluded that only Lamp-2a is an important receptor for the CMA pathway.

12.3.1 HSC70

HSC70 is a heat shock cognate protein of 70 kDa. It is a molecular chaperone that recognizes CMA substrates with KFERQ-like sequences. Once a substrate binds to HSC70, it is transported to the lysosomal membrane and interacts with the tails of Lamp-2a in the cytoplasm. Lamp-2a interacts with the substrate protein to form a multiprotein complex on the lysosomal membrane which causes the substrate protein to be transported into the lysosome. With the help of HSC70, the substrates begin to unfold and form the complex with Lamp-2a while crossing the lysosomal membrane. Substrate translocation requires the presence of HSC70 inside the lysosomal lumen (lys-HSC70), which may act by either pulling substrates into the lysosomes or preventing their return to the cytosol. The stability of HSC70 depends on the pH of the lysosome. Any slight increase in pH will promote the degradation of HSC70. After translocation, the substrate proteins are rapidly degraded by the lysosomal proteases.

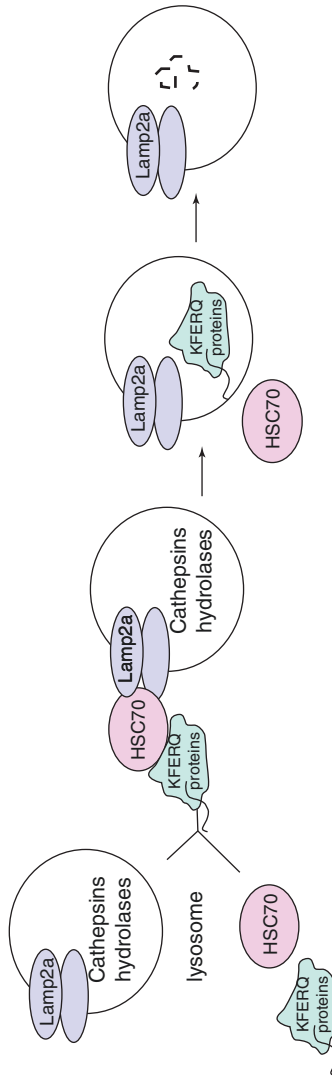


Fig. 12.2 The process of chaperone-mediated autophagy

12.3.2 *LAMP-2a*

Lysosomal membrane protein LAMP-2a is an important receptor of the CMA pathway. The LAMP-2a level is also a rate-limiting step in determining the efficiency of CMA in cells. For example, LAMP-2a knock-down causes the aggregation of glyceraldehyde 3-phosphate dehydrogenase (GAPDH), a substrate of CMA. LAMP-2a overexpression, on the other hand, causes a decrease of GAPDH level. Studies have shown that oxidative stress can up-regulate transcription of the LAMP-2a gene and activate the CMA pathway. Prolonged starvation causes a deceleration of the degradation rate of lamp-2a and activates the CMA pathway.

12.4 Biomarkers of Microautophagy

Endosomal microautophagy (eMI) has recently been identified in mammals as a process whereby endosomes engulf cytosolic material through the formation of multivesicular bodies (MVBs). The material is then degraded in late endosomes or upon the fusion with lysosomes. Cytosolic proteins degraded through eMI can be sequestered in bulk with other cytosolic components, or, if bearing a KFERQ motif, can be selectively targeted to this autophagy pathway. Therefore, microautophagy shares molecular components with both the endocytic and the CMA pathway.

12.4.1 *Rab7*

Ras-related protein 7 (Rab7) is a member of the GTPase family, containing 208 amino acids. Rab proteins control distinct vesicular transport steps. Along the endocytic pathway, Rab5a is a rate-limiting catalyst of internalization, and Rab7 controls the trafficking of late endosomes to lysosomes. Rab7 is one of the most important molecules participating in the fusion process between autophagosomes and lysosomes. It is also involved in the regulation of the transformation and maturation of early endosomes into late endosomes, and positive and negative transport to microtubules (Wang et al. 2011). Rab7 can also be located on the endoplasmic reticulum, the Golgi, and the mitochondrial membrane. In Parkin-mediated mitophagy, Rab7 can assist ATG9A vesicles to enter damaged mitochondria and promote vesicle formation. When exogenous Rab7 is overexpressed in cells, it can be used to observe lysosomal and mitochondrial functions and therefore evaluate the function of Rab7.

Detection methods: The localization of endogenous Rab7 to mitochondria and lysosomes is evident that Rab7 takes part in autophagy. The Rab7 protein level can be detected by Western blot, and an increased protein level indicates the activation of autophagy.

12.4.2 *Vac8*

Like lysosomes in mammalian systems, the yeast vacuole is an acidified organelle containing soluble proteolytic enzymes that degrade proteins, lipids, nucleic acids, and carbohydrates. The yeast vacuolar membrane protein (*Vac8*) is a scaffolding protein with a molecular weight of 63 kDa, consisting primarily of 11 armadillo repeats. *Vac8* is anchored in the membrane of the vacuole by its N-terminal myristate and palmitate moieties. Palmitoylation is an important form of post-translational modification of proteins. *Vac8* can in vitro and in vivo be palmitoylated by the DHHC protein Pfa3. Palmitoylation of *Vac8* is important for vacuolar membrane dynamics such as vacuolar membrane fusion. *Vac8* also has a role in nuclear autophagy (Mukherjee et al. 2016).

Detection methods: The level of palmitoylated protein can be determined by Western blot. However, other factors than abnormal palmitoylation can cause a dysfunction of *Vac8*. The determination of palmitoylation of endogenous *Vac8* may not provide a reliable evidence.

12.4.3 *Atg18*

Atg18 is a phosphoinositide-binding protein. *Atg18* is required for vesicle formation in autophagy and the cytoplasm-to-vacuole targeting (CVT) pathway. The mammalian homologs of *Atg18* include: WIPI1, WIPI2, WIPI3, and WIPI4/WDR45. The binding of a *Atg18*-*Atg2* complex to *Atg9* is crucial to form autophagic membranes (Obara et al. 2008). *ATG18* mutations cause blockage of the formation of the autophagosome. WIPI3 (also named *Wdr45b*) deficiency causes the accumulation of p62-positive and ubiquitin-positive aggregates in brain, and also causes motor deficits and learning and memory defects in mice (Ji et al. 2020).

Detection methods: The molecular weight of the *Atg2*-*Atg18* complex is more than 500 kD, which makes it hard to detect. Immunofluorescence analysis can be used to detect signal intensity. Focusing on the co-localization of *Atg18* and *Atg2*, the morphological characteristics of the complex can be observed by transmission electron microscope.

12.4.4 *ESCRT (VPS4)*

The ESCRT (endosomal sorting complex required for transport) machinery consists of a complex of cytosolic proteins, known as ESCRT-0, ESCRT-I, ESCRT-II, and ESCRT-III. It participates in a variety of cell autophagy processes, such as endosomal microautophagy and macroautophagy. The complex of ESCRT and several

accessory proteins lead to membranes budding away from the cytoplasm through a unique mode of membrane remodeling (Lefebvre et al. 2018). The accessory proteins mainly include five proteins, among which Vps4 is a member of type I AAA+ ATPase family and contains 430 amino acids. Vps4 is present in eukaryotes in a highly conserved form. It provides energy through hydrolysis of ATP to dissociate the ESCRT complex for recycling. In vitro studies have shown that a Vps4 dysfunction affects the entire ESCRT system. Vps4 plays a crucial role in the late endosomal maturation process and can be involved in membrane receptor transport to the lysosome for degradation.

Detection methods: As ESCRT contains multiple proteins, suitable proteins should be selected according to the research aim and objection. Vps4 and TSG101 can be detected by immunohistochemical staining and Western blot.

12.4.5 HSC70

Besides functioning as a chaperone to play a crucial role in chaperone-mediated autophagy, Hsc70 can also selectively bind to ESCRT, participating in a pathway similar to microautophagy (Tekirdag and Cuervo 2018). HSC70 can be detected with Western blot, and the band is about 79 kD on a SDS-PAGE gel. However, the stability of HSC70 depends on the pH value of the lysosome, in which the protein is easily degraded.

12.5 Lysosomal Markers

The lysosome is a membranous organelle. Since Christian DE Duve isolated and described the function of the lysosome in the 1950s, lysosomes have long been regarded merely as a waste dump. However, in recent years, with the increasing understanding of autophagy and the critical position of lysosomes in the autophagy pathway, research has demonstrated that lysosomes are involved in many cell processes closely related to health and disease (Huber and Teis 2016).

Because the process of autophagy is finally completed in the lysosome, lysosomal marker proteins have become important in the study of autophagy. After entering lysosomes, the autophagosome contents are degraded by acid hydrolytic enzymes. Proteins are degraded into peptides or amino acids, nucleic acids into nucleosides and phosphoric acids, carbohydrates into oligosaccharides or monosaccharides, and neutral fats into glycerol and fatty acids. The degraded soluble small molecules penetrate the cytoplasm via the lysosomal membrane and participate in the cell metabolism.

There are 25 membrane proteins in lysosomes that have been identified so far, all of which are hyperglycosylated. The most common membrane proteins are LAMP-1, LAMP-2, LIMP-2 (lysosomal integral membrane protein), and CD63. Glycosylated lysosomal proteins prevent the lysosomal membrane to be degraded by lysosomal enzymes in the lysosomal cavity.

LAMP-1 (lysosomal-associated protein 1) and LAMP-2 (lysosomal-associated protein 2) have 37% amino acid sequence homology. Both LAMP-1 and LAMP-2 have a transmembrane domain and a carboxyl terminal tail that are exposed to the cytoplasm. This tail consists of 11 amino acids, including a signal indicating the localization of LAMP-1. The polypeptide skeleton molecular weight is about 40–45 kD, and the glycosylated molecular weight is about 120 kD. LAMP-1 and LAMP-2 account for about 50% of the lysosomal membrane proteins.

There are three cleaved subtypes of LAMP-2: LAMPA-2a, LAMP-2b, and LAMP-2c. The distribution of the different LAMP-2 subtypes is tissue-specific. For example, LAMP-2b is mainly located in skeletal muscle. Mutations in the LAMP-2 gene cause hereditary lysosomal accumulation disease (Danon disease), and the main clinical syndromes are myocardial hypertrophy, skeletal muscle lesions, and mental retardation. The disease is characterized by an accumulation of autophagosomes in the myocardium and in skeletal muscle, and the accumulation of macromolecules in lysosomes due to the failure of normal degradation, which leads to the dysfunction of cells, tissues, and organs.

Detection methods: The expression levels of LAMP-1 and LAMP-2 in cells and tissues can be detected by Western blot, and their localization can be detected by immunohistochemistry. When the autophagy lysosomal pathway is activated, the expression levels of LAMP-1 and LAMP-2 increase and are located on perinuclear lysosomes.

Limitations: LAMP-1 and LAMP-2 are the main proteins on the lysosomal membrane, rather than direct markers of autophagic vesicles. Therefore, in the detection of autophagy activity, LAMP-1 and LAMP-2 should only be a reference, and other levels of autophagy-related proteins must be detected at the same time. For example, co-localization of LAMP-1 or LAMP-2 with autophagic vesicular proteins such as LC3 can be used. Additionally, the band of LAMP1 and LAMP2 on a Western blot may be heavy and during immunohistochemical staining, the proteins may form aggregates when the lysosomal function is inhibited, such as via chloroquine.

Conclusion: Autophagy biomarkers play an important role in the detection of autophagy. The described biomarkers may be used to detect the level of autophagy in cells in a dynamic, real-time, and quantitative manner. However, to measure the level of autophagy, it is critical to understand the significances, limitations, and preferred detection methods of the biomarkers. Controls (positive, negative, addition of autophagy inhibitors or stimulators, gene manipulation) must very carefully be considered to be able to confirm the autophagy level in cells.

References

- Bartlett BJ, et al. p62, Ref(2)P and ubiquitinated proteins are conserved markers of neuronal aging, aggregate formation and progressive autophagic defects. *Autophagy*. 2011;7(6):572–83.
- Cha-Molstad H, et al. p62/SQSTM1/Sequestosome-1 is an N-recognin of the N-end rule pathway which modulates autophagosome biogenesis. *Nat Commun*. 2017;8(1):102.
- Crighton D, et al. DRAM, a p53-induced modulator of autophagy, is critical for apoptosis. *Cell*. 2006;126(1):121–34.
- Cuervo AM, Wong E. Chaperone-mediated autophagy: roles in disease and aging. *Cell Res*. 2014;24(1):92–104.
- Dancourt J, Melia TJ. Lipidation of the autophagy proteins LC3 and GABARAP is a membrane-curvature dependent process. *Autophagy*. 2014;10(8):1470–1.
- Demishtein A, et al. SQSTM1/p62-mediated autophagy compensates for loss of proteasome poly-ubiquitin recruiting capacity. *Autophagy*. 2017;13(10):1697–708.
- Durcan TM, Fon EA. The three ‘P’s of mitophagy: PARKIN, PINK1, and post-translational modifications. *Genes Dev*. 2015;29(10):989–99.
- Fan W, Nassiri A, Zhong Q. Autophagosome targeting and membrane curvature sensing by Barkor/Atg14(L). *Proc Natl Acad Sci U S A*. 2011;108(19):7769–74.
- Galluzzi L, et al. Molecular definitions of autophagy and related processes. *EMBO J*. 2017;36(13):1811–36.
- Hanada T, Ohsumi Y. Structure–function relationship of Atg12, a ubiquitin-like modifier essential for autophagy. *Autophagy*. 2005;1(2):110–8.
- Huber LA, Teis D. Lysosomal signaling in control of degradation pathways. *Curr Opin Cell Biol*. 2016;39:8–14.
- Ji C, et al. Role of Wdr45b in maintaining neural autophagy and cognitive function. *Autophagy*. 2020;16(4):615–25.
- Jia S, et al. Mammalian Atg9 contributes to the post-Golgi transport of lysosomal hydrolases by interacting with adaptor protein-1. *FEBS Lett*. 2017;591(24):4027–38.
- Kirkin V, et al. NBR1 cooperates with p62 in selective autophagy of ubiquitinated targets. *Autophagy*. 2009;5(5):732–3.
- Klionsky DJ. For the last time, it is GFP-Atg8, not Atg8-GFP (and the same goes for LC3). *Autophagy*. 2011;7(10):1093–4.
- Klionsky DJ, et al. Guidelines for the use and interpretation of assays for monitoring autophagy (3rd edition). *Autophagy*. 2016;12(1):1–222.
- Lefebvre C, Legouis R, Culetto E. ESCRT and autophagies: endosomal functions and beyond. *Semin Cell Dev Biol*. 2018;74:21–8.
- Liu L, et al. Receptor-mediated mitophagy in yeast and mammalian systems. *Cell Res*. 2014;24(7):787–95.
- Mari M, et al. An Atg9-containing compartment that functions in the early steps of autophagosome biogenesis. *J Cell Biol*. 2010;190(6):1005–22.
- Mei Y, et al. Identification of BECN1 and ATG14 coiled-coil interface residues that are important for starvation-induced autophagy. *Biochemistry*. 2016;55(30):4239–53.
- Mizushima N, et al. A protein conjugation system essential for autophagy. *Nature*. 1998;395(6700):395–8.
- Mizushima N, Ohsumi Y, Yoshimori T. Autophagosome formation in mammalian cells. *Cell Struct Funct*. 2002;27(6):421–9.
- Mukherjee A, et al. Selective endosomal microautophagy is starvation-inducible in *Drosophila*. *Autophagy*. 2016;12(11):1984–99.
- Nascimbeni AC, et al. ER-plasma membrane contact sites contribute to autophagosome biogenesis by regulation of local PI3P synthesis. *EMBO J*. 2017;36(14):2018–33.
- Noda NN, et al. Structural basis of Atg8 activation by a homodimeric E1, Atg7. *Mol Cell*. 2011;44(3):462–75.

- Novak I, et al. Nix is a selective autophagy receptor for mitochondrial clearance. *EMBO Rep.* 2010;11(1):45–51.
- Obara K, et al. The Atg18-Atg2 complex is recruited to autophagic membranes via phosphatidylinositol 3-phosphate and exerts an essential function. *J Biol Chem.* 2008;283(35):23972–80.
- Romanov J, et al. Mechanism and functions of membrane binding by the Atg5-Atg12/Atg16 complex during autophagosome formation. *EMBO J.* 2012;31(22):4304–17.
- Runwal G, et al. LC3-positive structures are prominent in autophagy-deficient cells. *Sci Rep.* 2019;9(1):10147.
- Sahani MH, Itakura E, Mizushima N. Expression of the autophagy substrate SQSTM1/p62 is restored during prolonged starvation depending on transcriptional upregulation and autophagy-derived amino acids. *Autophagy.* 2014;10(3):431–41.
- Scheffner M, Nuber U, Huibregtse JM. Protein ubiquitination involving an E1-E2-E3 enzyme ubiquitin thioester cascade. *Nature.* 1995;373(6509):81–3.
- Shao Y, et al. Stimulation of ATG12-ATG5 conjugation by ribonucleic acid. *Autophagy.* 2007;3(1):10–6.
- Tekirdag K, Cuervo AM. Chaperone-mediated autophagy and endosomal microautophagy: joint by a chaperone. *J Biol Chem.* 2018;293(15):5414–24.
- Twig G, et al. Fission and selective fusion govern mitochondrial segregation and elimination by autophagy. *EMBO J.* 2008;27(2):433–46.
- Wang T, et al. Rab7: role of its protein interaction cascades in endo-lysosomal traffic. *Cell Signal.* 2011;23(3):516–21.
- Wirth M, Joachim J, Tooze SA. Autophagosome formation—the role of ULK1 and Beclin1-PI3KC3 complexes in setting the stage. *Semin Cancer Biol.* 2013;23(5):301–9.
- Wu JC, et al. The regulation of N-terminal Huntingtin (Htt552) accumulation by Beclin1. *Acta Pharmacol Sin.* 2012;33(6):743–51.
- Xu HD, Qin ZH. Beclin 1, Bcl-2 and autophagy. *Adv Exp Med Biol.* 2019;1206:109–26.
- Yu ZQ, et al. Dual roles of Atg8-PE deconjugation by Atg4 in autophagy. *Autophagy.* 2012;8(6):883–92.
- Zavodszky E, Vicinanza M, Rubinsztein DC. Biology and trafficking of ATG9 and ATG16L1, two proteins that regulate autophagosome formation. *FEBS Lett.* 2013;587(13):1988–96.

Chapter 13

Chemical Autophagy Regulators



Ya-Ping Yang, Fen Wang, and Chun-Feng Liu

Abstract Autophagy is a catabolic process that removes aggregated proteins and damaged organelles via lysosomal degradation. Increasing evidence suggests that dysfunction of autophagy is associated with a variety of human pathologies, including aging, cancer, neurodegenerative diseases, heart diseases, diabetes, and other metabolic diseases. Current research suggests that the regulation of autophagy may be a novel target for the treatment of these diseases. For this purpose, it is essential to have a deep understanding on the molecular details of autophagy and its regulatory network in each of the disease contexts. Over the years, a variety of chemical autophagy inducers and inhibitors has been developed. The application of these autophagy regulators can assist us in the exploration of the mechanism and therapeutic potential of autophagy regulation. In this chapter, we summarize the recent advances in chemical autophagy regulators to provide methodological support for autophagy research.

13.1 Autophagy Inducers

Many external stimuli (such as starvation and hormones) and intracellular stimuli (such as the accumulation of misfolded proteins and some small organelle damage) can induce autophagy. In autophagy-related studies, autophagy can be activated by

This work is an update of a previously published review paper (*Acta Pharmacol Sin* 34, 625–635 (2013). <https://doi.org/10.1038/aps.2013.5>).

Y.-P. Yang
Department of Neurology, The Second Affiliated Hospital of Soochow University,
Suzhou, China

F. Wang
Institute of Neuroscience, Soochow University, Suzhou, China

C.-F. Liu (✉)
Department of Neurology, The Second Affiliated Hospital of Soochow University,
Suzhou, China

Institute of Neuroscience, Soochow University, Suzhou, China
e-mail: liuchunfeng@suda.edu.cn

adding specific autophagy inducers to observe the role of autophagy in the development of disease. With the elucidation of the molecular mechanism of autophagy, we have increasingly recognized that simple activation of autophagy (increase in autophagosomes or autophagic vesicles) does not by itself promote the degradation of autophagosome-encapsulated proteins or damaged organelles. The imbalance between the induction and degradation of autophagy may lead to autophagic stress and thus exacerbate cell damage. Only completion of the entire process of autophagic flux can promote the degradation of autophagic substrates. Therefore, the use of autophagy inducers must take into account whether the inducer promotes completion of the entire autophagic flux process; various autophagy inducers are listed in Table 13.1.

13.1.1 Starvation Inducers

Initial studies on the molecular mechanisms of autophagy were based on the monitoring of vacuolar morphological changes and the role of autophagy-related proteins under starvation conditions. Autophagy is an important mechanism by which cells adapt to stress, such as elevated temperatures, high population densities, and nutrient deprivation. All cells in the body have internal nutrient storage for use during starvation. Under carbon and nitrogen starvation conditions, the activity of mammalian target of rapamycin (mTOR), the most important negative regulator of autophagy, is inhibited, and the subsequent up-regulation of autophagy provides degraded substrates for cell survival. When the body lacks energy, adenosine 5'-monophosphate (AMP)-activated protein kinase (AMPK), a key molecular regulator of bioenergy-related metabolic activity, is rapidly activated, which promotes autophagy. In addition, physiological levels of amino acid deprivation can also induce autophagy. It is now widely accepted that amino acid and serum starvation caused by amino acid- and serum-free Earle's balanced salt solution (EBSS) or Dulbecco's modified Eagle's medium (DMEM) can induce autophagy in different cells. Electron microscopy studies have also confirmed that complete deprivation of serum and amino acids provides a useful cellular model for autophagy. Receptor for activated C kinase 1 (RACK1) can increase protein folding under nutrient deprivation. This starvation-induced protein can be used as a potential scaffold protein in the process of autophagy activation. It has been reported that lack of Rack 1 can reduce the level of autophagy. Notably, in *in vitro* cell experiments, the half-life of glutamine in culture medium is approximately 2 weeks, resulting in the culture medium containing a low level of glutamine and a high concentration of ammonia, which affects autophagic flux (concentration-dependent inhibition or activation of autophagy). Therefore, the use of freshly prepared medium containing glutamine is suggested for cell autophagy studies to reduce discrepancies (Dobrenel et al. 2016).

Table 13.1 Autophagy activators

Name	Mechanism	Target point	Solubility
Earle's balanced salt solution (EBSS)	Starvation inducer	Autophagy induction	Water-soluble
Brefeldin A	ER stress inducer	Autophagy induction	Water-insoluble
Thapsigargin	ER stress inducer	Autophagy induction	Water-insoluble
Tunicamycin	ER stress inducer	Autophagy induction	Water-insoluble
Rapamycin	mTOR inhibitor	mTOR-dependent signaling pathway	Water-insoluble
CCI-779	mTOR inhibitor	mTOR-dependent signaling pathway	Water-insoluble
RAD001	mTOR inhibitor	mTOR-dependent signaling pathway	Water-insoluble
AP23576	mTOR inhibitor	mTOR-dependent signaling pathway	Water-insoluble
Small-molecule enhancer of rapamycin (SMER)	mTOR-independent activator	mTOR-independent signaling pathway	Water-insoluble
Trehalose	mTOR-independent activator	mTOR-independent signaling pathway	Water-soluble
Lithium chloride	IMPase inhibitor	mTOR-independent signaling pathway	Water-soluble
L-690,330	IMPase inhibitor	mTOR-independent signaling pathway	Water-soluble
Carbamazepine	IMPase inhibitor	mTOR-independent signaling pathway	Water-insoluble
Valproic acid sodium salt	IMPase inhibitor	mTOR-independent signaling pathway	Water-soluble
Xestospongine B	IP3R blocker	mTOR-independent signaling pathway	Water-insoluble
Xestospongine C	IP3R blocker	mTOR-independent signaling pathway	Water-insoluble
<i>N</i> -acetyl-D-sphingosine (C2-ceramide)	Class I PI3K inhibitor	mTOR-dependent signaling pathway	Water-insoluble
Penitrem A	Ca ²⁺ channel blocker	mTOR-independent signaling pathway	Water-insoluble
Calpastatin	Calpain inhibitor	mTOR-independent signaling pathway	Water-soluble

13.1.2 Endoplasmic Reticulum Stress Inducers

The endoplasmic reticulum (ER) is an important membranous organelle in mammalian cells. The ER mainly participates in the folding and modification of proteins and the storage and release of Ca²⁺. ER stress can be induced by hypoxic-ischemic

reperfusion, alcohol, drugs, poisoning, infection (bacteria, viruses, etc.), ultraviolet light, nutrient deficiency, and other physiological and pathological factors. ER stress activates the ER stress response or unfolded protein response (UPR). The UPR maintains the homeostasis of the ER by reducing the synthesis of nascent proteins, increasing the synthesis of chaperones, and the degradation of misfolded or unfolded proteins. Autophagy is an important metabolic process that eliminates, degrades, and reabsorbs intracellular macromolecules and damaged organelles. An increasing number of studies have shown that ER stress and UPR can induce autophagy in cells through a variety of molecular mechanisms, which will have an important impact on disease progression. The ER UPR mainly acts through three signaling pathways: PERK, ATF6, and IRE1. Activation of the PERK–eIF2 α –ATF4 signaling pathway can promote the expression of autophagy-related genes, while IRE1 mainly promotes autophagy by activating JNK. Conversely, defects in autophagy promote the development of the UPR and thus can relieve autophagic dysfunction. Sar1 and Rab1b are monomeric GTPases that regulate the transport from the ER to the Golgi apparatus, and it has been reported that the activity of these two proteins is essential for autophagosome formation. ER stress activates autophagy by negatively regulating the AKT/TSC/mTOR pathway. ER stress inducers such as brefeldin A, thapsigargin, and tunicamycin all promote the formation of autophagic vesicles. However, notably, some studies have obtained the opposite result: thapsigargin can inhibit autophagy, and the underlying mechanism may be related to the release of ER calcium stores by thapsigargin, which increases intracellular calcium levels. Another study has shown that thapsigargin does not affect autophagosome formation but instead causes mature autophagosome accumulation by blocking the fusion of autophagosomes with endocytic systems. The opposite effect of these ER stress inducers may be related to the interaction of ER stress and autophagy regulatory pathways. Whether an ER stress inducer can be used as an effective autophagy inducer should be determined by detecting the autophagic flux (Senft and Ronai 2015).

13.1.3 mTOR Inhibitors

13.1.3.1 Rapamycin and Its Derivatives

Rapamycin, also known as sirolimus, was extracted from the bacterium *Streptomyces hygroscopicus* in 1975. It is an unusual nitrogen-containing triene macrolide with a very large 31-membered lactone ring. Rapamycin possesses antifungal, antitumor, and immunosuppressive activity. The target protein of rapamycin in mammals is mTOR. mTOR is a member of phosphatidylinositol-associated kinase family and promotes phosphorylation of its substrates, such as ribosomal protein S6 kinase (p70S6K) and initiation factor 4E-binding protein 1 (eIF4E-binding protein, 1,4E-BP1). mTOR promotes the transcription process, leading to the synthesis of new proteins and enhancing cell proliferation, thereby acting as a key regulator of cell

growth and proliferation. mTOR includes two functional complexes: rapamycin-sensitive mTORC1 contains mTOR, raptor (an mTOR-associated protein), 40 kDa proline-rich Akt substrate (PRAS40), Deptor, mammalian lethal SEC13 protein (mammalian lethal with SEC13 protein 8, mLST8), Tti1, and Tel2. The other is rapamycin-insensitive mTORC2 comprising mTOR, rictor, mammalian stress-activated protein kinase-interacting protein 1 (Mammalian stress-activated protein kinase-interacting protein 1, mSin1), rotor1/2, Deptor, mLST8, Tti1, and Tel2. Rapamycin forms a complex with the immunophilin FK506-binding protein (FKBP12), which stabilizes raptor-mTOR binding and inhibits mTOR kinase activity. When the mTOR inhibitor rapamycin is added to cells rich in nutrient medium, autophagy is induced. This means that mTOR negatively regulates autophagy, while rapamycin induces autophagy by inhibiting mTOR. Rapamycin has been widely used in *in vitro* and *in vivo* autophagy studies and is recognized as an autophagy-inducing agent. However, a few studies have noted that rapamycin-induced autophagy in many cell lines is relatively slow or transient and has side effects. Notably, rapamycin also inhibits protein synthesis, so when identifying whether certain proteins are substrates for autophagy or degraded by autophagy, a control group should be set up to demonstrate that the reduction in protein levels is not due to suppression of the protein synthesis process (Saxton and Sabatini 2017).

Temsirolimus, also known as CCI-779, is a water-soluble derivative of rapamycin that is primarily metabolized to rapamycin. It has been reported that temsirolimus can reduce the formation of huntingtin protein aggregates in a mouse model of Huntington's disease, showing a certain neuroprotective effect. Rapamycin analogs similar to CCI-779 are everolimus (aka RAD001, oral drug) and AP23573 (intravenous formulation). These drugs have lower dose-limiting toxicities and are relatively safer than rapamycin. These rapamycin derivatives are likely to be effective therapeutic agents for tumors that target autophagy (Sarkar 2013).

13.1.3.2 Small-Molecule Enhancers of Rapamycin

The immunosuppressive side effects of rapamycin limit the role of this compound as an autophagy-targeted drug for the treatment of diseases such as cancer, and there is an urgent need to develop safe methods for inducing autophagy. In 2007, a small-scale chemical screen of autophagy regulators was used to identify small-molecule enhancers of rapamycin (SMERs), which are associated with mammalian autophagy. Three SMERs were screened from 50,729 complexes and were named SMER10, SMER18, and SMER28. SMER10 is an aminopyrimidinone, SMER18 is a vinylogous amide, and SMER28 is a bromo-substituted quinazoline. Further analysis of the effects of various chemical base substitutions on these three SMERs revealed that the rapamycin-related function of SMER10 is critical for the induction of autophagy; SMER10 can undergo a large number of base substitutions on the benzene to yield a tetrazolium hybrid, eliminating the activity of this compound. It is also important that the hydroxyl group on SMER18 is in the posterior position, because removal of this group from this position (and moving it to the ortho

position) causes SMER18 to lose its autophagy induction effect. After base substitution of SMER28, the efficacy of this compound was not enhanced, and most of the derivatives were resistant. The role of these SMERs as autophagy enhancers in yeast and mammals has also been confirmed. SMER has been shown to enhance the clearance of A53T α -synuclein, which is an autophagic substrate and a Parkinson's disease-related mutant, and to inhibit the accumulation and toxic effects of mutant huntingtin proteins in cellular and *Drosophila* models. This SMER-induced autophagy is not mTOR-dependent and may act on downstream factors of rapamycin targets or targets unrelated to mTOR. The combination of SMER10, SMER18, SMER28, and rapamycin has a significant effect on the clearance and toxicity of the agglutinin A53T α -synuclein and has a better therapeutic effect than the individual components. Notably, these SMERs do not affect the levels of autophagy regulators (such as Beclin-1, Atg6, Atg5, Atg7, and Atg12) or enhance the critical step in the formation of autophagosomes before binding to LC3, that is, the combination of Atg12 with Atg5. However, a study has proposed that during starvation or SMER28-induced autophagy, Atg5 plays an important role in the degradation of A β and APP-CTF, and SMER28 can reduce A β by the Atg5-dependent autophagy pathway (Sarkar 2013).

13.1.3.3 ATP-Competitive Small-Molecule mTOR Inhibitors

In addition to rapamycin and its derivatives, mTOR inhibitors also include ATP-competitive inhibitors, which usually consist of synthetic small molecules that target the catalytic site of the kinase. These small-molecule inhibitors can simultaneously inhibit the inhibition of mTORC1 and mTORC2. Due to their low molecular weights, it is easy for ATP-competitive small-molecule mTOR inhibitors to target the mTOR binding site. These inhibitors exhibit strong autophagy induction and lack the immunosuppression side effect of rapamycin. These small-molecule inhibitors can be classified according to their chemical structure and include AZD-8055, OSI-027, INK128, WYE-132, Torin 1, Torin2, and resveratrol (Liu et al. 2017). Use of most of the small molecules mentioned above in preclinical studies has been reported. Intensive research on such inhibitors will facilitate the development of autophagy inducers and their clinical applications.

13.1.4 Trehalose

Trehalose was first extracted from the ergot of rye by Wiggers in 1832 and is a non-reducing disaccharide composed of two glucose molecules with $\alpha,\alpha,1,1$ -glycosidic bonds. Trehalose is mainly found in nonmammals, such as bacteria, yeast, fungi, insects, and plants, and protects cells against various environmental stresses. Previous studies have shown that the protective effects of trehalose are mainly dependent on the characteristics of its chemical partner, and trehalose can directly

bind certain proteins to affect the folding of these proteins. In recent years, treatment with trehalose has been found to increase the level of autophagy in most mammalian cells, and these effects are regulated by intracellular trehalose. Trehalose significantly increased the LC3-II level of Atg5^{+/+} mouse embryonic fibroblasts but had no effect on autophagy-deficient Atg5^{-/-} mouse embryonic fibroblasts. It has been reported that trehalose inhibits the formation of amyloid in insulin in vitro and prevents the accumulation of β -amyloid peptide (A β) in Alzheimer's disease. In addition, trehalose can also increase the clearance rate of mutant huntingtin and the α -synuclein mutants A53T and A30P and inhibit the aggregation of mutant SOD1, thereby reducing the accumulation of mutant proteins or the toxicity of these mutants. Disease progression of Huntington's disease, Parkinson disease, and amyotrophic lateral sclerosis (ALS) can be delayed by the protective effect of trehalose, which is associated with autophagy. Unlike rapamycin, trehalose does not affect mTOR and AMPK activity but is an autophagy-inducing agent that is independent of mTOR. The combination of trehalose and the mTOR inhibitor rapamycin has a cumulative effect on phagocytosis. In addition to inducing autophagy, trehalose can protect cells by reducing mitochondrial dysfunction and attenuating cell apoptosis. This dual protection provided by trehalose and the low toxicity of this compound as a natural plant polysaccharide make it a promising autophagy-targeted drug for the treatment of neurodegenerative diseases such as Alzheimer's disease and prion diseases (Hosseinpour-Moghaddam et al. 2018).

13.1.5 *IMPase Inhibitors*

It has been shown that reducing intracellular inositol or inositol triphosphate (IP3) levels can induce autophagy. The emotional stabilizers lithium, carbamazepine, and sodium valproate can reduce the level of inositol, thereby inducing autophagy and clearing autophagic substrates, such as mutant huntingtin and the α -synuclein mutants A53T and A30P. Conversely, increasing the level of cellular inositol or increasing the level of IP3 attenuates the ability to clear autophagic substrates and attenuates the effects of lithium agents but does not alter the effects of rapamycin. Drugs that reduce IP3 levels do not reduce mTOR activity, whereas rapamycin has no effect on inositol levels, suggesting that inositol monophosphatase (IMPase) inhibitors are acting in a mTOR-independent manner, constituting the first mTOR-independent autophagy pathway in mammalian systems. Lithium is a noncompetitive inhibitor of IMPase because Li⁺ occupies the second Mg²⁺ binding site, which precludes binding of the phosphate group of the substrate. The induction of autophagy by lithium agents mainly occurs via IMPase inhibition. IMPase catalyzes the hydrolysis of inositol monophosphate (IP1) to free inositol, which requires the involvement of the phosphoinositide signaling pathway. In the phosphoinositide pathway, lithium inhibits IMPase and inositol polyphosphate-1-phosphatase (inositol). The activity of polyphosphate-1-phosphatase (IPPase) and its inhibitory effects are related to inhibition of inositol by IMPase, which leads to intracellular inositol

deficiency and decreased phosphoinositide cycle activity. L-690,330 is an IMPase bisphosphonate inhibitor that mimics the effects of lithium agents, leading to an increase in IP1 levels both *in vitro* and *in vivo*. Myo-inositol-1-phosphate (MIP) synthase is the rate-limiting enzyme that catalyzes inositol biosynthesis, and valproic acid reduces the level of inositol by inhibiting MIP synthase (Sarkar and Rubinsztein 2006).

It was revealed that glycogen synthase kinase-3 β (GSK-3 β) is another target of lithium, which has the opposite effect on autophagy regulation and can inhibit autophagy in mTOR-dependent manner. GSK-3 β is active in the nonphosphorylated form, and lithium agents specifically promote the phosphorylation of serine 9 of this protein, thereby inhibiting the activity of GSK-3 β . Lithium agents compete with Mg²⁺ for binding to GSK-3 β , though they are not competitive with respect to ATP binding. Induction of autophagy by GSK-3 β inhibitors does not depend on the target β -catenin but activates mTOR through phosphorylation of the nodular sclerosis protein subtype TSC2. Interestingly, lithium or L-690,300 reduced mutant huntingtin aggregates in GSK-3 β (-) cells, in which mTOR is active. This finding indicates that the induction of autophagy is determined by IMPase inhibition, even in the absence of GSK-3 β and independent of mTOR activity. In patients with ALS and in mouse models, lithium can increase patient survival and delay disease progression, likely owing to neuroprotective effects of lithium and also partly owing to autophagy induced by lithium. In addition, consistent with the role of IP3 in autophagy, IP3 receptor inhibitors such as xestospongin B/C can also act as mTOR-independent autophagy inducers (Sarkar and Rubinsztein 2006; Mancinelli et al. 2017; Sarkar 2013).

13.1.6 Class I PI3K Inhibitors

There are three types of phosphoinositide 3-kinases (PI3Ks) in mammals: PI3K-I is involved in autophagy regulation and is an autophagy inhibitor; PI3K-II is not associated with autophagy regulation; and PI3K-III is similar to Vps34 and plays an important role in the early stage of mammalian autophagosome formation. The PI3K-I/PKB pathway is involved in the negative regulation of autophagy and inhibits the occurrence of autophagy. When PI3K-I is activated, it can modify the cell membrane lipid phosphatidylinositol, phosphorylating PI(4)P and PI(4,5)P2 to PI(3,4)P2 and PI(3,4,5)P3. These lipids can recruit proteins required for autophagy to the early membrane of the autophagosome, and activate Akt/PKB through binding of their PH domain and Akt/PKB activator phosphatidylinositol-dependent kinase 1 (PDK1) domain. In addition, PDK1 also phosphorylates other kinases, such as p70S6. Expression of the active forms of PDK1 and PKB can activate the PI3K-I/PKB pathway and inhibit autophagy, while PTEN, which can hydrolyze PI(3,4,5)P3, alleviates the inhibition of PI3K-I/PKB. Activation of PI3K-I/PKB attenuates the inhibition of TSC1/TSC2 via the mTOR/p70S6 pathway, and TSC2

exhibits GTPase activity for the regulation of monomeric Rheb in mTOR/p70S6 kinase signaling. Although the regulation of autophagy by TSC1, TSC2, and the GTPase Rheb has not been directly confirmed, these proteins are most likely among the autophagy-related components upstream of mTOR, replacing other downstream signals of the PI3K-I pathway (Sarkar and Rubinsztein 2006; Shanware et al. 2013).

N-acetyl-D-sphingosine (C2-ceramide) is a biologically active ceramide that penetrates the cell membrane by interfering with the activation of interleukin-13-dependent protein kinase B (PKB) and promoting Beclin1 expression, alleviating the inhibition of the autophagy-related PI3K-I/PKB signaling pathway. These results suggest that ceramide has a novel function, that is, up-regulation of autophagy, as a PI3K-I inhibitor. It has been reported that CH5132799, GDC-0980, and GDC-0941 strongly inhibit the downstream signaling of PI3K and mTOR, but the proapoptotic mechanisms of these three novel PI3K-I inhibitors have not yet been fully elucidated. The role these inhibitors has yet to be confirmed by further research (Shanware et al. 2013; Russo and Russo 2018).

13.1.7 Other Activators

13.1.7.1 Calcium Channel Inhibitors and Calcium-Activating Enzyme Inhibitors

Ca²⁺ is an important intracellular second messenger that is involved in the regulation of many cellular processes. Autophagy can be inhibited by increasing intracellular Ca²⁺ levels in rat hepatocytes. Verapamil, which is used to treat hypertension, is an antagonist of the L-type Ca²⁺ channel, and induces autophagy and reduces cytotoxicity in the zebrafish HD model. Penicillin A is an irreversible inhibitor of intracellular large-conductance calcium-activated potassium channels and has been shown to activate autophagy by blocking calcium channels. Increased intracellular calcium activates calcium-activated enzymes in the calcium-dependent cysteine protease family, whereas calcium-activated enzymes are inhibited by cleavage of the alpha subunits of heterotrimeric G-proteins (G α). Therefore, calpastatin, a calcium-activating enzyme inhibitor, may also act as a potential autophagy-inducing agent (East and Campanella 2013).

13.1.7.2 Adenylate Cyclase Inhibitors

Drugs that regulate cyclic adenosine monophosphate (cAMP) levels include adenylate cyclase inhibitors such as 2,5-dideoxyadenosine, which reduces cAMP levels, induces autophagy, and promotes autophagic substrate clearance. Activators of cAMP (such as forskolin) or analogs of cAMP have the opposite effect. In the zebrafish model of Alzheimer's disease, the autophagy inducers clonidine and

2,5-dideoxyadenosine have been shown to have a protective effect, slowing rod cell photoreceptor degeneration and reducing mutant huntingtin protein levels (Noda and Inagaki 2015; Levine et al. 2015).

13.1.7.3 Paeoniflorin

Paeoniflorin is a single-glycoside compound and is a biologically active component in the dried root of peony (Fam. Ranunculaceae). Paeoniflorin regulates some key factors of the autophagy pathway. For example, paeoniflorin can up-regulate the expression of Hsp70, an important molecular chaperone that mediates chaperone-mediated autophagy (CMA), in human leukemia U937 cells; paeoniflorin can down-regulate nuclear factor-kappa B (NF- κ B), promoting the apoptosis of human gastric cancer cells, thus down-regulation of NF- κ B increases Beclin 1 expression and activates autophagy; Bcl-2 is a negative regulator of autophagy and paeoniflorin can up-regulate Bcl-2-antagonistic radiation-induced thymocyte apoptosis. However, it has not been reported whether paeoniflorin has a direct effect on autophagy. Our study shows that paeoniflorin has a significant regulatory effect on macroautophagy and CMA. When pathological factors cause LC3-II expression in PC12 cells to be inhibited, paeoniflorin can up-regulate LC3-II expression, then promote the survival of neurons; the diuretic amiloride also has a similar effect (Gros and Muller 2014; Russo and Russo 2018; Cao et al. 2010).

13.1.7.4 Hormones

Hormones also play an important role in the regulation of autophagy. Insulin can inhibit autophagy, and glucagon can activate autophagy. In addition, tyrosine kinase receptors, protein kinase A, casein kinase II, and mitogen-activated protein kinases are also present in the intricate regulatory network of autophagy, but the mechanisms are not well understood (Gros and Muller 2014).

13.2 Autophagy Inhibitors

Autophagy flux is divided into three phases: the autophagosome formation phase, characterized by a bilayer membrane; the autophagosome-lysosome fusion phase; and the degradation phase of the autolytic substrates in the lysosome. Autophagy can be inhibited at all stages of autophagic flux (Pasquier 2016). During the study of autophagy-related mechanisms, many chemical inhibitors have been identified and used in various cell and animal models (Table 13.2). However, most chemical inhibitors of autophagy are not entirely specific, and the findings obtained with the use of these compounds should be interpreted with caution, especially with respect to dose and incubation time.

Table 13.2 Autophagy inhibitors

Name	Mechanism	Target point	Solubility
3-Methyladenine	PI 3-kinase inhibitor	Autophagosome formation	Water-soluble
LY294002	PI 3-kinase inhibitor	Autophagosome formation	Water-insoluble
Wortmannin	PI 3-kinase inhibitor	Autophagosome formation	Water-insoluble
Cycloheximide	Protein synthesis inhibitor	Autophagosome formation	Water-insoluble
Bafilomycin A1	Vacuolar-type H(+)-ATPase inhibitor	Autophagolysosome formation	Water-insoluble
Hydroxychloroquine	Lysosomal lumen alkalizer	Lysosome	Water-soluble
Ammonium chloride	Lysosomal lumen alkalizer	Lysosome	Water-soluble
Lys05	Lysosomal lumen alkalizer	Lysosome	Water-soluble
Alkaloid	Lysosomal lumen alkalizer	Lysosome	Water-soluble
Pepstatin A	Acid protease inhibitor	Lysosome	Water-insoluble
Leupeptin	Acid protease inhibitor	Lysosome	Water-soluble
E64d	Acid protease inhibitor	Lysosome	Water-insoluble

13.2.1 Autophagosome Formation Inhibitors

13.2.1.1 PI3K-III Inhibitors

As described in the first section of this chapter, class III PI3K is an analog of vacuolar protein sorting 34 (Vps34), and the class III PtdIns3K catalytic subunit PIK3C3/Vps34 forms a protein complex with BECN1 and PIK3R4 and produces phospholipids. Phosphatidylinositol 3-phosphate (PtdIns3P), which is required for the initiation and progression of autophagy, plays an important role in the early stages of mammalian autophagosome formation. Localized formation of PI3K contributes to the recruitment of autophagy proteins on specific membrane domains in the early stages of autophagosome formation. In addition, the positioning of PI3K on the membrane can also make the membrane uneven or bent, finally forming the closed bilayer membrane structures of autophagosomes. The Beclin1/class III PI3K complex is involved in the formation of autophagosomes and induces autophagy; the PI3K inhibitor 3-methyladenine (3-MA) blocks this pathway and inhibits the formation of autophagosomes. 3-MA is the first PI3K inhibitor to be identified and widely used to inhibit autophagy. In as early as 1982, the PI3K inhibitor 3-MA was shown to inhibit the formation of autophagosomes in rat hepatocytes. Subsequent studies further confirmed that 3-MA and two other PI3K inhibitors (wortmannin and LY294002) can inhibit autophagy by inhibiting class III PI3K.

Because the class III PI3K required for activation of autophagy acts downstream of class I PI3K, which negatively regulates autophagy, the overall effect of PI3K inhibitors is thought to be inhibition of the autophagy process. However, studies

have shown that 3-MA has a dual role in the regulation of autophagy (Wu et al. 2010): in addition to inhibiting starvation-induced autophagy, the long-lasting action of 3-MA under nutrient-sufficient conditions promotes the completion of autophagic flux. The inhibitory effect of wortmannin is opposite to that of 3-MA. Short-term effects mainly affect class I PI3K-induced autophagy, and long-term effects mainly affect class III PI3K-mediated inhibition of inflammation. The results of this study suggest that wortmannin may be more suitable as an autophagy inhibitor than 3-MA, given the long-lasting inhibition of PI3K-III by wortmannin. It has also been reported that wortmannin is capable of inducing vacuolization, although this vacuole is a swollen late-endocytic compartment that is very similar to autophagosomes. In addition, studies have also confirmed that inhibition of autophagy with 3-MA or wortmannin has side effects on cytokine transcription, processing, and secretion, especially for IL-1 family members. 3-MA also inhibits the secretion of certain cytokines, such as TNF and IL-6, in a nonautophagy-dependent manner. Therefore, when studying the role of autophagy inhibitors in specific cellular processes, it is important to determine the accuracy of the results by other methods, such as RNAi-mediated inhibition of autophagy. Other studies have shown that LY294002 can activate autophagy by inhibiting the class I PI3K signaling pathway, which may be related to the LY294002-mediated increase in intracellular calcium levels, mobilization of intracellular calcium stores, and inhibition of calcium voltage transients. Therefore, calcium-related experiments should avoid the use of LY294002 as an autophagy inhibitor. Understanding the complex role of PI3K inhibitors in the autophagy pathway will help improve the selection of appropriate autophagy inhibitors for specific studies. Notably, 3-MA is the most appropriate for use in cells. In cellular experiments, 3-MA is usually dissolved directly into the medium and placed in a 37 °C incubator for 1 h for complete dissolution or heated in an oven to 50 °C. The solution, usually at a final concentration of 20 mM, is used after filtration and sterilization.

13.2.1.2 Protein Synthesis Inhibitors

Cycloheximide is an inhibitor of protein synthesis in eukaryotes and is produced by *Streptomyces griseus*. This compound hinders translation by interfering with the translocation steps in the protein synthesis process. Cycloheximide has been widely used in biomedical research because of its low cost and the rapid onset of its effects. In short-term experiments, cycloheximide exhibited no obvious inhibition of protein synthesis but could significantly inhibit the occurrence of autophagy. Western blot analysis showed that after incubation with cycloheximide for 24 h, the autophagy substrate protein P62 showed no significant degradation. Other studies have shown that cycloheximide can inhibit autophagy induced by high glucose or cadmium chloride levels in mouse pancreatic cancer cells, and the number of autophagic vacuoles of seminal vesicles is reduced after cycloheximide treatment. Cycloheximide has been shown to be a fast and potent inhibitor of autophagy, which may occur during isolation of the coated substrate from autophagic vacuoles formed

by autophagosomes. Although cycloheximide is now often used to inhibit autophagy pathways, once cycloheximide is removed, inhibition of autophagy degradation and lysosomal enzyme transport by cycloheximide is rapidly alleviated (Lawrence and Brown 1993). The mechanism of autophagy inhibition by cycloheximide in short-term experiments remains to be elucidated.

13.2.1.3 Other Autophagosome Formation Inhibitors

In the early stages of autophagosome formation, the isolation of autophagic substrate protein by autophagic membrane can be inhibited by intracellular and extracellular calcium chelators, such as ethylene glycol tetraacetic acid (EGTA). Vanadate also has the same effect, which may be caused by the lack of calcium in the cells. The effect of calcium on autophagic substrate protein isolation does not depend on calcium-dependent protein kinase activity because the inhibitors of these protein kinases, such as KN-62, do not directly regulate autophagic substrate protein isolation processes. Studies have shown that it is the release of intracellular calcium stores, rather than the increased calcium levels in the cytoplasm, that has an inhibitory effect on autophagy substrate protein isolation. ER is one of the intracellular calcium stores, so the ER Ca^{2+} -ATPase inhibitor thapsigargin can cause the release of intracellular calcium stores and inhibit autophagy. It has been found that phorbol myristate, calcium ionophore A23187, and phentolamine, which modify the calcium levels of lysosomes in vivo, can alter the total amounts of autophagic vacuoles.

13.2.2 Autolysosome Formation Inhibitors

Vesicular-type H^{+} -ATPase (V-ATPases) is present on the membranes of many organelles (such as lysosomes, inclusion bodies, and secretory vesicles) and plays an important role in maintaining the functions of these organelles. Bafilomycin A1 is a macrolide antibiotic derived from *S. griseus*; this compound has a molecular formula of $\text{C}_{35}\text{H}_{58}\text{O}_9$ and has antibacterial, antifungal, and antitumor effects. Bafilomycin A1 is a specific inhibitor of V-ATPase that disrupts the vesicle proton gradient and increases the pH of acidic vesicles. This effect prevents the fusion of autophagosomes and lysosomes, leading to the accumulation of autophagosomes (Nakamura and Yoshimori 2017). As early as 1998, it was reported that bafilomycin A1 can prevent the maturation of autophagic vacuoles in the rat hepatoma cell line H-4-II-E by inhibiting the fusion of autophagosomes and lysosomes. In colon cancer cells, inhibition of autophagy by bafilomycin A1 reduces cell proliferation and induces apoptosis. Similar to bafilomycin A1, another selective V-ATPase inhibitor, concanavalin A, also inhibits the fusion of autophagosomes and lysosomes to increase the accumulation of autophagosomes. This compound targets the early and late stages of the autophagy pathway by activating the mammalian target of rapamycin signaling and dissociating the Beclin 1-Vps34 complex, as well as by inhibiting

the formation of autolysosomes, all of which attenuate the functionality of autophagy.

However, another study shows a significantly different result, that is, bafilomycin A1 does not block the fusion of autophagosomes with lysosomes (Klionsky et al. 2008). It has been reported that bafilomycin A1 and rapamycin increase LC3 lipidation, while wortmannin and BECN1-specific shRNA inhibit LC3 lipidation. Because bafilomycin A1 and other vesicular H⁺-ATPase compounds increase lysosomal pH, this compound also has an indirect effect on other acidification chambers. In *in vitro* cellular experiments, treatment with bafilomycin A1 for more than 18 h caused significant mitochondrial damage. In plants, bafilomycin A1 or concanavalin A can cause Golgi swelling and increase tumor cell apoptosis. The final concentration of bafilomycin A1 is usually 100 nM, but low concentrations (such as 1 nM) appear to be sufficient to inhibit autolysosome degradation with few side effects. The most appropriate and effective inhibitor concentration also depends on the type of cells used in the experiment. Treatment with bafilomycin A1 increases autophagic flux by inhibiting mTOR and inhibits autophagic flux by inhibiting the fusion of autophagosomes and lysosomes (Dengjel et al. 2012). Therefore, perhaps other autophagic flux inhibitors are more suitable for autophagic flux detection.

Because bafilomycin A1 has a strong effect on LC3-II content, the treatment time of bafilomycin A1 is critical, and the half-life of the autophagosomes is only 20–30 min. Usually, bafilomycin A1 is applied for 4 h and can completely block autophagy.

In addition, microtubule inhibitors can also inhibit microtubule-dependent cell migration by interfering with the balance of microtubule dynamics, thereby inhibiting the fusion of autophagic vesicles and lysosomes. These drugs include vinblastine and nocodazole.

13.2.3 Lysosomal Inhibitors

Autophagosomes are eventually hydrolyzed by hydrolytic enzymes in lysosomes after fusion with lysosomes. The lysosome is acidified, and then the autophagic substrate is degraded by various proteases. The degradation products can be recycled in the cell. If the degradation process in lysosomes is inhibited, the autophagic substrate that should be degraded accumulates in the lysosome and cannot be recycled, which also inhibits autophagy.

13.2.3.1 Lysosomal Lumen Alkalizers

Lysosomal lumen alkalizers include chloroquine, hydroxylated chloroquine, ammonium chloride, cepharanthine (CEP), and neutral red. These substances can penetrate into lysosomes, increase the pH of lysosomes, inhibit lysosomal function, and

increase the autophagosome volume. For example, 20 mM NH_4Cl can alkalinize lysosomes and inactivate lysosomal enzymes. Among these compounds, chloroquine and its analog hydroxylated chloroquine are widely used in antimalarial and antirheumatic treatments. CEP is an alkaloid extracted from the genus *Astragalus* and acts as a novel autophagy inhibitor in nonsmall cell lung cancer (NSCLC) cells. This compound is currently in phase III clinical trials. Chloroquine has been widely used as an autophagy inhibitor for autophagy studies, but it should be noted that this compound may also activate autophagy at the beginning of its action. It has been reported in the literature that hydroxylated chloroquine-mediated autophagosome-lysosomal disorder increases the antitumor effect of this compound. However, a high concentration of hydroxylated chloroquine is required to block autophagy, and therefore, this compound cannot be used in clinical patients. Lys01 is a novel chloroquine dimer compound in which two chloroquine groups are linked by *N,N*-bis(2-aminoethyl)-methylamine, and autophagy inhibition by this compound is 10 times greater than that by hydroxylated chloroquine (Amaravadi and Winkler 2012). Lys05, the water-soluble salt of Lys01, can accumulate well in lysosomes to reduce lysosomal acidity, leading to autophagy and inhibition of tumor growth (McAfee et al. 2012). As a new lysosomal autophagy inhibitor, Lys05 has a good therapeutic index and has potential clinical applications as an autophagy-targeted therapeutic.

13.2.3.2 Acid Protease Inhibitors

Lysosomes are the final sites of autophagic substrate degradation, and lysosomal enzymes are involved in the degradation of autophagy substrates. Lysosomal cathepsin can help maintain the metabolic balance of cells by participating in the degradation of autophagosomes. Among lysosomal hydrolases and proteases, cathepsins play an important role. E64d is an inhibitor of lysosomal cathepsins B, H, and L, while pepstatin A is an inhibitor of cathepsins D and E, both of which inhibit autophagy by inhibiting lysosomal proteases (Moriyasu and Inoue 2008). Leupeptin is a naturally occurring protease inhibitor that inhibits serine and cysteine proteases, blocking autophagy at the step of lysosomal degradation of autophagic substrates, leading to the accumulation of autophagolysin. Lysosomal enzymes can be divided into three types of enzymes: cysteine, serine, and aspartic acid. Therefore, a single protease inhibitor may not be suitably effective. The use of a combination of lysosomal enzyme inhibitors has been previously recommended (Kominami et al. 1983), such as E64d and pepstatin A (1:1). Pepstatin A is a hydrophobic molecule that needs to be dissolved in DMSO or ethanol, so stimulation with this compound requires a long duration (>8 h) and high concentration (>50 g/mL), while for E64d, stimulation with only 10 g/mL for 1 h can inhibit lysosomal activity. It was reported that the combination of E64d and pepstatin A in colon cancer cell lines can significantly inhibit the degradation of lysosomes and block the progression of autophagy, while the formation of autophagosomes is not significantly affected. The reactivation of endogenous LC3-II in lysosomes can be observed after E64d- and

pepstatin A-mediated inhibition of autophagy. After starvation, the accumulation of LC3-positive staining spots on autophagosomes after E64d and pepstatin A treatment was observed, suggesting that starvation-induced autophagy was inhibited by E64d and pepstatin A, leading to autophagolysosome accumulation. However, it has recently been reported in the literature that the combination of E64d and pepstatin A promotes the degradation of GFP-LC3 in lysosomes and increases the number of free fragments of GFP in cells. The number of free fragments of GFP is thought to reflect the level of autophagic flux, so the above results suggest that E64d and pepstatin A promote autophagic flux, which is exactly the opposite of the results of previous studies. The reason for this contradictory result may be that under certain circumstances (e.g., unsaturated protease inhibitors), some lysosomal inhibitors only partially inhibit cathepsin activity; therefore, lysosomal degradation or GFP-LC3 is not completely inhibited.

13.3 Potential Applications of Autophagy Regulators

Autophagy is the main pathway for the degradation of long-lived proteins and cytoplasmic organelles in eukaryotic cells. Studies on many eukaryotic systems have shown that autophagy is conserved and that the mechanism of autophagy in higher eukaryotes is similar to that in yeast. As early as the 1970s, Christian de Duve, a Nobel Prize winner in physiology, predicted the importance of autophagy for animal physiology. Although autophagy was discovered nearly 50 years ago, studies in the field of autophagy have only recently gained popularity. Many problems regarding autophagy have not been well explained or solved. Research methods to study autophagy are constantly improving. Specific inducers and inhibitors of autophagy are constantly being discovered (Klionsky et al. 2016), as shown in Fig. 13.1. Confucius said, “If you want to do something good, you must first sharpen your tools.” The advancement of autophagy research methods and the discovery of specific regulators have an important impact on the study of autophagy mechanisms and have clinical value. However, there remain some issues associated with the use of autophagy regulators that require attention.

13.3.1 Specificity of Autophagy Inhibitors and Inducers

Autophagy inducers or inhibitors are frequently used in autophagy studies. Therefore, researchers must consider the specificity of these inducers and inhibitors. Most autophagy inducers and inhibitors are not 100% specific, so special attention needs to be paid to the side effects of these drugs.

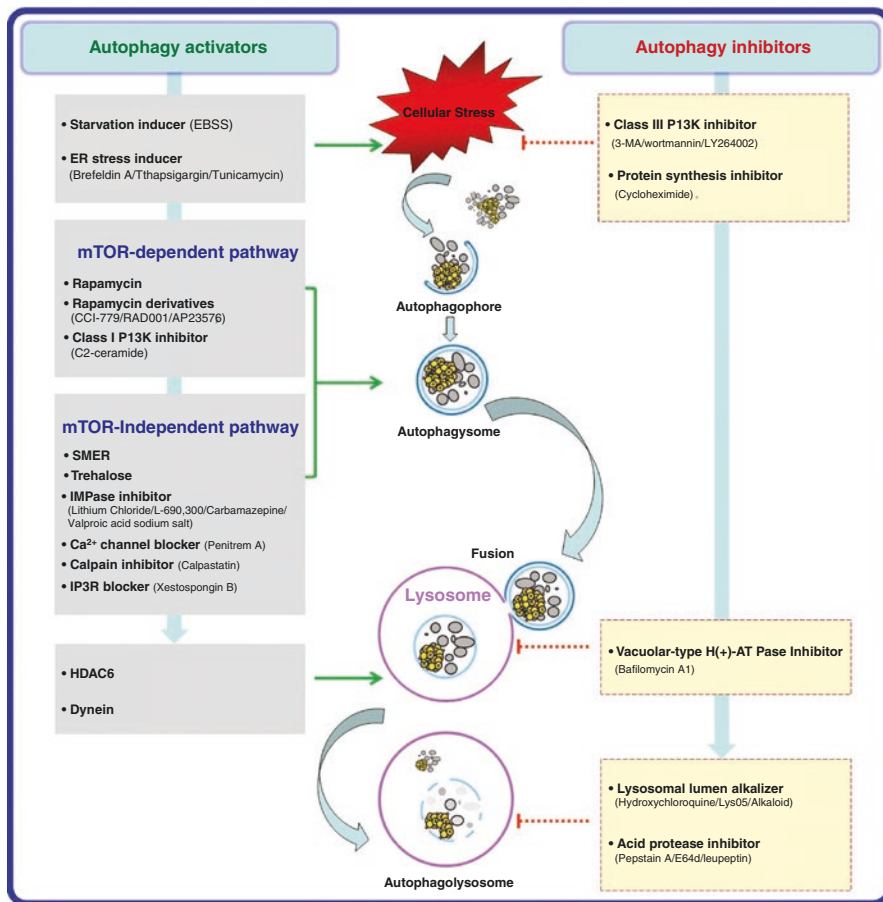


Fig. 13.1 Chemical autophagy regulators. Autophagy inducers activate autophagy in the stage of autophagosome formation, upstream signaling pathways, and autophagosome-lysosome fusion. Autophagy inhibitors decrease autophagy by inhibiting autophagosome formation, autophagosome-lysosome fusion, and autolysosomal degradation

With the help of the autophagy inducer rapamycin and the autophagy inhibitor bafilomycin A1, we can better understand the relationship between autophagy and disease. However, inhibition of mTOR signaling by rapamycin not only activates autophagy but also inhibits translational expression of a large number of proteins, resulting in immunosuppression, cell cycle arrest, and changes in cell shape. Similarly, bafilomycin A1 is a vesicular ATPase inhibitor. In addition to its role in the fusion of autophagosomes and lysosomes or the degradation of autophagosomes by lysosomes, this compound also plays a wide-ranging role in other vesicle fusion

events, so the side effects of this compound are also evident. The lysosomal basifying agents chloroquine and hydroxylated chloroquine may be more suitable for inhibiting autophagy than bafilomycin A1. However, it has been reported that in addition to preventing the accumulation of autophagic vacuoles formed by the fusion of autophagosomes and lysosomes, chloroquine can also stimulate an increase in autophagosome formation, but the reason is not clear. This process may be inhibited by lysosomal function, leading to a lack of amino acids stored in cells, which is associated with increased autophagy. This hypothesis has been confirmed in hepatocytes.

Due to the lack of specificity of autophagy inhibitors, appropriate controls must be used in the experiment. It is recommended that starvation or rapamycin be used to induce autophagy as a positive control for autophagy activation. However, in some cells, rapamycin exhibits slower onset of effects and may trigger other reactions. Due to the pleiotropic effects of the drug, it is necessary to verify that autophagy is indeed induced or inhibited prior to carrying out subsequent research. In addition, although inducers or inhibitors of autophagy can rapidly or artificially activate or inhibit autophagy, given the relative specificity of genetic intervention, it is best to use genetic methods to verify the relevant experimental results. A combination of chemical tools and genetic methods can be used to identify the main role of the autophagy pathway.

13.3.2 Difference Between Autophagy Activation and Autophagic Flux Completion

As the study of autophagy progresses from physiological homeostasis to pathological state, we should redefine autophagy and its related processes. The autophagy process has distinct stages. Because the autophagosome itself lacks enzymatic activity, fusion of autophagosome with lysosomes allows the degradation of the substrate protein in the lysosome, which is a decisive step in the completion of autophagic flux. Only completion of the entire autophagic flux can lead to the degradation of the autophagic substrate protein and completion of the autophagy process. Therefore, an increase in autophagosome levels does not necessarily indicate an up-regulation of autophagic activity but may instead reflect an imbalance between the autophagy substrate protein isolation and degradation. Autophagic stress refers to the imbalance between these two rates, for example, if the autophagosome formation rate exceeds the autophagy substrate protein degradation rate. An increasing number of studies have also shown that autophagy stress is closely related to cell death and neurodegeneration. Therefore, when using autophagy inducers, special attention must be paid to whether the inducer promotes the completion of the entire autophagic flux or only causes autophagic stress (Singh and Bhaskar 2019). In this regard, it may be necessary to consider the combined application of inducers or inhibitors targeting different phases of autophagy.

13.3.3 Combined Medication

Combinations of inducers or inhibitors at different stages of autophagy can enhance the effect of autophagy regulators on the whole process of autophagic flux. The combination of the autophagosome formation inhibitor cycloheximide and the lysosomal inhibitor leupeptin shows a strong inhibitory effect on autophagy. It can rapidly inhibit the formation of autophagic vacuoles and the isolation of cytoplasmic and lysosomal enzymes.

In addition, to counteract the negative regulation of autophagy induced by lithium-mediated mTOR activation, we can combine the mTOR-dependent autophagy inducer rapamycin and non-mTOR-dependent autophagy inducer lithium: rapamycin attenuates the activity of mTOR, lithium reduces the level of IP₃, and simultaneous induction of autophagy by these two agents greatly increases autophagy. It has been reported that these two drugs have synergistic effects on the clearance of mutant α -synucleins and huntingtin and on inhibition of neuronal cell death. This combination therapy may also benefit from the inhibition of GSK-3 β by lithium, which leads to activation of the β -catenin pathway. However, the combined use of rapamycin and other independent mTOR autophagy inducers other than lithium has yet to be further studied.

In general, combined medication will help increase the impact on autophagy levels compared to that of a single regulator. In addition, combined medication will also require lower amounts of each regulator, thus reducing the side effects of the regulator, making the regulator safer for long-term use. Therefore, we predict that the combination of drugs will be a hot spot in the study of autophagy regulation, and a new trend for the development of clinical applications of autophagy regulators in diseases such as neurodegenerative diseases.

References

- Amaravadi RK, Winkler JD. Lys05: a new lysosomal autophagy inhibitor. *Autophagy*. 2012;8:1383–4.
- Cao BY, Yang YP, Luo WF, Mao CJ, Han R, Sun X, Cheng J, Liu CF. Paoniflorin, a potent natural compound, protects PC12 cells from MPP+ and acidic damage via autophagic pathway. *J Ethnopharmacol*. 2010;131:122–9.
- Dengjel J, Hoyer-Hansen M, Nielsen MO, Eisenberg T, Harder LM, Schandorff S, Farkas T, Kirkegaard T, Becker AC, Schroeder S, Vanselow K, Lundberg E, Nielsen MM, Kristensen AR, Akimov V, Bunkenborg J, Madeo F, Jaattela M, Andersen JS. Identification of autophagosome-associated proteins and regulators by quantitative proteomic analysis and genetic screens. *Mol Cell Proteomics*. 2012;11:M111.014035.
- Dobrenel T, Caldana C, Hanson J, Robaglia C, Vincentz M, Veit B, Meyer C. TOR signaling and nutrient sensing. *Annu Rev Plant Biol*. 2016;67:261–85.
- East DA, Campanella M. Ca²⁺ in quality control: an unresolved riddle critical to autophagy and mitophagy. *Autophagy*. 2013;9:1710–9.
- Gros F, Muller S. Pharmacological regulators of autophagy and their link with modulators of lupus disease. *Br J Pharmacol*. 2014;171:4337–59.

- Hosseinpour-Moghaddam K, Caraglia M, Sahebkar A. Autophagy induction by trehalose: molecular mechanisms and therapeutic impacts. *J Cell Physiol.* 2018;233:6524–43.
- Klionsky DJ, Elazar Z, Seglen PO, Rubinsztein DC. Does bafilomycin A1 block the fusion of autophagosomes with lysosomes? *Autophagy.* 2008;4:849–50.
- Klionsky DJ, Abdelmohsen K, Abe A, Abedin MJ, Abeliovich H, Acevedo Arozena A, Adachi H, Adams CM, Adams PD, Adeli K, Adhietty PJ, Adler SG, Agam G, Agarwal R, Aghi MK, Agnello M, Agostinis P, Aguilar PV, Aguirre-Ghiso J, Airoidi EM, Ait-Si-Ali S, Akematsu T, Akporiaye ET, Al-Rubeai M, Albaiceta GM, Albanese C, Albani D, Albert ML, Aldudo J, Algul H, Alirezaei M, Alloza I, Almasan A, Almonte-Beceril M, Alnemri ES, Alonso C, Altan-Bonnet N, Altieri DC, Alvarez S, Alvarez-Erviti L, Alves S, Amadoro G, Amano A, Amantini C, Ambrosio S, Amelio I, Amer AO, Amessou M, Amon A, An Z, Anania FA, Andersen SU, Andley UP, Andreadi CK, Andrieu-Abadie N, Anel A, Ann DK, Anoopkumar-Dukie S, Antonoli M, Aoki H, Apostolova N, Aquila S, Aquilano K, Araki K, Arama E, Aranda A, Araya J, Arcaro A, Arias E, Arimoto H, Ariosa AR, Armstrong JL, Arnould T, Arsov I, Asanuma K, Askanas V, Asselin E, Atarashi R, Atherton SS, Atkin JD, Attardi LD, Auberger P, Auburger G, Aurelian L, Autelli R, Avagliano L, Avantaggiati ML, Avrahami L, Awale S, Azad N, Bachetti T, Backer JM, Bae DH, Bae JS, Bae ON, Bae SH, Baehrecke EH, Baek SH, Baghdiguiyan S, Bagniewska-Zadworna A, et al. Guidelines for the use and interpretation of assays for monitoring autophagy (3rd edition). *Autophagy.* 2016;12:1–222.
- Kominami E, Hashida S, Khairallah EA, Katunuma N. Sequestration of cytoplasmic enzymes in an autophagic vacuole-lysosomal system induced by injection of leupeptin. *J Biol Chem.* 1983;258:6093–100.
- Lawrence BP, Brown WJ. Inhibition of protein synthesis separates autophagic sequestration from the delivery of lysosomal enzymes. *J Cell Sci.* 1993;105(Pt 2):473–80.
- Levine B, Packer M, Codogno P. Development of autophagy inducers in clinical medicine. *J Clin Invest.* 2015;125:14–24.
- Liu Y, Wan WZ, Li Y, Zhou GL, Liu XG. Recent development of ATP-competitive small molecule phosphatidylinositol-3-kinase inhibitors as anticancer agents. *Oncotarget.* 2017;8:7181–200.
- Mancinelli R, Carpino G, Petrunaro S, Mammola CL, Tomaipitina L, Filippini A, Facchiano A, Ziparo E, Giampietri C. Multifaceted roles of GSK-3 in cancer and autophagy-related diseases. *Oxid Med Cell Longev.* 2017;2017:4629495.
- McAfee Q, Zhang Z, Samanta A, Levi SM, Ma XH, Piao S, Lynch JP, Uehara T, Sepulveda AR, Davis LE, Winkler JD, Amaravadi RK. Autophagy inhibitor Lys05 has single-agent antitumor activity and reproduces the phenotype of a genetic autophagy deficiency. *Proc Natl Acad Sci U S A.* 2012;109:8253–8.
- Moriyasu Y, Inoue Y. Use of protease inhibitors for detecting autophagy in plants. *Methods Enzymol.* 2008;451:557–80.
- Nakamura S, Yoshimori T. New insights into autophagosome-lysosome fusion. *J Cell Sci.* 2017;130:1209–16.
- Noda NN, Inagaki F. Mechanisms of autophagy. *Annu Rev Biophys.* 2015;44:101–22.
- Pasquier B. Autophagy inhibitors. *Cell Mol Life Sci.* 2016;73:985–1001.
- Russo M, Russo GL. Autophagy inducers in cancer. *Biochem Pharmacol.* 2018;153:51–61.
- Sarkar S. Regulation of autophagy by mTOR-dependent and mTOR-independent pathways: autophagy dysfunction in neurodegenerative diseases and therapeutic application of autophagy enhancers. *Biochem Soc Trans.* 2013;41:1103–30.
- Sarkar S, Rubinsztein DC. Inositol and IP3 levels regulate autophagy: biology and therapeutic speculations. *Autophagy.* 2006;2:132–4.
- Saxton RA, Sabatini DM. mTOR signaling in growth, metabolism, and disease. *Cell.* 2017;169:361–71.
- Senft D, Ronai ZA. UPR, autophagy, and mitochondria crosstalk underlies the ER stress response. *Trends Biochem Sci.* 2015;40:141–8.

- Shanware NP, Bray K, Abraham RT. The PI3K, metabolic, and autophagy networks: interactive partners in cellular health and disease. *Annu Rev Pharmacol Toxicol.* 2013;53:89–106.
- Singh B, Bhaskar S. Methods for detection of autophagy in mammalian cells. *Methods Mol Biol.* 2019;2045:245–58.
- Wu YT, Tan HL, Shui G, Bauvy C, Huang Q, Wenk MR, Ong CN, Codogno P, Shen HM. Dual role of 3-methyladenine in modulation of autophagy via different temporal patterns of inhibition on class I and III phosphoinositide 3-kinase. *J Biol Chem.* 2010;285:10850–61.

Chapter 14

Cell Models in Autophagy Research



Rui Huang and Shuyan Wu

Abstract Autophagy is highly conserved in organisms ranging from yeast to humans. *C. elegans*, *D. melanogaster*, zebrafish, and mice have been extensively used to study autophagy, though each of them has shortcomings. Suitable cell models are very important, and there is considerable potential for them to help advance autophagy research. Cell models have advantages in speed, stability, economy, etc. Moreover, experimental conditions are more easily controlled in cell models than in animal models. More than 40 *ATG* genes have been found in budding yeast and other fungi since 1992. As a model organism, yeast has a unique place in autophagy research and has become the most widely used cell model. It is almost equal to *E. coli* in terms of rapid proliferation, ease of culture, and handling. Yeast is also a good host for eukaryotic gene expression and can be used for screens that help clarify the function of unknown genes. However, as a lower unicellular organism, it is unable to show tissue-specific regulation of autophagy. Cells from higher organisms, such as humans or other animals, are indispensable. Deeper and more extensive study of autophagy using cell models such as nervous tissue-derived cell models, epithelial tissue-derived cell models, muscle tissue-derived cell models, blood cell, and immune cell models has made significant progress.

Although significant achievements in autophagy have been obtained in recent years, the problems that need to be solved have also become more and more complicated. Using suitable cell models to reveal the relationship between autophagy and disease has received increasing attention from autophagy researchers. Autophagy, firstly discovered by Christian de Duve in early 1960s, is highly conserved in organisms ranging from yeast to humans. In recent years, *C. elegans*, *D. melanogaster*, zebrafish, and mice have been extensively used to study autophagy due to their clear genetic background, short generational period, large numbers of offspring, mature

R. Huang · S. Wu (✉)
Medical School of Soochow University, Suzhou, China
e-mail: wushuyan@suda.edu.cn

Table 14.1 The advantages and disadvantages of model organisms to study autophagy

Model organisms	Advantages	Disadvantages
<i>C. elegans</i>	Easy to observe and detect due to its transparency; simple structured and defined cell lineages; genes are easily modified by RNAi; has two genders (male and hermaphrodite); fecund and easy to obtain mass mutants; extensively used to study mechanisms of autophagy regulation	Not as closely related to humans, and has highly nonrepetitive DNA; has only innate rather than adaptive immune system, so can not be used to establish systemic infectious models; some Atgs in yeast and mammals are lacking in nematodes
<i>D. melanogaster</i>	With plentiful phenotypes and many variants, mutant traits are easy to observe; highly homologous with human genes and can be used to study neurodegenerative disorders, tumor, infection, immunity, etc.	Has only innate rather than adaptive immune system, so can not be used to establish systemic infectious models to study immune disease
Zebrafish	Easy to observe due to transparency of embryo and larvae, so can be used to study the invasion, reproduction, and transmission of pathogens; nervous system, visceral organ, and blood circulatory system are highly homologous to humans on a genetic and developmental level, which is conducive to the study of relevant diseases; with both innate and adaptive immune systems, can be used to study the interaction between pathogens and host immune response	Some Atgs in yeast and mammals are lacking in zebrafish
Mouse	99% similar to humans at the genetic level; sensitive to stimulation and indispensable for biomedicine; can be used to study almost all autophagy-related diseases	Compared with other model organisms, have longer generational period and higher housing cost

phenotypic analysis, and genetic manipulation, all of which can help to solve remaining mysteries. However, each model organism has its shortcomings (Table 14.1). For example, *C. elegans* and *D. melanogaster* have only an innate, rather than adaptive, immune system and can not be used to establish systemic infection models to study diseases related to infection and immunity (Kuo et al. 2018). Some autophagy-related genes (*Atgs*) present in mammalian cells lack homologous genes in zebrafish (Varga et al. 2015). Compared with other model organisms, mice have longer generational periods and higher housing cost. Therefore, by virtue of the conservation of autophagy mechanisms, using suitable cell models help to avoid these problems. Compared with animal models, cell models have advantages in speed, stability, economy, etc. For instance, experimental conditions are more easily controlled, biochemical markers are more easily detected, and the morphology of living cells can be observed directly. This chapter will focus on the application of yeast and mammalian cell models in autophagy research.

14.1 Yeast in Autophagy Research

In the early 1990s, many biologists such as Y. Ohsumi and D. Klionsky made extensive efforts to screen relevant genes, and to study the cell biology and mechanisms of autophagy using *Saccharomyces cerevisiae* (budding yeast). More than 40 *ATGs* have been found in budding yeast and other fungi since 1992 and yeast has become the most widely used cell model to study mechanisms of cell autophagy.

14.1.1 Superiority of the Yeast Model in Autophagy

Yeast is a unicellular eukaryote almost equal to the prokaryote *Escherichia coli* (*E. coli*) in terms of rapid proliferation, ease of culture, and handling. As one of the best known model organisms, yeast is the first choice due to the conservation of processes such as autophagy, senescence, etc. with higher organisms. Yeast is also a good host for eukaryotic gene expression. Larger and more effective cloning systems, for example yeast artificial chromosomes (YAC), can be constructed by taking advantage of yeast chromosomes. The life cycle of yeast is suitable for classic genetic analysis, which makes it possible to construct subtle genetic maps. Foreign genes can be inserted into specific position in the yeast genome due to its high homologous recombination rate, which provides convenient to molecular biology techniques. In addition, yeast can be used for screens that help clarify the function of unknown genes by functional complementation of yeast mutants with heterologous genes. In addition, many genes related to hereditary human diseases are highly homologous in yeast. Therefore, studying the physiological function of proteins encoded by these genes and their interactions with other proteins can help to diagnose and cure relevant diseases.

14.1.2 Classification of Yeast Autophagy

There are many kinds of autophagy in yeast. Autophagy can be classified based on two different criteria: (1) macroautophagy, microautophagy, and chaperone-mediated autophagy based on way that the substrate is transported to lysosome, (2) selective and nonselective autophagy according to the nature of the substrates. In nonselective autophagy, the substances engulfed in the autophagosomes are chosen randomly and transported to the lysosome for degradation, reflecting bulk cytosol. Previously, nonselective autophagy was considered to be the primary pathway of autophagy. However, recent evidence suggests that selective autophagy also plays an important role in degrading substrates specifically. In 2013, Kuninori Suzuki

Table 14.2 Classification of selective autophagy in *Saccharomyces cerevisiae*

Autophagy types	Pathways	Targets	Characteristics
Atg11-dependent	The Cvt pathway	Intrinsic hydrolases	Targeted transport from cytoplasm to vacuole, Atg19 and Atg34 as receptor proteins and Atg11 as a scaffold protein
	Mitophagy	Mitochondria	Atg32 as a receptor protein and Atg11 as a scaffold protein
	Pexophagy	Peroxisomes	Atg30 and Atg36 as receptor proteins, and Atg11 and Atg17 as scaffold proteins
	Piecemeal microautophagy of the nucleus	NVJ	Dependent on core autophagy proteins and the interaction between vacuolar membrane Vac8 and outer nuclear membrane Nvj1
Atg11-independent	Ald6 degradation	Ald6	Dependent on core autophagy protein and active vacuole proteases
	Ribophagy	Ribosome	Occurred when ubiquitin proteases Ubp3 or Bre5 are deficient

classified selective autophagy in *Saccharomyces cerevisiae* into highly selective autophagy and less selective autophagy according to Atg11 dependence (Table 14.2) (Suzuki 2013). The former, highly selective category depending on Atg11 comprises the Cvt pathway, mitophagy, pexophagy, and piecemeal microautophagy of the nucleus; Autophagic degradation of acetaldehyde dehydrogenase 6 (Ald6) and ribophagy belong to the latter, less selective category, which is independent of Atg11. Atg11 is a protein found at the periphery of the preautophagosomal structure (PAS) and interacts with Atg1, Atg9, Atg29, Atg19, and Atg20 as an adapter and scaffold protein in selective autophagy. The following paragraphs will give a brief description of selective autophagy in *Saccharomyces cerevisiae*.

14.1.2.1 Atg11-Dependent Selective Autophagy

14.1.2.1.1 The Cvt Pathway

The Cvt pathway, which belongs to selective autophagy, is responsible for the transport of intrinsic hydrolases PrApel and Ams1 from cytoplasm to vacuole under nutrient-rich conditions. PrApel and Ams1 combine with the receptor protein Atg19 at different sites to form the Cvt complex, which is located at the PAS after the interplay between Atg19 and Atg11. Atg34, which is homologous to Atg19, transports Ams1 to vacuole as an Ams1 receptor during starvation.

14.1.2.1.2 Mitophagy

When exposed to external stresses such as reactive oxygen species (ROS), nutritional deficiency or cell senescence, damaged mitochondria are engulfed by autophagosome then delivered to the lysosome/vacuole to be degraded; this process is termed as mitophagy. In 2009, the Klionsky and Ohsumi labs found that the mitochondrial protein Atg32 functions as a mitochondria receptor, localizing to the PAS after interacting with Atg11. Atg32 also interacts with Atg8 to help in autophagosome formation.

14.1.2.1.3 Pexophagy

The function of peroxisome is to degrade lipids and cellular superoxide. Redundant or damaged peroxisomes can be degraded by autophagy. Peroxisomes are identified when receptor proteins Atg30 and Atg36 connect to Atg11, Atg17, and Pex14 (Pex14 is the peroxisomal surface marker used to recognize peroxisomes in yeast autophagy).

14.1.2.1.4 Piecemeal Microautophagy of the Nucleus

The nuclear membrane and nucleoplasm are invaginated and subsequently degraded by vacuolar hydrolases during nutritional deficiency, which is called piecemeal microautophagy of the nucleus (PMN). During PMN, the nucleus-vacuole junction (NVJ) is formed by interactions between vacuolar membrane-localized Vac8 and outer nuclear membrane localized Nvj1. Finally, the nucleus is degraded, assisted by core Atg protein Atg11 and other Atg proteins Atg17, Atg29, and Atg31.

14.1.2.2 Atg11-Independent Selective Autophagy

14.1.2.2.1 Ald6 Degradation

Ald6 is an enzyme that disappears after 24 h of nitrogen starvation in yeast. Ald6 is engulfed in autophagosomes then delivered to vacuole for degradation, with help of core Atg proteins and active vacuolar proteases. Researchers have found that the accumulation of active Ald6 could lead to the rapid death of autophagy-defective cells (Qin 2015).

14.1.2.2.2 Ribophagy

In *Saccharomyces cerevisiae* deficient in ubiquitin protease Ubp3 or Bre5, the degradation of ribosomes independent of Atg11 involves a novel type of selective autophagy termed ribophagy. In cells deficient in ribophagy, autophagy pathways other than ribophagy appear to be normal. However, the mechanisms remain unknown.

14.1.3 Molecular Mechanisms of Yeast Autophagy

The molecular mechanisms of autophagy have been investigated most thoroughly in yeast. The whole process of autophagy is regulated by different autophagy-related proteins. The genes that encode autophagy-related proteins are highly conserved in yeast and mammals. The deletion or mutation of any gene will result in dysregulation or even termination of autophagy. With continued study of autophagy, more and more new Atgs and the function of Atg homologs are being revealed. In addition, the functions of some core autophagy proteins are becoming well understood. The 18 core autophagy proteins can be classified into five multifunctional modules according to the different steps that they participate in (Fig. 14.1): the Atg1 kinase complex, vesicles containing the integral membrane protein Atg9, the class III phosphoinositide 3-kinase (PI3K) complex I, the Atg2-Atg18 complex, the Atg8-phosphatidylethanolamine (PE), and the Atg5-Atg12 conjugation systems (Farre and Subramani 2016; Suzuki et al. 2017).

14.1.3.1 The Atg1 Kinase Complex

The Atg1 kinase complex, also known as the autophagy initiation complex, is directly regulated by several kinases such as TOR kinase complex I and AMP-activated protein kinase. As the core of the PAS, the Atg1 kinase complex plays an upstream role in autophagy. The Atg1 kinase complex of budding yeast is

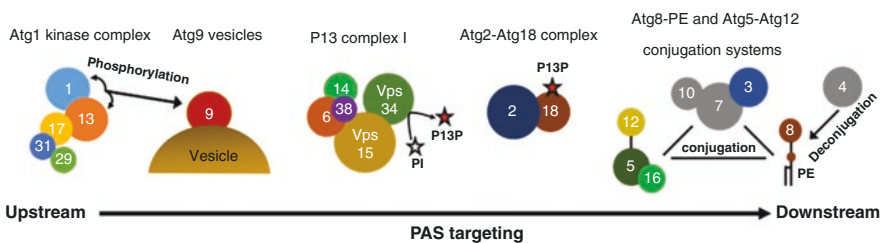


Fig. 14.1 Molecular mechanisms of yeast autophagy. Core Atg proteins in yeast are targeted to the PAS. Atg proteins are indicated by spheres with numbers (Suzuki et al. 2017)

comprised of five components: Atg1, Atg13, Atg17, Atg29, and Atg31. Atg1 is the only protein kinase among core autophagy proteins and is homologous with ULK1 in mammals, and binds to Atg13 to induce autophagy. Unlike the flexible structures seen for Atg1 and Atg13, Atg17 folds into a unique S-shaped homodimer. Atg29 and Atg31 form a stable heterodimer and bind to Atg17. Finally, the Atg17-Atg29-Atg31 complex is formed. However, the interaction of Atg17-Atg29-Atg31 complex with Atg1 and Atg13 is regulated by nutrient conditions. Under nutrient-rich conditions, the formation of the pentamer is impaired because of the serine phosphorylation in the binding regions, which inhibits autophagy.

14.1.3.2 Vesicles Containing the Integral Membrane Protein Atg9

Atg9 is the first Atg protein to be identified that locates to unique membrane structures in addition to the PAS. As the only integral membrane protein among core autophagy proteins, Atg9 has six transmembrane helical domains. It travels through the endoplasmic reticulum and Golgi complex, then cycles between the PAS and a pool of peripheral membrane structures that may be Golgi-derived. At the PAS, it participates in the expansion of the autophagosomal membrane expansion with the help of other autophagy-related proteins. The recruitment of Atg9 to the PAS depends on Atg17 during rapamycin or starvation induced autophagy, and Atg1 may regulate the assembly and disassembly of Atg9 in the PAS. The anterograde movement of Atg9 depends on Atg23 and Atg27, because Atg9 binds to Atg23 and Atg27 and this is required for its efficient transport to the PAS during starvation. In addition, Atg9 can bind to Atg2 and Atg18, and these proteins allow Atg9 to be transported back from the PAS to the peripheral structures, under the regulation of Atg1-Atg13 complex. In 2010, Muriel Mari found via immunoelectron microscopy that the peripheral structures were a novel compartment comprising clusters of vesicles and tubules (Mari et al. 2010). They also showed that these clusters were the same as the PAS in morphology, speculating that Atg9 was involved in the origin of the PAS. In 2016, Rao revealed the mechanism by which the autophagy initiation complex promoted Atg17-mediated tethering of Atg9-vesicles, and suggested that the membrane of autophagosome originated from the fusion of Atg9-vesicles (Rao et al. 2016).

14.1.3.3 The PI3K Complex I

The autophagy-specific PI3K complex, also known as PI3K complex I in yeast and class III PI3K complex I in mammals, comprises Vps34, Vps15, Atg6/Vps30 (Beclin 1 in mammals), Atg14, and the recently identified Atg38 (NRBF2 in mammals). Phosphatidylinositol (PI) can be phosphorylated by PI3K complex I to form Phosphatidylinositol-3-phosphate (PI3P), which plays an important role in autophagy initiation complex formation and determines the regulatory effect of downstream factors on autophagy. The PI3K complex I has a unique V-shaped architecture,

where one arm of the V is comprised of a parallel coiled-coil heterodimer of Atg6 and Atg14 and partial domain of Vps15, whereas the other arm is comprised of helical domains from Vps34 and Vps15. In addition, the homodimer of Atg38 is at the bottom of V. Based on this structure, when the PI3K complex I localizes to the PAS, the V shape faces the autophagosome membrane while the bottom is exposed to the cytoplasm. PI3K complex I recruits autophagy-related proteins by producing PI3P at the PAS in a manner dependent on the autophagy initiation complex and Atg9. PI3K complex II, which contains Vps34, Vps15, Vps38, and Atg6, mainly participates in the multivesicular body pathway rather than autophagy.

14.1.3.4 The Atg2-Atg18 Complex

Atg2 is a large soluble protein whose domains have been unclear for a long time. It was reported that Atg2 could localize to lipid droplets in mammals, suggesting it itself is capable of interacting with lipids. Atg18 is predicted to have two binding pockets for PI3P based on the structure of Hsv2, an Atg18 homolog. PI3P and Atg2 bind to the opposite side of Atg18. As a big protein, the interaction of Atg2 with the membrane and with membrane-bound Atg18 may happen simultaneously. Additionally, the location of Atg2-Atg18 complex at the expanding edge of the isolation membrane suggests that the complex plays a crucial role in both the elongation and closure of the isolation membrane.

14.1.3.5 The Atg8-PE and the Atg5-Atg12 Conjugation Systems

There are two ubiquitin-like conjugation systems involved in autophagy, the Atg8-PE and the Atg5-Atg12 conjugation systems. Eight of the eighteen Atg proteins that constitute the core autophagy machinery are in the Atg8-PE and Atg5-Atg12 conjugation systems. The resulting Atg8-PE and Atg5-Atg12 conjugates play important roles in the initialization and extension of autophagosome membrane. The Atg5-Atg12 conjugate contains one ubiquitin fold from Atg12 and two ubiquitin folds from Atg5. The two in Atg5 interact with each other to create a globular architecture. Together with Atg16, the Atg5-Atg12 conjugate rearranges the catalytic site of Atg3 (the E2-like conjugation enzyme) and acts as an E3-like enzyme in the conjugation of Atg8 to PE. Atg16 not only binds to Atg5, but also facilitates Atg8 attachment to PE by enhancing the membrane-binding activity of the Atg5-Atg12 conjugate. Additionally, through an interaction between Atg12 and Atg8, the Atg5-Atg12-Atg16 complex and Atg8-PE form a membrane scaffold to promote the formation of autophagosomes. One accepted function of the Atg8-PE conjugate is recognizing cargos as a receptor during selective autophagy. Besides cargo recognition, the Atg8-PE conjugate appears to have a critical role in autophagosome formation, including a probably role in the building of the autophagosome membrane.

14.1.4 *Autophagy in Other Types of Yeast*

In the early 1990s, biologists studied autophagy mainly in *Saccharomyces cerevisiae*, which is a type of budding yeast. However, whether or not the mechanisms were the same in other organisms remained unclear. Fission yeast is unicellular eukaryote, so named because it divides by fission instead of budding. Both it and *S.cerevisiae* belong to Sac fungi. However, fission yeast is very evolutionarily divergent from *S.cerevisiae*. The genome length of fission yeast is 13.8 Mb, and it contains 4824 genes distributed on three chromosomes. There are 50 genes similar to human disease-related genes and some are relevant to cancer genes. The fission yeast genome was sequenced in 2002 and there are 1000 fewer protein-encoding genes than in *S.cerevisiae*. In addition, many researchers have demonstrated that two yeasts above are different in cell cycle, rRNA biosynthesis, genetic structure, and regulation, etc. Fission yeast is a good model eukaryote due to its similarity to higher organisms. In 2013, two novel autophagy-related effectors were found from *Schizosaccharomyces pombe*, Ctl1, and Fsc1. *Ctl1* encoded a choline transporter-like (CTL) protein while *Fsc1* encoded a protein containing 5 fasciclin domains. By study of mutants using electron microscopy, subcellular localization, fluorescence loss in photobleaching (FLIP), etc., researchers found that Ctl1 was essential for the PAS assembly and required for autophagosome formation by interacting with Atg9. Autophagosomes were unable to fuse with vacuole normally in *Fsc1* knockout fission yeast, suggesting that Fsc1 was essential for autophagosome-vacuole fusion. Unlike in *S. cerevisiae*, Atg18 is essential for the targeting of the Atg5-Atg12 conjugate to the PAS in fission yeast, as shown using co-immunoprecipitation. In 2017, Nanji T found that the Atg1 complex of the fission yeast *Schizosaccharomyces pombe* was similar to budding yeast *S. cerevisiae*, and contained subunits of Atg1, Atg13, and Atg17 but not Atg29 and Atg31. However, unlike *S. cerevisiae*, it contained an Atg101 protein structurally similar to human ATG101. Therefore, *Schizosaccharomyces pombe* was a superb model to study the ULK1/2 complex of higher organisms due to its unique Atg1 complex (Nanji et al. 2017). Besides fission yeast, biologists have also studied autophagy in filamentous fungi during the past few years, finding that autophagy is an essential process to sustain high energy levels for filamentous growth and multicellular development even under nonstarvation conditions (Voigt and Poggeler 2013). These conclusions confirmed that other yeasts are also excellent model organisms to study the mechanisms of autophagy.

14.1.5 *Methods to Study Yeast Autophagy*

Many methods to study yeast autophagy have been previously described. Besides detection of the degradation of Atg8/LC3 by Western blot, fluorescently labeling of autophagy-related proteins and morphological observation by electron microscopy, there are also some specific methods to detect yeast autophagy.

14.1.5.1 The Pho8 Δ 60 Assay

The Pho8 Δ 60 assay, also called alkaline phosphatase (ALP) assay, is a method for quantitative detection of yeast autophagy. *Pho8* is the only gene encoding ALP in the yeast vacuole. The product of *Pho8*, which is a type II transmembrane protein, transits to the vacuole after being synthesized in the endoplasmic reticulum and processed by the Golgi complex, finally becoming activated ALP after its C-terminal peptide is excised by proteases in the vacuole. The 60 amino acids in N-terminal transmembrane domain, which mediate the transportation of pre-Pho8, can be excised to construct Pho8 Δ 60. Pho8 Δ 60 synthesized in the cytosol will be engulfed in autophagosomes then delivered to vacuole to be activated when autophagy occurs. Therefore, the magnitude of autophagy could be monitored by alkaline phosphatase activity.

14.1.5.2 Detection of mApel

PrApel (as mentioned above) usually enters the vacuole in the Cvt pathway. However, under starvation or adverse conditions, PrApel enters the vacuole via a nonselective autophagy pathway. Once in the vacuole it is processed to become mApel. Because the molecular weight of prApel and mApel is different, mApel can be detected by Western blot to evaluate autophagy or the Cvt pathway.

Autophagy is one of the hotspots in cellular biology. With an increasing number of laboratories entering this field, autophagy research has boomed in recent years. As a model organism, yeast has a unique role in the study of autophagy. However, as a lower unicellular organism, yeast is unable to communicate between cells or show tissue-specific regulation of autophagy. Thus, higher organisms are indispensable for further breakthroughs in autophagy research.

14.2 The Applications of Human or Animal Cell Models in Autophagy Research

As a unicellular fungus, yeast has a primitive evolutionary status, possessing a cell wall, cytoplasm with vacuoles, and reproduction by spores. There are obvious structural differences between yeast and human or animal cells. For example, there is no cell wall or obvious vacuole in the cytoplasm of human or animal cells. Therefore, in addition to yeast cells, the establishment of human and animal cell models also has a profound and lasting significance in revealing the mechanism of autophagy and the relationship between autophagy and disease.

14.2.1 The Applications of Nervous Tissue-Derived Cell Models in Autophagy Research

The nervous tissue consists of neurocytes and neurogliaocytes. Neurocytes, also named neurons, are capable of receiving stimuli, integrating information, and transmitting impulses. Neurocytes are the foundation of consciousness, memory, thought, and behavior. The accumulation of abnormal proteins in the cytoplasm of neurocytes can induce dysregulation of neurological function and cause neurodegenerative diseases, such as Alzheimer's disease (AD), Parkinson's disease (PD), Huntington's disease (HD), amyotrophic lateral sclerosis (ALS), and transmissible spongiform encephalopathies (TSEs) (Qin 2015). In the early stage of these diseases, autophagy could alleviate disease progression by promoting the clearance of abnormal proteins. However, as the disease progresses, the continuous activation of autophagy leads to autophagic death in neurocytes, which aggravates the disease. Neurogliaocytes provide support, protection, nutrition, and insulation for neurocytes, and participate in the metabolism of neurotransmitters and active substances. Glioma is a neuroglial cell-derived tumor with a grave prognosis, accounting for about half of the primary tumors of the central nervous system. The average survival time after diagnosis of malignant glioma is less than 1 year. In general, the autophagy level among the malignant glioma cells is low, thus radiotherapy and chemotherapy improve the therapeutic effect by inducing autophagic death of the glioma cells. In addition, neural stem cells in nerve tissue are capable of proliferation and multipotential differentiation, distributed in the subependymal area of hippocampus, brain, and spinal cord in adults. As reserve cells for nerve tissue, neural stem cells can repair the injured nerves. In neurodegenerative disease, the neural stem cells undergo programmed cell death, such as autophagic cell death (ACD), which are mostly disordered. Thus, autophagy may be closely related to the occurrence and development of nervous system diseases. It is of great value to study autophagy using cell models derived from nervous tissue.

The applications of nervous tissue-derived cell models in autophagy research are as follows:

14.2.1.1 Neurocytes and Neuron-Like Cells

Neurocytes and neuron-like cells include rat primary cortical neurons, primary hippocampal cells, mouse hippocampal nerve HT22 cell lines, human neuroblastoma SK-N-SH cell lines, mouse dopaminergic nerve SN4741 cell lines, rat pheochromocytoma PC12 cell lines, etc. In rat primary cortical neurons, researchers found that the lipid peroxidation product 4-hydroxynonenal (4-HNE) regulates autophagy by modifying autophagy-related proteins such as Beclin 1, LC3 I/II, ATG5, and ATG7, and their combined effects are responsible for neuronal metabolic dysfunction and

decreased cell survival, contributing to neurodegenerative disease progression (Dodson et al. 2017). In mouse hippocampal nerve HT22 cell lines, which are primary hippocampal cells, researchers found that Leukemia inhibitory factor (LIF), a novel myokine known to be associated with neural function via the Akt and ERK pathway, blocked amyloid β -mediated induction of the autophagy marker LC3 II. It can reduce the damage to nerve cells induced by amyloid β protein and provides a potential drug target for the treatment of AD (Lee et al. 2019). In the HT22 cells, a balance between autophagy markers (LC3 I/II and Beclin 1) and autophagy pathway factors (AKT, p-AKT, mTOR, and p-mTOR) is maintained by thymosin β 4 (T β 4) competitively against prion protein peptide (PrP). The reduction in PrP-induced neurotoxicity indicates that T β 4 is a potential therapeutic agent for preventing neurodegenerative diseases (Han et al. 2019). The SH-SY5Y cell line is a subline of SK-N-SH cell line, which has poor genetic differentiation while the morphology, physiological, and biochemical functions are similar to normal neurocytes. SH-SY5Y cells are dopaminergic neurons because they can synthesize dopamine (DA) and norepinephrine, as well as express active tyrosine hydroxylase, DA- β -hydroxylase, and DA transporter. When treated with 1-methyl-4-phenylpyridine (MPP⁺) or rotenone, SH-SY5Y cells undergo obvious degeneration, and are often used as a cell model to study PD. Rotenone can increase the accumulation of autophagosomes, inhibit the expression of heme oxygenase-1 (HO-1), and cause apoptosis of SH-SY5Y cells. Resveratrol, an antiviral substance produced by plants to resist pathogen invasion, blocks rotenone-induced apoptosis partially through the HO-1-dependent autophagy pathway. Sirtuin 3 (SIRT3), which has regulatory functions, protects rotenone-induced SH-SY5Y cells from injury through the LKB1-AMPK-mTOR pathway (Zhang et al. 2018). SN474 is also a subline of DA neurons. It was reported that autophagy could be induced in more than 75% of SN474 cells by treatment with various concentrations of the apoptosis agonist staurosporine. In contrast, cell viability decreased significantly upon treatment with autophagy inhibitor bafilomycin A1. Further research indicated that staurosporine treatment could result in activation of the PINK1-Parkin mitophagy pathway through mitochondrial translocation. The genetic blockade of the PINK1-Parkin pathway by the *PINK1* null mutation also dramatically increased staurosporine-induced cell death. Taken together, the data above suggest that staurosporine induces both mitophagy and autophagy, exerting a significant neuroprotective effect as well. In the PD cell model of MPP⁺-induced SN4741 cells, MPP⁺ prevented translocation of transcription factor EB (TFEB) through the nonreceptor tyrosine kinase Abelson-Glycogen synthase kinase-3B (c-Abl-GSk3b) pathway, subsequently damaged the autophagy-lysosomal pathway (ALP), and resulted in the accumulation of misfolded proteins, dysfunctional organelles, and even cell death (Ren et al. 2018). Pheochromocytoma cell PC12, a cell line derived from the rat adrenal medulla, is a chromaffin cell cultured under normal conditions. When treated with nerve growth factor (NGF), PC12 cells differentiate into neuron-like cells that are similar to chromaffin cells in physicochemical function. PC12 cells are used for the study of neurobiochemistry in vitro and are an ideal model of neurological disease. Oxygen and glucose deprivation (OGD) was used as a focal cerebral ischemic model in PC12 cells. A key finding

was that OGD decreased cell viability and increased LDH and ROS in PC12 cells. Moreover, astragalosides (AST), reported to be neuroprotective, blocked OGD-R-induced autophagy, functional impairment of mitochondria, and endoplasmic reticulum stress through intracellular oxidative stress during the reoxygenation phases. These data demonstrated that autophagy is an important feature of IRI-induced PC12 cell death.

14.2.1.2 Neurogliocytes

Neurogliocytes include glioblastoma U87MG cell lines, astrocytes, etc. Ursolic acid is a pentacyclic triterpenoid compound extracted from loquat leaves with anti-inflammatory, hepatoprotective, and anticancer activity. In the U87MG cells, researchers found that ursolic acid induced endoplasmic reticulum stress (ERS), ROS production, increased concentration of cytoplasmic calcium ($[Ca^{2+}]_{cyt}$), and resulted in autophagy activation through Ca^{2+} -MEK-AMPK-mTOR, pERK-eIF2a-CHOP, and IRE1a-JNK signaling pathways. In astrocytes, uncoordinated 51-like kinase (ULK2), an upstream autophagy initiator, was silenced by methylation in glioblastoma, and its ectopic expression inhibited astrocyte transformation and glioma cell growth through autophagy.

14.2.1.3 Neural Stem Cells

In adult rat hippocampal neural stem (HCN) cells, Valosin-containing protein (VCP), which is essential for autophagosome maturation in mammalian cells, was inactive in insulin-deprived HCN cells. Moreover, VCP significantly decreased ACD and down-regulated autophagy initiation signals with robust induction of apoptosis (Yeo et al. 2016). Further studies revealed the mechanism of autophagic death in HCN. Phosphorylation of autophagy-related protein p62 by AMP-activated protein kinase drove mitochondrial translocation and ACD (Ha et al. 2017). In addition, autophagic death of HCN was also regulated by intracellular Ca^{2+} (Chung et al. 2016).

14.2.2 *The Applications of Epithelial Tissue-Derived Cell Models in Autophagy Research*

Epithelial tissue (the epithelium for short) is composed of densely arranged epithelial cells and a small amount of extracellular matrix. It can be divided according to function into covering epithelium and glandular epithelium. Epithelia cover the body surface, the body cavity, and the surface of the organs and contribute to protection, absorption, secretion, and excretion, while glandular epitheliums are mainly

composed of secretory glandular cells. In addition, there are also a few specialized epithelia. Malignant tumors that originate from epithelial tissue are the most common type of cancer. Autophagy is closely related to the occurrence and development of cancer. Normal autophagy inhibits the growth of tumors while decreased autophagy or the knockout of autophagy-related genes leads to the formation of tumors. It has been found that the autophagy level in most cancer cells is lower than that in normal cells. However, cells from colorectal cancer, lung cancer, and human cervical cancer have high autophagic activity. By virtue of autophagy, cell survival in an adverse environment is improved, for example, autophagy can assist by weakening the pharmacological effects of anticancer drugs. In addition, autophagy increases the metastasis of cancer cells by reducing anoikis (apoptosis of cells due to the separation of extracellular matrix). Furthermore, autophagy is also closely related to the occurrence of cardiovascular diseases. Autophagy of cardiovascular endothelial cells is enhanced by various stimulating factors such as ischemia-reperfusion injury (IRI) or chronic hypoxia which lead to cell protective activities such as the promotion of cell repair. In contrast, recent studies showed that autophagy promoted cell death in ischemic and hypoxic diseases. IRI-induced cell death was reduced by interference with or drug inhibition of *beclin 1*. In conclusion, autophagy is a “double-edged sword” for cancer, cardiovascular disease, etc., and this research is also one of the hotspots in autophagy.

The applications of epithelial tissue-derived cell models in autophagy research are as follows:

14.2.2.1 Respiratory System

Respiratory system-derived epithelial cells include human lung adenocarcinoma A549 cell lines, human highly metastatic lung cancer 95D cell lines, human nonsmall cell lung cancer H1299 cell lines, human bronchial epithelial BEAS-2B cell lines, etc. When A549 and 95D cells are cultured in Earle’s balanced salt solution (EBSS) instead of 1640 medium during logarithmic growth, the expression of LC3 and Beclin1 increases, indicating that nutritional deficiency could induce autophagy in lung cancer cells. Treatment with bromoconduiritol, a selective inhibitor of the beta subunit of glucosidase II (GluII β), resulted in the induction of autophagy in A549 cells, H1299 cells, and BEAS-2B cells, indicating that GluII β could block autophagy in lung cancer cells (Khaodee et al. 2017).

14.2.2.2 Digestive System

Digestive system-derived epithelial cells include human oral squamous cell carcinoma OECM1 cell lines, human tongue cancer SAS cell lines, human pharyngeal squamous cell carcinoma FaDu cell lines, human esophageal adenocarcinoma OE19 EAC cell lines, human gastric cancer MGC803 cell lines, human colon cancer HCT116 cell lines, human colon cancer HT29 cell lines, human colon

adenocarcinoma Caco-2 cell lines, hepatoblastoma HepG2 cell lines, etc. In OECM1, SAS and FaDu cells, prodigiosin (PG)-primed autophagy could induce oral squamous cell carcinoma cells apoptosis by promoting doxorubicin (Dox) influx (Lin and Weng 2018). In OE19 EAC cells, autophagy might contribute to acquired resistance to human epidermal growth factor receptor 2 (Her2)-targeted therapy in EAC, and the combination of Her2 and autophagy inhibition might be beneficial for EAC patients. In MGC803 cells, treatment with either Gefitinib or GSK126 alone induced a significant increase in cell apoptosis and autophagy, whereas the combination of the two induced a further increase. Pretreated with an autophagy inhibitor, 3-methyladenine (3-MA), prevented the apoptosis. This study provided evidence that the combined use of GSK126 and Gefitinib exerted a synergic effect on inhibiting tumor growth through an increased level of autophagy. Thus, this is being considered as a potential strategy in enhancing chemotherapy for cancer in clinic (Yang et al. 2018). Researchers treated HCT-116 and HT-29 cells with autophagy inhibitor chloroquine (CQ) and found that CQ increased the sensitivity of these two cancer cell lines to radiotherapy or chemotherapy, suggesting that inhibiting autophagy could improve the effect of radiotherapy and chemotherapy in colorectal cancer. Octreotide (OCT) affected autophagy through up-regulating miR-101 in LPS-treated Caco-2 cells, suggesting that OCT protects the monolayer permeability and tight junction level (Li et al. 2018b). Hepatocellular carcinoma (HCC) cells are more tolerant to ERS than normal hepatocytes, which contributes to multidrug resistance in HCC. In the HepG2 cell model, the autophagy and autophagic flux were increased by the ERS inducer tunicamycin in a time-dependent and dose-dependent manner. Further research demonstrated that autophagy inhibitor 3-MA treatment increased ERS-induced HepG2 cell death, indicating that the enhanced autophagy activity is an important mechanism for HepG2 cells to resist ERS. Studies revealed that autophagy induction by insulin significantly promoted chemotherapeutic drug resistance in hepatoma cells. Autophagy was found to be a potential treatment of inherent insulin resistance (IR)-mediated chemoresistance in HCC (Li et al. 2018a).

14.2.2.3 Genitourinary System

Genitourinary system-derived epithelial cells include human cervical cancer Hela cell lines, human ovarian cancer A2780 cell lines, human ovarian adenocarcinoma SKOV3 cell lines, etc. It was reported that concanavalin A (Con A), a mannose or glucose-specific legume lectin, suppressed the PI3K-Akt-mTOR and up-regulated the MEK-ERK pathway leading to the activation of autophagy in Hela cells. In addition, previous research suggested that hYF127c/cu, a copper complex, induced protective autophagy through the activation of p38 MAPK pathway in Hela cells. Further findings indicated that in A2780 and SKOV3 cells, down-regulation of *O*-*N*-acetylglucosamine (GlcNAc) transferase (OGT) enhanced cisplatin-induced autophagy, resulting in cisplatin-resistant cancer.

14.2.2.4 Cardiovascular System

Cardiovascular system-derived epithelial cells include dermal microvascular endothelial cells (ECs), cardiac microvascular endothelial cells (CMECs), human umbilical vein endothelial cells (HUVECs), etc. High mobility group box 1 (HMGB1), one of the endogenous ligands for innate immunity, was released by ECs, and then autophagy occurred in response to hypoxia or nutrition depletion. HMGB1 and autophagy are likely to play an interdependent role in promoting the angiogenic behavior of ECs. Tongxinluo (TXL), a traditional Chinese medicine, was shown to be vascular protective in the proper concentration, and could promote autophagy through activation of the mitogen-activated protein kinase and extracellular signal-regulated kinase (MEK-ERK) pathway and protect CMECs from IRI. In addition, autophagy was induced by IRI in HUVECs as shown by accumulation of ROS and increased expression of Beclin 1 and LC3 I/II. This was also accompanied by increased p65 expression and cell death.

14.2.2.5 Other Systems

In normal human epidermal keratinocytes (NHEKs), researchers demonstrated that a low dose of caffeine-activated autophagy, thus facilitating the elimination of ROS through a series of sequential events, starting with the inhibition of its target adenosine A2a receptor (A2AR), then an increase in the protein level of SIRT3 and the activation of 5' adenosine monophosphate-activated protein kinase (AMPK). A low dose of caffeine suppressed cell senescence by 2, 2'-Azobis (2-amidinopropane) dihydrochloride (AAPH) induction. In human keratinocyte HaCaT, researchers showed an antioxidant effect of opioid receptor agonist remifentanyl, which could decrease autophagy induced through IRI or hydrogen peroxide stimulation and protect cells from oxidative stress injury as a result (Li et al. 2018c).

14.2.3 *The Applications of Blood Cell and Immune Cell Models in Autophagy Research*

Blood flows through the cardiovascular system. Blood cells account for about 45% of blood volume. Leukemia and infectious disease are two main types of blood cell-related diseases related to autophagy. Leukemia is a kind of neoplastic disease that presents as a clonal hyperplasia that usually originates from genic mutation of hematopoietic stem cells. Autophagy is involved in the occurrence, treatment, and drug resistance of leukemia that can be induced by drugs, poisons, vitamins, biotoxins, and light exposure. Autophagy was found in the bone marrow of leukemia patients, and its activity varied depending on the type and chemotherapy stage of leukemia. Thus autophagy is involved in the regulation of leukemia cell survival and

drug resistance. As an innate immune mechanism, autophagy degrades pathogens and controls inflammation and homeostasis, which can be initiated by various cytokines. For example, IFN- γ could induce macrophage autophagy to resist the invasion of *Mycobacterium* and other pathogens. However, pathogens such as *Salmonella* could evade or even create favorable conditions for self-replication and survival by virtue of autophagy through specific mechanisms, so as to resist the host immune response. Overall, autophagy is strongly linked with leukemia and infectious diseases.

The applications of blood cell and immune cell models in autophagy research are as follows:

14.2.3.1 Granulocyte Cell Lines

Common granulocytes include human promyelocytic leukemia HL-60 cell lines, human acute promyelocytic leukemia NB4 cell lines, human eosinophilic leukemia EoL-1 cell lines, etc. HL-60 cells are widely used to study the molecular events and physiologic effects of myeloid differentiation for its phagocytosis and chemotaxis. The results showed that the expression of autophagy-related LC3 protein was up-regulated with lower lysosomal pH in neutrophils from synovial fluid of rheumatoid arthritis (RA) and changed under stimulation by CQ and transfection of small interfering RNAs (siRNAs) against Atg5. Further investigation showed that the concentration of IL-6, IL-8, IL-10, and MCP-1 was high, which might regulate the pathogenesis of RA via cytokine-cytokine receptor interactions. Previous research also indicated that MCP-1 was regulated by cytokine-inducible MEK6-p38 and MAPK pathways in RA (Zhang et al. 2015). IL-6, a major regulator of the differentiation of Th17 cells, activated the IL-17 signaling pathway when highly expressed. In RA, NOD1 and NOD2 could be up-regulated by TLR ligands via p38 and NF- κ B signaling pathways. In synovial tissues of RA, NOD1 and NOD2 were detected together with the expression of IL-6, IL-8, and IL-10, predominantly at the sites of invasion into articular cartilage, which encouraged researchers to further explore the relation between nucleotide-binding oligomerization domain-like receptors (NLRs) and RA. The above research suggests that specific inhibitors of neutrophil autophagy would improve the therapeutic effect of RA in clinical practice in future (An et al. 2018).

14.2.3.2 Lymphocyte Cell Lines

Common lymphocyte cell lines include leukemia Jurkat, Clone E6-1, U266, NCI-H929, Molt-4, CCRF-CEM cell lines, etc. Granulysin is a protein in the granules of human CTL and NK cells, with cytolytic activity against microbes and tumors. Previous studies demonstrated that granulysin-induced apoptosis was prevented in Jurkat cells which over-expressed Bcl-x_L or Bcl-2, or were lacking Bak, Bax or Bim

expression. In addition, granulysin induced the cleavage of ATG5 from the ATG5-ATG12 complex, without affecting autophagy. In a conclusion, granulysin induced the apoptosis of hematological tumor cells and the dissociation of autophagy regulator ATG5.

14.2.3.3 Macrophage Cell Lines

Common macrophage cell lines include mouse mononuclear macrophages J774A.1 and RAW 264.7 cell lines, human monocytic leukemia THP-1 cell lines, and human lymphoma U937T cell lines. Unlike J774A.1 cells, RAW 264.7 cells lack the apoptosis-associated speck-like protein containing CARD (ASC). Therefore, J774A.1 cells are best used if ASC is involved in the autophagy-related pathway. Macrophages recognize pathogen-associated molecular patterns (PAMPs) on the surface of pathogens. The pattern recognition receptors (PRRs) such as TLRs and scavenger receptors (SRs) are known to be involved in innate immunity in devouring, killing, and clearing pathogens. According to recent research, J774A.1 cells were co-cultured with *Salmonella* Typhimurium (*S. Typhimurium*) wild type, mutant, and complemented strains (*spvB* or complemented with *spvB*) at a multiplicity of infection (MOI) of 100:1, while rapamycin was used as an agonist and CQ as an inhibitor. Results indicated that *spvB* could suppress autophagosome formation through depolymerizing actin, and aggravate inflammatory injury of the host in response to *S. Typhimurium* infection (Chu et al. 2016).

14.2.3.4 Reticulocytes

Reticulocytes are transitional cells between orthochromatic normoblasts and erythrocytes, whose number in peripheral blood reflects the generating function of the erythrocytes. Thus reticulocytes have great significance for the diagnosis and treatment of blood diseases. There are no mitochondria in most mature erythrocytes, and damaged or unnecessary mitochondria must be effectively cleared during the development process to ensure normal cell activity. Too high or too low level of mitochondrial autophagy would cause disease. Therefore, it is very important to elucidate the mechanism of mitochondrial autophagy in erythrocyte development. Research indicates that Ulk1-dependent, Atg5-independent macroautophagy is the dominant process of mitochondrial clearance from fetal definitive reticulocytes. NIX (BNIP3L), a Bcl-2-related protein, is a key protein during terminal erythroid differentiation (Honda et al. 2014). A recent report highlighted the synergy between mitochondrial clearance and the removal of CD71 in the terminal period of erythroid maturation, which may have a role in the pathogenesis of myelodysplastic syndromes (MDS) (Zhang et al. 2019).

14.2.3.5 The Other Cell Lines

Dendritic cells (DCs) are the most efficient antigen-presenting cells (APCs) in terms of processing and presenting antigens. Kaposi's Sarcoma associated HerpesVirus (KSHV) can infect monocytes and DCs and impair their function as a result. However, the underlying mechanism is not yet completely elucidated. Previous studies indicated that DC exposure to active or UV-inactivated KSHV resulted in Signal Transducers and Activators of Transcription (STAT3) phosphorylation, which was also correlated with a block of autophagy in DCs, as indicated by LC3 II reduction and p62 accumulation. The release of IL-10, IL-6, and IL-23 was overcome by inhibiting STAT3 phosphorylation. ENdosome-Mediated Autophagy (ENMA), an unconventional APC-specific type of autophagy, was a major type of autophagy in DCs found by Vangelis Kondyli. ENMA mediates the processing and presenting of cytosolic antigens by MHC class II molecules, and selectively cleared toxins produced by ROS/RNS in activated DCs, thereby promoting their survival.

14.2.4 The Applications of Muscle Tissue-Derived Cell Models in Autophagy Research

14.2.4.1 Adipocyte Cell Lines

Mouse embryonic fibroblast (preadipocyte) 3T3-L1 cells are widely used to study the function and metabolism of adipocytes. The process of differentiation into mature adipocytes is accompanied by changes in cell morphology, expression of various differentiation-related transcription factors, and lipid metabolism-related enzymes, as well as deposition of lipids. 3T3-L1 preadipocytes were differentiated in medium containing insulin, dexamethasone, and 1-methyl-3-isobutylxanthine, a nonspecific phosphodiesterase inhibitor of AMP and GMP. It was reported that α -lipoic acid, which scavenges free radicals in mitochondria, specifically suppressed activation of AMPK. Furthermore, α -lipoic acid decreased the intracellular accumulation of lipid droplets by blocking the production of autophagic vacuoles and reducing the expression of autophagy-related proteins and adipocyte-stimulating factors. These data suggested that α -lipoic acid significantly attenuated adipocyte differentiation via an AMPK-dependent pathway and consequently decreased intracellular fat deposit of adipocytes.

14.2.4.2 Cardiomyocyte Cell Lines

Rat myocardial cell line H9C2, a cardiac myoblast derived from embryonic rat ventricular tissues, has nicotinic receptor on its surface and can synthesize muscle-specific creatine phosphokinase. According to one study, H9C2 cells pretreated with LPS resulted in decreased superoxide dismutase (SOD) activation, excessive

PKC β 2, and autophagy activation. All these changes were attenuated by remifentanyl intervention, which protected H9C2 cells from LPS-induced oxidative injury, as a result of down-regulating PKC β 2 activation and inhibiting autophagy (Kim et al. 2017).

14.2.4.3 Skeletal Muscle Cell

Skeletal muscle is mainly composed of muscle cells with contraction and relaxation functions that are necessary in any body's activities. Autophagy plays an important role in the homeostasis of skeletal muscle, and absence of autophagy is closely related to various diseases of skeletal muscle. The lack of autophagy can induce abnormal glucose and lipid metabolism as well as insulin resistance in skeletal muscle. Myoblasts, which exist in adult skeletal muscle tissue, are precursor cells that rebuild muscle tissue after trauma and have good differentiation ability. C2C12 is a common myoblast, which is widely used to study muscle development and differentiation in vitro. It was reported that the lncRNA Pvt1 impacts mitochondrial respiration and morphology and affects mito/autophagy, apoptosis, and myofiber size. This work corroborated the importance of lncRNAs in the regulation of metabolism and neuromuscular pathologies, and offered a valuable resource to study the metabolism in single cells characterized by pronounced plasticity (Alessio et al. 2019).

14.2.5 Deficiencies of Cell Models

Though autophagy is of great significance in biology, its role in neurodegenerative disease, tumor, cardiovascular disease, infectious disease, immune, and metabolic disease is still controversial. The function of autophagy-related genes, the mechanism of autophagy occurrence, and the regulation of autophagy still remain to be further investigated. As we continue to discover new details about autophagy using cell models, we will undoubtedly gain new insights into the regulation of autophagy, which might open novel avenues for disease prevention and therapeutic intervention. However, there are differences between any cell model and the real human body in protein expression and biological characteristics. The dynamic changes of autophagy in humans can not be exactly reflected by cell models.

14.2.6 Prospects of Cell Models

With the development of molecular biology, the study of autophagy has made significant progress since it was discovered 50 years ago. Autophagy is involved in a wide range of biological processes from cell differentiation to death and is of great

significance and with broad prospects. Although some research has already been done, there are still many problems that need to be explored in this field, such as the mechanism of autophagy regulation, the origin of the autophagic membrane, and its role in the development of related diseases. In conclusion, there is considerable potential for cell models to help advance autophagy research. With the recent accelerating pace of pharmacological and genetic technology, we are looking forward to an even deeper and more extensive investigation of autophagy in cell models. Moreover, by regulating autophagy, it should be possible to slow down the progression of related diseases and even reverse disease outcomes.

References

- Alessio E, Buson L, Chemello F, Peggion C, Grespi F, Martini P, Massimino ML, Pacchioni B, Millino C, Romualdi C, Bertoli A, Scorrano L, Lanfranchi G, Cagnin S. Single-cell analysis reveals the involvement of the long non-coding RNA Pvt1 in the modulation of muscle atrophy and mitochondrial network. *Nucleic Acids Res.* 2019;47:1653–70.
- An Q, Yan W, Zhao Y, Yu K. Enhanced neutrophil autophagy and increased concentrations of IL-6, IL-8, IL-10 and MCP-1 in rheumatoid arthritis. *Int Immunopharmacol.* 2018;65:119–28.
- Chu Y, Gao S, Wang T, Yan J, Xu G, Li Y, Niu H, Huang R, Wu S. A novel contribution of *spvB* to pathogenesis of *Salmonella* Typhimurium by inhibiting autophagy in host cells. *Oncotarget.* 2016;7:8295–309.
- Chung KM, Jeong EJ, Park H, An HK, Yu SW. Mediation of autophagic cell death by type 3 ryanodine receptor (RyR3) in adult hippocampal neural stem cells. *Front Cell Neurosci.* 2016;10:116.
- Dodson M, Wani WY, Redmann M, Benavides GA, Johnson MS, Ouyang X, Cofield SS, Mitra K, Darley-Usmar V, Zhang J. Regulation of autophagy, mitochondrial dynamics, and cellular bioenergetics by 4-hydroxynonenal in primary neurons. *Autophagy.* 2017;13:1828–40.
- Farre JC, Subramani S. Mechanistic insights into selective autophagy pathways: lessons from yeast. *Nat Rev Mol Cell Biol.* 2016;17:537–52.
- Ha S, Jeong SH, Yi K, Chung KM, Hong CJ, Kim SW, Kim EK, Yu SW. Phosphorylation of p62 by AMP-activated protein kinase mediates autophagic cell death in adult hippocampal neural stem cells. *J Biol Chem.* 2017;292:13795–808.
- Han HJ, Kim S, Kwon J. Thymosin beta 4-induced autophagy increases cholinergic signaling in PrP (106-126)-treated HT22 cells. *Neurotox Res.* 2019;36(1):58–65.
- Honda S, Arakawa S, Nishida Y, Yamaguchi H, Ishii E, Shimizu S. Ulk1-mediated Atg5-independent macroautophagy mediates elimination of mitochondria from embryonic reticulocytes. *Nat Commun.* 2014;5:4004.
- Khaodee W, Inboot N, Udomsom S, Kumsaiyai W, Cressey R. Glucosidase II beta subunit (GluIIbeta) plays a role in autophagy and apoptosis regulation in lung carcinoma cells in a p53-dependent manner. *Cell Oncol (Dordr).* 2017;40:579–91.
- Kim CH, Jeong SS, Yoon JY, Yoon JU, Yu SB, Kim EJ. Remifentanyl reduced the effects of hydrogen peroxide-induced oxidative stress in human keratinocytes via autophagy. *Connect Tissue Res.* 2017;58:597–605.
- Kuo CJ, Hansen M, Troemel E. Autophagy and innate immunity: insights from invertebrate model organisms. *Autophagy.* 2018;14:233–42.
- Lee HJ, Lee JO, Lee YW, Kim SA, Seo IH, Han JA, Kang MJ, Kim SJ, Cho YH, Park JJ, Choi JJ, Park SH, Kim HS. LIF, a novel myokine, protects against amyloid-beta-induced neurotoxicity via Akt-mediated autophagy signaling in hippocampal cells. *Int J Neuropsychopharmacol.* 2019;22:402–14.

- Li L, Liu X, Zhou L, Wang W, Liu Z, Cheng Y, Li J, Wei H. Autophagy plays a critical role in insulin resistance-mediated chemoresistance in hepatocellular carcinoma cells by regulating the ER stress. *J Cancer*. 2018a;9:4314–24.
- Li Y, Wang S, Gao X, Zhao Y, Li Y, Yang B, Zhang N, Ma L. Octreotide alleviates autophagy by up-regulation of MicroRNA-101 in intestinal epithelial cell line Caco-2. *Cell Physiol Biochem*. 2018b;49:1352–63.
- Li YF, Ouyang SH, Tu LF, Wang X, Yuan WL, Wang GE, Wu YP, Duan WJ, Yu HM, Fang ZZ, Kurihara H, Zhang Y, He RR. Caffeine protects skin from oxidative stress-induced senescence through the activation of autophagy. *Theranostics*. 2018c;8:5713–30.
- Lin SR, Weng CF. PG-priming enhances doxorubicin influx to trigger necrotic and autophagic cell death in oral squamous cell carcinoma. *J Clin Med*. 2018;7:375.
- Mari M, Griffith J, Rieter E, Krishnappa L, Klionsky DJ, Reggiori F. An Atg9-containing compartment that functions in the early steps of autophagosome biogenesis. *J Cell Biol*. 2010;190:1005–22.
- Nanji T, Liu X, Chew LH, Li FK, Biswas M, Yu ZQ, Lu S, Dong MQ, Du LL, Klionsky DJ, Yip CK. Conserved and unique features of the fission yeast core Atg1 complex. *Autophagy*. 2017;13:2018–27.
- Qin Z. *Autophagy-biology and disease*. Science Press, The Basic Volume; 2015. p. 464–75.
- Rao Y, Perna MG, Hofmann B, Beier V, Wollert T. The Atg1-kinase complex tethers Atg9-vesicles to initiate autophagy. *Nat Commun*. 2016;7:10338.
- Ren Y, Chen J, Wu X, Gui C, Mao K, Zou F, Li W. Role of c-Abl-GSK3 β signaling in MPP $^{+}$ -induced autophagy-lysosomal dysfunction. *Toxicol Sci*. 2018;165:232–43.
- Suzuki K. Selective autophagy in budding yeast. *Cell Death Differ*. 2013;20:43–8.
- Suzuki H, Osawa T, Fujioka Y, Noda NN. Structural biology of the core autophagy machinery. *Curr Opin Struct Biol*. 2017;43:10–7.
- Varga M, Fodor E, Vellai T. Autophagy in zebrafish. *Methods*. 2015;75:172–80.
- Voigt O, Poggeler S. Autophagy genes *Smatg8* and *Smatg4* are required for fruiting-body development, vegetative growth and ascospore germination in the filamentous ascomycete *Sordaria macrospora*. *Autophagy*. 2013;9:33–49.
- Yang Y, Zhu F, Wang Q, Ding Y, Ying R, Zeng L. Inhibition of EZH2 and EGFR produces a synergistic effect on cell apoptosis by increasing autophagy in gastric cancer cells. *Oncotargets Ther*. 2018;11:8455–63.
- Yeo BK, Hong CJ, Chung KM, Woo H, Kim K, Jung S, Kim EK, Yu SW. Valosin-containing protein is a key mediator between autophagic cell death and apoptosis in adult hippocampal neural stem cells following insulin withdrawal. *Mol Brain*. 2016;9:31.
- Zhang L, Yu M, Deng J, Lv X, Liu J, Xiao Y, Yang W, Zhang Y, Li C. Chemokine signaling pathway involved in CCL2 expression in patients with rheumatoid arthritis. *Yonsei Med J*. 2015;56:1134–42.
- Zhang M, Deng YN, Zhang JY, Liu J, Li YB, Su H, Qu QM. SIRT3 protects rotenone-induced injury in SH-SY5Y cells by promoting autophagy through the LKB1-AMPK-mTOR pathway. *Aging Dis*. 2018;9:273–86.
- Zhang Q, Steensma DP, Yang J, Dong T, Wu MX. Uncoupling of CD71 shedding with mitochondrial clearance in reticulocytes in a subset of myelodysplastic syndromes. *Leukemia*. 2019;33:217–29.

Chapter 15

Autophagy in *Drosophila* and Zebrafish



Xiuying Duan and Chao Tong

Abstract Autophagy is a highly conserved cellular process that delivers cellular contents to the lysosome for degradation. It not only serves as a bulk degradation system for various cytoplasmic components but also functions selectively to clear damaged organelles, aggregated proteins, and invading pathogens (Feng et al., *Cell Res* 24:24–41, 2014; Galluzzi et al., *EMBO J* 36:1811–36, 2017; Klionsky et al., *Autophagy* 12:1–222, 2016). The malfunction of autophagy leads to multiple developmental defects and diseases (Mizushima et al., *Nature* 451:1069–75, 2008). *Drosophila* and zebrafish are higher metazoan model systems with sophisticated genetic tools readily available, which make it possible to dissect the autophagic processes and to understand the physiological functions of autophagy (Lorincz et al., *Cells* 6:22, 2017a; Mathai et al., *Cells* 6:21, 2017; Zhang and Baehrecke, *Trends Cell Biol* 25:376–87, 2015). In this chapter, we will discuss recent progress that has been made in the autophagic field by using these animal models. We will focus on the protein machineries required for autophagosome formation and maturation as well as the physiological roles of autophagy in both *Drosophila* and zebrafish.

X. Duan

MOE Key Laboratory for Biosystems Homeostasis and Protection and Innovation Center for Cell Signaling Network, Life Sciences Institute, Zhejiang University, Hangzhou, Zhejiang, China

C. Tong (✉)

MOE Key Laboratory for Biosystems Homeostasis and Protection and Innovation Center for Cell Signaling Network, Life Sciences Institute, Zhejiang University, Hangzhou, Zhejiang, China

The Second Affiliated Hospital, School of Medicine, Zhejiang University, Hangzhou, Zhejiang, China

e-mail: ctong@zju.edu.cn

15.1 Overview

There are three types of autophagy, known as macroautophagy, microautophagy, and chaperone-mediated autophagy (CMA) (Galluzzi et al. 2017; Mizushima et al. 2008, 2010). Macroautophagy is the most studied type of autophagy in which cytosolic materials are degraded through the formation of double-membraned autophagosomes, maturation, and fusion with lysosomes (Mizushima 2011; Mizushima and Komatsu 2011; Feng et al. 2014; Klionsky et al. 2016). Different from yeast, but similar to mammalian cells, the formation of autophagosomes in flies and zebrafish is initiated via the simultaneous formation of isolation membranes at multiple sites (Zhang and Baehrecke 2015). These membrane cisterns elongate and finally enclose cargoes to form double-membraned autophagosomes. These nascent autophagosomes fuse with endosomes and multivesicular bodies (MVBs). In this way, hybrid organelles are formed, which are named amphisomes (Lamb et al. 2013). The amphisomes fuse with lysosomes to form autolysosomes. The cargoes are digested in these autolysosomes, and nutrition is released to the cytosol. After that, the lysosomes are regenerated through a process called autophagic lysosome reformation (ALR) (Yu et al. 2010).

Microautophagy is a type of autophagy that is mainly found in yeasts and plants. During microautophagy, cytosolic materials are directly taken up by the vacuole through vacuole membrane invagination. In mammalian cells and flies, a similar process, known as “endosomal microautophagy”, was found, in which endosomes engulf cytosolic material through the formation of MVBs (Huber and Teis 2016; Mijaljica et al. 2011).

CMA is an autophagic process to deliver specific cytosolic proteins to the lysosome for degradation (Kaushik and Cuervo 2018). Proteins destined for the lysosome contain a KFERQ-motif that binds to the chaperone proteins HSPA8/HSC70 to form a complex. The lysosomal membrane protein LAMP2A binds to the chaperone complex and translocates the protein into the lysosome for degradation (Kaushik and Cuervo 2012). LAMP2A is conserved in birds and mammals. Therefore, CMA was presumed to be restricted to the tetrapod clade. Recently, genes encoding proteins that are very similar to mammalian LAMP2A have been identified in several fish species, including zebrafish. This suggests that fish might also have CMA pathway (Lescat et al. 2018). Recent studies in flies and mammals indicated that proteins containing KFERQ-motif are degraded via endosomal microautophagy. This process also requires HSPA8/HSC70, suggesting that endosomal microautophagy as it exists in flies might be an ancient form of CMA known in birds and mammals (Issa et al. 2018; Mukherjee et al. 2016).

Since there have been very few studies about microautophagy and CMA in fly and zebrafish, we will mainly focus on macroautophagy in this chapter. Macroautophagy will be referred to as “autophagy” hereafter.

Table 15.1 (continued)

	<i>S.cerevisiae</i>	<i>D.Melanogaster</i>	<i>D. rerio</i>	<i>H. sapiens</i>
HOPS complex	<i>VPS11</i> , <i>VPS16</i> , <i>VPS18</i> , <i>VPS33</i> , <i>VPS39</i> , <i>VPS41</i>	<i>Vps11/CG32350</i> , <i>Vps16A</i> , <i>Vps18/dor</i> , <i>Vps33A/car</i> , <i>Vps39/CG7146</i> , <i>Vps41/lt</i>	<i>vps11</i> , <i>vps16</i> , <i>vps18</i> , <i>vps33a</i> , <i>vps39</i> , <i>vps41</i>	<i>VPS11</i> , <i>VPS16</i> , <i>VPS18</i> , <i>VPS33A</i> , <i>AC048338.1</i> , <i>VPS39</i> , <i>VPS41</i>
Rab GTPase and effectors	\ \ \	<i>Rab7</i> , <i>Rab2</i> , <i>epg5</i>	<i>rab7a</i> , <i>rab7b</i> , <i>zgc:100918</i> <i>rab2a</i> <i>epg5</i>	<i>RAB7A</i> , <i>RAB2A</i> , <i>Rab2B</i> <i>EPG5</i>
SNARE proteins	<i>VAM3</i> , <i>VTI1</i> , <i>Vam7</i> <i>SEC9*</i> \ \ <i>YKL196C</i>	<i>Syx17</i> , <i>Vti1a</i> , <i>Vti1b</i> \ <i>Ubisnap</i> <i>Vamp7</i> \ <i>Ykt6</i>	<i>stx17</i> , <i>vti1a</i> , <i>vti1b</i> , <i>gosr2</i> \ <i>snap29</i> <i>vamp7</i> <i>vamp8</i> <i>ykt6</i>	<i>STX17</i> , <i>VTI1A</i> , <i>VTI1B</i> , <i>GOSR2</i> , <i>AC005670.2</i> \ <i>SNAP29</i> <i>VAMP7*</i> <i>VAMP8</i> <i>YKT6</i>

*These genes encode proteins have not been reported as a component of the indicated complex

\The ortholog does not exist in the indicated species

15.2.1 Proteins Required for Autophagosome Formation

15.2.1.1 Atg1 Complex

In metazoan, the target of rapamycin (TOR), a serine/threonine kinase, functions as a primary nutrient and energy sensor (Gonzalez and Hall 2017; Wullschleger et al. 2006). When nutrients are sufficient, TOR suppresses autophagy by phosphorylating and inhibiting Atg1, a serine/threonine kinase whose kinase activity is required for the initiation of autophagy. Upon starvation stimuli, TOR is inactivated, which facilitates the assembly and activation of the Atg1 complex, a multiprotein complex containing Atg1, Atg13, Atg17, and Atg101. Null mutant flies of *Atg1*, *Atg13*, or *Atg17* are able to reach adulthood, but the majority of animals fail to enclose from the pupal case (Chang and Neufeld 2009; Kim et al. 2013b; Nagy et al. 2014b). The lack of each of these proteins abolishes starvation and development induced autophagosome formation. The overexpression of *Atg1* induces autophagy in the absence of starvation stimuli. It inhibits cell growth and TOR signaling and finally leads to cell death (Lee et al. 2007; Scott et al. 2007). *Atg17* functions upstream of *Atg1*. The knockdown of *Atg17* prevents the formation of the characteristic starvation-induced punctate mCherry-Atg1 localization. *Atg17* overexpression-induced autophagy

depends on *Atg1* (Nagy et al. 2014b). Atg13 directly binds to Atg1, Atg17, and Atg101 (Hegedus et al. 2014). Upon starvation, Atg13 is hyperphosphorylated by Atg1 in *Drosophila*, which can be blocked in *Atg17* mutants. Atg13 stimulates the autophagy inducing activity of Atg1. However, overexpression of *Atg13* decreases the stability of Atg1 and facilitates Atg1's inhibitory phosphorylation by TOR. As a result, overexpression of *Atg13* inhibits autophagosome expansion (Chang and Neufeld 2009).

15.2.1.2 VPS34 Complex and PI3P Effectors

Upon starvation stimuli, the activation of the Atg1 complex facilitates the recruitment of the VPS34 complex to the isolation membranes (Ktistakis and Tooze 2016). The core VPS34 complex contains Atg6, the catalytic subunit of Class III PI3K Vps34, and its regulatory subunit Vps15. The VPS34 complex does not only play an important role in autophagy but is also essential for endocytosis. When Atg14 is bound to the core VPS34 complex components, it forms an autophagy-specific complex, but when Uvrag protein forms a complex with the core components, it regulates endocytosis (Itakura et al. 2008; Kim et al. 2013a). Null mutants of *Atg6*, *Vps34*, or *Vps15* die as early as *third instar* larvae, and only a few *Atg6* mutants are able to initiate pupariation (Juhasz et al. 2008). The loss of *Vps34* not only impairs autophagosome formation but also disrupts endocytosis. The kinase-dead form of Vps34 functions dominant negatively to reduce autophagosome formation upon stimuli. However, autophagosomes still form at a slow rate when the activity of Vps34 is lost, suggesting that there is a pathway to compensate for the loss of Class III PI3K activity. The overexpression of *Vps34* induces the formation of Atg8 puncta but not lysotracker positive structures in fed fat body tissue, which indicates that extra Vps34 is not sufficient to fully activate autophagy process (Juhasz et al. 2008). Vps15 is required for stress-induced or development programmed autophagosome formation and protein aggregate degradation. *Vps15* mutant animals are defective in the antibacterial immune-response and more susceptible to bacterial infection. Besides this, Vps15 is required for efficient salivary gland protein secretion (Anding and Baehrecke 2015b). Vps15 protein has a serine/threonine kinase domain, but whether its kinase activity is required for its function in autophagy is not known. As explained before, Atg14 and Uvrag bind mutually exclusive to the core VPS34 complex to form two functionally distinctive complexes. In fed fat body cells, the loss of *Atg14* does not significantly influence the patterns of PI3P positive vesicles, but the loss of *Uvrag* leads to a complete lack of PI3P in these cells. In contrast, the loss of *Atg14* abolishes starvation-induced PI3P formation in fat body cells, whereas *Uvrag* mutant cells form PI3P positive vesicles just as the controls upon starvation stimuli (Lorincz et al. 2014; Takats et al. 2014). The Uvrag containing class III PI3K complex is essential for the downregulation of *Patched* through the endolysosomal pathway to regulate axon pruning during neural development (Issman-Zecharya and Schuldiner 2014).

PI3P generated on the isolation membrane can recruit its effectors to regulate autophagosome formation. In yeast, Atg18 is an effector of PI3P. Atg18 forms a complex with Atg2 to regulate the recycling of Atg9, the only transmembrane protein encoded by *ATG* genes, from PAS (Reggiori et al. 2004). In worms and mammals, Atg2 appears to function downstream of the Atg8 family proteins (Polson et al. 2010). In flies, there is one gene encoding Atg2 and there are three genes encoding Atg18 like proteins: *Atg18a*, *Atg18b*, and *CG11975*. The functions of *Atg18b* and *CG11975* are not known. Both *Atg2* and *Atg18a* mutants are late pupal/pharate adult lethal. The lack of *Atg18a* abolishes the recruitment of Atg9 to the Ref(2)P concrete substrate upon starvation. In starved fat body tissues, Atg8 puncta are significantly reduced in *Atg18a* mutants. However, the patterns of both Atg9 and Atg8 are not influenced by the loss of *Atg2* (Nagy et al. 2014a). The Atg18 family proteins contain a WD40 domain with seven β -propellers, which enable their interaction with multiple proteins. In flies, both Atg2 and Atg9 show interaction with Atg18a (Nagy et al. 2014a). A lack of *Atg9* in flies is semilethal. Survivors are sterile and have locomotor defects, a reduced lifespan, and increased susceptibility to stress (Tang et al. 2013; Wen et al. 2017). The lack of *Atg9* abolished both starvations induced and developmental programmed autophagy. In addition to its autophagy functions, the loss of *Atg9* leads to an aberrant adult midgut morphology at the physiological condition. Atg9 also interacts with *Drosophila* tumor necrosis factor receptor-associated factor 2 (dTRAF2) to regulate ROS-induced c-Jun N-terminal kinase (JNK) signaling (Tang et al. 2013).

In mammals, a FYVE domain protein called DFPC1 binds to PI3P and labels omegasomes and autophagosome precursors (Matsunaga et al. 2010). There is no clear ortholog of DFPC1 in *Drosophila melanogaster*. However, other *Drosophila* species such as *Drosophila willistoni* and the *virilism* have DFPC1 orthologs. A tagged form of mammalian DFPC1 can be used as a marker to label early autophagosomal structures that are positive for PI3P in flies (Liu et al. 2018).

15.2.1.3 Ubiquitin-Like Protein and Its Conjugation System

Atg8 and Atg12 are two ubiquitin-like modifiers that need two ubiquitin-like conjugation systems. Phosphatidylethanolamine (PE) modified Atg8 labels autophagic vacuoles throughout different stages, from early isolation membranes to late autolysosomes (Ichimura et al. 2000; Matsushita et al. 2007). It is the most used autophagic marker to label autophagic vacuoles. Atg8 is cleaved by a cysteine protease Atg4 at the C-terminus to expose a glycine residue. Subsequently, the cleaved Atg8 is conjugated to an E1-like enzyme, Atg7, followed by its transfer to the E2-like Atg3. Similarly, with the help of Atg7 and an E2-like enzyme Atg10, Atg5 conjugates to Atg12 and finally forms a complex with Atg16. The Atg5-Atg12-Atg16 complex enhances the covalent conjugation of Atg8 to PE (Nakatogawa et al. 2007). There are two *Atg8* genes in flies: *Atg8a* and *Atg8b*. *Atg8a* is ubiquitously expressed in most tissues, whereas *Atg8b* is specifically expressed in testis. Mutants of *Atg7*, *Atg8a*, and *Atg16* are viable (Juhász et al. 2007; Mulakkal et al. 2014; Simonsen

et al. 2008). They have a shorter lifespan and are more sensitive to different types of stress. There are two *Atg4* genes in *Drosophila*: *Atg4a* and *Atg4b*. It is not known whether both of them are required for Atg8 cleavage.

15.2.1.4 Autophagy Receptor Proteins

Many selective receptors or adaptors for autophagy cargo recognition have been identified in higher organisms (Deng et al. 2017). They all have orthologs in zebrafish, but only a few have *Drosophila* orthologs. In flies, Ref(2)P (the fly ortholog of SQSTM1/p62) acts as a selective receptor to recognize cargo during autophagy (Nezis et al. 2008). The Ref(2)P C-terminus has a ubiquitin-binding domain that binds to ubiquitin-modified cargoes. Ref(2)P multimerizes and triggers the formation of ubiquitin-positive protein aggregates both under physiological conditions and when healthy protein turnover is inhibited. Ref(2)P contains an Atg8-interacting motif that might help to enclose cargoes with Atg8 positive membranes. Homozygous *ref(2)P* null mutants are viable, but males are sterile with degenerated mitochondria in spermatids (Dezelee et al. 1989). In vertebrates, there are two oxidation-sensitive cysteine residues on SQSTM1 to sense stress and activate prosurvival autophagy. Although they are not conserved, introducing these oxidation-sensitive cysteine residues into the fly Ref(2)P protein increases protein turnover and stress resistance in flies (Carroll et al. 2018).

Alfy is an autophagy adaptor that is associated with the clearance of protein aggregates (Simonsen et al. 2004). Alfy is a very large protein. It binds to PI3P and interacts with LC3 through an LC3 binding motif. It can also associate with SQSTM1 and the ATG5-ATG12 complex (Isakson et al. 2013). In flies, the ortholog of *Alfy* is named *blue cheese* (*bchs*) after the brain morphology is observed in mutant flies (Finley et al. 2003). *bchs* is required for autophagic degradation of Ref(2)P-associated ubiquitinated proteins. *bchs* mutants are viable but have a reduced adult life span. In the mutant animals, protein aggregates containing ubiquitinated proteins and amyloid precursor-like protein accumulate in the CNS in an age-dependent manner. The size of the CNS is reduced, and it shows extensive neuronal apoptosis (Finley et al. 2003; Lim and Kraut 2009).

Huntingtin (Htt), the protein encoded by the gene mutated in Huntington disease, was recently identified as a scaffold to regulate autophagy (Ochaba et al. 2014; Rui et al. 2015). It binds to SQSTM1 to facilitate the engulfment of ubiquitinated cargoes by LC3 positive membranes. Htt also binds to ULK1 to promote its activation. In flies, *htt* mutant animals are viable with no visible developmental defects. However, the life span and locomotor ability of *htt* mutants are reduced with aging. Lack of endogenous *htt* significantly enhances the neurodegenerative phenotypes associated with polyglutamine Htt toxicity (HD-Q93) (Zhang et al. 2009). Besides, *htt* and autophagy genes have genetic interaction in flies (Rui et al. 2015). Loss of *htt* in *Drosophila* disrupts starvation-induced autophagy (Ochaba et al. 2014).

For the autophagy receptor UBQLN2, there are several low homology orthologs in flies. However, their function has not been studied. There is no fly ortholog for autophagy receptors such as OPTN/Optineurin, NBR1, and NDP52 (Deng et al.

2017). For these genes, zebrafish might be an excellent model to study the *in vivo* functions.

15.2.2 Proteins Required for Autophagosome and Lysosome Fusion

Autophagosomes fuse with endosomes and lysosomes to deliver their cargo for degradation. The fusion requires Rab GTPases to label the membranes (Stenmark 2009), a tethering complex to facilitate docking and association between two organelles, and a complex of soluble *N*-ethylmaleimide-sensitive fusion attachment protein receptors (SNARE) proteins to mediate fusion (Hong 2005).

15.2.2.1 Rab GTPases

Rab7 and Rab2 are essential small GTPases mediating autophagosome-lysosome fusion. Rab7 is localized on endosomes, lysosomes, and autophagosomes. A lack of Rab7 leads to the abolishment of fusion between autophagosomes and lysosomes. The localization of Rab7 to the autophagosome does not depend on Rab5 and the autophagosome-lysosome tethering complex: the HOPS complex (see the below paragraph for a more detailed description of the function of this complex). The Rab7 guanine nucleotide exchange factor (GEF) Mon1–Ccz1 complex is required for the fusion process (Cabrera et al. 2014; Lawrence et al. 2014; Poteryaev et al. 2010). The Mon1–Ccz1 complex binds to the PI3P produced by the VPS34 complex to promote Rab7 recruitment to the autophagosomes (Cabrera et al. 2014; Hegedus et al. 2016; Lawrence et al. 2014). Rab2 is known to mediate the trafficking between the ER and the Golgi. Recently, it was shown to be required for autophagosome-lysosome fusion and the proper trafficking of lysosomal hydrolases (Csizmadia et al. 2018; Fujita et al. 2017; Lorincz et al. 2017b). The GTP-binding form of Rab2 (Rab2-GTP) localizes to the autolysosome. Overexpression of Rab2-GTP enhances the fusion between autophagosomes and lysosomes (Lorincz et al. 2017b). Both Rab7 and Rab2 bind to the tethering complex HOPS, to coordinate the fusion process (Lorincz et al. 2017b). PLEKHM1, the effector of Rab7, is also required for the fusion between autophagosomes and lysosomes (Csizmadia et al. 2018; McEwan et al. 2015). EPG5, initially identified in worms, is identified as an Rab7 effector that regulates autophagosome-lysosome fusion (Tian et al. 2010). In flies, the reduction of the *EPG5* ortholog *Epg5* leads to abnormal autophagy and progressive neurodegeneration (Byrne et al. 2016).

15.2.2.2 The HOPS Complex

The homotypic fusion and vacuole protein sorting (HOPS) complex is the tethering complex required for the fusion between the autophagosome and the lysosome (Solinger and Spang 2013; Spang 2016). In flies, *Vps11*, *Vps16A*, *Vps39*, *Vps18/dor*, *Vps33A/car*, and *Vps41/lt* encode proteins that form the HOPS complex (Lindmo et al. 2006). *Vps18/dor*, *Vps33A/car*, and *Vps41/lt* are classical eye color mutants (Lloyd et al. 1998). Hypomorphic mutations of these genes impair the biogenesis of eye pigment granules and lead to eye color defects. Null mutants in these genes lead to early instar lethality. Loss of *dor* or *car* or a hypomorphic mutation of *lt* also leads to defects in endocytosis, and similar phenotypes have been reported based on RNA interference (RNAi) analysis of *Vps16A* (Akbar et al. 2009; Pulipparacharuvil et al. 2005; Sevrioukov et al. 1999; Swetha et al. 2011). The HOPS complex binds to Rab7 and Rab2 to tether autophagosomes and lysosomes. It also interacts with the autophagosomal Qa SNARE Syntaxin 17 (Syx17) to trigger SNARE complex assembly (Jiang et al. 2014; Takats et al. 2014).

15.2.2.3 The SNARE Complex

SNARE proteins mediate membrane fusion events. They are divided into four sub-families: QA-SNARES, QB-SNARES, QC-SNARES, and R-SNARES. A tetrameric complex of one of each type of SNARES triggers membrane fusion (Hong and Lev 2014). In flies, mature autophagosomes have a Qa SNARE Syntaxin 17 (Syx17), which forms a complex with the Qbc SNARE Ubisnap (SNAP29 in mammals) and the R SNARE Vamp7 (VAMP8 in mammals) located on late endosomes and lysosomes (Itakura et al. 2012; Takats et al. 2013). Ykt6 is another R-SNARE localized on lysosomes. Ykt6 and Vamp7 compete to form a SNARE complex with Syx17 and Ubisnap. Both Vamp7 and Ykt6 bind to the HOPS complex and are required for the fusion between autophagosome and lysosome (Takats et al. 2018). It has been reported that ATG14 also binds to Syntaxin17 to promote the fusion events in mammals (Diao et al. 2015). It is not known whether Atg14 has a similar function in flies or not.

15.3 The Physiological Roles of Autophagy in *Drosophila* and Zebrafish

Autophagy plays important physiological roles in the development and tissue homeostasis in flies. Autophagy is required for tissue remodeling during metamorphosis, for ovary development, for neuronal homeostasis, and for the clearance of paternal mitochondria. During stress, such as starvation, autophagy also functions as a lifesaving strategy to remobilize nutrition to the proliferating tissues (Lorincz et al. 2017a).

15.3.1 Autophagy in the Fat Body of *Drosophila*

The *Drosophila* fat body is similar to the human liver and white adipose tissues and functions both as a metabolic organ and as a tissue for the storage of energy (Zheng et al. 2016). The larval fat body is the most used model system to study autophagy in *Drosophila* (Scott et al. 2004). It consists of a single layer of cells. From embryonic stage 16 to the third *instar* larvae stage, the fat cell number remains constant at about 2200 cells per animal. At the embryonic stage, the size of the fat body is small. With feeding, the size of the fat body increases dramatically and the cells reach enormous sizes, but the cell number remains unchanged. The DNA in the fat body cells is endoreplicated to reach a ploidy level of 256-512n at the mid-third *instar* larval stage. Autophagy is induced at the initiation of the metamorphosis when the third *instar* larvae reach the wandering stage and crawl out of their food to start pupariation. Cytoplasmic components within the fat body are degraded by autophagy to provide nutrients to develop imaginal tissues (Butterworth et al. 1988; Juhasz et al. 2003; Rusten et al. 2004).

In addition to the programmed induction of autophagy during metamorphosis, autophagy can be induced in fat body tissues at the early third *instar* stage by starvation. When early third instar larvae are soaked in 20% sucrose for several hours (3–6 h), autophagy will be induced in the fat body tissue. The induction of autophagy can be observed by examining the patterns of lysotracker staining. Without autophagy induction, fat body cells only have a diffused background level of lysotracker staining. However, once autophagy is induced, a large amount of lysotracker positive puncta can be observed in the early third *instar* larval fat body tissues (Fang et al. 2016; Scott et al. 2004). Multiple autophagy markers, such as Atg5, Atg6, Atg8, Atg9, Atg16, Atg18, Syntaxin17, Rab7, and Ref(2)P, change patterns upon the induction of autophagy. Ectopic tagging of these proteins and examining their patterns or examining the endogenous proteins by immunostaining help to analyze whether there is a defect in autophagy. TEM analysis has been used to analyze autophagic vacuoles. Autophagosomes, amphisomes, and autolysosomes have distinct morphologies in this tissue and can be easily analyzed. The fusion between the autophagosome and the lysosome has been monitored by GFP- and RFP (mCherry)-double tagged Atg8a. Similar to mammalian cells, the GFP signals are observed to be quenched once the autophagosome fused with the lysosome, whereas the RFP signals remain. In the well-fed early third *instar* larval fat body, both the GFP and RFP signals were diffused. Occasionally, small RFP puncta could be observed. Upon starvation, GFP signals are still diffused, but a large amount of RFP puncta emerge. When autophagosomes fail to fuse with lysosomes or the acidification of the lysosome is defective, yellow puncta are observed upon induction of autophagy (Mauvezin et al. 2014; Nagy et al. 2015).

By using FRT-/FLP-mediated mitotic recombination, it is possible to generate mosaic tissues with both mutant cells and wild-type control cells in fat body tissues. This technique can also be used to overexpress a particular protein or RNAi knock down a gene's expression in a few cells surrounded by wild-type cells. Analyses on

this material make it possible to compare markers for autophagy in mutant cells and wild-type controls in the same piece of tissue. The internal control facilitates the analysis of mild defects caused by the loss or the gain of a gene's expression (Nagy et al. 2015).

15.3.2 Autophagy in the Salivary Gland of *Drosophila*

Autophagy is a self-protection mechanism promoting cell survival under stress conditions. However, it is also involved in cell death in animals (Anding and Baehrecke 2015a; Nelson and Baehrecke 2014). The *Drosophila* larval salivary glands die at the early pupal stage. A small ring of diploid cells located at the anterior end of the larval salivary glands divides and differentiates to form the adult salivary glands (Andrew et al. 2000). The elimination of larval salivary glands depends on a cell death mechanism that requires both autophagy and caspases (Berry and Baehrecke 2007; Martin and Baehrecke 2004).

The larval salivary gland is composed of two major cell types, secretory cells and duct cells. Secretory cells synthesize and secrete proteins and duct cells form tubes connecting the secretory cells to the mouth. The majority of salivary gland cells are polyploid cells with an enormous cell size. These cells have differentiated without further cell division, and their polyploidy level can reach 1024 *n*. At the end of the third *instar* stage, larvae crawl out of their food and search a suitable site to pupate. Glue is secreted from the salivary glands to the duct and out of the mouth and is used to adhere the pupa to their pupation place. About 10–12 h after puparium formation, a pulse of a steroid hormone 20-hydroxyecdysone (ecdysone) induces autophagy and prompts the destruction of the salivary glands (Berry and Baehrecke 2007; Lee and Baehrecke 2001; Martin and Baehrecke 2004).

The death of the salivary gland cells requires both caspases and autophagy. The expression of the majority of *Drosophila Atg* and *caspase* genes are induced. Dying salivary gland cells contain a large number of autophagosomes (Lee and Baehrecke 2001; Martin and Baehrecke 2004). Sixteen hours after puparium formation, the larval salivary glands are degraded. In most *Atg* gene mutants, such as the mutants of *Atg1*, *Atg2*, *Atg3*, *Atg6*, *Atg7*, *Atg8a*, *Atg12*, or *Atg18a*, the salivary glands are not properly degraded. Similarly, the reduction of caspase activity leads to an incomplete degradation of the salivary glands. A combined inhibition of caspases and autophagy further blocks gland degradation. A provocation of autophagy by the induction *Atg1* expression leads to a premature destruction of the salivary gland. Interestingly, this *Atg1*-triggered autophagy is sufficient to induce salivary gland cell death without the requirement of caspase activity (Berry and Baehrecke 2007).

During salivary gland cell death, autophagy is regulated by calcium and inositol-1,4,5 trisphosphate (IP3) signaling pathway components. IP3 binds to the IP3 receptor to trigger calcium release from the ER (Nelson et al. 2014). The calcium ions bind to **Calmodulin** to activate autophagy. miR14 was found to target IP3 kinase 2 to regulate autophagy in salivary glands (Nelson et al. 2014). Recently, it has been

shown that Hermes, a proton-coupled monocarboxylate transporter, is required for autophagy during steroid-triggered salivary gland cell death. Hermes preferentially transports pyruvate over lactate. In *Hermes* mutant flies, mTOR signaling is elevated and the salivary glands cannot be adequately degraded. The cell death defect could be suppressed by decreasing the mTOR function (Velentzas et al. 2018).

The death and elimination of salivary glands is a cell-autonomous process, and no phagocytosis is involved. Surprisingly, autophagy-induced salivary gland cell death and phagocyte-mediated clearance of dying cell corpses use a similar machinery. Draper, an immunoreceptor, is required for autophagy in the salivary gland. Loss of draper prevents autophagy in dying salivary glands and leads to an incomplete larval salivary gland degradation (McPhee et al. 2010). Draper is also known as the critical engulfment receptor to recognize cell debris during phagocytosis. Draper-dependent phagocytic activity is mediated by Src and Syk family kinase signaling in glial cells (Ziegenfuss et al. 2008). Interestingly, these factors downstream of Draper are also required for autophagy during salivary gland cell death.

The elimination of salivary gland could be examined by histochemistry. The induction of autophagy could be monitored by TEM and the immunostaining of various autophagy markers.

15.3.3 Autophagy in the Intestine of *Drosophila*

Autophagy-induced cell death also occurs in the larval intestine. A pulse of ecdysone in the late third *instar* larvae induces a wave of autophagy in midgut cells. The elimination of these cells begins after puparium formation. Small islands of imaginal cells that are committed to forming the future adult gut surround the larval midgut cells. They proliferate and enclose the condensed degenerating larval midgut. The dead midgut cells form the yellow body, which is excreted as meconium right after adult flies enclose (Denton et al. 2009; Lee et al. 2002).

The death of the larval midgut cells occurs with many features similar to the cell death in salivary glands, including the formation of autophagosomes, DNA fragmentation, and caspase activation. Disrupting *Atg* genes such as *Atg1*, *Atg2*, *Atg18a*, as well as blocking the initiation of autophagy by modulating growth signaling, delays midgut cell death. However, different from autophagic cell death in salivary glands, caspase activity is not required for larval midgut cell death (Denton et al. 2009; Xu et al. 2015). The inhibition of caspases fails to enhance the *Atg* mutant phenotype in the midgut, suggesting that autophagy is required for larval midgut cell death, but caspases are not. Surprisingly, not all the *Atg* genes encoding the core machinery of autophagy are required. The E1-activating enzyme *Atg7* and the E2-conjugating enzyme *Atg3* are required for *Atg8* lipidation. Although *Atg8* is essential for midgut cell death, *Atg3* and *Atg7* are dispensable for this process. Instead, the E1-activating enzyme encoded by *Uba1* is required for autophagy and the reduction of cell size during midgut cell death. These data indicate that there is

a specific mechanism regulating the process of autophagy in midgut cell death (Chang et al. 2013).

In addition to the larval cell death, several *Atg* genes are required for the homeostasis of the adult midgut. The *Drosophila* adult midgut is a tubular structure with monolayered epithelium cells surrounded by visceral muscles (Micchelli and Perrimon 2006). Intestinal stem cells (ISCs) divide asymmetrically to generate renewal ISCs and enteroblasts (EBs). The EBs differentiate further to produce either absorptive enterocytes (ECs) or secretory enteroendocrine cells (EEs). The ablation of *Atg9* leads to a significantly shortened and thickened adult midgut in the posterior region. *Atg9* acts on ECs to control their size and morphology (Wen et al. 2017). Similar midgut defects can be observed when *Atg1*, *Atg13*, and *Atg17* encode components of Atg1 kinase complex, but not when *Atg7*, *Atg12*, *Atg16*, *Atg18a*, or *Vps34* is reduced in ECs (Wen et al. 2017). Further study found that the defects are likely due to an increased TOR activity since inhibiting it could primarily rescue the midgut growth defects in *Atg9* mutants. Although *Atg9* functions downstream of the Atg1 complex during autophagy, it seems to use different mechanisms to inhibit TOR activity in ECs (Wen et al. 2017).

A lack of *Atg16* leads to a shorter and thicker posterior midgut in adult flies. The differentiation of EE cells is compromised. However, the lack of *Atg8a* and *Atg5* does not influence EE differentiation. The WD40 domain on *Atg16* is not required for autophagy but is essential for EE differentiation. Together, it suggests that *Atg16* plays an autophagy-independent role in adult midguts (Nagy et al. 2017). The functions of *Atg9* and *Atg16* in adult midguts are not directly related to the autophagy process, and it needs further efforts to elucidate whether autophagy per se plays a role in the adult midgut homeostasis.

The clearance of the larval midgut could be analyzed by histochemistry. The adult midgut morphology, cell proliferation, cell death, ISC self-renew, and differentiation could be monitored by immunostaining of specific markers. Autophagy markers such as mCherry-tagged *Atg8* and Ref2(P) could also be analyzed via immunostaining and western blots in this tissue.

15.3.4 Autophagy in the Ovary of *Drosophila*

The adult fly ovary contains 15–20 ovarioles with developing egg chambers. Each egg chamber consists of one oocyte and 15 nurse cells surrounded by a layer of somatic follicle cells (King 1970; Spradling 1993). During the late stage of oogenesis, the nurse cells transfer their cytoplasmic contents to the oocyte to support its growth. Then, the nurse cells undergo programmed cell death. This process depends on the autophagy-mediated degradation of Bruce, an inhibitor of apoptosis. The degradation of Bruce enables caspase activation and cell death (Nezis et al. 2009).

In addition to this late-stage developmental cell death, nutrient starvation or other stresses can induce the egg chambers to die at two earlier stages, during gerarium formation (in region 2) and mid-oogenesis (Drummond-Barbosa and

Spradling 2001; McCall 2004). This stress-induced cell death requires caspases to activate high levels of autophagy. Therefore, autophagy seems to function either upstream or downstream of caspases in the cell death of fly ovary (Hou et al. 2008).

The cell death during mid-oogenesis is accompanied by the remodeling of the mitochondrial network in the dying nurse cells followed by the fragmentation of nurse cells and engulfment of their clustered mitochondria and the cytoplasm by the surrounding follicle cells. The lack of *Atg* genes such as *Atg1* or *Atg7* interferes with the engulfment of the fragments of nurse cells by follicle cells and cell death. The remodeling of mitochondria is a pivotal mechanism to regulate autophagy flux and cell death during mid-oogenesis (DeVorkin et al. 2014).

Autophagy can be modulated at the translational level during oogenesis. *Orb*, the fly ortholog of mammalian translation regulator *CPEB*, prevents cell death through the repression of autophagy. It does so by directly repressing the translation of *Atg12* mRNA (Rojas-Rios et al. 2015).

Autophagy not only plays a role in germ cell death but also triggers the loss of follicle stem cells (FSCs). Hedgehog signaling-induced autophagy drives FSC loss and premature sterility. During aging, Hh-dependent autophagy increases. Insulin-IGF signaling (IIS) suppresses Hh-induced autophagy and promotes a stable proliferative state. The balance between cell proliferation and autophagy determines the reproductive lifespan of flies (Singh et al. 2018).

In *Drosophila* ovaries, *bam* mutant stem cells function as tumor-like stem cells to promote tumor growth. Autophagy is low in wild-type stem cells but elevated in *bam* mutant stem cells. Loss of either *Atg6* or *Atg17* decreases the *bam* mutant stem cell niche occupancy, slows the cell cycle, and inhibits *bam* mutant-induced tumor growth in the ovary (Zhao et al. 2018).

15.3.5 Autophagy in the Nerve System of *Drosophila*

Developmentally programmed autophagy mostly occurs in polyploid cells, as we mentioned above. These polyploid cells undergo autophagic cell death in response to specific signals. Environmental stimuli such as starvation can prematurely induce autophagic responses in these polyploid cells. *Drosophila* neurons are diploid cells. Autophagy cannot be induced by starvation in these cells (Mulakkal et al. 2014). However, a basal level of autophagy is critical for neuronal homeostasis. Autophagy is particularly crucial for neurons since they are long-lived cells with a complex morphology and lengthy processes. The loss of most *Atg* genes or factors required for autophagy results in neurodegeneration in flies. For example, the loss of *Atg7*, *Atg8a*, *Atg5*, *Epg5*, *Ref(2)P*, *bchs*, or *htt* leads to neurodegeneration (Chang and Neufeld 2010; Mulakkal et al. 2014).

Because of the importance of autophagy for neuronal survival, neurons have developed some specific mechanisms to regulate the autophagy process locally at the synapses. Cacophony (*Cac*), a *Drosophila* voltage-gated calcium channel

(VGCC), is required for the fusion between autophagosomes and lysosomes in neurons. Photoreceptor terminals mutated in *Cac* accumulate a large number of autophagosomal structures. In cultured cerebellar neurons from mice, the protein encoded by the *cac* ortholog *CACNA1A* localizes on lysosomes and is required for lysosomal fusion (Tian et al. 2015). The presynaptic lipid phosphatase Synaptojanin is required for macroautophagy. In flies that contain a Parkinson's disease mutation *synaptojanin*^{R258Q} knock-in, Atg18a is accumulated on nascent synaptic autophagosomes. Autophagosome maturation is blocked in the synapses of these flies (Vanhouwaert et al. 2017). Endophilin A, a protein that is highly enriched at the synapse of flies, induces macroautophagy at the synapses. Kinase LRRK2 phosphorylates the BAR domain of Endophilin A to promote the formation of highly curved membranes, which serve as docking stations for autophagic factors (Soukup et al. 2016).

15.3.6 Autophagy in Zebrafish

Although most genes participating in autophagy are highly conserved between zebrafish and human, the study of autophagy in zebrafish is still at an early stage. It is relatively easy to study embryogenesis and organogenesis in zebrafish since the embryos and larvae are small and transparent and develop *ex utero*. These characteristics make zebrafish an excellent system to generate disease models and discover the underlying mechanisms (Mathai et al. 2017). For example, polyglutamine expansion diseases, such as Huntington's disease (Williams et al. 2008), tauopathy (Bai et al. 2007), and amyotrophic lateral sclerosis (ALS) (Ramesh et al. 2010), have been successfully modeled in zebrafish.

The functions of most zebrafish autophagy genes were revealed by morpholino-mediated knockdown experiments. The reduction of *atg5*, *atg7*, *beclin1*, *atg4da*, *ambra1a*, and *ambra1b* all leads to developmental defects during embryogenesis. One of the common phenotypes seen is a cardiac defect, suggesting that autophagy plays a specific role in cardiac development (Benato et al. 2013; Hu et al. 2011; Kyostila et al. 2015; Lee et al. 2014). Transient depletion of *sqstm1* in zebrafish embryos increases the susceptibility to bacterial infection (Mostowy et al. 2013; van der Vaart et al. 2014). The ablation of *sqstm1* causes a specific locomotor defect (Lattante et al. 2015). The knockdown of *optineurin* also leads to motor axonopathy, an increase of protein aggregates, defective vesicle trafficking, and an increased susceptibility to bacterial infection (Chew et al. 2015; Korac et al. 2013; Paulus and Link 2014). Morpholino-mediated depletion of *spns1*, a lysosomal transporter, increases embryonic cellular senescence, and the phenotype is reversed by the depletion of the lysosomal v-ATPase (Sasaki et al. 2014, 2017). *Sorting nexin 14* knockdown causes defective autophagic degradation and neurodegeneration in zebrafish (Akizu et al. 2015).

The development of genome editing techniques greatly facilitated mutant generation. Recently, an *epg5* knockout zebrafish was generated. The zebrafish

epg5^{-/-} mutants were viable and without visible developmental defects. The *epg5*^{-/-} mutants developed age-dependent locomotor defects and muscle thinning, together with the accumulation of nondegradative autophagic vacuoles. The human *EPG5* mutation leads to Vici syndrome. Zebrafish *epg5*^{-/-} mutants could serve as a model to study this disease (Meneghetti et al. 2019).

15.4 Mitophagy in *Drosophila*

Mitophagy is the most studied type of selective autophagy in *Drosophila*. The Parkinson disease-related genes *PINK1* and *PARKIN* are well-known as mitophagy regulators in cultured mammalian cells (Durcan and Fon 2015). Upon damage of mitochondria, the kinase PINK1 phosphorylates the E3 ubiquitin (Ub) ligase PARKIN to stimulate PARKIN activation and translocation to damaged mitochondria. Mitochondrial proteins such as MFN are ubiquitinated. The mitochondrial surface polyUb chain is also phosphorylated by PINK1, and that phosphorylated polyUb chain facilitates mitophagy (Pickles et al. 2018). In flies, the functions of *Pink1* and *park* (the fly ortholog of *PARKIN*) are required to maintain proper mitochondrial morphology and activity. The loss of *Pink1* or *park* leads to male infertility and the degeneration of dopaminergic neurons and muscles (Guo 2012). However, whether *Pink1* and *park* participate in the mitophagic process in flies is still controversial. Using live imaging monitor mt-Keima signals and correlative light and electron microscopy (CLEM), one group showed that mitophagy occurred and increased with aging in muscle cells and dopaminergic neurons. However, the age-dependent increase of mitophagy was abrogated by the loss of *Pink1* or *park* (Cornelissen et al. 2018). Another group using a similar tool observed that basal mitophagy occurred in multiple tissues, but the loss of *Pink1* and *park* had little effects on mitophagy (Lee et al. 2018). These controversial results are likely due to the low basal mitophagy level under physiological conditions. In addition to *Pink1/park*, the mitophagy receptor FUNDC1 also has orthologs in flies (Liu et al. 2014). However, their functions have not been studied.

It has been reported that elevating autophagy by *Atg1* overexpression can significantly rescue mitochondrial defects in *Pink1* and *park* mutants in *Drosophila* (Ma et al. 2018). This suggests that defective mitochondria quality control is the leading cause of the mitochondrial defects in *Pink1/park* mutants. A knockdown of the mitochondrial deubiquitinating enzyme USP30 or the inhibition of USP14 improves the mitochondrial integrity in *park*- or *Pink1*-deficient flies (Bingol et al. 2014; Chakraborty et al. 2018). Mitochondrial ubiquitin ligase 1 (MUL1, also known as MAPL or MULAN), an E3 protein ligase, functions in parallel with *Pink1/park* to regulate the Marf level. Overexpression of *MUL1* rescues the mitochondrial defects of the *Pink1/park* mutants (Yun et al. 2014). A mitochondrial protein Clueless (*clu*) binds to VCP/p97 and promotes the degradation of Marf. An overexpression of *clu* complements the *Pink1* mutant defects (Wang et al. 2016).

In addition to the basal level of mitophagy that maintains the homeostasis of adult fly tissues such as neurons and muscles, there are also developmental processes that require mitophagy. The paternal mitochondria are eliminated after fertilization through a process displaying multiple features of the endocytic and autophagic pathways in flies. Park is not required for this process. However, the ubiquitin pathway and Ref(2)P are required (Politi et al. 2014).

At the onset of larval midgut cell death during intestine development, autophagy is required for the reduction of the cell size and for mitochondrial clearance in the dying cells. *Vps13D* mutant cells retain their mitochondria, indicating a defect in mitochondrial clearance. The autophagy function of *Vps13D* is context dependent since no defect is observed in starvation or rapamycin-induced autophagy in the fat body or intestine. *Vps13D* also regulates mitochondrial fission downstream of known mitochondrial fusion regulators such as Drp1 and Mff. It is still not clear how *Vps13D* regulates autophagy/mitophagy (Anding et al. 2018).

In cells, mutant mtDNA often coexists with the wild-type mtDNA, a phenomenon known as heteroplasmy. By studying a fly model that carries a heteroplasmic lethal mtDNA deletion (mtDNA^A) in adult muscle, one group found that stimulation of autophagy, activation of the Pink1/park pathway, or decreased levels of Marf resulted in a selective decrease in mtDNA^A. It suggests that mitophagy may help to eliminate damaged mtDNA selectively (Kandul et al. 2016).

References

- Akbar MA, Ray S, Kramer H. The SM protein Car/Vps33A regulates SNARE-mediated trafficking to lysosomes and lysosome-related organelles. *Mol Biol Cell*. 2009;20:1705–14.
- Akizu N, Cantagrel V, Zaki MS, Al-Gazali L, Wang X, Rosti RO, Dikoglu E, Gelot AB, Rosti B, Vaux KK, et al. Biallelic mutations in SNX14 cause a syndromic form of cerebellar atrophy and lysosome-autophagosome dysfunction. *Nat Genet*. 2015;47:528–34.
- Anding AL, Baehrecke EH. Autophagy in cell life and cell death. *Curr Top Dev Biol*. 2015a;114:67–91.
- Anding AL, Baehrecke EH. Vps15 is required for stress induced and developmentally triggered autophagy and salivary gland protein secretion in *Drosophila*. *Cell Death Differ*. 2015b;22:457–64.
- Anding AL, Wang C, Chang TK, Sliter DA, Powers CM, Hofmann K, Youle RJ, Baehrecke EH. Vps13D encodes a ubiquitin-binding protein that is required for the regulation of mitochondrial size and clearance. *Curr Biol*. 2018;28:287–295.e6.
- Andrew DJ, Henderson KD, Seshaiiah P. Salivary gland development in *Drosophila melanogaster*. *Mech Dev*. 2000;92:5–17.
- Bai Q, Garver JA, Hukriede NA, Burton EA. Generation of a transgenic zebrafish model of Tauopathy using a novel promoter element derived from the zebrafish *eno2* gene. *Nucleic Acids Res*. 2007;35:6501–16.
- Benato F, Skobo T, Gioacchini G, Moro I, Ciccocanti F, Piacentini M, Fimia GM, Carnevali O, Dalla Valle L. Ambra1 knockdown in zebrafish leads to incomplete development due to severe defects in organogenesis. *Autophagy*. 2013;9:476–95.
- Berry DL, Baehrecke EH. Growth arrest and autophagy are required for salivary gland cell degradation in *Drosophila*. *Cell*. 2007;131:1137–48.

- Bingol B, Tea JS, Phu L, Reichelt M, Bakalarski CE, Song Q, Foreman O, Kirkpatrick DS, Sheng M. The mitochondrial deubiquitinase USP30 opposes parkin-mediated mitophagy. *Nature*. 2014;510:370–5.
- Butterworth FM, Emerson L, Rasch EM. Maturation and degeneration of the fat body in the *Drosophila* larva and pupa as revealed by morphometric analysis. *Tissue Cell*. 1988;20:255–68.
- Byrne S, Jansen L, U-King-Im JM, Siddiqui A, Lidov HG, Bodi I, Smith L, Mein R, Cullup T, Dionisi-Vici C, et al. EPG5-related Vici syndrome: a paradigm of neurodevelopmental disorders with defective autophagy. *Brain*. 2016;139:765–81.
- Cabrera M, Nordmann M, Perz A, Schmedt D, Gerondopoulos A, Barr F, Piehler J, Engelbrecht-Vandre S, Ungerermann C. The Mon1-Ccz1 GEF activates the Rab7 GTPase Ypt7 via a longin-fold-Rab interface and association with PI3P-positive membranes. *J Cell Sci*. 2014;127:1043–51.
- Carroll B, Otten EG, Manni D, Stefanatos R, Menzies FM, Smith GR, Jurk D, Kenneth N, Wilkinson S, Passos JF, et al. Oxidation of SQSTM1/p62 mediates the link between redox state and protein homeostasis. *Nat Commun*. 2018;9:256.
- Chakraborty J, von Stockum S, Marchesan E, Caicci F, Ferrari V, Rakovic A, Klein C, Antonini A, Bubacco L, Ziviani E. USP14 inhibition corrects an in vivo model of impaired mitophagy. *EMBO Mol Med*. 2018;10(11):e9014.
- Chang YY, Neufeld TP. An Atg1/Atg13 complex with multiple roles in TOR-mediated autophagy regulation. *Mol Biol Cell*. 2009;20:2004–14.
- Chang YY, Neufeld TP. Autophagy takes flight in *Drosophila*. *FEBS Lett*. 2010;584:1342–9.
- Chang TK, Shrivage BV, Hayes SD, Powers CM, Simin RT, Wade Harper J, Baehrecke EH. Uba1 functions in Atg7- and Atg3-independent autophagy. *Nat Cell Biol*. 2013;15:1067–78.
- Chew TS, O’Shea NR, Sewell GW, Oehlers SH, Mulvey CM, Crosier PS, Godovac-Zimmermann J, Bloom SL, Smith AM, Segal AW. Optineurin deficiency in mice contributes to impaired cytokine secretion and neutrophil recruitment in bacteria-driven colitis. *Dis Model Mech*. 2015;8:817–29.
- Cornelissen T, Vilain S, Vints K, Gouonko N, Verstreken P, Vandenbergh W. Deficiency of parkin and PINK1 impairs age-dependent mitophagy in *Drosophila*. *Elife*. 2018;7:e35878.
- Csizmadia T, Lorincz P, Hegedus K, Szeplaki S, Low P, Juhasz G. Molecular mechanisms of developmentally programmed crinophagy in *Drosophila*. *J Cell Biol*. 2018;217:361–74.
- Deng Z, Purtell K, Lachance V, Wold MS, Chen S, Yue Z. Autophagy receptors and neurodegenerative diseases. *Trends Cell Biol*. 2017;27:491–504.
- Denton D, Shrivage B, Simin R, Mills K, Berry DL, Baehrecke EH, Kumar S. Autophagy, not apoptosis, is essential for midgut cell death in *Drosophila*. *Curr Biol*. 2009;19:1741–6.
- DeVorkin L, Go NE, Hou YC, Moradian A, Morin GB, Gorski SM. The *Drosophila* effector caspase Dcp-1 regulates mitochondrial dynamics and autophagic flux via SesB. *J Cell Biol*. 2014;205:477–92.
- Dezelee S, Bras F, Contamine D, Lopez-Ferber M, Segretain D, Teninges D. Molecular analysis of ref(2)P, a *Drosophila* gene implicated in sigma rhabdovirus multiplication and necessary for male fertility. *EMBO J*. 1989;8:3437–46.
- Diao J, Liu R, Rong Y, Zhao M, Zhang J, Lai Y, Zhou Q, Wilz LM, Li J, Vivona S, et al. ATG14 promotes membrane tethering and fusion of autophagosomes to endolysosomes. *Nature*. 2015;520:563–6.
- Drummond-Barbosa D, Spradling AC. Stem cells and their progeny respond to nutritional changes during *Drosophila* oogenesis. *Dev Biol*. 2001;231:265–78.
- Durcan TM, Fon EA. The three ‘P’s of mitophagy: PARKIN, PINK1, and post-translational modifications. *Genes Dev*. 2015;29:989–99.
- Fang X, Zhou J, Liu W, Duan X, Gala U, Sandoval H, Jaiswal M, Tong C. Dynamin regulates autophagy by modulating lysosomal function. *J Genet Genomics = Yi chuan xue bao*. 2016;43:77–86.
- Feng Y, He D, Yao Z, Klionsky DJ. The machinery of macroautophagy. *Cell Res*. 2014;24:24–41.

- Finley KD, Edeen PT, Cumming RC, Mardahl-Dumesnil MD, Taylor BJ, Rodriguez MH, Hwang CE, Benedetti M, McKeown M. Blue cheese mutations define a novel, conserved gene involved in progressive neural degeneration. *J Neurosci.* 2003;23:1254–64.
- Fujita N, Huang W, Lin TH, Groulx JF, Jean S, Nguyen J, Kuchitsu Y, Koyama-Honda I, Mizushima N, Fukuda M, et al. Genetic screen in *Drosophila* muscle identifies autophagy-mediated T-tubule remodeling and a Rab2 role in autophagy. *Elife.* 2017;6:e23367.
- Galluzzi L, Baehrecke EH, Ballabio A, Boya P, Bravo-San Pedro JM, Cecconi F, Choi AM, Chu CT, Codogno P, Colombo MI, et al. Molecular definitions of autophagy and related processes. *EMBO J.* 2017;36:1811–36.
- Gonzalez A, Hall MN. Nutrient sensing and TOR signaling in yeast and mammals. *EMBO J.* 2017;36:397–408.
- Guo M. *Drosophila* as a model to study mitochondrial dysfunction in Parkinson's disease. *Cold Spring Harb Perspect Med.* 2012;2:a009944.
- Hegedus K, Nagy P, Gaspari Z, Juhasz G. The putative HORMA domain protein Atg101 dimerizes and is required for starvation-induced and selective autophagy in *Drosophila*. *Biomed Res Int.* 2014;2014:470482.
- Hegedus K, Takats S, Boda A, Jipa A, Nagy P, Varga K, Kovacs AL, Juhasz G. The Ccz1-Mon1-Rab7 module and Rab5 control distinct steps of autophagy. *Mol Biol Cell.* 2016;27:3132–42.
- Hong W. SNAREs and traffic. *Biochim Biophys Acta.* 2005;1744:120–44.
- Hong W, Lev S. Tethering the assembly of SNARE complexes. *Trends Cell Biol.* 2014;24:35–43.
- Hou YC, Chittaranjan S, Barbosa SG, McCall K, Gorski SM. Effector caspase Dcp-1 and IAP protein Bruce regulate starvation-induced autophagy during *Drosophila melanogaster* oogenesis. *J Cell Biol.* 2008;182:1127–39.
- Hu Z, Zhang J, Zhang Q. Expression pattern and functions of autophagy-related gene atg5 in zebrafish organogenesis. *Autophagy.* 2011;7:1514–27.
- Huber LA, Teis D. Lysosomal signaling in control of degradation pathways. *Curr Opin Cell Biol.* 2016;39:8–14.
- Ichimura Y, Kirisako T, Takao T, Satomi Y, Shimonishi Y, Ishihara N, Mizushima N, Tanida I, Kominami E, Ohsumi M, et al. A ubiquitin-like system mediates protein lipidation. *Nature.* 2000;408:488–92.
- Isakson P, Holland P, Simonsen A. The role of ALFY in selective autophagy. *Cell Death Differ.* 2013;20:12–20.
- Issa AR, Sun J, Pettigac C, Mesquita A, Dulac A, Robin M, Mollereau B, Jenny A, Cherif-Zahar B, Birman S. The lysosomal membrane protein LAMP2A promotes autophagic flux and prevents SNCA-induced Parkinson disease-like symptoms in the *Drosophila* brain. *Autophagy.* 2018;14:1898–910.
- Issman-Zecharya N, Schuldiner O. The PI3K class III complex promotes axon pruning by downregulating a Ptc-derived signal via endosome-lysosomal degradation. *Dev Cell.* 2014;31:461–73.
- Itakura E, Kishi C, Inoue K, Mizushima N. Beclin 1 forms two distinct phosphatidylinositol 3-kinase complexes with mammalian Atg14 and UVRAG. *Mol Biol Cell.* 2008;19:5360–72.
- Itakura E, Kishi-Itakura C, Mizushima N. The hairpin-type tail-anchored SNARE syntaxin 17 targets to autophagosomes for fusion with endosomes/lysosomes. *Cell.* 2012;151:1256–69.
- Jiang P, Nishimura T, Sakamaki Y, Itakura E, Hatta T, Natsume T, Mizushima N. The HOPS complex mediates autophagosome-lysosome fusion through interaction with syntaxin 17. *Mol Biol Cell.* 2014;25:1327–37.
- Juhasz G, Csikos G, Sinka R, Erdelyi M, Sass M. The *Drosophila* homolog of Aut1 is essential for autophagy and development. *FEBS Lett.* 2003;543:154–8.
- Juhasz G, Erdi B, Sass M, Neufeld TP. Atg7-dependent autophagy promotes neuronal health, stress tolerance, and longevity but is dispensable for metamorphosis in *Drosophila*. *Genes Dev.* 2007;21:3061–6.
- Juhasz G, Hill JH, Yan Y, Sass M, Baehrecke EH, Backer JM, Neufeld TP. The class III PI(3)K Vps34 promotes autophagy and endocytosis but not TOR signaling in *Drosophila*. *J Cell Biol.* 2008;181:655–66.

- Kandul NP, Zhang T, Hay BA, Guo M. Selective removal of deletion-bearing mitochondrial DNA in heteroplasmic *Drosophila*. *Nat Commun.* 2016;7:13100.
- Kaushik S, Cuervo AM. Chaperone-mediated autophagy: a unique way to enter the lysosome world. *Trends Cell Biol.* 2012;22:407–17.
- Kaushik S, Cuervo AM. The coming of age of chaperone-mediated autophagy. *Nat Rev Mol Cell Biol.* 2018;19:365–81.
- Kim J, Kim YC, Fang C, Russell RC, Kim JH, Fan W, Liu R, Zhong Q, Guan KL. Differential regulation of distinct Vps34 complexes by AMPK in nutrient stress and autophagy. *Cell.* 2013a;152:290–303.
- Kim M, Park HL, Park HW, Ro SH, Nam SG, Reed JM, Guan JL, Lee JH. *Drosophila* Fip200 is an essential regulator of autophagy that attenuates both growth and aging. *Autophagy.* 2013b;9:1201–13.
- Kling RC. The meiotic behavior of the *Drosophila* oocyte. *Int Rev Cytol.* 1970;28:125–68.
- Klionsky DJ, Abdelmohsen K, Abe A, Abedin MJ, Abeliovich H, Acevedo Arozena A, Adachi H, Adams CM, Adams PD, Adeli K, et al. Guidelines for the use and interpretation of assays for monitoring autophagy (3rd edition). *Autophagy.* 2016;12:1–222.
- Korac J, Schaeffer V, Kovacevic I, Clement AM, Jungblut B, Behl C, Terzic J, Dikic I. Ubiquitin-independent function of optineurin in autophagic clearance of protein aggregates. *J Cell Sci.* 2013;126:580–92.
- Ktistakis NT, Tooze SA. Digesting the expanding mechanisms of autophagy. *Trends Cell Biol.* 2016;26:624–35.
- Kyostila K, Syrja P, Jagannathan V, Chandrasekar G, Jokinen TS, Seppala EH, Becker D, Drogemuller M, Dietschi E, Drogemuller C, et al. A missense change in the ATG4D gene links aberrant autophagy to a neurodegenerative vacuolar storage disease. *PLoS Genet.* 2015;11:e1005169.
- Lamb CA, Yoshimori T, Tooze SA. The autophagosome: origins unknown, biogenesis complex. *Nat Rev Mol Cell Biol.* 2013;14:759–74.
- Lattante S, de Calbiac H, Le Ber I, Brice A, Ciura S, Kabashi E. Sqstm1 knock-down causes a locomotor phenotype ameliorated by rapamycin in a zebrafish model of ALS/FTLD. *Hum Mol Genet.* 2015;24:1682–90.
- Lawrence G, Brown CC, Flood BA, Karunakaran S, Cabrera M, Nordmann M, Ungermann C, Fratti RA. Dynamic association of the PI3P-interacting Mon1-Ccz1 GEF with vacuoles is controlled through its phosphorylation by the type 1 casein kinase Yck3. *Mol Biol Cell.* 2014;25:1608–19.
- Lee CY, Baehrecke EH. Steroid regulation of autophagic programmed cell death during development. *Development.* 2001;128:1443–55.
- Lee CY, Cooksey BA, Baehrecke EH. Steroid regulation of midgut cell death during *Drosophila* development. *Dev Biol.* 2002;250:101–11.
- Lee SB, Kim S, Lee J, Park J, Lee G, Kim Y, Kim JM, Chung J. ATG1, an autophagy regulator, inhibits cell growth by negatively regulating S6 kinase. *EMBO Rep.* 2007;8:360–5.
- Lee E, Koo Y, Ng A, Wei Y, Luby-Phelps K, Juraszek A, Xavier RJ, Cleaver O, Levine B, Amatruda JF. Autophagy is essential for cardiac morphogenesis during vertebrate development. *Autophagy.* 2014;10:572–87.
- Lee JJ, Sanchez-Martinez A, Zarate AM, Beninca C, Mayor U, Clague MJ, Whitworth AJ. Basal mitophagy is widespread in *Drosophila* but minimally affected by loss of Pink1 or parkin. *J Cell Biol.* 2018;217:1613–22.
- Lescat L, Herpin A, Mouro B, Veron V, Guiguen Y, Bobe J, Seiliez I. CMA restricted to mammals and birds: myth or reality? *Autophagy.* 2018;14:1267–70.
- Lim A, Kraut R. The *Drosophila* BEACH family protein, blue cheese, links lysosomal axon transport with motor neuron degeneration. *J Neurosci.* 2009;29:951–63.
- Lindmo K, Simonsen A, Brech A, Finley K, Rusten TE, Stenmark H. A dual function for Deep orange in programmed autophagy in the *Drosophila melanogaster* fat body. *Exp Cell Res.* 2006;312:2018–27.

- Liu L, Sakakibara K, Chen Q, Okamoto K. Receptor-mediated mitophagy in yeast and mammalian systems. *Cell Res.* 2014;24:787–95.
- Liu W, Duan X, Fang X, Shang W, Tong C. Mitochondrial protein import regulates cytosolic protein homeostasis and neuronal integrity. *Autophagy.* 2018;14:1293–309.
- Lloyd V, Ramaswami M, Kramer H. Not just pretty eyes: *Drosophila* eye-colour mutations and lysosomal delivery. *Trends Cell Biol.* 1998;8:257–9.
- Lorincz P, Lakatos Z, Maruzs T, Szatmari Z, Kis V, Sass M. Atg6/UVRAG/Vps34-containing lipid kinase complex is required for receptor downregulation through endolysosomal degradation and epithelial polarity during *Drosophila* wing development. *Biomed Res Int.* 2014;2014:851349.
- Lorincz P, Mauvezin C, Juhasz G. Exploring autophagy in *Drosophila*. *Cells.* 2017a;6:22.
- Lorincz P, Toth S, Benko P, Lakatos Z, Boda A, Glatz G, Zobel M, Bisi S, Hegedus K, Takats S, et al. Rab2 promotes autophagic and endocytic lysosomal degradation. *J Cell Biol.* 2017b;216:1937–47.
- Ma P, Yun J, Deng H, Guo M. Atg1 mediated autophagy suppresses tissue degeneration in pink1/parkin mutants by promoting mitochondrial fission in *Drosophila*. *Mol Biol Cell.* 2018;29(26):3082–92. <https://doi.org/10.1091/mbc.E18-04-0243>.
- Martin DN, Baehrecke EH. Caspases function in autophagic programmed cell death in *Drosophila*. *Development.* 2004;131:275–84.
- Mathai BJ, Meijer AH, Simonsen A. Studying autophagy in zebrafish. *Cells.* 2017;6:21.
- Matsunaga K, Morita E, Saitoh T, Akira S, Kistakis NT, Izumi T, Noda T, Yoshimori T. Autophagy requires endoplasmic reticulum targeting of the PI3-kinase complex via Atg14L. *J Cell Biol.* 2010;190:511–21.
- Matsushita M, Suzuki NN, Obara K, Fujioka Y, Ohsumi Y, Inagaki F. Structure of Atg5-Atg16, a complex essential for autophagy. *J Biol Chem.* 2007;282:6763–72.
- Mauvezin C, Ayala C, Braden CR, Kim J, Neufeld TP. Assays to monitor autophagy in *Drosophila*. *Methods.* 2014;68:134–9.
- McCall K. Eggs over easy: cell death in the *Drosophila* ovary. *Dev Biol.* 2004;274:3–14.
- McEwan DG, Popovic D, Gubas A, Terawaki S, Suzuki H, Stadel D, Coxon FP, Miranda de Stegmann D, Bhogaraju S, Maddi K, et al. PLEKHM1 regulates autophagosome-lysosome fusion through HOPS complex and LC3/GABARAP proteins. *Mol Cell.* 2015;57:39–54.
- McPhee CK, Logan MA, Freeman MR, Baehrecke EH. Activation of autophagy during cell death requires the engulfment receptor Draper. *Nature.* 2010;465:1093–6.
- Meneghetti G, Skobo T, Chrisam M, Facchinello N, Fontana CM, Belleso S, Sabatelli P, Raggi F, Cecconi F, Bonaldo P, et al. The *egg5* knockout zebrafish line: a model to study Vici syndrome. *Autophagy.* 2019;15(8):1438–54.
- Micchelli CA, Perrimon N. Evidence that stem cells reside in the adult *Drosophila* midgut epithelium. *Nature.* 2006;439:475–9.
- Mijaljica D, Prescott M, Devenish RJ. Microautophagy in mammalian cells: revisiting a 40-year-old conundrum. *Autophagy.* 2011;7:673–82.
- Mizushima N. Autophagy in protein and organelle turnover. *Cold Spring Harb Symp Quant Biol.* 2011;76:397–402.
- Mizushima N, Komatsu M. Autophagy: renovation of cells and tissues. *Cell.* 2011;147:728–41.
- Mizushima N, Levine B, Cuervo AM, Klionsky DJ. Autophagy fights disease through cellular self-digestion. *Nature.* 2008;451:1069–75.
- Mizushima N, Yoshimori T, Levine B. Methods in mammalian autophagy research. *Cell.* 2010;140:313–26.
- Mostowy S, Boucontet L, Mazon Moya MJ, Sirianni A, Boudinot P, Hollinshead M, Cossart P, Herbomel P, Levraud JP, Colucci-Guyon E. The zebrafish as a new model for the in vivo study of *Shigella flexneri* interaction with phagocytes and bacterial autophagy. *PLoS Pathog.* 2013;9:e1003588.
- Mukherjee A, Patel B, Koga H, Cuervo AM, Jenny A. Selective endosomal microautophagy is starvation-inducible in *Drosophila*. *Autophagy.* 2016;12:1984–99.

- Mulakkal NC, Nagy P, Takats S, Tusco R, Juhasz G, Nezis IP. Autophagy in *Drosophila*: from historical studies to current knowledge. *Biomed Res Int*. 2014;2014:273473.
- Nagy P, Hegedus K, Pircs K, Varga A, Juhasz G. Different effects of Atg2 and Atg18 mutations on Atg8a and Atg9 trafficking during starvation in *Drosophila*. *FEBS Lett*. 2014a;588:408–13.
- Nagy P, Karpati M, Varga A, Pircs K, Venkei Z, Takats S, Varga K, Erdi B, Hegedus K, Juhasz G. Atg17/FIP200 localizes to perilyosomal Ref(2)P aggregates and promotes autophagy by activation of Atg1 in *Drosophila*. *Autophagy*. 2014b;10:453–67.
- Nagy P, Varga A, Kovacs AL, Takats S, Juhasz G. How and why to study autophagy in *Drosophila*: it's more than just a garbage chute. *Methods*. 2015;75:151–61.
- Nagy P, Szatmari Z, Sandor GO, Lippai M, Hegedus K, Juhasz G. *Drosophila* Atg16 promotes enteroendocrine cell differentiation via regulation of intestinal Slit/Robo signaling. *Development*. 2017;144:3990–4001.
- Nakatogawa H, Ichimura Y, Ohsumi Y. Atg8, a ubiquitin-like protein required for autophagosome formation, mediates membrane tethering and hemifusion. *Cell*. 2007;130:165–78.
- Nakatogawa H, Suzuki K, Kamada Y, Ohsumi Y. Dynamics and diversity in autophagy mechanisms: lessons from yeast. *Nat Rev Mol Cell Biol*. 2009;10:458–67.
- Nelson C, Baehrecke EH. Eaten to death. *FEBS J*. 2014;281:5411–7.
- Nelson C, Ambros V, Baehrecke EH. miR-14 regulates autophagy during developmental cell death by targeting ip3-kinase 2. *Mol Cell*. 2014;56:376–88.
- Nezis IP, Simonsen A, Sagona AP, Finley K, Gaumer S, Contamine D, Rusten TE, Stenmark H, Brech A. Ref(2)P, the *Drosophila melanogaster* homologue of mammalian p62, is required for the formation of protein aggregates in adult brain. *J Cell Biol*. 2008;180:1065–71.
- Nezis IP, Lamark T, Velentzas AD, Rusten TE, Bjorkoy G, Johansen T, Papassideri IS, Stravopodis DJ, Margaritis LH, Stenmark H, et al. Cell death during *Drosophila melanogaster* early oogenesis is mediated through autophagy. *Autophagy*. 2009;5:298–302.
- Ochaba J, Lukacsovich T, Csikos G, Zheng S, Margulis J, Salazar L, Mao K, Lau AL, Yeung SY, Humbert S, et al. Potential function for the Huntingtin protein as a scaffold for selective autophagy. *Proc Natl Acad Sci U S A*. 2014;111:16889–94.
- Paulus JD, Link BA. Loss of optineurin in vivo results in elevated cell death and alters axonal trafficking dynamics. *PLoS One*. 2014;9:e109922.
- Pickles S, Vignie P, Youle RJ. Mitophagy and quality control mechanisms in mitochondrial maintenance. *Curr Biol*. 2018;28:R170–85.
- Politi Y, Gal L, Kalifa Y, Ravid L, Elazar Z, Arama E. Paternal mitochondrial destruction after fertilization is mediated by a common endocytic and autophagic pathway in *Drosophila*. *Dev Cell*. 2014;29:305–20.
- Polson HE, de Lartigue J, Rigden DJ, Reedijk M, Urbe S, Clague MJ, Tooze SA. Mammalian Atg18 (WIPI2) localizes to omegasome-anchored phagophores and positively regulates LC3 lipidation. *Autophagy*. 2010;6:506–22.
- Poteryaev D, Datta S, Ackema K, Zerial M, Spang A. Identification of the switch in early-to-late endosome transition. *Cell*. 2010;141:497–508.
- Pulipparacharuvil S, Akbar MA, Ray S, Sevrioukov EA, Haberman AS, Rohrer J, Kramer H. *Drosophila* Vps16A is required for trafficking to lysosomes and biogenesis of pigment granules. *J Cell Sci*. 2005;118:3663–73.
- Ramesh T, Lyon AN, Pineda RH, Wang C, Janssen PM, Canan BD, Burghes AH, Beattie CE. A genetic model of amyotrophic lateral sclerosis in zebrafish displays phenotypic hallmarks of motoneuron disease. *Dis Model Mech*. 2010;3:652–62.
- Reggiori F, Tucker KA, Stromhaug PE, Klionsky DJ. The Atg1-Atg13 complex regulates Atg9 and Atg23 retrieval transport from the pre-autophagosomal structure. *Dev Cell*. 2004;6:79–90.
- Rojas-Rios P, Chartier A, Pierson S, Severac D, Dantec C, Busseau I, Simonelig M. Translational control of autophagy by orb in the *Drosophila* germline. *Dev Cell*. 2015;35:622–31.
- Rui YN, Xu Z, Patel B, Chen Z, Chen D, Tito A, David G, Sun Y, Stimming EF, Bellen HJ, et al. Huntingtin functions as a scaffold for selective macroautophagy. *Nat Cell Biol*. 2015;17:262–75.

- Rusten TE, Lindmo K, Juhasz G, Sass M, Seglen PO, Brech A, Stenmark H. Programmed autophagy in the *Drosophila* fat body is induced by ecdysone through regulation of the PI3K pathway. *Dev Cell*. 2004;7:179–92.
- Sasaki T, Lian S, Qi J, Bayliss PE, Carr CE, Johnson JL, Guha S, Kobler P, Catz SD, Gill M, et al. Aberrant autolysosomal regulation is linked to the induction of embryonic senescence: differential roles of Beclin 1 and p53 in vertebrate Spns1 deficiency. *PLoS Genet*. 2014;10:e1004409.
- Sasaki T, Lian S, Khan A, Llop JR, Samuelson AV, Chen W, Klionsky DJ, Kishi S. Autolysosome biogenesis and developmental senescence are regulated by both Spns1 and v-ATPase. *Autophagy*. 2017;13:386–403.
- Scott RC, Schuldiner O, Neufeld TP. Role and regulation of starvation-induced autophagy in the *Drosophila* fat body. *Dev Cell*. 2004;7:167–78.
- Scott RC, Juhasz G, Neufeld TP. Direct induction of autophagy by Atg1 inhibits cell growth and induces apoptotic cell death. *Curr Biol*. 2007;17:1–11.
- Sevrioukov EA, He JP, Moghrabi N, Sunio A, Kramer H. A role for the deep orange and carnation eye color genes in lysosomal delivery in *Drosophila*. *Mol Cell*. 1999;4:479–86.
- Simonsen A, Birkeland HC, Gillooly DJ, Mizushima N, Kuma A, Yoshimori T, Slagsvold T, Brech A, Stenmark H. Alfy, a novel FYVE-domain-containing protein associated with protein granules and autophagic membranes. *J Cell Sci*. 2004;117:4239–51.
- Simonsen A, Cumming RC, Brech A, Isakson P, Schubert DR, Finley KD. Promoting basal levels of autophagy in the nervous system enhances longevity and oxidant resistance in adult *Drosophila*. *Autophagy*. 2008;4:176–84.
- Singh T, Lee EH, Hartman TR, Ruiz-Whalen DM, O'Reilly AM. Opposing action of hedgehog and insulin signaling balances proliferation and autophagy to determine follicle stem cell lifespan. *Dev Cell*. 2018;46:720–734.e6.
- Solinger JA, Spang A. Tethering complexes in the endocytic pathway: CORVET and HOPS. *FEBS J*. 2013;280:2743–57.
- Soukup SF, Kuenen S, Vanhauwaert R, Manetsberger J, Hernandez-Diaz S, Swerts J, Schoovaerts N, Vilain S, Gounko NV, Vints K, et al. A LRRK2-dependent EndophilinA phosphoswitch is critical for macroautophagy at presynaptic terminals. *Neuron*. 2016;92:829–44.
- Spang A. Membrane tethering complexes in the endosomal system. *Front Cell Dev Biol*. 2016;4:35.
- Spradling AC. Position effect variegation and genomic instability. *Cold Spring Harb Symp Quant Biol*. 1993;58:585–96.
- Stenmark H. Rab GTPases as coordinators of vesicle traffic. *Nat Rev Mol Cell Biol*. 2009;10:513–25.
- Swetha MG, Sriram V, Krishnan KS, Oorschot VM, ten Brink C, Klumperman J, Mayor S. Lysosomal membrane protein composition, acidic pH and sterol content are regulated via a light-dependent pathway in metazoan cells. *Traffic*. 2011;12:1037–55.
- Takats S, Nagy P, Varga A, Piracs K, Karpati M, Varga K, Kovacs AL, Hegedus K, Juhasz G. Autophagosomal Syntaxin17-dependent lysosomal degradation maintains neuronal function in *Drosophila*. *J Cell Biol*. 2013;201:531–9.
- Takats S, Piracs K, Nagy P, Varga A, Karpati M, Hegedus K, Kramer H, Kovacs AL, Sass M, Juhasz G. Interaction of the HOPS complex with Syntaxin 17 mediates autophagosome clearance in *Drosophila*. *Mol Biol Cell*. 2014;25:1338–54.
- Takats S, Glatz G, Szenci G, Boda A, Horvath GV, Hegedus K, Kovacs AL, Juhasz G. Non-canonical role of the SNARE protein Ykt6 in autophagosome-lysosome fusion. *PLoS Genet*. 2018;14:e1007359.
- Tang HW, Liao HM, Peng WH, Lin HR, Chen CH, Chen GC. Atg9 interacts with dTRAF2/TRAF6 to regulate oxidative stress-induced JNK activation and autophagy induction. *Dev Cell*. 2013;27:489–503.
- Tian Y, Li Z, Hu W, Ren H, Tian E, Zhao Y, Lu Q, Huang X, Yang P, Li X, et al. *C. elegans* screen identifies autophagy genes specific to multicellular organisms. *Cell*. 2010;141:1042–55.
- Tian X, Gala U, Zhang Y, Shang W, Nagarkar Jaiswal S, di Ronza A, Jaiswal M, Yamamoto S, Sandoval H, Duraine L, et al. A voltage-gated calcium channel regulates lysosomal fusion

- with endosomes and autophagosomes and is required for neuronal homeostasis. *PLoS Biol.* 2015;13:e1002103.
- van der Vaart M, Korbee CJ, Lamers GE, Tengeler AC, Hosseini R, Haks MC, Ottenhoff TH, Spaink HP, Meijer AH. The DNA damage-regulated autophagy modulator DRAM1 links mycobacterial recognition via TLR-MYD88 to autophagic defense [corrected]. *Cell Host Microbe.* 2014;15:753–67.
- Vanhauwaert R, Kuenen S, Masius R, Bademosi A, Manetsberger J, Schoovaerts N, Bounti L, Gontcharenko S, Swerts J, Vilain S, et al. The SAC1 domain in synaptojanin is required for autophagosome maturation at presynaptic terminals. *EMBO J.* 2017;36:1392–411.
- Velentzas PD, Zhang L, Das G, Chang TK, Nelson C, Kobertz WR, Baehrecke EH. The proton-coupled monocarboxylate transporter hermes is necessary for autophagy during cell death. *Dev Cell.* 2018;47:281–293.e4.
- Wang ZH, Clark C, Geisbrecht ER. *Drosophila* clueless is involved in Parkin-dependent mitophagy by promoting VCP-mediated Marf degradation. *Hum Mol Genet.* 2016;25:1946–64.
- Wen JK, Wang YT, Chan CC, Hsieh CW, Liao HM, Hung CC, Chen GC. Atg9 antagonizes TOR signaling to regulate intestinal cell growth and epithelial homeostasis in *Drosophila*. *Elife.* 2017;6:e29338.
- Williams A, Sarkar S, Cuddon P, Ttofi EK, Saiki S, Siddiqi FH, Jahreiss L, Fleming A, Pask D, Goldsmith P, et al. Novel targets for Huntington's disease in an mTOR-independent autophagy pathway. *Nat Chem Biol.* 2008;4:295–305.
- Wullschlegel S, Loewith R, Hall MN. TOR signaling in growth and metabolism. *Cell.* 2006;124:471–84.
- Xu T, Nicolson S, Denton D, Kumar S. Distinct requirements of Autophagy-related genes in programmed cell death. *Cell Death Differ.* 2015;22:1792–802.
- Yu L, McPhee CK, Zheng L, Mardones GA, Rong Y, Peng J, Mi N, Zhao Y, Liu Z, Wan F, et al. Termination of autophagy and reformation of lysosomes regulated by mTOR. *Nature.* 2010;465:942–6.
- Yun J, Puri R, Yang H, Lizzio MA, Wu C, Sheng ZH, Guo M. MUL1 acts in parallel to the PINK1/parkin pathway in regulating mitofusins and compensates for loss of PINK1/parkin. *Elife.* 2014;3:e01958.
- Zhang H, Baehrecke EH. Eaten alive: novel insights into autophagy from multicellular model systems. *Trends Cell Biol.* 2015;25:376–87.
- Zhang S, Feany MB, Saraswati S, Littleton JT, Perrimon N. Inactivation of *Drosophila* Huntingtin affects long-term adult functioning and the pathogenesis of a Huntington's disease model. *Dis Model Mech.* 2009;2:247–66.
- Zhao S, Fortier TM, Baehrecke EH. Autophagy promotes tumor-like stem cell niche occupancy. *Curr Biol.* 2018;28:3056–3064.e3.
- Zheng H, Yang X, Xi Y. Fat body remodeling and homeostasis control in *Drosophila*. *Life Sci.* 2016;167:22–31.
- Ziegenfuss JS, Biswas R, Avery MA, Hong K, Sheehan AE, Yeung YG, Stanley ER, Freeman MR. Draper-dependent glial phagocytic activity is mediated by Src and Syk family kinase signalling. *Nature.* 2008;453:935–9.

Chapter 16

Screening for Genes Involved in Autophagy



Kefeng Lu and Huihui Li

Abstract Autophagy is an important intracellular lysosomal degradation process in cells, which is highly conserved from yeast to mammals. The process of autophagy is roughly divided into the following key steps: the formation of a membrane structure called ISM (isolated membrane) after stimulation, the biogenesis and maturation of autophagosomes, and finally the degradation of autophagosomes. A number of proteins are required to function in the whole process of autophagy. Since the initial genetic screening in yeast cells, multiple genes that play pivotal roles in autophagy have been discovered. These molecules have been named ATG genes (AuTophagy related genes). The screening for new key molecules involved in autophagy has greatly promoted the characterization of the mechanism of the autophagy machinery and provides multiple targets for the development of autophagy-based regulatory drugs.

In this section, we will summarize the screening methods used to find autophagy genes, represented in chronological order, including the screening in yeast cells and screening in mammalian cells. We apologize for some screening researches that have not been introduced due to space limitations.

16.1 Overview of the Multispecies Conservation of the Process of Autophagy and the Early Screens for Genes Involved in the Process

The process of autophagy is highly conserved in almost all eukaryotes, from simple single-cell yeast cells to multicellular mammals such as human. The conserved mechanism of autophagy is due to the conservative existence of molecules involved

K. Lu (✉) · H. Li
State Key Laboratory of Biotherapy, West China Hospital, Sichuan University,
Chengdu, China
e-mail: lukf@scu.edu.cn; lihuihui@scu.edu.cn

in the autophagy machinery. Since the first screening of autophagy genes in yeast cells in 1993, subsequent screening in various model organisms such as *Arabidopsis*, tobacco, nematodes, fruit flies, mice, etc. has shown clearly that autophagy genes are highly conserved across all eukaryotes.

16.1.1 Autophagy Genes in the Model Organism *Saccharomyces cerevisiae*

In 1992, Yoshinori Ohsumi discovered that when yeast cells were treated with nutrient limitations, a large number of autophagosomes appeared in the cells. This was the first time that autophagy was observed in yeast cells. The Ohsumi laboratory subsequently screened for autophagy mutants and found a series of yeast mutants associated with autophagy deficiency and identified 15 autophagy genes. Later on, more ATG genes were revealed. There are currently 37 ATG genes in the yeast database SGD, which are named ATG1 to ATG42 (lacking are ATG25, ATG28, ATG30, ATG35, and ATG37).

16.1.1.1 Introduction to the Yeast *Saccharomyces cerevisiae*

The mostly used yeast in research is *Saccharomyces cerevisiae*, also known as baker's yeast or budding yeast. It can be used not only for the production of food such as bread and wine but also as a very effective model organism commonly used in molecular biology and cell biology. The morphology of *Saccharomyces cerevisiae* cells is spherical or ovate and about 5–10 μm in diameter. Offspring reproduction is carried out by budding. *Saccharomyces cerevisiae* cells can occur in haploid and diploid condition. Haploid cells are propagated by germination after mitosis. Haploid cells have two mating types, named a and alpha, which can in combination form diploid cells by mating. Diploid cells are an advantageous form of yeast, and they are also propagated by simple mitosis under normal culture conditions. In the case of external stress such as nutrient deficiencies, diploid cells undergo meiosis to produce haploid spores, which can survive harsh conditions and that become haploid cells when the yeast is shifted back to nutrient-rich conditions. Whole genome sequencing of *S. cerevisiae* was completed in 1996 as the first eukaryotic organism being genomically sequenced. *Saccharomyces cerevisiae* cells are genetically composed of 16 sets of chromosomes containing a total of approximately 12 million base pairs. *S. cerevisiae* cells possess at least 6275 genes, of which about 5800 genes have known biological functions. It is estimated that approximately 23% of its genes are homologous to human genes. Because *Saccharomyces cerevisiae* cells have many of the same structural and biological processes as other eukaryotic cells such as animals and plant cells and also its culture and genetic manipulations are very simple and reliable, it is widely used as a model organism.

16.1.1.2 The Discovery of Autophagy Genes in *Saccharomyces cerevisiae* Cells

In 1992, the Ohsumi laboratory found that when in yeast cells, genes were knocked out that coded for proteolytic enzymes in the vacuole, nitrogen starvation could induce a large number of autophagic vesicles in the vacuole. These autophagic vesicles can be directly observed by ordinary phase contrast microscopy. The accumulation of autophagic vesicles was also observed after treatment with the hydrolase inhibitor phenylmethanesulfonyl fluoride (PMSF). In 1993 and later, based on the above phenomenon, the Ohsumi laboratory screened for genes related to autophagy. In 1994 and 1995, scientists such as Thumm (Wolf Laboratories) and Harding (Klionsky Laboratories) also screened for genes involved in the autophagy process or in the CVT pathway (cytoplasm to vacuole targeting and a selective degradation type of autophagy) and identified more autophagy related genes. There was a large intersection between the autophagy genes identified by their separate screenings, but the initial nomenclature was quite different. In order to facilitate the communication between autophagy scientists and for a clear definition of the autophagy genes, in 2003, many scientists organized by Klionsky and Ohsumi jointly published a paper to unify the naming of the autophagy genes in *Saccharomyces cerevisiae* and named as *ATG* genes (AuTophagy-related genes).

16.1.2 Autophagy Genes in Animal Cells and in Other Species

Since the first autophagy genes were identified in *Saccharomyces cerevisiae* in 1993, a lot of work has been done. Currently, at least 37 autophagy-related genes have been identified in yeast. Due to the conservation of the autophagy process, autophagy-related genes are highly conserved among multiple model organisms. The existence and conserved functions of *ATG* homologues were discovered in *Arabidopsis*, tobacco, nematodes, fruit flies, zebrafish, mice, human cells, and other organisms. More conserved *ATG* genes will be discovered, and their functions will be clarified in more new model organisms such as the planarian.

16.1.2.1 The Discovery of Genes Involved in Autophagy in Mammalian Cells and Their Functions

Mammalian autophagy genes are named similar to those in yeast and are mostly named Atg. However, there are also several differences, for instance, the yeast *ATG8* is called LC3 in mammals and the yeast *ATG6* is named Beclin 1 in mammals. Moreover, it is found that most of the autophagy-related genes known in yeast have multiple homologues in mammal, for example, the mammalian homologous molecules of the yeast *ATG1* gene include Ulk1, Ulk2, and Ulk3 and the mammalian LC3 has at least seven homologous genes. This aspect demonstrates the

conservation of the autophagy process and more importantly suggests the functional diversity and complexity of the autophagy process in mammalian cells. Autophagy is involved in numerous physiological and pathological processes in mammals such as cancer, inflammatory immunity, development, and aging. Studies have also shown that autophagy is involved in neurodegenerative diseases such as Alzheimer disease (AD). In recent years, some potential therapeutic drugs have been discovered that may improve AD by regulating autophagy. In addition, a number of small molecules that extend the lifespan of model organisms, such as resveratrol and Rapamycin, have been found to activate autophagy.

16.1.2.2 Autophagy Gene Discovery and Function Studies in Other Species

In recent years, several key genes of autophagy have been identified in the plant *Arabidopsis thaliana* and in crops such as rice (*Oryza sativa*) and maize (*Zea mays*). Autophagy plays an important role in the resistance of plants against nutrient deficiencies, abiotic stresses such as drought and high temperatures, and pathogens. As a multicellular organism, *Caenorhabditis elegans* has become a good model organism to be used for studying basic life phenomena such as cell differentiation, apoptosis, neurodevelopment, sex differentiation, and aging. In recent years, the study on autophagy in *C. elegans* has also been greatly developed, especially after the autophagy screening that was carried out in Hong Zhang's Laboratory. More and more autophagy molecules in *C. elegans* have been discovered and revealed for their functions. The zebrafish (*Danio rerio*) is a commonly used model that serves as a powerful tool for studying organ development and regeneration. Many autophagy-related genes have been found to have homologous molecules in zebrafish, and they have been shown to play an important role in fighting pathogens, cellular immunity, and body and organ development. The successful use of the CRISPR/Cas9-based gene editing technology in zebrafish has accelerated zebrafish autophagy research in recent years.

16.2 Screening for Autophagy Genes

The biological importance of the function of autophagy is increasingly recognized. Professor Yoshinori Ohsumi's winning of the 2016 Nobel Prize in Physiology and Medicine for his research on autophagy has demonstrated a high level of recognition for the significance of autophagy. At present, with the results of various autophagy gene screening assays available, the mechanism of autophagy is gradually becoming clear in more and more detail. However, the screening of new autophagy key molecules will help to reveal specific information in the initiation, maturation, and transportation processes of autophagy. The discovery of new key molecules for autophagy will truly complement our perception of autophagy, and the clarification

of new molecular functions will also enrich and reveal the biological function of autophagy in specific physiological and pathological processes. This section summarizes the initial and latest autophagy gene screenings and provides autophagy scientists with suggestive information for future screening.

16.2.1 Screening for Autophagy Genes in *Saccharomyces cerevisiae*

Saccharomyces cerevisiae, as a widely used eukaryotic model organism, has made a crucial contribution to the initial discovery of autophagy genes. Even in the current study of autophagy, *Saccharomyces cerevisiae* is still favored by autophagy scientists because of its unique advantages. First, the activity of autophagy in yeast cells can be significantly regulated. Under the conditions of adequate nutrient culture, the autophagy activity in yeast cells is very low. When the cells are transferred to conditions in which there is nitrogen source starvation or carbon source starvation, or when the cells are treated with rapamycin, the autophagy activity is significantly enhanced. In other model organisms, due to the high activity of basal autophagy, this distinct regulation of autophagy is relatively difficult to achieve. In addition, all the known autophagy genes are present as single copies in yeast cells, so after an autophagy key gene is knocked out in a haploid yeast culture, a complete blockade of autophagy can be achieved, thereby verifying the function of autophagy genes. In other model organisms, especially in mammalian cells, autophagy genes mostly have multiple homologous molecules. Therefore, after knocking down or knocking out one gene alone, the activity of autophagy may not be changed due to the complementation of its homologous genes. At present, all autophagy key genes in yeast cells are found to have homologue genes in mammalian animals. Therefore, by screening for autophagy related genes in yeast and analyzing their mammalian homologous sequences, the finding of new key genes of autophagy in mammals can effectively be promoted. The screening for autophagy-related genes in yeast is broadly divided into two categories. One is the long-standing approach, with the use of chemical reagents to create gene mutations and the screening for cells affected in autophagy to identify related genes. The second category is screens using a yeast knockout mutant library to find new autophagy related genes. Using these techniques, genes that are involved in the machinery of general and selective autophagy can be found.

16.2.1.1 The Initial Discovery of Autophagy Genes

In 1992, Takeshige et al. from the Ohsumi Laboratory knocked out the hydrolase proteases A and B (proteinase A and B) and carboxypeptidase Y, proteases that are normally functioning in yeast vacuoles, and then placed the cells in media with a

nitrogen or carbon deficiency. It was found that nutrient deficiencies induced the accumulation of autophagic vesicles in vacuoles (Takeshige et al. 1992). Subsequently, in 1993, Tsukada from the Ohsumi laboratory used the above phenotype to screen for genes involved in autophagy. First, gene mutation was induced by adding ethyl methanesulfonate (EMS) to the culture and then under nutrient deficiency, and the autophagy-blocked cells had a decreased viability due to the inability to undergo autophagy. Yeast cells that died after starvation were selected by staining with phloxine B. A second round of screening was then performed through observation of the presence of autophagic vesicles in the vacuoles by light microscopy. A total of 15 autophagy genes were identified by selecting strains that could not form autophagic vacuoles in their cells and by subsequent complementation assays with a yeast gene library, which were named *APG1-APG15* (Tsukada and Ohsumi 1993).

In 1994, Thumm from the Wolf lab also conducted a screening for autophagy-related genes (Thumm et al. 1994). Thumm used the cytoplasmic protein fatty acid synthase as an autophagic degradation marker. This synthase is transported into vacuoles via autophagy and is degraded in autophagy activated conditions. The induction of gene mutation was also carried out by EMS treatment, and a fatty acid synthase antibody was used to screen for mutant strains in which this synthase could not be transported to the vacuole for degradation. Using this method, Thumm identified three autophagy genes and named *AUT1-AUT3* (Thumm et al. 1994).

In 1995, Harding et al. from the Klionsky lab also used chemical reagents to induce genetic mutations to search for autophagy genes (Harding et al. 1995). Klionsky had previously discovered that the precursor of the aminopeptidase I (Ape I) protein (pro-ApeI) becomes an active aminopeptidase when it is transported from the cytoplasm to the vacuole. ApeI is first translated as a 61 kD soluble cytoplasmic localized precursor molecule. After being transported to the vacuole, the amino-terminal signal peptide is removed by proteinase B to produce a mature 50 kD ApeI hydrolase. Harding et al. induced gene mutations using ethyl methanesulfonate (EMS) and then used ApeI specific serum antibody to screen for a mutant strain in which a mature form of ApeI could not be formed. They found and named a number of autophagy-related genes, *CVT1-CVT8*. As it turned out, the *CVT* (cytoplasm to vacuole protein targeting) pathway is a special form of autophagy in which the uptake of pro-ApeI is propagated by wrapping the substrate pro-ApeI and transporting it to the vacuole in an autophagic fashion.

The classic autophagy gene screenings clarified above were carried out in succession in the 1990s. Subsequent screenings gradually increased the number of autophagy genes. Since then, the discovery of autophagy genes has greatly promoted the understanding of the mechanism and function of autophagy. At the beginning, the names of autophagy-related genes obtained by each screening were different. For example, the Ohsumi laboratory termed their discovered genes *APG* genes, Thumm et al. used the acronym *AUT*, and the Klionsky laboratory labeled the genes as *CVT* genes. All these autophagy genes were then unified as *ATG* genes (Klionsky et al. 2003).

16.2.1.2 New Screening of Autophagy Genes

In the autophagy gene screening assays conducted in the early 90s, all researchers used EMS to chemically induce gene mutations in order to identify strains blocked in autophagy. In later years, the ease of genetic manipulation of yeast cells allowed gene knockout libraries to be implemented. A knockout library of approximately 5000 genes was generated by collaboration between multiple yeast laboratories around the world. Subsequent autophagy-related screenings were mostly based on this library. Most of the genes in yeast cells (about 5000) can be knocked out without causing cell death. Likewise, the knockout of an autophagy gene has almost no effect on the viability of cells under normal culture conditions, but after prolonged nutrition starvation, the blocked autophagy causes cell death.

In 2001, Barth from the Thumm lab used the yeast gene knockout library for a new screen for genes involved in autophagy (Barth and Thumm 2001). The screening method was based on the fact that after the autophagy is blocked, the yeast cells die after being starved by lack of a nitrogen source and the phloxine B dye can specifically display the dead cells. Using this method, Barth screened the yeast knockout library and discovered a new autophagy gene named *AUT8* (i.e., *ATG2*).

In 2005, the Ohsumi laboratory also used a yeast gene knockout library for a new screen (Kawamata et al. 2005). The same phenomenon was observed by staining dead cells after nutritional starvation, and 250 knockout strains were selected. After the known autophagy genes were removed from the selection, the potentially new autophagy genes were further identified by detecting the accumulation of autophagosomes. Among them, they found a new autophagy gene named *ATG29*.

In 2013, Sun from the Du lab screened the knockout library of *Schizosaccharomyces pombe* for new autophagy genes (Sun et al. 2013). They obtained information on the autophagy genes of fission yeast by screening for mating defects in strains, caused by deletions in autophagy genes. In addition to the autophagy genes known in *S. cerevisiae*, some new fission yeast specific autophagy genes were identified.

In 2014, Kida from the Noda lab screened the yeast knockout library by using the alkaline phosphatase (ALP) method (Kira et al. 2014). The yeast gene *PHO8* is the only alkaline phosphohydrolase in the yeast cell vacuole. The Pho8 precursor protein has no activity after synthesis in the cytoplasm and the signal peptide composed of 60 amino acids at the N-terminus directs its transfer to vacuole, in which the C-terminus of the Pho8 protein is cleaved by other hydrolases in the vacuole to become the active form of Pho8. When the N-terminal 60 amino acid signal peptide of Pho8 is removed, the Pho8 Δ 60 protein can only enter the vacuole and become the mature form via autophagy. Therefore, the autophagic activity of yeast cells can be detected by the quantification of Pho8 Δ 60 alkaline phosphatase activity. Kira et al. used the ALP method to screen the yeast knockout library. In addition to the discovery of known autophagy genes, new autophagy-related genes, *NPR2* and *NPR3*, were discovered. Both genes regulate autophagy by controlling the activity of the TORC1 complex.

In 2013, Shiraama-Noda from the Noda lab used the alkaline phosphatase method to screen for autophagy genes after the knockdown of essential genes in

yeast (Shirahama-Noda et al. 2013). Of the more than 6000 genes in yeast, about 5000 genes can be knocked out and about 1000 genes cannot be knocked out, indicating them as essential genes for survival. Shirahama-Noda et al. screened autophagy-related genes using a library of strains in which the mRNA stability of the essential genes was reduced. They found that Transport Protein Particle III (TRAPP III) participates in autophagy by circulating Atg9 lipid vesicles between the Golgi and the autophagosomes.

In the beginning, autophagy was considered to be nonselective. Later, various selective autophagy phenomena were revealed, targeting specific substrates to the vacuole. Currently, a variety of selective autophagy pathways are known, such as mitochondrial autophagy, ribosome autophagy, peroxisome autophagy, protein aggregate autophagy, and pathogenic autophagy. After the extensive disclosure of the key genes in general autophagy, the screening of genes involved in selective autophagy has gradually become the trend of autophagy screening.

In 2009, the Ohsumi lab and the Klionsky lab performed a screen for genes involved in the specific autophagy of mitochondria (Okamoto et al. 2009; Kanki et al. 2009a, b). After fusion of the mitochondrial localization signal or fusion of mitochondrial proteins with GFP, the autophagic transfer of the GFP protein into the vacuole was monitored. In the case of autophagy blockage, the GFP fusion protein cannot enter the vacuole. The GFP fusion protein was expressed in the yeast knock-out library for screening. Based on these screenings, the two laboratories have intensively verified many new genes and consistently discovered the mitochondrial autophagy receptor molecule Atg32.

In 2014, Bockler from the Westermann lab used a set of mitochondrial respiratory abnormal strains to screen for mitochondrial autophagy-related genes (Bockler and Westermann 2014).

Bockler fused the fluorescent protein Rosella to the mitochondrial targeting signal sequence (mtRosella) and checked the phenotype of the strains in starvation conditions. It was found that the endoplasmic reticulum mitochondria encounter structure (ERMES) molecules Mdm10, Mdm12, Mdm34, and Mmm1 that play important roles in mitochondrial autophagy.

In 2015, Muller from the Reichert lab used a yeast gene knockout library to screen for mitochondrial autophagy-related genes using a synthetic quantitative array (SQA) (Muller et al. 2015). This method relies on the expression of mitochondria localized inactive alkaline phosphatase precursor ALP (mtALP). After induction of mitochondrial autophagy, a portion of mtALP is delivered to the vacuole and activated. Thereby, the extent of mitochondrial autophagy can be quantified. Endogenous PHO8 was knocked out in the yeast knockout library using the SGA (synthetic genetic array) method, and the mtALP vector was expressed. By this method, they screened for multiple mitochondrial autophagy positive and negative regulatory genes. Among them, they verified and further studied the negative regulation of mitochondrial autophagy by the ubiquitin hydrolase Ubp3-Bre5 complex.

In 2016, Bernard et al. from the Klionsky lab used a yeast DNA-binding protein knockout library for autophagy gene screening (Bernard et al. 2015). Autophagy genes such as *ATG8* are significantly upregulated at the transcriptional level upon

activation of autophagy. By analyzing the transcriptional activation of multiple *ATG* genes, Bernard et al. screened for autophagy-related transcriptional regulatory molecules in the library and discovered positive and negative transcriptional regulatory molecules of multiple autophagy genes such as *Gcn4*, *Gln3*, and *Gat1*.

In 2016, Zhu from the Xie lab used a kinase mutant library to screen for autophagy-related genes in yeast and found that the *Ccl1*–*Kin28* kinase complex regulates the expression of *Atg29* and *Atg31* (Zhu et al. 2016). Their screening method was to express GFP-*Atg8* in kinase knockout or mutant strains to observe the autophagic transport of GFP-*Atg8* to the vacuole by fluorescence microscopy.

In addition to screening by experimental methods, new autophagy gene information can be obtained by bioinformatic analysis based on autophagy protein interaction networks and gene expression under autophagy activation conditions. In 2017, Kramer et al. from the Ideker lab used a generalized progressive program and interaction network construction to analyze the hierarchical structure and biological function annotation of autophagy-related molecules (Kramer et al. 2017). Based on these bioinformatics results, they deeply verified and analyzed the role of *Gyp1* in autophagosome assembly, the role of *Atg24* in substrate encapsulation, the role of *Atg26* in CVT, and the function of *Ssd1* and *Did4* in selective autophagy.

16.2.2 Screening for Autophagy Genes in Mammalian Cells

Considering the high conservation of autophagy in all eukaryotes, autophagy genes were rapidly screened in higher eukaryotes, especially mammalian cells, after the discovery of autophagy-related genes in yeast. At present, for all the key autophagy genes in yeast, corresponding homologous molecules have been found in mammalian cells. In addition, autophagy genes specific for multiple multicellular organisms have been revealed. Autophagy screening in multicellular organisms, including mammalian cells, is relatively complex: for performing a gene knockout, both alleles need to be knocked out simultaneously. There is also a high requirement for knockdown specificity and efficiency of the target gene, since most of the autophagy genes have several homologous molecules, such as the yeast *ATG8* gene having at least seven homologous molecules in mammalian cells (the *LC3* subfamily and the *GABARAP/GATE-16* subfamily) and the yeast *ATG4* gene having four homologous molecules (*ATG4A/B/C/D*) in mammalian cells. The autophagy phenomenon in mammalian cells is relatively complicated compared to that in yeast cells. Large-scale autophagy detection in animal cells usually uses fluorescently labeled *LC3* or a fluorescently labeled autophagy substrate. Large-scale automatic fluorescence image acquisition is costly and has less uniformity and accuracy than other methods, resulting in a low overlap of results between different screens. However, considering the close relationship between autophagy and numerous physiological and pathological processes in mammals such as humans like cancer, neurodegenerative diseases, inflammatory immunity, development, aging, etc., screening for the identification of autophagy genes in multicellular organisms has become a trend.

This section only deals with the screening for autophagy in mammalian cells. Autophagy screening and research in other species such as nematodes, fruit flies, and other multicellular organisms will be introduced in other relevant parts of this book. The techniques used for the screening for autophagy-related genes in mammalian cells are broadly divided into two categories: siRNA/shRNA-mediated gene knockdown and CRISPR-CAS9-mediated gene knockout. This section will summarize the screens performed in chronological order. The corresponding screening methods can be used as a reference for future screening and research of autophagy genes.

16.2.2.1 Autophagy Gene Screening in Mammalian Cells Based on Gene Knockdown

In 2007, Chan et al. from the Tooze lab used an HEK293 cell line stably expressing GFP-LC3 to screen for genes involved in amino acid starvation-induced autophagy (Chan et al. 2007). The screening range was an siRNA library containing 753 kinase genes. This screening confirmed that the homologous molecule of the yeast Atg1, ULK1, acts as an upstream autophagy molecule involved in activating the autophagy process.

In 2010, Lipinski et al. from the Yuan lab used an siRNA library at the genome-wide level for autophagy screening (Lipinski et al. 2010). LC3-GFP was stably expressed in the H4 cell line and then a whole-genome-covering siRNA library was transfected. After fixing and staining, large-scale acquisition of cell fluorescence images was performed to observe the number of autophagosomes. In the first round, a total of 574 potential autophagy genes were obtained after screening 21,121 siRNA knockdowns and then, in the second round, siRNAs based on 4 different loci per gene were designed for the 574 selected genes. A total of 236 candidate genes were vetted, including knockdowns of 219 candidate genes inducing an increase of autophagy and knockdowns of 17 candidate genes inducing a decrease of autophagy. The scientists continued to analyze the results and revealed that type III phosphatidylinositol 3 phosphate (PI3K) plays an important role in the activity of autophagy under basal culture conditions. Based on this screening, Lipinski et al. found that reactive oxygen species (ROS) can act as an upstream signal of type III PI3K to activate autophagy.

In 2011, Martin from the MacKeigan lab used EGFP-2xFYVE as an autophagy marker to screen between 200 phosphatase gene siRNAs (Martin et al. 2011). The FYVE (Fab1, YOTB, Vac1, and EEA1) domain specifically recognizes phosphatidylinositol 3-phosphate (PtdIns3P and PI3P), which is highly abundant in autophagic vesicles. After subsequent validation and in-depth analysis, they found that PTPsigma, a dual-domain protein tyrosine phosphatase (PTP), negatively regulates autophagy by hydrolyzing PI3P.

In 2011, Szyniarowski from the Jaattela lab used an siRNA library of human kinase genes to screen for autophagy-regulated kinases (Szyniarowski et al. 2011). The screening method is as follows: siRNA targeting 726 kinase genes was

transfected into the MCF-7 cell line expressing EGFP-LC3 and then the level of autophagy was detected by fluorescence microscopy of EGFP-LC3 fluorescent spots (representing autophagy vesicles). They screened out ten new kinases that regulate autophagy in the human breast cancer cell line MCF-7. These kinases can be divided into two groups: those participating in autophagy via the mTOR kinase pathway and those participating in autophagy via the mTOR kinase independent pathway.

In 2011, Orvedahl et al. from the Levine lab screened for genes involved in the selective autophagy of viruses through a high-throughput, imaging-based, and genome-wide coverage siRNA library (Orvedahl et al. 2011). The sindbis virus capsid protein was labeled with red fluorescent protein, and the researchers detected for colocalization with the autophagosome-tagged GFP-LC3. They selected 141 genes that could influence the selective autophagy of the virus and found that 96 of them were also involved in Parkin-mediated mitochondrial autophagy. They further validated and analyzed the SMURF1 protein and found that SMURF1 binds phospholipids to promote selective autophagy degradation of the virus through its N-terminal C2 domain.

In 2012, McKnight from the Tokze lab used an HEK293 cell line stably expressing GFP-LC3 to screen for genes involved in amino acid starvation-induced autophagy (McKnight et al. 2012). After the siRNA knockdown of genes, they discovered several new autophagy genes through automated imaging and automated analysis of autophagic spots. Afterward, it was further analyzed that the short coiled-coil protein (SCOC) was activated by recruiting the autophagy initiation complex containing ULK1, UVRAG (UV radiation resistance-associated gene), and FEZ1 (fasciculation and elongation protein zeta 1).

In 2012, Rong from the Yu lab screened for autophagy genes involved in autophagic lysosome reformation (ALR) (Rong et al. 2012). The activation of autophagy, such as by nutrient starvation, causes the formation of new lysosomes via the ALR pathway. They purified ALR tubes through immunoprecipitation, identified proteins that bind to ALR tubes by mass spectrometry, and then knocked down the corresponding genes via siRNA to verify that the proteins were involved in ALR. They found that clathrin and phosphatidylinositol-4, 5-bisphosphate (PtdIns(4,5)P₂) act as central regulators of the ALR process.

In 2015, Strohecker from the White lab screened for autophagy genes by monitoring the protein level of the autophagy substrate p62/SQSTM1 under metabolic stress (hypoxia plus hypoglycemia) (Strohecker et al. 2015). By screening RNAi gene knockdown strains of 1361 vesicle transport-associated kinases and GTP hydrolases (GTPases), they found 186 knockdowns that resulted in a blockade of autophagy and 67 gene knockdowns that lead to the activation of autophagy. They further confirmed that the knockdown of PFKFB4 (6-phosphofructo-2-kinase/fructose-2,6-biphosphatase 4) in prostate cancer cell lines leads to an increase in p62 and reactive oxygen species, but promotes the autophagy process.

Subsequent siRNA- or shRNA-based autophagy gene screenings were similar to the above-mentioned screenings. Hale et al. from the Carlisle lab screened based on the detection of the autophagy substrate p62 (Hale et al. 2016). In 2016, Lassen

et al. from the Xavie lab monitored intracellular bacterial growth and autophagy targeting for their autophagy gene screening, (Lassen et al. 2016) and in 2017, Jung et al. from the Behrends lab used multiple autophagy markers (WIPI2, ATG12, LC3B, GABARAP, and STX17) for an autophagy gene screening (Jung et al. 2017). In 2018, the Sheng lab used an MDC staining (monodansylcadaverine staining) for autophagy gene screening (Guo et al. 2018); in 2018, Lubas et al. from the Frankel lab used GFP-LC3B for autophagy gene screening (Lubas et al. 2018); in 2018, Pengo et al. from the Ketteler lab detected cleavage of the autophagy marker LC3B by ATG4 for their autophagy gene screening (Pengo et al. 2018); in 2018, Ebner et al. from the Ikeda lab used dual fluorescent label LC3B (mCherry-EGFP-LC3B) for screening, (Ebner et al. 2018) and New et al. from the Tooze lab in 2019 performed an autophagy gene screening by detecting endogenous LC3B-forming autophagy spots (New et al. 2019).

16.2.2.2 CRISPR-CAS9-Based Screening for Autophagy Genes in Mammalian Cells

siRNA- or shRNA-mediated gene knockdown is widely used in autophagy gene screening, but the gene knockdown efficiency may have an effect on the screening results. With the rise of the new gene editing technology CRISPR-CAS9, its unique gene knockout specificity and high efficiency make this technology highly popular for autophagy researchers in mammalian autophagy gene screening. CRISPR (Clustered Regularly Interspaced Short Palindromic Repeat) is an immunity system found in bacteria and archaea. As used in the lab, it consists of a single-stranded gRNA (guide RNA) and a Cas 9 protein with endonuclease activity. The designed gRNA recognizes the target gene by complementary binding, and then, the Cas9 enzyme thereto cleaves the targeted gene to cause a double-strand DNA break. Subsequent repair causes an indel, leading to a frameshift mutation causing loss of gene expression.

In 2016, DeJesus et al. from the Nyfeler lab (Novartis Institute of Biomedical Research) used the CRISPR-mediated genome editing tool for forward genetic screening combined with an FACS (fluorescence automated cell sorting)-based cell selection method to screen for autophagy-related genes, using the autophagy substrate protein p62/sqstm1 as a marker (DeJesus et al. 2016). They established a glioma H4 cell line that stably expresses CAS9 and green fluorescent protein (GFP)-tagged p62. The sgRNA-encoding library was introduced into the H4-CAS9-GFP-p62 cell line by lentivirus infection, and the cells were separated into GFP high or GFP low groups using FACS. Genomic DNA was isolated from these cell populations and analyzed by deep sequencing to identify the targeted genes. They found that the CRISPR screening method is superior to RNAi-mediated screening. This screening for new p62 regulatory molecules identified HNRNPM, SLC39A14, SRRD, PGK1, and ufmylation pathway molecules as new autophagy genes.

In 2017, Shoemaker from the Denic lab at Harvard University used CRISPR-mediated gene knockout to screen for new genes in autophagy (Shoemaker et al.

2017). They detected changes in selective autophagy substrates including LC3B, p62, NBR1, TAX1BP1, and NDP52 with tandem fluorescent RFP-GFP. They found several new ATG genes of mammalian cells, including the endoplasmic reticulum protein TMEM41B, which was found to mediate autophagosome membrane expansion and/or closure. In addition, they found that some autophagy substrates can be transported to the lysosome via autophagy in the absence of ATG7 or other LC3-PE conjugating enzymes.

In 2017, Goodwin from the Murphy lab in the Novartis Institutes for BioMedical Research screened for new autophagy genes by detecting the autophagy substrate GFP-NCOA4 (nuclear receptor coactivator-4) in CRISPR gene knockout cells (Goodwin et al. 2017). They found that a noncanonical autophagy-lysosomal pathway can mediate the degradation of NCOA4. This pathway requires the autophagy genes FIP200, ATG9A, VPS34, and TAX1BP1, but does not require LC3-PE conjugation enzymes.

In 2018, two labs used the CRISPR method to screen for autophagy genes and further validated the function of the endoplasmic reticulum protein TMEM41B in autophagy. Morita et al. from the Mizushima lab in the University of Tokyo and Moretti et al. from the Nyfeler lab, respectively, tested the protein level of GFP-LC3-RFP, p62, and NDP52 to screen for autophagy genes in CRISPR/CAS9 knockout cells (Morita et al. 2018; Moretti et al. 2018). Interestingly, the two screenings simultaneously selected and analyzed the endoplasmic reticulum protein TMEM41B for its function in autophagy. They found that after a knockout of TMEM41B, autophagy was blocked at the early stages and that autophagic substrate lipid droplets accumulated in cells. TMEM41B localizes to the endoplasmic reticulum and promotes the development of the early events of autophagy by forming a complex with VMP1.

References

- Barth H, Thumm M. A genomic screen identifies AUT8 as a novel gene essential for autophagy in the yeast *Saccharomyces cerevisiae*. *Gene*. 2001;274(1–2):151–6.
- Bernard A, et al. A large-scale analysis of autophagy-related gene expression identifies new regulators of autophagy. *Autophagy*. 2015;11(11):2114–22.
- Bockler S, Westermann B. Mitochondrial ER contacts are crucial for mitophagy in yeast. *Dev Cell*. 2014;28(4):450–8.
- Chan EY, Kir S, Tooze SA. siRNA screening of the kinome identifies ULK1 as a multidomain modulator of autophagy. *J Biol Chem*. 2007;282(35):25464–74.
- DeJesus R, et al. Functional CRISPR screening identifies the ufmylation pathway as a regulator of SQSTM1/p62. *Elife*. 2016;5:e17290.
- Ebner P, et al. The IAP family member BRUCE regulates autophagosome-lysosome fusion. *Nat Commun*. 2018;9(1):599.
- Goodwin JM, et al. Autophagy-independent lysosomal targeting regulated by ULK1/2-FIP200 and ATG9. *Cell Rep*. 2017;20(10):2341–56.
- Guo S, et al. A large-scale RNA interference screen identifies genes that regulate autophagy at different stages. *Sci Rep*. 2018;8(1):2822.

- Hale CM, et al. Identification of modulators of autophagic flux in an image-based high content siRNA screen. *Autophagy*. 2016;12(4):713–26.
- Harding TM, et al. Isolation and characterization of yeast mutants in the cytoplasm to vacuole protein targeting pathway. *J Cell Biol*. 1995;131(3):591–602.
- Jung J, et al. Multiplex image-based autophagy RNAi screening identifies SMCR8 as ULK1 kinase activity and gene expression regulator. *Elife*. 2017;6:e23063.
- Kanki T, et al. Atg32 is a mitochondrial protein that confers selectivity during mitophagy. *Dev Cell*. 2009a;17(1):98–109.
- Kanki T, et al. A genomic screen for yeast mutants defective in selective mitochondria autophagy. *Mol Biol Cell*. 2009b;20(22):4730–8.
- Kawamata T, et al. Characterization of a novel autophagy-specific gene, ATG29. *Biochem Biophys Res Commun*. 2005;338(4):1884–9.
- Kira S, et al. Reciprocal conversion of Gtr1 and Gtr2 nucleotide-binding states by Npr2-Npr3 inactivates TORC1 and induces autophagy. *Autophagy*. 2014;10(9):1565–78.
- Klionsky DJ, et al. A unified nomenclature for yeast autophagy-related genes. *Dev Cell*. 2003;5(4):539–45.
- Kramer MH, et al. Active interaction mapping reveals the hierarchical organization of autophagy. *Mol Cell*. 2017;65(4):761–774.e5.
- Lassen KG, et al. Genetic coding variant in GPR65 alters lysosomal pH and links lysosomal dysfunction with colitis risk. *Immunity*. 2016;44(6):1392–405.
- Lipinski MM, et al. A genome-wide siRNA screen reveals multiple mTORC1 independent signaling pathways regulating autophagy under normal nutritional conditions. *Dev Cell*. 2010;18(6):1041–52.
- Lubas M, et al. eIF5A is required for autophagy by mediating ATG3 translation. *EMBO Rep*. 2018;19(6):e46072.
- Martin KR, et al. Identification of PTPsigma as an autophagic phosphatase. *J Cell Sci*. 2011;124(Pt 5):812–9.
- McKnight NC, et al. Genome-wide siRNA screen reveals amino acid starvation-induced autophagy requires SCOC and WAC. *EMBO J*. 2012;31(8):1931–46.
- Moretti F, et al. TMEM41B is a novel regulator of autophagy and lipid mobilization. *EMBO Rep*. 2018;19(9):e45889.
- Morita K, et al. Genome-wide CRISPR screen identifies TMEM41B as a gene required for autophagosome formation. *J Cell Biol*. 2018;217(11):3817–28.
- Muller M, et al. Synthetic quantitative array technology identifies the Ubp3-Bre5 deubiquitinase complex as a negative regulator of mitophagy. *Cell Rep*. 2015;10(7):1215–25.
- New M, et al. Identification and validation of novel autophagy regulators using an endogenous readout siGENOME screen. *Methods Mol Biol*. 2019;1880:359–74.
- Okamoto K, Kondo-Okamoto N, Ohsumi Y. Mitochondria-anchored receptor Atg32 mediates degradation of mitochondria via selective autophagy. *Dev Cell*. 2009;17(1):87–97.
- Orvedahl A, et al. Image-based genome-wide siRNA screen identifies selective autophagy factors. *Nature*. 2011;480(7375):113–7.
- Pengo N, et al. Identification of kinases and phosphatases that regulate ATG4B activity by siRNA and small molecule screening in cells. *Front Cell Dev Biol*. 2018;6:148.
- Rong Y, et al. Clathrin and phosphatidylinositol-4,5-bisphosphate regulate autophagic lysosome reformation. *Nat Cell Biol*. 2012;14(9):924–34.
- Shirahama-Noda K, et al. TRAPPIII is responsible for vesicular transport from early endosomes to Golgi, facilitating Atg9 cycling in autophagy. *J Cell Sci*. 2013;126(Pt 21):4963–73.
- Shoemaker CJ, Huang TQ, Weir NR, Polyakov N, Denic V. A CRISPR screening approach for identifying novel autophagy-related factors and cytoplasm-to-lysosome trafficking routes. *BioRxiv [PREPRINT]*. 2017. <https://doi.org/10.1101/229732>.
- Stroecker AM, et al. Identification of 6-phosphofructo-2-kinase/fructose-2,6-bisphosphatase as a novel autophagy regulator by high content shRNA screening. *Oncogene*. 2015;34(45):5662–76.

- Sun LL, et al. Global analysis of fission yeast mating genes reveals new autophagy factors. *PLoS Genet.* 2013;9(8):e1003715.
- Szyniarowski P, et al. A comprehensive siRNA screen for kinases that suppress macroautophagy in optimal growth conditions. *Autophagy.* 2011;7(8):892–903.
- Takeshige K, et al. Autophagy in yeast demonstrated with proteinase-deficient mutants and conditions for its induction. *J Cell Biol.* 1992;119(2):301–11.
- Thumm M, et al. Isolation of autophagocytosis mutants of *Saccharomyces cerevisiae*. *FEBS Lett.* 1994;349(2):275–80.
- Tsukada M, Ohsumi Y. Isolation and characterization of autophagy-defective mutants of *Saccharomyces cerevisiae*. *FEBS Lett.* 1993;333(1–2):169–74.
- Zhu J, et al. The Ccl1-Kin28 kinase complex regulates autophagy under nitrogen starvation. *J Cell Sci.* 2016;129(1):135–44.

Chapter 17

Proteomics and Autophagy Research



Kefeng Lu and Huihui Li

Abstract Autophagy is an evolutionarily conserved intracellular degradation process. Autophagy is closely involved in human health and diseases. In recent years, mass spectrometry-based proteomic methods have become important and powerful tools for autophagy studies. These types of techniques have been especially helpful to reveal the range of degradation substrates of autophagy through large-scale, unbiased analysis of cellular proteomes. At present, a variety of mass spectrometry-based proteomics methods have been successfully applied to autophagy research.

In this part, we will introduce the principles of mass spectrometry, proteomic labeling and nonlabeling methods, and the application of mass spectrometry in the identification of autophagy complexes and related post-translational modifications (PTMs).

17.1 Overview of Proteomics and Autophagy Research

Autophagy is a complex intracellular biological process. It starts from the formation of an autophagic bilayer membrane structure, and then, the contents to be degraded are wrapped in this structure to form intact autophagosomes, which are transported to lysosomes (vacuoles in yeast and plants) for degradation. The autophagy process requires the participation of numerous autophagy molecules to form the autophagic machinery. Mass spectrometry-based proteomics methods can not only identify the degradation content in the autophagosome but also analyze the component molecules of the autophagy machinery, i.e., the key molecules of autophagy and their corresponding dynamic PTM changes.

K. Lu (✉) · H. Li
State Key Laboratory of Biotherapy, West China Hospital, Sichuan University,
Chengdu, China
e-mail: lukf@scu.edu.cn; lihuihui@scu.edu.cn

17.1.1 Introduction to Mass Spectrometry

Mass spectrometry technology has demonstrated strong identification capabilities since its inception. With the development of mass spectrometry instruments, the identification speed, coverage, and accuracy for various biological materials such as proteins, lipids, and metabolites have been greatly improved. Autophagy research also benefits from the advancements of the mass spectrometry technology, which promotes the discovery of autophagy molecules, dynamics, and degradation substrates.

17.1.1.1 Introduction to Mass Spectrometry

Mass spectrometry (MS) analyzes the material size of substances by ionization in the gas phase. Mass spectrometer machines include an ion source, a mass analyzer, and a detector. MS-based proteomic studies have improved significantly over the past two decades. MS-based proteomics analysis can be divided into top-down or bottom-up types. The top-down approach is to directly analyze intact proteins or peptides by mass spectrometry. After the protein is subjected to ionization (via Electrospray Ionization (ESI) or Matrix-assisted Laser Desorption/Ionization (MALDI)), the complete protein is analyzed by mass spectrometry. Bottom-up proteomics requires proteolytic enzymes (usually trypsin) to digest complex protein mixtures into peptides. The peptides are separated by liquid chromatography, and finally, the peptides are detected by tandem mass spectrometry (MS/MS). Size analysis then confers the identification of proteins by matching mass spectral data to theoretical spectra from proteome databases generated by theoretical cleavage with specific proteolytic enzymes.

17.1.1.2 Introduction to Mass Spectrometry-Based Proteomics

Mass spectrometry-based proteomics can identify proteins from various systems such as intracellular, subcellular, and extracellular secretion systems and identify proteins in samples at different times and conditions to reveal dynamic biological processes in cells. In the early stages, two-dimensional gel electrophoresis (2D-GE) and two-dimensional fluorescence difference in gel electrophoresis (2D-DIGE) were important methods in proteomics research, which were used for protein separation, identification, and quantification. Later, LC-MS methods based on chromatographic techniques have gradually become mainstream. The LC-MS method can, contrary to 2D-GE methods, effectively detect low-abundance proteins in samples. It also has higher resolution and higher repeatability than 2D-GE methods.

17.1.2 Protein Labeling and Label-Free Methods in Proteomics Research

Proteomics methods can be generally divided into two categories: labeling and non-labeling. Labeling refers to incorporating labeled tags into cells during culture or adding a label after sample collection. The advantage of the labeling method is that subsequent mass spectrometry analysis of different samples can be performed simultaneously, reducing errors in the mass spectrometry analysis. The disadvantage of the labeling method is that culture conditions are not completely consistent with the normal conditions and the labeling method also has a labeling efficiency problem. Label-free methods are currently becoming a trend. Label-free method-based mass spectrometry analysis is performed by normal culture or processing of samples. Advances in mass spectrometry instruments and analytical methods have made relative quantification possible even when measurements are run sequentially.

17.1.2.1 Protein Labeling Methods

Protein labeling techniques refer to the incorporation of stable isotopic labels into proteins or polypeptides to distinguish and compare differences between samples in an experiment. The labeled proteins exhibit the same properties as the nonlabeled proteins and thus do not affect the biological activity of cells under the labeling conditions and the differentially labeled polypeptides that are retrieved after the procedure can be distinguished by MS. Isotopes can be incorporated by metabolic or chemical means. In metabolic labeling, the commonly used SILAC (stable isotope labeling by amino acids in cell culture) method refers to cells being labeled with a normal or “heavy” (^{13}C and/or ^{15}N) amino acid. SILAC is generally considered as the “golden standard” for isotope labeling methods. Its advantage is that labeling and sample mixing are performed much earlier than in other labeling methods, eliminating possible errors or deviations from downstream sample processing. Chemical labeling methods are becoming increasingly popular due to their advantages in terms of diversification capabilities and target versatility. Chemical labeling methods mainly include isotope coded affinity tag (ICAT) and isobaric labeling. The latter includes TMT (tandem mass tag) and iTRAQ (isobaric tags for relative and absolute quantification). The chemical tag labels the target protein, usually in cysteine (in the case of ICAT) or primary amine (e-amino on lysine or N-terminal amino for TMT and iTRAQ). In the case of ICAT, normal and “heavy” markers allow two samples to be compared by MS detection via a mass shift of 8 Da. For multiple TMT and iTRAQ, the labels contain a unique mass of reporter groups and are balanced by equilibrium groups of different masses to obtain the same total mass. Commercially available isobaric labels allow for greater flexibility in research, with up to 10 (TMT) and 8 (iTRAQ) different markers for a comparison of multiple samples. Because there is no need for metabolic incorporation of isotopic labels, various samples including body fluids and tissues can be directly labeled by

chemical methods. There are great advantages for its application in clinically relevant experiments. But in contrast to metabolic labeling, chemical labeling methods may introduce errors or deviations into the downstream sample processing procedure.

17.1.2.2 Label-Free Methods

Label-free (also called protein nonlabeling) methods make it possible to do quantification analysis without using isotopic labels. Significant advantages of this method are high convenience and low costs, since there is no need for special sites in proteins for labeling and also expensive labeling reagents are unnecessary. The label free method is the only multiplexed and ultra-large-scale mass spectrometry-based proteomic method that is currently widely used for clinical testing. Previously, the label-free method was somewhat disadvantageous in terms of quantification compared to the labeling methods. However, with the improvement of analysis software, the purpose of relative quantification can be achieved by quantifying spectral counts and ionic strengths from the mass spectra. Despite these advantages, label-free methods are still limited by precision. Compared with isotope labels, they are prone to induce experimental variations and errors from different samples in different LC-MS analysis runs. Errors and differences in workflows may also result in reduced accuracy of quantitative information. However, label-free methods are still extremely attractive due to their simplicity and speed. When the experimental group is expected to have significant changes in protein levels, especially with further improvement of data processing analysis methods and mass spectrometers, quantitative proteomics with label-free methods have evolved into a viable and reliable protein qualitative and quantitative analysis method.

17.2 Application of Mass Spectrometry-Based Proteomics in Autophagy Research

The whole process of autophagy is roughly divided into three stages: (1) in the case of nutrient deficiency, oxidative stress, external pressure, etc., membrane components that derive from the endoplasmic reticulum, Golgi, and other sources in cell form a separated structure surrounded by autophagosomal substrates (intracellular damaged organelles, misfolded proteins, etc.); (2) the membrane gradually extends to completely encapsulate the substrates to form intact autophagosomes; and (3) autophagosomes fuse to the lysosome to form autolysosomes and the inclusions are degraded. Mass spectrometry-based proteomic methods have been widely used in autophagy studies. Applications can be broadly categorized as follows: (1) The identification of proteins and protein interaction partners of basal or induced autophagy machineries; (2) The study of intracellular protein dynamics affected by

autophagy, including basal or induced protein synthesis and degradation; and (3) The detection of PTMs of autophagy machine molecules and autophagic substrates.

17.2.1 The Identification of Autophagy Machinery Molecules by Proteomic Methods

Autophagy is an intracellular process of membrane structure formation and occurs as a dynamic response following signal stimulation. The molecules involved in autophagy have a significant increase of expression after the activation of autophagy. By using mass spectrometry, it is possible to shed light on changes in intracellular protein expression under the condition of autophagy activation. In this way, new molecules of the autophagy machinery can be identified. The molecules that form the autophagy machine can also be analyzed by purifying autophagosomes, especially during autophagy activation conditions such as amino acid starvation, rapamycin treatment, or concanamycin (ConA) treatment.

17.2.1.1 The Discovery of Autophagy Machine Molecules by Proteomics

Affinity-purification and MS-based proteomic methods enable unbiased large-scale determination of comprehensive protein networks. During the process of autophagy, the interaction network of autophagy molecules promotes the autophagy progress in time and space. Affinity purification-mass spectrometry (AP-MS) has caused a breakthrough in the clarification of the construction of the molecular network of autophagy. In a groundbreaking paper published in 2010 in *Nature*, Behrends et al. first established a comprehensive autophagy interaction network (AIN) (Behrends et al. 2010). A label-free quantitative proteomics method was used to quantify changes in intracellular proteome levels after Torin1 treatment that inhibits mTOR. The identified network contains 751 pairs of interaction partners and another 409 pairs of potential protein interactions occurring during basal autophagy. The scientists started with 32 known autophagy proteins and isolated and identified their copurified proteins by affinity separation. Through MS identification and bioinformatics analysis, 2553 interacting proteins were obtained. Comparative proteomics analysis was performed using CompPASS software. Using this software, it is possible to identify new protein interactions with a high reliability. The scientists built a complete AIN network and deduced ten interconnected functional subnetworks. By comparing the CompPASS analysis data with databases of protein interactions including BIOGRID, MINT, and STRING, the scientists identified 429 pairs of new potential protein-protein interaction pairs, including known autophagy-related proteins, new autophagy molecules, and unknown complex subunit molecules. The scientists validated the newly revealed interacting protein molecules, via *in vitro* experiments and RNAi interference and verified their function in autophagy. The

impact of this landmark study on autophagy networks suggests that MS-based proteomics combined with bioinformatics can help scientists understand complex networks of protein interactions within cells. It is worth noticing that in this work, MS is mainly used as a qualitative tool for protein identification rather than for quantitative purposes. In this case, the addition of quantitative elements in the experiment would effectively reduce nonspecific data and thereby further improve the stability of the data by removing the effects of nonspecific binding contaminants. In addition to overall analysis of the entire interaction network of autophagy, AP-MS can be used to identify interacting proteins of specific autophagy-related molecules, which also contributes to the understanding of the autophagy machine. In addition, protein interaction studies can serve as a natural extension of proteomics research regarding protein expression. For example, Mancias et al. used an SILAC-based quantitative method to identify autophagosome proteins that were obtained by gradient separation (Mancias et al. 2014). After cell labeling based on SILAC, different treatments with wortmannin (autophagosome formation inhibitor) or chloroquine (lysosomal inhibitor to obtain the maximum number of autophagosomes) were given to influence the amount of autophagosomes in the cells. Lightly labeled cells were treated with wortmannin, while heavily labeled cells were treated with chloroquine. By calculating the ratio heavy to light, proteins involved in the autophagosomal machinery could be identified. In this way, a PANC1 pancreatic cancer cell line and a MCF7 breast cancer cell line were quantitatively analyzed to identify 50 highly reliable autophagosome-specific molecules. Among them, NCOA4 (nuclear receptor coactivator 4) was found to be highly enriched. The NCOA4 interacting proteins were further studied by AP-MS plus CompPASS analysis. It finally revealed the role of NCOA4 as a receptor protein to mediate autophagic degradation of ferritin. These studies have clearly demonstrated that MS-based interaction proteomics can be a powerful tool for the study of autophagy machine molecules.

17.2.1.2 Identifying the Modification of Autophagy Molecules by Proteomics

PTMs are critical for many signaling pathways. Autophagy machinery molecules are also regulated by extensive PTMs. Current studies discovered clear examples of regulation of autophagy molecules by phosphorylation, acetylation, ubiquitination, and glycosylation (Xie et al. 2015). Although the involvement of these modifications on autophagy has been well-determined, the mechanisms of specific functions caused by PTMs and the global dynamics of protein modifications during autophagy are still incomplete. MS-based quantitative proteomic techniques enable a global detection of PTM events, including the identification of modified proteins and the protein sites affected by the modifications. Quantitative comparisons of various modifications at whole cell and specific organelle level make it possible to clarify the PTM changes involved in autophagy.

Phosphorylation is a well-characterized PTM. Many studies have shown that in the LC3-interacting region (LIR) of autophagy receptor molecules, phosphorylation

often occurs to change the acidic environment of this region to effectively bind LC3. Such modified receptor molecules include SQSTM1 (i.e., p62) and the mitochondrial autophagy receptor BNIP3. In addition, autophagy core proteins such as in the ULK1 initiation complex are regulated by significant phosphorylation. Rigbolt et al. applied quantitative phosphorylation proteomics to study early signal transduction in autophagy (Rigbolt et al. 2014). SILAC-labeled MCF7 cells were used to compare short-term (5 min) and long-term (30 min) modification changes by inducing starvation- and rapamycin-induced autophagy. The study found 930 phosphorylation sites on a total of 590 proteins. These included 435 rapamycin-activated modification sites, 406 starvation-activated sites, and 74 modification sites that were activated by both stimuli. It is worth noticing that 230 sites were found to undergo more than a twofold change after only 2 min of activation, indicating that phosphorylation modification is immediately induced in cells following autophagy stimulation. Further analysis by GO (gene ontology) analysis and IPA (ingenuity pathway analysis) revealed the phosphorylation of the mTOR regulatory axis and the phosphorylation of LC3-interacting proteins.

In another study, Harder et al. used an SILAC-based quantitative phosphorylation proteomics approach to compare cells that were induced for autophagy, via either rapamycin or starvation. They specifically looked at the difference between mTOR-dependent and nondependent autophagy initiation signaling responses (Harder et al. 2014). This study revealed 626 specific phosphorylation sites, providing a large-scale autophagy protein phosphorylation dataset. Studies have shown that the unfolded protein response plays a pivotal role in mTOR-independent autophagy induction. In starvation-induced activation of autophagy, DDIT3, a marker protein of endoplasmic reticulum stress (ER stress), is markedly elevated. At the level of autophagy-specific subpathways, Papinski et al. used SILAC-based phosphorylation proteomics to explore the regulation of Atg9 in yeast after autophagy initiation via Atg1 kinase (Papinski et al. 2014). Feng et al. identified Atg1-independent Atg9 phosphorylation by comparing wild-type and Atg1-deficient yeast strains with the SILAC method (Feng et al. 2016). Heo et al. and Richter et al. used TMT or SILAC-mediated quantitative phosphorylation to analyze the function of TBK1-mediated phosphorylation of the autophagy receptor OPTN (optineurin) in mitochondrial autophagy (Heo et al. 2015; Richter et al. 2016). Based on SILAC phosphorylation proteomics, scientists have also analyzed the role of the longevity-related agents resveratrol and spermidine in autophagy, in relation with mTOR signaling and in cross talk between autophagy and apoptotic pathways (Bennetzen et al. 2012; Alayev et al. 2014). Protein ubiquitination is currently known to be involved in the regulation of numerous ATG proteins, including BECN1 (beclin1) and ULK1. The relation between ubiquitination modification and autophagy, especially selective autophagy, has gradually become one of the focuses of autophagy research. Among many types of selective autophagy, mitochondrial autophagy is a representative example of selective degradation of autophagy substrates. The PINK1-PARK2 signaling pathway has been discovered to be involved in mitochondrial autophagy. During mitochondrial autophagy, PINK1 (PTEN-induced putative kinase 1) activates PARK2 ubiquitin ligase and then targets depolarized

mitochondria for degradation via autophagy. Using a supplementation with unique bi-glycine (diGLY) ubiquitin-modifying protein peptides and a quantitative labeling SILAC approach, Sarraf et al. quantified diGLY (QdiGLY) enrichment and analysis of ubiquitinated proteins. A comprehensive detection of PARK2-dependent ubiquitination substrates indicated dynamic changes in ubiquitin modifications in CCCP-induced mitochondrial autophagy (Sarraf et al. 2013). Combined with AP-MS-mediated analysis of PARK2 interacting proteins, hundreds of ubiquitination-modifying sites and proteins, including mitochondrial membrane proteins, cytoplasmic proteins, proteasome subunits, and autophagy receptors, were further identified. Considering the fact that ubiquitin itself can further be ubiquitinated (polyubiquitination) and the effect of phosphorylation on ubiquitination, the interaction between ubiquitination and phosphorylation is prominent in the mitochondrial autophagy pathway. In addition, deubiquitinating enzymes have been found to play an important role in selective autophagy. By detecting and quantifying specific ubiquitin chain isoforms catalyzed by the deubiquitinating enzyme USP8 in mitochondrial autophagy, USP8 was revealed as a specific and key regulator to remove the K6-type of PARK2-mediated ubiquitination. The series of studies discussed above demonstrates the power of quantitative proteomics in accurate, dynamic, comprehensive, and in-depth, analysis of protein modifications that regulate autophagy. Similar to phosphorylation modification, ubiquitin modification in other types of selective autophagy is still lacking in-depth understanding, such as in xenophagy (pathogenic microbial autophagy) and ribosome autophagy (ribosome autophagy degradation). In addition to phosphorylation and ubiquitination, there are other types of modifications such as acetylation and PTM10 modification, which are also revealed by quantitative proteomics methods. Other types of modifications in autophagy such as glycosylation, lipidation, and redox modification will be interesting challenges in the study of autophagy.

17.2.2 The Discovery of Autophagic Substrates by Proteomics Methods

As one of the two highly conserved degradation mechanisms in cells, the autophagy process was originally considered to be a nonselective bulk degradation process, in contrast to the high specificity of ubiquitin-proteasome system. It was initially believed that intracellular contents such as proteins, organelles, and membrane structures could be randomly encapsulated by autophagic structures and transported to the lysosome for degradation. However, this view has been altered because of subsequent studies, that is, autophagy is a strictly regulated cellular clearance process, which specifically targets substrates for degradation and is linked with many physiological and pathological processes, such as cancer, innate and adaptive immunity, and neurodegenerative diseases. The variety of autophagy functions is closely related to the selection of its substrates. Accordingly, the disclosure of autophagic substrates can help to understand the physiological functions of autophagy.

17.2.2.1 The Identification of Autophagy Substrates by Isolation Methods

Proteomic methods are combined more and more with the separation of various organelles or subcellular components. The advantage of this strategy is that it provides information of the proteome in time and space and the corresponding data analysis can be more detailed. Critical information can be obtained about the specific locations and time points in which researched biological processes occur within cells. The disadvantage of the strategy is that cross-contamination between organelles or subcellular components may occur because of low separation efficiency during sample preparation. Separated organelles and subcellular components are typically captured or enriched using gradient centrifugation in a sucrose or nycodenz gradient matrix.

The isolation of autophagosomes can provide direct information on the substrates of autophagy and partial information of the autophagic machinery. A series of studies have revealed information on the types and amount of proteins that are contained in or bound by autophagosomes. One of the earliest reported methods of autophagosome separation was reported by Stromhaug et al., which was also known as the basis for most subsequent proteomics studies based on autophagosome separation (Stromhaug et al. 1998). After nycodenz gradient centrifugation, an autophagosome-enriched fraction was purified, using the autophagosome membrane protein LC3, which was GFP-labeled. This method purifies autophagosomes very effectively (Stromhaug et al. 1998). Autophagosome purification can also be achieved to some extent by using only gradient centrifugation or only immunological recruitment using GFP-LC3. Dengjel et al. have fully revealed the overall information of proteins contained in autophagosomes. Their work has found that different activation conditions can produce different autophagosomal contents (Dengjel et al. 2012). They used a protein correlation profile (PCP) to analyze the components obtained by density gradient centrifugation. The PCP method assumes that proteins/polypeptides from the same organelle will have a largely similar distribution in different isolated components. The scientists used Hank's Balanced Salt Solution (HBSS) to cause amino acid starvation, rapamycin to induce autophagosome production, and concanamycin A to induce autophagosome accumulation. Dengjel et al. identified a total of 728 specific proteins in the collected autophagosomes, 94 of which were specific for one of the three stimuli that were used. The results of proteomics studies of autophagosomes by Overbye et al. and Gao et al. revealed that the number of different substrate proteins in autophagosomes may not be as high as thought before. These two studies have found that 39 and 101 proteins, respectively, are specifically enriched in autophagosomes (Overbye et al. 2007; Gao et al. 2010). The overlap between the above three studies is very small, which may be due to different experimental methods. Overbye et al. and Gao et al. mainly analyzed autophagosome membrane-associated proteins, while Dengjel et al. focused on whole autophagosomes. In addition, the work by Overbye is based on rat primary hepatocytes and the induction condition was nutritional starvation. The work of Gao was carried out in KEK293 and HCT116 cells, and autophagy was induced by calcium phosphate stimulation. In the work of Dengjel et al., concanamycin A was used to

treat starved cells in order to diminish the interference of nonautophagosome components. After concanamycin A blockage of the degradation of autophagosomes, a large number of mature autophagosomes accumulate in the cells. Dengjel et al. found that compared to rapamycin treatment or concanamycin A treatment, autophagy-related proteins such as LC3B, p62/SQSTM1, and GABARAPL2 were found to be less abundant in autophagosomes isolated after starvation treatment. This suggests that the proteins that are present in autophagosomes during starvation may rapidly detach after autophagosome formation. Mancias et al. also isolated and analyzed autophagosomes during their identification of nuclear receptor coactivator 4 (NCOA4) (Mancias et al. 2014). In their work, a density gradient separation and purification of autophagosomes were performed with SILAC-labeled PANC-1 and PA-TU-8988T pancreatic cells and MCF7 breast cancer cells. In addition, chloroquine treatment was used to block the fusion of autophagosomes and lysosomes to increase the number of autophagosomes in cells. This work revealed 94 proteins that bind specifically to autophagosomes.

These autophagosome isolation and identification methods do not only provide information on autophagosome membrane proteins and substrate proteins of autophagy but also confer implications for the process of autophagy. Dengjel et al. showed, using mass spectrometry-based autophagosome proteomics analysis, that autophagy and degradation via the proteasome are related to each other. These two intracellular degradation pathways are not independent, but interact with each other and regulate each other. This study found that after various autophagy activation stimuli, the level of proteasome components decreased significantly. This decline was blocked when autophagy was inhibited by 3-methyladenine (3-MA) treatment. After analyzing autophagosome proteins, Mancias et al. found that NCOA4 binds very strongly and specifically to autophagosomes, thus revealing that NCOA4 acts as an autophagy receptor to effectively mediate autophagy degradation of ferritin. NCOA4 was also identified in the work of Dengjel et al., but the credibility was in the low-confidence category. The autophagosome proteins isolated and identified by Dengjel et al. were divided into group A and other groups. Group A referred to high-confidence autophagosome proteins because this group of proteins excluded nonautophagosomal membrane components such as endoplasmic reticulum, Golgi, and endosome proteins. In the model organism *Saccharomyces cerevisiae*, Suzuki et al. monitored the isolation and purification efficiency of autophagosomes by observing the autophagy substrate GFP-Ape1. The isolated and purified autophagosomes were then subjected to protein identification analysis, and numerous autophagy substrate proteins were discovered (Suzuki et al. 2014).

17.2.2.2 The Lysosomal Separation Method Used to Identify Autophagy Substrates

Lysosomes are single-membrane organelles that serve in one of the two major degradation pathways. Lysosomes function by providing hydrolytic enzymes for autophagosome degradation. The optimal environment for the lysosomal hydrolytic

enzymes is acidic, and many drugs inhibit lysosomal degradation by increasing the pH values of lysosomes. Lysosomes also play a role in the endocytosis degradation pathway. Lysosomes have been found to be involved in a wide range of human diseases and pathological processes, such as lysosomal storage diseases (LSDs), Alzheimer's disease, neuronal ceroid lipofuscinoses (NCLs), and cancers (Bagshaw et al. 2004; Lübke et al. 2009). Many LSDs have also been shown to be associated with defects in the autophagy pathway (Lieberman et al. 2012). Using classical biochemical methods, the protein components in lysosomes have been extensively studied, but the functional molecules of lysosomes are not yet fully identified. By combining mass spectrometry-based proteomics, affinity-based purification techniques, and subcellular fractionation methods, the number of lysosomal proteins that are identified is gradually increasing. Jaquinod et al. have outlined methods for the purification of lysosomes, based on an affinity enrichment method. This method provides a basic principle for studying lysosomal soluble proteins (Jaquinod et al. 2008). Bagshaw et al. conducted a proteomics study to determine the proteins contained inside the lysosomes. Cytochrome P450 enzymes such as CYP2A1, CYP2C13, CYP2D3, and CYP4A3 and various ATP synthase subunits including α , β , and F1 complex O and γ chain subunits were identified (Bagshaw et al. 2004). Leighton et al. used the Triton WR-1339 method to isolate and identify 215 lysosomal membrane proteins, some of which were not found in previous studies (Leighton et al. 1968).

Other proteomic studies based on lysosomal separation also help us in understanding the lysosomal protein composition and its functional relevance, such as its association with autophagy. Chapel et al. identified 734 lysosomal proteins by differential centrifugation and density gradient separation of rat liver lysosomes (Chapel et al. 2013). Of these, 207 proteins were well-defined or predicted lysosomal-associated proteins and the remaining 527 proteins were not previously found to be related to the lysosome. Forty-six potential lysosomal transporters were also identified, 12 of which were confirmed to be lysosomal membrane molecules by overexpression and colocalization observation in HeLa cells. Della Valle et al. identified high-confidence lysosomal proteins using iTRAQ labeling and two-dimensional peptide separation combined with MALDI-TOF (Della Valle et al. 2011). The method also involved differential centrifugation and sucrose gradient density centrifugation after Triton-WR1339 treatment. The highly reliable lysosomal proteins they identified include cathepsin D (CTSD), lysosomal acid phosphatase 2 and 5 (acid phosphatases 2 and 5, ACP2 and ACP5), and lysosomal-associated membrane protein 2 (lysosomal associated membrane protein 2, LAMP2). Sleat et al. identified the mannose-6-phosphate receptor by comparing brain detergent extracts from patients with advanced infantile neuropiloidosis (CLCL) with healthy controls. Mannose-6-phosphate modifications were enriched and detected in a variety of lysosomal matrices (Sleat et al. 2006). Naureckiene et al. found that human epididymis-specific protein 1 (HE1) is specifically localized in lysosomes as a cholesterol-binding protein, which suggests that it may be involved in lysosomal cholesterol storage-associated diseases (Naureckiene et al. 2000).

17.2.2.3 Whole-Cell Proteomics-Based Identification of Autophagy Substrates

Given the degradation function of autophagy, information on autophagy substrates can also be provided by analyzing changes of the overall proteome within cells. The high-throughput MS method can be used to quantify the effect of autophagy on intracellular proteome dynamics or protein homeostasis. Kristensen et al. analyzed the dynamics of the cell proteome after amino acid starvation-induced autophagy activation, using mass spectrometry (Kristensen et al. 2008). In this work, MCF7 cells were labeled using SILAC and proteomic changes were analyzed at various time points (0, 3, 6, 18, and 36 h) after amino acid starvation. A total of 1486 proteins were found to change with autophagy activation. Through GO analysis, it was found that protein degradation is correlated with the subcellular distribution of proteins. Free cytosolic and proteasome proteins are rapidly degrading substrates, with ribosomal protein and mitochondrial protein degradation slightly delayed, while endoplasmic reticulum and nuclear-related proteins remain relatively stable. It is worth noticing that proteasome-related proteins are rapidly degraded, while lysosomal proteins remain unchanged or even increase. Subsequent comparison of proteasome inhibition with autophagy inhibition, based on SILAC validation, confirmed that autophagy is the major intracellular degradation pathway under starvation conditions. In addition to its function in stress responses, autophagy is also an important aspect of cellular homeostasis. Zhang et al. used ATG5 knockout and ATG7 knockout fibroblasts to quantify the kinetics of autophagy degradation of proteins (Zhang and Ghaemmaghami 2016). The SILAC method was used to label normal and autophagy blocked cells followed by subsequent whole cell proteome analysis. Cells were allowed to enter the resting phase under normal culture conditions and then changed to the labeling medium for 6 days. LC-MS/MS analysis was performed after collecting cells at different time points, so that progressive degradation of whole cell proteins over time could be observed. GO analysis and further validation indicated that basal autophagy, similar to induced autophagy, also exhibits selectivity for its degradation substrates. Notably, certain organelle-specific autophagy processes, such as ribosome autophagy, rarely occurred in basal autophagy, suggesting that the selective autophagy degradation of such substrates involves specific signaling molecules.

Another method that can label proteins for proteomics study is called bio-orthogonal noncanonical amino acid tagging (BONCAT) (Zhang et al. 2014). This method was used to label intracellular proteins and observe their degradation by autophagy, leading to the identification of many autophagic substrates. The BONCAT method is based on the intracellular integration of amino acids labeled with bioreactive groups into proteins. One representative of such labeled amino acids is azidohomoalanine (AHA), an azide-modified methionine substitute that can be chemically linked to an alkyne-containing label. In the absence of methionine, AHA is integrated into newly synthesized proteins, which can then be labeled with a fluorescent dye or by conjugating biotin for subsequent affinity enrichment. The

AHA-based BONCAT method provides a viable new alternative for radioisotopes for use in quantitative autophagy analysis.

The iTRAQ method was also used to quantify the degradation kinetics of autophagy substrate proteins. Zhuo et al. studied whole-cell proteome changes in wild-type MEF (mouse embryonic fibroblasts) and ATG7 knockout MEF using iTRAQ and LC-MS (Zhuo et al. 2013). In their work, 1234 changed proteins were found, with 66 upregulated and 48 downregulated proteins verified. In a similar study, Mathew et al. compared whole-cell proteome changes in wild-type and autophagy deficient cells (Mathew et al. 2014). In this work, autophagy has been found to have a dramatic effect on the intracellular proteome, especially stress survival-related proteins. In addition, it was also found that an autophagy blockade leads to the accumulation of DDX58/RIG-I immune pathway molecules, suggesting that autophagy may inhibit immunity and interferon response by degrading immune pathway molecules.

References

- Alayev A, Doubleday PF, Berger SM, Ballif BA, Holz MK. Phosphoproteomics reveals resveratrol-dependent inhibition of Akt/mTORC1/S6K1 signaling. *J Proteome Res.* 2014;13:5734–42.
- Bagshaw RD, Mahuran DJ, Callahan JW. A proteomic analysis of lysosomal integral membrane proteins reveals the diverse composition of the organelle. *Mol Cell Proteomics.* 2004;4:133–43.
- Behrends C, Sowa ME, Gygi SP, Harper JW. Network organization of the human autophagy system. *Nature.* 2010;466:68–76.
- Bennetzen MV, Marino G, Pultz D, Morselli E, Færgeman NJ, Kroemer G, Andersen JS. Phosphoproteomic analysis of cells treated with longevity-related autophagy inducers. *Cell Cycle.* 2012;11:1827–40.
- Chapel A, Kieffer-Jaquinod S, Sagne C, Verdon Q, Ivaldi C, Mellal M, Thirion J, Jadot M, Bruley C, Garin J, Gasnier B, Journet A. An extended proteome map of the lysosomal membrane reveals novel potential transporters. *Mol Cell Proteomics.* 2013;12:1572–88.
- Della Valle MC, Sleat DE, Zheng H, Moore DF, Jadot M, Lobel P. Classification of subcellular location by comparative proteomic analysis of native and density-shifted lysosomes. *Mol Cell Proteomics.* 2011;10:1–14.
- Dengjel J, Høyer-Hansen M, Nielsen MO, Eisenberg T, Harder LM, Schandorff S, Farkas T, Kirkegaard T, Becker AC, Schroeder S, Vanselow K, Lundberg E, Nielsen MM, Kristensen AR, Akimov V, Bunkenborg J, Madeo F, Jäättelä M, Andersen JS. Identification of autophagosome-associated proteins and regulators by quantitative proteomic analysis and genetic screens. *Mol Cell Proteomics.* 2012;11:1–17.
- Feng Y, Backues SK, Baba M, Heo JM, Harper JW, Klionsky DJ. Phosphorylation of Atg9 regulates movement to the phagophore assembly site and the rate of autophagosome formation. *Autophagy.* 2016;12:648–58.
- Gao W, Kang JH, Liao Y, Ding WX, Gambotto AA, Watkins SC, Liu YJ, Stolz DB, Yin XM. Biochemical isolation and characterization of the tubulovesicular LC3-positive autophagosomal compartment. *J Biol Chem.* 2010;285:1371–83.
- Harder LM, Bunkenborg J, Andersen JS. Inducing autophagy a comparative phosphoproteomic study of the cellular response to ammonia and rapamycin. *Autophagy.* 2014;10:339–55.
- Heo JM, Ordureau A, Paulo JA, Rinehart J, Harper JW. The PINK1-PARKIN Mitochondrial Ubiquitylation pathway drives a program of OPTN/NDP52 recruitment and TBK1 activation to promote mitophagy. *Mol Cell.* 2015;60:7–20.

- Jaquinod SK, Chapel A, Garin J, Journet A. Affinity purification of soluble lysosomal proteins for mass spectrometric identification. *Methods Mol Biol.* 2008;432:243–58.
- Kristensen AR, Schandorff S, Høyer-Hansen M, Nielsen MO, Jatela M, Dengjel J, Andersen JS. Ordered organelle degradation during starvation-induced autophagy. *Mol Cell Proteomics.* 2008;7:2419–28.
- Leighton F, Poole B, Beaufoy H, Baudhuin P, Coffey JW, Fowler S, De Duve C. The large-scale separation of peroxisomes, mitochondria, and lysosomes from the livers of rats injected with triton WR-1339. Improved isolation procedures, automated analysis, biochemical and morphological properties of fractions. *J Cell Biol.* 1968;37:482–513.
- Lieberman AP, Puertollano R, Raben N, Slaugenhaupt S, Walkley SU, Ballabio A. Autophagy in lysosomal storage disorders. *Autophagy.* 2012;8:719–30.
- Lübke T, Lobel P, Sleat DE. Proteomics of the lysosome. *Biochim Biophys Acta Mol Cell Res.* 2009;1793:625–35.
- Mancias JD, Wang X, Gygi SP, Harper JW, Kimmelman AC. Quantitative proteomics identifies NCOA4 as the cargo receptor mediating ferritinophagy. *Nature.* 2014;509:105–9.
- Mathew R, Khor S, Hackett SR, Rabinowitz JD, Perlman DH, White E. Functional role of autophagy-mediated proteome remodeling in cell survival signaling and innate immunity. *Mol Cell.* 2014;55:916–30.
- Naureckiene S, Sleat DE, Lackland H, Fensom A, Vanier MT, Wattiaux R, Jadot M, Lobel P. Identification of HE1 as the second gene of Niemann-Pick C disease. *Science.* 2000;290:2298–301.
- Overbye A, Fengersrud M, Seglen PO. Proteomic analysis of membrane-associated proteins from rat liver autophagosomes. *Autophagy.* 2007;3:300–22.
- Papinski D, Schuschnig M, Reiter W, Wilhelm L, Barnes CA, Maiolica A, Hansmann I, Pfaffenwimmer T, Kijanska M, Stoffel I, et al. Early steps in autophagy depend on direct phosphorylation of Atg9 by the Atg1 Kinase. *Mol Cell.* 2014;53:471–83.
- Richter B, Sliter DA, Herhaus L, Stolz A, Wang C, Beli P, Zaffagnini G, Wild P, Martens S, Wagner SA, et al. Phosphorylation of OPTN by TBK1 enhances its binding to Ub chains and promotes selective autophagy of damaged mitochondria. *Proc Natl Acad Sci.* 2016;113:4039–44.
- Rigbolt KTG, Zarei M, Sprenger A, Becker AC, Diedrich B, Huang X, Eiselein S, Kristensen AR, Gretzmeier C, Andersen J, et al. Characterization of early autophagy signaling by quantitative phosphoproteomics. *Autophagy.* 2014;10:356–71.
- Saraf SA, Raman M, Guarani-Pereira V, Sowa ME, Huttlin EL, Gygi SP, Harper JW. Landscape of the PARKIN-dependent ubiquitylome in response to mitochondrial depolarization. *Nature.* 2013;496:372–6.
- Sleat DE, Zheng H, Qian M, Lobel P. Identification of sites of mannose 6-phosphorylation on lysosomal proteins. *Mol Cell Proteomics.* 2006;5:686–701.
- Stromhaug PE, Berg TO, Fengersrud M, Seglen PO. Purification and characterization of autophagosomes from rat hepatocytes. *Biochem J.* 1998;335:217–24.
- Suzuki K, Nakamura S, Morimoto M, Fujii K, Noda NN, Inagaki F, Ohsumi Y. Proteomic profiling of autophagosome cargo in *Saccharomyces cerevisiae*. *PLoS One.* 2014;9:1–9.
- Xie Y, Kang R, Sun X, Zhong M, Huang J, Klionsky DJ, Tang D. Posttranslational modification of autophagy-related proteins in macroautophagy. *Autophagy.* 2015;11:28–45.
- Zhang T, Ghaemmaghami S. Global analysis of cellular protein flux quantifies the selectivity of basal autophagy. *Autophagy.* 2016;12:1411–2.
- Zhang J, Wang J, Ng S, Lin Q, Shen HM. Development of a novel method for quantification of autophagic protein degradation by AHA labeling. *Autophagy.* 2014;10:901–12.
- Zhuo C, Ji Y, Chen Z, Kitazato K, Xiang Y, Zhong M, Wang Q, Pei Y, Ju H, Wang Y. Proteomics analysis of autophagy-deficient *Atg7^{-/-}* MEFs reveals a close relationship between F-actin and autophagy. *Biochem Biophys Res Commun.* 2013;437:482–8.

Chapter 18

Bioinformatics Technologies in Autophagy Research



Yu Xue, Dong Wang, and Di Peng

Abstract Autophagy is an important and dynamic biological process, and provides an ideal application scenario for bioinformatics to develop new data resources, algorithms, tools and computational or mathematic models for a better understanding of complex regulatory mechanisms in cells. In the past decade, great efforts have been taken on the development of numerous bioinformatics technologies in autophagy research, and a comprehensive summarization of these important studies will provide a timely reference for both biologists and bioinformaticians who are working in the field of autophagy. In this book chapter, we first introduce bioinformatics technologies that allow sequence analysis of autophagy genes. We briefly summarize the mainstream algorithms in sequence alignment for the identification of homologous autophagy genes and emphasize the computational identification of potential orthologs and paralogs, as well as the evolutionary analysis of autophagy gene families. Three methods for the recognition of autophagy-related sequence motifs are introduced: regular expression, position-specific scoring matrix (PSSM) and group-based prediction system (GPS). Second, we carefully summarize recent progress in the analysis of autophagy-related omics data. We discuss how two major types of computational methods, enrichment analysis and network analysis can be used to analyze omics data, including transcriptomics, non-coding RNAomics, epigenomics, proteomics, phosphoproteomics and protein lysine modification (PLM) omics data. Finally, we summarize several important autophagy-related data resources, including both autophagy gene databases and autophagy-related RNA databases. We anticipate that more useful bioinformatics technologies will be developed and play an ever-more-important role in the analysis of autophagy.

Y. Xue (✉) · D. Peng

Key Laboratory of Molecular Biophysics of Ministry of Education, Hubei Bioinformatics and Molecular Imaging Key Laboratory, Center for Artificial Intelligence Biology, College of Life Science and Technology, Huazhong University of Science and Technology, Wuhan, China
e-mail: xueyu@hust.edu.cn; pengdi@hust.edu.cn

D. Wang

Department of Bioinformatics, School of Basic Medical Sciences, Southern Medical University, Guangzhou, China
e-mail: wangdong79@smu.edu.cn

© Science Press 2021

Z. Xie (ed.), *Autophagy: Biology and Diseases*, Advances in Experimental Medicine and Biology 1208, https://doi.org/10.1007/978-981-16-2830-6_18

387

Bioinformatics is a newly emerged interdisciplinary field that merges the knowledge from life science, biomedical science, computer science, information technology, mathematics, physics, chemistry and statistics. The major research areas in bioinformatics cover the collection, integration, quality control, annotation, maintenance and sharing of biological and biomedical big data. Related research areas also include abstraction and modeling from distinct data types to transform biological questions into resolvable and computable problems, as well as the combination of approaches from mathematics, physics, computer science and statistics to develop novel bioinformatics algorithms and corresponding tools. When focused on specific biological phenomena or processes such as autophagy, bioinformaticians also conduct high-throughput omics profilings and computational analyses to infer potential key regulatory factors for addressing important scientific questions. In this regard, data, algorithms and applications are the three main branches in the current field of bioinformatics, and none of them is dispensable.

One of the earliest bioinformatics studies can be traced to a paper entitled “The negentropy intake of biological systems (As shown by the problems of protein nutrition),” which was written in 1962 by Dr. Ching-Hua Hsu, a principle investigator at Institute of Biochemistry, Academia Sinica, Shanghai of China at that time, and published in *Acta Biochimica et Biophysica Sinica* (Hsu 1962). In the paper, based on amino acid frequencies of proteins in foods, the author presented potentially useful informatics method to calculate the negentropy intake of eaters such as children, young adults and rats. The predictions were very consistent with known experimental results, and the work is one of the earliest studies on protein sequence analysis. When the international Human Genome Project (HGP) started in 1980s, bioinformatics obtained a great opportunity for its development, as it exhibited a particular superiority in analyzing the flood of sequencing data and efficiently pushed the completion of HGP. During the following two decades, two trends existed in bioinformatics studies. First, due to the increase of data types, mainstream computational research was gradually expanded from nucleotide or protein sequence analysis to the analysis of omics profiling data and biomedical image data, and the diversity of research topics was dramatically increased. Second, mainstream bioinformaticians went much deeper into detailed branches of the biological and biomedical fields, and paid more and more attention to the combination of theoretical computation together with experimental validation. More efforts were directed toward making important biological findings, and bioinformatics was actively merged into the mainstream study of life and biomedical sciences.

Autophagy is an important and highly conserved biological process, whose stages include initiation and activation, phagophore formation, autophagosome formation, the fusion of autophagosome and lysosome, and lysosome re-formation, all to deliver cytoplasmic contents into the lysosome or vacuole for degradation. In contrast to periodic processes such as the cell cycle and circadian rhythm, autophagy is a typical non-periodic biological process. Thus, autophagy serves as an excellent model for bioinformatics, and it can be anticipated that related computational analyses might provide a relatively general solution for similar biological processes. After only about 30 min under starvation conditions, the occurrence of autophagy

can be readily and robustly detected in yeast, indicating a rapid response of autophagy. The specifically regulatory mechanisms remain to be explored. Autophagy can be roughly classified into two types: nonselective and selective autophagy. How to distinguish the two types is still a great challenge. In addition, technical innovation is strongly encouraged in the field of autophagy (Klionsky et al. 2016), as well as the generous sharing of experimental materials, reagents and/or antibodies. There are close and mutual communications among peers, and the field is welcoming to newcomers. Therefore, bioinformaticians can quickly acclimatize and begin making important contributions even if they lack background knowledge of autophagy biology.

In 2016, Dr. Daniel J. Klionsky, a famous professor at the University of Michigan in the USA, together with additional 2466 authors, published a paper entitled “Guidelines for the use and interpretation of assays for monitoring autophagy (3rd edition)” in *Autophagy* (Klionsky et al. 2016). The paper contained a special chapter on “Interpretation of in silico assays for monitoring autophagy,” which summarized the progresses in autophagy-related bioinformatics studies covering three aspects, including “Sequence comparison and comparative genomics approaches,” “Web-based resources related to autophagy” and “Dynamic and mathematical models of autophagy.” In this chapter, Sect. 18.1, corresponds to the first aspect of “Sequence comparison and comparative genomics approaches.” Also, the basic rationales for the computational recognition of LC3-interacting region (LIR) motifs will be briefly introduced, as well as the prediction of post-translational modification (PTM) sites. In recent years, autophagy-related omics identification studies have been widely conducted. Thus, Sect. 18.2 carefully introduces computational analyses for different layers of autophagy-related omics data, such as transcriptomics, epigenomics, proteomics and PTMomics. Section 18.3 corresponds to the topic of “Web-based resources related to autophagy,” to introduce autophagy gene databases and autophagy-related RNA databases. The third topic, “Dynamic and mathematical models of autophagy,” is not discussed here since these studies are still far from mature.

18.1 The Sequence Analysis of Autophagy Genes

Sequence analysis is the most fundamental and key aspect of bioinformatics, with techniques including pairwise sequence alignment, multiple sequence alignment, evolutionary and phylogenetic analysis, and sequence pattern recognition. All these computational approaches are widely applicable in the field of autophagy. In this section, we took the Atg8 protein in *Saccharomyces cerevisiae* as an example to introduce the use of various sequence analysis methods. Yeast Atg8 protein is an important molecular marker of autophagy and localizes to the outer and inner membranes of autophagosome during its formation. After the fusion of the autophagosome and vacuole, Atg8 located on the inner membrane can be degraded by acidic hydrolytic enzymes within the vacuole.



Fig. 18.1 (a) UniProt database contains two sub-databases including Swiss-Prot and TrEMBL. The former is manually annotated and reviewed, whereas the latter is automatically annotated without review. (b) The online service of BLAST at ExPASy

Before proceeding with a formal description, several important basic concepts should be introduced. First, the protein sequence database UniProt (<https://www.uniprot.org/>) used in this section contains two sub-databases: the manually annotated and reviewed Swiss-Prot, and the automatically annotated and not reviewed TrEMBL (Fig. 18.1a). Because manual annotation and review is quite time-consuming and labor-intensive, the number of protein sequences in Swiss-Prot is much fewer than in TrEMBL. Second, the Basic Local Alignment Search Tool (BLAST) is one of the most commonly used tools for searching protein or nucleotide sequences, and here, we used the BLAST maintained by ExPASy at Swiss Institute of Bioinformatics (<https://web.expasy.org/blast/>) (Fig. 18.1b). Third, a fundamental hypothesis of sequence alignment is that similar sequences may have similar functions. Similar sequences with similar functions are called homologs and are usually conserved during evolution. Thus, the meanings of the terms “similarity,” “homology” and “conservation” of sequences are similar. Homologs can be classified into two types: orthologs and paralogs. The former refers to the appearance of two genes during speciation events, whereas the latter denotes the appearance of two genes through gene duplication events in the same species. For example, human ULK1 and yeast Atg1 are reciprocal orthologs, where human ULK1, ULK2, ULK3 and ULK4 are paralogs with each other.

18.1.1 The Homologous Identification of Autophagy Genes

When “Atg8” is entered in the search field of UniProt, the first returned result is Atg8 in *S. cerevisiae*, with its UniProt accession number as P38182 (Fig. 18.2a). By clicking on the link <https://www.uniprot.org/uniprot/P38182>, Atg8-related annotations can be retrieved (Fig. 18.2b). Through visiting the page <https://www.uniprot.org/uniprot/P38182.fasta>, the Atg8 protein sequence can be obtained (Fig. 18.2c).

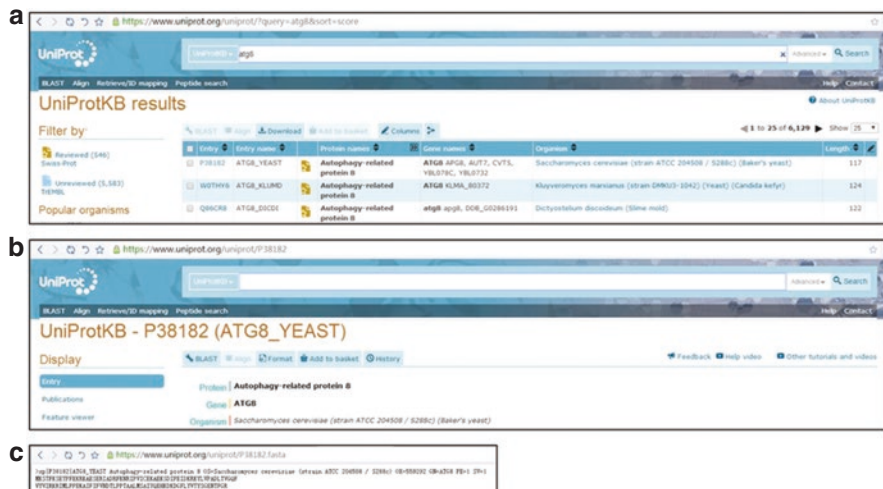


Fig. 18.2 (a) Inputting “atg8” into UniProt search tool gives yeast Atg8 as the first result. (b) The annotation page of yeast Atg8. (c) The sequence of yeast Atg8 in the FASTA format

In mainstream biological sequence databases, the standard sequence storage format is FASTA, in which the first line is the annotation line (starting with a “>” character) followed by one or multiple lines of sequences. Sequences in FASTA format can be easily manipulated by a computer. For example, in Perl or Python scripting languages, a protein sequence can be retrieved by recognizing a line started with “>”, and the next “>” indicates the beginning of the next sequence. Therefore, FASTA is a compact format for storing multiple sequences. For example, the first line in the UniProt FASTA file of Atg8 yeast is “>sp|P38182| atg8_adaptive autophagy-related protein 8 OS=Saccharomyces cerevisiae (strain ATCC 204508 / S288c) OX=559292 GN= Atg8 PE=1 SV=1”, in which “sp” refers to the sequence derived from the Swiss-Prot sub-database, “P38182” is the UniProt accession number, “ATG8_YEAST” is the sequence name, “autophagy-related protein 8” is the full protein name, “OS=Saccharomyces cerevisiae (strain ATCC 204508 / S288c)” is the species name, “OX = 559292” is the taxonomic identifier, and “GN = ATG8” refers to gene name (Fig. 18.2c).

18.1.1.1 Algorithms in Sequence Alignment

By entering the yeast Atg8 protein sequence and choosing *Homo sapiens* in the species selection bar of ExPASy BLAST (<https://web.expasy.org/blast/>), potential homologs of yeast Atg8 in human proteome can be searched. (Alternatively, the UniProt accession number of P38182 can be directly inputted for yeast Atg8 instead of the FASTA sequence) (Fig. 18.3a). In ExPASy BLAST, the UniProt database is used. Since one gene can be translated into multiple protein sequences, different

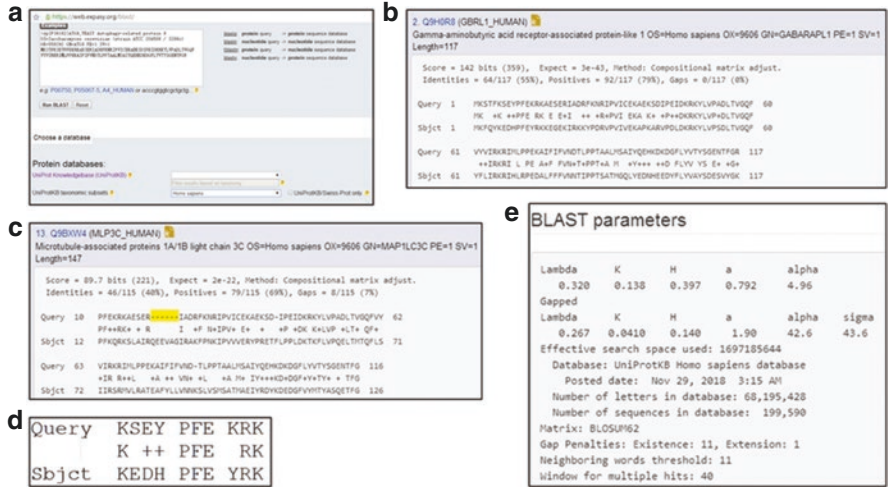


Fig. 18.3 (a) Inputting the sequence of yeast Atg8 to query human proteome by BLAST. (b) The minor isoforms were not considered, and the second result from BLAST is the human homolog of yeast Atg8 with the highest score. (c) Insertion/deletions in sequence alignment. (d) The rationale of scoring strategy in BLAST. (e) Parameters provided by BLAST

types of alternative splicing isoforms exist in the UniProt database. Here, only major isoforms were taken into consideration. The first search result “1. A0A024RAP5 (A0A024RAP5_HUMAN)” is a minor isoform of GABARAPL1, while the second result “2. Q9H0R8 (GBRL1_HUMAN)” is the major isoform of GABARAPL1. Thus, the human GABARAPL1 is a homologous sequence of the yeast Atg8 (Fig. 18.3b).

How is a protein sequence alignment result produced for yeast Atg8 and human GABARAPL1? How should this result be interpreted? How can we judge whether or not two proteins are potential homologs? The rationale of BLAST-based sequence alignment is that a submitted protein sequence will be pairwise aligned to protein sequences pre-stored in the database. Thus, such a procedure contains multiple pairwise sequence alignments, and here, we should introduce the algorithms on pairwise sequence alignments. A protein’s function is determined by its three-dimensional (3D) structure. Thus, two protein sequences with similar lengths and conserved functions might exhibit similar 3D structures. If we maximally align two protein 3D structures together, each pair of aligned positions might contain a matching pair of amino acid residues, an insertion or a deletion. In this example, the first residue “M” of yeast Atg8 is aligned with the first residue “M” of human GABARAPL1, and the “M-M” pair is denoted as a match. The third residue “S” of yeast Atg8 is aligned with the third residue “F” of human GABARAPL1, and the “S-F” pair is also a match. For the insertion or deletion, we can refer to the 13th result of “13.Q9BXW4 (MLP3C_HUMAN)”, in which six “-” characters exist between the 20th “R” and the 21st “I” in yeast Atg8, whereas “R-----I” was aligned to “RQEEVAGI” of

human GABARAPL1 starting from the 22nd “R” and the 29th “I” residues (Fig. 18.3c).

These alignments present two problems. First, how should matches be defined? Based on biological experience, when sequences with similar functions are aligned, a good alignment should have identical amino acid residues aligned together. Because there is no difference in the “M-M” pair, it can be anticipated that the protein function will be not altered, and such a pair should be a “good” match. However, in the “S-F” pair, “S” is substituted by “F” or vice versa, and such a substitution might affect the protein function. Thus, the “S-F” pair is a “bad” match. For bioinformatics, biological experiences and intuitions should be transformed into quantitative and computable values, by constructing amino acid substitution matrices, such as the most commonly used BLOSUM62 scoring matrix (Fig. 18.4). The BLOSUM 62 matrix is symmetric and is used to evaluate the matching scores of amino acid pairs. In the “M-M” pair, the two amino acid residues are identical, and their substitution score, 5, is found by searching the BLOSUM 62 matrix. In the “S-F” pair, the two amino acid residues are different, and their physicochemical properties also differ. Thus, their substitution score is -2 . A higher score represents a higher conservation of an amino acid pair. The second problem is how to deal with the insertions or deletions, which won’t be represented in the BLOSUM 62 matrix.

```
# Matrix made by matblas from blosum62.iij
# * column uses minimum score
# BLOSUM Clustered Scoring Matrix in 1/2 Bit Units
# Blocks Database = /data/blocks_5.0/blocks.dat
# Cluster Percentage: >= 62
# Entropy = 0.6979, Expected = -0.5209
# A R N D C Q E G H I L K M F P S T W Y V B Z X *
A 4 -1 -2 -2 0 -1 -1 0 -2 -1 -1 -1 -1 -1 -2 -1 1 0 -3 -2 0 -2 -1 0 -4
R -1 5 0 -2 -2 -3 1 0 -2 0 -3 -2 2 -1 -3 -2 -2 -1 -3 -2 -3 -1 0 -1 -4
N -2 0 6 1 -3 0 0 0 1 -3 -3 0 -2 -3 -2 1 0 -4 -2 -3 3 0 -1 -4
D -2 -2 1 6 -3 0 2 -1 -1 -3 -4 -1 -3 -3 -1 0 -1 -4 -3 -3 4 1 -1 -4
C 0 -3 -3 -3 9 -3 -4 -3 -3 -1 -1 -3 -1 -2 -3 -1 -1 -2 -2 -1 -3 -3 -2 -4
Q -1 1 0 0 -3 5 2 -2 0 -3 -2 1 0 -3 -1 0 -1 -2 -1 -2 0 3 -1 -4
E -1 0 0 2 -4 2 5 -2 0 -3 -3 1 -2 -3 -1 0 -1 -3 -2 -2 1 4 -1 -4
G 0 -2 0 -1 -3 -2 -2 6 -2 -4 -4 -2 -3 -3 -2 0 -2 -2 -3 -3 -1 -2 -1 -4
H -2 0 1 -1 -3 0 0 -2 8 -3 -3 -1 -2 -1 -2 -1 -2 -2 2 -3 0 0 -1 -4
I -1 -3 -3 -3 -1 -3 -3 -4 -3 4 2 -3 1 0 -3 -2 -1 -3 -1 3 -3 -3 -1 -4
L -1 -2 -3 -4 -1 -2 -3 -4 -3 2 4 -2 2 0 -3 -2 -1 -2 -1 1 -4 -3 -1 -4
K -1 2 0 -1 -3 1 1 -2 -1 -3 -2 5 -1 -3 -1 0 -1 -3 -2 -2 0 1 -1 -4
M -1 -1 -2 -3 -1 0 -2 -3 -2 1 2 -1 5 0 -2 -1 -1 -1 -1 1 -3 -1 -1 -4
F -2 -3 -3 -3 -2 -3 -3 -3 -1 0 0 -3 0 6 -4 -2 -2 1 3 -1 -3 -3 -1 -4
P -1 -2 -2 -1 -3 -1 -1 -2 -2 -3 -3 -1 -2 -4 7 -1 -1 -4 -3 -2 -2 -1 -2 -4
S 1 -1 1 0 -1 0 0 0 -1 -2 -2 0 -1 -2 -1 4 1 -3 -2 -2 0 0 0 -4
T 0 -1 0 -1 -1 -1 -1 -2 -2 -1 -1 -1 -1 -2 -1 1 5 -2 -2 0 -1 -1 0 -4
W -3 -3 -4 -4 -2 -2 -3 -2 -2 -3 -2 -3 -1 1 -4 -3 -2 11 2 -3 -4 -3 -2 -4
Y -2 -2 -2 -3 -2 -1 -2 -3 2 -1 -1 -2 -1 3 -3 -2 -2 2 7 -1 -3 -2 -1 -4
V 0 -3 -3 -3 -1 -2 -2 -3 -3 3 1 -2 1 -1 -2 -2 0 -3 -1 4 -3 -2 -1 -4
B -2 -1 3 4 -3 0 1 -1 0 -3 -4 0 -3 -3 -2 0 -1 -4 -3 -3 4 1 -1 -4
Z -1 0 0 1 -3 3 4 -2 0 -3 -3 1 -1 -3 -1 0 -1 -3 -2 -2 1 4 -1 -4
X 0 -1 -1 -1 -2 -1 -1 -1 -1 -1 -1 -1 -1 -1 -2 0 0 -2 -1 -1 -1 -1 -1 -4
* -4 -4 -4 -4 -4 -4 -4 -4 -4 -4 -4 -4 -4 -4 -4 -4 -4 -4 -4 -4 -4 -4 -4 1
```

Fig. 18.4 The BLOSUM62 matrix

From the viewpoint of biologists, the easiest solution in theory is the introduction of the score penalty, which subtracts a corresponding score if met with a gap. Bioinformaticians also followed this linear score penalty; however, such a strategy is quite stringent. For example, in BLAST, a score of 11 will be subtracted for the first gap, and only 1 will be subtracted for any additional gaps. Following this way, when the “R-----I” in yeast Atg8 was aligned to the “RQEEVAGI” in human GABARAPL1, the similarity score can be calculated as follows: 5 (the substitution score of “R-R” pair) -11 (the penalty of the first gap) -5 (The penalty score of the following 5 gaps) $+4$ (the substitution score of “I-I” pair) $= -7$. Therefore, the similarity score can be calculated by aligning two protein sequences together.

So how to align two protein sequences? The classical pairwise alignment algorithms were derived from the dynamic programming algorithm, and included the Needleman–Wunsch algorithm of global pairwise alignment and the Smith–Waterman algorithm of local pairwise alignment. The concepts of the two algorithms are quite clear, and their manipulation procedures are elegant. However, due to their low speed, the two algorithms were rarely used in reality, instead appearing primarily in textbooks. Examples in textbooks should be simple, clear and aesthetic, in order to be easily mastered by students. These two classical algorithms are the core of all sequence analysis. In practice, various adaptations are used to improve and optimize the algorithms for more sophisticated usage. In fact, the BLAST algorithm was derived from the Smith–Waterman algorithm, with additional optimization and adjustments. First, a database for searching protein sequences is constructed. During this process, the similarity scores between any two 3 amino acid (aa) peptides will be pre-calculated based on the BLOSUM62 matrix and threshold values pre-defined to filter unnecessary results. When a protein sequence is inputted into BLAST, 3 aa peptides will be sequentially segmented from N- to C-termini, with 1 aa per step. Then, each 3 aa peptide will be queried in the pre-calculated scoring list, and only results higher than the threshold values are retained. For each retained 3 aa pair, the alignment will be bidirectionally extended to calculate the similarity score. Then, high-scoring segment pairs (HSP) are retained, and the algorithm will attempt to connect these fragments into as long of a sequence as possible. Here, we used the pairwise sequence alignment between yeast Atg8 (Query) and human GABARAPL1 as an example. In the first step of searching the scoring list, e.g., the similarity score of “PFE” between the two sequences is $7 + 6 + 5 = 18$, which exceeds the threshold. The bi-directional extension will be conducted. The left side is the KSEY-KEDH pair, and the similarity score is $5 + 0 + 2 + 2 = 9$. The right side is KRK-YRK pair, and the score is $-2 + 5 + 5 = 8$. So the total score is $18 + 9 + 8 = 35$ (Fig. 18.3d). In the first round, a number of isolated HSPs will be computed, and gaps will be added. If the total similarity score is higher than either of two neighboring HSPs after adding gaps, such a manipulation will be adopted. Such a procedure will be iteratively performed until no HSPs can be conjugated any longer. Thus, multiple alignment results might be output from BLAST, if low complexity regions existed in protein sequences. The results should be carefully interpreted. One of the advantages of BLAST algorithm is that it is much faster than the Needleman–Wunsch and

Smith–Waterman algorithms, while the computational accuracy is not significantly influenced.

Let's come back to the alignment result between yeast Atg8 and human GABARAPL1 (Fig. 18.3) and discuss what its parameters mean. In the first item of “Score = 142 bits (359)”, the “359” in parentheses is computed by adding substitution scores in the BLOSUM 62 matrix, and such a score is called the “raw score” and represented by R . The “Score” is a bit score, which refers to the ratio of matched: unmatched probabilities between two sequences, after the logarithmic normalization with a base 2. If “Score = 0”, the ratio of matched: unmatched probabilities would be equal to be 1, and the matched vs. unmatched probability between the two sequences is 50%. Therefore, the “Score = 142” means that the matched probability: the unmatched probability = $2^{142} = 5.6 \times 10^{42}$. Thus, the probability that the two sequences to be unmatched is extremely low.

Although the probability is very low, this comparison is complicated by the nature of multi-sample statistics, because the queried protein sequence has been pairwise compared with all the sequences in the database. Thus, bioinformaticians will ask a second question: given a computed score, is it statistically significant? That is to say, if the bit score of yeast Atg8 and human GABARAPL1 is calculated as “Score = 142 bits”, how do we calculate the probability that the two sequences might still be unmatched? The result can be found in the second item of “Expect = $3e-43$ ”, which estimates the unmatched probability (expected probability) for a bit score of Score = 142 and is denoted as E . The relations among the “raw score” R , bit score S and expected probability E were originally calculated by the two formulas shown below:

$$E(S) \approx Kmne^{-\lambda S} = mn2^{-S}, S = \frac{\lambda R - \ln(K)}{\ln(2)}$$

The λ or K in the two formulas was previously estimated in the BLAST. For the alignment results of yeast Atg8 in human proteome, users can refer to the bottom of the page, and the two parameters will be shown in the “BLAST parameters” (Fig. 18.3e). Because gapped BLAST was used, we can find under the line “Gapped” that Lambda (λ) = 0.267 and $K = 0.0410$. Using the two parameters, we first calculate the bit score S based on $R = 359$ as below:

$$S = \frac{0.267 * 359 - \ln(0.041)}{\ln(2)} \approx \frac{95.9 - (-3.2)}{0.7} = \frac{99.1}{0.7} \approx 142$$

Then according to the bit score of Score/ $S = 142$, the expected probability E -value of can be calculated by using the formulas, in which “ m ” refers to the length of the query sequence. Since the length of yeast Atg8 is 117 aa, $m = 117$ in this case. The “ n ” presents the effective length of the searched sequences. In the “Number of letters in database” option of “BLAST parameters”, its effective length is $n = 68,195,428$. Using the m and n values, the calculation is as below:

$$E(142) = 117 * 68195428 * 2^{-142} = 1.43 * 10^{-33}$$

Obviously, we can see that the E -value calculated by the formula is inconsistent with “Expect = 3e-43” provided by the website. It was found that the original E -values calculated by the formula in the earlier versions of ExPASy BLAST were too stringent in practical applications. Thus, the third item, “Method: Compositional matrix adjustment” indicates the adjustment of original E -values to increase the sensitivity to allow more homologs to be detected. The fourth term “Identities = 64/117 (55%)” means that 64 aa pairs in the total of 117 aa pairs for the two sequences are identical without any substitutions of different amino acids, and the corresponding amino acids in the middle lines are shown in the below results of Query and Sbjct. The fifth item “Positives = 92/117 (79%)” refers to the aa pairs with positive scores in the BLOSUM 62 matrix, and these pairs also include the identical aa pairs. For the substitution between two different amino acids, if the score is positive, the symbol of “+” is used in the middle line of the alignment results. The sixth item of “Gaps = 0/117 (0%)” means the number of gaps in the alignment result is 0.

18.1.1.2 The Identification of Orthologs and Paralogs

All life on earth has evolved from a common ancestor, and thus, all proteins will exhibit some degree of homologous relationship. Therefore, in theory, all retrieved results from BLAST are homologs of the queried sequence. However, the aim of sequence alignment is finding proteins with similar functions from sequence similarity, and a general search of all homologous sequences is meaningless. Instead, an analysis of protein families is necessary. The members of a protein family usually share similar primary sequences, similar 3D structures and conformations, as well as similar biological functions. However, the definition of a protein family is not very strict. For example, the human genome encodes about 520 protein kinase genes, which contain conserved functional domains for catalyzing the protein phosphorylation reaction. Actually, these protein kinases belong to the same protein family, but were arbitrarily classified into three levels: the protein kinase super-family, family and sub-family, due to the large number of protein kinases. How to properly define a protein family depends on distinct scientific problems, and here, we do not discuss it in depth. For convenience, we can simply regard a conserved protein family as containing multiple members, some of which have functionally identical or similar homologs in other species.

Thus, we need to introduce the concepts of ortholog and paralog. The keyword for the former is “speciation,” whereas the keyword for the latter is “gene duplication.” It can be expected that genes/proteins existing before the speciation event will keep their conserved functions after the speciation event, and the sequence similarity of orthologs among different species will be higher. For paralogs, due to the divergence and economics of biological evolution, it is difficult for a species to

maintain two genes/proteins with identical functions. After a gene duplication event, perhaps one gene preserved the original function and the other evolved new functions, or both genes preserved parts of original functions and evolved new functions. Two hypotheses have been proposed and supported by molecular evolutionary analyses. The former is called neofunctionalization, whereas the latter is called subfunctionalization. No matter which hypothesis more accurately describes the process followed by genes during their evolution after the duplication, the protein sequences would have considerable changes due to the generation of new functions. Thus, the similarity of paralogs is usually lower than that of orthologs. Herein, the most important goal of sequence alignment is to determine the ortholog of the inputted sequence in other species, because orthologous sequences in various species usually share identical or highly similar functions. Then, potentially paralogous sequences can be inferred, and the protein family should be well defined for further analysis.

Here, we discuss the first question on how to determine the orthologs of yeast Atg8 in the human proteome. One of the most widely used computational method is Reciprocal Best Hits (RBHs) (Tatusov et al. 1997) (Fig. 18.5). In the procedure of RBHs, a protein sequence a in the species A is searched for homologs in the species B by BLAST, and b achieves the highest score in the results. Then, the protein sequence b in the species B was used for reversely searching homologs in the species A . If a also achieves the highest score in the BLAST results, it can be demonstrated that a in the species A and b in the species B reciprocally find each other as the optimal result. Thus, a and b are a potential orthologous pair. The RBHs approach was proposed in 1997, and its core rationale has never been altered during the past two decades, although some minor adaptations have been added. For yeast Atg8, since minor isoforms were not considered, human GABARAPL1 was computationally determined as the best match to yeast Atg8. Then, we input the UniProt accession number Q9H0R8 of human GABARAPL1 into BLAST and select the species as *Saccharomyces cerevisiae* (Fig. 18.6a). From the results, we find that yeast Atg8 had the highest score (Fig. 18.6b). Therefore, the yeast Atg8 and human GABARAPL1 are mutually orthologous sequences.

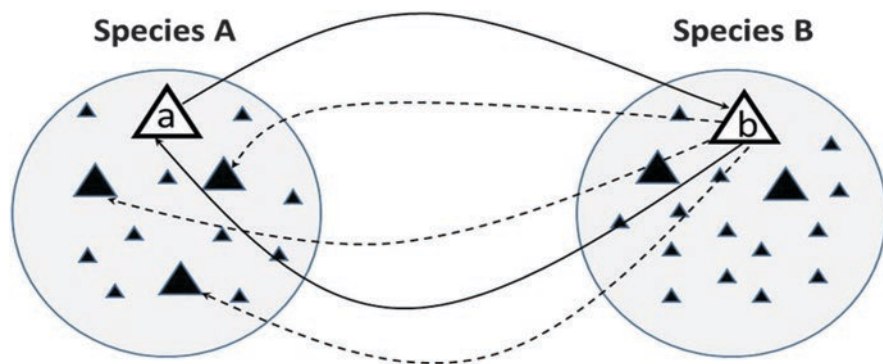


Fig. 18.5 The reciprocal best hits (RBHs) approach for the detection of orthologs in different species

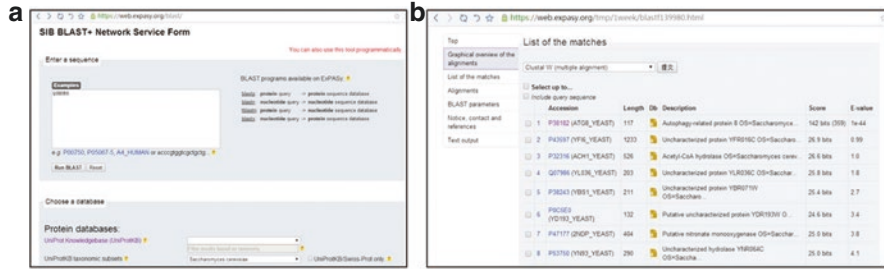


Fig. 18.6 (a) Inputting the sequence of human GABARAPL1 to search homologs in yeast proteome. (b) The homolog of human GABARAPL1 with the highest score in budding yeast is Atg8

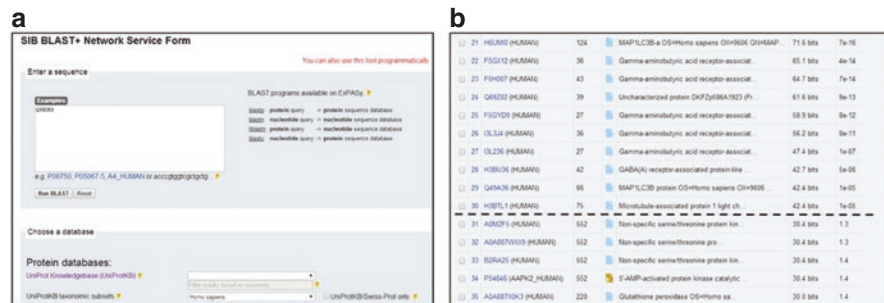


Fig. 18.7 (a) Inputting the sequence of human GABARAPL1 to query in the human proteome. (b) BLAST bit scores will dramatically decrease between paralogs and unrelated sequences

Are there any problems with this result? No errors occurred in the process of computation, yet the result was incorrect, because previously experimental studies have indicated that mammalian MAP1LC3B/LC3B, rather than GABARAPL1, performs the function most similar to yeast Atg8. The orthologs determined by RBHs are mostly reliable, but not for all cases. For this reason, the predictions require further experimental validations. Actually, human MAP1LC3B is a paralog of GABARAPL1, and so how can we find paralogous sequences? Using BLAST, we can adopt the human GABARAPL1 to search the human proteome (Fig. 18.7a) and then check the results carefully.

In our experience, there are several simple rules to judge potential paralogs. First, paralogs are usually similar to the inputted sequence, which must exhibit low similarity with unrelated sequences. Thus, if the bit score is dramatically reduced and expected probability *E*-value significantly increased, results above this position are potential paralogs (Fig. 18.7b). Second, minor isoforms and fragments should be ignored. Third, paralogs usually share similar functions, and this can be judged from their corresponding genes names and UniProt annotations. No fool-proof approach exists for the identification of paralogs, but users can identify seven human genes (GABARAP, GABARAPL1, GABARAPL2, GABARAPL3, MAP1LC3A,

MAP1LC3B and MAP1LC3C) to be mutually paralogous sequences based on the described rules.

18.1.1.3 The Evolutionary Analysis of Autophagy Gene Families

Based on the rules described in the above section, we can identify the orthologs and paralogs of yeast Atg8 in *Homo sapiens*, *Mus musculus*, *Drosophila melanogaster*, *Caenorhabditis elegans*, *Schizosaccharomyces pombe* and *Arabidopsis thaliana* (Fig. 18.8a). Using their UniProt accession numbers, we obtained their protein sequences in FASTA format: a compact, mainstream and common format for storing single or multiple sequences. For each sequence, we modified its name by using the abbreviation of the species name plus gene name; e.g., yeast Atg8 was changed to ScATG8. Then, all protein sequences were stored in a single text file, and the suffix name of the file was changed to “.fas” (Fig. 18.9a).

There are numerous software packages developed for phylogenetic or molecular evolutionary analyses, and MEGA is one of the most commonly used tools. Here, we downloaded the latest version of MEGA software (<https://www.megasoftware.net/>) (Fig. 18.8b). After installing MEGA X, users can open the software, click on ALIGN, then click on “Edit/Build Alignment” in the menu that appears (Fig. 18.9b), select “Retrieve a sequence from a file” in the dialog box (Fig. 18.9c) and import the saved sequence file, such as the file “Atg8.fas”. Then in the text form that appears, users can click on “Alignment” and select “Align by ClustalW”. Then, multiple sequence alignments will be performed by using the ClustalW software pre-embedded in MEGA (Fig. 18.9d). Such a procedure is necessary before constructing an evolutionary tree.

a

<i>S. cerevisiae</i>		<i>H. sapiens</i>		<i>M. musculus</i>		<i>D. melanogaster</i>		<i>C. elegans</i>		<i>S. pombe</i>		<i>A. thaliana</i>	
Name	UniProt	Name	UniProt	Name	UniProt	Name	UniProt	Name	UniProt	Name	UniProt	Name	UniProt
ATG8	P38182	GABARAP	O95166	Gabarap	Q9DCD6	Atg8a	Q9W2S2	lgg-1	Q09490	atg8	O94272	ATG8A	Q8LEM4
		GABARAPL1	Q9H0R8	Gabarapl1	Q8R3R8	Atg8b	Q9VEG5	lgg-2	Q23536			ATG8B	Q9XE85
		GABARAPL2	P60520	Gabarapl2	P60521							ATG8C	Q85927
		GABARAPL3	Q9BY60									ATG8D	Q95L04
		MAP1LC3A	Q9H492	Map1c3a	Q91VR7							ATG8E	Q85926
		MAP1LC3B	Q9GZQ8	Map1c3b	Q9CQV6							ATG8F	Q8VYK7
		MAP1LC3C	Q9BXW4									ATG8G	Q9LZZ9

b

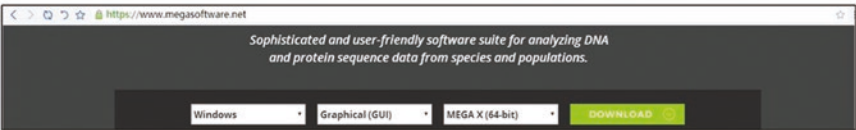


Fig. 18.8 (a) Paralogs and orthologs of yeast Atg8 in multiple model organisms. (b) The website for MEGA, a tool for analyzing molecular evolution



Fig. 18.9 (a) Protein sequences in FASTA format for members of the Atg8 family. (b) Choose “Edit/Build Alignment”; (c) Choose “Retrieve a sequence from a file”. (d) Choose “Align by ClustalW”. (e) Click on “Export Alignment” and choose “MEGA Format”

After performing the multiple sequence alignment, please do not choose the “save file” option. Instead, users should select “Export Alignment”, then select “MEGA Format”, export the alignment results and save the results into the “Atg8.Meg” file (Fig. 18.9e). MEGA uses a specific suite of file formats and will not process files in other formats. Then, users can close the text form of the multiple sequence alignment, return to the main interface, drag the saved “Atg8.Meg” file into the main interface of MEGA by mouse, select “PHYLOGENY” and then choose “Construct/Test neighbor-joining Tree” (Fig. 18.10a). MEGA implements five algorithms for the construction of phylogenetic trees or molecular evolution trees, and three most commonly used algorithms are the maximum likelihood method, the neighbor-joining method and minimum-evolution method. Each algorithm has its own advantages and disadvantages. The maximum likelihood method is suitable for phylogenetic analysis of remote sequences, but the computational speed is quite low. The rationales of the neighbor-joining method and minimum-evolution method are similar to each other, and both are rapid with accuracy not significantly lower than the maximum likelihood method. Here, we choose the neighbor-joining method. From the dialog box that appears, users should select “Bootstrap method” in the option “Test of Phylogeny”, then change the number to 5000 and click on OK for the computation (Fig. 18.10b). Here, we only care about “Bootstrap consensus tree.”

The construction of molecular evolutionary trees is not so simple, and the results must be properly interpreted. If the results are not consistent with known experimental knowledge, additional attempts should be conducted. For example, in this

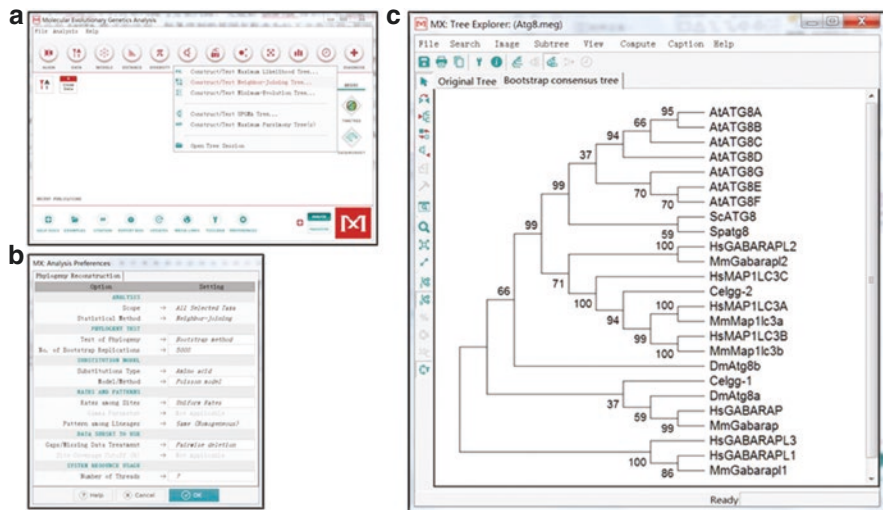


Fig. 18.10 (a) The neighbor-joining tree will be constructed. (b) Parameters should be properly set. (c) The Bootstrap consensus tree

case, we find that ScATG8 of budding yeast and Spatg8 of fission yeast are closely related, whereas the seven genes of ATG8A-G in *A. thaliana* might have independently evolved after the speciation of fungi, plants and animals (Fig. 18.10c). However, the evolutionary pattern in animals is quite complicated, and actually, the seven human Atg8 homologs can be classified into four subfamilies, including GABARAPL2, MAP1LC3A/B/C, GABARAP and GABARAPL1/3. The evolutionary patterns of the seven human genes in the phylogenetic tree are not very consistent with the speciation events, and it will be difficult to use the RBHs approach to predict potentially orthologs, or to infer the functionally identical complement of yeast Atg8. In this regard, computational prediction can efficiently narrow down potential candidates, but cannot replace experimental results. In addition, the “Bootstrap method” option provides resampling tests, which is a commonly used method to test the reliability of a molecular evolutionary tree, and should be usually selected. For example, in this analysis, one of the divergence points of two evolutionary branches has a bootstrap value of 37, which indicates the reliability of its correct topology to only be 37% (Fig. 18.10c). However, most of bootstrap values are greater than 50 in our tree, indicating that the result is generally reliable. If the reliability of a molecular evolutionary tree is not high, or inconsistent with experimental evidence, two approaches can be adopted. First, more species can be added to find orthologs and paralogs in more species, and these new sequences should be added into the phylogenetic analysis. Second, different methods for constructing trees can be tested. If different methods can generate relatively consistent trees, this indicates a reliable result.

18.1.2 *The Recognition of Autophagy-Related Sequence Motifs*

In this section, three methods will be introduced for computational identification of sequence motifs: regular expression, the position-specific scoring matrix (PSSM) algorithm and the GPS algorithm. Short linear motifs in protein sequences are important functional elements. It should be noted that motifs are different from functional domains. Functional domains usually have distinct biological functions, exhibit integrative and independent 3D structures, and have a length of tens or hundreds of amino acid residues. Insertions/deletions or gaps are allowed in functional domains. In contrast, motifs usually have specific biological functions, but do not necessarily have integrative and independent 3D structures, and have a length of several or tens of amino acid residues. For the prediction of functional domains, usually multiple sequence alignment should be conducted for members in a same family, and hidden Markov models (HMMs) can then be constructed by using *hmm-build* in HMMER (<http://www.hmmerr.org/>) software package. Then, *hmmsearch* will be used for searching candidate sequences by using pre-constructed HMMs. In public databases such as UniProt, pre-calculated functional domains are usually provided in annotations. Thus, users can directly refer to the annotation information. However, there are few public databases maintained for annotating protein motifs, because too many potential motifs can be found and it is difficult to annotate all of them. Second, new motifs are continuously being defined, and it is difficult to collect these new motifs in time. One of best annotated databases of protein motifs is ELM (<http://elm.eu.org/>).

Here, we only discuss the recognition and prediction of autophagy-related motifs. To date, two autophagy-related motifs have been widely studied (Klionsky et al. 2016). First, chaperone-mediated autophagy (CMA) substrates often contain a motif with the five amino acid residues “KFERQ,” which can be specifically recognized by a chaperone protein HSPA8/HSC70 (Human UniProt accession number: P11142) and transported to lysosome for degradation. Another, more important motif is named the LIR motif or Atg8 family interacting motif (AIM), which contains the consensus sequence “WXXL” (X represents any amino acid). Previous studies demonstrated that LIR/AIM motifs exist in the sequences of numerous Atg proteins and autophagy regulators, and can be specifically recognized by LC3B/Atg8 to mediate protein–protein interactions. A mainstream hypothesis is that macroautophagy (hereafter autophagy) can be classified as either nonselective or selective autophagy. One of the fundamental elements of selective autophagy might be LIR/AIM motifs, which mediate the physical interaction of specific proteins and LC3B/Atg8, recruit the autophagy substrates to autophagosome and deliver them into lysosome/vacuole for degradation. The classic LIR/AIM motif is not very rigorous, and too many false-positive results will be generated if used for the prediction. Thus, an extended LIR-motif (xLIR) was proposed, namely,

x(2)-[WFY]-x(2)-[LIV], in which x represents an acidic amino acid (Klionsky et al. 2016). However, a more exact motif used is [DE][DEST][WFY][DELIV]X[ILV] (Kalvari et al. 2014).

18.1.2.1 Regular Expression

The first method of sequence pattern finding searches all candidate protein sequences that contain a given sequence pattern and returns the start and end position. In previous studies, Ioanna Kalvari et al. established an online tool iLIR (<http://repeat.biol.ucy.ac.cy/iLIR/>) for the LIR/AIM prediction, and collected 34 experimentally validated LIR/AIM motifs as the training dataset (Kalvari et al. 2014). To simplify our example, here we only selected three known human proteins that contain LIR motifs for further analysis: ATG13, CALR/Calreticulin and FUNDC1 (Fig. 18.11a). Each of the three proteins contains an experimentally verified LIR motif. From the UniProt database, we individually obtained their protein sequences, and copy and pasted them into a single text file named “LIR.txt” (Fig. 18.11b).

In the Perl scripting language, a sequence motif is called a “regular expression,” and a search based on regular expression is pattern matching. For example, the experimentalists defined a LIR/AIM motif as “[DE][DEST][WFY][DELIV]X[ILV]”, which should be translated into a regular expression in Perl as “[DE][DEST][WFY][DELIV].[ILV]”. The square brackets mean that one of the characters should be matched, and the “.” is a wildcard character in Perl to represent any character. Based on a reference code (<http://liucheng.name/1285/>), a small script was written in Perl for searching LIR/AIM motifs from the multiple protein sequences. Before using this script, the software package ActivePerl should be downloaded (<https://www.activestate.com/products/activeperl/>) as a Perl interpreter (Fig. 18.11c). After installation, users can refer to the following code:



Fig. 18.11 (a) Three experimentally identified and known LIR/AIM motifs were adopted for an example of motif finding methods. (b) The protein sequences in FASTA format. (c) ActivePerl is an interpreter of Perl. (d) Finding LIR/AIM motifs by regular expression

```

#A LIR/AIM motif finding script
open(Fh,"LIR.txt"); #Open the sequence file for searching motifs
open(In,">Motif.txt"); #Open the output file
my $motif="[DE][DEST][WFY][DELIV].[ILV]"; #The LIR/AIM motif
$/ = ">"; # A global variable of Perl to separate lines by ">"
print In "ID\tMotif\tStart\tEnd\tLength\n"; #Output the
title line
while(<Fh>){
  if($_ =~ /(.*?)\s(.*)/ms){ # The first brackets match the ID,
  and the second ones match the sequence
    $id = $1; #Sequence ID
    $seq = $2; # Sequence
    $seq =~ s/\s//g; #Delete all line breaks to get a single
line of the sequence
    while ($seq =~ m/($motif)/g) { #Match the motif
      $len = length($1); #Return the motif length
      $end = pos($seq); #Return the end position of motif
      $start = $end - $len + 1; #Calculate the start
position
      print In "$id\t$1\t$start\t$end\t$len\n"; #Output
the results
    }
  }
}
close(Fh);#Close the sequence file to release memory
close(In);#Close the output file

```

Readers can copy the contents between the two lines of “*” characters into a new text file and change the file suffix “.pl” instead of “.txt”. After double-clicking on this file, the results will automatically be generated into the file of “motif.txt” (Fig. 18.11d). This script is not limited to searching for LIR/AIM motifs. Users can change the regular expression in the third line to search for customized motifs. It will be quite helpful for experimentalists to learn a little programming. Various scripting languages such as Perl or Python are much easier than C++ or Java, but quite powerful in dealing with text files. One introductory book entitled *Beginning Perl For Bioinformatics* (By James Tisdall, Release Date: February 2009, Publisher: O’Reilly Media) consists of 13 chapters. For readers who learned C++ in their undergraduate courses, it would not be difficult to learn one chapter per day. In this way basic Perl programming can be roughly learned in about 2 weeks. Also, writing code or programming is different from performing experiments. The reuse and extension of existing code is important, and excellent programmers usually use 80% to 90% open-source code, adopt various functions, and only write the key parts by themselves to resolve problems. “Don’t reinvent the wheel” is the basic rationale of programming.

acids are 0. For the second column, D appears in the first two motifs, but S appears in the third motif. Thus, the frequencies of D and S are 0.67 and 0.33, respectively. By using such a simple approach, a PSSM can be constructed (Fig. 18.12b). Because this matrix is derived from the known LIR/AIM motifs, it is called the foreground (“+”). Also, the background (“-”) matrix should be built by various methods. For example, 6 aa peptides can be randomly retrieved from the UniProt database to consist a negative dataset (most of them will be expected not to be LIR/AIM motifs), and then, a matrix will be formed to calculate amino acid frequencies for each position. The simplest approach is to directly count amino acid frequencies in a public database, as the background. For example, in this case, if we pre-calculated the amino acid frequencies of D, S, W, V and I of all protein sequences in UniProt as 0.05, 0.07, 0.01, 0.06 and 0.04, the PSSM ratio score R of “DSWDVI” can be calculated as below:

$$R = \frac{P(\text{"DSWDVI"}|+)}{P(\text{"DSWDVI"}|-)} = \frac{1 * 0.33 * 0.33 * 0.33 * 0.33 * 0.33}{0.05 * 0.07 * 0.01 * 0.05 * 0.06 * 0.04} \approx 931795$$

$$\log_2(R) \approx 19.8$$

$P(\text{"DSWDVI"}|+)$ refers to the probability of “DSWDVI” in the foreground matrix. According to the constructed matrix, the probability of D in the first position is 1, the probability of the S in the second position is 0.33, and the probability of W in the third position is 0.33. The final result is the multiplied probabilities of all amino acid residues. $P(\text{"DSWDVI"}|-)$ refers to the background probability. Since we did not construct a background PSSM, the probability of each randomly appearing amino acid in UniProt can be multiplied. Because the raw R score is usually a large number, a logarithmic normalization with a base 2 will be conducted. Thus, a higher score represents a high probability of a potential peptide being a real LIR/AIM motif. In the iLIR tool, all candidate 6 aa peptides with >13 logarithmic scores from PSSM were predicted as potential LIR/AIM motifs (Klionsky et al. 2016; Kalvari et al. 2014). In addition, the ANCHOR tool (<https://iupred2a.elte.hu/>) was integrated and utilized to predict disordered regions of proteins. The authors suggest that if more than three residues of a LIR/AIM motif are located in a disordered region of the protein, its tertiary structure might be stabilized through the interaction with LC3B/Atg8. Such a prediction provides additional information for judging LIR/AIM motifs, whereas the online tool iLIR mainly uses PSSM to predict LIR/AIM motifs. The iLIR online tool of is easy to use. For example, if we submit the protein sequence of human FUNDC1 into the server (<http://repeat.biol.ucey.ac.cy/cgi-bin/iLIR/iLIR.cgi>) (Fig. 18.12c), five predicted results and the corresponding PSSM logarithmic scores will be returned, including two results following the xLIR motif and three results following the classical “WXXL” motif (Fig. 18.12d). Finally, computational predictions cannot fully replace experiments. Whether predicted results are real LIR/AIM motifs, and whether they really interact with LC3B/Atg8, as well as their functions, should be experimentally validated.

18.1.2.3 Group-Based Prediction System

In 2004, one of the authors of this chapter designed the GPS algorithm for the prediction of kinase-specific phosphorylation sites. At that time, the full name of GPS was the “group-based phosphorylation predicting and scoring method,” and current name of “group-based prediction system” was adopted for simplicity. The series of GPS algorithms are continuously updated and improved, with a number of different versions. However, the fundamental rationale of the scoring strategy has never been changed. Focusing on PTMs, the CUCKOO workgroup (<http://www.biocuckoo.org/>) has released 14 prediction tools (Fig. 18.13a), including GPS for sequence-based prediction of kinase-specific phosphorylation sites, iGPS for the prediction of site-specific kinase and substrate relationships by combining sequence profiles with protein–protein interactions, GPS-MSP for the prediction of protein arginine and lysine methylation sites, CSS-Palm for predicting *S*-palmitoylation sites, GPS-SUMO for predicting SUMOylation sites and SUMO binding motifs, GPS-SNO for *S*-nitrosylation site prediction, GPS-YNO2 for nitration site prediction, GPS-CCD for the prediction of calpain cleavage sites, GPS-Polo for predicting PLK phosphorylation and binding sites, GPS-PUP for pupylation site prediction, GPS-MBA for epitope prediction, GPS-ARM for the prediction of an E3 ubiquitin ligase complex APC/C substrates, GPS-TSP for sulfation site prediction and GPS-PAIL for acetyltransferase-specific site prediction. The authors also developed a series of visualization tools and databases, which can be accessed by clicking on buttons of the left column in homepage of the CUCKOO workgroup (Fig. 18.13a).

The basic assumption of the GPS algorithm is that similar peptides may have similar biological functions. Thus, the GPS algorithm considers the overall similarity between different peptides. Here, we again used the three known human LIR/AIM motifs as the training data to illustrate that how the GPS algorithm predicts the peptide of “DSWDVI” (Fig. 18.13b). First, based on the BLOSUM62 matrix, we individually compared the “DSWDVI” peptide with the three known LIR/AIM motifs and calculated each similarity score. For the “DDFVMI” from ATG13, the first match with the sequence of “DSWDVI” was D-D, and the substitution score was 6 according to the BLOSUM62 matrix. The second match was D-S, and the substitution score was 0. In this manner, the overall similarity score of the two peptides was calculated to be 9. Following the same method, the overall similarity scores of “DSWDVI” peptide compared with the other two motifs were calculated as 24 and 20, respectively. Therefore, the “average global similarity” between “DSWDVI” and the three known LIR/AIM motifs was $(9 + 24 + 20)/3 = 17.7$. A higher score indicates a higher similarity between the given peptide and known motifs, and means a higher probability that the peptide is a real LIR/AIM motif. Although the authors have not yet applied the GPS algorithm to develop any prediction tools for LIR/AIM motifs, a study was published in 2012 for the prediction of the E3 ligase complex APC/C substrates, in which KEN-box (KEN) or D-box (RXXL) motifs are contained and can be computationally found by the approach described above.

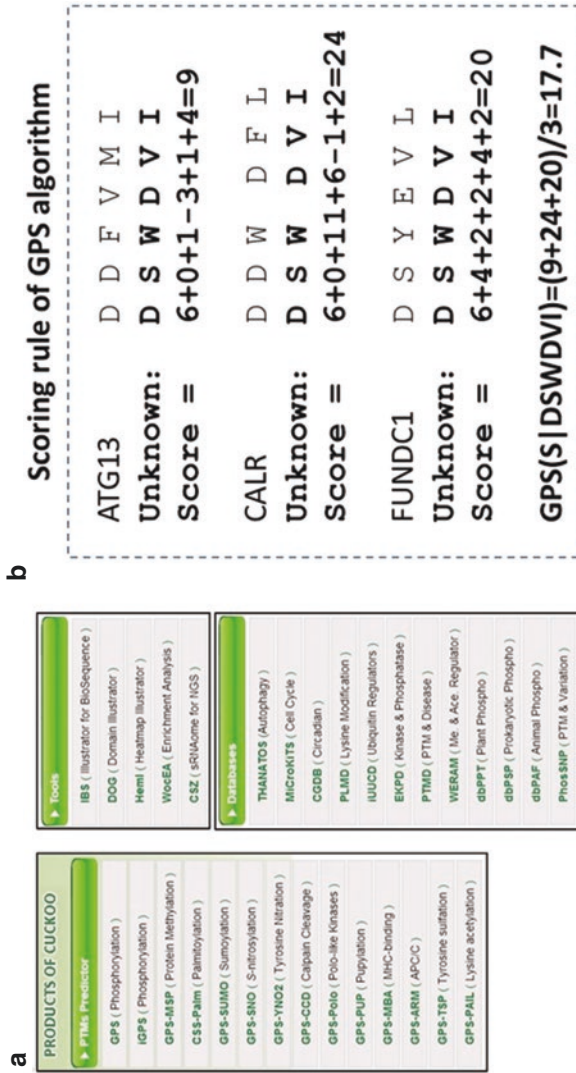


Fig. 18.13 (a) The authors developed a number of PTM-regulated tools and databases. (b) The scoring strategy in GPS algorithms

For predicting PTMs sites, the same rationale was used in GPS algorithms. However, a question arises as to whether or not it is appropriate to use bioinformatics tools to directly predict protein PTM sites. Unfortunately, it is not, largely because the accuracy of predicting PTM sites from protein sequences is still very low, with a high rate of false-positive hits. Recently, a large number of papers have been published reporting high-throughput PTMomics profiling, and flood of reported PTM substrates and sites have been detected by mass spectrometry. To analyze protein PTM sites, we recommend that the first step should be the search of public databases to find known and experimentally identified PTM sites. For example, to search phosphorylation substrates and sites in human, animals or fungi, users can access the dbPAF database (<http://dbpaf.biocuckoo.org/>), which contains 483,001 known phosphorylation sites of 54,148 phosphoproteins collected from seven model organisms, including *H. sapiens*, *M. musculus*, *R. norvegicus*, *D. melanogaster*, *C. elegans*, *S. pombe* and *S. cerevisiae*. To find plant phosphorylated substrates, users can search the dbPPT database (<http://dbppt.biocuckoo.org/>), which contains 82,175 phosphorylation sites in 31,012 known phosphoproteins from 20 plants. To search PTMs occurring at lysine residues such as ubiquitination and acetylation, the PLMD database (<http://plmd.biocuckoo.org/>) can be accessed, which contains 284,780 known PTM sites in 53,501 proteins for 20 types of lysine modifications.

Finding known and experimentally verified PTM sites from a public database is only the first step of a long journey. Further analyses and experimental verifications are required to determine which PTM enzymes regulate the sites, as well as the biological function of the PTMs. For phosphorylation sites, GPS or iGPS can be applied to predict potential upstream kinases for these specific sites. For acetylation sites, GPS-PAIL is available to predict potential acetyltransferases that modify the site, whereas GPS-Polo can predict phosphorylated substrates and phospho-binding proteins of the Plk kinase family. For the ubiquitinated substrates of APC/C, GPS-ARM is accessible. The prediction of regulatory enzyme–substrate relations is much more difficult than the prediction of PTM sites, and there are currently only a few tools available.

When using the GPS software, the number of candidate kinases that potentially modify the phosphorylation sites should be narrowed down, either by identifying protein kinases that physically interact with the given substrates through immunoprecipitation or by only considering kinases that were reported to be involved in distinct processes. For example, we input the protein sequences of mouse Map11c3a and Map11c3b into the GPS 2.1.2 software (Fig. 18.14a). When all kinases were selected, a larger number of prediction results were generated, and such a prediction would be less helpful for subsequent experiments. However, by checking the literature, we found that the protein kinase PKA has been demonstrated to be involved in the regulation of autophagy. If only PKA was selected in GPS, only a single residue of S12 would be predicted as phosphorylated by PKA, and such a prediction will be much useful as a guide for further experimentation (Fig. 18.14b). Currently, only a few kinases, such as PKA, Akt, mTOR and AMPK, have been reported to function in autophagy. Thus, these kinases should be prioritized for prediction. The iGPS software considers both sequence motifs and the interactions between kinases and substrates. In theory, narrowing down candidate kinases is not necessary. However,

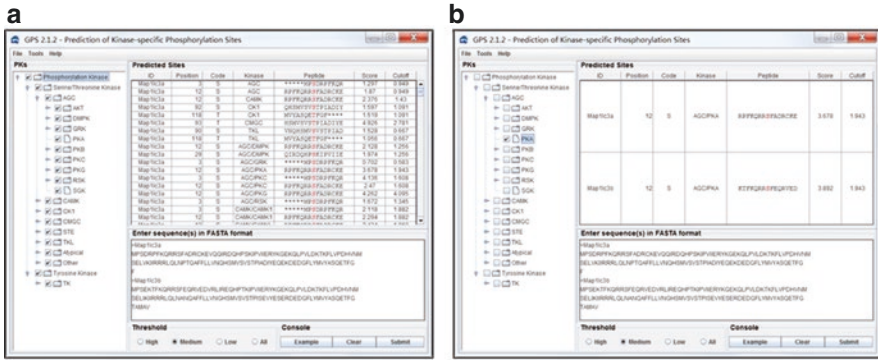


Fig. 18.14 (a) In GPS 2.1.2, all kinases were selected. (b) Only protein kinase PKA was selected

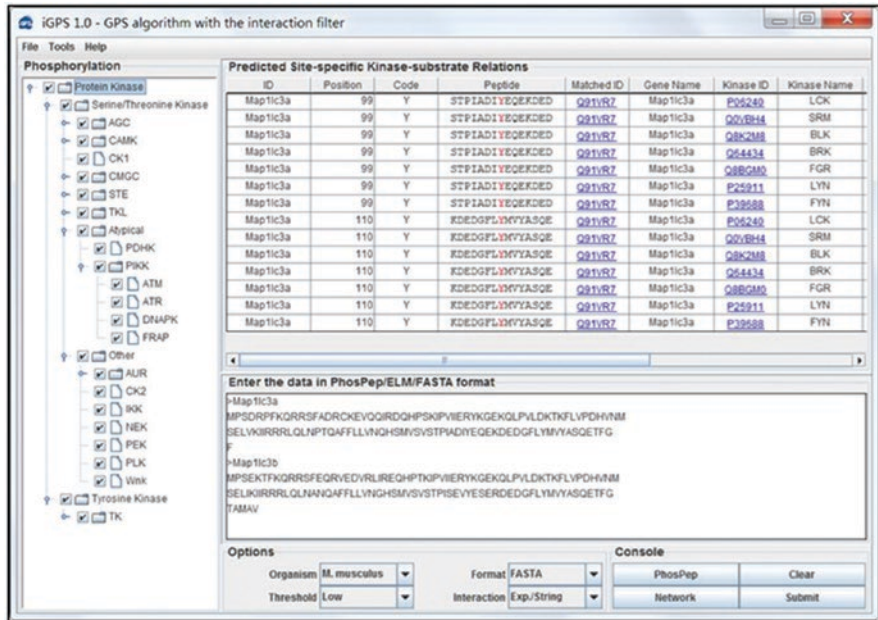


Fig. 18.15 The prediction results of iGPS

two problems exist in practice. First, the protein–protein interaction (PPI) information used in iGPS was taken from multiple public databases, which might contain errors and be not fully applicable. Thus, bona fide site-specific kinase–substrate relationships might not be always predicted. Second, if all kinases are selected, the number of predicted kinases might be still an unreasonably large number. For example, we submitted the protein sequences of mouse Map11c3a and Map11c3b to iGPS 1.0 for prediction and selected all kinases (Fig. 18.15). The results showed that Y99 and Y110 of Map11c3a were potentially phosphorylated by multiple tyrosine

kinases, whereas the real kinase-specific site in Map11c3a/b phosphorylated by PKA was not predicted. In this regard, the prediction results of GPS and iGPS should be balanced to get the best results. When using other prediction tools, similar strategies should be considered. Any predictions should be carefully analyzed before further experimentation. Because a variety of resources have been generated by our group, we have also summarized 233 other existing tools and related databases (<http://www.biocuckoo.org/link.php>), which are all valuable for computational analyses of PTMs.

18.2 The Analysis of Autophagy-Related Omics Data

18.2.1 Computational Methods in Omics Data Analysis

The rise of high-throughput sequencing technology and large-scale applications allow the convenient generation of experimental biological data for a large number of different species and different omics, and how to establish effective relationships between big data and biological phenomena has emerged as a key challenge that is becoming ever more important. For this reason, gene function enrichment analysis and network analysis has experienced a rapid sequence of development through stages from online platforms to application software based on databases. The emergence and application of single-cell sequencing technology has led to even more rapid development and progress in this field, and is helping biologists carry out systematic research on functional pathways and regulatory networks involving multiple genes.

18.2.1.1 Enrichment Analysis

Enrichment analysis is mostly based on differential expression analysis. According to the annotation information of differentially expressed genes, they are clustered into different functional clusters, which are often used to analyze case-control data. The most commonly used annotation databases for function enrichment are GO and KEGG, and there are many online methods, such as DAVID, GStat, GenMAPP and GoMiner. A large number of software and language packages have been developed around enrichment analysis, such as GSEA, MetaCore, GSA and clusterProfiler. Here, GSEA is used as an example.

The principle of gene set enrichment analysis (GSEA) (Subramanian et al. 2005) is to search for genes from the gene set S (a priori defined before the analysis) in the already sorted differentially expressed gene set L . When a gene from the S gene set is encountered in L , the statistic is increased, and when a gene in the non- S gene set is encountered, the statistic is reduced, and then an enrichment score (ES) is calculated. After the standardization of the enrichment scores, the false-positive rate

(FPR) is adjusted by the false-discovery rate (FDR). Next, using the acquired gene information and position information, it is determined whether the gene set S is randomly distributed in L or concentrated at the top or bottom of L . Since the gene set L is sorted according to the expression correlation and classification between genes, if S is randomly distributed in L , the effect of L on the phenotype is not significant, while if it is concentrated at the top/bottom of L , then the gene set is closer to the phenotypic classification represented by the top/bottom. It should be noted that the increase or decrease of the statistic is relative, not absolute, and its magnitude depends on the correlation between the gene and the phenotype.

The GSEA software is publicly available online at the URL <http://software.broadinstitute.org/gsea/downloads.jsp>. The software running environment is based on Java and can be installed on any desktop system that supports Java 8 (Windows, macOS, Linux, etc.). It is currently not supported in Java 9 and above. The desktop version has four kinds of memory capacity (1G–8G) which is available according to actual needs. Confirm that Java has been installed on the system, and select the appropriate GSEA version (32/64-bit) before installation. After opening the software, you can see that there are four partitions on the left side of the running interface, which are Steps in GSEA analysis, Tools, Analysis history and GSEA reports (Fig. 18.16a).

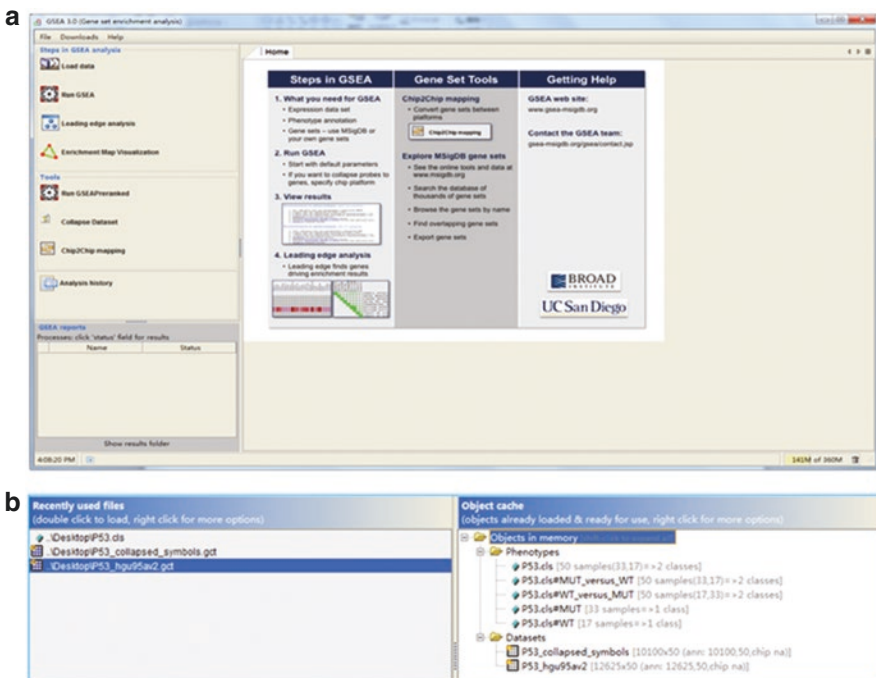


Fig. 18.16 GSEA initial page. (a) 4 partitions on the running interface. (b) Datasets uploaded

18.2.1.1.1 Uploading Data

- Four types of input files need to be prepared before the GSEA performs the analysis:
- Expression dataset file: .res, .gct, .pcl and .txt format files
- Phenotype labels file: .cls format file
- Gene sets file: .gmx or .gmt format file
- Chip (array) annotation file: .chip format file.

Among the four types of files, the gene sets file can be selected online in the software, or the latest version can be downloaded from the GSEA website. At the bottom of the software download page are all data from the MSigDB gene set and various types of data supporting GSEA analysis, including gene ontology (GO) gene sets, KEGG gene sets and motif gene sets. The Expression dataset file can be downloaded as the processed dataset from a database such as GEO or TCGA. It can also be original data or the user's own dataset as long as it has been processed into the required format. If the input Expression dataset file is normalized, the Chip (array) annotation file can be left blank. For those who are new to GSEA software, the GSEA website (<http://software.broadinstitute.org/gsea/datasets.jsp>) provides case data for download and practice. Here, take the p53 data as an example and download the P53_hgu95av2.gct, P53_collapsed.gct, and P53.cls files. Here "collapsed" means that the dataset identifier (i.e., affymetrix probe set ID) has been replaced by a symbol. It is important to understand the data format requirements by reference to the case data (http://software.broadinstitute.org/cancer/software/gsea/wiki/index.php/Data_formats). Click the Load data button to upload the data. You can see the data in the left and right areas in the software (Fig. 18.16b).

18.2.1.1.2 Running GSEA

Click the Run GSEA button, and select the P53_collapsed.gct file in the Expression dataset (Fig. 18.17a). Choose the online resource for Gene sets or select the local data resource. Note here that the larger the background set is, the larger the memory capacity will be needed. For example, if all the data of the MSigDB gene set is selected here, but the installed version of GSEA is a memory version that only supports 1G, there will be an "OutOfMemoryError" (Fig. 18.17b). Changing it to a relatively small dataset as "c2.cp.kegg.v6.2.symbols.gmt" allows it to run successfully (Fig. 18.17c, d). Therefore, it is necessary to consider the maximum memory capacity when choosing the GSEA version.

The number of permutations can be selected up to 1000. The higher the number, the higher the accuracy and the longer the running time. When running a gene set analysis for the first time, selecting a small number (say, 10) will facilitate the timely detection of errors. Then, choose the recommended 1000 permutations after one successful operation to avoid wasting time. For "collapse dataset to gene symbols," select "false" because "Expression dataset" has already uploaded the "collapsed"

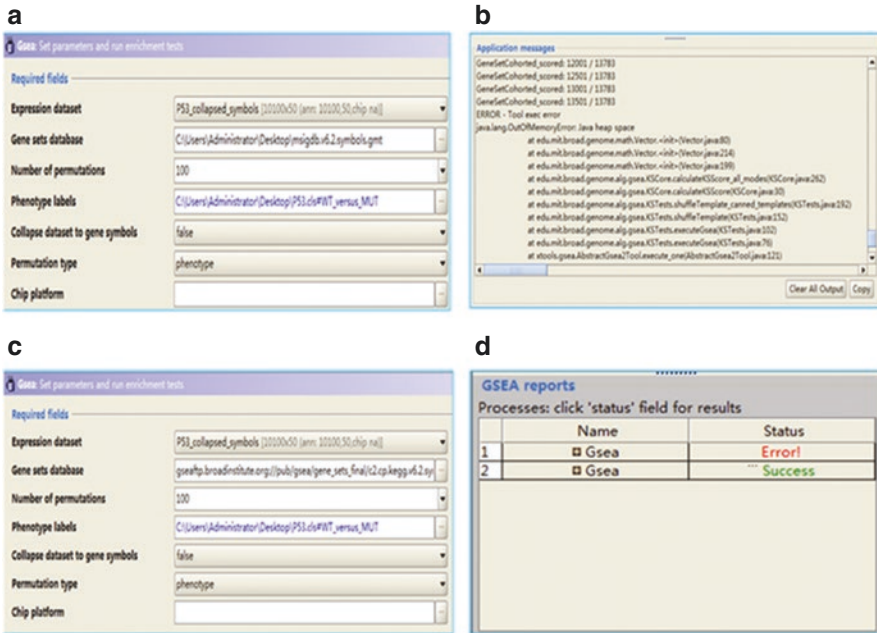


Fig. 18.17 Gene set selection and operation results. (a, c) Two different combinations of input datasets. (b, d) Two different results

file. “Permutation type” can be either “phenotype” or “gene_set”. It is better to select “phenotype” when the number of samples per group is greater than 7. Otherwise, it is better to select “gene_set”. In this dataset, there were 17 wild-type samples and 33 mutant samples, so “phenotype” was chosen. Fill in the necessary input information and click the run button below. For each successful GSEA report, click “Success” to view the results report online (Fig. 18.17d); the results report is stored in the local folder and viewed on the pop-up page in the address bar or in the Basic fields area above the run button.

Taking the combination of “c2.all.v6.2.symbols.gmt”, “false” and “phenotype” as an example (Fig. 18.18a), the phenotypic enrichment results of wild type (17 samples) and mutant type (33 samples) were more important than other results in the report (Fig. 18.18b). The results showed that in a total of 3363 gene sets, 1503 genes were upregulated in WT and 1860 in MUT. Eight and one gene sets were significantly enriched with a FDR < 0.25 in WT and MUT, respectively. In contrast, if the criteria for “significant” enrichment are taken as a nominal p -value < 0.05 , then there are 115 and 60 gene sets significantly enriched in WT and MUT, respectively. Click “Snapshot” to view the enrichment map (Fig. 18.18c). “Advanced fields” at

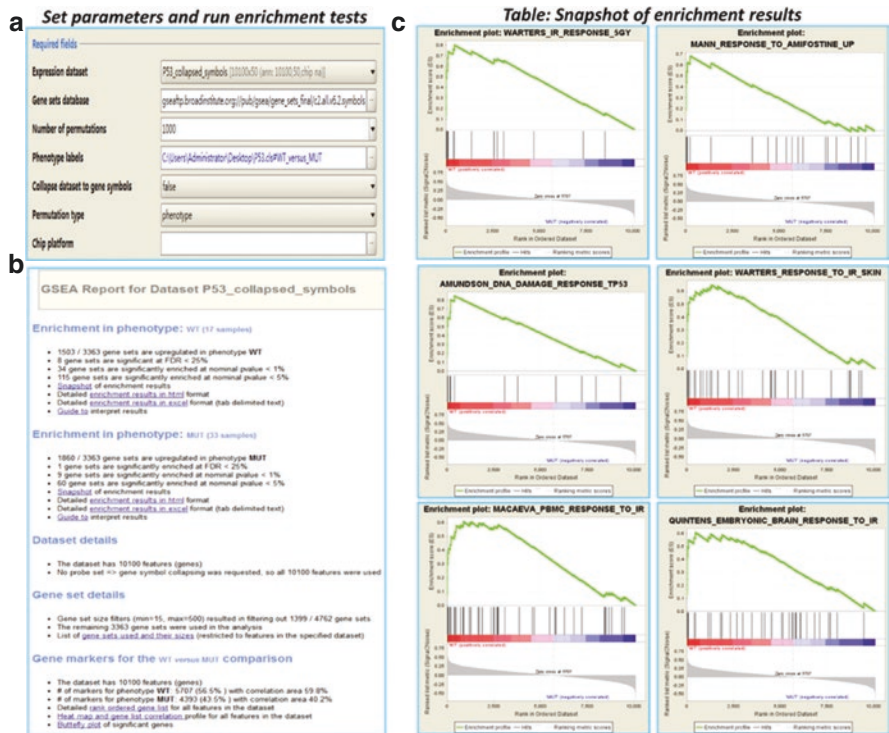


Fig. 18.18 Results report. (a) Sample combinations of required fields. (b) GSEA report. (c) Snapshot of enrichment results

the bottom of the “Run GSEA” page shows the first 20 enrichment results by default, or you can define the number of displays.

Click on the small chart to see more detailed information. If you want to see all enrichment results, you can view them locally in the folder where the results report is stored. Select the MACAEVA_PBMC_RESPONSE_TO_IR of 8 gene sets enriched with $FDR < 0.25$ in WT. The normalized enrichment score (NES) is 2.1433039, and FDR is 0.013515615 (Fig. 18.19a). This indicates that the genes in this gene set are significantly enriched at the top of the list and is more associated with wild type (Fig. 18.19b). A total of 46 genes were obtained after dataset filtering, of which 18 were located on the left side of the ES value (marked “Yes” in the table, with a background color of green). The “RUNNING ES” column shows the cumulative contribution of the 18 genes to the ES value (Fig. 18.19c). You can see that the final ES value reaches 0.6083 and then begins to decline, and that all the genes in the gene set form the leading edge subset. In the heat map formed by the gene expression value in the gene set, the color transition from red to blue indicates the expression value from high to low. Finally, the random ES distribution is given (Fig. 18.19d, e).

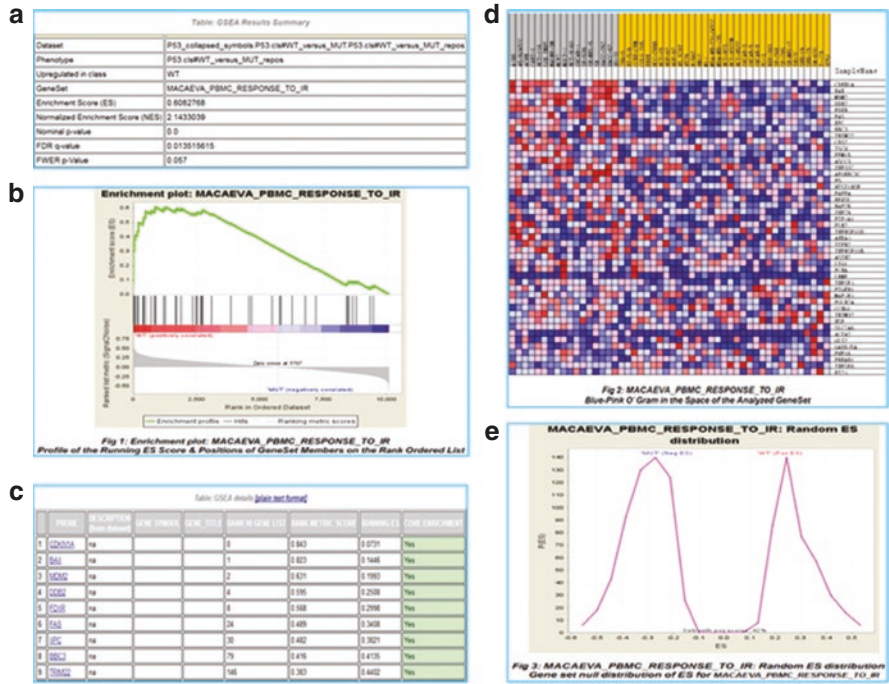


Fig. 18.19 Significantly enriched gene sets. (a) Results summary. (b) Gene set enrichment plot. (c) The ranked gene list of the gene set. (d) Heatmap. (e) Random ES distribution

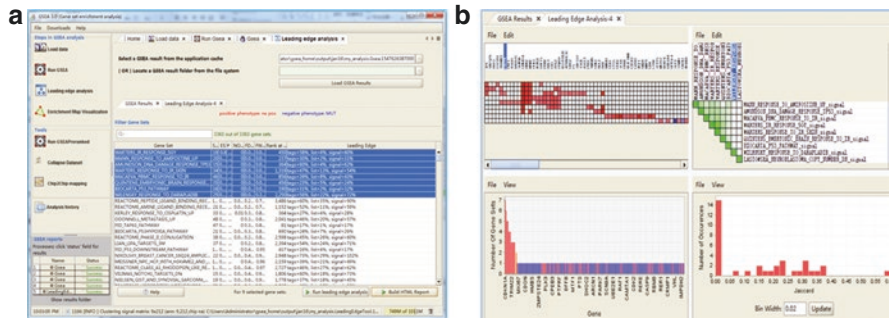


Fig. 18.20 Leading edge analysis. (a) GSEA results. (b) Leading edge analysis results

18.2.1.1.3 Leading Edge Analysis

Leading edge analysis refers to the screening of genes of interest by selecting one or more significantly enriched gene sets and observing the expression of the leading edge subset of genes and the gene overlap among them (Fig. 18.20a). There are four colors in the heat map: red, pink, light blue and dark blue, representing high, moderate, low and lowest expression values, respectively (Fig. 18.20b). The triangle

diagram in the upper right corner shows the intersection between different gene sets. The deeper the green is, the more the gene intersects. The lower left corner is the gene distribution in the subset, the horizontal axis represents the gene, and the vertical axis shows that the gene appears in several subsets. The graph in the lower right corner shows that most subsets have no overlap (Jacquard = 0).

18.2.1.1.4 Enrichment Network Visualization

The visualization steps used by the nested Cytoscape software interface (Shannon et al. 2003) in GSEA software to enrich the network analysis will be introduced in detail in the second part, “Network analysis.”

18.2.1.2 Network Analysis

18.2.1.2.1 STRING

Based on protein-level network analysis, STRING (Snel et al. 2000) has been updated several times since 2000. The current version is V10.5, which was updated in March 2017. It can be accessed via <https://string-db.org/>. The page is simple. The search page supports single or multiple protein names or sequences, species, protein families and other forms of input (Fig. 18.21a), making it very flexible.

For yeast Atg8, for example, you could use a single protein name search, which allows you to select “automatic detection” and specific species. In the results of the search, you can select the desired species and the interacting protein information, such as “*Saccharomyces cerevisiae*,” based on your interests. Select and go to the next step (Fig. 18.21b). The default display of the system is Network, where the points in the network can be moved at will. Redistributing the positions between the points according to the important nodes that you want to highlight will not affect the layout of the overall network lines. Click on each node and line in the network for further information, including a three-dimensional structure map of proteins with proven structures, and a list of protein sequences and homology. The area below the network diagram has a number of buttons (Fig. 18.21c) that can manipulate the presentation and content of the network, as follows:

Viewers: network graphics display mode (network, cooccurrence, coexpression and so on) (Fig. 18.21d, e), listing relevant information, such as experiments, databases from *Saccharomyces cerevisiae* and other species related experimental data, information and related database information such as related information mined from the literature, fusion gene information, adjacent protein information and so on.

Legend: legend information, such as the meaning of nodes and lines in the network display mode, whether there are known or predicted 3D structures, the description of different display modes, the current input protein name, a brief introduction, predicted functional partners and current species information, etc. The legend will also change after switching display mode.

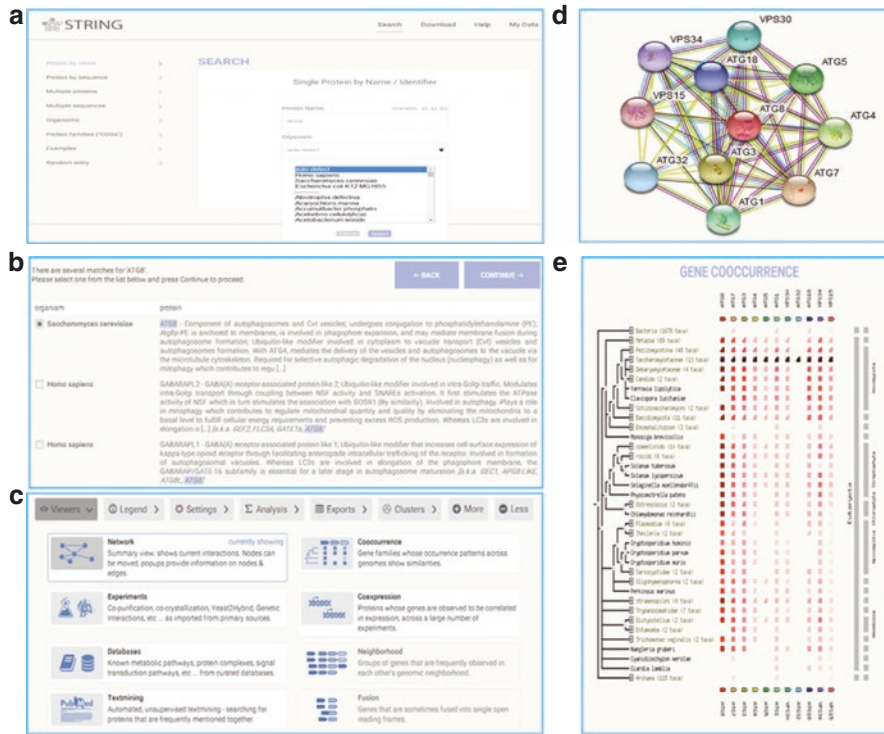


Fig. 18.21 STRING search page. (a) Search single protein by name/identifier. (b) Select organism. (c) Options for different types of viewers. (d) Protein–Protein interactions network. (e) Gene family cooccurrence patterns

Settings: sets the network display parameters. There are three different ways to display a network connection in the basic setup: “evidence” is evidence of interaction between proteins using lines that do not use colors (Fig. 18.21d), which are divided into known interactions, predicted interactions and others. Detailed identification can be seen in legend information; “confidence” denotes the strength of the data support, indicated by the thickness of the lines, while “molecular action” represents the relationships between genes such as activation, inhibition, interaction, binding and transcriptional regulation, indicated by different color lines and arrowheads. The minimum threshold (maximum confidence = 0.9, high confidence = 0.7, middle confidence = 0.4, low confidence = 0.15, custom) can be set. If there are too few interacting genes to be mapped, the number of interacting proteins in the network can be increased. Advanced settings allow the user to switch between png diagram and interactive SVG mode, hide the point identifications or hide unconnected points on the network.

Analysis: query the network function enrichment information, including the GO and KEGG pathways. This can be downloaded to the local computer.

Exports: downloads the result diagram to the local computer in eight ways for subsequent analysis. The SVG model is convenient for further processing with AI

and other software. The TSV mode can be opened in TXT or Excel to see the scores and total scores between specific interactions, or to view the annotated interactions and ratings directly below in tabular form (Fig. 18.22).

Clusters: shows the nodes in the network into clusters, *k*-means clustering and MCL clustering. The default is three clusters (Fig. 18.23a), and the proteins in the

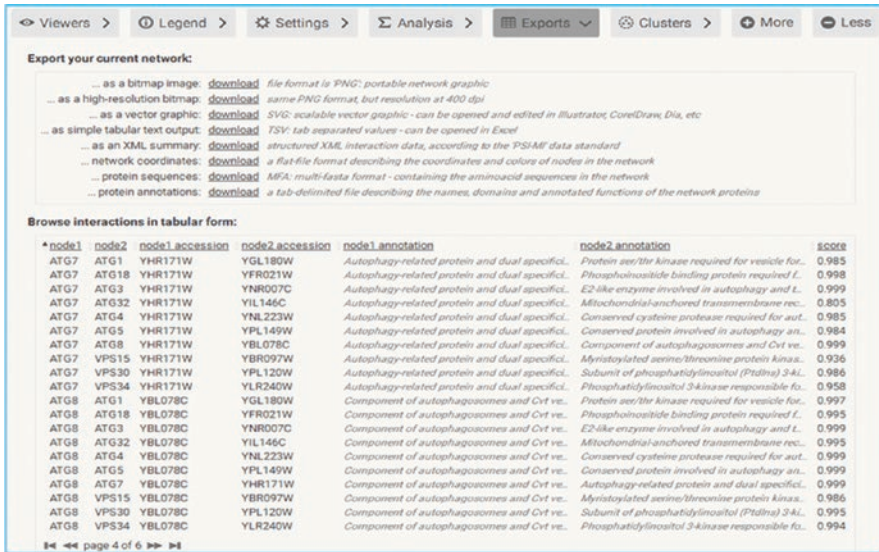


Fig. 18.22 Result output mode

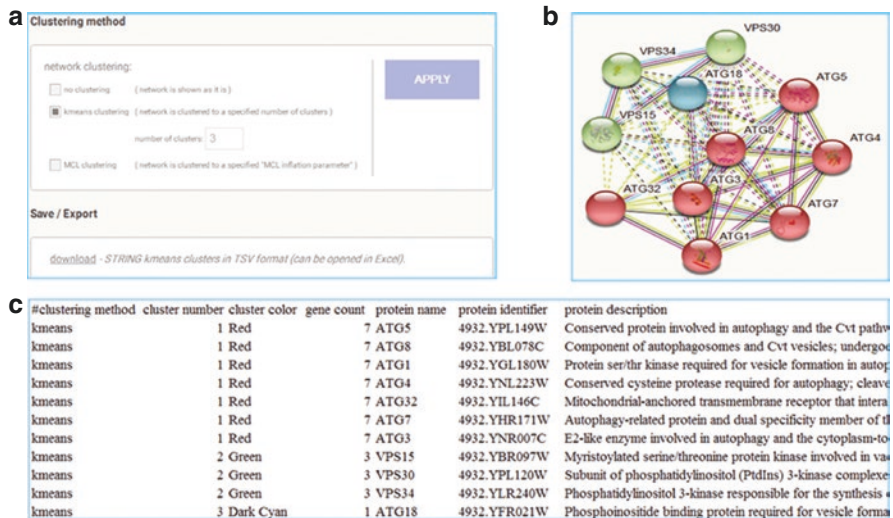


Fig. 18.23 The clustering method. (a) Optional clustering method. (b) K-means clustering plot. (c) Clustering results table

same cluster are represented by the same color dots (Fig. 18.23b). The results can be downloaded into TSV format for easy viewing in Excel (Fig. 18.23c), where the description of protein can help with understanding its function and the commonalities and differences within and among clusters.

To input multiple genes into STRING for network analysis, simply switch to the search page to select the “Multiple proteins” option to enter the gene name or upload the file. Only one gene name can be written in each line, and multiple lines can be entered in succession. If you choose to upload a file for searching, you need to provide a file that conforms to the input format, such as a single line of TXT documents listed separately by gene. Otherwise, the system may fail to recognize the file. The subsequent analysis is very similar to that of a single gene search.

18.2.1.2.2 Cytoscape

Cytoscape is different from the simple bar plots provided by GO enrichment and KEGG enrichment. The visual network diagram provided by the Cytoscape software integrates the data and makes the whole network more intuitive and vivid through the setting of points and edges. Compared with STRING, Cytoscape has many different Mini Programs for various output embedded in the graphic display, making it quite attractive and giving the user a lot of control. Users can get download links from <https://cytoscape.org/>, and the current version is 3.7.1, running in the Java environment. Currently, it supports the Java 8 but not Java 9 or above, and the official website is currently running version 3.7.0. After downloading and installing the program, go directly to the main page (Fig. 18.24).

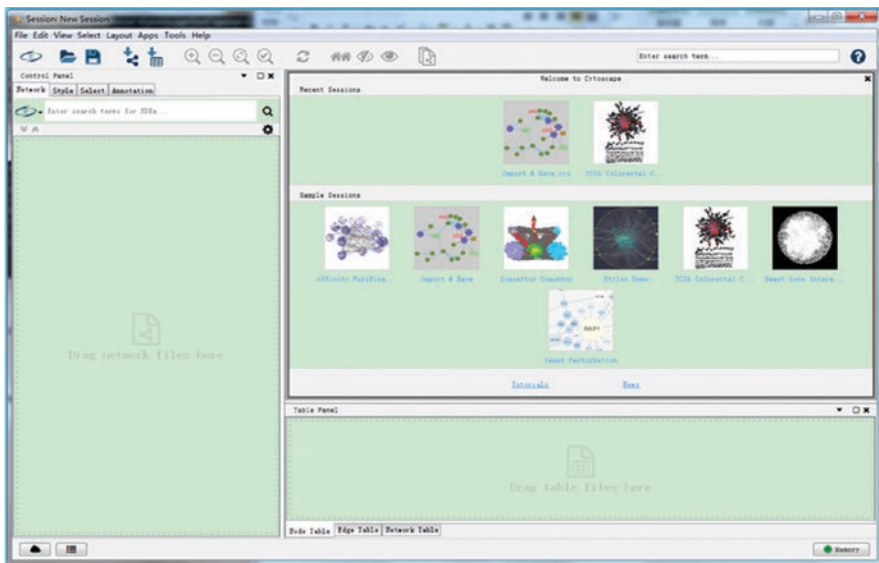


Fig. 18.24 Cytoscape home page

18.2.1.2.2.1 Import Data

Users can choose to import data from the network or upload data files that they want for network analysis. If you import data over the network, select “File”—“import”—“network from NDEX” to enter the network import data page (Fig. 18.25a). Enter “autophagy” in the search bar, search for 41 pieces of data sorted by correlation, and select the desired data results, such as data from UC San Diego Center for Computational Biology & Bioinformatics, ucscdcbb, named “TCGA-THYM [miRNA vs RNA] GO: negative regulation of autophagy [2040000731]”. The data, which include 36 points and 79 edges, is relatively new and was generated in July 2017. Note that it will initially take a lot of time to import data with thousands or even hundreds of thousands of edges.

When the data are successfully imported, the interactive network diagram is displayed directly on the page (Fig. 18.25b). To allow movement or modification of the points and edges in the network, click on the two small icons in the lower right corner. You can see the complex interactions between miRNAs and RNAs in the diagram, with three miRNAs at the center, hsa-mir-155, hsa-mir-484 and hsa-mir-425 (Fig. 18.25c). If you want further detail on the single regulatory network formed by each of the three miRNAs, you can find the icon for that in the menu bar

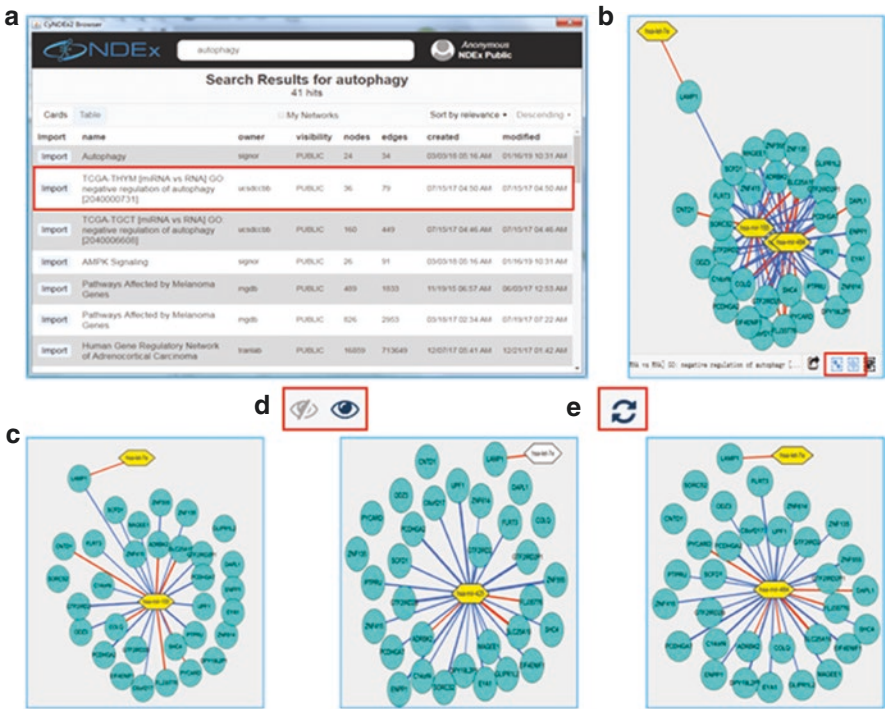


Fig. 18.25 Data import, hiding and recovery. (a) Data import. (b) Interactions network. (c) Networks with some nodes and edges being hidden. (d) Hide icon. (e) Reset icon

(Fig. 18.25d), and the small icon on the left can hide the selected point with and its connections. In this way, the separate regulatory network for each miRNA can be clearly displayed. There are no further editing or visualization operations just to make all edges and points uncovered; small icons on the right can be used to redisplay hidden points and edges. If you feel dissatisfied with the rearrangement of the graphics, you can use the reset icon (Fig. 18.25e) in the menu bar to reset the display to the default.

18.2.1.2.2.2 Control Panel

The first row of icons at the bottom of the menu bar are the operation shortcut keys. The functions from left to right are: import from network, open folder, save, import from file, import form, enlarge, shrink, appropriate page display, display selection, restore the status quo ante, show the first layer neighbor node of the selected point, hide, show and rebuild the network with the selected point and all involved edges (Fig. 18.26a). Each time the network is rebuilt, a lower layer of the network appears in the region of the gene set formed after the original data are imported to the left, including the number of points and edges contained. If you do not want a certain layer of network, you can right-click and select “Destroy Network” to delete it. If you want to change the display style, select “Apply Style” to replace the display style after right-clicking on the layer where the network is located (Fig. 18.26b-d).

After selecting the style, you can further adjust the detailed style of the point, line and network until you achieve the desired effect (Fig. 18.27a-f), including the size, color, shape, border and border color of the dot, the font size of the dot label, the color of the dot label, the thickness, direction, color of the edges and color of the background, and the style with dynamic effects. It is important to clearly display the network interaction relationship and node information so as to avoid obscuring

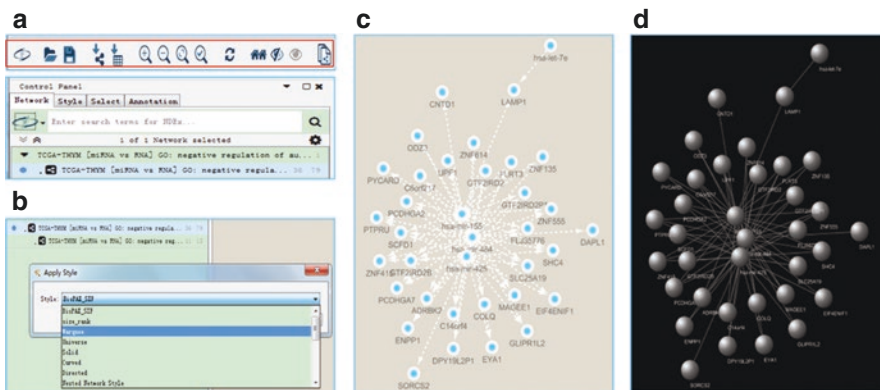


Fig. 18.26 Selection of network presentation styles. (a) Control panel. (b-d) Style and pattern diagram

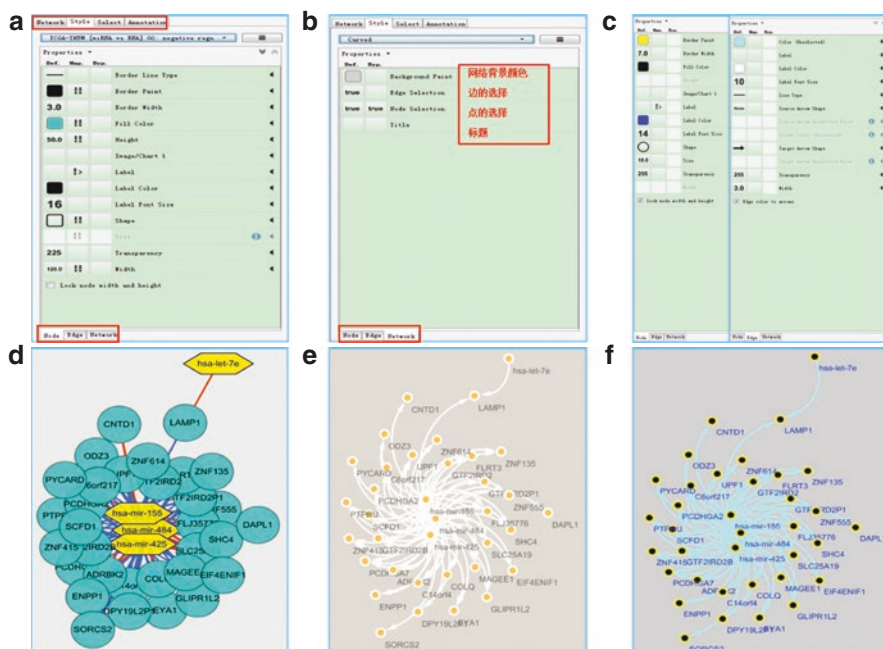


Fig. 18.27 Selection of patterns of points, lines and networks. (a) Option bar of point style. (b) Option bar of network style. (c) Point style VS line style. (d–f) Different styles and pattern diagrams

some of the information and thus affecting the subsequent analysis. By adjusting the position of the points in Fig. 18.27f, the number of lines connected with each point can be seen intuitively so as to understand the number of nodes interacting with each node, and the nodes on both sides can be easily observed by clicking on each edge.

18.2.1.2.2.3 Export Results

At the bottom of the network diagram, there are three tabular descriptions of points, lines and detailed parameters in the network. The tabular information of points includes gene name, expression value and molecular type; edge table information contains correlation score and p -value; network table information contains data source, GO ID, disease information, GO enrichment Q value, method information, species information and so on. Table information and network diagrams are available through “File”-“Export”-“Table to File...” or “Network to...” in the menu bar. The results are exported locally (Fig. 18.28a), or through the shortcut key between the network diagram and the table. The format exported from the network diagram is selected according to the actual needs. For further processing in AI graphics processing software, select SVG mode (Fig. 18.28b–d). Save the path and rename it. Otherwise, the save may fail or the file might not be able to be found.

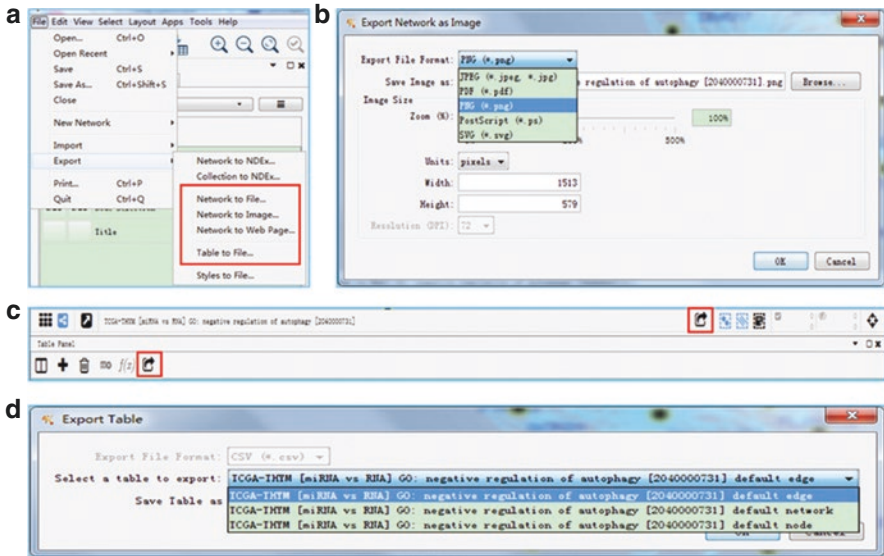


Fig. 18.28 Export results. (a) Optional export mode. (b) Network diagram export. (c) Export icon. (d) Table export

18.2.2 The Analysis of Autophagy-Related Transcriptomics and Epigenomics Data

Transcriptome research and analysis have been a very important part of biological research. Transcription reflects the expression of genes and affects the translation of proteins. Different transcripts and variable shear events affect the phenotypic and evolutionary direction of the human and indeed all species. Autophagy transcriptomics is an important branch of transcriptomics. Autophagy is the key to maintaining the homeostasis of organisms and is involved in cellular processes from the beginning of embryonic development in early life. How can we analyze the role of autophagy genes in development based on RNA-seq data? In this section, we will discuss the analysis of autophagy transcriptome data in the field of stem cells. Two papers published in a journal of *Autophagy* are taken as examples to explain the strategies of RNA-seq and single-cell RNA-seq analysis.

Epigenetics also has a significant impact on species diversity. DNA with the same sequence is affected by allelic methylation, acetylation and other modifications, and the effect is hereditary and self-sustaining. Some apparent differences between twins, parents and siblings may also be the subtle effects of histone modification, which has both positive and negative effects on the risk of disease. The relationship between N⁶-methyladenosine (m⁶A) RNA modification and autophagy is discussed here.

18.2.2.1 RNA-seq Data Analysis

From the single transcript analysis of Northern blot, through quantitative PCR to the application of gene chips then RNA-seq, transcriptomics has progressed through many rounds of ever-improving technologies. RNA-seq is a second-generation sequencing technology that has emerged as a cutting-edge single-cell sequencing technology. The development of transcriptomics technology has provided a huge amount of data for basic research and created a need for bioinformatic “big data” analysis. Large sequencing companies continue to work hard to improve the accuracy and speed of each generation of sequencers, and a large number of sequencing kits have been developed accordingly, so that the stability of laboratory sequencing can be improved. For small sample data and scarce sample data, researchers have developed single-cell isolation and sequencing techniques, which have further promoted the development of transcriptomics research. Currently, RNA-seq data analysis is the first step in many new studies at the frontiers of the scientific research and ultimately affects clinical practice by boosting our understanding of diseases and making possible targeted therapies.

As an example, we here describe the transcriptional study of the temporal expression pattern of autophagy genes during monocyte and granulocyte differentiation (Huang et al. 2018). During the differentiation of hematopoietic stem progenitor cells (hematopoietic stem and progenitor cells, HSPCs), HSPCs gradually differentiate into various types of lymphoid and myeloid cells through different differentiation procedures under the control of many interacting factors. It has been shown that autophagy is involved in the regulation of various types of stem cells, especially HSPC, and that autophagy plays a particularly extensive role in shaping the characteristics and functions of myeloid cells. Monocytes and granulocytes are the most common myeloid cells in the blood, so this study combined RNA-seq data from CD34 HSPCs monocytes and granulocytes. The temporal expression of autophagy genes during monocyte and granulocyte differentiation was analyzed. Using a self-organizing map (SOM) algorithm, 22 autophagy genes showed different roles in the process of monocyte and granulocyte differentiation. These autophagy genes may play important roles in the differentiation of myeloid progenitor cells into monocytes and granulocytes.

The study was based on the RNA-seq data of CD34+ HSPCs samples on days 5, 10 and 15 of mononuclear and granulocyte differentiation in human blood. A list of 747 human autophagy genes was extracted from three databases: Autophagy Regulatory Network (ARN), Autophagy Database and Human Autophagy Database (HADb), and the expression of these 747 human autophagy genes was measured in the RNA-seq data. Using the SOM algorithm and the distance correlation statistics, it was found that the expression of 13 genes was enhanced during granulocyte differentiation, but decreased during monocyte differentiation. In contrast, the expression of 9 other genes increased gradually during monocyte differentiation, but decreased in granulocyte differentiation. Furthermore, the expression levels of four genes from RNA-seq results was verified by qRT-PCR analysis, and all four of them showed the same pattern of expression changes as in the RNA-seq data during the

process of single cell and granulocyte differentiation. All together, these 22 autophagy genes have different roles in the differentiation of monocytes and granulocytes, suggesting that these genes may be important regulatory factors for the differentiation of granulocyte-monocyte progenitor cells.

The most difficult aspect of this research was the experimental work, and the selection of hematopoietic stem progenitor cells that met the requirements of the study. The key to the RNA-seq data analysis involved here is the selection of reference databases (i.e., background sets) and the selection of analytical methods. A critical factor is the preprocessing and standardization of the obtained RNA-seq data from the raw data. First, because the whole experiment is focused on autophagy-related genes, the background set must have been obtained from an autophagy database, and using several large recognized autophagy databases can naturally add to the reliability of the background set, which seems to be well understood. The choice of the self-organizing mapping (SOM) algorithm is mainly for its unsupervised learning model, which simulates the perception-response model of biological neural network, and compares the input information by distance and cosine similarity to extract the most representative features. Competitive learning allows the best solution to win out, so it has a natural advantage in reducing dimensionality during feature construction and choice, which allows the classification result to better capture the essential features of the data. In addition, it is also a good clustering method.

The process of selecting a method for bioinformatic analysis can seem very daunting to a researcher who is new to the field, particularly since many articles, especially top articles describing a very comprehensive approach, cannot include everything that went into making that pipeline. Just as with experimentation, when a final pipeline is described in a paper, it seems so easy and straightforward, but in fact, its selection is the end product of a groping process of experimental design. There are many things that a researcher must consider when choosing a method; even simple things like where to download the software or which version to use can be daunting. Often one ends up using something just because it is what everyone uses, and it is undeniable that imitating established methods is a useful strategy and can greatly reduce the chance of heading off on a wrong direction in the early stages of learning. However, there are many confounding factors that may make it inappropriate to blindly copy the methods used in another paper, including different species, different research groups (particularly when using the data from multiple groups), the type of sequencing technology used, whether the sequencing is single-terminal or two-terminal, and how the gene symbol is represented in the sequencing results. For example, one important issue to consider is which methods should be used to standardize the data and whether the assumptions of the proposed standardization methods regarding the data distribution are consistent with (or close to) the actual characteristics of the data, and whether standardization will lead to excessive deletion of real data or even the elimination of actual differences and so on. Just as one example: If you use a t-test to judge the significance of an effect, but forget that the t-test assumes that the data are normally distributed, you might use a t-test on data that is skewed or deviates from a normal distribution, in which case the results would not be valid. So the statistical methods chosen must be appropriate to the

characteristics of the data. It is generally understood, but key to remember, that just because a program generates a result and doesn't report any errors doesn't necessarily mean that it is a good analysis. If the front-end data processing was done in an inappropriate way, then the subsequent analysis, however beautiful, may not reflect the facts. Therefore, if you really want to understand what bioinformatics can do, you should take some time to study the software and algorithms that are commonly used, and get to know the underlying data and basis for the algorithms. Since there are endless new technologies and methods becoming available, we can find the most suitable method for ourselves and our research as quickly as possible when we have some basic understanding of the techniques. In doing so, we must keep to the principles of reliable data processing and take care to minimize the distortion of the data.

The emergence of single-cell transcriptional RNA-seq technology is a boon for small sample data, especially for cell types that are difficult to obtain in large numbers under experimental conditions. Even the powerful research groups cannot afford to waste materials. From 8 single cell (Tang et al. 2009) in 2009 to 10 X GENOMICS single cell gene expression database (Kiselev et al. 2019) 7 years later, all kinds of pipelines for single cell RNA-seq data analysis have been developed.

The second example article we will consider is a study of the transcriptional activity of autophagy-related genes in mouse embryonic hematopoietic stem cell formation based on single cell RNA-seq data (Hu et al. 2017). Hematopoietic stem cells (HSCs) are isolated from embryonic hematopoietic endothelial cells and/or precursor HSCs at an early developmental stage. They are rare and difficult to isolate effectively. The demand for high-throughput single-cell RNA sequencing is high. During mouse embryogenesis, the standard HSC potential initially appears in the E10.5 AGM region, later than the head, placenta and yolk sac. At E11.5, mature HSCs at these blood degree sites begin to migrate to the fetal liver for further expansion. Five cell populations related to the formation of HSCs during mouse embryogenesis were selected for single cell RNA sequencing; all five populations are classes of endothelial cells (ECs). The five populations chosen are PTPRC/CD45- and PTPRC/CD45 precursors of PTPRC/CD45- and PTPRC/CD45 in the Aortic-gonadal mesonephric (AGM) region and HSCs in the mature liver of the E14 fetus.

The dynamic expression of autophagy-related genes at the single cell level in 678 mouse embryos during HSC formation was extracted from Autophagy Database. Among them, 82 autophagy-related genes showed significant changes among adjacent cell types and formed six clusters. When ECs differentiated into precursor HSCs, transcriptional activity increased sharply, and the expression of more than half of autophagy-related genes increased significantly between ECs and T1 precursor HSCs. Compared with ECs, 13 downregulated autophagy-related genes and 44 upregulated autophagy-related genes were observed in T1 precursor HSCs, suggesting that autophagy activity was significantly increased during the process of HSCs specialization in the presumed endothelial precursor cells. It has been shown that the Notch signaling pathway is an important regulatory factor in the maintenance and differentiation of stem cells during embryonic development and plays a key role in the lineage orientation of HSCs. The authors tried to detect the expression of several autophagy essential genes (ATG 5 + ATG 7 Sqstm 1/p62 and Ulk1) and

multiple Notch target genes (*Myc/c-Myc*, *Ccnd1* [cyclinD 1], *Hes1* and *Hey1*). The expression profiles of 17 precursors of HSCs were analyzed by hierarchical clustering and correlation analysis. The results showed that the expression of essential autophagy genes was negatively correlated with the expression of Notch target genes, suggesting that the autophagic activity of precursor HSCs might be related to the downregulation of the Notch signal during the development of mouse HSCs. This was an application of hierarchical clustering and correlation analysis, and is a very basic analytical method. In biological research, the dynamic changes of cells and complex interactions make the application of some complex analytical methods unsatisfactory. Part of the reason is that the more complex the design, the more rigorous the assumptions must be, and the more regular the studied changes must be. But often the variations in complex diseases lead to more uncertainty. Therefore, choosing simple and effective analytical methods can to some extent reduce the influence of complex operations on data results. Grasping and applying these analytical methods flexibly is also an area that requires learning and practice.

18.2.2.2 Epigenomic Data Analysis

If the mechanism under investigation involves epigenomics, experimental verification will need to be a large proportion of the whole article as the study will involve a large number of reagents and many experimental verification methods. Take, for example, a 2018 *Cell Research* article on the relationship between m⁶A RNA modification and autophagy (Jin et al. 2018) in which it is necessary to understand the functions and roles of various proteins and reagents before trying to establish a mechanism:

N⁶-methyladenosine (m⁶A): an important dynamic mRNA modification regulated by methyltransferase complex, demethylase and RNA binding protein. The m⁶A modification is promoted by different treatments during cell differentiation, embryonic development and stress response. Translation and attenuation groups mRNA and directs mRNA to different destinies.

Unc-51-like kinase 1(ULK1): a protein kinase activated by autophagy, which is essential for recruiting other autophagy-related proteins to autophagy formation sites.

Fat mass and obesity associated (FTO): a positive autophagy regulatory factor

Autophagy marker light chain 3B (LC3B): used to detect autophagy levels

Bafilomycin A1(Baf A1): can block autophagy at a late step

p62/SQSTM1: autophagy substrates

YTHDF2: proteins that mainly bind to m⁶A to mediate mRNA degradation

YTHDF2 protein can recognize m⁶A modified ULK1 mRNA to mediate the degradation of mRNA and block the translation of ULK1 into protein, thus blocking autophagosome formation. FTO can remove the m⁶A methylation modification, so that ULK1 mRNA can be translated into protein efficiently, and ULK1 protein can recruit other autophagy-related proteins to the autophagy formation site, thus initiating autophagy. Small interfering RNA (siRNA) was used to target the gene that

regulates m⁶A, and FTO protein was recognized as a positive autophagy regulator. FTO-specific siRNA could block the effect of FTO on m⁶A. Therefore, relatively few LC3B spots could be observed in FTO siRNA #1 and FTO siRNA #2 cells. If FTO was mutated to FTO RQ (R316Q, which has low catalytic activity), it could not play an effective role. Therefore, the positive regulatory effect of FTO on autophagy was dependent on enzymatic activity. Similarly, the m⁶A site on the ULK 1 transcripts is a direct substrate for demethylation catalyzed by FTO. If the m⁶A site is mutated, the wild-type FTO will not be able to recognize it. If FTO is damaged, m⁶A modified ULK1 mRNA is recognized and degraded by the YTHDF2 protein, which reduces ULK1 protein levels. In YTHDF2 knockout cells, the effect of FTO damage on the reduction of ULK1 protein was almost eliminated, suggesting that YTHDF2 targeted m⁶A-labeled ULK1 transcripts. In general, the change in m⁶A modification induced by FTO may affect the stability of ULK1 transcripts through YTHDF2-dependent degradation, thus affecting autophagy.

Turning to transcriptome data analysis, a recent article in a journal of *Autophagy* identified new autophagy regulators by analyzing the transcriptional and epigenetic characteristics of nutritionally deficient cells (Peeters et al. 2019). By RNA-seq and ChIP-seq of human autophagy normal cells and autophagy deficient cells which were deprived of nutrition, the researchers found that nutritional deficiency caused both types of cells to transcribe a large number of autophagy-related genes. This change was reflected in the level of epigenetic modifications (H3K4me3, H3K27ac and H3K56ac) and was independent of autophagy flux. EGR1 (early growth response 1; aka early growth factor 1) was used as a candidate transcription regulator for autophagy. The results showed that EGR1 could affect autophagy-related gene expression and autophagy flux. The researchers believe the data could be used to identify autophagy regulators.

This study deals with some commonly used bioinformatics analysis tools, including RNA-seq analysis, ChIP-seq analysis, motif enrichment analysis and GSEA.

(a) *RNA-seq analysis*

STAR version 2.4.2a: Used to compare the sequencing data with the reference genomic GRCh37.

Picard's AddOrReplaceReadGroups (v1.98): Used to add read groups to a BAM file.

Sambamba v0.4.5: Used to sort BAM files.

HTSeq-count version 0.6.1p1: Quantifies the abundance of transcripts by Joint pattern.

edgeR's RPKM: Calculate RPKMs.

ESeq2: Identify differentially expressed genes.

(b) *ChIP-seq analysis*

Cisgenome 2.0: Peak calling for ChIP-seq data.

DESeq: Identify Peaks with differential occupancy.

(c) *Motif enrichment analysis*

AME: Motif enrichment analysis of overlapping peaks.

(d) *GSEA*

GSEA: The enrichment significance of autophagy-related genes identified in human autophagy database was calculated by GSEA with 1000 permutations.

Different combinations of algorithms, R packets and online analysis tools can bring into play the powerful computing and data processing capabilities of all kinds of analytical tools, effectively shortening the necessary time and providing a more accurate range of candidate gene sets. As scientific research progresses, the integration of various disciplines is bound to become a trend, as is the combination of dry and wet experiments, physics, chemistry, biology, mathematics, computer; even optics, machinery and other kinds of knowledge are fused together; each subject is a tool. At the same time, all of these are complementary to each other, so that scientific progress and technological breakthroughs can be rapidly promoted.

18.2.3 The Analysis of Autophagy-Related Proteomics and PTMomics Data

Autophagy-related proteomics or PTMomics studies are mainly focused on the profiling of gene products with significant changes in protein expression level or PTM level under different treatments or during autophagy process. Mass spectrometry is still the mainstream technology for proteomic and PTMomic identifications. Combined with chemical labeling such as stable isotope labeling with amino acids in cell culture (SILAC), isobaric tags for relative and absolute quantitation (iTRAQ), tandem mass tag (TMT), and label-free techniques, quantitative proteomics and PTMomics have become mainstream research plans. Here, we took three published papers as examples to introduce the commonly used strategies of autophagy-related proteomics, phosphorylation data analysis and acetylomics data analysis. Each paper was intended to solve a distinct scientific problem, and the corresponding analysis strategies cannot be simply used as is for novel studies. Additional refinement should be added for addressing other questions.

18.2.3.1 Proteomics Data Analysis

In 2014, Joseph D. Mancias et al. found using the quantitative proteomics technology that the human nuclear receptor coactivator NCOA4 is highly enriched on autophagosomes and interacts with ATG8 family members to recruit cargo-receptor complex to autophagosomes (Mancias et al. 2014). NCOA4 interacts with heavy and light chains of ferritin and mediates its degradation by autophagy. Thus, NCOA4 is a new selective receptor for ferritinophagy.

In this study, the authors chose three human cell lines, including two pancreatic cancer cell lines, PANC-1 and PA-TU-8988T, which require autophagy for the survival, and a breast cancer cell line MCF7, which does not require autophagy for the survival. In the study, SILAC technology was adopted for labeling cells, and

differentially labeled cells were mixed by the ratio of 1:1 and then quantified by mass spectrometry. The “light labeling” was used to label human cancer cells treated with phosphoinositide 3-kinase (PI3K) inhibitor Wortmannin, which inhibits autophagosome formation, while the “heavy labeling” was utilized to label cells treated with the lysosome inhibitor chloroquine, which significantly increases autophagosome accumulation. The molecular formula of lysine is $C_6H_{12}ON_2$ and that of arginine is $C_6H_{12}ON_4$, the two isotopes of carbon are C^{12} and C^{13} , and the two isotopes of nitrogen are N^{14} and N^{15} . So the “light labeling” is the use of C^{12} and N^{14} to label lysine and arginine residues in protein sequences, whereas the “heavy labeling” is the addition of C^{13} - and N^{15} -labelled lysine and arginine into the culturing medium that lacks normal lysine and arginine residues for a substitution. Thus, the molecular weights of lysine and arginine with the heavy labeling are 8 and 10 Da higher than that with the light labeling, respectively. In this article, single-label refers to the heavy labeling of only lysine residues, and double-label refers to the heavy labeling of both lysine and arginine residues. SILAC is a relatively quantitative technique, and the ratio of \log_2 (heavy labeling vs. light labeling) was considered in this paper. The samples with the light labeling have fewer autophagosomes, while the samples with the heavy labeling have more autophagosomes. When the ratio of \log_2 (heavy: light) is >1 , the ratio of heavy labeling: light labeling is >2 .

By using the autophagosome fractions derived from single-labelled PANC-1 cells treated with chloroquine for 4 or 16 h and autophagosomes retrieved from double-labeled PANC-1 and MCF7 cells treated with chloroquine for 16 h, the authors totally quantified over 2000 proteins. The number was too large to identify proper candidate genes for further experiments. Thus, the authors carefully analyzed the proteomics results and selected the proteins with \log_2 (heavy: light) > 1 in MCF7 cells treated by chloroquine for 16 h, proteins with \log_2 (heavy: light) > 1.5 in PANC-1 cells treated by chloroquine for 16 h, or proteins with \log_2 (heavy: light) > 0.5 in PANC-1 and PA-TU-8988T treated by chloroquine for 4 h. Also, each selected protein must be identified by at least two peptides. In this way, about 600 proteins were selected in each dataset. Next, abundantly expressed proteins that are unrelated to autophagy were discarded. The authors also respectively quantified the total proteomes of MCF7, PANC-1 and PA-TU-8988T cells, and individually compared these to the autophagosome proteomes by using the two-tail student's t-test (p -value < 0.05). After this processing, about 150 proteins remained in each dataset. Three biological replicates were provided for PANC-1 cells treated with chloroquine for 16 h, and 86 proteins were mutually quantified in all the three replicates. Two biological replicates were provided for MCF7 cells, and 102 proteins were simultaneously detected in both experiments. The overlap of the PANC-1 and MCF7 datasets has 33 proteins, while 122 proteins were exclusively detected in PANC-1 or MCF7. Thus, the authors defined the 155 proteins as Class 1 candidate autophagosomal proteins, and further defined the top 50 proteins simultaneously quantified in at least three independent experiments or known to function in autophagy as Class 1A candidates. Among the Class 1A candidates, there were two paralogs of ATG8 (GABARAPL2 and MAP1LC3B), four known autophagy cargo receptors (SQSTM1, CALCOCO2, OPTN and NBR1), and four ATG8-interacting

cargo receptors (KEAP1, TMEM59, FYCO1 and STX17). NCOA4 ranked 7th among the 50 Class 1A candidates in significance. Since there had been less previous research for NCOA4, it became the starting point for additional studies.

Taken together, in terms of quantitative proteomics data analysis, the computational analyses in this study were not very complicated. However, the data analyses were designed very carefully and efficiently reduced the false positive rate of proteomics identification, thus allowing important biological discoveries.

18.2.3.2 Phosphoproteomics Data Analysis

In 2017, the author cooperated with the research group of Professor Min Li, who works at the Hong Kong Baptist University, to focus on two neuroprotective autophagy inducers obtained from a Chinese herbal medicine *Uncaria rhynchophylla* (Gouteng): Corynoxine (Cory) and Cory B. Quantitative phosphoproteomics was conducted on cells treated with Cory and Cory B, and 5413 phosphorylation sites were identified (Chen et al. 2017). By using bioinformatics approaches, potential kinases that specifically modify these sites were predicted, and a kinase-substrate regulatory network was reconstructed. We developed a new algorithm for in silico Kinome Activity Profiling (iKAP), which predicted a number of protein kinases specifically regulated by Cory or Cory B. Further experimental verifications showed that Cory upregulated the kinase activity of MAP2K2/MEK2 and PLK1 to induce autophagy and promote the lysosomal degradation of disease-associated proteins. As introduced in the previous section, $^{12}\text{C}_6^{14}\text{N}_2$ -lysine and $^{12}\text{C}_6^{14}\text{N}_4$ -arginine were used in the light labeling for SILAC and denoted as “K0, R0,” whereas $^{13}\text{C}_6^{15}\text{N}_2$ -lysine and $^{13}\text{C}_6^{15}\text{N}_4$ -arginine were used for the heavy labeling and denoted as “K8, R10.” For the middle labeling, $^{13}\text{C}_6^{14}\text{N}_2$ -lysine and $^{13}\text{C}_6^{14}\text{N}_4$ -arginine were adopted and denoted as “K4, R6,” as the molecular weights of lysine and arginine are 4 and 6 Da higher than that in the light labeling. In this study, we chose the mouse neuroblastoma cell line N2a and labeled N2a cells with Cory and Cory B treatment for 3 h by the light labeling and middle labeling, respectively. The cells without any treatment were adopted for the heavy labeling as a control. Three types of labeled cells were mixed at a ratio of 1:1:1, and 5328 phosphopeptides were detected and quantified in three samples by mass spectrometry. These peptides were mapped to the mouse proteome, and we obtained 5413 phosphorylation sites in 2233 phosphoproteins, including 4749 phospho-serine (87.7%), 643 phospho-threonine (11.9%) and 21 phospho-tyrosine (0.4%) residues, respectively. Based on these results, we found that Cory upregulates 126 phosphorylation sites and downregulates 103 phosphorylation sites, whereas Cory B upregulates 91 phosphorylation sites and downregulates 98 phosphorylation sites. By using GSEA (Subramanian et al. 2005), we determined that Cory and Cory B are preferentially involved in distinct biological processes. The iGPS software, which was introduced in Sect. 18.1.2.3, was adopted to predict potential kinases that specifically regulate all phosphorylation sites. We also constructed a kinase-phosphorylation site network, containing 360 kinases and 1524 phosphorylation sites. In the iKAP algorithm, for substrates of each protein

kinase, the sum of the quantitative values of all upregulated sites was denoted as x , and the sum of reciprocals of the quantitative values of all downregulated sites was denoted as y . For all the 1524 phosphorylation sites, the sums of the quantitative values of all up- and downregulated sites were denoted as X and Y , respectively. Thus, the problem was transformed into a 2×2 table, and the statistical significance was tested by the chi-squared test (<http://www.quantpsy.org/chisq/chisq.htm>). The analysis of upregulated or downregulated kinases with significant changes can be regarded as alternative enrichment analysis. Combining the iKAP predictions and literature evidence, we finally predicted that Cory upregulated 7 kinases and downregulated 12 kinases, while Cory B upregulated 2 kinases and downregulated 11 kinases, respectively. Through a comparison, we found that two kinases, MAP2K2 and PLK1, might be exclusively upregulated by Cory but not Cory B. The relationship between these two kinases and autophagy were not well understood, and thus, they were selected as candidates for further experiments.

In this study, the phosphoproteomics experimental design was quite simple and direct. For the data analysis, a novel algorithm was designed, but without a complicated rationale, and still belonging to the category of enrichment analyses. The development of new algorithms, new tools or new data resources frequently appears in collaborative papers published by bioinformaticians and biologists. There are two reasons for this. First, bioinformaticians receive the pressure from their peers to innovate, and the development of new algorithms cannot be neglected. Second, each bioinformatician is familiar with her/his field. The development of new algorithms is helpful for obtaining better predictions and contributes to the field of bioinformatics.

18.2.3.3 Protein Lysine Modification Omics Data Analysis

There are various types of lysine modifications, such as acetylation, ubiquitination and SUMOylation. Here, we took the analysis of autophagy-related acetylome as an example to introduce the relevant approaches for analyzing the lysine modifications. In 2011, Eugenia Morselli et al. found that the acetyltransferase inhibitor spermidine could induce autophagy in humans, yeast and *C. elegans* (Morselli et al. 2011). Unlike resveratrol, another autophagy inducer, spermidine-induced autophagy, is independent of NAD-dependent protein deacetylase sirtuin-1 (SIRT1). Through a quantitative analysis of acetylomes, the author found that both compounds promoted the deacetylation of cytoplasmic proteins but enhanced the acetylation of nuclear proteins, and the two compounds have similar mechanisms for regulating acetylation.

This study mainly revealed that spermidine-induced autophagy is independent of SIRT1, while autophagy induced by resveratrol depends on SIRT1. Also, the mechanism of spermidine-induced autophagy is conserved in eukaryotes. To explore the detailed mechanisms of how the two compounds modulate acetylation, the authors labeled HCT 116 human colon cancer cells by SILAC. For sample preparation, heavy labeling (K8, R10) was adopted for cells treated with 100 μ M spermidine for

2 h, middle labeling (K4, R6) was chosen for cells treated with 100 μ M resveratrol for 2 h, and light labeling was adopted for untreated cells as control. The three labeled cells were mixed in a ratio of 1:1:1, and then, subcellular fractions including cytoplasm, mitochondria and nucleus were separated and prepared. Eventually, acetylpeptides were identified and quantified by mass spectrometry. Using this method, the authors found that spermidine or resveratrol induced changes at 560 acetylation sites in 375 acetylated proteins. Here, “change” was defined as an upregulation or downregulation of an acetylation site by at least a factor of 1.2 in cells treated by the two compounds as compared to than that in cells without treatment. Among the results, 170 proteins could be found in a previously reported human autophagy protein network, and 89 proteins could interact with at least 10 proteins of this network, indicating their importance in the network. The authors found that acetylation or deacetylation of autophagy substrates such as ATG5 and LC3 was regulated by spermidine or resveratrol. A sequence motif extraction and visualization software, Motif-x (<http://motif-x.med.harvard.edu/>), was used to analyze the sequence motif K(F/Y) of acetylation sites regulated by spermidine or resveratrol. Here, the number of cytoplasmic proteins with upregulated acetylation levels was denoted as x , and the number of downregulated acetylated proteins was defined as y . The number of nuclear proteins with upregulated acetylation levels was defined as X , and the number of downregulated acetylated proteins was defined as Y . Thus, this question was transformed into a 2×2 table, and the significance was testified by the chi-squared test. With the help of this method, the authors detected the acetylated proteins with significant changes in cytoplasm and nucleus (p -value < 0.001) and found that spermidine and resveratrol mainly promoted deacetylation of cytoplasmic proteins, but also elevated acetylation of nuclear proteins. Moreover, a GO-based enrichment analysis was performed using a Fisher’s exact test (<http://www.langsrud.com/fisher.htm>), and the results showed that deacetylated proteins were significantly enriched in the metabolism-related biological process.

In summary, the computational analysis of the acetylome is not much different from of the proteome and phosphoproteome. After obtaining the omic dataset generated by mass spectrometry, proteins or PTM peptides showing significant changes should be first identified. What threshold to use for significance depends on the distinct scientific question being asked, and twofold is not always appropriate for all studies. In addition, the enrichment analysis is quite useful, since many problems in analyzing proteomics and PTMomics data can be transformed into a 2×2 table to calculate the statistical significance. The chi-squared test, Fisher’s exact test and hypergeometric test are simple but effective statistical methods.

18.3 Autophagy-Related Data Resources

Autophagy-related data resources are related to many aspects of molecular biology, including gene protein, sequence, structure and interaction, each of which has its own particular angle and direction, and many of which are available online.

Bioinformatics itself is an interdisciplinary fusion, so the application of various research products, including databases, algorithms, tools and software, is not limited to researchers in a single field. Bioinformatics can be a tool, but is also an important area of basic research in its own right. The establishment, maintenance and updating of all kinds of biological resource databases is the embodiment of bioinformatics for the integration of information resources in a field. For biological databases, two important features are regular updating and quality data and annotations. Two key web-based autophagy-related resources are (1) the Human Autophagy Database (HADb, <http://autophagy.lu/>) (Moussay et al. 2011), which was published in 2011, listing more than 200 human genes/proteins associated with autophagy. However, no further updates have been made to this database; (2) Autophagy Database developed by the National Genetics Institute of Japan (<http://www.tanpaku.org/autophagy/index.html>), which is regularly updated and, as of January 2017, contains 582 reviewed protein entries plus more than 52,000 homologous/homologous protein items and predicted homologous proteins (Homma et al. 2011). Various newly developed autophagy-related database resources continue to emerge, and the quality of the databases and the amount of information they cover are reaching ever higher standards. The 2016 edition of the journal *autophagy*, led by Daniel J Klionsky of the University of Michigan in the United States, contains a paper signed by 2467 authors, “Guidelines for the use and interpretation of autophagy Analysis (Third Edition)” (Klionsky et al. 2016). Two aspects of autophagy-related data resources are emphasized: one is whether it provides the possibility to identify new autophagy-related proteins, and the other is whether it describes the characteristics that may link specific proteins to autophagy processes. Example cases of autophagy-related RNA database application are described in the second part of this section. The introduction to the databases in this section does not involve the underlying platform code and algorithms, but instead is focused on basic content and practical applications. Readers who are interested in website building and other aspects can find this information in the referenced literature or websites. In order to best introduce the databases, this section includes many graphics.

18.3.1 Autophagy Gene Databases

18.3.1.1 The THANATOS Database

Autophagy is a highly conserved “self-eating” process, which controls the degradation of lysosomes and cytoplasm in vacuoles and ensures the homeostasis of cells and the circulation of macromolecules. In some states, autophagy can induce programmed cell death (PCD) by excessive degradation of cell inclusions. In addition to autophagic cell death, apoptosis and necrosis can lead to cell suicide, two other types of PCDs. There is complex crosstalk between autophagy, apoptosis and necrosis to determine cell survival or suicide. In addition to autophagy-related (ATG) genes, many regulatory factors and various post-translational modifications (PTMs)

are involved in autophagy. *ATG* genes and autophagy are regulated by both transcription and PTMs. Post-transcriptional regulation and protein–protein interactions (PPIs) are widely controlled. Hundreds of small chemicals can induce or inhibit autophagy. The THANATOS database is a collection of 4237 proteins regulated in autophagy and cell death pathways based on the literature. By calculating the potential congeners to recognize known proteins, a comprehensive database of The Autophagy, Necrosis, Apoptosis OrchestratorS (THANATOS) was constructed, which contains 191,543 proteins that may be related to 164 eukaryotic autophagy death pathways (Deng et al. 2018).

18.3.1.1.1 Interface Introduction

URL link: <http://thanatos.biocuckoo.org>. Links below the “home” button link to the collection of the existing work of the group, including PTMs prediction software, tools and databases. The first database under the database section is the THANATOS database.

18.3.1.1.2 Search

The search interface (Fig. 18.29) on the home page of the database allows the user to type a query and submit it by clicking “submit”. In addition, the user can optionally narrow the scope of the search by ID, species, gene or protein names, and

Please search the **THANATOS** database with one or multiple keywords to find the related information:

Any Field

ONLY experimentally identified THANATOS proteins

Any Field dropdown menu: Any Field, THANATOS Accession, Ensembl ID, UniProt ID, Species, Gene/Protein Name, Function

THANATOS proteins: 2 Experimental (2)

Evidence	Accession	Gene Name	Species
	ANA-HSA-112028	AT09B: APOB2; NOS3AS	Homo sapiens (human)
	ANA-HSA-112072	AT09A: APOB1	Homo sapiens (human)

Content

Tag	THANATOS ID	ANA-HSA-112072
Ensembl ID	ENSPP00000355173.4; ENSG00000198925.10	
Uniprot	Q3VU65; ATG9A_HUMAN; Q72320; Q9H6L1; Q6PON7; Q8NDK6; Q7Z3C6; Q7Z317; Q9HAG7; Q9BVL5; Q3ZAO6	
Accession	79065	
Entrez ID	BC065534; AC068946; BX538198; BC021202; BK004018; BC001098; BX538192; CH471063; AK025822; AK027448; AK021732; AI833865; BX537984	
Genbank	EAW70706.1; CAD38723.1; AAH01098.2; BAB15246.1; AAH65534.1; CAD98061.1; BAB13882.1; CAD98064.1; AAH21202.2; BAB55119.1; CAD97944.1; NOT_ANNOTATED_CDS; DAA05199.1	
Protein ID	Autophagy-related protein 9A; APG9-like 1; mATG9	
Gene Name	ATG9A; APG9L1	
Organism	Homo sapiens (Human)	
Taxonomy ID	9606	

Fig. 18.29 THANATOS database

functions. The example provided on the page provides the input format: “Atg9 human”. After submission, you can see the protein entries corresponding to the input key. Each entry is marked with a pentagonal symbol in the “Evidence” column. Select protein items of interest for further details.

Take TANAATAS ID: ANA-HSA-112157 as an example. The details include the different numbers (ID) of the protein on the main public platform, providing a one-click direct link. The details of the other parts are as follows:

“ANA regulation” refers to the classification of the regulated proteins regarding the three main types of PCD: “autophagy, necrosis, apoptosis,” for example AT+: autophagy positive/positive regulation, NE-: necrotic negative/negative regulation and AP+: Apoptosis positive/positive regulation (Fig. 18.30a);

PTM: Post-translational modification showing the PTM-related kinases involved with the protein being queried;

PPI: A network of interactions between each protein and other proteins that can be displayed. The red dot is the queried protein; the other connected dots will provide the corresponding THANATAS ID below when selected and can be clicked to jump to the protein details page (Fig. 18.30b).

KEGG, GO: Provides KEGG and GO enrichment path links;

Ortholog Gene: Lists the orthologous genes of the query gene and provides links to view the details.

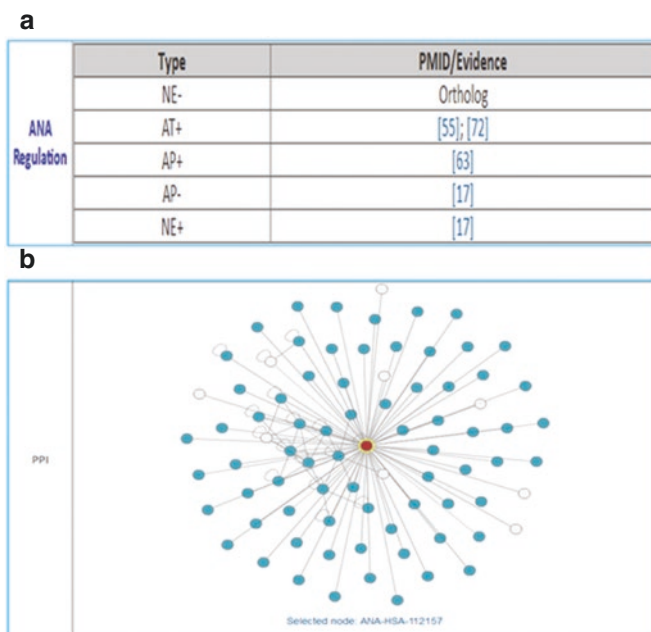


Fig. 18.30 (a) ANA regulation type. (b) PPI network

18.3.1.1.3 Browse

You can choose to browse by process and browse by species.

The process involves three processes: autophagy, apoptosis and necrosis. Autophagy includes 2501 experimentally validated unique proteins with AT+ and AT- function in 10 species; apoptosis includes 2700 experimentally validated unique proteins with AP+ and AP- function in eight species; necrosis includes 8575 experimentally validated unique proteins with NE+ and NE- functions in one species. If the test validation option is not checked, the results can be expanded to a total of 164 species (Fig. 18.31). Species are provided according to three major categories (animals, plants and fungi), and each category is further classified according to the classification of PCD process regulation (Fig. 18.32).

18.3.1.1.4 Advanced Search

Advanced search options can increase the search constraints and further customize various combinations of options of interest, such as a list of proteins associated with autophagy function under experimentally validated conditions, or which proteins associated with a specific gene (e.g., TP53) under experimentally validated conditions are involved in functions other than autophagy (Fig. 18.33).

1. Browse process: 👤

ONLY experimentally identified THANATOS proteins

• There are **2691** unique proteins with the function(s) of **AT+; AT-** for **10** species.

<i>Arabidopsis thaliana</i> (thale cress) (51)	<i>Caenorhabditis elegans</i> (roundworm) (65)	<i>Danio rerio</i> (zebrafish) (30)
<i>Drosophila melanogaster</i> (fruit fly) (132)	<i>Homo sapiens</i> (human) (1087)	<i>Xenopus laevis</i> (clownfish) (4)
<i>Macaca mulatta</i> (rhesus monkey) (1)	<i>Mus musculus</i> (house mouse) (736)	<i>Rattus norvegicus</i> (norway rat) (236)
<i>Saccharomyces cerevisiae</i> (baker's yeast) (179)		

• There are **2700** unique proteins with the function(s) of **AP+; AP-** for **8** species.

<i>Arabidopsis thaliana</i> (thale cress) (20)	<i>Caenorhabditis elegans</i> (roundworm) (41)	<i>Danio rerio</i> (zebrafish) (29)
<i>Drosophila melanogaster</i> (fruit fly) (81)	<i>Homo sapiens</i> (human) (1389)	<i>Mus musculus</i> (house mouse) (820)
<i>Rattus norvegicus</i> (norway rat) (269)	<i>Saccharomyces cerevisiae</i> (baker's yeast) (51)	

• There are **676** unique proteins with the function(s) of **NE+; NE-** for **8** species.

<i>Arabidopsis thaliana</i> (thale cress) (1)	<i>Caenorhabditis elegans</i> (roundworm) (9)	<i>Danio rerio</i> (zebrafish) (18)
<i>Drosophila melanogaster</i> (fruit fly) (22)	<i>Homo sapiens</i> (human) (225)	<i>Mus musculus</i> (house mouse) (212)
<i>Rattus norvegicus</i> (norway rat) (81)	<i>Saccharomyces cerevisiae</i> (baker's yeast) (9)	

1. Browse process: 👤

ONLY experimentally identified THANATOS proteins

• There are **120683** unique proteins with the function(s) of **AT+; AT-** for **164** species.

• There are **118503** unique proteins with the function(s) of **AP+; AP-** for **164** species.

• There are **18536** unique proteins with the function(s) of **NE+; NE-** for **164** species.

Fig. 18.31 Browse process

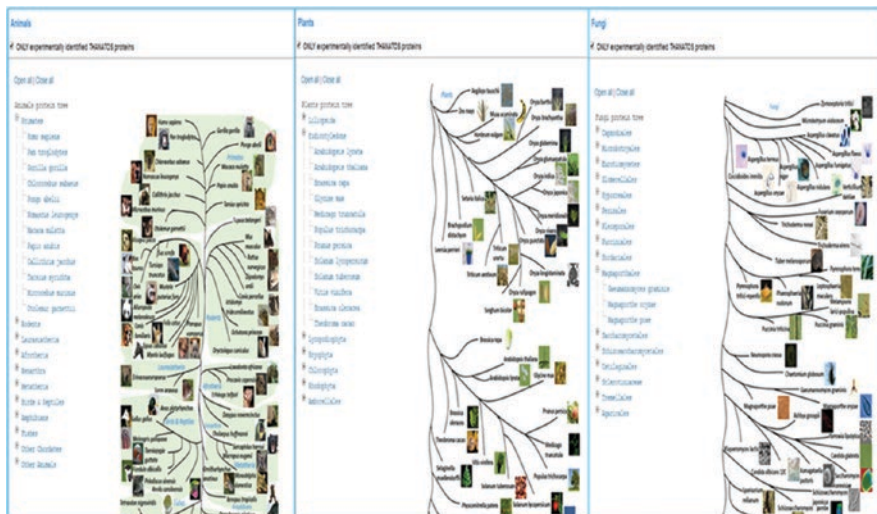


Fig. 18.32 Browse by species

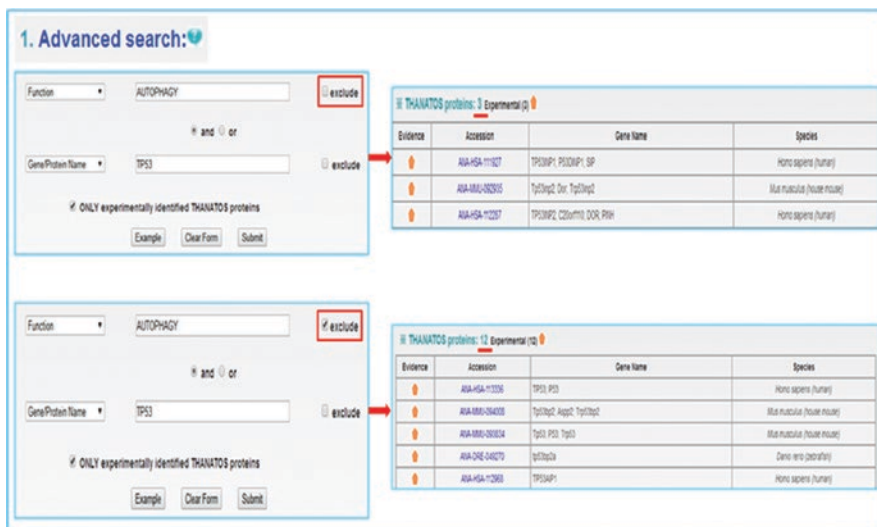


Fig. 18.33 Advanced search

Batch search: Provides combined keyword browsing;

BLAST search: When an unknown protein sequence is entered in FASTA format, similar proteins are matched in the database to provide similarity evaluation. Taking the sequence information of ANA-HSA-112772 as an example (Fig. 18.34), the similar gene rankings and scores given below can be seen. ANA-HSA-112772 is in the first row, with 100% similarity and the highest score.

3. BLAST search:
Please input a **PROTEIN** sequence in **FASTA** format:

```

MWLEELNQ LHFLLILLS MHTRANFLON MLRSAGLN VTKKEDGS
TAFIPFPRYL KCKRHRKPE DYNBDC3TD 80
GCVTFREED DSGLPPTFS CGLGKSRQK CREDIPFNR KSIEOCTRN
KCRNLRPL FLKKNDFVD GPIDKALLI 160
DVTWCLLLV LILLCPTFY KRGSTFRYS SLSGQETTY PFGESLNDI
RQGSVSSSS GLPLNWTI AKQIKWQI 240
GKRGTEVM GKWGEYAV KYFFTEAS WFRTEIVQI VLMDKHWLG
PIAADKRGIS DPTLVLTD YHRSGLDVT 320
LKSITLDRS RELAYDVSY GLCRHEIEF STQKFAIAH NDKSKHWLY
KMGTCIAD LGLAWKPID TNGVDFPRT 400
KNGKTYRFP EYLDSELRN RQGGYIRAH YSFLILWEV ANRCVSGGLV
BEYGLPTDL YPSFPTYEM KEIVLRLK 480
PSPFRWSD ECLGKALK YCWANRPA S KLTALRYKKT LAKMSEQDI KL 532
    
```

E-Value: 0.01 ONLY experimentally identified THANATOS proteins

Example Clear Form Submit

THANATOS proteins: 254 Experimental (254)

Evidence	Accession	Species	Gene Name	Identity	E-value	Score (bits)
●	ANA-HSA-112772	Homo sapiens (human)	BMP1RB	100.00%	0.0	1050
●	ANA-RNO-151400	Rattus norvegicus (norway rat)	Tgfbt1	54.04%	1e-140	494
●	ANA-HSA-113058	Homo sapiens (human)	TGFBR1, ALKS, SKR4	53.96%	3e-138	486
●	ANA-DME-158178	Drosophila melanogaster (fruit fly)	babo, CG5224, Dmel, CG5224	48.63%	1e-133	471
●	ANA-HSA-110949	Homo sapiens (human)	ACVR1C, ALK7	52.78%	1e-127	451
●	ANA-MMU-094171	Mus musculus (house mouse)	Acv2b	52.69%	1e-99	225
●	ANA-HSA-112282	Homo sapiens (human)	BMP2, PPH1	31.90%	4e-57	217
●	ANA-HSA-111138	Homo sapiens (human)	AMHR2, AHR2, MSR2	33.12%	2e-41	163
●	AQA-HSA-112297	Homo sapiens (human)	ZAK, MLTK, HCC54	27.27%	3e-20	84.7
●	ANA-HSA-112159	Homo sapiens (human)	FYN	27.43%	1e-19	92.4
●	ANA-MMU-093675	Mus musculus (house mouse)	Fyn	27.43%	1e-19	92.4
●	ANA-MMU-092083	Mus musculus (house mouse)	Braf B-raf	30.36%	2e-19	91.3
●	ANA-HSA-111437	Homo sapiens (human)	BRAF, BRAF1, RAFB1	30.36%	2e-19	90.9
●	ANA-HSA-112253	Homo sapiens (human)	SRG, SRG1	27.05%	6e-19	90.1
●	ANA-MMU-093590	Mus musculus (house mouse)	Srg	26.74%	1e-18	89.0
●	ANA-HSA-112771	Homo sapiens (human)	RAF1, RAF	30.24%	2e-18	88.2
●	ANA-MMU-092043	Mus musculus (house mouse)	Raft, C'raf	30.10%	2e-18	88.2
●	ANA-MMU-092225	Mus musculus (house mouse)	PKS, Ssk	26.74%	4e-18	87.8

Fig. 18.34 BLAST search

18.3.1.2 The Human Autophagy Database (HADb)

Website link: <http://autophagy.lu/>. The database contains more than 200 human gene/protein entries related to autophagy, from manual collection of biomedical literature and other online resources. The database was released in 2011, and there is no information showing further updates (Moussay et al. 2011).

The home page is a brief introduction to the concept of autophagy and basic information about the database. In the module of the home page, there is no content under the Database module. Several search methods are available under the Gene Find module: “Symbol or Synonym”, “Accession”, “Chromosome” and “Keyword” (Fig. 18.35).

In the “Symbol or Synonym” mode, take the *WIP12* gene that is used as a default by the website as an example. In the only piece of information returned, click on the gene name line in the red font above to view the details of the gene (Fig. 18.35). The details are presented in four ways: genes, transcripts, exons and proteins, which can be viewed separately (Fig. 18.36). When viewing the gene mode, the ensemble link and sequence information are provided below (can be switched between FASTA format and continuous base format). When selecting a transcript, each transcript line can be clicked to switch to the corresponding transcript details below, such as basic information, exon information (providing a link to detailed information), mutated information (providing a link to detailed information) and sequence information (Switch between FASTA format and continuous base format). The exon method corresponds to the exon under the transcript. In the protein mode, it provides various external links, functional annotation information, protein information

Fig. 18.35 Look for gene module

Fig. 18.36 Gene details in the “Symbol or Synonym” mode



Fig. 18.37 Clustering module

under different transcripts, and sequence annotation information (such as repeat region, position, length, variation and amino acid modification) and sequence information.

The “Clustering” module is divided into two modes: gene list and protein. The gene list is indexed in English alphabetical order and clicks to enter the same page as the gene search function. The protein model is further divided into three categories: “motifs motif,” “domains domain” and “sites locus” (Fig. 18.37), and the proteins corresponding to these three types of structures are separately classified and displayed. In structural biology, the term “motif” corresponds to the secondary structure of the protein and designates a short region with a specific spatial conformation and specific function, while the term “domain” corresponds to the tertiary structure of the protein, and is an independently folding region with a stable structure and independent function. Each protein can be clicked to enter the same page as the gene search function and will not be repeated here.

18.3.1.3 The Autophagy Database

Website link: <http://www.tanpaku.org/autophagy/index.html> (Homma et al. 2011), supported by the National Institute of Genetics of Japan in the Ministry of Education, Culture, Sports, Science and Technology (MEXT) Targeted Protein Research Program. This database is continually being updated, and the latest autophagy-related information provided contains protein structure information. As of January 18, 2017, 582 reviewed autophagy-related protein entries and 42,007 entries for predicted homologs have been included, for a total of 52,021 entries. In my hands,

Firefox worked better with this website than Google Chrome, so if you encounter a problem in using this website you might try a different browser.

18.3.1.3.1 Autophagy-Related Protein List

The autophagy-related protein list includes six species: Protista, Fungi, Plantae, Invertebrata, Chordata and Mammalia, a total of 69 species (Fig. 18.38).

Taking *Saccharomyces cerevisiae* as an example, when only the “Synonyms” option is selected, 11 lines of information including other information are listed, each of which includes functions, clusters, names, synonyms (e.g., different names representing the same gene) and PDB Structure (linking to Protein Data Bank Japan (PDBj)) (Fig. 18.39).

If all the items displayed by the information are clicked, some of the items originally in the name link will be displayed directly on the page, and the protein interaction information and DICHOT results can be further viewed.

18.3.1.3.2 Homologs of Autophagy-Related Genes

This function is used to discover which proteins in each species may be functional homologs of specific autophagy-related proteins in other species. The protein list is listed separately for 69 species, while the gene homology portion is listed for

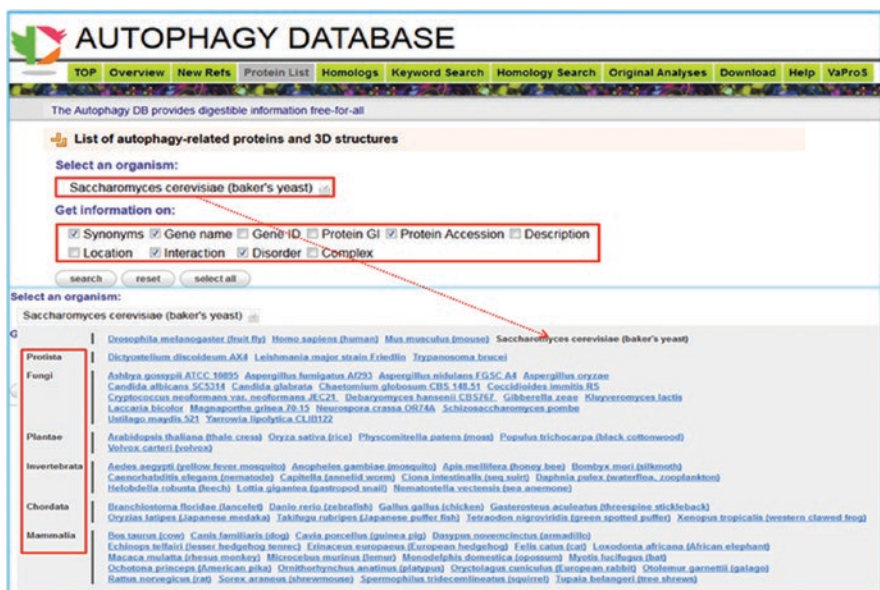


Fig. 18.38 All species in the protein list

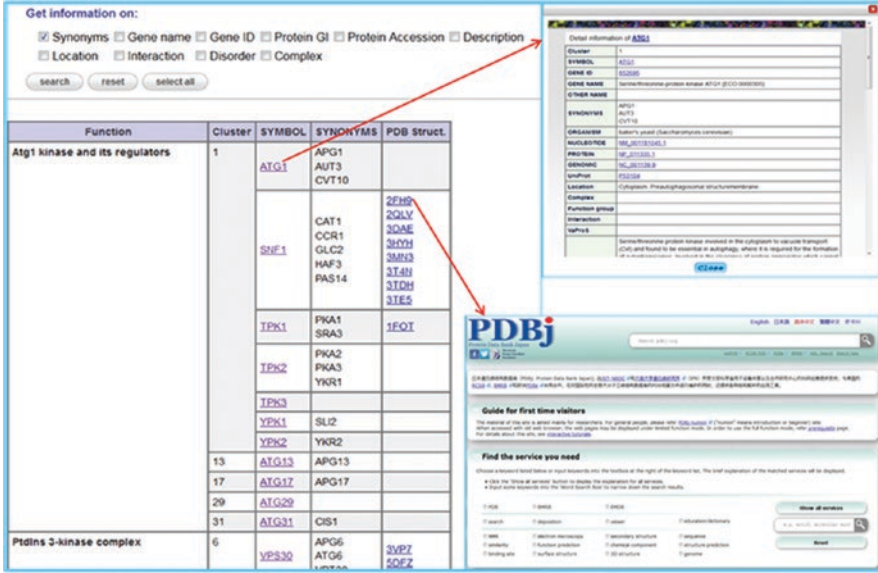


Fig. 18.39 *Saccharomyces Cerevisiae* Protein List

selection of the species of interest among 69 species. Take *Homo sapiens* and *Mus musculus* as an example (Fig. 18.40). The homologous gene entries examined in the legend are marked in black, the orthologous gene entries are in blue, the homologous gene entries are in green, and the other entries are gray font. Four types of gene entries can be seen simultaneously in the Atg8 binding system. Even if the homology list of all 69 species is selected at the same time, the page feedback information can be obtained relatively quickly.

When taking Atg8 as an example, the keyword search selects the exact matching gene/protein name, performs an unfiltered species search and returns 17 results, which correspond to proteins of different species that perform the function of Atg8. A homologous search can be performed by entering an amino acid sequence to find a protein. The website provides two examples: “sample1: ATG1 yeast; sample2: ULK2 human”. Select the second example, and use the Homo sapiens species as the filter to obtain the homologous gene results for the sequence sought. The rightmost “score” is the scoring of the results (Fig. 18.41).

18.3.1.4 The Autophagy Regulatory Network (ARN)

The URL link: <http://arn.elte.hu/> (Turei et al. 2015), focuses on the analysis of the database of autophagy protein regulatory networks. The website statistics show that a total of 14,018 proteins and 386 miRNAs are stored, providing autophagy regulators and interactions and their predictions, a one-step network of autophagy proteins, transcription factors and interactions, miRNAs and interactions.

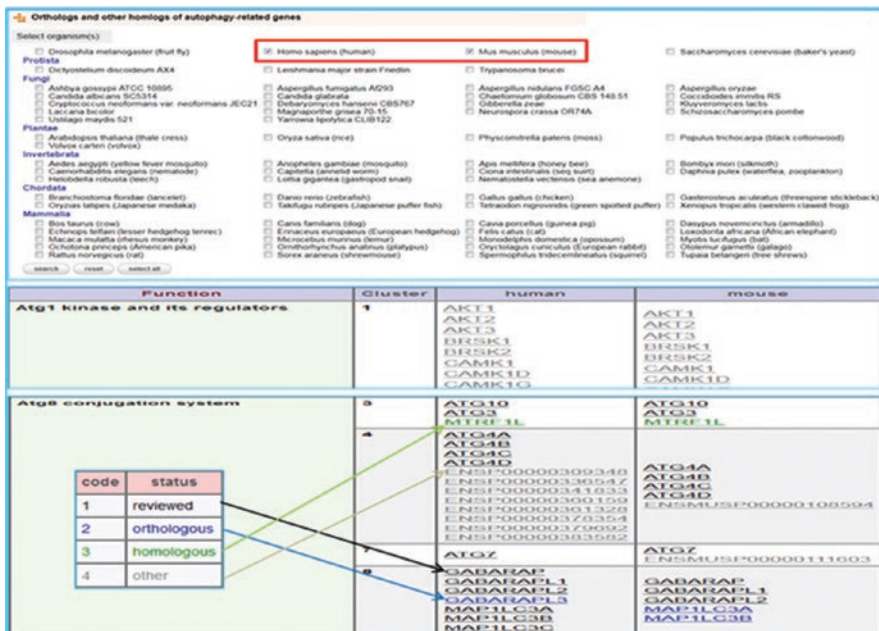


Fig. 18.40 Homologous gene legend

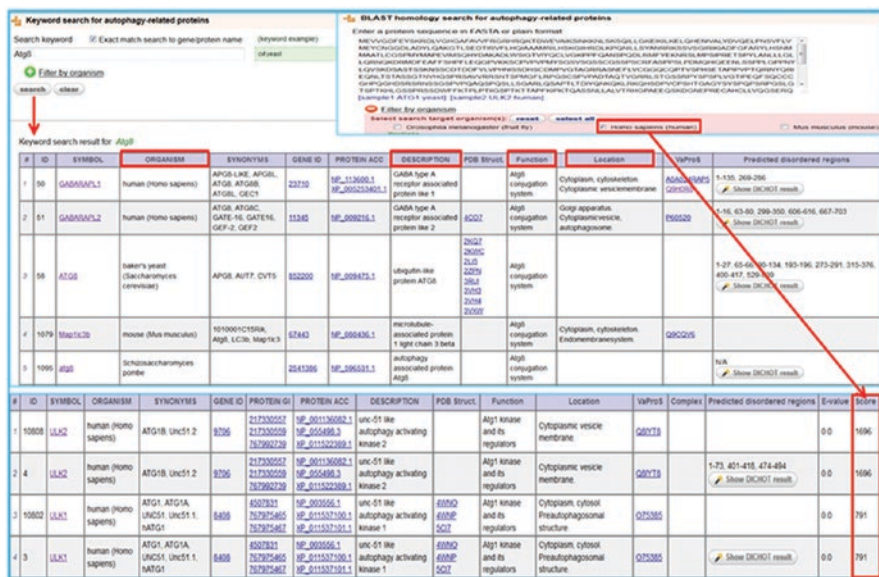


Fig. 18.41 Keywords search autophagy-related gene Atg8

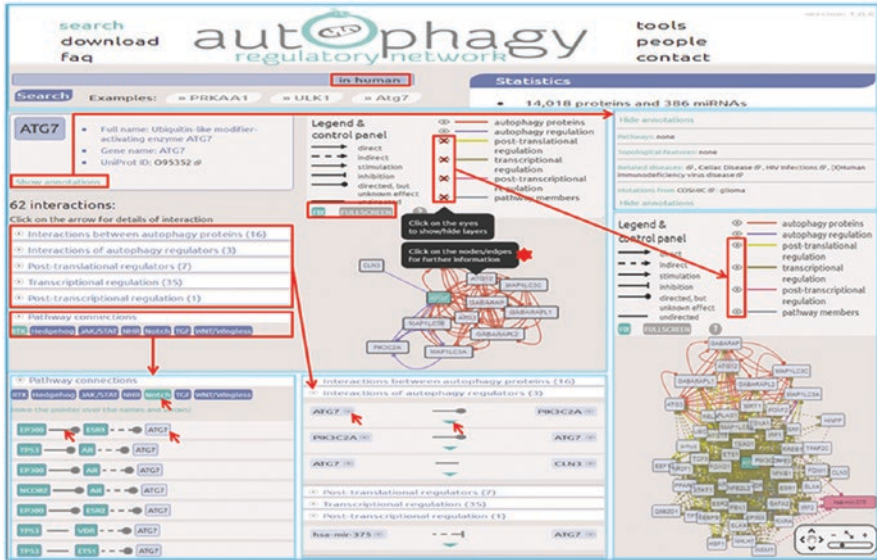


Fig. 18.42 ARN website search for ATG7 results

A total of 397,764 interactions are included, including transcription factors and interactions, and pathway proteins and interactions. Only the search page is introduced here.

In the case of Atg7, only Homo sapiens species searches are available (Fig. 18.42). In addition to external links, almost all display pages are available in a single view, so no location will be overlooked:

There are hidden annotations under the “ATG7” gene information. Each of the five categories of 62 interactions has a drop-down page, and the first level drop-down page has a triangular arrow symbol for the second level drop-down menu. In addition to the drop-down menus, pathway connections also have toggle buttons for different paths, such as the “RTK” path, the “Notch” path and the “TGF” path. Each gene name and direction arrow in the pathway will appear with annotation information when moused-over, and clicking the control arrow can link to the new page to provide information on the regulatory relationship in both the positive and negative directions. The basic interaction network shows only autophagy proteins and autophagy regulators. The other four items can be viewed by clicking on the eye-shaped icon in the legend next to each item you would like to display. The open interaction network after the open display is large and complex, practical and not tall. Of note, the visualization of the network image requires Adobe Flash to run. You can click on the points and edges in the network map to get further information, or you can view it in full screen and stretch the network into the shape you want.

18.3.2 *Autophagy-Related RNA Databases*

18.3.2.1 **The ncRNA-Associated Cell Death Database (ncRDeathDB)**

Non-coding RNAs (ncRNAs) are a broad range of RNA molecules, including miRNAs, lncRNAs and snoRNAs. They are not converted to proteins, but play an important regulatory role in the expression of coding genes. There is increasing evidence that abnormal expression of ncRNAs regulates different pathways of PCD. The ncRDeathDB database developed by miRDeathDB (Xu and Li 2012) has a larger amount of data than miRDeathDB, storing more than 4600 ncRNA-mediated PCD entries in 12 species (Wu et al. 2015). By retrieving more references, increasing homology predictions and covering more RNA types such as lncRNA and snoRNA, these resources will help visualize and explore knowledge about cell death and autophagy non-coding RNA components, revealing the general organizing principles of ncRNA-regulated cell death pathways and producing valuable biological insights.

18.3.2.1.1 Interface Introduction

Website link: <http://www.rna-society.org/ncrdeathdb/index.php>. The home page contains three sections: introductions, statistics and other sister databases for the group. The statistical information is presented in terms of miRNA, lncRNA and snoRNA-related entry statistics, as well as statistics on apoptosis, autophagy and necrosis-related entries.

18.3.2.1.2 Search

The search page is divided into three search methods: keyword search, death pathway (apoptosis, autophagy and necrosis) search and advanced search.

18.3.2.1.2.1 Search by Keyword

The types of keywords that can be used include ncRNA names, protein names, species and death pathways, and fuzzy queries are supported. Using ATG7 as an example, 152 ncRNA entries interacting with ATG7 were obtained. The entry information contains the ncRNA name, RNA species, species, death pathway, PubMed ID supported by the literature, or predicted entries identified by “prediction.” Select the detailed information of the first item, let-7a, to view more; the detailed information contains three parts: Basic, Binding and Network (Fig. 18.43).

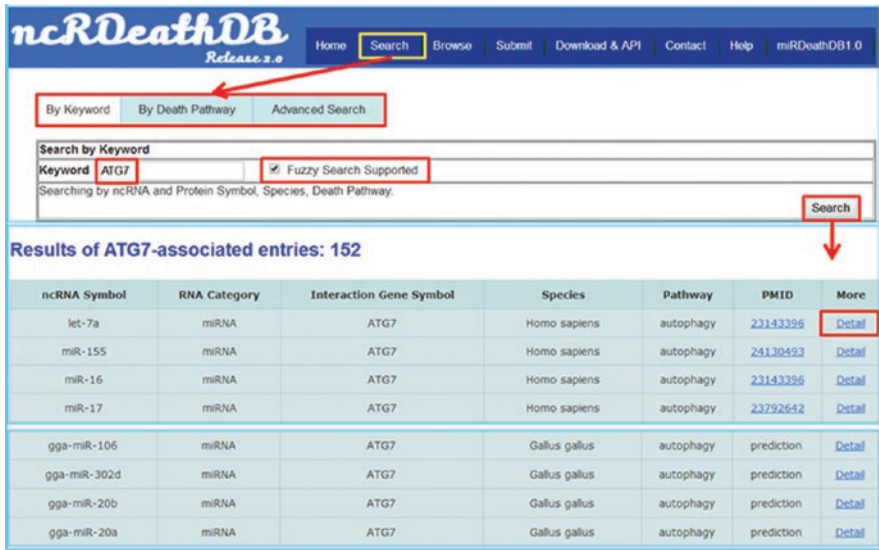


Fig. 18.43 Search by keyword in ncRDeathDB

Detail shows the path of death involved in interaction (autophagy), expression up and down direction (down, down), species (Homo sapiens) and tissue (Hella cells, human cervical cancer cells, HeLa cell) The details are described in the reference as a description of the interaction between the two (Fig. 18.44). Click on the let-7a name and the ATG7 name to get separate description links, and you can continue to track the various links provided according to your interests, such as the link to the miRBase interface of the precursor miRNA and mature miRNA of let-7a and the KEGG and GO information in the functional analysis. There are enrichment pathway interface links, such as ATG7 interaction gene and network visualization information. Binding based on RIssearch provides predictive binding sites between different transcripts of mature and interacting genes of the ncRNA under different names, and scores (Fig. 18.45); Network allows visualization which can be controlled by selecting the center point and the number of neighbor layers.

18.3.2.1.2.2 Search by Death Pathway

Taking Homo sapiens autophagy as an example, a total of 619 entries were returned. The details are the same as the keyword search (Fig. 18.46).

Search by Death Pathway

Species: **Homo sapiens** | Death Pathway: **Autophagy**

Searching by Apoptosis, Autophagy, Necrosis

Results by Homo sapiens and autophagy : 619

ncRNA Symbol	RNA Category	Interaction Gene Symbol	Species	Pathway	PMID	More
BANCR	lncRNA	MAP1LC3A	Homo sapiens	autophagy	23289082	Detail
BANCR	lncRNA	MAP1LC3B	Homo sapiens	autophagy	23289082	Detail
FLJ13182	lncRNA	ATG13				
HECC	lncRNA					
HECC3	lncRNA	MAP1LC3B				
MI-7	miRNA	MTOR				
MI-7a	miRNA	ATG5				
MI-7b	miRNA	ATG7				

Results by Homo sapiens and necrosis : 7

ncRNA Symbol	RNA Category	Interaction Gene Symbol	Species	Pathway	PMID	More
BC200	lncRNA		Homo sapiens	necrosis	25645324	Detail
HOTAIR	lncRNA		Homo sapiens	necrosis	22543869	Detail
TUG1	lncRNA		Homo sapiens	necrosis	25645324	Detail
miR-155	miRNA	RIPK1	Homo sapiens	necrosis	20550618	Detail
miR-155g	miRNA		Homo sapiens	necrosis	25645324	Detail
miR-24	miRNA	BCL2L1	Homo sapiens	necrosis	22098654	Detail
miR-674	miRNA	CASP8	Homo sapiens	necrosis	23828572	Detail

Results by Homo sapiens and apoptosis : 2054

ncRNA Symbol	RNA Category	Interaction Gene Symbol	Species	Pathway	PMID	More
7SK	lncRNA					
h007479	lncRNA	BNP1				
AF118081	lncRNA					
AFAP1-AS1	lncRNA		Homo sapiens	apoptosis	23322111	Detail
ANIL	lncRNA	CDKN2B	Homo sapiens	apoptosis	20729237	Detail
ANIL	lncRNA	CDKN2B	Homo sapiens	apoptosis	23084255	Detail

Fig. 18.46 Search by death pathway

Advanced Search (Result of your interesting ncRNA and gene symbols by associated option of species and death pathway)

Species: **All** | Death pathway: **All**

Result Presentation: Just List Result Visualize Direct Network Visualize Indirect Network

ncRNA Symbol: 7SK, h007479, AF118081, AFAP1-AS1, ANIL, ASLN04080, ASlncmRNAs, BIALR-2, BANCR, bantam, BC200, hsa007-7

Gene Symbol: 14-3-3sigma, AATK, ABCA1, ABCB1, ABCB9, ABCC1, ABCC2, ABL1, ADAM17, ADAMTS7, Adey5, Adrb1

Selected Items: 7SK, BANCR, 14-3-3sigma

Results by associated options of ncRNA/gene symbols: 11

ncRNA Symbol	RNA Category	Interaction Gene Symbol	Species	Pathway	PMID	More
BANCR	lncRNA	MAP1LC3A	Homo sapiens	autophagy	25289082	Detail
BANCR	lncRNA	MAP1LC3B	Homo sapiens	autophagy	25289082	Detail
7SK	lncRNA		Homo sapiens	apoptosis	25492483	Detail
BANCR	lncRNA	CDH1	Homo sapiens	apoptosis	24655544	Detail
BANCR	lncRNA	CDH2	Homo sapiens	apoptosis	24655544	Detail
BANCR	lncRNA	MAP2K7	Homo sapiens	apoptosis	25661343	Detail
BANCR	lncRNA	MAPK11	Homo sapiens	apoptosis	25661343	Detail
BANCR	lncRNA	MAPK9	Homo sapiens	apoptosis	25661343	Detail
BANCR	lncRNA	MAPK9	Homo sapiens	apoptosis	25661343	Detail
BANCR	lncRNA	MAPK9	Homo sapiens	apoptosis	25661343	Detail
BANCR	lncRNA	VIM	Homo sapiens	apoptosis	24655544	Detail
miR-134a	miRNA	14-3-3sigma	Homo sapiens	apoptosis	186272110	Detail

Fig. 18.47 Advanced search

18.3.2.1.2.3 Advanced Search

Users can select species and death pathways through the drop-down box in the advanced search mode and display the results in three different ways: “Just List Result”, “Visualize Direct Network” and “Visualize Indirect Network” (Fig. 18.47), which displays the results through the list, visualizes the direct interacting

Browse by ncRNA category...

[MiRNA](#) (4373 miRNA-associated cell death entries)
[LncRNA](#) (230 lncRNA-associated cell death entries)
[SnoRNA](#) (12 snoRNA-associated cell death entries)

Browse by species...

[Homo sapiens](#) (H.sapiens; 2680 ncRNA-associated entries between 569 ncRNAs and 622 target genes)
[Mus musculus](#) (M.musculus; 480 ncRNA-associated entries between 212 ncRNAs and 161 target genes)
[Rattus norvegicus](#) (R.norvegicus; 300 ncRNA-associated entries between 139 ncRNAs and 86 target genes)
[Macaca mulatta](#) (M.mulatta; 282 ncRNA-associated entries between 99 ncRNAs and 52 target genes)
[Pan troglodytes](#)(P.troglodytes; 272 ncRNA-associated entries between 97 ncRNAs and 50 target genes)
[Bos taurus](#) (B.taurus; 240 ncRNA-associated entries between 94 ncRNAs and 44 target genes)
[Gallus gallus](#) (G.gallus; 242 ncRNA-associated entries between 48 ncRNAs and 34 target genes)
[Canis familiaris](#) (C.familiaris; 215 ncRNA-associated entries between 83 ncRNAs and 48 target genes)
[Danio rerio](#) (D.rerio; 22 ncRNA-associated entries between 15 ncRNAs and 16 target genes)
[Drosophila melanogaster](#) (D.melanogaster; 17 ncRNA-associated entries between 8 ncRNAs and 9 target genes)
[Caenorhabditis elegans](#) (C.elegans; 4 ncRNA-associated entries between 3 ncRNAs and 3 target genes)
[Xenopus](#) (Xenopus; 4 ncRNA-associated entries between 2 ncRNAs and 4 target genes)

Browse by cell death pathway...

[Apoptosis](#) (2403 ncRNA-associated entries between 480 ncRNAs and 750 target genes)
[Autophagy](#) (2205 ncRNA-associated entries between 848 ncRNAs and 425 target genes)
[Necrosis](#) (7 ncRNA-associated entries between 7 ncRNAs and 4 target genes)

Fig. 18.48 Browse

sub-network associated with the input ncRNAs or genes, and visualizes the direct and secondary interacting sub-network associated with the input ncRNAs or genes, respectively.” The names of the ncRNAs and genes on both sides are placed in the intermediate region by selecting the add key, and the entries with an interaction relationship are listed after the submission.

18.3.2.1.3 Browse

The content can be browsed directly by ncRNA category, species and by death cell pathway. Browsing can be performed by clicking on the link (Fig. 18.48).

References

- Chen LL, Wang YB, Song JX, Deng WK, Lu JH, Ma LL, Yang CB, Li M, Xue Y. Phosphoproteome-based kinase activity profiling reveals the critical role of MAP2K2 and PLK1 in neuronal autophagy. *Autophagy*. 2017;13:1969–80.
- Deng W, Ma L, Zhang Y, Zhou J, Wang Y, Liu Z, Xue Y. THANATOS: an integrative data resource of proteins and post-translational modifications in the regulation of autophagy. *Autophagy*. 2018;14:296–310.

- Homma K, Suzuki K, Sugawara H. The Autophagy Database: an all-inclusive information resource on autophagy that provides nourishment for research. *Nucleic Acids Res.* 2011;39:D986–90.
- Hsu CH. The negentropy intake of biological systems (As shown by the problems of protein nutrition). *Acta Biochim Biophys Sin Shanghai.* 1962;2:11–20.
- Hu Y, Huang Y, Yi Y, Wang H, Liu B, Yu J, Wang D. Single-cell RNA sequencing highlights transcription activity of autophagy-related genes during hematopoietic stem cell formation in mouse embryos. *Autophagy.* 2017;13:770–1.
- Huang Y, Tan P, Wang X, Yi Y, Hu Y, Wang D, Wang F. Transcriptomic insights into temporal expression pattern of autophagy genes during monocytic and granulocytic differentiation. *Autophagy.* 2018;14:558–9.
- Jin S, Zhang X, Miao Y, Liang P, Zhu K, She Y, Wu Y, Liu DA, Huang J, Ren J, Cui J. m(6)A RNA modification controls autophagy through upregulating ULK1 protein abundance. *Cell Res.* 2018;28:955–7.
- Kalvari I, Tsompanis S, Mulakkal NC, Osgood R, Johansen T, Nezis IP, Promponas VJ. iLIR: a web resource for prediction of Atg8-family interacting proteins. *Autophagy.* 2014;10:913–25.
- Kiselev VY, Andrews TS, Hemberg M. Challenges in unsupervised clustering of single-cell RNA-seq data. *Nat Rev Genet.* 2019;20:273–82.
- Klionsky DJ, Abdelmohsen K, Abe A, Abedin MJ, Abeliovich H, Acevedo Arozena A, Adachi H, Adams CM, Adams PD, Adeli K, Adhietty PJ, Adler SG, Agam G, Agarwal R, Aghi MK, Agnello M, Agostinis P, Aguilar PV, Aguirre-Ghiso J, Airoidi EM, Ait-Si-Ali S, Akematsu T, Akporiaye ET, Al-Rubeai M, Albaiceta GM, Albanese C, Albani D, Albert ML, Aldudo J, Algul H, Alirezai M, Alloza I, Almasan A, Almonte-Beceril M, Alnemri ES, Alonso C, Altan-Bonnet N, Altieri DC, Alvarez S, Alvarez-Erviti L, Alves S, Amadoro G, Amano A, Amantini C, Ambrosio S, Amelio I, Amer AO, Amessou M, Amon A, An Z, Anania FA, Andersen SU, Andley UP, Andreadi CK, Andrieu-Abadie N, Anel A, Ann DK, Anoopkumar-Dukie S, Antonioli M, Aoki H, Apostolova N, Aquila S, Aquilano K, Araki K, Arama E, Aranda A, Araya J, Arcaro A, Arias E, Arimoto H, Ariosa AR, Armstrong JL, Arnould T, Arsov I, Asanuma K, Askanas V, Asselin E, Atarashi R, Atherton SS, Atkin JD, Attardi LD, Auburger P, Auburger G, Aurelian L, Autelli R, Avagliano L, Avantiaggiati ML, Avrahami L, Awale S, Azad N, Bachetti T, Backer JM, Bae DH, Bae JS, Bae ON, Bae SH, Baehrecke EH, Baek SH, Baghdiguian S, Bagniewska-Zadworna A, et al. Guidelines for the use and interpretation of assays for monitoring autophagy (3rd edition). *Autophagy.* 2016;12:1–222.
- Mancias JD, Wang X, Gygi SP, Harper JW, Kimmelman AC. Quantitative proteomics identifies NCOA4 as the cargo receptor mediating ferritinophagy. *Nature.* 2014;509:105–9.
- Morselli E, Marino G, Bennetzen MV, Eisenberg T, Megalou E, Schroeder S, Cabrera S, Benit P, Rustin P, Criollo A, Kepp O, Galluzzi L, Shen S, Malik SA, Maiuri MC, Horio Y, Lopez-Otin C, Andersen JS, Tavernarakis N, Madeo F, Kroemer G. Spermidine and resveratrol induce autophagy by distinct pathways converging on the acetylproteome. *J Cell Biol.* 2011;192:615–29.
- Moussay E, Kaoma T, Baginska J, Muller A, van Moer K, Nicot N, Nazarov PV, Vallar L, Chouaib S, Berchem G, Janji B. The acquisition of resistance to TNFalpha in breast cancer cells is associated with constitutive activation of autophagy as revealed by a transcriptome analysis using a custom microarray. *Autophagy.* 2011;7:760–70.
- Peeters JGC, Picavet LW, Coenen S, Mauthe M, Vervoort SJ, Mocholi E, de Heus C, Klumperman J, Vastert SJ, Reggiori F, Coffey PJ, Mokry M, van Loosdregt J. Transcriptional and epigenetic profiling of nutrient-deprived cells to identify novel regulators of autophagy. *Autophagy.* 2019;15:98–112.
- Shannon P, Markiel A, Ozier O, Baliga NS, Wang JT, Ramage D, Amin N, Schwikowski B, Ideker T. Cytoscape: a software environment for integrated models of biomolecular interaction networks. *Genome Res.* 2003;13:2498–504.
- Snel B, Lehmann G, Bork P, Huynh MA. STRING: a web-server to retrieve and display the repeatedly occurring neighbourhood of a gene. *Nucleic Acids Res.* 2000;28:3442–4.

- Subramanian A, Tamayo P, Mootha VK, Mukherjee S, Ebert BL, Gillette MA, Paulovich A, Pomeroy SL, Golub TR, Lander ES, Mesirov JP. Gene set enrichment analysis: a knowledge-based approach for interpreting genome-wide expression profiles. *Proc Natl Acad Sci U S A*. 2005;102:15545–50.
- Tang F, Barbacioru C, Wang Y, Nordman E, Lee C, Xu N, Wang X, Bodeau J, Tuch BB, Siddiqui A, Lao K, Surani MA. mRNA-Seq whole-transcriptome analysis of a single cell. *Nat Methods*. 2009;6:377–82.
- Tatusov RL, Koonin EV, Lipman DJ. A genomic perspective on protein families. *Science*. 1997;278:631–7.
- Turei D, Foldvari-Nagy L, Fazekas D, Modos D, Kubisch J, Kadlecsek T, Demeter A, Lenti K, Csermely P, Vellai T, Korcsmaros T. Autophagy Regulatory Network—a systems-level bioinformatics resource for studying the mechanism and regulation of autophagy. *Autophagy*. 2015;11:155–65.
- Wu D, Huang Y, Kang J, Li K, Bi X, Zhang T, Jin N, Hu Y, Tan P, Zhang L, Yi Y, Shen W, Huang J, Li X, Xu J, Wang D. ncRDeathDB: a comprehensive bioinformatics resource for deciphering network organization of the ncRNA-mediated cell death system. *Autophagy*. 2015;11:1917–26.
- Xu J, Li YH. miRDeathDB: a database bridging microRNAs and the programmed cell death. *Cell Death Differ*. 2012;19:1571.